BIOMECHANICS, AGING, EXERCISE AND OTHER INTERVENTIONS

EDITED BY: Rafael Reimann Baptista, Marcus Fraga Vieira, Chiarella Sforza and Rezaul Begg
PUBLISHED IN: Frontiers in Bioengineering and Biotechnology, Frontiers in Physiology and Frontiers in Sports and Active Living

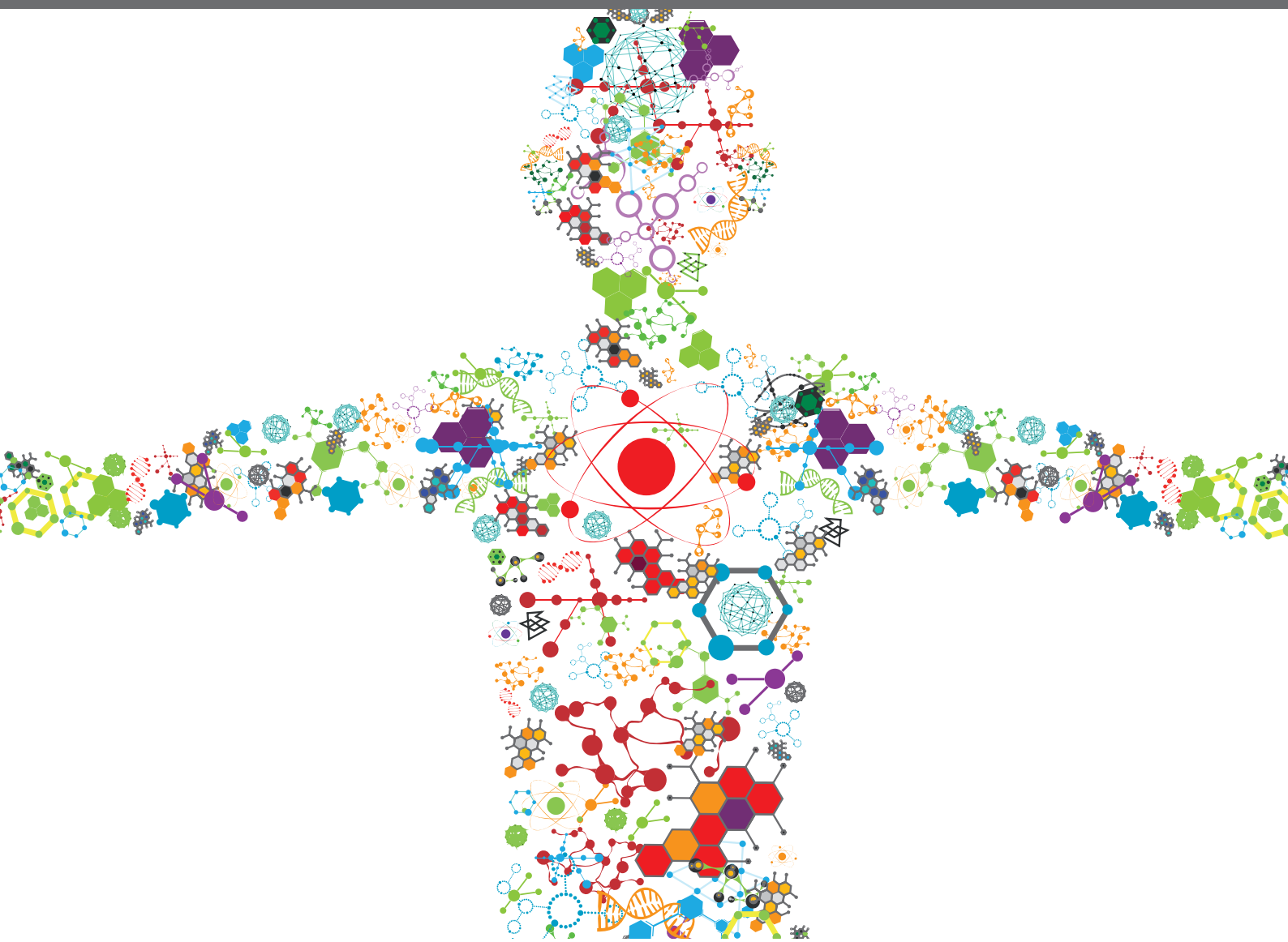

frontiers Research Topics

frontiers

ISSN 1664-8714
ISBN 978-2-83250-824-4
DOI 10.3389/978-2-83250-824-4

About Frontiers

Frontiers is more than just an open-access publisher of scholarly articles: it is a pioneering approach to the world of academia, radically improving the way scholarly research is managed. The grand vision of Frontiers is a world where all people have an equal opportunity to seek, share and generate knowledge. Frontiers provides immediate and permanent online open access to all its publications, but this alone is not enough to realize our grand goals.

Frontiers Journal Series

The Frontiers Journal Series is a multi-tier and interdisciplinary set of open-access, online journals, promising a paradigm shift from the current review, selection and dissemination processes in academic publishing. All Frontiers journals are driven by researchers for researchers; therefore, they constitute a service to the scholarly community. At the same time, the Frontiers Journal Series operates on a revolutionary invention, the tiered publishing system, initially addressing specific communities of scholars, and gradually climbing up to broader public understanding, thus serving the interests of the lay society, too.

Dedication to Quality

Each Frontiers article is a landmark of the highest quality, thanks to genuinely collaborative interactions between authors and review editors, who include some of the world's best academicians. Research must be certified by peers before entering a stream of knowledge that may eventually reach the public - and shape society; therefore, Frontiers only applies the most rigorous and unbiased reviews.
Frontiers revolutionizes research publishing by freely delivering the most outstanding research, evaluated with no bias from both the academic and social point of view. By applying the most advanced information technologies, Frontiers is catapulting scholarly publishing into a new generation.

What are Frontiers Research Topics?

Frontiers Research Topics are very popular trademarks of the Frontiers Journals Series: they are collections of at least ten articles, all centered on a particular subject. With their unique mix of varied contributions from Original Research to Review Articles, Frontiers Research Topics unify the most influential researchers, the latest key findings and historical advances in a hot research area! Find out more on how to host your own Frontiers Research Topic or contribute to one as an author by contacting the Frontiers Editorial Office: frontiersin.org/about/contact

BIOMECHANICS, AGING, EXERCISE AND OTHER INTERVENTIONS

Topic Editors:
Rafael Reimann Baptista, Pontifical Catholic University of Rio Grande do Sul, Brazil
Marcus Fraga Vieira, Universidade Federal de Goiás, Brazil
Chiarella Sforza, University of Milan, Italy
Rezaul Begg, Victoria University, Australia

Citation: Baptista, R. R., Vieira, M. F., Sforza, C., Begg, R., eds. (2022). Biomechanics, Aging, Exercise and Other Interventions. Lausanne: Frontiers Media SA. doi: 10.3389/978-2-83250-824-4

Table of Contents

frontiers | Frontiers in Bioengineering and Biotechnology

TYPE Editorial
PUBLISHED 07 November 2022
DOI 10.3389/fbioe.2022.1056547

OPEN ACCESS

EDITED AND REVIEWED BY
Markus O. Heller,
University of Southampton,
United Kingdom

*CORRESPONDENCE
Rafael Reimann Baptista,
rafael.baptista@pucrs.br

SPECIALTY SECTION
This article was submitted to Biomechanics, a section of the journal Frontiers in Bioengineering and Biotechnology

RECEIVED 29 September 2022
ACCEPTED 24 October 2022
PUBLISHED 07 November 2022

CITATION
Baptista RR, Vieira MF, Begg R and Sforza C (2022), Editorial: Biomechanics, aging, exercise and other interventions.
Front. Bioeng. Biotechnol. 10:1056547.
doi: 10.3389/fbioe.2022.1056547

Editorial: Biomechanics, aging, exercise and other interventions

Rafael Reimann Baptista[1]*, Marcus Fraga Vieira[2], Rezaul Begg[3] and Chiarella Sforza[4]

[1]Pontifical Catholic University of Rio Grande do Sul, Porto Alegre, Brazil, [2]Universidade Federal de Goiás, Goiânia, Brazil, [3]Victoria University, Melbourne, VIC, Australia, [4]Department of Biomedical Sciences for Health, Università degli Studi di Milano, Milan, Italy

KEYWORDS

aging, older adults, exercise, interventions, kinesiology

Editorial on the Research Topic
Biomechanics, aging, exercise and other interventions

Physiological and biomechanical changes observed during human aging are related to several factors, but alterations in physical health and deficits in motor control are among the most frequent. In this Research Topic we collected some investigations describing the normal modifications occurring in older adults, as well as the effect of specific interventions to counteract the side effects and complications of aging.

Due to the increase in life expectancy, people over the age of 65 years are increasing rapidly. According to a 2019 worldwide estimate, about 16% of the population will be older adults by 2050 compared to 9% less than 5 years ago. In the same timespan (2019–2050) the number of people aged 80 years or over is expected to increase from 143 million to 426 million (United Nations, 2022).

Non-pharmacological treatments, such as exercise, have been highlighted in several studies. Exercise can be proposed in multiple forms, from sport, outdoor walking, indoor gyms, and dedicated classes to private home facilities, but, on all occasions, there should be control of the performance and the effect of the intervention. Before the COVID-19 pandemic, controlled training and rehabilitation coaching were directly provided during the classes or in dedicated laboratories, using conventional optoelectronic motion-capture systems or inertial measurement units. Lockdown weeks showed the necessity to continue to control the effects of home physical exercise on the locomotor system using new, simplified, and low-cost devices. The effectiveness of such devices was evaluated in the current Research Topic. For example, Lee and Park devised a 2-TV camera system that can effectively be used for assisting home exercises.

Delbes et al. proposed a head-mounted display for overground walking during fully immersive virtual training sessions in older adults. The authors showed that older adults adopted the same gait adaptability behavior despite the use of a real vs. virtual environment. Besides, the older adults that participated in the study exhibited good acceptance of the virtual reality device, opening the possibility to design training programs in virtual reality to prevent falls in older adults.

Of course, motion capture is just one of the many tools that can help exercise planning and evaluation. The effectiveness of dynamometers, force platforms, surface EMG, and body composition instruments was investigated in the current Research Topic (Čretnik et al.). Also, exercise planning in older adults should consider age-related characteristics and cannot be directly imported from protocols devised for younger persons.

For example, the most classical form of exercise is sport, and indeed, sports practice should be safe at all ages, with physiological modifications contributing to athletic performance. Unfortunately, some sports include activities with potentially negative implications that can jeopardize an athletic career and should be known by athletes, coaches, and health professionals for screening and injury prevention perspectives. Muscles, tendons, cartilages, and bones are frequently involved, as reported for Taekwondo (Xu et al.) and the alpine sky (Götschi et al.).

During running, fatigue can affect joint biomechanics dramatically. Quan et al. found that there was no proximal shift in knee joint mechanics in amateur female runners after prolonged running. The variations in running fatigue were related to the redistribution of joint work. The authors suggest that to reduce the risk of injuries associated with long-distance running, athletes should also train their muscles.

Tennis training is another popular sport used for fitness maintenance during the lifespan. While evaluating children between the ages of 7 and 8 beginning to play tennis, Wang et al. observed that when introduced to childhood tennis beginners during a sensitive period, regular tennis training combined with a neuromuscular training program could produce greater improvement in a player's sprint and ability to change direction than tennis class intervention alone.

Fatigue is not the only aspect that a physiologist should consider when studying human performance. The Recovery Rate is also important, and this was addressed by Markus et al.. They found that following an exercise-induced muscle damage downhill protocol, young and middle-aged male amateur athletes recover comparably. These findings suggest that trainees of both ages can use similar recovery strategies after completing an aerobic-based exercise-induced muscle damage protocol.

For assessing knee joint disorders, not only deficits in quadriceps flexibility are a risk factor, but their stiffness should also be considered. Chang et al. have shown that patients with knee osteoarthritis (KO) exhibited greater vastus lateralis (VL) stiffness compared to age-matched healthy adults. Furthermore, the authors found a positive correlation between VL stiffness and the Western Ontario and McMaster University's Osteoarthritis Index in patients with KO. These findings suggest an additional evaluation of quadriceps muscle for a proper KO patient follow-up.

In another study published in the current Research Topic, Chen et al. analyzed the effect of plantar-flexion motion on the stiffness of the lumbar and lower limb tissues. Healthy humans participated in this study and performed isometric plantar flexion against different resistance conditions. Their data showed a significant effect of isometric plantar flexion on the stiffness of the lumbar soft tissue and gastrocnemius.

Our Research Topic was not sorely dedicated to exercise physiology. Clinical biomechanics was also addressed as can be observed by the study of De La Fuente et al.. They present interesting data suggesting that crutches on the elbows change how the gluteus medius (GM) activates when climbing stairs. The number of crutches, the lateral usage of the crutches, and whether the leg is loaded or unloaded when going up the stairs were analyzed in detail. Their findings may help those who currently use or plan to use crutches to activate their GM.

Biomechanical modeling was also addressed in this Research Topic. Kumar et al. studied the sit-to-stand adaptations due to muscle strength deficits and the corresponding assistance trajectories adopted in those adaptations using an open-loop single shooting optimization framework and musculoskeletal models. The authors showed that vasti muscle saturation leads to reduced activation of hamstring muscles and gluteus maximus saturation, suggesting that vasti muscle weakness is responsible for sit-to-stand failure. Besides, external assistance can be used when needed to complement strength deficits for a successful sit-to-stand. Such a model can help to design an intervention and novel sit-to-stance assistance devices.

Advanced modeling techniques such as machine learning are being applied to predict internal biomechanical data and as well as data patterns. Using the deep learning method, Boukhennoufa et al. have predicted internal knee abduction impulses from body kinematics and kinetics data. The study found transfer learning to be the best-performing model, achieving a mean absolute percentage error of 8.28%. Since knee joint abduction moments provide an indirect measure of knee joint loading during locomotion, this type of machine learning-based prediction offers the possibility of many clinical applications.

Other authors have proposed challenging situations to improve postural control in older adults. Tsai et al. have studied the effects of stroboscopic vision (SV) on postural fluctuations and cortical processing during stance. SV induced greater postural fluctuations and reduced EEG power in the mid-frontal theta cluster but enhanced in the visual dorsal and frontal-occipital loops of the right hemisphere. The authors concluded that SV adds challenge to postural control and suggest that older adults shift their great dependence on visual inputs to control with more non-visual awareness.

Regarding the improvement of older adults' fitness, strength training is considered as one of the best interventions for this population. Čretnik et al. performed a Systematic Review with Meta-Analysis to examine how traditional or concentric exercise affects older persons' muscle strength, body composition, and

functional performance in comparison to eccentric exercise modalities. Their research showed eccentric exercise is preferable to concentric exercise, or at least just as effective, for maintaining general health and function in older persons.

In this sense, Zhao et al. have studied the effects of low-intensity resistance exercise combined with blood flow restriction in hypertension older adults. They showed that compared to high-intensity resistance exercise and low-intensity resistance exercise, low-intensity resistance exercise combined with blood flow restriction could effectively decrease systolic pressure in hypertension older adults performing quadriceps femoris resistance exercise after 12 weeks of training.

Surgical treatment sometimes is a necessary intervention, especially in older adults. Total hip arthroplasty, dubbed "the operation of the century," has been proven to be incredibly successful for decades. But today's patients want more from their surgeons; if not adequately advised, they now anticipate a painless joint restoration and a quick return to work and sports. Bender et al. discovered evidence to support the need to give patients critical feedback regarding their expectations for returning to work and athletic activities to address this topic. Patients returning to more demanding sports should be closely watched and counseled to prevent overloading as much as possible.

The importance of an active life as well as the relevant role of physical activity in the health and well-being of people of all ages is now well recognized by the scientific, medical, and civil society in general. Physical activity plays an important role in healthy aging, prolonging life by reducing the onset of chronic diseases that affect both physical and mental health.

Overall, the investigations collected by the current Research Topic provided a set of new information that may help the definition of novel exercise protocols (Čretnik et al.; Zhao et al.) specifically suited for elderly people such as the successful use of virtual reality to improve postural control (Delbes et al.) and of stroboscopic vision (Tsai et al.). Activity can then be detected by low-cost devices thus helping to test and training (Lee and Park). The Research Topic also introduced several biomechanical models of the knee joint and the lower limb muscles that represent the theoretical background for the definition of safe and effective training in both healthy and diseased people (Wang et al.; Markus et al.; Chang et al.; Kumar et al.; De La Fuente et al.). From this point of view, current investigations are more and more studying the active part of the locomotor system also thanks to suitable instruments for their assessment (Chen et al.; De La Fuente et al.).

Another important result is the growing attention to injury prevention and evaluation (Xu et al.; Götschi et al.), with a special focus on the effects of fatigue (Quan et al.; Bender et al.). One of the most advanced study mixed biomechanics and artificial intelligence using a deep learning method to predict internal knee forces (Boukhennoufa et al.). The method can be potentially applied to several contexts providing more reliable and predictive models of the joints and muscles. It represents the first step for future investigations.

Author contributions

All authors listed have made a substantial, direct, and intellectual contribution to the work and approved it for publication.

Conflict of interest

The authors declare that the research was conducted in the absence of any commercial or financial relationships that could be construed as a potential conflict of interest.

Publisher's note

Reference

United Nations (2022). Peace, dignity and equality on a healthy planet. Available at: https://www.un.org/en/global-issues/ageing#:~:text=Globally%2C%20the%20population%20aged%2065,11%20in%202019%20(9%25) (Accessed on Sept 03, 2022).

frontiers in Bioengineering and Biotechnology

ORIGINAL RESEARCH
published: 24 September 2021
doi: 10.3389/fbioe.2021.746761

Effects of Fatigue Running on Joint Mechanics in Female Runners: A Prediction Study Based on a Partial Least Squares Algorithm

Wenjing Quan[1,2], Feng Ren[1], Datao Xu[1], Fekete Gusztav[2], Julien S Baker[3] and Yaodong Gu[1]**

[1]Faculty of Sports Science, Ningbo University, Ningbo, China, [2]Savaria Institute of Technology, Eötvös Loránd University, Szombathely, Hungary, [3]Centre for Health and Exercise Science Research, Department of Sport and Physical Education, Hong Kong Baptist University, Hong Kong, China

OPEN ACCESS

Edited by:
Rafael Reimann Baptista, Pontifical Catholic University of Rio Grande do Sul, Brazil

Reviewed by:
Sai Wei Yang, National YangMing ChiaoTung University, Taiwan
Diane Wagner, Indiana University, Purdue University Indianapolis, United States

***Correspondence:**
Fekete Gusztav
fg@inf.elte.hu
Yaodong Gu
guyaodong@nbu.edu.cn

Specialty section:
This article was submitted to Biomechanics, a section of the journal Frontiers in Bioengineering and Biotechnology

Received: *24 July 2021*
Accepted: *13 September 2021*
Published: *24 September 2021*

Citation:
Quan W, Ren F, Xu D, Gusztav F, Baker JS and Gu Y (2021) Effects of Fatigue Running on Joint Mechanics in Female Runners: A Prediction Study Based on a Partial Least Squares Algorithm. Front. Bioeng. Biotechnol. 9:746761. doi: 10.3389/fbioe.2021.746761

Background: Joint mechanics are permanently changed using different intensities and running durations. These variations in intensity and duration also influence fatigue during prolonged running. Little is known about the potential interactions between fatigue and joint mechanics in female recreational runners. Thus, the purpose of this study was to describe and examine kinematic and joint mechanical parameters when female recreational runners are subject to fatigue as a result of running.

Method: Fifty female recreational runners maintained running on a treadmill to induce fatigue conditions. Joint mechanics, sagittal joint angle, moment, and power were recorded pre- and immediately post fatigue treadmill running.

Result: Moderate reductions in absolute positive ankle power, total ankle energy dissipation, dorsiflexion at initial contact, max dorsiflexion angle, and range of motion of the joint ankle were collected after fatigue following prolonged fatigue running. Knee joint mechanics, joint angle, and joint power remained unchanged after prolonged fatigue running. Nevertheless, with the decreased ankle joint work, negative knee power increased. At the hip joint, the extension angle was significantly decreased. The range motion of the hip joint, hip positive work and hip positive power were increased during the post-prolonged fatigue running.

Conclusion: This study found no proximal shift in knee joint mechanics in amateur female runners following prolonged fatigue running. The joint work redistribution was associated with running fatigue changes. As for long-distance running, runners should include muscle strength training to avoid the occurrence of running-related injuries.

Keywords: joint work, kinetics, partial least-squares regression, fatigue, prolonged running

INTRODUCTION

Running can be considered one of the most popular recreational physical activities worldwide that promote aerobic capacity and reduce the risk of cardiovascular disease (Chakravarty et al., 2008; Stamatakis and Chaudhury, 2008; Dempster et al., 2021). Running-related injuries have been identified as a common overuse injury in competitive and recreational runners. As a cyclical

movement, long-distance running can cause overuse-related injuries due to the extended heavy impacts between the lower limb and the ground. It has been shown that the risk of running-related injury has increased from 6.9 to 92.4% per 1,000 h of running (Van Gent et al., 2007; Videbæk et al., 2015). In addition, female runners are subjected to a higher risk of overuse running injuries than male runners (Taunton et al., 2002; Boling et al., 2010). However, the mechanism of female running joint work distributed for fatigue running was still unclear.

Recently, some studies have focused on joint work distribution after long-distance running. Previous investigations have reported that the ankle energy generation significantly decreased in recreational runners compares to competitive runners. With an increase in running distance, the positive work contribution could shift from distal (ankle) to proximal (knee, hip) joints. The possible interpretation of this phenomenon is the following: runners who are subjected to fatigue due to intensive sports activities such as running, the ankle, plantar flexors might cause the ankle energy generation and ankle joint moment reduced (Sanno et al., 2018). This evidence shows that a redistribution occurs in the joint work, which can be considered as a primary factor in improving the metabolic cost during prolonged running. Simultaneously, the muscular capacity of competitive runners was significantly greater than the recreational runners, which might result in less plantarflexor after fatigue running. Evidence has demonstrated that the foot and ankle play an essential role during running, constituting more than 50% of the joint absorption and joint energy generation (Kelly et al., 2018; Cigoja et al., 2019). Interestingly, a previous study found that well-trained rearfoot strike runners did not show a proximal positive joint work shift followed by prolonged running (Melaro et al., 2021). It is worth mentioning that different running strike pattern designs were used in the study, which may have caused different results. However, there is little research about joint work in female runner's fatigue running biomechanics. Future studies should consider the type of sex and distance when calculating the changes in joint work following fatigue induced from prolonged running (Melaro et al., 2021).

Additionally, fatigue running was the main factor that modify running biomechanics parameters. (Derrick et al., 2002). In 1999, Dutto et al. reported that after fatigue running, dorsiflexion at heel contact was more reduced than pre-fatigue; in 1981, Elliot et al. showed an increase in rearfoot motion after prolonged running, possibly due to fatigue (Elliot and Ackland, 1981; Dutto et al., 1997). Generally, fatigue might lead to a decline in the motor control ability of the musculoskeletal system and increase the risk of sports injuries (Lieber, 2018; Zheng, 2021). With respect to kinematic parameters, previous studies have pointed out that impact acceleration, trunk tilt, and ankle eversion angle were increased after prolonged running due to fatigue (Mizrahi et al., 2000). For example, after exhaustive running, the plantarflexion moment and external rotation moments were decreased (Benson and O'Connor, 2015; Hashish et al., 2016). Simultaneously, the knee and hip angular abduction impulses were significantly increased (Willson et al., 2015).

As for the running kinematics variables, it has been shown that the ankle and knee initial contact angle was crucial for joint stability (Bazuelo-Ruiz et al., 2018). Regarding IC (initial foot contact), contradictive studies have been published, where some authors claimed that the ankle angle is linearly influenced by joint absorption during running (Breine et al., 2017), while others stated that the connection was nonlinear (Chambon et al., 2015). There is limited research on how the initial angle affects joint work. Bastiaan Breine et al. found that the foot angle at initial contact during the rearfoot strike had the highest correlation with the vertical instantaneous loading rate (VILR) (Breine et al., 2017). This indicates that a greater foot angle or more pronounced rearfoot strike corresponded with a lower vertical instantaneous loading rate (VILR). Furthermore, following exhaustive treadmill running, knee flexion at foot contact was significantly increased (Derrick et al., 2002). Therefore, lower limb kinematics' modification following fatigue-induced running was associated with ankle initial foot contact and joint energy.

To the best of our knowledge, little work has been done on the effects of fatigue on joint work during the impact phase of long-distance running. Thus, the purpose of this study was to describe and examine kinematic and joint mechanical parameters when female recreational runners were subjected to fatigue after long-distance running. The analysis was carried out using the Partial Least Square Algorithm (PLSR) to investigate if a linear relationship existed between the initial joint angle, ankle joint work, and knee joint work. Our first hypothesis was that ankle work would decrease due to fatigue after prolonged running. Our second hypothesis was that joint work would have a greater relationship with the initial angle of the ankle and knee.

MATERIALS AND METHODS

Participants

Fifty female recreational runners (23.89 ± 1.27 years, 65.39 ± 22.47 kg, 163.22 ± 15.01 cm) were recruited from the university running clubs, while flyers were distributed around the university campus for this investigation. Participants were screened to include individuals aged between 18 and 27 years, ran between 5 and 10 km per week, and did not have any low limb musculoskeletal injuries in the previous 6 months prior to data collection. All participants were rearfoot strikers and without any vigorous exercise 24 h before data capture. All subjects provided their signed informed consent, while ethical approval was obtained from the Sports Science Faculty at Ningbo University.

Instrumentation

The kinematic data was acquired using a British-made Vicon infrared 3D motion capture system (Oxford Metric Ltd., Oxford, United Kingdom), including eight high-speed infrared cameras with Nexus analysis software. The sampling frequency for this study was 200 Hz. Ground reaction force (GRF) data were measured using a 90*58*10 cm force platform at 1000 Hz (9281B, Kistler Instruments AG, Switzerland). During the test process, heel strike and toe-off phases were defined when the vertical GRF crossed a 30 N threshold (Maas et al., 2018). Kinematic and kinetic data were collected simultaneously before the running started and when the person reached the point of exhaustion or fatigue. This point was detected by a heart rate monitor (Polar RS100, Polar Electro Oy, Woodbury, NY, United States), which was compulsory for all participants while running on the motorized treadmill (h/p/cosmos sports and medical GmbH, Germany). The subjects used conventional running shoes during the running experiments. Thirty-six retroreflective markers, with 14 mm-diameter, were attached to the right and left lower extremities to define the ankle, knee, and hip joints using a 6DOF market set flowing the previous study (Zhou et al., 2021).

Running Fatigue Protocol

Prior to data collection, subjects were familiarized with the running protocol and the Borg Scale RPE 6–20. The Borg Scale RPE 6–20 and heart rate monitor were used to record subjective fatigue and heart rate changes during the running intervention. First, the subjects warmed up at 6 km/h for 3 min. Then, the operator increased the treadmill speed to 14.4 km/h. Subjects were required to run at 14.4 km/h on the treadmill until they could not continue. They were then considered in a fatigued state. Fatigue was defined when all the following conditions were met: 1) the heart rate of the participants reached 90% maximum heart rate of their age-calculated maximum heart rate (HRmax = 220-age), 2) the participants could not continue running, and 3) a rating on the Borg scale exceeded RPE > 17 (very hard) (Koblbauer et al., 2014).

Experimental Protocol

There are two testing sessions in this study, which include the pre-fatigue and post-fatigue protocols. Before the test, all subjects had to wear uniform pants, T-shirts, socks, and running shoes. They used to jump and running activities for the warm-up session. In the pre-fatigue section, the participants ran through the force plate across a 15 m runway at 3.3 m/s to capture the kinematic and ground reaction force data. All participants performed the fatigue intervention on the treadmill in the post-fatigue section and then immediately ran over the force plate at 3.3 m/s to capture the kinematics and ground reaction force. For each subject, six successful running trials were collected. Using the speed measuring instrument (Smart speed, Fusion Sport Inc., Burbank, CA, United States) to control every subject running speed at 3.3 m/s. A successful trial was defined when a participant ran through the force platform using the right foot and the running speed was 3.3 m/s ±0.05.

TABLE 1 | The average value (X_{ave}), maximum value (X_{max}), minimum value (X_{min}) and the difference between the maximum and minimum values (X_{dif}) of predictive variables X.

X	X1 (ankle IC)	X2 (knee IC)	X3 (ROM ankle)	X4 (ROM knee)
X_{ave}	8.21	19.22	43.82	27.01
X_{max}	16.58	29.85	80.41	37.51
X_{min}	1.97	8.44	22.53	18.34
X_{dif}	14.61	21.41	57.88	19.17

Data Analysis

Sagittal Plane Kinematics

The kinematic data was preprocessed using Vicon Nexus software, capturing a full running stance phase, completing any missing mark points, and removing any incorrect or redundant mark points during the process. After preprocessing, the biomechanical data was imported into Visual3D software (v6; C-Motion, Inc., Germantown, MD, United States) for processing and calculation. The kinematic and kinetic data were processed using a fourth-order Butterworth low-pass filter with cutoff frequencies of 15 and 50 Hz, respectively (Bezodis et al., 2008). Joint angles, joint moments, joint power, and joint work were normalized to the gait cycle over 101-time points. Ankle, knee and hip angles were calculated using Cardan angles in the sagittal plane (positive-flexion/dorsiflexion; negative-extension/plantarflexion) (Quan et al., 2021).

Joint Kinetics

The joint moments, including the maximum moment values of the ankle, knee, and hip joints, were calculated using an inverse dynamics approach. Joint power, including the maximum power values of the ankle, knee, and hip joints, was defined as the dot product of the joint moment and the angular velocity. The ankle joint dorsiflexion moment, knee joint flexion moment, and hip flexion moment are positive (+), and the corresponding ankle joint plantarflexion moment and hip joint extension moment are negative (−). The positive value (+) of the ankle, knee, and hip joint power indicates energy production. The negative value (−) of the ankle, knee and hip joint power indicates the energy absorption of the ankle, knee, and hip joints.

$$\mathbf{P_j} = \mathbf{M_j} \cdot \boldsymbol{\omega_j}$$

M_j is the joint moment of the ankle, knee, and hip joint, while ω_j is the joint angular velocity of the ankle, knee, or hip. The joint work is obtained by integrating the joint power over time. In this paper, the trapezoidal method was used for numerical integration. Energy generation (E_g) or energy absorption (E_a) was calculated by the integral of the positive and negative areas of joint angular power at a time using a custom program over the stance phase in MATLAB (Version: R2019a, The MathWorks,

TABLE 2 | The predictors of each predictive variable.

X	X1 (ankle IC)	X2 (knee IC)	X3 (ROM ankle)	X4 (ROM knee)
X_{min}-10%X_{dif}	1.78	7.60	20.27	16.51
X_{min}	1.97	8.44	22.53	18.34
X_{min}+10%X_{dif}	3.44	10.58	28.31	20.26
X_{min}+20%X_{dif}	4.90	12.73	34.10	22.18
X_{min}+30%X_{dif}	6.36	14.87	39.89	24.09
X_{min}+40%X_{dif}	7.82	17.01	45.68	26.01
X_{min}+50%X_{dif}	9.28	19.15	51.47	27.93
X_{min}+60%X_{dif}	10.74	21.29	57.25	29.84
X_{min}+70%X_{dif}	12.20	23.43	63.04	31.76
X_{min}+80%X_{dif}	13.66	25.57	68.83	33.68
X_{min}+90%X_{dif}	15.12	27.71	74.62	35.59
X_{max}	16.58	8.44	80.41	37.51
X_{max}+110%X_{dif}	33.16	16.89	160.81	75.02

Note: X: predictor variables, X1: initial ankle angle, X2: initial knee angle, X3: range motion of ankle angle, X4: range motion of knee angle.
*Note: X: *significant difference between pre-fatigue running and post-fatigue ($p \leq 0.05$).*

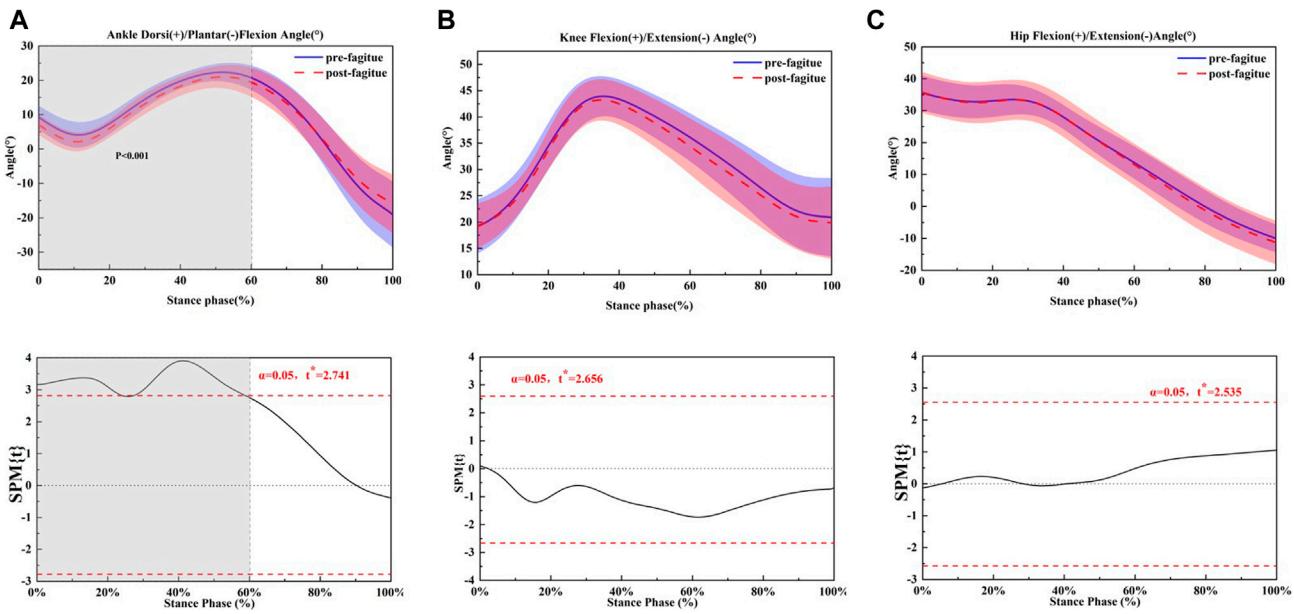

FIGURE 1 | Comparing the mean values of ankle, knee and hip joint angle from all participants between fatigue conditions (pre-fatigue; post-fatigue). *$p \leq 0.05$.

Natick, MA, United States). Total joint work was calculated by integrating the joint power time curves over the stance phase, respectively (Koblbauer et al., 2014; Xu et al., 2021).

$$E_i = W_i = \int_{t1}^{t2} P_j \cdot dt = \int_{t1}^{t2} M_j \cdot \omega_j \cdot dt$$

Where $i = a$ as absorption or g as generation, t_1 to t_2 is the time of running stance; W is the total work on a joint during the running stance; P_j is the instantaneous power of a joint. The joint moment, power, and work were all divided by body weight for normalization.

Partial Least Squares Regression Method

Partial least squares regression (PLSR) is a regression mathematical modeling approach applied to multiple independent variables to various dependent variables (responses Y) and multiple independent variables (predictors X) to a single dependent variable (Wu et al., 2014). Partial least squares regression (PLSR) was used to compare four predictors, including initial joint angle and joint motion of the knee and ankle, and six responses, including positive and negative joint work, total joint work of the knee, and the ankle. The predictive variables included initial ankle joint angle (X1), initial knee joint angle (X2), range motion of the ankle (X3), and range motion of the knee (X4). The response variables included ankle positive work (Y1), ankle negative work (Y2), total work of the ankle (Y3), knee positive work (Y4), knee negative work (Y5) and total work of the knee (Y6).

Data standardization processing was carried out on the original data matrix X, Y to facilitate the use of formulas in subsequent operations and to express the corresponding data while reducing the error. The corresponding matrix was obtained after processing.

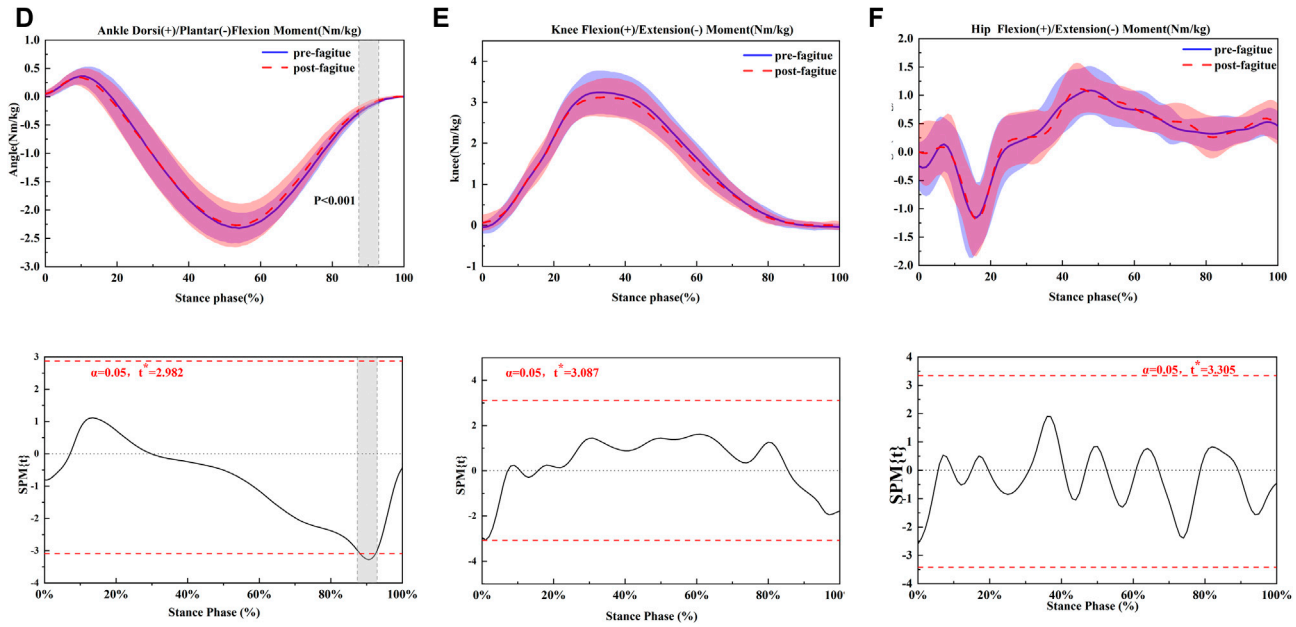

FIGURE 2 | Comparing the mean values of ankle, knee and hip joint moment from all participants between fatigue conditions (pre-fatigue; post-fatigue). *$p \leq 0.05$.

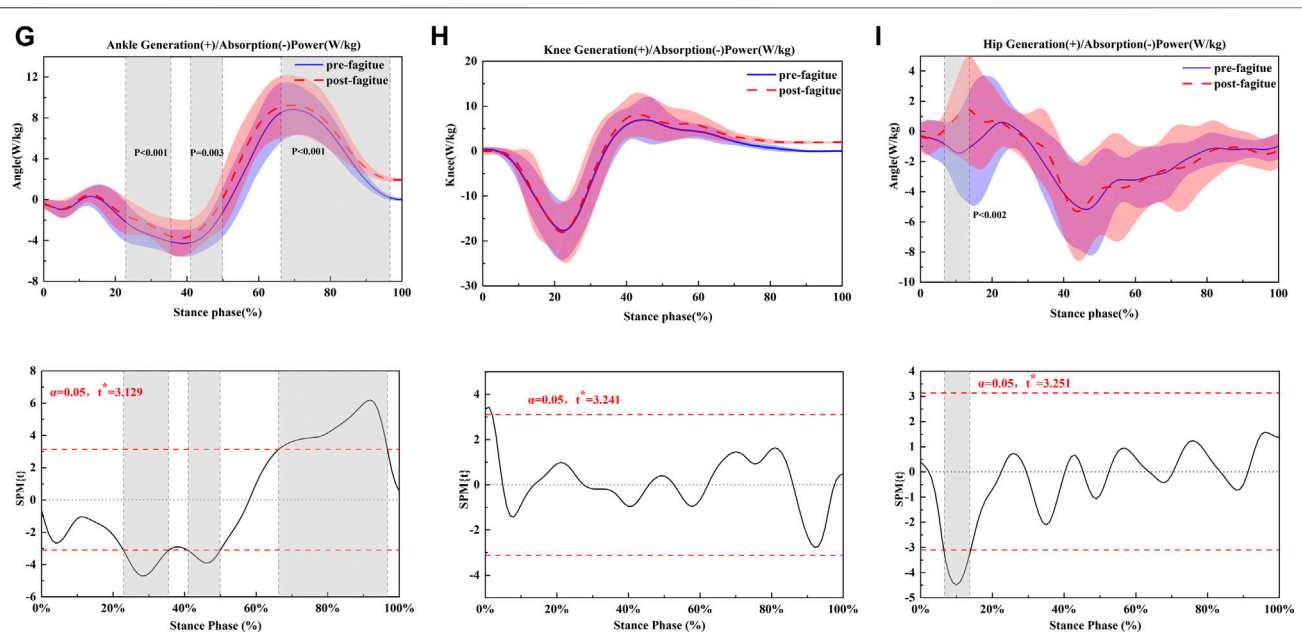

FIGURE 3 | Comparing the mean values of ankle, knee and hip joint power from all participants between fatigue conditions (pre-fatigue; post-fatigue). *$p \leq 0.05$.

Considering a $(\boldsymbol{N} \times \boldsymbol{K})$ matrix of the mean-centered input space (X) and a $(\boldsymbol{N} \times \boldsymbol{J})$ matrix of the mean-centered output space (Y), where K is the number of independent variables (factors) per observation (4 joint angles), J is the number of dependent variables per observation (6 joint work), and N is the number of the observations (50 training samples from the total of runners in this study) and subscript L is the number of components. **P** matrix and **Q** matrix are the so-called loading matrices, **E** and **F** are the residual matrices. T and U are the projection matrices. PLSR method decomposes the **X** and **Y** matrices into a bilinear structural model, consisting of a linear combination of the score and the loading matrix.

$$\boldsymbol{X}_{NK} = \boldsymbol{T}_{NL} \cdot \boldsymbol{P}_{KL}^{T} + \boldsymbol{E}_{NK}$$
$$\boldsymbol{Y}_{NJ} = \boldsymbol{U}_{NL} \cdot \boldsymbol{Q}_{JL}^{T} + \boldsymbol{F}_{NJ}$$

Step 1. The original data matrix X, Y will be normalized to facilitate the expression of the corresponding data by the formula

TABLE 3 | Lower extremity joint kinematics pre-fatigue running and post-prolonged fatigue running (x ± SD).

Variables	Pre-fatigue	Post-fatigue	*p*-value
Ankle IC (◦)	9.23 ± 3.44	7.19 ± 3.00	**0.002***
Max dorsiflexion angle (◦)	22. 20.66 ± 3.31	20.66 ± 3.31	**0.001***
Max plantarflexion angle (◦)	−19.16 ± 9.43	−18.52 ± 8.24	0.513
Range of ankle joint motion (◦)	41.74 ± 8.28	39.18 ± 13.00	**0.023***
Knee IC (◦)	19.17 ± 5.12	19.27 ± 4.24	0.902
Max flexion angle (◦)	44.13 ± 3.87	43.54 ± 3.83	0.271
Range of knee joint motion (◦)	27.23 ± 4.28	26.78 ± 4.29	0.511
Max hip flexion angle (◦)	35.87 ± 5.24	36.15 ± 6.47	0.693
Max hip extension angle (◦)	−9.98 ± 4.39	−11.26 ± 6.86	**0.026***
Range of hip joint motion (◦)	45.86 ± 4.03	47.41 ± 4.49	**0.001***

*Note: *significant difference between pre-fatigue running and post-fatigue running (p ≤ 0. 05). IC: initial contact angle.*

in the subsequent operation while reducing the error between data volumes, and the corresponding matrix will be obtained after processing. The $\mathbf{E_{NK}}$ is the corresponding matrix for $\mathbf{X_{NK}}$ and $\mathbf{F_{NJ}}$ is the corresponding matrix for $\mathbf{Y_{NJ}}$ for repeated iterative operations(Xu et al., 2020).

Step 2. After obtaining the corresponding normalized matrix, the corresponding components need to be extracted. In this regression PLSR model, the number k principal components extracted for modeling is determined by the cross-validity test. Thus, H principal components are extracted, where Y_j is the *j*th dependent variable. The squared sum of the prediction error is shown in the following equation, where p is the total number of reaction factors:

$$\boldsymbol{PRESS}(\boldsymbol{H}) \sum_{i=k}^{p} \boldsymbol{PRESS}_j(\boldsymbol{H})$$

The squared sum of errors of the dependent variable set Y is:

$$\boldsymbol{SS}(\boldsymbol{H}) \sum_{j=k}^{p} \boldsymbol{SS}_j(\boldsymbol{H})$$

According to the principal component analysis, the corresponding components should satisfy PRESS (H) while it reaches the minimum value. Generally, PRESS (H) is larger than SS (H), While SS (H) is lesser than SS (H-1). Consequently, the smaller PRESS(H)/SS(H-1) is the better. The limit value is commonly set as 0.05 (29,32).

$$\boldsymbol{Q}_H^2 = 1 - \boldsymbol{PRESS}(\boldsymbol{H})/\mathbf{SS}(\mathbf{H}-1) = 1 - 0.952 = 0.0975$$

For this reason, the model meets the accuracy requirement when the cross validity $Q_H^2 < 0.0975$, while the extraction of components is stopped.

This PLSR algorithm model (Version: R2019a, The MathWorks, Natick, MA, United States) uses 80% of the data set sample size as the training set, and 20% sample size as the test set. Firstly, the training set is cross-checked by leave-one-out cross-validation analysis. Second, after cross-checking the model's training set, the new data set was used to verify the model. The average X_{ave}, maximum X_{max}, minimum X_{min}, the difference between the maximum and minimum X_{dif} (X_{max}-X_{min}) of each predictive variable is shown in **Table 1**. The incremental perturbation action of a predictor variable was taken to X_{min} - $10\%X_{dif}$, X_{min}, X_{min} + $10\%X_{dif}$, X_{min} + $20\%X_{dif}$, X_{min} + $30\%X_{dif}$, X_{min} + $40\%X_{dif}$, X_{min} + $50\%X_{dif}$, X_{min} + $60\%X_{dif}$, X_{min} + $70\%X_{dif}$, X_{min} + $80\%X_{dif}$, X_{min} + $90\%X_{dif}$, X_{max}, X_{max} + $100\%X_{dif}$ in **Table 2**.

Statistical Analysis

Statistical analyses were performed to determine significant differences in ankle and knee joint work, joint angle, joint moment, and joint power during the stance phase. Shapiro–Wilk's tests were performed for normal distribution. We used the paired *t*-test in SPSS 23.0 (SPSS Inc., Chicago, IL) to assess data differences for kinematic and kinetic parameters. The significance alpha level was set to 0.05. One-dimensional, one-way repeated measures Statistical Parametric Mapping (SPM) (a = 0.05) was used to assess differences in joint angle, joint moment, and joint power throughout the running stance.

RESULT

The joint kinematics and kinetics of ankle, knee, and hip of pre-post fatigue running are shown in **Figures 1–3** and **Table 3**; **Table 4**; **Table 5**, respectively.

TABLE 4 | Lower extremity joint moment, power pre-fatigue running and post-prolonged fatigue running (x ± SD).

Variables	Pre-fatigue	Post-fatigue	*p*-value
Max ankle PF moment (Nm/kg)	-2.34 ± 0.07	−2.30 ± 0.39	0.337
Max ankle DF moment (Nm/kg)	0.42 ± 0.12	0.40 ± 0.14	0.385
Max knee flexion moment (Nm/kg)	3.34 ± 0.51	3.24 ± 0.41	0.093
Max hip flexion moment (Nm/kg)	1.37 ± 0.44	1.38 ± 0.36	0.885
Max hip extension moment (Nm/kg)	−1.58 ± 0.56	−1.57 ± 0.42	0.982
Max ankle positive power (Watt/kg)	9.42 ± 2.44	8.74 ± 2.89	**0.034***
Max ankle negative power (Watt/kg)	−5.27 ± 1.13	−5.43 ± 1.71	0.535
Max knee positive power (Watt/kg)	9.48 ± 3.97	9.91 ± 4.53	0.455
Max knee negative power (Watt/kg)	−21.45 ± 6.02	−23.65 ± 6.43	**0.050***
Max hip positive power (Watt/kg)	2.63 ± 2.24	3.61 ± 2.74	**0.045**
Max hip negative power (Watt/kg)	−7.80 ± 2.73	−7.43 ± 3.90	0.521

*Note: *significant difference between pre-fatigue running and post-fatigue running (p ≤ 0. 05).*

TABLE 5 | Lower extremity joint work pre-fatigue running and post-prolonged fatigue running (x ± SD).

Variables	Pre-fatigue	Post-fatigue	*p*-value
Ankle positive work (J/kg)	0.63 ± 0.17	0.53 ± 0.17	**0.044***
Ankle negative work (J/kg)	−0.32 ± 0.08	−0.33 ± 0.08	0.733
Ankle total work (J/kg)	0.31 ± 0.21	0.25 ± 0.16	**0.046***
Knee positive work (J/kg)	0.60 ± 0.16	0.55 ± 0.16	0.273
Knee negative work (J/kg)	−0.78 ± 0.21	−0.81 ± 0.21	0.223
Knee total work (J/kg)	0.28 ± 0.17	0.26 ± 0.18	0.543
Hip positive work (J/kg)	0.06 ± 0.05	0.09 ± 0.06	**0.050***
Hip negative wok (J/kg)	−0.57 ± 0.18	−0.55 ± 0.28	0.590
Hip total work (J/kg)	−0.51 ± 0.20	−0.46 ± 0.28	0.203

Kinematic Variables

Ankle dorsiflexion angle at initial contact significantly decreased when the pre-fatigue condition and post-prolonged running condition were compared (p = 0.002) (**Figure 1A**). The maximum dorsiflexion angle was also significantly greater than post-prolonged running in the sagittal ankle plane. Due to the dorsiflexion angle decrease, the ROM of the ankle was significantly larger after prolonged running (p = 0.001). There were no differences present in the knee flexion angle and in ROM regarding the sagittal plane. At the hip fatigue, prolonged running had a more significant effect on the max hip extension, and the max hip extension angle was decreased when all participants after prolonged running (p = 0.026) (**Figure 1C**), but hip flexions observed no change. The range of motion of the hip was increased during the post-prolonged running (p = 0.001).

Peak Torque and Power

Moderate reductions in peak positive ankle power (p = 0.034) (**Figure 2D**) were observed following the prolonged running fatigue protocol in **Table 4**. During running, a significantly higher knee negative power (p = 0.05) (**Figure 2E**) was found after the prolonged running fatigue protocol in **Table 4**. For the hip, the positive power (p = 0.045) (**Figure 2F**) was significantly increased in the fatigue and prolonged running condition, respectively (**Table 4**). All other peak joint moments and peak positive and negative joint powers remained unchanged following the prolonged running fatigue protocol.

Joint Work

Relative positive ankle work was significantly increased after prolonged running (p = 0.044). A moderate reduction in the absolute total of ankle work was observed after prolonged running (p = 0.046). Relative negative knee work and knee positive work were moderately unchanged following the prolonged running fatigue protocol (**Table 4**). In addition, the hip positive work was significantly greater when participants after prolonged running (p = 0.050).

PLSR Model

PLSR models for female amateur runners (**Figure 4**) were trained separately for ankle positive work (Y1), ankle negative work (Y2), total work of the ankle (Y3), knee positive work (Y4), knee negative work (Y5) and total work of the knee (Y6). A "leave-one-out" analysis showed a response variable prediction accuracy of 93.31% for the training set and 91.73% for the test set. The results of the sensitivity analysis of the PLSR model based on the independent variable set disturbance factor are shown in **Figure 5**.

Under the control of other independent variable sets, we can find 1) with increased initial ankle angle, under the same conditions, the joint work for runners after fatigue running, Y2 and Y6 were reduced, and the joint work for runners after fatigue running Y1, Y3, Y4 and Y5 were increased. 2) with increased initial knee angle, under the same conditions, the joint work for runners after fatigue running Y5 and Y6 were reduced, and the joint work for runners after fatigue running Y1, Y3 were increased. 3) with the increased motion of the ankle, under the same conditions, the joint work for runners after fatigue running Y2, Y5, and Y6 were reduced, and the joint work for runners after fatigue running Y1, Y3 and Y4 were increased. 4) with the increased motion of the knee, under the same conditions, the joint work for runners after fatigue running Y2 was reduced, and the joint work for runners after fatigue running Y3, Y4, Y5 and Y6 were increased.

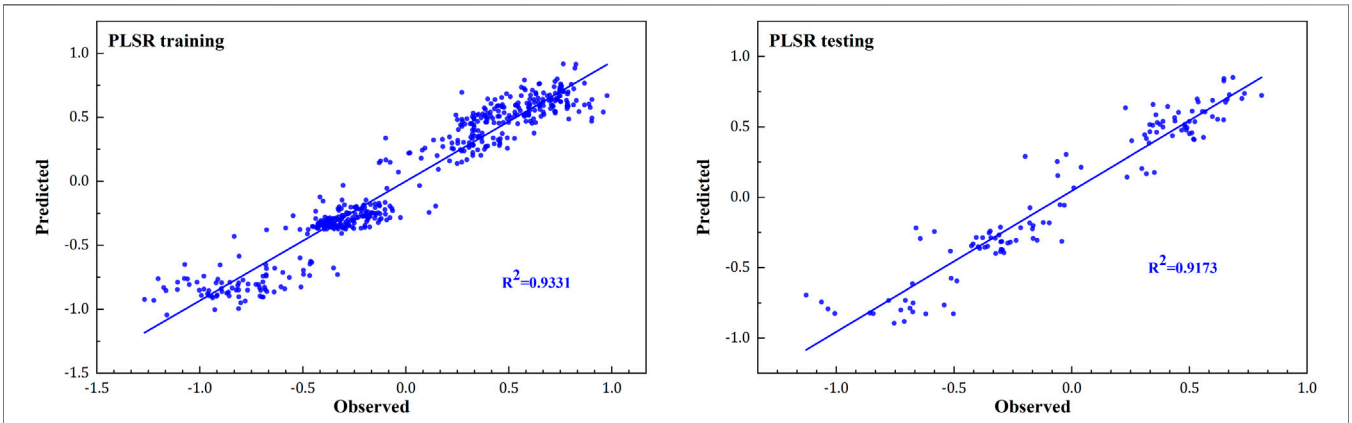

FIGURE 4 | Training (left) and testing (right) accuracy of special skills assessment results of observed and predicted from the PLSR model in the female runners.

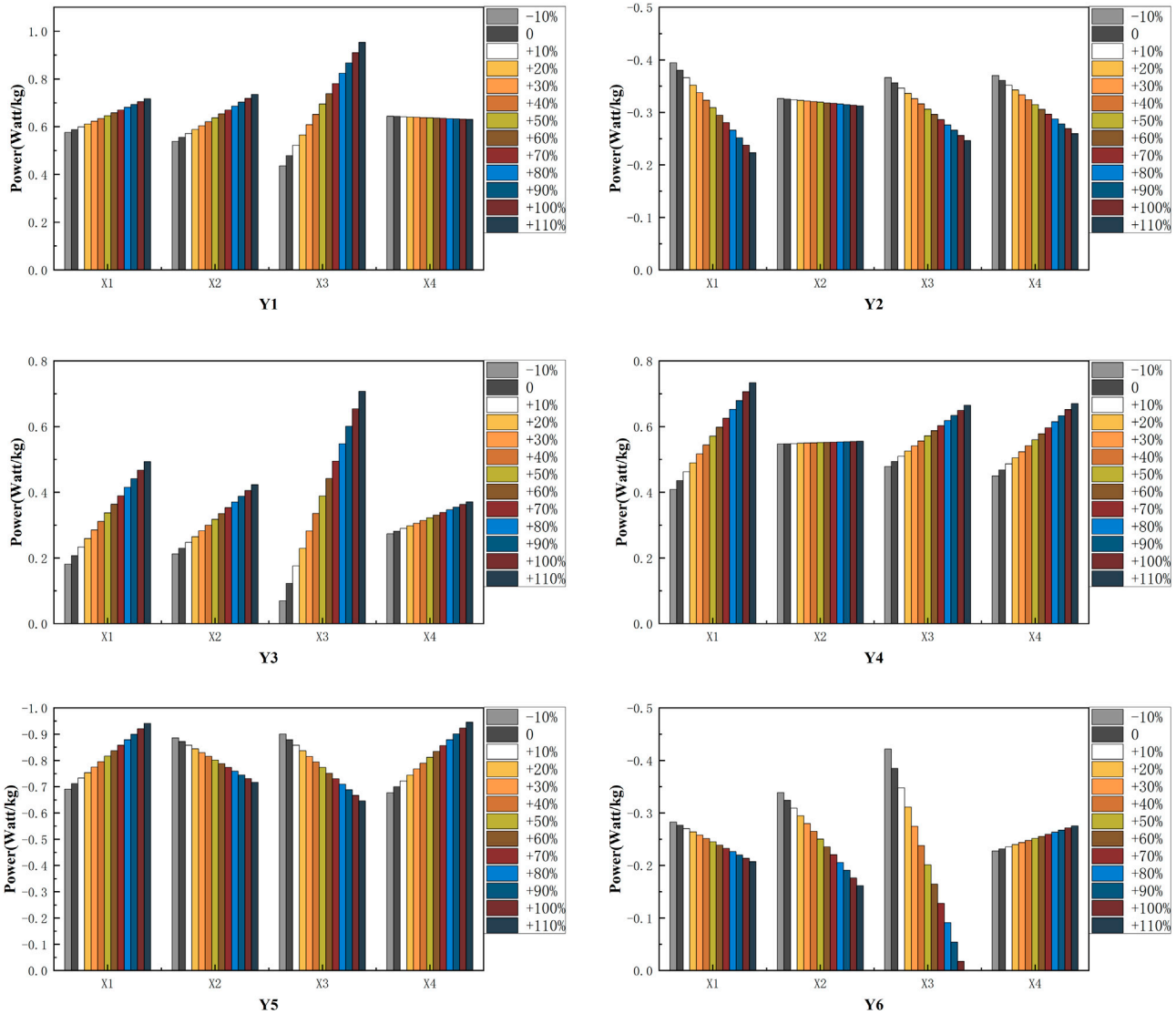

FIGURE 5 | The predicted results of the response variables base on the PLSR model. Ankle positive work (Y1), ankle negative work (Y2), total work of the ankle (Y3), knee positive work (Y4), knee negative work (Y5) and total work of the knee (Y6). Initial ankle joint angle (X1), initial knee joint angle (X2), range motion of the ankle (X3), and range motion of the knee (X4).

DISCUSSION

This study aimed to describe and examine the kinematic and joint mechanical parameters of female recreational runners who sustained prolonged running until reaching the point of fatigue. This study's primary findings are the following: decreased ankle initial contact angle and range of motion of the ankle was found following fatigue running, which agrees with our hypothesis. At the hip joint, the extension angle was significantly decreased, but the motion of the hip increased in the fatigue prolonged running condition. Furthermore, skeletal joint work was significantly reduced regarding the kinetics, including positive ankle work and total ankle work. However, fatigue running resulted in increased hip positive power and hip positive work. When comparing the knee parameters, negative knee power was higher following prolonged running compared to the initial status. However, there was no significant change in the joint angle, positive power, and joint work of knee parameters in this study.

In the present study, significant fatigue effects on lower limb kinematics and kinetics were found following prolonged running as highlighted in the lower limb kinematics: pre-running and post-fatigue running presented different joint angles, joint power, and joint work change trends. A recent study has compared joint work following prolonged running and found that joint work decreased in the distal lower limb joints (Sanno et al., 2018). After

prolonged running, the ankle plantar flexor muscle activity was significantly reduced, which led to joint work redistribution in the ankle joint. Our results are consistent with this finding. With the distal ankle work decreased proximally, hip power significantly increased in the fatigue running condition. Several factors were identified as the underlying mechanisms that caused joint work redistribution following fatigue-induced prolonged running. First, the initial contact angle, max dorsiflexion angle, and range of ankle motion during the stance were significantly decreased in the prolonged fatigue condition compared with the pre-fatigue condition. The decrease in ankle dorsiflexion angle will reduce the moment arm of the ankle joint. A combination of smaller dorsiflexion initial contact and a smaller range of motion of the ankle resulted in smaller positive power, and therefore more minor positive joint work and total energy dissipation at the joint. Moreover, the running distance, sex, and the runner's ability level might affect joint work redistribution following prolonged fatigue running. During the stance of running, the energy distribution of the lower limbs follows the conservation of energy. After a fatigue prolonged running, a decrease in the work done by the distal ankle joint results in an increase in the work and power done by the hip joint. In this study finding, the hip ROM was significantly increased when runners in post-fatigue prolonged running. The study by Winter et al. is that the ROM of the hip joint increases significantly after fatigue, which also supports this result (Winter et al., 2016).

However, there was no change in knee joint work moment and angle in our study. After fatigue prolonged running, the knee flexion with no changes might be due to fatigue running not being associated with knee flexion. Accordingly, the knee was a vital joint during the running stance, absorbing shock and dissipating the ground reaction force (Zhang et al., 2000). In the current study, it has been found that knee negative power was increased in the fatigue prolonged running condition. It has also been demonstrated that there were no changes of the knee and hip joint positive work following a fatiguing treadmill running for the well-trained runners (Melaro et al., 2021).

In addition, it has been noted that following prolonged running, the muscle of the foot also undergoes modification (Christina et al., 2001), which inverts or dorsiflexes following fatigue. It has been found that prolonged fatigue running might lead to dorsiflexor fatigue, increasing the lower extremity attenuation capability to heel impacts (Duquette and Andrews, 2010). Therefore, if the dorsiflexors are fatigued, the initial dorsiflexion contact angle and max dorsiflexion angle are smaller in the fatigue condition, which was consistent with our results. The decreased positive joint work and total joint work of the ankle may result from muscular fatigue. However, we did not collect any muscle change data prior to and after the prolonged running fatigue protocol. In the future, researchers should consider muscle fatigue and investigate the relationship between joint work redistribution.

It should be noted that while the PLSR method has been used to predict plantar pressure (Mei et al., 2019b), foot posture, joint kinematics, joint moments, and joint contact forces in gait analysis (Mei et al., 2019a), this is the first study which applies PLSR models to correlate initial angles with prolonged running fatigue joint work in amateur female runners.

Our model observed that the ankle angle at IC decreased in the fatigue prolonged running, and the joint work showed a high linear correlation, which is consistent with the previous study. Furthermore, with the dorsiflexion decreased, the ankle work and total ankle work were also smaller than the pre-fatigue condition (Sanno et al., 2018; Melaro et al., 2021). Moreover, after prolonged fatigue running, knee flexion may increase more than pre-running. The increased knee flexion angle will decrease the arm of the proximal joint, and the knee joint work will also be smaller than pre-running. This model can be used to analyze the angle changes after fatigued running, which can predict the redistribution and alteration of the work of the ankle and knee joint. Using this prediction model, it is possible to understand the change of work in lower limb joints following prolonged running.

There are also some limitations to our study. First, all subjects were amateur female runners, therefore we need to consider different levels of runners to compare the joint work before and after prolonged running in the future. A considerable variance existed in knee outcome measures. Additional measurement trials may help to overcome this problem. In the future, more attention needs to be paid to muscle fatigue and running economy tests. We used a subjective measure (RPE) and heart rate to rate physical fatigue following treadmill running. While these measures are accurate and valid, we cannot be 100% certain that all participants were totally exhausted at the end of the running fatigue protocol.

CONCLUSION

This study shows an investigation of the changes in joint mechanics, joint kinematics, joint moments, and joint power in the lower extremity following a fatiguing treadmill run in 50 female recreational runners. A relationship between knee and ankle initial angle and joint work was developed. It was found that moderate reductions in absolute positive ankle power, total ankle energy dissipation, dorsiflexion at initial contact, max dorsiflexion angle, and range of motion of the joint ankle were observed after fatigue following prolonged running. Knee joint mechanics, joint angle, and joint power were unchanged following prolonged running. However, with the decreased ankle joint work, negative knee power, increased hip positive work, and hip positive power were increased during initial foot contact following running due to fatigue. These results suggest no proximal shift in knee joint mechanics in female recreational runners following a prolonged run. The joint work redistribution was associated with running fatigue changes. To improve running performance, long-distance runners should include ankle muscle strength training to avoid running-related injuries.

DATA AVAILABILITY STATEMENT

The datasets generated for this study are available on request to the corresponding author.

ETHICS STATEMENT

The studies involving human participants were reviewed and approved by Ethics Committee of Ningbo University (protocol code RAGH20200716). The patients/participants provided their written informed consent to participate in this study.

AUTHOR CONTRIBUTIONS

Conceptualization, WQ and FR; methodology, WQ, DX, and JS; software, FG and YG; validation, WQ, FR, and YG; investigation, WQ, DX, and JS.; writing—original draft preparation, WQ, FG, and DX; writing—review and editing, JS and FR; All authors have read and agreed to the published version of the manuscript.

FUNDING

This study was funded by the by-Key Project of the National Social Science Foundation of China (19ZDA352), National Natural Science Foundation of China (No. 81772423), NSFC-RSE Joint Project (81911530253), János Bolyai Research Scholarship of the Hungarian Academy of Sciences (BO/00047/21/6) and K. C. Wong Magna Fund in Ningbo University.

REFERENCES

Bazuelo-Ruiz, B., Durá-Gil, J. V., Palomares, N., Medina, E., and Llana-Belloch, S. (2018). Effect of Fatigue and Gender on Kinematics and Ground Reaction Forces Variables in Recreational Runners. *PeerJ* 6, e4489. doi:10.7717/peerj.4489

Benson, L. C., and O'Connor, K. M. (2015). The Effect of Exertion on Joint Kinematics and Kinetics during Running Using a Waveform Analysis Approach. *J. Appl. Biomech.* 31 (4), 250–257. doi:10.1123/jab.2014-0138

Bezodis, I. N., Kerwin, D. G., and Salo, A. I. T. (2008). Lower-Limb Mechanics during the Support Phase of Maximum-Velocity Sprint Running. *Med. Sci. Sports Exerc.* 40 (4), 707–715. doi:10.1249/mss.0b013e318162d162

Boling, M., Padua, D., Marshall, S., Guskiewicz, K., Pyne, S., and Beutler, A. (2010). Gender Differences in the Incidence and Prevalence of Patellofemoral Pain Syndrome. *Scand. J. Med. Sci. Sports* 20 (5), 725–730. doi:10.1111/j.1600-0838.2009.00996.x

Breine, B., Malcolm, P., Van Caekenberghe, I., Fiers, P., Frederick, E. C., and De Clercq, D. (2017). Initial Foot Contact and Related Kinematics Affect Impact Loading Rate in Running. *J. Sports Sci.* 35 (15), 1556–1564. doi:10.1080/02640414.2016.1225970

Chakravarty, E. F., Hubert, H. B., Lingala, V. B., and Fries, J. F. (2008). Reduced Disability and Mortality Among Aging Runners. *Arch. Intern. Med.* 168 (15), 1638–1646. doi:10.1001/archinte.168.15.1638

Chambon, N., Rao, G., Guéguen, N., Berton, E., and Delattre, N. (2015). Foot Angle at Touchdown Is Not Linearly Related to the Loading Rate during Running. *Footwear Sci.* 7, S37–S38. doi:10.1080/19424280.2015.1038314

Christina, K. A., White, S. C., and Gilchrist, L. A. (2001). Effect of Localized Muscle Fatigue on Vertical Ground Reaction Forces and Ankle Joint Motion during Running. *Hum. Mov. Sci.* 20 (3), 257–276. doi:10.1016/S0167-9457(01)00048-3

Cigoja, S., Firminger, C. R., Asmussen, M. J., Fletcher, J. R., Edwards, W. B., and Nigg, B. M. (2019). Does Increased Midsole Bending Stiffness of Sport Shoes Redistribute Lower Limb Joint Work During Running? *J. Sci. Med. Sport* 22 (11), 1272–1277. doi:10.1016/j.jsams.2019.06.015

Dempster, J., Dutheil, F., and Ugbolue, U. C. (2021). The Prevalence of Lower Extremity Injuries in Running and Associated Risk Factors: A Systematic Review. *Phys. Act. Health* 5 (1), 133–145. doi:10.5334/paah.109

Derrick, T. R., Dereu, D., and McLean, S. P. (2002). Impacts and Kinematic Adjustments during an Exhaustive Run. *Med. Sci. Sports Exerc.* 34 (6), 998–1002. doi:10.1097/00005768-200206000-00015

Duquette, A. M., and Andrews, D. M. (2010). Tibialis Anterior Muscle Fatigue Leads to Changes in Tibial Axial Acceleration after Impact when Ankle Dorsiflexion Angles are Visually Controlled. *Hum. Mov. Sci.* 29 (4), 567–577. doi:10.1016/j.humov.2010.03.004

Dutto, D. J., Levy, M., Lee, K. K., Sidthalaw, S., and Smith, G. A. (1997). Effect of Fatigue and Gender on Running Mechanics 469. *Med. Sci. Sports Exerc.* 29 (5), 82. doi:10.1097/00005768-199705001-00468

Elliot, B., and Ackland, T. (1981). Biomechanical Effects of Fatigue on 10,000 Meter Running Technique. *Res. Q. Exerc. Sport* 52 (2), 160–166. doi:10.1080/02701367.1981.10607853

Hashish, R., Samarawickrame, S. D., Baker, L., and Salem, G. J. (2016). The Influence of a Bout of Exertion on Novice Barefoot Running Dynamics. *J. Sports Sci. Med.* 15 (2), 327–334.

Kelly, L. A., Cresswell, A. G., and Farris, D. J. (2018). The Energetic Behaviour of the Human Foot across a Range of Running Speeds. *Sci. Rep.* 8 (1), 1–6. doi:10.1038/s41598-018-28946-1

Koblbauer, I. F., van Schooten, K. S., Verhagen, E. A., and van Dieën, J. H. (2014). Kinematic Changes during Running-Induced Fatigue and Relations with Core Endurance in Novice Runners. *J. Sci. Med. Sport* 17 (4), 419–424. doi:10.1016/j.jsams.2013.05.013

Lieber, R. L. (2018). Biomechanical Response of Skeletal Muscle to Eccentric Contractions. *J. Sport Health Sci.* 7 (3), 294–309. doi:10.1016/j.jshs.2018.06.005

Maas, E., De Bie, J., Vanfleteren, R., Hoogkamer, W., and Vanwanseele, B. (2018). Novice Runners Show Greater Changes in Kinematics with Fatigue Compared with Competitive Runners. *Sports Biomech.* 17 (3), 350–360. doi:10.1080/14763141.2017.1347193

Mei, Q., Gu, Y., Xiang, L., Baker, J. S., and Fernandez, J. (2019a). Foot Pronation Contributes to Altered Lower Extremity Loading after Long Distance Running. *Front. Physiol.* 10, 573. doi:10.3389/fphys.2019.00573

Mei, Q., Gu, Y., Xiang, L., Yu, P., Gao, Z., Shim, V., et al. (2019b). Foot Shape and Plantar Pressure Relationships in Shod and Barefoot Populations. *Biomech. Model. Mechanobiol.* 19, 1211–1224. doi:10.1007/s10237-019-01255-w

Melaro, J. A., Gruber, A. H., and Paquette, M. R. (2021). Joint Work Is Not Shifted Proximally after a Long Run in Rearfoot Strike Runners. *J. Sports Sci.* 39 (1), 78–83. doi:10.1080/02640414.2020.1804807

Mizrahi, J., Verbitsky, O., and Isakov, E. (2000). Fatigue-related Loading Imbalance on the Shank in Running: A Possible Factor in Stress Fractures. *Ann. Biomed. Eng.* 28 (4), 463–469. doi:10.1114/1.284

Quan, W., Ren, F., Sun, D., Fekete, G., and He, Y. (2021). Do Novice Runners Show Greater Changes in Biomechanical Parameters? *Appl. Bionics Biomech.* 2021, 1–8. doi:10.1155/2021/8894636

Sanno, M., Willwacher, S., Epro, G., and Brüggemann, G.-P. (2018). Positive Work Contribution Shifts from Distal to Proximal Joints during a Prolonged Run. *Med. Sci. Sports Exerc.* 50 (12), 2507–2517. doi:10.1249/MSS.0000000000001707

Stamatakis, E., and Chaudhury, M. (2008). Temporal Trends in Adults' Sports Participation Patterns in England between 1997 and 2006: the Health Survey for England. *Br. J. Sports Med.* 42 (11), 601–608. doi:10.1136/bjsm.2008.048082

Taunton, J. E., Ryan, M. B., Clement, D., McKenzie, D. C., Lloyd-Smith, D., and Zumbo, B. (2002). A Retrospective Case-Control Analysis of 2002 Running Injuries. *Br. J. Sports Med.* 36 (2), 95–101. doi:10.1136/bjsm.36.2.95

Van Gent, R. N., Siem, D., van Middelkoop, M., Van Os, A. G., Bierma-Zeinstra, S. M. A., Koes, B. W., et al. (2007). Incidence and Determinants of Lower Extremity Running Injuries in Long Distance Runners: a Systematic Review * Commentary. *Br. J. Sports Med.* 41 (8), 469–480. doi:10.1136/bjsm.2006.033548

Videbæk, S., Bueno, A. M., Nielsen, R. O., and Rasmussen, S. (2015). Incidence of Running-Related Injuries Per 1000 H of Running in Different Types of Runners: a Systematic Review and Meta-Analysis. *Sports Med.* 45 (7), 1017–1026. doi:10.1007/s40279-015-0333-8

Willson, J. D., Loss, J. R., Willy, R. W., and Meardon, S. A. (2015). Sex Differences in Running Mechanics and Patellofemoral Joint Kinetics Following an Exhaustive Run. *J. Biomech.* 48 (15), 4155–4159. doi:10.1016/j.jbiomech.2015.10.021

Winter, S., Gordon, S., and Watt, K. (2017). Effects of Fatigue on Kinematics and Kinetics during Overground Running: a Systematic Review. *J. Sports Med. Phys. Fitness.* 57 (6), 887–899. doi:10.23736/s0022-4707.16.06339-8

Wu, T., Martens, H., Hunter, P., and Mithraratne, K. (2014). Emulating Facial Biomechanics Using Multivariate Partial Least Squares Surrogate Models. *Int. J. Numer. Meth. Biomed. Engng.* 30 (11), 1103–1120. doi:10.1002/cnm.2646

Xu, D., Song, Y., Meng, Y., István, B., and Gu, Y. (2020). Relationship between Firefighter Physical Fitness and Special Ability Performance: Predictive Research Based on Machine Learning Algorithms. *Ijerph* 17 (20), 7689. doi:10.3390/ijerph17207689

Xu, D., Lu, Z., Shen, S., Fekete, G., C. Ugbolue, U., and Gu, Y. (2021). The Differences in Lower Extremity Joints Energy Dissipation Strategy during Landing between Athletes with Symptomatic Patellar Tendinopathy (PT) and without Patellar Tendinopathy (UPT). *Mol. Cel. Biomech.* 18 (2), 107–118. doi:10.32604/MCB.2021.015453

Zhang, S.-N., Bates, B. T., and Dufek, J. S. (2000). Contributions of Lower Extremity Joints to Energy Dissipation during Landings. *Med. Sci. Sports Exerc.* 32 (4), 812–819. doi:10.1097/00005768-200004000-00014

Zheng, K. (2021). Research on the Physiological Monitoring and Evaluation of Pre-Competition Altitude Training for Zhejiang Elite Swimmers. *Phys. Act. Health* 5 (1), 64–70. doi:10.5334/paah.91

Zhou, H., Xu, D., Chen, C., Ugbolue, U. C., Baker, J. S., and Gu, Y. (2021). Analysis of Different Stop-Jumping Strategies on the Biomechanical Changes in the Lower Limbs. *Appl. Sci.* 11 (10), 4633. doi:10.3390/app11104633

Conflict of Interest: The authors declare that the research was conducted in the absence of any commercial or financial relationships that could be construed as a potential conflict of interest.

Publisher's Note: All claims expressed in this article are solely those of the authors and do not necessarily represent those of their affiliated organizations, or those of the publisher, the editors, and the reviewers. Any product that may be evaluated in this article, or claim that may be made by its manufacturer, is not guaranteed or endorsed by the publisher.

frontiers in Bioengineering and Biotechnology

ORIGINAL RESEARCH
published: 17 January 2022
doi: 10.3389/fbioe.2021.790764

Real-Time Motion Analysis System Using Low-Cost Web Cameras and Wearable Skin Markers

*Kun-Do Lee and Hyung-Soon Park**

Neuro-Rehabilitation Engineering Laboratory, Korea Advanced Institute of Science and Technology, Dept. Mechanical Engineering, Daejeon, South Korea

COVID-19 has restricted outdoor exercise and hospital visits for rehabilitation therapy. Home-based training and rehabilitation coaching systems have emerged as a way to overcome these circumstances. Conventional optical motion-capture systems, such as VICON, have been used for measuring precise movement and providing posture feedback during exercise or rehabilitation; however, its application is limited to professional facilities because of its high cost and space requirement. To extend the applicability to home-based use, we designed wearable skin markers (WSMs) with body segment-specific patterns that can be detected by low-cost web cameras. WSMs are band-shaped and stretchable and thus can be worn like cloth, with minimal effort for placement. The body segment-specific patterns enable real-time data processing, which reduces the marker data post-processing time. A 6-degree-of-freedom (DOF) pose for each WSM is obtained by recognizing the segment-specific patterns; the 3D configuration of the contoured corners of the patterns found by triangulation is then utilized to construct the coordinates of each WSM. The WSM system was validated *via* three experiments. The robustness of marker recognition was evaluated by measuring the false-positive and false-negative rates of WSM. For accuracy validation, the angle estimation results were obtained for the mechanical joint of a 3-DOF gimbal and lower-limb joints of a walking human subject and compared to the reference systems. The gimbal experiment was included to evaluate the accuracy of our system in the condition with no skin movement artifact. The maximum standard deviation of the difference between WSM and the encoder was 0.9° for the gimbal experiment, and that between WSM and VICON was 5.0° for the human experiment. The accuracy was comparable to the reference systems, making it suitable for home environment application.

Keywords: wearable skin marker, home rehabilitation, image motion analysis, motion capture, image processing

OPEN ACCESS

Edited by:
Chiarella Sforza,
University of Milan, Italy

Reviewed by:
Matteo Zago,
Politecnico di Milano, Italy
Matteo Lancini,
University of Brescia, Italy

****Correspondence:***
Hyung-Soon Park
hyungspark@kaist.ac.kr

Specialty section:
This article was submitted to Biomechanics, a section of the journal Frontiers in Bioengineering and Biotechnology

Received: *07 October 2021*
Accepted: *06 December 2021*
Published: *17 January 2022*

Citation:
Lee K-D and Park H-S (2022) Real-Time Motion Analysis System Using Low-Cost Web Cameras and Wearable Skin Markers. Front. Bioeng. Biotechnol. 9:790764. doi: 10.3389/fbioe.2021.790764

1 INTRODUCTION

OPTICAL motion-capture systems that include high-end infrared cameras, such as VICON (Vicon Motion Systems, Oxford, United Kingdom) and OptiTrack (NaturalPoint, Inc., OR, United States) systems, are considered to be gold-standard systems for motion-analysis research. They are employed in biomechanics laboratories and in large hospitals that conduct studies on the pathological movement patterns of patients. The kinematic data acquired from these systems are applied in medical and sports applications to analyze and evaluate the quality of human movement.

These systems can also be used in domains such as robotic research and the film industry. However, the applicability of these systems is limited by their high cost and the technical skills required to collect and analyze data.

The protracted COVID-19 pandemic has highlighted the need for home-based training and rehabilitation systems. Such a system would require that motion-capture systems be designed for home-based use, as they play an important role in pose feedback during exercise. The ideal motion-capture system in a home environment should not only be able to provide accurate pose estimation but also be affordable and simple enough to be used by individuals who are unfamiliar with the motion-capture technique. Several low-cost motion-capture systems are introduced in the following paragraphs.

One of the most widely used low-cost motion-analysis systems utilizes inertial measurement units (IMUs) composed of accelerometers and gyroscopes that provide information about body position and orientation. In the case of gait analysis, the angular kinematics (e.g., pelvis tilt and hip flexion/extension) and spatiotemporal gait parameters (e.g., step length and speed) can be analyzed by attaching IMUs to different segments of the lower half of the body, such as the pelvis, thigh, or shank. Unlike optical motion-capture systems, IMU-based motion-analysis systems must integrate the raw data to obtain the absolute pose of the segments. However, the integrated sensor noise contributes to the steadily reduced positional and rotational data accuracy over time (Brennan et al., 2011; Seaman and McPhee, 2012; Filippeschi et al., 2017; Zhang et al., 2017). Brennan et al. determined the maximum angular drift of an IMU on a 3-degree-of-freedom (DOF) gimbal to be 1°/min; they reported it to considerably affect joint-angle estimation accuracy (Brennan et al., 2011). Thus, marker-based optical motion-capture systems are better equipped than IMU-based systems to accurately determine the absolute position and orientation of body segments.

There are markerless motion-capture systems that can be used with low-cost cameras. Convolutional neural network-based motion-capture systems, such as OpenPose, have been developed. Implementation of these systems with multiple cameras allows the positions of the body joints in 3D space to be obtained via triangulation (Cao et al., 2017; Slembrouck et al., 2020). Kinect sensors (Microsoft Corp., NM, United States) have also been used to determine joint location without the use of body markers (Pfister et al., 2014; Bilesan et al., 2019). Although these types of systems are convenient, in that the users are not required to wear any markers, because they only provide joint location data, it is difficult to determine the joint rotation angle in the transverse plane (e.g., forearm supination/pronation and internal/external rotation of shoulder/knee/hip joints) (Bilesan et al., 2019). There is another type of motion-capture system that extracts the human body silhouette from captured images and then fits the 3D human skeletal model to obtain the kinematic parameters (Corazza et al., 2006; Becker and Russ, 2015). However, this method is also inadequate in terms of its ability to determine the joint rotation angle in the transverse plane because the changes in the silhouette during rotation are not sufficiently large to enable precise motion tracking.

FIGURE 1 | Marker positioning. WSMs and retroreflective markers were positioned on the lower limb to evaluate the joint-angle estimation accuracy of the WSM system.

Some researchers have utilized augmented reality (AR) markers to track specific movements (Mostashiri et al., 2018; Nagymáté and Kiss, 2019). Nagymáté et al. developed an affordable AR marker-based gait-analysis system (Nagymáté and Kiss, 2019). A total of five AR markers were attached to the pelvis, thighs, and shanks, and the locations of the virtual anatomical points were calibrated relative to the AR markers. The locations of the virtual anatomical points and orientations of the segments were obtained by tracking the poses of the AR markers. Their approach only requires one camera to determine the AR marker poses. However, accurate pose estimation requires that the AR markers be sufficiently large and composed of a rigid material, creating conditions that may negatively impact the gait of patients with walking disorders.

In this study, we propose wearable skin markers (WSMs) that can be recognized by ordinary RGB cameras for low-cost and accurate motion analysis. The WSM pattern was printed on stretchable span fabric. To ensure comprehensive evaluation of the WSM-based system, the robustness of WSM recognition was assessed by false-positive (FP) and false-negative (FN) analyses, and two types of experiments were conducted for pose estimation accuracy evaluation using a 3-DOF gimbal and with a healthy human subject.

The primary purpose of this study was to introduce a new method for low-cost optical motion analysis. Specifically, the WSM concept was designed in this study to enable 6-DOF kinematic analysis of body segments. WSMs can be detected by low-cost web cameras, thereby reducing the cost of motion-capture systems. Moreover, they can be stretched according to the size of body segments, allowing them to be worn like cloth to reduce preparation time. The second aim was to evaluate the accuracy of the proposed system by comparing to well-known measurement systems (e.g., digital encoder and a professional optical motion-capture system).

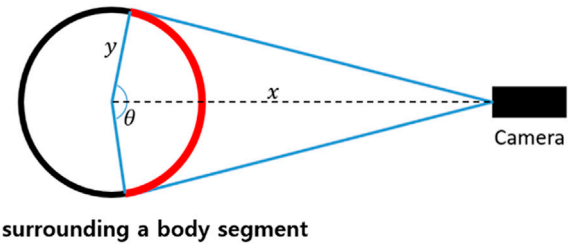

FIGURE 2 | The number of pattern IDs needed for a WSM was decided by considering that at least two pattern IDs should be visible in the red region, thereby ensuring that at least one pattern ID can be recognized from any direction.

2 METHODS

2.1 Wearable Skin Marker Design

2.1.1 Overall Design of Wearable Skin Markers

Figure 1 shows the human subject wearing WSMs and the retroreflective markers for the experiment. WSMs were made in the shape of a skinny band to ensure that they would not impede natural movement and to widen the area for camera locations where the markers are visible. The material is span fabric, allowing it to stretch and shrink according to the size of the subject's body parts. On WSM, a continuous pattern of triangles with or without the black dots inside is printed. Each WSM has its own body-segment-specific pattern so that it allows the cameras to recognize and distinguish each WSM. When two or more cameras detect the same pattern of a WSM, the 3D configuration of triangle vertices that compose the WSM can be obtained. Vertex configuration is used to determine the body segment poses defined relative to it. Thus, even when all of the vertex positions are not detected during motion analysis, multilateration and the least squares method can be used to estimate the 6-DOF pose of each body segment. The detailed procedure for pose estimation is described in **sections 2.2** and **2.3**, and the following paragraphs describe the detailed design decision process of WSM.

2.1.2 Adopting Equilateral Triangle as a Basic Polygon to Compose the Pattern of Wearable Skin Markers

The Ramer–Douglas–Peucker (RDP) algorithm, which approximates contours as polygons by specifying the locations of vertices, was implemented for polygon recognition to enable robust pattern recognition, even under the conditions of curved surfaces that result in distortion of the marker pattern in the image (Saalfeld, 1999). If the internal angle of polygons that compose the marker pattern is large, the vertex might be missed during the line simplification procedure of the RDP algorithm. Therefore, each pattern was designed with equilateral triangles as smaller internal angles help robust recognition of vertices in the RDP algorithm in the presence of marker pattern distortion. The triangles were arranged to meet at a point to form hexagons, and the continuous pattern covered the marker surface.

2.1.3 Required Number of Pattern IDs in Wearable Skin Markers

To obtain the vertex configurations of a WSM, multiple patterns should be employed, each with their own ID, as this would allow each WSM to be individually recognized by cameras at different locations. Regarding the process of determining a suitable number of pattern IDs for a single WSM, we assumed that at least two IDs should be able to fit in the red region shown in **Figure 2** to ensure that at least one ID would be able to be recognized by each camera. The red region denotes the area on a WSM that is visible by a camera. To determine θ, which reflects the range of the red region, the following three additional assumptions were made: (1) the transverse section of each body segment is circular, (2) the marker is at least 1 m away from all cameras (i.e., x is larger than 1 m), and (3) the radius of any body segment y is less than 23 cm, as obtained from the results of an anthropometric survey of United States Army personnel (Gordon et al., 1989). Thus, the smallest possible θ is 153°. Additionally, to ensure reliability, when at least two IDs were able to fit within a 120° range, each WSM was required to have six IDs.

2.1.4 Definition of Pattern ID

We first considered the hexagonal patterns shown in **Figure 3A**. These patterns can be identified by decoding clockwise the sequence of triangles with or without the interiorly positioned black dots. To ensure that each triangle making up each hexagon could be distinguished, radially symmetric patterns were avoided. As such, nine hexagonal patterns were found to be possible (**Figure 3A**). However, this number is insufficient when there is more than one body segment to be analyzed. Therefore, we decided to use two neighboring hexagons to define an ID (**Figure 3B**). Consequently, a total of 384 pattern IDs were found to be possible following analysis of the patterns of single hexagons and all of the patterns that can be generated by merging and rotating neighboring hexagons in 60° increments. Note that the number of pattern IDs could be increased by adding the number of dots in a single triangle, instead of merging two neighboring hexagonal patterns; however, this could lead to marker ID confusion when the dots overlap in the image because of the pattern distortion in the image caused by the curved surface.

2.1.5 Size of Triangles Required for Robust Wearable Skin Marker Pattern Recognition

The camera resolution and distance between the cameras and subject of motion analysis should be considered when deciding the size of the pattern triangles. According to the theory behind the pinhole camera model, the relationship between the actual size and pixel size of the triangles can be described as

$$\frac{A}{T^2} = \frac{A_{pixel}}{f_x f_y}$$

where A and A_{pixel} are the actual area and pixel area of the triangles, respectively, and T is the actual distance between the focal center of the camera and the pattern triangle. f_x and f_y are the

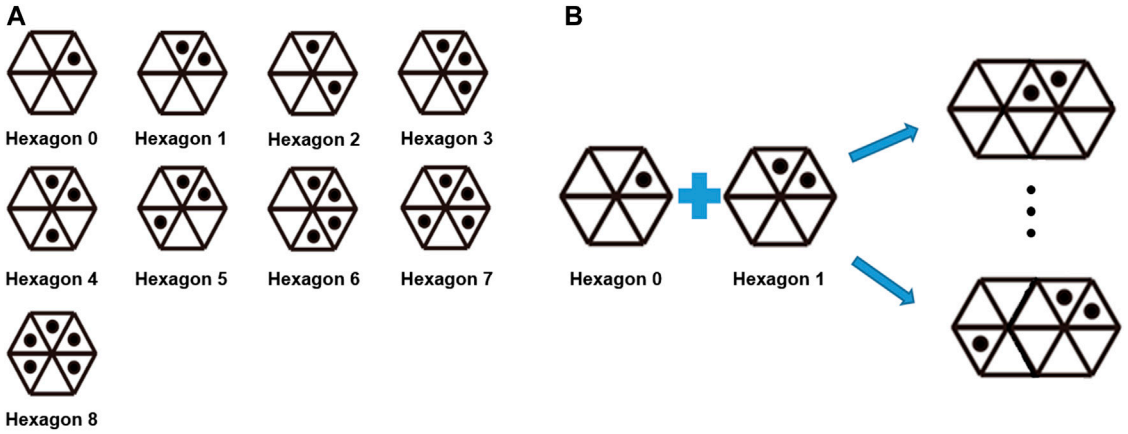

FIGURE 3 | (A) Pattern IDs implemented in the WSM system. Note that radially symmetric patterns were avoided within a single hexagon. **(B)** A total of 384 pattern IDs can be used when two adjacent hexagons are used to compose an ID.

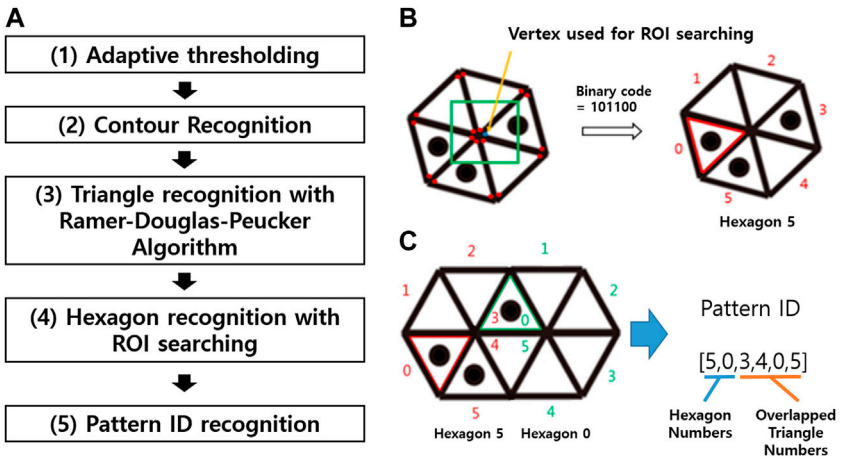

FIGURE 4 | (A) Flow chart summarizing the steps to pattern recognition. (1) Binarize the original RGB images using an adaptive thresholding method. (2) Recognize the boundaries of binarized images to obtain the contours. (3) Use the Ramer–Douglas–Peucker algorithm to identify the triangles and vertex locations from the contours. (4) Identify the hexagonal patterns by decoding the binary code. (5) Recognize the pattern ID by determining which and how the neighboring hexagons are integrated. **(B)** Individual hexagonal pattern identification process. Using the square ROI centered about the triangle vertices found in Step 3, when six vertices are included in the ROI, the binary code for the triangles is read clockwise, beginning with the vertex corresponding to the ROI center. The binary code is used to recognize the hexagonal patterns and each corresponding triangle, because the hexagonal patterns are not radially symmetric. **(C)** Integrated hexagonal pattern identification process. The final pattern ID can be recognized by identifying the overlapping triangles. Here, Triangles 3 and 4 of Hexagon 5 are overlapping with 0 and 5 of Hexagon 0.

horizontal and vertical focal lengths of the camera, respectively, in pixels. The size of the triangle was decided after determining T and the smallest triangle pixel area that would allow for robust recognition. Thus, an experiment was performed to confirm the smallest pixel area of each triangle required for robust recognition of WSM; the results revealed that an area larger than 80 pixels was required. The detailed experiment is described in **sections 3.1** and **4.1**. The focal length parameters for the camera were determined by using the "calibrateCamera" function of OpenCV and a chessboard pattern plate. Consequently, f_x and f_y were calculated to be 1,452.59 and 1,439.01, respectively. The cameras around the treadmill were positioned to be a maximum of 2 m from the WSMs on the moving subject. Thus, the triangle area was required to be at least 1.53 cm^2. In this study, equilateral triangles, each with a side length of 2 cm and an area of 1.73 cm^2, were used to make up the patterns.

2.2 Marker Recognition Algorithm

As described by the flow chart shown in **Figure 4A**, the marker recognition process consists of five steps. In Step 1, the adaptive thresholding method is used to create binary images. The processes of contour recognition and triangle recognition are respectively performed in Steps 2 and 3 based on the binary images. In Step 4, the binary code for the hexagon and a region-of-interest (ROI) searching technique are used to identify the individual hexagonal pattern (**Figure 3A**). Specifically, a square

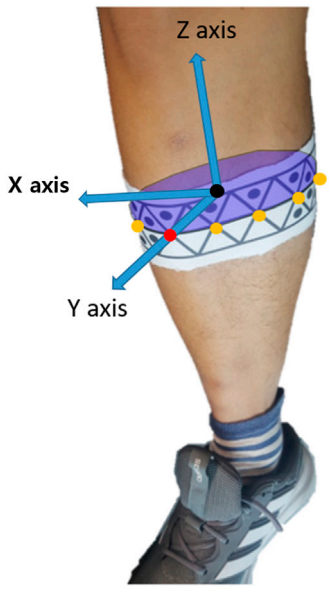

FIGURE 5 | Example of the pose estimation referencing system. Each body segment was defined with respect to the anterior (positive *Y* axis) and proximal (positive *Z* axis) directions. The positive X axis corresponds to the cross product of *Y* and *Z* axes.

ROI that is centered at the vertex and has the same side length as the corresponding triangle is defined for each triangle vertex. When the ROI contains six vertices, the binary code for the hexagon is scanned clockwise, beginning with the triangle associated with the ROI center (**Figure 4B**). This binary code is then utilized to identify the individual hexagonal pattern and, consequently, the comprising triangles. Lastly, in Step 5, the overlapping triangles of the neighboring hexagons are identified, and the final pattern ID is determined (**Figure 4C**). When two or more cameras output the same ID, the 3D locations of the vertices of the pattern can be determined by triangulation.

2.3 Pose Estimation for Wearable Skin Markers

2.3.1 Static Step

The pose estimation process comprised two steps: the static step and motion-analysis step. In the static step, the geometric parameters of the body segments with applied WSMs were calculated as the user stood still in the predetermined area for motion analysis. As shown in **Figure 5**, the positive *Y* axis of the body segments corresponded to the anterior direction, and the positive *Z* axis corresponded to the proximal direction. **Figure 6** provides insight into the static step, showing how the geometric parameters were determined relative to the pose of the WSM on a body segment. For each WSM, there was one hexagonal pattern that was predefined as the anterior or posterior part of each body segment, and the center of each of these hexagons was positioned as the center of the corresponding anterior or posterior body segment. The positive *Y* axis has been defined as the vector extending from the center of the posterior hexagon to the center of the anterior hexagon. The positive *Z* axis has been defined as the normal vector of the plane fitted to the center of all hexagons on each WSM; the origin of the coordinate system has been defined as the midpoint between the centers of the posterior and anterior hexagons.

After the coordinates were defined, the distance from the origin was calculated for each WSM vertex. Then, in the motion-analysis step, these data were implemented in a multilateration process to estimate the origin. Multilateration is the process of determining the position of a point in 3D space by measuring and referencing its relative distances from more than two known points (Blewitt, 1997). The angles between the *Y* axis and the vector from origin to each of the hexagon centers are also calculated in the static step. These angles were used to find the *Y* axis in the motion-analysis step when the posterior or anterior hexagon was not recognized.

2.3.2 Motion-Analysis Step

It should be noted that, because the motion-analysis step does not ensure that the posterior and anterior hexagons can be recognized by cameras while the subject is in motion, the origin and *Y* axis

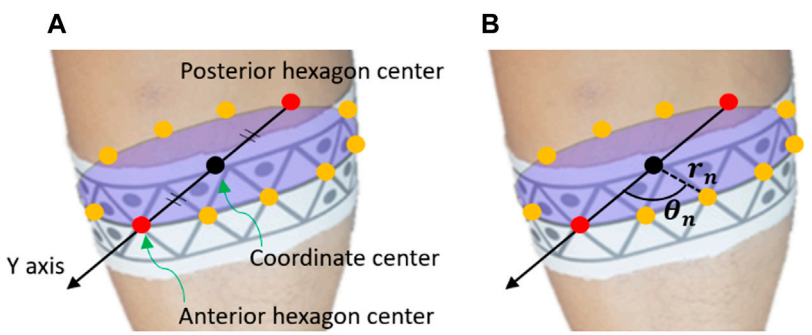

FIGURE 6 | Illustrative example of how the pose estimation referencing system was utilized to determine the geometric parameters of a body segment. In the static step, the geometric parameters of each body segment are collected. As shown in **(A)**, the positive *Y* axis corresponded to the anterior direction of body segments; it was defined as the vector extending from the center of the posterior hexagon to the center of the anterior hexagon. These centers were predefined as the respective centers of the anterior and posterior points of each body segment and were thus positioned as such. The origin was defined as the midpoint between the centers of the posterior and anterior hexagons. As shown in **(B)**, the distance between the origin and each vertex of each marker (i.e., not only the hexagon centers) was denoted as r_n. Additionally, the angles between the positive *Y* axis and the vectors for each hexagon center were determined (θ_n). r_n and θ_n were utilized in the motion-analysis step to reconstruct the positive *Y* axis and origin when the anterior and posterior hexagons could not be recognized.

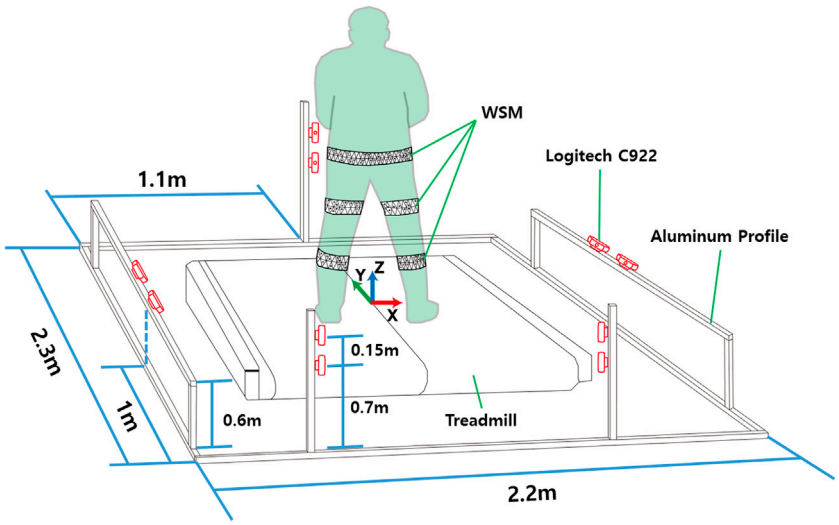

FIGURE 7 | Camera locations for 3-DOF gimbal and human subject experiments. The world coordinates were defined on the center of the treadmill.

were estimated based on the information obtained in the static step. To summarize the process of the motion-analysis step, first, the position of the origin is determined by using multilateration based on the location of vertices of the WSM currently found. Then, by fitting the plane to the centers of identified hexagons and the estimated origin, the normal vector of the plane is established as the positive *Z* axis. Lastly, the *Y* axis is identified in the motion-analysis step by rotating the vector extending from one of the identified hexagon centers about the *Z* axis according to the aforementioned angles determined in the static step.

3 EXPERIMENT DESIGN FOR SYSTEM VALIDATION

3.1 Experiment 1: Robustness of Marker Recognition

We analyzed the FP and FN rates of WSM to evaluate its robustness of recognition. The FP rate is the proportion of falsely detected markers in the LabelMe dataset (Russell et al., 2008). LabelMe is composed of 207,913 images of various indoor and outdoor scenes that do not contain WSM images.

The FN rate is the proportion of undetected WSMs when there are WSMs in the image. We attached a WSM around a cylinder with 7 cm diameter. We fixed the size of the marker, and the length of one side of the equilateral triangles constituting the pattern was 2 cm. We obtained the minimum pixel area of a WSM for robust marker recognition adjusting the distance between WSM and the camera.

3.2 Experiment 2: Joint-Angle Estimation for a 3-DOF Gimbal

For Experiments 2 and 3, the motion-capture area was surrounded by 10 Logitech C922 webcams (68 USD each) for the WSM system as shown in **Figure 7** and eight infrared cameras (i.e., camera types: five VICON T40-S, two T160, and one T040) for the VICON-based system. The webcams were placed in pairs for correspondence-based triangulation. Five pairs of webcams were placed as shown in **Figure 7**.

To evaluate system accuracy, joint-angle estimation tests were conducted using a 3-DOF gimbal and on the lower body of a healthy subject. A 3-DOF gimbal test was included to eliminate the effects of skin movement artifacts, which consequently reduce the accuracy of marker-based motion-analysis systems (Ferrari et al., 2008; Gao and Zheng, 2008). Gao and Zheng (2008) conducted a study in which 20 healthy subjects performed a walking task with retroreflective marker clusters attached to the same body segment with different locations; they consequently found that skin movement caused maximum discrepancy between the marker clusters on the thighs and shanks approximately 19.6° and 8.6° in the transverse plane, 12.0° and 2.6° in the sagittal plane, and 5.9° and 2.7° in the frontal plane. Because, in this study, the WSMs and retroreflective markers needed to be positioned on the same body segment, but at different locations to prevent obstruction, the results of the human subject experiment were presumed to be susceptible to skin movement artifacts. Thus, a gimbal experiment was performed to enable comparison of the proposed system to a VICON-based system under the condition of no skin movement artifacts.

For the gimbal experiment, the gimbal was positioned in the designated motion-analysis area. Retroreflective marker clusters and WSMs were attached to it as shown in **Figure 8**. With the gimbal encoder output set as the reference, the joint-angle estimation errors for the proposed WSM system and VICON-based system were compared. As shown in **Figure 8A**, the pose of the upper segment relative to the lower segment of the gimbal was represented by XYZ Euler angles to enable comparison of the estimated joint angles. Additionally, the rotations about the X, Y,

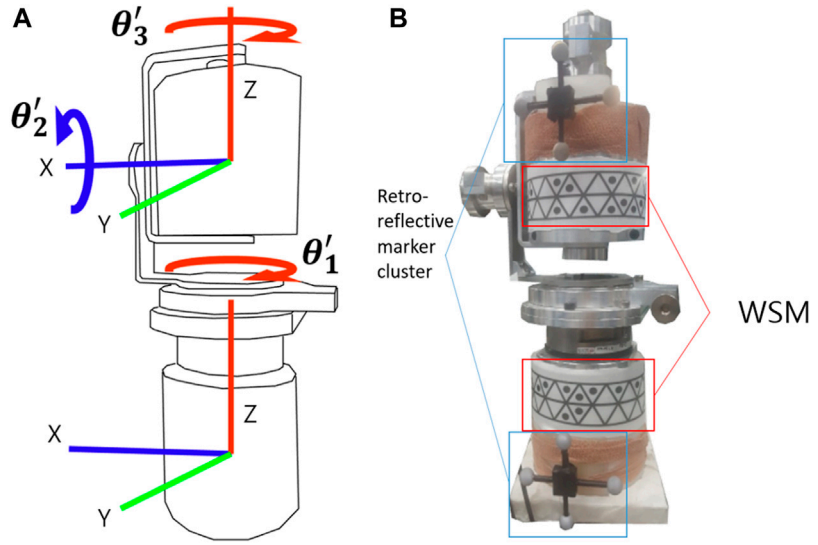

FIGURE 8 | (A) Schematic of the gimbal coordinate system. The gimbal had 3 DOFs, and the joint angles were obtained by measuring the position of the upper segment relative to the lower segment. **(B)** Retroreflective cluster and WSM placement on the gimbal. Each cluster and WSM had defined coordinates.

and *Z* axes were respectively equated to flexion/extension (Fle/Ext), abduction/adduction (Abd/Add), and rotation (Rot) in this study. The upper part of the gimbal was manually rotated as the joint-angle trajectories captured by the encoders and WSM and VICON-based systems were recorded. Relatively wide and narrow ranges of motion (ROMs) were applied in this experiment. For the narrow ROM test, the gimbal was rotated to maintain a joint-angle ROM equivalent of approximately 5°. For the wide-ROM test, the ROM was adjusted such that the joint-angle equivalent was consistently larger than 10°.

3.3 Experiment 3: Joint-Angle Estimation for Lower Limb of a Healthy Human Subject

In the healthy human subject experiment, a modified Helen Hayes marker set methodology was applied for the retroreflective markers (Collins et al., 2009; Charalambous, 2014). Specifically, a total of three retroreflective markers were placed over the sacrum and right and left halves of the anterior superior iliac spine to define the pelvis segment. A total of two markers were placed directly lateral and medial to each knee, and one marker each was placed laterally and medially on the ankle, over the first and fifth digits of the foot, and on the heel of the foot (**Figure 1**). The marker clusters were also positioned on the thighs and shanks to increase orientation-tracking accuracy. The WSMs were positioned on the pelvis, thighs, and shanks as shown in **Figure 1**. The predefined anterior and posterior hexagons of each WSM were positioned to be directly anterior and posterior to each segment. The relative camera locations were the same as those for the gimbal experiment, and the subject was asked to walk on a treadmill in the designated motion-analysis area. The XYZ Euler angles obtained by determining the orientation of the distal segment relative to the proximal segment were implemented for joint-angle estimation. For pelvis angle estimation, the coordinates corresponding to the center of the treadmill were set as the proximal segment reference as shown in **Figure 7**. The joint-angle estimation of the WSM system was compared to the VICON-based system.

The root mean square error (RMSE), standard deviation of difference (SD of Diff), and Pearson correlation coefficient (*r*) were derived for each comparison. Note that a large RMSE does not necessarily indicate a large error, because the different methods used to define the body segment coordinates of the systems introduced a baseline angular offset. According to the paper of Kainz et al. (2017) that compared joint angle estimated from four different clinical marker placing, models using VICON, "PiG-DK", and "6-DOF-DK" showed about 7° RMSE on hip rotation, and "PiG-DK" and "3-1-1-DOF-IK" showed more than 10° of RMSE in hip flexion/extension. Therefore, RMSE might vary according to the motion-capture method or marker placing protocol. SD of Diff represents the discrepancy between the two systems when the angular offset is ignored. Lastly, the Pearson correlation coefficient indicates the strength of the relationship between the reference and estimated joint trajectories.

To establish a method to assess the accuracy of the proposed WSM system in the presence of skin movement artifacts, we referenced several studies that compared the joint-angle trajectory results obtained as a result of implementing different marker sets in an infrared marker-based system (Ferrari et al., 2008; Collins et al., 2009; Kainz et al., 2017). Ferrari et al. (2008) compared various joint angles estimated for five different retroreflective marker sets; with the exception of the hip rotation and knee abduction/adduction and rotation results that yielded negative correlations, the correlations varied between 0.7 and 1.0. Additionally, Collins et al. (2009) compared the performance of a marker set referred to as the

TABLE 1 | FN rate analysis for WSMs.

Pixel area of WSM	3,000~2,000	2,000~1,500	1,500~1,000	1,000~800	800~500	500~400
FN rate (%)	0	0	0	0	0.5	45.3

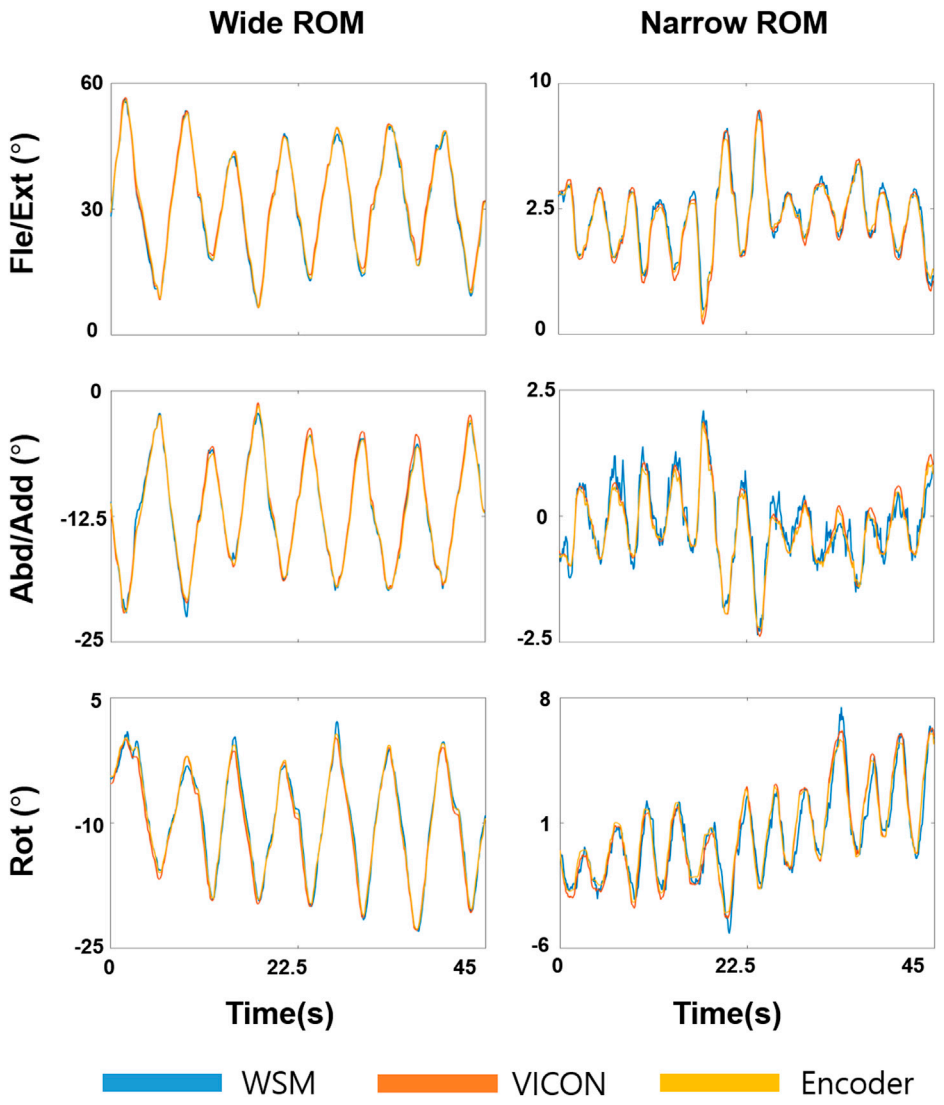

FIGURE 9 | Joint-angle estimation results for the 3-DOF gimbal experiment. Fle/Ext, Abd/Add, and Rot angles were obtained for wide and narrow ROMs. Yellow, orange, and blue respectively denote the encoder, VICON-based system, and WSM system results.

"6-DOF marker set" to that of the Helen Hayes marker set; they found the knee flexion angle to have the largest SD of Diff (3.61°). Kainz et al. (2017) compared four different clinical marker sets, and it showed the largest standard deviation of RMSD of about 5.0° on knee rotation. Their varied results indicate that it is difficult to accurately estimate joint angles if the system is susceptible to skin movement artifacts, because the estimations may vary according to the retroreflective marker set. Thus, we aimed to determine high correlation coefficients and low SD of Diff values that indicated a good result. Specifically, using the results reported by Ferrari et al., Collins et al., and Kainz et al. as references, a correlation coefficient value 0.70 or higher was set as the criterion for a good correlation, whereas an SD of Diff value 5.0° or lower was set as the criterion for a good SD of Diff. These criteria were applied in the analysis of the human experiment results.

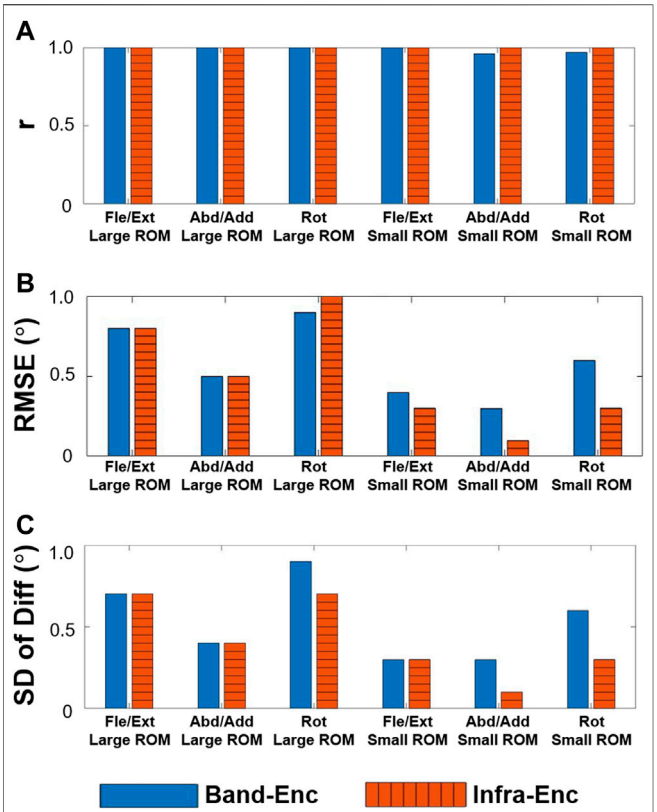

FIGURE 10 | WSM-Enc (blue solid) and Infra-Enc (orange striped) comparison results. High correlation coefficients **(A)** and relatively small discrepancies, as shown by the RMSE **(B)** and SD of Diff **(C)** results, were consistently observed between the two systems.

Data collection for the human subject was approved by the Institutional Review Board at the Korea Advanced Institute of Science and Technology (KH 2019-113).

4 RESULTS

4.1 Experiment 1: Robustness of Marker Recognition

We applied the WSM recognition algorithm on the images of the LabelMe dataset, and 27 markers were falsely detected, resulting in a 0.013% (27/207,913 × 100) FP rate. As shown in **Table 1**, we could observe that the FN rate started to grow as the pixel area of a WSM became smaller than 800 pixels, showing a 0.5% FN rate. When the pixel area became smaller than 500 pixels, FN became 45.3%, indicating that it is hardly usable at the 0–500 pixel area range. As one WSM is composed of 10 triangles, the result indicates that the pixel area of each triangle should be larger than 80 in the image for robust recognition.

4.2 Experiment 2: Joint-Angle Estimation for a 3-DOF Gimbal

The results of the gimbal experiment are presented in **Figures 9** and **10**. The blue solid bars in **Figure 10** denote the WSM and encoder system comparison results (WSM-Enc), and the orange striped bars denote the infrared camera-based (VICON-based) and encoder system comparison results (Infra-Enc). It is worth noting that r was higher than 0.95, and RMSE and SD of Diff were 1.0° or less for all joint-angle estimations (**Figure 10**). The WSM-Enc result yielded the largest SD of Diff at Rot with a large ROM, which was 0.9°, while the Infra-Enc result yielded 0.7°. Additionally, even though the Infra-Enc result showed a better or similar SD of Diff result for all joint-angle estimations, the differences of the SD of Diff values between WSM-Enc and Infra-Enc were consistently less than 0.3° (**Figure 10C**).

4.3 Experiment 3: Joint-Angle Estimation for Lower Limb of a Healthy Human Subject

The results of the healthy subject gait analysis experiment are shown in **Figures 11** and **12**. As shown in **Figure 12A**, with the exception of the right and left hip rotation results ($r = 0.58$ and 0.65 respectively), r was consistently above 0.70; moreover, as can be seen in **Figure 12C**, all of the SD of Diff values satisfied the criteria for good SD of Diff that we set in **section 3.3**. The highest SD of Diff for both sides was on Fle/Ext for the knee joints, showing 4.6° and 5.0° on the right and left sides, respectively, but they are still in the range of the criteria for good SD of Diff. RMSE varied from 1.4° to 8.2°, and it might be attributable to the different way of defining coordinates of body segments between the WSM and infrared camera-based systems.

5 DISCUSSION

We evaluated the performance of the WSM system through three experiments. Experiment 2 and Experiment 3 showed that the accuracy of the WSM system is comparable to that of the VICON-based system. In Experiment 2, which is the gimbal-based experiment, the difference between the SD of Diff values for the WSM-Enc and Infra-Enc comparisons was consistently below 0.3°. A previous study that focused on quantifying the error associated with the application of a VICON 370 system to estimate the joint angles for a static leg-like object revealed that the error varied between 0.1° and 0.4° owing to changes in the position of the object in the designated motion-analysis area (Dorociak and Cuddeford, 1995). Thus, the error level of the proposed system is within the range of the error for VICON-based systems. Furthermore, the IMU 3-DOF gimbal test reported by Brennan et al. (2011) yielded a 3.19° maximum SD of Diff compared to the potentiometer, whereas the largest WSM-Enc SD of Diff (0.9°) was considerably smaller, indicating that a WSM-based system has the potential to become a general-use motion-analysis system. In Experiment 3, which is the human gait experiment, all of the SD of Diff results satisfied the criteria of high accuracy that we set based on previous studies showing an SD of Diff of 5.0° or less. This result indicates that

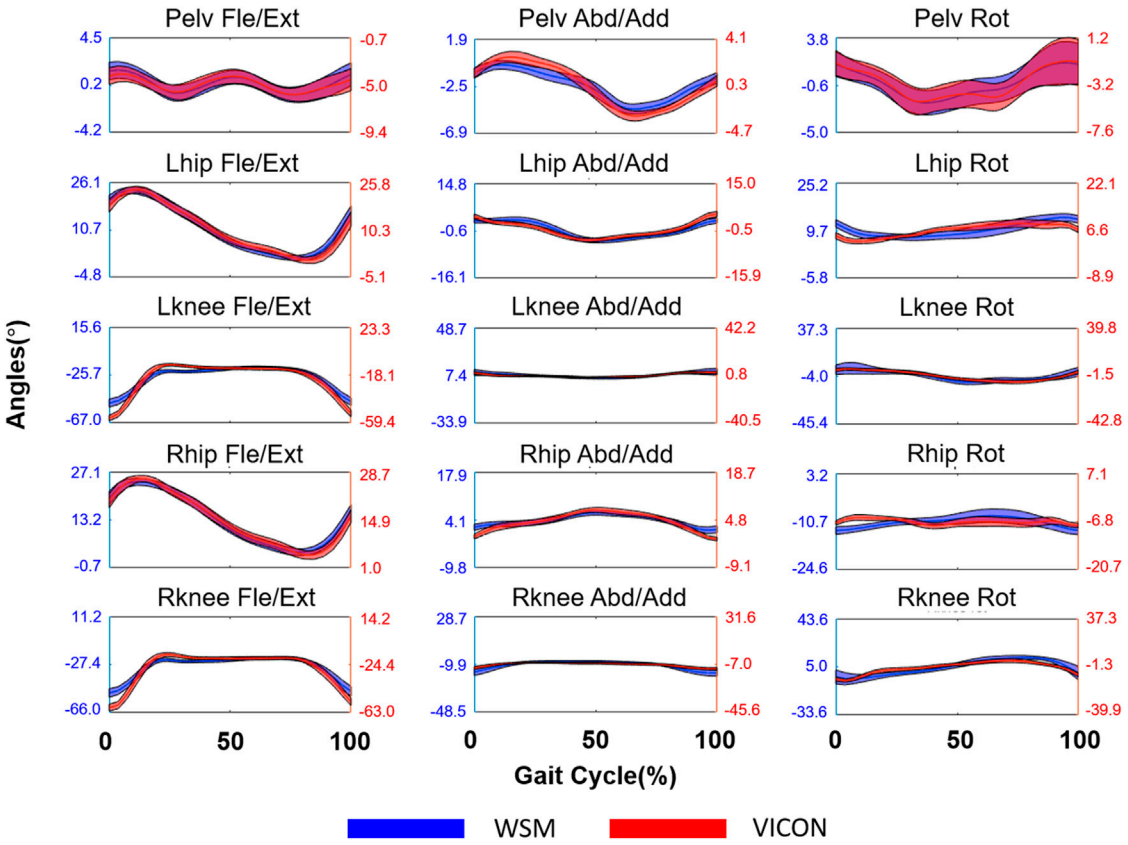

FIGURE 11 | Joint-angle estimation results for the lower limbs of a human subject walking on a treadmill. The blue and red lines respectively denote the WSM and infrared camera-based systems (VICON). The X axis denotes the gait cycle percentage (%), and the *Y* axis denotes the estimated joint angle in degrees (°), which was averaged over all gait cycles.

WSM has a high tracking accuracy comparable to the practically used marker sets of the VICON system.

For the gimbal experiment, the largest WSM-Enc SD of Diff (0.9°) was obtained for the wide-ROM Rot. This may be attributable to coordinate system misalignment. There were three coordinate systems for each segment in the 3-DOF gimbal experiment that were each defined through the use of retroreflective marker clusters, WSMs, and encoders. Ideally, they would have been perfectly aligned for direct comparison; however, because the markers were attached by hand, perfect alignment was not possible. It is for this reason that the Rot SD of Diff increased as the ROM was extended.

Regarding the human subject experimental results, the RMSE values for the proposed and infrared camera-based systems varied between 1.4° and 8.2°. As mentioned in section 3, a large RMSE value does not indicate poor pose estimation performance, as it is an effect of employing different techniques to define the coordinates of the two systems; this resulted in misaligned segment coordinates. Although RMSE was not considered to be an indicator of system performance in this study, the marker placement protocol for the WSM-based system needs to be improved to enable robust definition of segment coordinates. The method used in this study entailed positioning the WSMs such that a specific hexagon center is positioned at the anterior or posterior body segment center. To improve segment coordinate definition, additional guidelines that take into account bony landmarks should be established in future work.

Although all joint-angle estimation satisfied the criterion for good SD of Diff, the knee Fle/Ext showed the largest SD of Diff on both sides. This may have been largely attributable to skin movement artifacts. As previously mentioned, comparisons of the joint-angle results obtained through the use of retroreflective markers and WSMs that cannot be simultaneously positioned on body segments at the same location will be subject to the influence of skin movement artifacts. Gao and Zheng (2008) reported the effects of these artifacts on the thigh and shank to be up to 19.6° and 8.6°, respectively. Their results indicate that differential marker placement can manifest as large deviations in the results. In this study, the hip rotation angle results indicated the lowest correlation ($r = 0.58$); this finding is consistent with the results of previous studies that investigated the implementation of different marker sets in an infrared camera-based system

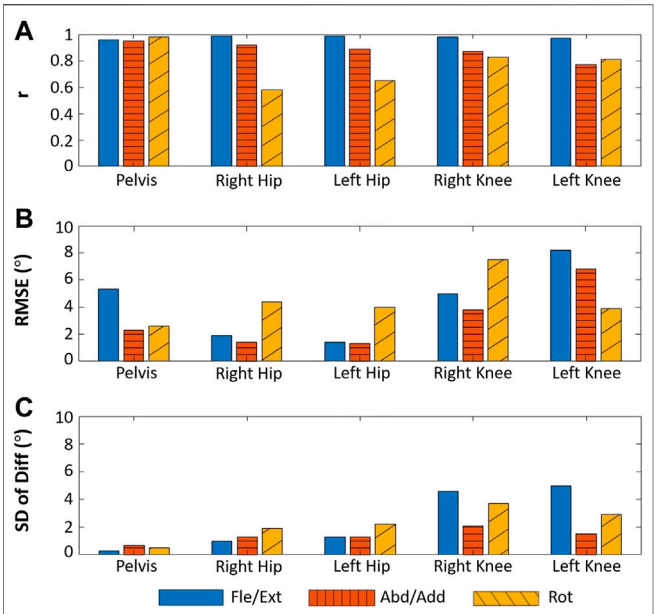

FIGURE 12 | Results for the human subject joint-angle estimation experiment. The blue solid bars denote rotation in the sagittal plane (pelvic tilt, hip Fle/Ext, and knee Fle/Ext), the orange striped bars denote rotation in the frontal plane (pelvic obliquity, hip Abd/Add, and knee Abd/Add), and the yellow diagonally striped bars denote rotation in the transverse plane (pelvic Rot, hip Rot, and knee Rot).

(Ferrari et al., 2008; Collins et al., 2009). Ferrari et al. analyzed the kinematic results obtained through the use of five different marker sets; in some cases, they found negative correlations for hip rotation. Furthermore, in a study performed by Collins et al. that compared the Helen-Hayes set and their "6-DOF marker set", the results for the hip joint angle in the transverse plane revealed opposing joint-angle trajectory trends, indicating a large discrepancy.

In Experiment 1, we evaluated the robustness of recognition for WSM as it is a newly designed marker. AprilTag and AprilTag2, which are two of the most widely used and robust fiducial markers, were also evaluated on the LabelMe dataset (Wang and Olson, 2016). AprilTag and AprilTag2 respectively showed FP rates of 0.034% (145/421,049 × 100) and 0.0014% (6/421,049 × 100) (the number of images was different from the version that we downloaded). WSM showed an FP rate lower than that of AprilTag but higher than that of AprilTag2, indicating that WSM has comparable robustness to widely used fiducial markers. The reason for an FP higher than that of AprilTag2 might be the deformability of WSM. AprilTag2 is used on planar surfaces, so it can reject the deformed candidates in the sample images, resulting in a low FP rate, while WSM does not reject those candidates as it is designed to be used on curved surfaces. For the FN rate, the result in **Table 1** could be the guideline for deciding the size of the motion-capture area and WSM pattern. The size of the WSM pattern in Experiment 2 and Experiment 3 was chosen according to this result.

6 FUTURE STUDY

In this study, we focused on introducing the main concept of the WSM system and evaluating its accuracy in the environment that has a sufficient number of cameras for stable recognition of WSM. Ten low-cost web cameras were placed around a 2.2 m × 2.3 m space. However, the applicability of an optical motion-capture system for home-based use is highly related to the number of cameras and calibration procedure. Therefore, we are planning to evaluate the performance of the WSM system by reducing the number of cameras from ten to two. If the WSM system with a reduced number of cameras still results in acceptable accuracy, it will reduce the system cost, required space, and calibration procedure. Especially with two cameras, it might require only an initial calibration if the relative pose is fixed. Moreover, we will investigate on the light condition and improve the wearing part of WSMs to make the WSM system more suitable for home-based use. The second goal of future studies should be to establish a human experiment protocol that can minimize the effects of skin movement artifacts. This may be achieved by using retroreflective markers with intra-cortical pins or by establishing a protocol based on the 3D bone reconstructions that were obtained via fluoroscopic imaging (Benoit et al., 2006; Zheng et al., 2006; Kurazume et al., 2009). Although the intra-cortical pin method requires surgical preparation and a fluoroscopic imaging system is difficult to apply for continuous joint-angle estimation, these methods may yield the most reliable results for WSM-based systems. Alternatively, methods similar to the point cluster technique and optimal common shape technique have been developed and applied to minimize skin movement artifacts in infrared camera-based systems (Taylor et al., 2005). These techniques take into account the fact that the original marker configuration will change as a subject moves; this discrepancy is quantified and subsequently taken into account in body segment coordinate calculations. This approach can also be applied to WSM pattern vertices to reduce skin movement artifacts. Lastly, a marker placement protocol based on bony landmarks needs to be established for the WSM system.

7 CONCLUSION

A method for affordable optical motion analysis was developed in this study. The use of webcams can reduce the cost of such systems, thereby extending the applicability of optical motion-capture systems to include home-based applications, such as posture correction for at-home training, accurate body tracking for virtual-reality gaming, and remote monitoring for home rehabilitation. WSMs that can be recognized by webcams were designed, and the pose estimation accuracy of the resulting system was evaluated. The results of the human subject experiment revealed a relatively low correlation for left and right hip rotations; we interpreted the main source of error to be skin movement artifacts. Except these results, all of the

other joint-angle results met the criteria of high accuracy that we set based on previous studies. The results of the gimbal experiment, which was not subject to skin movement artifacts, revealed the accuracy of the proposed WSM system to be comparable to that of an infrared camera-based system under the condition of encoder output as the reference. The WSM system can be a good solution in the field of home-based motion analysis that requires high accuracy as well as low cost.

DATA AVAILABILITY STATEMENT

The raw data supporting the conclusion of this article will be made available by the authors, without undue reservation.

ETHICS STATEMENT

The studies involving human participants were reviewed and approved by the Institutional Review Board at the Korea Advanced Institute of Science and Technology. The patients/participants provided their written informed consent to participate in this study.

AUTHOR CONTRIBUTIONS

K-DL contributed to the design and development of wearable skin markers, conducted the experiment, and drafted the article. K-DL and H-SP designed the experiment protocol. H-SP supervised this study. All authors contributed to the article and approved the submitted version.

FUNDING

This work was supported by the ICT R&D program of MSIP/IITP under Grant 2020-0-00114 Problem Solving in Military Camp Life: the Safety and Reliability of Human Resources Management.

REFERENCES

Becker, L., and Russ, P. (2015). *Evaluation of Joint Angle Accuracy Using Markerless Silhouette Based Tracking and Hybrid Tracking Against Traditional Marker Tracking*. Unterschleissheim, Germany: Poster für Masterarbeit bei Simi Reality Motion Systems GmbH und der Otto-von-Guericke-Universität Magdeburg.

Benoit, D. L., Ramsey, D. K., Lamontagne, M., Xu, L., Wretenberg, P., and Renström, P. (2006). Effect of Skin Movement Artifact on Knee Kinematics During Gait and Cutting Motions Measured *In Vivo*. *Gait & Posture.* 24 (2), 152–164. doi:10.1016/j.gaitpost.2005.04.012

Bilesan, A., Behzadipour, S., Tsujita, T., Komizunai, S., and Konno, A. (2019). "Markerless Human Motion Tracking Using Microsoft Kinect SDK and Inverse Kinematics," in 2019 12th Asian Control Conference (ASCC) (IEEE), 504–509.

Blewitt, G. (1997). *Basics of the GPS Technique: Observation Equations*. Geodetic applications of GPS, 10–54.

Brennan, A., Zhang, J., Deluzio, K., and Li, Q. (2011). Quantification of Inertial Sensor-Based 3D Joint Angle Measurement Accuracy Using an Instrumented Gimbal. *Gait & Posture.* 34 (3), 320–323. doi:10.1016/j.gaitpost.2011.05.018

Cao, Z., Simon, T., Wei, S. E., and Sheikh, Y. (2017). "Realtime Multi-Person 2d Pose Estimation Using Part Affinity fields," in Proceedings of the IEEE conference on computer vision and pattern recognition, 7291–7299. doi:10.1109/cvpr.2017.143

Charalambous, C. P. (2014). "Measurement of Lower Extremity Kinematics during Level Walking," in *Classic Papers in Orthopaedics* (London: Springer), 397–398. doi:10.1007/978-1-4471-5451-8_100

Collins, T. D., Ghoussayni, S. N., Ewins, D. J., and Kent, J. A. (2009). A Six Degrees-Of-Freedom Marker Set for Gait Analysis: Repeatability and Comparison With a Modified Helen Hayes Set. *Gait & Posture.* 30 (2), 173–180. doi:10.1016/j.gaitpost.2009.04.004

Corazza, S., Mündermann, L., Chaudhari, A. M., Demattio, T., Cobelli, C., and Andriacchi, T. P. (2006). A Markerless Motion Capture System to Study Musculoskeletal Biomechanics: Visual Hull and Simulated Annealing Approach. *Ann. Biomed. Eng.* 34 (6), 1019–1029. doi:10.1007/s10439-006-9122-8

Dorociak, R. D., and Cuddeford, T. J. (1995). Determining 3-D System Accuracy for the VICON 370 System. *Gait & Posture.* 3 (2), 88. doi:10.1016/0966-6362(95)93468-r

Ferrari, A., Benedetti, M. G., Pavan, E., Frigo, C., Bettinelli, D., Rabuffetti, M., et al. (2008). Quantitative Comparison of Five Current Protocols in Gait Analysis. *Gait & Posture.* 28 (2), 207–216. doi:10.1016/j.gaitpost.2007.11.009

Filippeschi, A., Schmitz, N., Miezal, M., Bleser, G., Ruffaldi, E., and Stricker, D. (2017). Survey of Motion Tracking Methods Based on Inertial Sensors: A Focus on Upper Limb Human Motion. *Sensors.* 17 (6), 1257. doi:10.3390/s17061257

Gao, B., and Zheng, N. (2008). Investigation of Soft Tissue Movement during Level Walking: Translations and Rotations of Skin Markers. *J. Biomech.* 41 (15), 3189–3195. doi:10.1016/j.jbiomech.2008.08.028

Gordon, C. C., Churchill, T., Clauser, C. E., Bradtmiller, B., and McConville, J. T. (1989). *Anthropometric Survey of US Army Personnel: Methods and Summary Statistics 1988*. Yellow Springs, OH: Anthropology Research Project Inc.

Kainz, H., Graham, D., Edwards, J., Walsh, H. P. J., Maine, S., Boyd, R. N., et al. (2017). Reliability of Four Models for Clinical Gait Analysis. *Gait & Posture.* 54, 325–331. doi:10.1016/j.gaitpost.2017.04.001

Kurazume, R., Nakamura, K., Okada, T., Sato, Y., Sugano, N., Koyama, T., et al. (2009). 3D Reconstruction of a Femoral Shape Using a Parametric Model and Two 2D Fluoroscopic Images. *Computer Vis. Image Understanding.* 113 (2), 202–211. doi:10.1016/j.cviu.2008.08.012

Mostashiri, N., Dhupia, J. S., Verl, A. W., and Xu, W. (2018). A Novel Spatial Mandibular Motion-Capture System Based on Planar Fiducial Markers. *IEEE Sensors J.* 18 (24), 10096–10104. doi:10.1109/jsen.2018.2873349

Nagymáté, G., and Kiss, R. M. (2019). Affordable Gait Analysis Using Augmented Reality Markers. *PloS one.* 14 (2), e0212319. doi:10.1371/journal.pone.0212319

Pfister, A., West, A. M., Bronner, S., and Noah, J. A. (2014). Comparative Abilities of Microsoft Kinect and Vicon 3D Motion Capture for Gait Analysis. *J. Med. Eng. Technology.* 38 (5), 274–280. doi:10.3109/03091902.2014.909540

Russell, B. C., Torralba, A., Murphy, K. P., and Freeman, W. T. (2008). LabelMe: a Database and Web-Based Tool for Image Annotation. *Int. J. Comput. Vis.* 77 (1-3), 157–173. doi:10.1007/s11263-007-0090-8

Saalfeld, A. (1999). Topologically Consistent Line Simplification With the Douglas-Peucker Algorithm. *Cartography Geogr. Inf. Sci.* 26 (1), 7–18. doi:10.1559/152304099782424901

Seaman, A., and McPhee, J. (2012). Comparison of Optical and Inertial Tracking of Full Golf Swings. *Proced. Eng.* 34, 461–466. doi:10.1016/j.proeng.2012.04.079

Slembrouck, M., Luong, H., Gerlo, J., Schütte, K., Van Cauwelaert, D., De Clercq, D., et al. (2020). "Multiview 3d Markerless Human Pose Estimation from Openpose Skeletons," in International Conference on Advanced Concepts for Intelligent Vision Systems (Cham: Springer), 166–178. doi:10.1007/978-3-030-40605-9_15

Taylor, W. R., Ehrig, R. M., Duda, G. N., Schell, H., Seebeck, P., and Heller, M. O. (2005). On the Influence of Soft Tissue Coverage in the Determination of Bone Kinematics Using Skin Markers. *J. Orthop. Res.* 23 (4), 726–734. doi:10.1016/j.orthres.2005.02.006

Wang, J., and Olson, E. (2016). "AprilTag 2: Efficient and Robust Fiducial Detection," in 2016 IEEE/RSJ International Conference on Intelligent Robots and Systems (IROS) (IEEE), 4193–4198.

Zhang, R., Yang, H., Hoflinger, F., and Reindl, L. M. (2017). Adaptive Zero Velocity Update Based on Velocity Classification for Pedestrian Tracking. *IEEE Sensors J.* 17 (7), 2137–2145. doi:10.1109/jsen.2017.2665678

Zheng, G., Ballester, M. Á. G., Styner, M., and Nolte, L.-P. (2006). "Reconstruction of Patient-specific 3D Bone Surface From 2D Calibrated Fluoroscopic Images and Point Distribution Model," in International conference on medical image computing and computer-assisted intervention (Berlin, Heidelberg: Springer), 25–32. doi:10.1007/11866565_4

Conflict of Interest: K-DL and H-SP are inventors of the patent application (KR10-2273276), registered on June 30th, 2021, for the proposed motion capture system.

Publisher's Note: All claims expressed in this article are solely those of the authors and do not necessarily represent those of their affiliated organizations, or those of the publisher, the editors, and the reviewers. Any product that may be evaluated in this article, or claim that may be made by its manufacturer, is not guaranteed or endorsed by the publisher.

frontiers in Physiology

ORIGINAL RESEARCH
published: 10 February 2022
doi: 10.3389/fphys.2022.831248

Effects of Integrative Neuromuscular Training Combined With Regular Tennis Training Program on Sprint and Change of Direction of Children

*Zhi-Hai Wang, Rui-Cheng Pan, Meng-Ru Huang and Dan Wang**

School of Physical Education and Sport Training, Shanghai University of Sport, Shanghai, China

Objective: The aim of this study was to investigate the effects of integrative neuromuscular training (NMT) on sprint and the ability to change direction for children who are between the ages of 7 and 8 and beginning to play tennis.

Methods: Thirty-two participants were randomized into a training group (TG; $n = 16$) and a control group (CG; $n = 16$). All participants attended tennis classes twice a week for a continuous 8 weeks. In addition, the TG received NMT (e.g., 20-m sprints, running at four corners, rope ladder drills, etc.), which progressed in difficulty every 2 weeks. Pre-intervention and post-intervention measurements, including a 30-m sprint test, a 5–10–5 test, and a 3 × 10 m shuttle run test, were assessed by a Smartspeed laser timing gate system, while the spider agility test was evaluated with a stopwatch.

Results: Two-way repeated measures ANOVA found significant differences in the interaction between time and group among variables measured. Results were as follows: time in the 30 m sprint ($F = 13.467$, 95% CI = 7.163–7.506, $p = 0.001$, $\eta^2_p = 0.310$, $\Delta = 0.42$ s); 5–10–5 test ($F = 13.975$, 95% CI = 8.696–9.017, $p = 0.001$, $\eta^2_p = 0.318$, $\Delta = 0.78$ s); 3 × 10 m shuttle run ($F = 7.605$, 95% CI = 11.213–11.642, $p = 0.01$, $\eta^2_p = 0.202$, $\Delta = 0.77$ s); and spider agility test ($F = 34.555$, 95% CI = 28.258–29.670, $p < 0.001$, $\eta^2_p = 0.535$, $\Delta = 3.96$ s). The results demonstrated a greater decrease in sprint and change of direction (COD) time among the TG than the CG from pre-intervention to post-intervention.

Conclusion: A regular tennis training combined with NMT program could produce greater improvement in a player's sprint and ability to change direction when introduced to childhood tennis beginners in a sensitive period, compared to tennis class intervention only.

Keywords: sensitive period, physical fitness, movement, performance, child

OPEN ACCESS

Edited by:
Rafael Reimann Baptista, Pontifical Catholic University of Rio Grande do Sul, Brazil

Reviewed by:
Giovani Dos Santos Cunha, Federal University of Rio Grande do Sul, Brazil
Corrado Lupo, University of Turin, Italy

****Correspondence:***
Dan Wang
wangdan@sus.edu.cn

Specialty section:
This article was submitted to Exercise Physiology, a section of the journal Frontiers in Physiology

Received: *08 December 2021*
Accepted: *19 January 2022*
Published: *10 February 2022*

Citation:
Wang Z-H, Pan R-C, Huang M-R and Wang D (2022) Effects of Integrative Neuromuscular Training Combined With Regular Tennis Training Program on Sprint and Change of Direction of Children. Front. Physiol. 13:831248. doi: 10.3389/fphys.2022.831248

INTRODUCTION

Tennis is a high-intensity and demanding sport, requiring players to repeatedly engage in a sequence of intense activities, such as accelerations, decelerations, COD, and strokes during a variable period of competition time (on average 90 min; Fernandez-Fernandez et al., 2017). Players commonly complete more than 1,000 CODs in each competitive match (Kovacs, 2009).

Tennis players must move an average distance of 8–15 m, complete four COD movements, and hit the ball an average of 4–5 times for every one point scored (Murias et al., 2007). Typically, players must move quickly in linear directions (i.e., acceleration) and react quickly in both lateral and multiple directions (Fernandez-Fernandez et al., 2014). This requires attaining a high level of speed and COD ability (Fernandez-Fernandez et al., 2014). A previous study showed that speed and COD are decisive factors for tennis performance, and maximizing such abilities promotes on-court success (Fernandez-Fernandez et al., 2014). The 30 m sprint, 3 × 10 m shuttle run, spider agility, and 5–10–5 tests have been widely used to assess tennis players' speed and COD ability (Kramer et al., 2016; Rossi et al., 2017; Cheng, 2018; Vigh-Larsen et al., 2021). The 30 m sprint and 3 × 10 m shuttle run tests assess a tennis player's ability to accelerate in a straight line and run forward and backward from baseline to net, respectively. The combination of the two tests provides a more comprehensive assessment of a tennis player's speed ability than either alone. The spider agility and 5–10–5 tests assess different routes of movement in a tennis player's ability, such as lateral, forward, and backward, as well as the ability to move sideways along the back line of the court (known as the baseline). Combining these two tests provides a comprehensive assessment of a tennis player's full-court COD ability. Given the good neuroplasticity of 7–8 years old, training related to neural adaptation may be beneficial (Rumpf et al., 2012; Lloyd et al., 2013). Generally, sprint and COD training for children (7–8 years old) is effective and safe (Lupo et al., 2019). For example, Alonso-Aubin et al. (2021) reported significant improvements in dominant and non-dominant hand-eye coordination, core muscular endurance and sprinting ability in rugby players aged 6–14 years after 8 weeks of NMT (including sprint training, etc.). Similarly, Michailidis et al. (2019) conducted a 1-year sprint training intervention (including soccer training program) for school children aged 8–10, and found that the scores of anthropometries (e.g., body weight and body fat et al.), 30 m sprint and standing long jump were significantly improved. As for the trainability of COD during childhood, directly related literature are sparse. However, the Youth Physical Development model suggests the need for COD training (Lloyd et al., 2013) throughout childhood and adolescence (Lloyd and Oliver, 2012). Lloyd et al. (2013) considered that both children and adolescent athletes should receive training program including fundamental movement skills, COD and reactive agility training, but the percentage of time should be allocated according to different stages (e.g., 25% COD training in prepubertal stage).

The term "sensitive period" was originally used by Dutch biologist Hugo de Vries in his studies of animal growth. At the beginning of the last century, the Italian physician Maria Montessori, during her long-time work with children, discovered certain periods of sensitivity to special environmental stimuli that affect growth (Edwards, 2006). The long-term athlete development (LTAD) model suggests that children and adolescents during the sensitive period are more sensitive to training-induced adaptation (Balyi and Hamilton, 2004). Studies showed the first sensitive period for developing linear, lateral, and multi-directional speed (i.e., COD) occurs between the ages of 6 and 8 for girls and between 7 and 9 for boys (Balyi and Hamilton, 2004; Balyi and Way, 2005; Rumpf et al., 2012). If children fail to develop these skills during this period, young players might lose the opportunity to reach their full potential (Balyi and Hamilton, 2004). On the contrary, research shows that most fitness parameters are trainable throughout childhood and should not be restricted to sensitive period at different stages of development (Ford et al., 2011; Rumpf et al., 2012). For instance, Rumpf et al. (2012) suggest that prepubertal children (male: 7–12 years; female: 7–11 years) gain more speed performance improvements from high levels of neural activation training (e.g., sprint training). Also, children at this stage possess better neuroplasticity, and the development of sport-specific movements including COD performance is necessary at an early childhood (Lloyd et al., 2013). Lloyd et al. (2013) suggested that both children and adolescent athletes should receive training program including fundamental movement skills (FMS), COD and reactive agility training (RAT), but the percentage of time should be allocated according to different stages (e.g., prepubertal stage: 60% FMS training, 25% COD training and 15% RAT; circumpubertal stage: 30% FMS training, 40% COD training and 30% RAT). These may support the concept of a sensitive period in which sprint and COD training should be trained throughout childhood, but different training adaptations predominate differently. In addition, most studies also show that 6–12 years old is the golden period of motor skill learning and motor development, which is often referred to as the sensitive or critical period of motor skill learning and motor development (Hirtz and Starosta, 2002; Watanabe et al., 2007; Ireland et al., 2019; Solum et al., 2020). For example, one study showed that musicians who started training early showed better performance on tasks (keystroke accuracy and response synchronization), which could be due to the fact that children's neurodevelopment is not fully mature and the brain has greater plasticity during sensitive period of motor skill learning and motor development (Knudsen, 2004; Watanabe et al., 2007). It was considered that brain plasticity was likely highest in childhood and gradually decreased thereafter (Johansson, 2004). The potential reasons could be that in early childhood increased myelination in motor pathways leads to reduced reaction time and increased motor speed, which is associated with improved motor skills (Penhune, 2011). In addition, children develop stronger synapses between nerve cells as well as getting rid of those that are less adaptive (Knudsen, 2004). Overall, during the sensitive period of motor skill learning and motor development, the nervous system is particularly sensitive to related stimuli and is more prone to change when stimulated (Penhune, 2011). The brain develops new neural circuits during sensitive periods, laying the groundwork for later learning. Therefore, 7–8 years old seems to be a sensitive period for children's motor development and motor learning, and targeted training should be able to better promote the improvement of fitness.

At present, some of the research focused on determining which training interventions can maximize speed and COD performance in young tennis players. These interventions are mainly NMT (Salonikidis and Zafeiridis, 2008; Barber-Westin et al., 2010, 2015; Fernandez-Fernandez et al., 2016, 2018). NMT

is a complementary training program that includes both general (e.g., fundamental movements) and specific (e.g., exercises targeted to motor control) strength and conditioning activities, such as resistance, dynamic stability, core focused strength, plyometric and agility, that are designed to enhance health and skill-related components of physical fitness (Myer et al., 2011). It is a critical intervention for adolescents with high plasticity, starting in mid-childhood (approximately 7–10 years of age) and continuing throughout adolescence (Myer et al., 2011). For example, Fernandez-Fernandez et al. (2016) performed neuromuscular training (e.g., COD drills training, chasing training and ladder drills training) for 5 weeks before regular tennis training and observed a significant improvement in tennis players' (12.9 ± 0.4 years) speed (5–20 m sprint) and COD (5-0-5 agility test) performance. In addition, Salonikidis and Zafeiridis (Salonikidis and Zafeiridis, 2008) compared the effects of plyometric training (PT), tennis-specific training, and combined training (PT combined tennis-specific training) on tennis players (21.1 ± 1.3 years), and observed that combined training (e.g., sprint training, repetition COD training) combined the advantages of both regimens and significantly improved speed (4 and 12 m sprint) performance compared to PT and tennis-specific training alone. Similarly, Fernandez-Fernandez et al. (2016) observed that adding PT (e.g., jump training and multidirectional movements) to regular tennis training resulted in a significant improvement in 10-m sprint time and COD (5-0-5 agility test) performance compared to tennis training alone (12–13 years). Generally, most studies have shown that NMT training (e.g., sprint training, multidirectional movements) combined with tennis specific training can significantly improve sprint and COD performance in 12–21 years old tennis players. However, to our knowledge, no studies have examined whether a combination of reglue tennis training and NMT for tennis beginners aged 7–8 has a similar effect.

Therefore, the purpose of this study was to compare the effects of an 8-week NMT combined with a regular tennis training program on the sprint and COD ability of tennis beginners aged 7–8 to a control group taking only regular tennis training. It was hypothesized that NMT combined with regular tennis training could produce greater improvements in sprint and COD ability among tennis beginners 7–8 years old when compared with regular tennis training only.

MATERIALS AND METHODS

Study Design

This study was designed to compare the effects on tennis beginners of 8 weeks of NMT combined with regular tennis training for sprint and COD ability. Sprint and COD ability tests were carried out before (pre-test) and after training (post-test), including: (a) 30 m sprint test, (b) 3 × 10 shuttle run test, (c) 5–10–5 test, and (d) spider agility test.

Participants

Thirty-two participants were randomized into a training group (TG: eight females and eight males) and a control group (CG: eight females and eight males; see **Table 1**). The inclusion criteria were as follows: (1) no previous participation in tennis lessons, NMT and (2) no physical or mental defects or congenital diseases. The TG underwent a training program that incorporated tennis lessons, NMT between 15:30 and 17:00 (at a tennis court) on Mondays and Tuesdays for eight continuous weeks. The CG underwent only tennis-specific training from 15:30 to 17:00 on Wednesdays and Thursdays for eight continuous weeks. All participants completed two familiarization sessions before baseline measurements were taken (i.e., pre-test). All participants signed informed consent forms with the help of parents/teachers and were informed that they could withdraw from the experiment at any time. The study was approved by the Human Research Ethics Committee of Shanghai University of Sports.

Measurements

Speed Tests

30 m Sprint Test

The 30 m sprint test was used to assess straight line acceleration ability. After a warm-up, participants were instructed to sprint as fast as possible from a standing start just behind the Smartspeed laser timing gate system (Fusion Sports, Inc., Milton, Australia). Time was automatically recorded by the timing gate system. The participants each performed two trials with 2 min of rest in between, and each participant's best performance was used for subsequent statistical analysis.

3 × 10 m Shuttle Test

Each participant sprinted from the start line, completely crossed the finish line (10 m away from the start line), then turned 180° to sprint back to the start line, followed by another immediate sprint back to the finish line. Total time was automatically recorded using the Smartspeed laser timing gate system. Two trials with 2 min of rest in between were conducted, and each participant's shorter times were recorded for subsequent analysis.

COD Tests

5–10–5 Test

Three marker barrels (A, B, and C) were placed five yards apart on a track and field court. The participants started at the first marker barrel (A), and upon command, sprinted left and touched the second marker barrel (B); the participant

TABLE 1 | Demographic characteristics of the participants (Mean ± SD).

	TG ($n = 16$)		CG ($n = 16$)	
	Females ($n = 8$)	Males ($n = 8$)	Females ($n = 8$)	Males ($n = 8$)
Age (years)	7.4 ± 0.5	7.2 ± 0.4	7.2 ± 0.5	7.2 ± 0.4
Height (m)	1.19 ± 0.48	1.19 ± 0.57	1.19 ± 0.51	1.21 ± 0.44
Body mass (kg)	21.0 ± 2.71	21.3 ± 2.91	21.5 ± 2.76	22.3 ± 2.63

TG, training group; CG, control group.

then turned 180° and sprinted to touch the far-right marker barrel (C), followed by another sprint back to the first marker barrel (A; Rossi et al., 2017). Time was automatically recorded using the Smartspeed laser timing gate system. The participants performed two trials separated by 3 min of rest. The faster trials of each participant were used for subsequent data analysis.

Spider Agility Test

Five tennis balls were placed on the sidelines and along the service line. Participants started from the middle of the baseline (M), ran to pick up a ball, and ran back to leave the ball at M. Each ball was retrieved in a clockwise manner. The time when the last ball was placed at M was recorded in seconds to two decimal places with a Tianfu stopwatch timer (Fuhai Chemical Glass Instrument Co., Ltd., Shenzhen, China; Kramer et al., 2016, 2017). The participants each performed two trials separated by a 5 min rest. The shorter times for each participant were used for subsequent data analysis.

Training Program

The TG program included training in sprints, coordination, and COD in addition to the tennis lessons (see **Table 2**). Considering the young age of the participants and the complexity of the training contents, the strength and conditioning coach organized one meeting every 2 weeks to introduce the methods of training progression such as increasing the difficulty of the movements, changing the movements from single direction to multi-direction, and increasing the training load every 2 weeks. Proper techniques were demonstrated by the strength and conditioning coaches and maintained *via* verbal cues. The extra training for the TG was conducted as a 15–20 min component of the twice-weekly 90-min tennis classes. Each member of the TG strictly followed the training program and completed all sessions.

CG only attended 90-min tennis instruction (e.g., small steps in place with a racket, combination of small step and split step, swing practice in multi-directions, etc.) twice a week for eight continuous weeks.

Statistical Analyses

Descriptive statistics (mean ± SD) for the different variables were conducted. The Kolmogorov–Smirnov test and the Levene test for equality of variances were used to determine normal distribution. Two-way repeated measures analysis of variance (ANOVA) were used for data analysis [2 time-points (pre-test vs. post-test) *two group (TG vs. CG)]. Partial eta squared (η^2) was used as the effect size (ES) estimation for the time by group interaction effect with its strength being interpreted as the following: small < 0.06; moderate < 0.14; large ≥ 0.14 (Cohen, 1988). The level of significance was set at $p < 0.05$. The sphericity of the data was validated by Mauchly's W statistic. If this test were violated, the Greenhouse–Geisser correction would have been used for adjustment.

TABLE 2 | Eight-week neuromuscular training program.

Week	Exercise activities	Sets (*n*)	Reps (*n*)	Rests (sets)	Exercises (*n*)
1–2	5 m sprint	1	2	1 min	2
	2 in forward	1	4	1 min	2
	2 in lateral	1	4	1 min	2
	Frontal 2 in 2 out	1	4	1 min	2
	Later 2 in 2 out	1	4	1 min	2
	Sprint back and forth	1	2	1 min	2
	Left sideline shuttle run	1	2	1 min	2
	Right sideline shuttle run	1	2	1 min	2
	Hexagon jump(40 cm)	4	2	1 min	2
3–4	10 m sprint	1	2	1 min	2
	1 lateral (back and forth)	1	4	1 min	2
	Lateral lckey shuffle	1	4	1 min	2
	Side step	1	4	1 min	2
	Crossover step	1	4	1 min	2
	Sprint off left sideline in forward	1	2	1 min	2
	Sprint off right sideline in forward	1	2	1 min	2
	Hexagon jump (40 cm)	4	2	1 min	2
5–6	20 m sprint	1	2	1 min	2
	Frontal 2 in 2 out forward	1	4	1 min	2
	Frontal 2 in 2 out backward	1	4	1 min	2
	Frontal 1 in 1 out forward	1	4	1 min	2
	Frontal 1 in 1 out backward	1	4	1 min	2
	Throwing and catching balls over the net	1	4	1 min	2
	Four-corners run	1	2	1 min	2
	Hexagon jump (50 cm)	4	2	1 min	2
7–8	20 m sprint	1	2	1 min	2
	Rope ladder drills	1	4	1 min	2
	Throwing and catching balls over the net	1	4	1 min	2
	Four-corners run	1	2	1 min	2
	Hexagon jump (60 cm)	4	2	1 min	2

RESULTS

No significant differences were observed between the TG and CG in any of the variables analyzed pre-intervention. Significant differences in the interaction between time and group were found in the following: 30 m sprint test ($F = 13.467$, 95% CI = 7.163–7.506, $p = 0.001$, $\eta^2_p = 0.310$); 5–10–5 test ($F = 13.975$, 95% CI = 8.696–9.017, $p = 0.001$, $\eta^2_p = 0.318$); 3 × 10 m shuttle

run test ($F = 7.605$, 95% CI = 11.213–11.642, $p = 0.01$, $\eta^2_p = 0.202$); and spider agility test ($F = 34.555$, 95% CI = 28.258–29.670, $p < 0.001$, $\eta^2_p = 0.535$; see **Figure 1**).

DISCUSSION

The current study aimed to investigate the effects of an 8-week NMT combined with regular tennis training for beginning tennis players aged 7–8. To our knowledge, this is the first study conducted in 7–8 years old tennis beginners about NMT combined with regular tennis training. Significant improvements were observed in speed (30 m sprint test and 3 × 10 m test) and COD ability (5–10–5 test and spider agility test) for the TG, demonstrating the importance of NMT combined with regular tennis to speed and COD ability in tennis beginners during the first sensitive period. The results suggest that NMT combined with regular tennis training appears to be an effective method of improving these abilities in this particular age group.

The speed (30 m sprint test and 3 × 10 m test) and COD (5–10–5 test and spider agility test) performances improved for the TG as a result of the 8-week training program intervention when compared to the CG. These differences may be related to the lack of sufficient training stimulation to increase neural drive in CG. Due to the size of the court and the specific technique movements only in regular tennis training, children are rarely exposed to sprint distances over 10 m and COD training. Therefore, NMT combined with regular tennis training may provide an additional advantage when compared to regular tennis training. In addition, the improvement of various neuromuscular adaptations in children may be the important factor for the enhancement of sprint and COD performance after NMT combined with regular tennis training. Preadolescence (male: 7–12 years; female: 7–11 years) is considered to be a period of rapid development (Borms, 1986) and high plasticity of children's neuromuscular system (Ford et al., 2011). Studies have shown that children (7–8 years old) benefit most from training related to neural adaptation (Fernandez-Fernandez et al., 2016). The structure or function of the brain is sensitive to specific external stimuli and more likely to establish nervous motor circuits (Thomas and Johnson, 2008). NMT is a vital intervention program for children with high plasticity of cognitive and motor capabilities (Kraemer et al., 1989). The NMT program in this study mainly includes sprinting (e.g., 5–20 m sprint), coordination training (e.g., ladder drills), and multidirectional movements (e.g., four-corner run). It can effectively improve children's neural

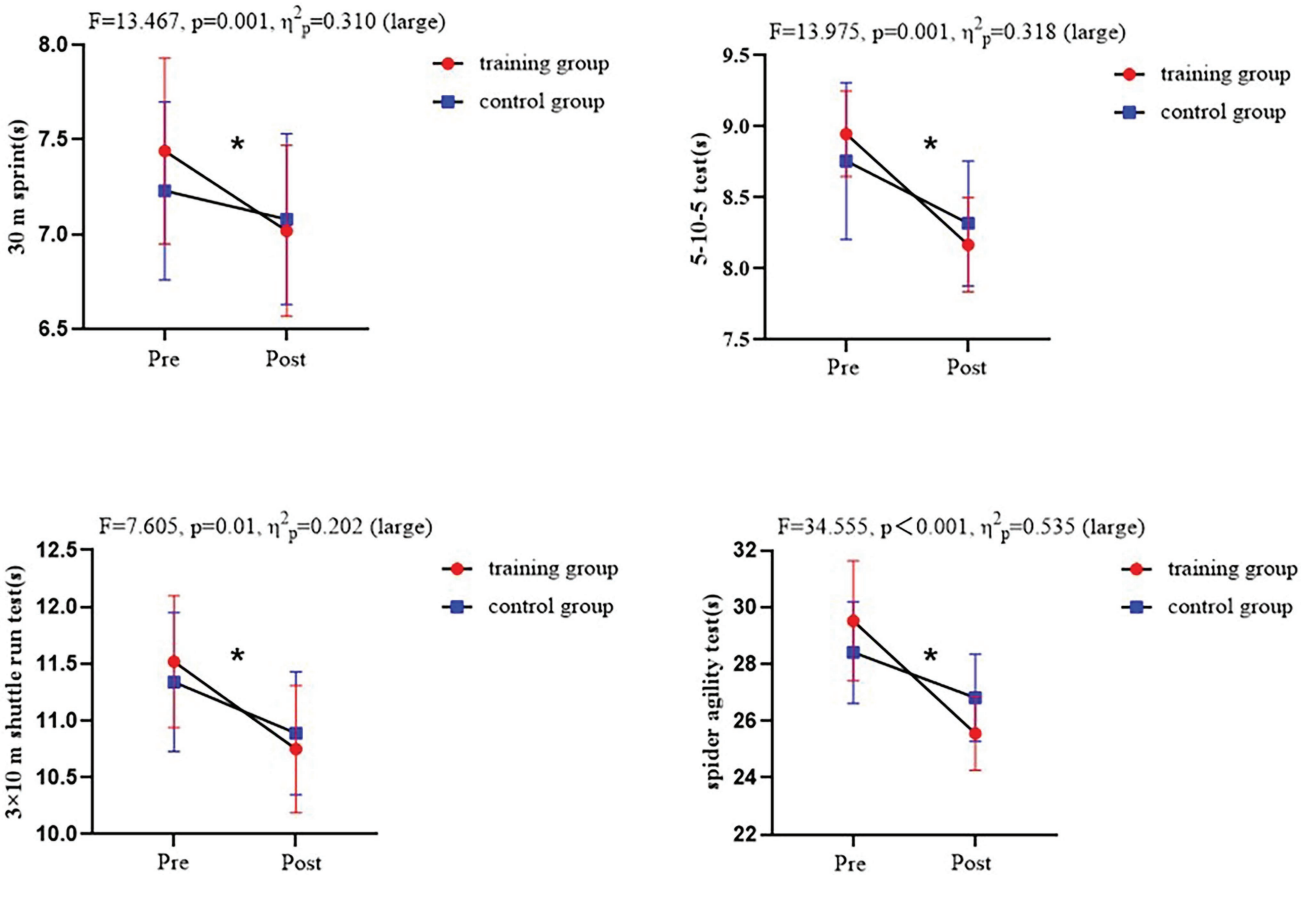

FIGURE 1 | Comparison of training group and control group pre-and post-intervention. *Significant difference from pre-test within the group.

adaptation, such as an increase in motor unit activation and synchronization, as well as an increase in motor unit recruitment and excitation frequency (Baechle and Earle, 1994).

The 30 m sprint and 3 × 10 m shuttle sprint performances improved for the TG as a result of the 8-week training program intervention when compared to the CG. Van Praagh (1998) suggested training methods that aim to improve coordination, movement efficacy, or velocity should be used to optimize the effectiveness of speed training before puberty. Speed is reflected in linear sprints. Speed performance may be highly influenced by technique (Faigenbaum et al., 2007), balance (Chaouachi et al., 2014), anthropometrics (height, body mass, etc.; Meyers et al., 2017), motor performance, and coordination (Behringer et al., 2011). An increase in coordination and a decrease in sprint time may have been important factors for improved speed in the current study. The TG NMT program incorporated sprint training and intermuscular coordination training, such as 5–20 m sprint and some ladder drills training. The evidence suggests that the most efficient training method for improving sprint performance is sprint training (Padrón-Cabo et al., 2020). Sprint-based activities, such as sprinting 5–20 m at maximum speed, involved heavy use of stretch-shortening-cycle movements, and thus may increase rate of force development, impulse production and stiffness of muscles which are associated with optimal sprint performance (Haff and Triplett, 2006). Sprinting is divided into three phases: initial acceleration, transition, and maximum velocity phases (von Lieres Und Wilkau et al., 2020). Sprint training may increase the velocity of the acceleration phase, resulting in significant decreases in ground contact time, which may allow children to achieve increases in stride rate and thus improve sprint performance (Kotzamanidis, 2006). One study indicated that a 10-week sprint training program could improve 20 m sprint performance for 11-year-old children (Kotzamanidis, 2006). A study by Venturelli et al. (2008) also reported improvements in 20 m sprint performances for male soccer players following 12 weeks of sprint training. In addition, coordination training (e.g., ladder drills training, hexagon jump) also seems to be a suitable method for improving speed performance (Venturelli et al., 2008; Padrón-Cabo et al., 2020), possibly providing a greater neural stimulus that results in better intramuscular and intermuscular coordination, and thus improvement in speed performance.

The 5–10–5 and spider agility tests also showed improved COD performance for the TG over 8 weeks compared to the CG. Our training program incorporated coordination exercises (e.g., ladder drills and hexagon jump) and multi-directional training (e.g., four-corner run) to improve intermuscular coordination, as well as acceleration and deceleration ability. Coordination training may improve intermuscular coordination and provide better synchronization of body segments to effect an improvement in COD ability. Multi-directional training may improve the speed and force of muscle contraction (e.g., eccentric strength) and enables the players to switch between deceleration and acceleration motions. This is critical for COD performance and another factor that affects COD ability (Balyi and Way, 2005; Brughelli et al., 2008; Barber-Westin et al., 2015). Meanwhile, the improvement of linear sprint speed may also contribute to the improvement of children's COD performance. Improving the sprint speed in short distance can benefit the initial and exit velocity in COD (Vanrenterghem et al., 2012). However, the contribution of sprint speed to COD performance may vary with the magnitude and amount of angle changed during a number of the direction changes (Young et al., 2002). Pettersen and Mathisen (2012) reported that the COD performance of 11–12 years old boys were significantly improved after 6 weeks of short distance sprint training, and also found that there was a significant transfer effect between the performance of straight-line sprint and COD performance ($r = 0.68–0.75$).

The significant improvement of sprint and COD ability may help children improve motor competence and physical fitness. On the one hand, the improved sprint and COD ability can help children further enhance their performance in tennis competitions. It also can help children achieve faster directional transitions, reach a point on the court faster and/or answer to a tennis ball faster. On the other hand, it provides a better basis for children to use targeted strength and conditioning training program to improve their physical fitness in tennis. Based on the current findings, improved speed and COD performance may help athletes achieve better long-term development and provide more lasting benefits, such as improved physical fitness, tennis skills and competitive performance. However, to know whether there are long term benefits of participating in such a training program was beyond the scope of current research, and future research should be conducted to investigate this issue. It would be useful if the same group of children were followed up some time after the intervention to check whether the positive changes reported here were maintained.

CONCLUSION AND LIMITATIONS OF THE STUDY

Conclusion

NMT combined with regular tennis training program could produce greater improvement in sprint and COD ability among sensitive period childhood tennis beginners when compared to regular tennis training intervention only. In view of the current results, when tennis coaches design training programs for children during the first sensitive period, it is recommended that specific tennis NMT be added to the program to improve speed and COD ability.

Limitations of the Study

A limitation in the current study that should be addressed is that it did not explore the underlying mechanisms of improved speed and COD, such as neuromuscular and lower limb force changes, after the training program. Therefore, further study

is needed to examine the effects of neuromuscular adaptation and lower limb force following NMT combined with regular tennis training program.

Practical Applications

Researchers have found similar benefits of NMT combined with tennis training on sprint and COD performance in other age groups of 12–13 and 21 years old. However, to our knowledge, this is the first study conducted in 7–8 years old tennis beginners about NMT combined with regular tennis training. Overall, our results demonstrate the potential value of incorporating an injuries-free, time-saving, inexpensive and developmentally appropriate NMT program into regular tennis training for children aged 7–8 years. Meanwhile, the results extend previous research work advocating the use of NMT program in children (e.g., 8–12 years), confirming that participation in the NMT program combined with regular tennis training was an effective approach to better improve sprint and COD performance of children aged 7–8 years. The performance improvements shown in current study are of great interest to tennis coaches and are directly applicable to childhood tennis beginners aged 7–8 years. It is recommended that tennis coaches implement NMT to improve players' performance. The results of the study could help coaches and sports scientists develop better guidelines and recommendations for childhood tennis beginners' training prescription and competition preparation.

DATA AVAILABILITY STATEMENT

The original contributions presented in the study are included in the article/supplementary material, further inquiries can be directed to the corresponding author.

ETHICS STATEMENT

The studies involving human participants were reviewed and approved by the Human Research Ethics Committee of Shanghai University of Sports. Written informed consent to participate in this study was provided by the participants' legal guardian/next of kin.

AUTHOR CONTRIBUTIONS

Z-HW, R-CP, and M-RH performed all the experiments. DW designed the experiments. Z-HW and DW analysed the experimental results. Z-HW wrote the manuscript. All authors reviewed and approved the submission of the manuscript.

FUNDING

This research was funded by a grant from Program for Overseas High-level Talents at Shanghai Institutions of Higher Learning under Grant No. TP2019072, the Natural Science Foundation of the Higher Education Institutions of Jiangsu Province under Grant No. 17KJB320008, and Shanghai Key Lab of Human Performance (Shanghai University of Sport) under Grant No. 11DZ2261100.

ACKNOWLEDGMENTS

The authors thank those who contributed to the development of this research. The authors would also like to thank all the children and teachers.

REFERENCES

Alonso-Aubin, D. A., Picón-Martínez, M., Rebullido, T. R., Faigenbaum, A. D., Cortell-Tormo, J. M., and Chulvi-Medrano, I. (2021). Integrative neuromuscular training enhances physical fitness in 6- to 14-year-old Rugby players. *J. Strength Cond. Res.* 35, 2263–2271. doi: 10.1519/JSC.0000000000003995

Baechle, T. R., and Earle, R. W. (1994). *Essentials of Strength Training and Conditioning.* Champaign, IL: Human Kinetics.

Balyi, I., and Hamilton, A. (2004). Long-term athlete development: trainability in childhood and adolescence. *Olympic Coach* 16, 4–9.

Balyi, I., and Way, R. (2005). The role of monitoring growth in long-term athlete development. *Canadian Sport for Life* 2, 47–64.

Barber-Westin, S. D., Hermeto, A. A., and Noyes, F. R. (2010). A six-week neuromuscular training program for competitive junior tennis players. *J. Strength Cond. Res.* 24, 2372–2382. doi: 10.1519/JSC.0b013e3181e8a47f

Barber-Westin, S. D., Hermeto, A., and Noyes, F. R. (2015). A six-week neuromuscular and performance training program improves speed, agility, dynamic balance, and core endurance in junior tennis players. *J. Athl. Enhanc.* 4:1. doi: 10.4172/2324-9080.1000185

Behringer, M., Vom Heede, A., Matthews, M., and Mester, J. (2011). Effects of strength training on motor performance skills in children and adolescents: a meta-analysis. *Pediatr. Exerc. Sci.* 23, 186–206. doi: 10.1123/pes.23.2.186

Borms, J. (1986). The child and exercise: an overview. *J. Sports Sci.* 4, 3–20. doi: 10.1080/02640418608732093

Brughelli, M., Cronin, J., Levin, G., and Chaouachi, A. (2008). Understanding change of direction ability in sport: a review of resistance training studies. *Sports Med.* 38, 1045–1063. doi: 10.2165/00007256-200838120-00007

Chaouachi, A., Othman, A. B., Hammami, R., Drinkwater, E. J., and Behm, D. G. (2014). The combination of plyometric and balance training improves sprint and shuttle run performances more often than plyometric-only training with children. *J. Strength Cond. Res.* 28, 401–412. doi: 10.1519/JSC.0b013e3182987059

Cheng, L. (2018). Study on the influence of speed quality training on the bottom line movement ability of tennis majors in Yuncheng University. master's thesis. Shanxi: Shanxi Normal University.

Cohen, J. (1988). *Statistical Power Analysis for the Behavior Science: Lawrance Eribaum Association*. Cambridge: Academic Press Books-Elsevier.

Edwards, C. P. (2006). Montessori education and its scientific basis. *J. Appl. Dev. Psychol.* 27, 183–187. doi: 10.1016/j.appdev.2005.12.012

Faigenbaum, A. D., McFarland, J. E., Keiper, F. B., Tevlin, W., Ratamess, N. A., Kang, J., et al. (2007). Effects of a short-term plyometric and resistance training program on fitness performance in boys age 12 to 15 years. *J. Sports Sci. Med.* 6:519. doi: 10.1016/j.jsams.2006.09.004

Fernandez-Fernandez, J., Granacher, U., Sanz-Rivas, D., Sarabia Marín, J. M., Hernandez-Davo, J. L., and Moya, M. (2018). Sequencing effects of

neuromuscular training on physical fitness in youth elite tennis players. *J. Strength Cond. Res.* 32, 849–856. doi: 10.1519/JSC.0000000000002319

Fernandez-Fernandez, J., Saez de Villarreal, E., Sanz-Rivas, D., and Moya, M. (2016). The effects of 8-week plyometric training on physical performance in young tennis players. *Pediatr. Exerc. Sci.* 28, 77–86. doi: 10.1123/pes.2015-0019

Fernandez-Fernandez, J., Sanz, D., Sarabia, J. M., and Moya, M. (2017). The effects of sport-specific drills training or high-intensity interval training in young tennis players. *Int. J. Sports Physiol. Perform.* 12, 90–98. doi: 10.1123/ijspp.2015-0684

Fernandez-Fernandez, J., Ulbricht, A., and Ferrauti, A. (2014). Fitness testing of tennis players: how valuable is it? *Br. J. Sports Med.* 48(Suppl 1), i22–i31. doi: 10.1136/bjsports-2013-093152

Ford, P., De Ste Croix, M., Lloyd, R., Meyers, R., Moosavi, M., Oliver, J., et al. (2011). The long-term athlete development model: physiological evidence and application. *J. Sports Sci.* 29, 389–402. doi: 10.1080/02640414.2010.536849

Haff, G. G., and Triplett, N. T. (eds.) (2006). *Essentials of Strength Training and Conditioning. 4th Edn.* Illinois: Human Kinetics Publishers Inc.

Hirtz, P., and Starosta, W. (2002). Sensitive and critical periods of motor co-ordination development and its relation to motor learning. *J. Hum. Kinet.* 7, 19–28.

Ireland, K., Iyer, T. A., and Penhune, V. B. (2019). Contributions of age of start, cognitive abilities and practice to musical task performance in childhood. *PLoS One* 14:e0216119. doi: 10.1371/journal.pone.0216119

Johansson, B. B. (2004). Brain plasticity in health and disease. *Keio J. Med.* 53, 231–246. doi: 10.2302/kjm.53.231

Knudsen, E. I. (2004). Sensitive periods in the development of the brain and behavior. *J. Cogn. Neurosci.* 16, 1412–1425. doi: 10.1162/0898929042304796

Kotzamanidis, C. (2006). Effect of plyometric training on running performance and vertical jumping in prepubertal boys. *Strength Cond. J.* 20, 441–445. doi: 10.1519/R-16194.1

Kovacs, M. S. (2009). Movement for tennis: The importance of lateral training. *Strength Cond. J.* 31, 77–85. doi: 10.1519/SSC.0b013e3181afe806

Kraemer, W. J., Fleck, S. J., Callister, R., Shealy, M., Dudley, G. A., Maresh, C. M., et al. (1989). Training responses of plasma beta-endorphin, adrenocorticotropin, and cortisol. *Med. Sci. Sports Exerc.* 21, 146–153

Kramer, T., Huijgen, B. C., Elferink-Gemser, M. T., and Visscher, C. (2016). A longitudinal study of physical fitness in elite junior tennis players. *Pediatr. Exerc. Sci.* 28, 553–564. doi: 10.1123/pes.2016-0022

Kramer, T., Huijgen, B. C., Elferink-Gemser, M. T., and Visscher, C. (2017). Prediction of tennis performance in junior elite tennis players. *J. Sports Sci. Med.* 16, 14–21.

Lloyd, R. S., and Oliver, J. L. (2012). The youth physical development model: a new approach to long-term athletic development. *Strength Cond. J.* 34, 61–72. doi: 10.1519/SSC.0b013e31825760ea

Lloyd, R. S., Read, P., Oliver, J. L., Meyers, R. W., Nimphius, S., and Jeffreys, I. (2013). Considerations for the development of agility during childhood and adolescence. *Strength Cond. J.* 35, 2–11. doi: 10.1519/SSC.0b013e31827ab08c

Lupo, C., Ungureanu, A. N., Varalda, M., and Brustio, P. R. (2019). Running technique is more effective than soccer-specific training for improving the sprint and agility performances with ball possession of prepubescent soccer players. *Biol. Sport* 36, 249–255. doi: 10.5114/biolsport.2019.87046

Meyers, R. W., Oliver, J. L., Hughes, M. G., Lloyd, R. S., and Cronin, J. B. (2017). Influence of age, maturity, and body size on the spatiotemporal determinants of maximal Sprint speed in boys. *J. Strength Cond. Res.* 31, 1009–1016. doi: 10.1519/JSC.0000000000001310

Michailidis, Y., Metaxas, T. I., Stefanidis, P., and Christoulas, K. (2019). Fitness effects of one-year soccer training of 8-10 and 10-12-year-old school children. *J. Sports Med. Phys. Fitness* 59, 725–732. doi: 10.23736/S0022-4707.18.08612-7

Murias, J. M., Lanatta, D., Arcuri, C. R., and Laiño, F. A. (2007). Metabolic and functional responses playing tennis on different surfaces. *Strength Cond. J.* 21, 112–117. doi: 10.1519/00124278-200702000-00021

Myer, G. D., Faigenbaum, A. D., Ford, K. R., Best, T. M., Bergeron, M. F., and Hewett, T. E. (2011). When to initiate integrative neuromuscular training to reduce sports-related injuries and enhance health in youth? *Curr. Sports Med. Rep.* 10, 155–166. doi: 10.1249/JSR.0b013e31821b1442

Padrón-Cabo, A., Rey, E., Kalén, A., and Costa, P. B. (2020). Effects of training with an agility ladder on Sprint, agility, and dribbling performance in youth soccer players. *J. Hum. Kinet.* 73, 219–228. doi: 10.2478/hukin-2019-0146

Penhune, V. B. (2011). Sensitive periods in human development: evidence from musical training. *Cortex* 47, 1126–1137. doi: 10.1016/j.cortex.2011.05.010

Pettersen, S. A., and Mathisen, G. E. (2012). Effect of short burst activities on sprint and agility performance in 11- to 12-year-old boys. *J. Strength Cond. Res.* 26, 1033–1038. doi: 10.1519/JSC.0b013e31822e58c8

Rossi, F. E., Landreth, A., Beam, S., Jones, T., Norton, L., and Cholewa, J. M. (2017). The effects of a sports nutrition education intervention on nutritional status, sport nutrition knowledge, body composition, and performance during off season training in NCAA division I baseball players. *J. Sports Sci.* 16, 60–68.

Rumpf, M. C., Cronin, J. B., Pinder, S. D., Oliver, J., and Hughes, M. (2012). Effect of different training methods on running sprint times in male youth. *Pediatr. Exerc. Sci.* 24, 170–186. doi: 10.1123/pes.24.2.170

Salonikidis, K., and Zafeiridis, A. (2008). The effects of plyometric, tennis-drills, and combined training on reaction, lateral and linear speed, power, and strength in novice tennis players. *J. Strength Cond. Res.* 22, 182–191. doi: 10.1519/JSC.0b013e31815f57ad

Solum, M., Lorås, H., and Pedersen, A. V. (2020). A Golden age for motor skill learning? Learning of an unfamiliar motor task in 10-year-olds, young adults, and adults, when starting From similar baselines. *Front. Psychol.* 11:538. doi: 10.3389/fpsyg.2020.00538

Thomas, S. C., and Johnson, M. H. (2008). New advances in understanding sensitive periods in development. *Curr. Dir. Psychol.* 17, 1–5. doi: 10.1111/j.1467-8721.2008.00537.x

van Praagh, E. (1998). *Pediatric Anaerobic Performance.* Champaign, IL: Human Kinetics Publisher, Inc.

Vanrenterghem, J., Venables, E., Pataky, T., and Robinson, M. A. (2012). The effect of running speed on knee mechanical loading in females during side cutting. *J. Biomech.* 45, 2444–2449. doi: 10.1016/j.jbiomech.2012.06.029

Venturelli, M., Bishop, D., and Pettene, L. (2008). Sprint training in preadolescent soccer players. *Int. J. Sport Physiol. Perform.* 3, 558–562. doi: 10.1123/ijspp.3.4.558

Vigh-Larsen, J. F., Haverinen, M. T., Knudsen, C. B., Daasbjerg, A., Beck, J. H., Overgaard, K., et al. (2021). The relationship between age and fitness profiles in elite male ice hockey players. *J. Sports Med. Phys. Fitness* 61, 512–518. doi: 10.23736/S0022-4707.20.11313-6

von Lieres Und Wilkau, H. C., Irwin, G., Bezodis, N. E., Simpson, S., and Bezodis, I. N. (2020). Phase analysis in maximal sprinting: an investigation of step-to-step technical changes between the initial acceleration, transition and maximal velocity phases. *Sport. Biomech.* 19, 141–156. doi: 10.1080/14763141.2018.1473479

Watanabe, D., Savion-Lemieux, T., and Penhune, V. B. (2007). The effect of early musical training on adult motor performance: evidence for a sensitive period in motor learning. *Exp. Brain Res.* 176, 332–340. doi: 10.1007/s00221-006-0619-z

Young, W. B., James, R., and Montgomery, I. (2002). Is muscle power related to running speed with changes of direction? *J. Sports Med. Phys. Fitness* 42, 282–288.

Conflict of Interest: The authors declare that the research was conducted in the absence of any commercial or financial relationships that could be construed as a potential conflict of interest.

Publisher's Note: All claims expressed in this article are solely those of the authors and do not necessarily represent those of their affiliated organizations, or those of the publisher, the editors and the reviewers. Any product that may be evaluated in this article, or claim that may be made by its manufacturer, is not guaranteed or endorsed by the publisher.

frontiers in Bioengineering and Biotechnology

ORIGINAL RESEARCH
published: 10 February 2022
doi: 10.3389/fbioe.2021.781672

Modulation in the Stiffness of Specific Muscles of the Quadriceps in Patients With Knee Osteoarthritis and Their Relationship With Functional Ability

*Tian-Tian Chang[1], Yuan-Chun Zhu[2], Zhe Li[3], Feng Li[1], Ya-Peng Li[1], Jia-Yi Guo[1], Xue-Qiang Wang[2,4] and Zhi-Jie Zhang[1]**

[1]Rehabilitation Therapy Center, Luoyang Orthopedic Hospital of Henan Province, Orthopedic Hospital of Henan Province, Luoyang, China, [2]Department of Sport Rehabilitation, Shanghai University of Sport, Shanghai, China, [3]The First Clinical Medical School, Shaanxi University of Chinese Medicine, Xi'an, China, [4]Department of Rehabilitation Medicine, Shanghai Shangti Orthopaedic Hospital, Shanghai, China

Deficits in the flexibility of the quadriceps are one of the risk factors for developing knee joint disorders. No studies have investigated the changes in the stiffness of the quadriceps muscle among patients with knee osteoarthritis (OA). Therefore, the purpose of this study was to investigate changes in the stiffness of specific-muscle of the quadriceps in patients with knee OA and their relationship with functional ability. Twenty-five patients with knee OA and 25 healthy, asymptomatic subjects were recruited in this study. The stiffness of the vastus lateralis (VL), vastus medialis (VM) and rectus femoris (RF) in all participants was evaluated using MyotonPRO at 60° and 90° flexion of the knee joint. The results of this study showed a greater VL stiffness in patients with knee OA than in healthy subjects at both 60° and 90° of knee flexion ($p < 0.05$). Significant differences in VL, VM and RF stiffness were obtained at different knee joint angles in individuals with and without knee OA ($p < 0.05$). In addition, there was a positive correlation between VL stiffness and the Western Ontario and McMaster Universities Osteoarthritis Index (WOMAC) scores in patients with Knee OA (60° of knee flexion: $r = 0.508$, $p = 0.010$; 90° of knee flexion: $r = 0.456$, $p = 0.022$). These results indicate that there is an increase in VL stiffness in patients with knee OA compared with healthy, asymptomatic subjects, and the quadriceps stiffness was increased with knee flexion in both healthy subjects and patients with knee OA. VL stiffness is associated with WOMAC scores in patients with knee OA.

Keywords: stiffness, quadriceps, osteoarthritis, knee, vastus lateralis, WOMAC

OPEN ACCESS

Edited by:
Marcus Fraga Vieira, Universidade Federal de Goiás, Brazil

Reviewed by:
Fu-Lien Wu, University of Illinois at Urbana-Champaign, United States
Rafael Reimann Baptista, Pontifical Catholic University of Rio Grande do Sul, Brazil

****Correspondence:***
Zhi-Jie Zhang
sportspt@163.com

Specialty section:
This article was submitted to Biomechanics, a section of the journal Frontiers in Bioengineering and Biotechnology

Received: *23 September 2021*
Accepted: *13 December 2021*
Published: *10 February 2022*

Citation:
Chang T-T, Zhu Y-C, Li Z, Li F, Li Y-P, Guo J-Y, Wang X-Q and Zhang Z-J (2022) Modulation in the Stiffness of Specific Muscles of the Quadriceps in Patients With Knee Osteoarthritis and Their Relationship With Functional Ability. Front. Bioeng. Biotechnol. 9:781672. doi: 10.3389/fbioe.2021.781672

INTRODUCTION

Osteoarthritis (OA) is the most common joint disorder around the world and it can affect many joints but most frequently occurs in the knee (Du et al., 2019). Knee osteoarthritis, characterized by knee joint degeneration, usually occurs during middle to older age (Michael et al., 2010). It is estimated that approximately 37% of individuals (aged > 45 years) are affected by knee OA (Dillon et al., 2006). Furthermore, the prevalence of knee OA has increased because of the increasingly older and obese population worldwide (Hunter and Bierma-Zeinstra, 2019). As a result, knee OA results in a significant social and economic burden (Liu Q et al., 2018). The costs of medical care, indirect costs

due to work loss and premature retirement caused by knee OA are escalating (Cross et al., 2014; Safiri et al., 2020). There are many risk factors for knee OA, including a high body mass index (BMI), quadriceps weakness, frequent kneeling and squatting, and participation in sports (Simic et al., 2021; Szilagyi et al., 2021).

The quadriceps muscle plays an important role in shock absorption and knee joint stability during walking and running (Davis et al., 2019; Ebihara et al., 2020). The reduced flexibility of the quadriceps may be one of the risk factors for the development of anterior knee pain, including patellofemoral pain syndrome and patellar tendinopathy, and tight quadriceps muscles may contribute to increasing knee joint stress during functional activities (Witvrouw et al., 2000; Witvrouw et al., 2001; Piva et al., 2005). Previous studies have used the knee range of motion to reflect the flexibility of the quadriceps in patients with knee OA (Cho et al., 2015; Lu et al., 2018; Perlman et al., 2019). However, this method is used to quantify the flexibility of groups of muscles, not individual muscles. The joint range of motion is influenced not only by skeletal muscle but also by noncontractile structures such as skin, tendons and the joint capsule (Geertsen et al., 2015; Andrade et al., 2016; Nordez et al., 2017). Thus, the method used to quantify the joint range of motion could not provide insight into changes in the stiffness of individual muscles. Furthermore, several studies have demonstrated that the stiffness of each individual muscle may be influenced by various factors, such as contraction (Avrillon et al., 2018), stretching (Hirata et al., 2016) and pathology (Zhang et al., 2014; Zhou et al., 2020). In recent years, some studies compared the difference in the stiffness of soft tissues between healthy subjects and patients with musculoskeletal disorders (such as low back pain, neck pain, and patellar tendinopathy) and explored the mechanical properties of soft tissue in these patients (Ishikawa et al., 2017; Breda et al., 2020; Koppenhaver et al., 2020). One study has investigated quadriceps tendon stiffness in patients with knee OA and they found the passive stiffness of the quadriceps tendon was negatively correlated to the maximum knee flexion angle in patients with knee OA and speculated that the increased soft tissues stiffness may contribute to functional impairment (Ebihara et al., 2020). Although patients with knee OA often experience pathological changes in the muscles around the knee (Rice et al., 2011; Noehren et al., 2018), to the best of our knowledge, no studies have investigated the muscles stiffness in patients with knee OA. Therefore, it is necessary to directly compare the differences in quadriceps stiffness between the healthy subjects and patients with knee OA to obtain a comprehensive understanding of the biomechanical properties of the muscle and to develop an appropriate rehabilitation program for patients with knee OA.

Quantitative assessment of muscle stiffness usually uses biomechanical methods to evaluate changes in the muscle-tendon length-tension relationship (Rieder et al., 2016). However, it evaluates the stiffness of the entire muscle group and cannot assess changes in the stiffness of individual muscles. A handheld device, MyotonPRO, can measure changes in individual muscle stiffness conveniently and quickly (Chang et al., 2020; Amirova et al., 2021). In our previous studies, we demonstrated that MyotonPRO is a reliable method for assessing the stiffness of the gastrocnemius (Feng et al., 2018) and upper trapezius (Liu CL et al., 2018). Chen et al. (2019) observed good intra- and interrater reliability of MyotonPRO for measuring the stiffness of the superficial quadriceps [vastus lateralis (VL), vastus medialis (VM) and rectus femoris (RF)] (ICC >0.84). Therefore, we compared the differences in the quadriceps stiffness between healthy people and patients with Knee OA using MyotonPRO.

The objectives of this study were to 1) compare the stiffness of the superficial quadriceps (RF, VL, and VM) between healthy individuals and patients with knee osteoarthritis; 2) examine differences of quadriceps stiffness at different angles of the knee joint; and 3) evaluate the correlations between the quadriceps (RF, VL, and VM) stiffness and joint dysfunction in patients with Knee OA.

MATERIALS AND METHODS

Subjects

This study had a cross-sectional design. Twenty-five patients with knee OA and 25 healthy, asymptomatic, age-matched subjects were recruited for this study. The sample size was calculated based on a pilot study of 14 subjects. The effect size between the patients with knee OA and healthy controls for VL stiffness was 0.77. Taking α at 5% and power at 80%, the estimated sample size was 22 subjects per group. All patients applied to outpatient clinics with knee pain and received an initial clinical assessment (including knee X-rays) to support the clinical diagnosis of knee OA. The patients were included if they met the following criteria (Vaz et al., 2013; Devrimsel et al., 2019): 1) Age greater than 45 years old; 2) clinically diagnosed with knee OA; 3) patients diagnosed with grade 2 or 3 knee osteoarthritis according to the criteria proposed by Kellgren and Lawrence; 4) visual analog scale (VAS) > 3 points in daily activity; and 5) no skin lesions above the measuring regions. Patients' exclusion criteria for this study were based on the following factors: a history of knee or hip or ankle surgery, previous musculoskeletal or joint injuries of lower limb in addition to knee OA, acute inflammation or pain with edema, metabolic diseases, severe deformity of the lower limbs, and BMI >30 kg/m^2.

Equipment

In the present study, MyotonPRO (Myoton AS, Tallinn, Estonia) was used to quantify the quadriceps stiffness. The device's basic principles are as follows (Gavronski et al., 2007; Schneider et al., 2015): five short mechanical impulses (the tap interval was 0.8 s) were implemented automatically by the device after precompressing the tissue, and these impulses cause mechanical oscillations in the soft tissue being evaluated. Then, MyotonPRO recorded the oscillation information and calculated the soft tissue mechanical parameters. One of these parameters is stiffness (newtons/meter, N/m). The stiffness value was calculated as the maximum acceleration of the oscillation/maximum displacement of the tissue. The larger the value, the stiffer the tissue. Any data with a coefficient of variation greater than 3% in any measurement on quintuple scanning mode were remeasured.

TABLE 1 | The characteristics of the subjects.

Women/Men (n)	Patients with knee OA (M ± SD)	Healthy subjects (M ± SD)	*p*
	17/8	17/8	
Age (years)	62.20 ± 8.30	59.44 ± 5.33	0.168
Height (m)	1.62 ± 0.06	1.63 ± 0.06	0.873
Weight (kg)	63.92 ± 7.14	62.64 ± 8.13	0.557
BMI (kg/m^2)	24.22 ± 1.96	23.67 ± 2.67	0.55
WOMAC	103.48 ± 27.73	—	—

WOMAC, the Western Ontario and McMaster Universities Osteoarthritis Index scores.

TABLE 2 | Stiffness of the RF, VL, and VM between the patients with Knee OA and the healthy subjects.

Knee flexion		Patients with knee OA (M ± SD)	Healthy subjects (M ± SD)	*p*
60°	RF	268.68 ± 37.21	262.96 ± 31.10	0.558
	VL	288.80 ± 29.78	254.88 ± 29.33	0.001**
	VM	260.92 ± 30.68	246.80 ± 30.56	0.110
90°	RF	292.48 ± 37.86	286.32 ± 34.42	0.987
	VL	321.92 ± 27.47	289.88 ± 26.81	0.001**
	VM	290.36 ± 39.22	291.40 ± 40.07	0.926

RF, rectus femoris; VL, vastus lateralis; VM, vastus medialis. **p < 0.05.

Procedures

Demographic information such as age, sex, weight, height, and BMI were recorded before the experiment. The Western Ontario and McMaster Universities Osteoarthritis Index (WOMAC) was used to assess the severity of the symptoms and physical functional disability among the knee OA patients (Salaffi et al., 2003). The questionnaire included 24 questions divided into three subscales: pain, stiffness and physical function. Each question was answered based on a validated 10-point numerical rating scale. The WOMAC has demonstrated acceptable validity and reliability in individuals with Knee OA (Bellamy et al., 1988). The total WOMAC scores were defined as the sum of 24 items, ranging from 0 to 240.

Measurement of the Quadriceps Stiffness

The room temperature was maintained at 25°C throughout all tests. The quadriceps was subdivided into the rectus femoris (RF), vastus lateralis (VL), vastus medialis (VM), and vastus intermedius (VI). Because the VI is deep inside the RF, the stiffness of the VI cannot be measured by the MyotonPRO. According to previous studies, the measurement region for RF stiffness was two-thirds of the length between the anterior superior iliac spine (ASIS) and the superior pole of the patella (Agyapong-Badu et al., 2016; Chen et al., 2019). The stiffness of the VL and VM was measured at the most salient point of the muscle belly (near the knee joint) (Chen et al., 2019). The measurement sites were marked by the same experienced physical therapist. The symptomatic knees of the patients with knee OA were used for all measurements. When both knees were symptomatic, the most affected knee was evaluated (León-Ballesteros et al., 2020). We measured the stiffness of the soft tissues in the dominant legs in healthy participants. The dominant leg of the subject was determined by which leg they used when they were asked to kick a ball (Lenskjold et al., 2015).

Before the stiffness assessment, the participants were allowed to rest for 5 min. The stiffness measurement was taken with the participant in the sitting position with the knee bent at 60° and 90°. The knee angle was maintained by an angle-adjustable knee orthosis. The order of stiffness measurements was RF, VL, and VM. The MyotonPRO was applied perpendicular to the surface of the muscle being examined. The subjects were asked to refrain from talking, to remain relaxed, and to avoid any muscle contraction during the stiffness measurements.

Statistical Analysis

SPSS Version 22.0 software (IBM, Armonk, NY, United States) was used for the data analysis. The demographic information was calculated by descriptive statistics. The Shapiro–Wilk test was used to assess the normal distribution of the data. Homogeneity of variances was tested using Levene's test. Independent t tests were performed to compare the demographic data between individuals with and without knee OA. Comparisons between RF, VL, and VM stiffness in the healthy subjects and the patients with knee OA were evaluated using an independent sample *t*-test. A paired-sample *t*-test was performed for quadriceps stiffness differences at different knee angles. The correlation between RF, VL, VM stiffness, and WOMAC scores was demonstrated by Pearson correlation analysis (r). All measurement data are expressed as the mean ± standard deviation, and all $p < 0.05$ indicated a significant level.

RESULTS

Demographic Information

Demographic information for all participants regarding age, weight, height, and BMI is depicted in **Table 1**. The clinical assessment report regarding WOMAC is also presented in **Table 1**. There were no significant differences in age, height, weight, or BMI ($p > 0.05$).

RF, VL, and VM Stiffness Between the Patients With Knee OA and Healthy Subjects

The mean stiffness values of the RF, VL and VM in the patients with knee OA and healthy controls are summarized in **Table 2**. The VL stiffness of patients with knee OA was greater than that of the healthy subjects at flexion 60° of the knee joint ($p < 0.05$). Similarly, compared with the healthy subject group, the patients in the knee OA group had greater VL stiffness at 90° of knee flexion ($p < 0.05$). However, no between-group differences were observed in the RF and VM stiffness measured at 60° and 90° of knee flexion ($p > 0.05$).

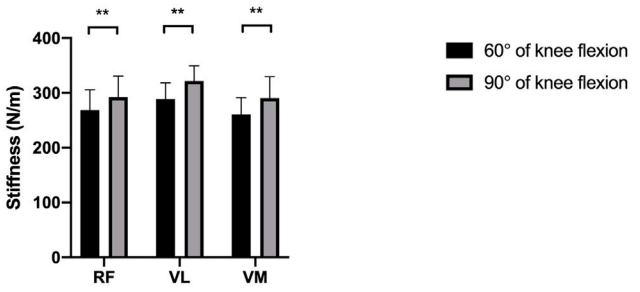

FIGURE 1 | The difference between the mean stiffness of the quadriceps at 60° and 90° of knee flexion in patients with knee OA. **$p < 0.05$.

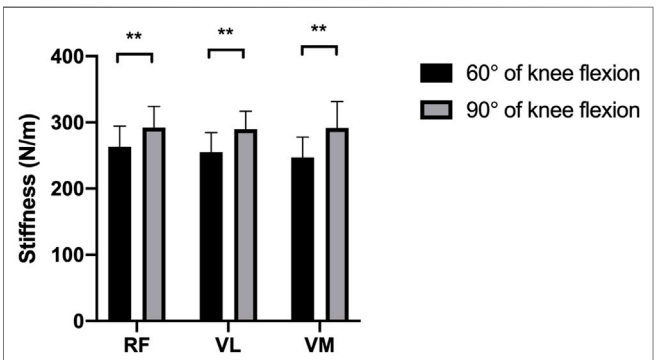

FIGURE 2 | The difference between the mean stiffness of the quadriceps at 60° and 90° of knee flexion in healthy subjects. **$p < 0.05$.

TABLE 3 | Correlation of RF, VL, and VM stiffness and WOMAC scores.

Knee flexion		WOMAC	
		r	p
60°	RF	0.297	0.149
	VL	0.508	0.010**
	VM	0.284	0.169
90°	RF	0.283	0.170
	VL	0.456	0.022**
	VM	0.328	0.110

RF, rectus femoris; VL, vastus lateralis; VM, vastus medialis; WOMAC, the Western Ontario and McMaster Universities Osteoarthritis Index scores. **p < *0.05.*

RF, VL, and VM Stiffness at Different Degrees of Knee Flexion

Figures 1, **2** reveal the stiffness of RF, VL, and VM at 60° and 90° of knee flexion in patients with knee OA and healthy subjects, respectively. A significant difference was found in the RF, VL, and VM stiffness between the 60° of knee flexion and 90° flexion of the knee joint in the patients with knee OA ($p < 0.05$). Similarly, in the healthy subject group, there was a significant increase in the RF, VL, and VM stiffness at 90° flexion of the knee joint compared with that at 60° of knee flexion ($p < 0.05$).

The Correlation Between RF, VL, VM Stiffness, and WOMAC Scores

In patients with Knee OA, Pearson correlation analysis tests were used to indicate the relationship between RF, VL, VM stiffness, and WOMAC scores. As shown in **Table 3**, there was a significant positive correlation ($r = 0.508$, $p = 0.010$) between the WOMAC scores and the VL stiffness measured at 60° of knee flexion. At 90° of knee joint flexion, a significant positive correlation was found between the WOMAC scores and the VL stiffness ($r = 0.456$, $p = 0.022$). However, no significant correlation was apparent between RF and VM stiffness and WOMAC scores, regardless of knee position ($p > 0.05$). The stiffer the VL is, the greater the level of physical dysfunction in knee OA patients.

DISCUSSION

This is the first study to compare the stiffness of the VL, RF and VM between subjects with Knee OA and healthy controls. The present study aimed to investigate the difference in the stiffness of the VL, RF and VM between subjects with and without knee OA. The main results of the study demonstrated that increased VL stiffness was found in subjects with knee OA compared to healthy controls. Furthermore, the findings from this study revealed that the quadriceps stiffness increased with knee flexion. More importantly, our study also established a relationship between the stiffness of the VL, RF and VM and the degree of disability among subjects with knee OA. We found a significant positive correlation between the VL stiffness index and WOMAC scores.

We observed the VL stiffness among subjects with Knee OA was higher than that among healthy controls. The VL stiffness was increased by 11.8% at 60° of knee flexion and by 10.0% at 90° of knee flexion compared to the control group. Although no previous studies have made a direct comparison as in our study, previous studies have reported that a reduction in muscle flexibility may be associated with anterior knee pain (Witvrouw et al., 2000; Piva et al., 2005). A 2-year prospective study revealed that there was significantly less flexibility of the quadriceps in subjects with patellofemoral pain (Witvrouw et al., 2000). They found that the flexibility of the quadriceps in subjects with patellofemoral pain was reduced by 6.1% compared to the control group. Similarly, Piva et al. (2005) observed that patients with patellofemoral pain syndrome had a reduced knee range of motion. In the study of Witvrouw et al. (2001), significantly lower flexibility of the quadriceps in individuals with patellar tendinitis was obtained as compared with the control group (Witvrouw et al., 2001). A recent study evaluated the stiffness of the RF and VL in athletes with patellar tendinopathy using shear wave elastography, and they observed that the VL stiffness was increased by 26.5% in athletes with patellar tendinopathy (Zhang et al., 2017). More recently, Zhou et al. (2020) reported that a stiffer medial gastrocnemius but not the lateral gastrocnemius was found in individuals with plantar fasciitis. The knee extensor plays an important role in dissipating kinetic energy during walking, running and landing (Decker et al., 2003), and a decrease in the flexibility of the quadriceps

muscle might contribute to increasing the loading on the patellofemoral joint (Piva et al., 2005). Some studies have investigated the effects of soft tissue release in patients with knee OA (Tarabichi and Tarabichi, 2010; Atkins and Eichler, 2013). Atkins and Eichler, 2013 conducted a randomized controlled trial and observed a significant difference in the WOMAC score between the self-massage intervention group (applied on the quadriceps) and the control group after intervention. And Field (2016) suggested the massage therapy on quadriceps and hamstrings could reduce pain and increase the knee ROM. Tarabichi and Tarabichi (2010) also found a significant increase in knee ROM after quadriceps release alone in patients with knee OA. The findings from the present study indicate that releasing the quadriceps (especially VL muscle) may have a positive effect on the prevention and treatment of patients with knee OA. Therefore, additional studies need to be conducted to investigate the effectiveness of releasing the tightness of the VL for subjects with knee OA.

As shown in **Figure 1** and **Figure 2**, the stiffness of RF, VL, and VM in 90° flexion of the knee joint was significantly higher than that in 60° flexion of the knee, regardless of whether patients with knee OA or healthy subjects were included. Similarly, Coombes et al. (2018) reported that the stiffness of the quadriceps muscle quantified with shear wave elastography increased with knee flexion. Xu et al. (2018) observed that the passive tension of RF, VL and VM started to increase at 51°, 48°, and 45° flexion, respectively, of the knee joint in rowers (Xu et al., 2018). These cases demonstrate the straining-stiffening behavior of soft tissue after the fibers become tight (DeWall et al., 2014). Chen et al. (2019) measured the stiffness of RF, VL and VM in young healthy participants at different angles of knee flexion using MyotonPRO, and they observed an increase of 11.38 and 18.59% in VL stiffness and VM stiffness in the nondominant limb from 60° to 90° flexion of the knee, respectively, while there was no significant difference in RF stiffness. Their results for VL and VM stiffness are similar to our results. In the present study, changing from 60 to 90° flexion of the knee resulted in 13.73 and 18.07% VL and VM stiffness in the control group, respectively, but we also found an increase of 8.88% in RF stiffness. Possible reasons for different variations in RF stiffness measurements may include the different measurement methodologies and the differences in the participants being studied.

In the present study, we also detected a positive correlation between VL stiffness and WOMAC scores in patients with knee OA. To the best of our knowledge, this is the first study to investigate the correlation between quadriceps stiffness and the level of function of patients with knee OA. Some previous studies also focused on the correlations between soft tissue stiffness and pain intensity or the functional level of the patients (Zhang et al., 2014; Koppenhaver et al., 2020; Zhou et al., 2020). In the study of Koppenhaver et al. (2020), lumbar muscle stiffness was greater in individuals with low back pain than in asymptomatic participants and was associated with pain intensity as quantified with the numeric pain rating scale and the level of disability measured by the Oswestry Disability Index (Koppenhaver et al., 2020). Zhou et al. (2020) observed that the stiffness of the medial gastrocnemius was positively correlated with pain intensity in patients with plantar fasciitis. Significant correlations were found between the elastic properties of the patellar tendon and pain and dysfunctions in athletes with patellar tendinopathy (Zhang et al., 2014). The above evidence indicates that soft tissue stiffness may be related to some functional outcomes in patients with musculoskeletal disorders. Chino and Takahashi et al. (2015) and Chino and Takahashi et al. (2016) found that increased muscle stiffness can contribute to an increase in passive joint stiffness. Miyamoto and Hirata (2019) found that muscle stiffness was negatively correlated with joint ROM. Ebihara et al. (2020) investigated the correlation between the passive stiffness of the quadriceps tendon and the gait parameters in the swing phase during gait, and they found that there was a negative correlation between the stiffness of the quadriceps tendon and gait speed and step length in patients with knee OA. Therefore, we speculate that the positive correlation between VL stiffness and WOMAC scores may be caused by the increased VL stiffness leading to decreased knee ROM or increased knee joint stiffness or further increased difficulty in performing activities of daily living in patients with knee OA.

There are some limitations of this study. First, only one point each in the RF, VL and VM was assessed, and our findings could not be generalized to other regions of the quadriceps muscle. Second, although we suggested that subjects be completely relaxed during the stiffness measurements, electromyography was not used to monitor the quadriceps muscle activity and ensure it was not firing. Third, the order of stiffness measurement of quadriceps was not randomized, which may introduce potential bias. In addition, due to the limitations of MyotonPRO, we did not investigate the stiffness of the vastus intermedius. Finally, this study indicated that the VL stiffness was related to the WOMAC score. However, it was not clear whether the VL stiffness affected the level of function in patients with knee OA. A prospective study is necessary to ascertain the cause and effect relationship between passive muscle stiffness and the degree of function in patients with knee OA.

CONCLUSION

Patients with knee OA have an increase in the stiffness of the vastus lateralis, and the stiffness of the quadriceps is increased with knee flexion in individuals with and without knee OA. In addition, the stiffness of the vastus lateralis is associated with the WOMAC score in patients with knee OA.

DATA AVAILABILITY STATEMENT

The raw data supporting the conclusion of this article will be made available by the authors, without undue reservation.

ETHICS STATEMENT

This study was approved by the Human Subjects Ethics Committee of Luoyang Orthopaedic Hospital of Henan Province (KY2020-003-02). Prior to this study, all participants

provided written informed consent, and the experimental procedure was fully explained to each subject. All of the experimental procedures adhered to the principles of the Declaration of Helsinki.

AUTHOR CONTRIBUTIONS

T-TC, Y-CZ and FL carried out the experiments and collection data. Z-JZ, J-YG and ZL designed the experiments. Z-JZ, Y-PL and X-QW analyzed the experimental results. T-TC and Y-CZ drafted the manuscript. All authors reviewed and approved the submission of the manuscript.

FUNDING

This study were supported by Project of Science Research of Traditional Chinese Medicine of Henan Province of China (2019ZY1028) and key project of decision-making consultation research of Shanghai Municipal People's government (2021-A-047).

REFERENCES

Agyapong-Badu, S., Warner, M., Samuel, D., and Stokes, M. (2016). Measurement of Ageing Effects on Muscle Tone and Mechanical Properties of Rectus Femoris and Biceps Brachii in Healthy Males and Females Using a Novel Hand-Held Myometric Device. *Arch. Gerontol. Geriatr.* 62, 59–67. doi:10.1016/j.archger.2015.09.011

Amirova, L. E., Plehuna, A., Rukavishnikov, I. V., Saveko, A. A., Peipsi, A., and Tomilovskaya, E. S. (2021). Sharp Changes in Muscle Tone in Humans under Simulated Microgravity. *Front. Physiol.* 12, 661922. doi:10.3389/fphys.2021.661922

Andrade, R. J., Lacourpaille, L., Freitas, S. R., McNair, P. J., and Nordez, A. (2016). Effects of Hip and Head Position on Ankle Range of Motion, Ankle Passive Torque, and Passive Gastrocnemius Tension. *Scand. J. Med. Sci. Sports* 26, 41–47. doi:10.1111/sms.12406

Atkins, D. V., and Eichler, D. A. (2013). The Effects of Self-Massage on Osteoarthritis of the Knee: A Randomized, Controlled Trial. *Int. J. Ther. Massage Bodyw.* 6, 4–14. doi:10.3822/ijtmb.v6i1.119

Avrillon, S., Hug, F., and Guilhem, G. (2018). Between-muscle Differences in Coactivation Assessed Using Elastography. *J. Electromyogr. Kinesiol.* 43, 88–94. doi:10.1016/j.jelekin.2018.09.007

Bellamy, N., Buchanan, W. W., Goldsmith, C. H., Campbell, J., and Stitt, L. W. (1988). Validation Study of WOMAC: a Health Status Instrument for Measuring Clinically Important Patient Relevant Outcomes to Antirheumatic Drug Therapy in Patients with Osteoarthritis of the Hip or Knee. *J. Rheumatol.* 15, 1833–1840.

Breda, S. J., van der Vlist, A., de Vos, R.-J., Krestin, G. P., and Oei, E. H. G. (2020). The Association between Patellar Tendon Stiffness Measured with Shear-Wave Elastography and Patellar Tendinopathy-A Case-Control Study. *Eur. Radiol.* 30, 5942–5951. doi:10.1007/s00330-020-06952-0

Chang, T.-T., Li, Z., Wang, X.-Q., and Zhang, Z.-J. (2020). Stiffness of the Gastrocnemius-Achilles Tendon Complex between Amateur Basketball Players and the Non-athletic General Population. *Front. Physiol.* 11, 606706. doi:10.3389/fphys.2020.606706

Chen, G., Wu, J., Chen, G., Lu, Y., Ren, W., Xu, W., et al. (2019). Reliability of a Portable Device for Quantifying Tone and Stiffness of Quadriceps Femoris and Patellar Tendon at Different Knee Flexion Angles. *PloS one* 14, e0220521. doi:10.1371/journal.pone.0220521

Chino, K., and Takahashi, H. (2015). The Association of Muscle and Tendon Elasticity with Passive Joint Stiffness: *In Vivo* Measurements Using Ultrasound Shear Wave Elastography. *Clin. Biomech.* 30, 1230–1235. doi:10.1016/j.clinbiomech.2015.07.014

Chino, K., and Takahashi, H. (2016). Measurement of Gastrocnemius Muscle Elasticity by Shear Wave Elastography: Association with Passive Ankle Joint Stiffness and Sex Differences. *Eur. J. Appl. Physiol.* 116, 823–830. doi:10.1007/s00421-016-3339-5

Cho, H.-y., Kim, E.-H., Kim, J., and Yoon, Y. W. (2015). Kinesio Taping Improves Pain, Range of Motion, and Proprioception in Older Patients with Knee Osteoarthritis. *Am. J. Phys. Med. Rehabil.* 94, 192–200. doi:10.1097/PHM.0000000000000148

Coombes, B. K., Ziegenfuss, B., David, M., Badya, R., van den Hoorn, W., Hug, F., et al. (2018). Heterogeneity of Passive Elastic Properties within the Quadriceps Femoris Muscle-Tendon Unit. *Eur. J. Appl. Physiol.* 118, 213–221. doi:10.1007/s00421-017-3763-1

Cross, M., Smith, E., Hoy, D., Nolte, S., Ackerman, I., Fransen, M., et al. (2014). The Global burden of Hip and Knee Osteoarthritis: Estimates from the Global burden of Disease 2010 Study. *Ann. Rheum. Dis.* 73, 1323–1330. doi:10.1136/annrheumdis-2013-204763

Davis, H. C., Luc-Harkey, B. A., Seeley, M. K., Troy Blackburn, J., and Pietrosimone, B. (2019). Sagittal Plane Walking Biomechanics in Individuals with Knee Osteoarthritis after Quadriceps Strengthening. *Osteoarthr. Cartil.* 27, 771–780. doi:10.1016/j.joca.2018.12.026

Decker, M. J., Torry, M. R., Wyland, D. J., Sterett, W. I., and Richard Steadman, J. (2003). Gender Differences in Lower Extremity Kinematics, Kinetics and Energy Absorption during landing. *Clin. Biomech.* 18, 662–669. doi:10.1016/s0268-0033(03)00090-1

Devrimsel, G., Metin, Y., and Serdaroglu Beyazal, M. (2019). Short-term Effects of Neuromuscular Electrical Stimulation and Ultrasound Therapies on Muscle Architecture and Functional Capacity in Knee Osteoarthritis: a Randomized Study. *Clin. Rehabil.* 33, 418–427. doi:10.1177/0269215518817807

DeWall, R. J., Slane, L. C., Lee, K. S., and Thelen, D. G. (2014). Spatial Variations in Achilles Tendon Shear Wave Speed. *J. Biomech.* 47, 2685–2692. doi:10.1016/j.jbiomech.2014.05.008

Dillon, C. F., Rasch, E. K., Gu, Q., and Hirsch, R. (2006). Prevalence of Knee Osteoarthritis in the United States: Arthritis Data from the Third National Health and Nutrition Examination Survey 1991-94. *J. Rheumatol.* 33, 2271–2279.

Du, C., Smith, A., Avalos, M., South, S., Crabtree, K., Wang, W., et al. (2019). Blueberries Improve Pain, Gait Performance, and Inflammation in Individuals with Symptomatic Knee Osteoarthritis. *Nutrients* 11, 290. doi:10.3390/nu11020290

Ebihara, B., Fukaya, T., and Mutsuzaki, H. (2020). Relationship between Quadriceps Tendon Young's Modulus and Maximum Knee Flexion Angle in the Swing Phase of Gait in Patients with Severe Knee Osteoarthritis. *Medicina* 56, 437. doi:10.3390/medicina56090437

Feng, Y. N., Li, Y. P., Liu, C. L., and Zhang, Z. J. (2018). Assessing the Elastic Properties of Skeletal Muscle and Tendon Using Shearwave Ultrasound Elastography and MyotonPRO. *Sci. Rep.* 8, 17064. doi:10.1038/s41598-018-34719-7

Field, T. (2016). Knee Osteoarthritis Pain in the Elderly Can Be Reduced by Massage Therapy, Yoga and Tai Chi: A Review. *Complement. Therapies Clin. Pract.* 22, 87–92. doi:10.1016/j.ctcp.2016.01.001

Gavronski, G., Veraksitš, A., Vasar, E., and Maaroos, J. (2007). Evaluation of Viscoelastic Parameters of the Skeletal Muscles in Junior Triathletes. *Physiol. Meas.* 28, 625–637. doi:10.1088/0967-3334/28/6/002

Geertsen, S. S., Kirk, H., Lorentzen, J., Jorsal, M., Johansson, C. B., and Nielsen, J. B. (2015). Impaired Gait Function in Adults with Cerebral Palsy Is Associated with Reduced Rapid Force Generation and Increased Passive Stiffness. *Clin. Neurophysiol.* 126, 2320–2329. doi:10.1016/j.clinph.2015.02.005

Hirata, K., Miyamoto-Mikami, E., Kanehisa, H., and Miyamoto, N. (2016). Muscle-specific Acute Changes in Passive Stiffness of Human Triceps Surae after Stretching. *Eur. J. Appl. Physiol.* 116, 911–918. doi:10.1007/s00421-016-3349-3

Hunter, D. J., and Bierma-Zeinstra, S. (2019). Osteoarthritis. *Lancet* 393, 1745–1759. doi:10.1016/S0140-6736(19)30417-9

Ishikawa, H., Muraki, T., Morise, S., Sekiguchi, Y., Yamamoto, N., Itoi, E., et al. (2017). Changes in Stiffness of the Dorsal Scapular Muscles before and after Computer Work: a Comparison between Individuals with and without Neck and Shoulder Complaints. *Eur. J. Appl. Physiol.* 117, 179–187. doi:10.1007/s00421-016-3510-z

Koppenhaver, S., Gaffney, E., Oates, A., Eberle, L., Young, B., Hebert, J., et al. (2020). Lumbar Muscle Stiffness Is Different in Individuals with Low Back Pain Than Asymptomatic Controls and Is Associated with Pain and Disability, but Not Common Physical Examination Findings. *Musculoskelet. Sci. Pract.* 45, 102078. doi:10.1016/j.msksp.2019.102078

Lenskjold, A., Kongsgaard, M., Larsen, J. O., Nielsen, R. H., Kovanen, V., Aagaard, P., et al. (2015). The Influence of Physical Activity during Youth on Structural and Functional Properties of the Achilles Tendon. *Scand. J. Med. Sci. Sports* 25, 25–31. doi:10.1111/sms.12143

León-Ballesteros, S., Espinosa-Morales, R., Clark-Peralta, P., Gómez-Pineda, A. G., and Guadarrama-Becerril, J. H. (2020). Kinesiotape and Quadriceps Strengthening with Elastic Band in Women with Knee Osteoarthritis and Overweight or Obesity. A Randomized Clinical Trial. *Reumatol. Clín.* 16, 11–16. doi:10.1016/j.reuma.2018.03.001

Liu CL, C. L., Feng, Y. N., Zhang, H. Q., Li, Y. P., Zhu, Y., and Zhang, Z. J. (2018). Assessing the Viscoelastic Properties of Upper Trapezius Muscle: Intra- and Inter-tester Reliability and the Effect of Shoulder Elevation. *J. Electromyogr. Kinesiol.* 43, 226–229. doi:10.1016/j.jelekin.2017.09.007

Liu Q, Q., Wang, S., Lin, J., and Zhang, Y. (2018). The burden for Knee Osteoarthritis Among Chinese Elderly: Estimates from a Nationally Representative Study. *Osteoarthr. Cartil.* 26, 1636–1642. doi:10.1016/j.joca.2018.07.019

Lu, Z., Li, X., Chen, R., and Guo, C. (2018). Kinesio Taping Improves Pain and Function in Patients with Knee Osteoarthritis: A Meta-Analysis of Randomized Controlled Trials. *Int. J. Surg.* 59, 27–35. doi:10.1016/j.ijsu.2018.09.015

Michael, J. W.-P., Schlüter-Brust, K. U., and Eysel, P. (2010). The Epidemiology, Etiology, Diagnosis, and Treatment of Osteoarthritis of the Knee. *Deutsches Arzteblatt Int.* 107, 152–162. doi:10.3238/arztebl.2010.0152

Miyamoto, N., and Hirata, K. (2019). Moderate Associations of Muscle Elasticity of the Hamstring with Hip Joint Flexibility. *Int. J. Sports Med.* 40, 717–724. doi:10.1055/a-0981-7282

Noehren, B., Kosmac, K., Walton, R. G., Murach, K. A., Lyles, M. F., Loeser, R. F., et al. (2018). Alterations in Quadriceps Muscle Cellular and Molecular Properties in Adults with Moderate Knee Osteoarthritis. *Osteoarthr. Cartil.* 26, 1359–1368. doi:10.1016/j.joca.2018.05.011

Nordez, A., Gross, R., Andrade, R., Le Sant, G., Freitas, S., Ellis, R., et al. (2017). Non-Muscular Structures Can Limit the Maximal Joint Range of Motion during Stretching. *Sports Med.* 47, 1925–1929. doi:10.1007/s40279-017-0703-5

Perlman, A., Fogerite, S. G., Glass, O., Bechard, E., Ali, A., Njike, V. Y., et al. (2019). Efficacy and Safety of Massage for Osteoarthritis of the Knee: a Randomized Clinical Trial. *J. Gen. Intern. Med.* 34, 379–386. doi:10.1007/s11606-018-4763-5

Piva, S. R., Goodnite, E. A., and Childs, J. D. (2005). Strength Around the Hip and Flexibility of Soft Tissues in Individuals with and without Patellofemoral Pain Syndrome. *J. Orthop. Sports Phys. Ther.* 35, 793–801. doi:10.2519/jospt.2005.35.12.793

Rice, D. A., McNair, P. J., and Lewis, G. N. (2011). Mechanisms of Quadriceps Muscle Weakness in Knee Joint Osteoarthritis: the Effects of Prolonged Vibration on Torque and Muscle Activation in Osteoarthritic and Healthy Control Subjects. *Arthritis Res. Ther.* 13, R151. doi:10.1186/ar3467

Rieder, F., Wiesinger, H.-P., Kösters, A., Müller, E., and Seynnes, O. R. (2016). Whole-body Vibration Training Induces Hypertrophy of the Human Patellar Tendon. *Scand. J. Med. Sci. Sports* 26, 902–910. doi:10.1111/sms.12522

Safiri, S., Kolahi, A.-A., Smith, E., Hill, C., Bettampadi, D., Mansournia, M. A., et al. (2020). Global, Regional and National burden of Osteoarthritis 1990-2017: a Systematic Analysis of the Global Burden of Disease Study 2017. *Ann. Rheum. Dis.* 79, 819. doi:10.1136/annrheumdis-2019-216515

Salaffi, F., Leardini, G., Canesi, B., Mannoni, A., Fioravanti, A., Caporali, R., et al. (2003). Reliability and Validity of the Western Ontario and McMaster Universities (WOMAC) Osteoarthritis Index in Italian Patients with Osteoarthritis of the Knee. *Osteoarthr. Cartil.* 11, 551–560. doi:10.1016/s1063-4584(03)00089-x

Schneider, S., Peipsi, A., Stokes, M., Knicker, A., and Abeln, V. (2015). Feasibility of Monitoring Muscle Health in Microgravity Environments Using Myoton Technology. *Med. Biol. Eng. Comput.* 53, 57–66. doi:10.1007/s11517-014-1211-5

Simic, M., Harmer, A. R., Agaliotis, M., Nairn, L., Bridgett, L., March, L., et al. (2021). Clinical Risk Factors Associated with Radiographic Osteoarthritis Progression Among People with Knee Pain: a Longitudinal Study. *Arthritis Res. Ther.* 23 (1), 160. doi:10.1186/s13075-021-02540-9

Szilagyi, I. A., Waarsing, J. H., Schiphof, D., van Meurs, J. B. J., and Bierma-Zeinstra, S. M. A. (2021). Towards Sex-specific Osteoarthritis Risk Models: Evaluation of Risk Factors for Knee Osteoarthritis in Males and Females. *Rheumatology (Oxford)*, keab378. doi:10.1093/rheumatology/keab378

Tarabichi, S., and Tarabichi, Y. (2010). Can an Anterior Quadriceps Release Improve Range of Motion in the Stiff Arthritic Knee? *J. Arthroplasty* 25, 571–575. doi:10.1016/j.arth.2009.04.015

Vaz, M. A., Baroni, B. M., Geremia, J. M., Lanferdini, F. J., Mayer, A., Arampatzis, A., et al. (2013). Neuromuscular Electrical Stimulation (NMES) Reduces Structural and Functional Losses of Quadriceps Muscle and Improves Health Status in Patients with Knee Osteoarthritis. *J. Orthop. Res.* 31, 511–516. doi:10.1002/jor.22264

Witvrouw, E., Lysens, R., Bellemans, J., Cambier, D., and Vanderstraeten, G. (2000). Intrinsic Risk Factors for the Development of Anterior Knee Pain in an Athletic Population: A Two-Year Prospective Study. *Am. J. Sports Med.* 28, 480–489. doi:10.1177/03635465000280040701

Witvrouw, E., Bellemans, J., Lysens, R., Danneels, L., and Cambier, D. (2001). Intrinsic Risk Factors for the Development of Patellar Tendinitis in an Athletic Population. *Am. J. Sports Med.* 29, 190–195. doi:10.1177/03635465010290021201

Xu, J., Hug, F., and Fu, S. N. (2018). Stiffness of Individual Quadriceps Muscle Assessed Using Ultrasound Shear Wave Elastography during Passive Stretching. *J. Sport Health Sci.* 7, 245–249. doi:10.1016/j.jshs.2016.07.001

Zhang, Z. J., Ng, G. Y.-f., Lee, W. C., and Fu, S. N. (2014). Changes in Morphological and Elastic Properties of Patellar Tendon in Athletes with Unilateral Patellar Tendinopathy and Their Relationships with Pain and Functional Disability. *PloS one* 9, e108337. doi:10.1371/journal.pone.0108337

Zhang, Z. J., Ng, G. Y. F., Lee, W. C., and Fu, S. N. (2017). Increase in Passive Muscle Tension of the Quadriceps Muscle Heads in Jumping Athletes with Patellar Tendinopathy. *Scand. J. Med. Sci. Sports* 27, 1099–1104. doi:10.1111/sms.12749

Zhou, J.-P., Yu, J.-F., Feng, Y.-N., Liu, C.-L., Su, P., Shen, S.-H., et al. (2020). Modulation in the Elastic Properties of Gastrocnemius Muscle Heads in Individuals with Plantar Fasciitis and its Relationship with Pain. *Sci. Rep.* 10, 2770. doi:10.1038/s41598-020-59715-8

Conflict of Interest: The authors declare that the research was conducted in the absence of any commercial or financial relationships that could be construed as a potential conflict of interest.

Publisher's Note: All claims expressed in this article are solely those of the authors and do not necessarily represent those of their affiliated organizations, or those of the publisher, the editors and the reviewers. Any product that may be evaluated in this article, or claim that may be made by its manufacturer, is not guaranteed or endorsed by the publisher.

frontiers in Bioengineering and Biotechnology

ORIGINAL RESEARCH
published: 11 February 2022
doi: 10.3389/fbioe.2021.810250

Effects of Isometric Plantar-Flexion on the Lower Limb Muscle and Lumbar Tissue Stiffness

Baizhen Chen[1,2], *Shaoyang Cui*[3], *Mingzhu Xu*[4], *Zhijie Zhang*[5]* and *Chunlong Liu*[1]*

[1]Clinical Medical College of Acupuncture Moxibustion and Rehabilitation, Guangzhou University of Chinese Medicine, Guangzhou, China, [2]The Second Affiliated Hospital, Guangzhou University of Chinese Medicine, Guangzhou, China, [3]Shenzhen Hospital, Guangzhou University of Chinese Medicine (Futian), Shenzhen, China, [4]Shenzhen Hospital, Southern Medical University, Shenzhen, China, [5]Luoyang Orthopedics Hospital of Henan Province, Luoyang, China

Purpose: This study investigated the effects of isometric plantar-flexion against different resistances on the thoracolumbar fascia (TLF), erector spinae (ES), and gastrocnemius stiffness by shear wave elastography (SWE). The purpose was to explore the interaction between the lower limb muscle and lumbar tissue in the myofascial tensegrity network.

Methods: Twenty healthy young female were recruited in this study. The stiffness of the TLF, ES, medial gastrocnemius (MG), and lateral gastrocnemius (LG) was measured by SWE under four isometric plantar-flexion resistance conditions. The resistance conditions involved 0% maximum voluntary isometric contraction (MVIC), 20% MVIC, 40% MVIC, and 60% MVIC.

Results: There was a strong correlation between the stiffness change of MG and that of TLF (r = 0.768–0.943, $p < 0.001$) and ES (r = 0.743–0.930, $p < 0.001$), while it was moderate to strong correlation between MG and that of LG (r = 0.588–0.800, $p < 0.001$). There was no significant difference in the stiffness between the nondominant and dominant sides of TLF and ES under the resting position ($p > 0.05$). The increase in stiffness of the TLF, ES, MG, and LG, with MVIC percentage ($p < 0.05$), and the stiffness of TLF and ES on the nondominant side is much higher than that on the dominant side.

Conclusions: Our data shows that isometric plantar-flexion has a significant effect on the stiffness of the lumbar soft tissue and gastrocnemius. The gastrocnemius has a strong correlation with the stiffness changes of TLF and ES, which provides preliminary evidence for exploring the myofascial tensegrity network between the dorsal side of the lower limb muscle and lumbar tissue.

Keywords: thoracolumbar fascia, gastrocnemius, shear wave elastography, myofascial continuity, isometric plantar-flexion, tensegrity network

OPEN ACCESS

Edited by:
Rezaul Begg,
Victoria University, Australia

Reviewed by:
Hanatsu Nagano,
Victoria University, Australia
Alessandro Garofolini,
Victoria University, Australia

***Correspondence:**
Zhijie Zhang
sportspt@163.com
Chunlong Liu
lcl05mpt@gzucm.edu.cn

Specialty section:
This article was submitted to Biomechanics, a section of the journal Frontiers in Bioengineering and Biotechnology

Received: *06 November 2021*
Accepted: *29 December 2021*
Published: *11 February 2022*

Citation:
Chen B, Cui S, Xu M, Zhang Z and Liu C (2022) Effects of Isometric Plantar-Flexion on the Lower Limb Muscle and Lumbar Tissue Stiffness. Front. Bioeng. Biotechnol. 9:810250. doi: 10.3389/fbioe.2021.810250

INTRODUCTION

The fascia is a connective tissue network that envelops and links the muscles, blood vessels, nerves, and viscera of the whole body (Wilke et al., 2016; Bordoni et al., 2019). Fascia is mainly responsible for transmitting and absorbing loads to connective tissues, depending on its viscoelasticity, thereby building an extensive tensegrity network linking the various human tissues (Huijing, 2009). In recent

years, biomechanical and anatomical studies have found that the interactions among different tissues is realized through the connection of muscle and fascia—for example, pectoralis major, latissimus dorsi, and deltoid transfer interact through the brachial fascia, thereby playing a synergistic role in upper arm movement (Stecco et al., 2008); dorsiflexion of the ankle joint can cause the joint displacement of the gastrocnemius, semimembranosus, and quadriceps femoris (Huang et al., 2018; Wilke et al., 2020); the contraction of gluteus maximus (GMax) can affect the contralateral latissimus dorsi through the thoracolumbar fascia (TLF) and erector spinae (ES) (Carvalhais et al., 2013). These studies show that the different human tissues interact by the myofascial tensegrity network, which provides solid evidence for the existence of the tensegrity network. However, the *in vivo* behavior of the tensegrity network lacks specific numerical data, so it is necessary to conduct clinical human trials of tensegrity networks in human tissues.

Anatomical studies have demonstrated a structural continuity between the lumbosacral portion and the lower limb. The TLF radiates outward along the L3-S3 spinous process and connects with GMax (Barker et al., 2014). GMax is continuous with fascia lata, iliotibial tract, and lateral muscle septum (Stecco et al., 2013). The hamstring and gastrocnemius are connected through a deep fascia of popliteal fossa (Tuncay et al., 2007). These anatomical studies provide a substantial way for the interaction between the dorsal side of lower limb muscle and lumbar tissue. Considering the existence of anatomical continuity between the lumbosacral and lower limbs, the change in lower limb strength may have a long-distance effect on the lumbar tissue. The gastrocnemius includes the medial gastrocnemius (MG) and lateral gastrocnemius (LG), which together with the soleus form the triceps surae. The triceps surae make an important contribution to human walking, running, and jumping by controlling the plantar-flexion movement (Fukunaga et al., 2001; Weinfeld, 2014). Fukunaga *et al.* found that the triceps surae are the largest synergist among plantar-flexors (Fukunaga et al., 1992). During plantar-flexion, these three muscles produce tension and act on the Achilles tendon (Rosager et al., 2002). Creswell *et al.* found that the gastrocnemius produces had the highest percentage of plantar-flexion torque knee extension position and that plantar-flexion can maximize gastrocnemius activity (Cresswell et al., 1995). Similarly, isometric contraction can maximize muscle activity. Therefore, we chose isometric plantar flexion in the prone position to maximize gastrocnemius tension in order to better observe the effects of isometric plantar-flexion on the dorsal side of lower limb muscle and lumbar tissue stiffness.

In the human body, the fascia is an important buffer structure and force transmitter. Its function depends on its own tension element, and tissue stiffness is one of the important indexes to evaluate tissue tension (Swanson, 2013). Shear wave elastography (SWE) is a new evaluation technology of tissue stiffness, which has the characteristics of being noninvasive, painless, fast, and accurate. SWE quantifies tissue stiffness and draws a colored image of tissue stiffness using shear wave generated by acoustic radiation force pulse and ultra-high speed imaging technology (Creze et al., 2018; Gennisson et al., 2013). Our previous research shows that SWE is a reliable tool for quantifying TLF, MG, and LG stiffness and monitoring its dynamic changes (Chen et al., 2021; Liu et al., 2020). Therefore, we used SWE to quantify the stiffness of TLF, ES, and gastrocnemius during isometric plantar-flexion in this experiment.

The purpose of this study was to assess the variations in stiffness of MG, LG, TLF, and ES at isometric plantar-flexion against different resistances by using the SWE. We put forward the following assumptions around the purpose of the study: (1) the stiffness of nondominant and dominant lumbar tissues increased asymmetrically with the increase of isometric plantar-flexion resistance; (2) the stiffness of gastrocnemius increased with the increase of isometric plantar-flexion resistance, and the stiffness of MG and LG increased unevenly; and (3) there was a significant correlation between the stiffness changes of the lower leg and the back tissue.

METHODS

Ethical Approval

This study received approval by the ethics committee of the Guangdong Provincial Hospital of Chinese Medicine (YE 2020-131-01). This research follows the principles of the Helsinki Declaration. Before the experiment, all the participants fully understood the safety of SWE, the basic rights of the participants, the experimental purpose, and the process by a written agreement, and they signed an informed consent.

Participants

The researchers recruited 20 healthy young female participants from Guangzhou University of Chinese Medicine from November 2020 to March 2021 (mean age: 21.1 ± 1.7 years, 19–23 years; mean height: 1.61 ± 0.04 m, 1.53–1.69 m; mean mass: 49.5 ± 5.1 kg, 41–59 kg; MVIC: 31.08 ± 4.79 kg). The location of the study was the Department of Ultra-sound Imaging of the Second Affiliated Hospital of Guangzhou University of Chinese Medicine. The inclusion criteria were that (1) all participants had no pain or trauma to their feet, lower limbs, and waist that affected their lives and work for, at least, the past 6 months; (2) all the participants had no history of surgery on their feet, lower limbs, and waist and had no history of neuromuscular diseases and joint diseases; and (3) with the right hands and feet on the dominant side (the dominant leg of the participants was determined by kicking a ball, and the dominant hand was determined by writing preference). The participants were instructed to abstain from physical activity for 48 h before the start of the experiment.

Equipment and Parameter Settings

The study was conducted using an Aixplorer ultrasound device (Aixplorer Supersonic Imagine, France). A 40-mm linear array sensor (SL10-2, Supersonic Imagine, France) is selected for the instrument that was a handheld device. Musculoskeletal mode and SWE mode were selected for device mode. The equipment parameter settings were as follows : conventional preset enhancement mode, image display of 85% opacity, and

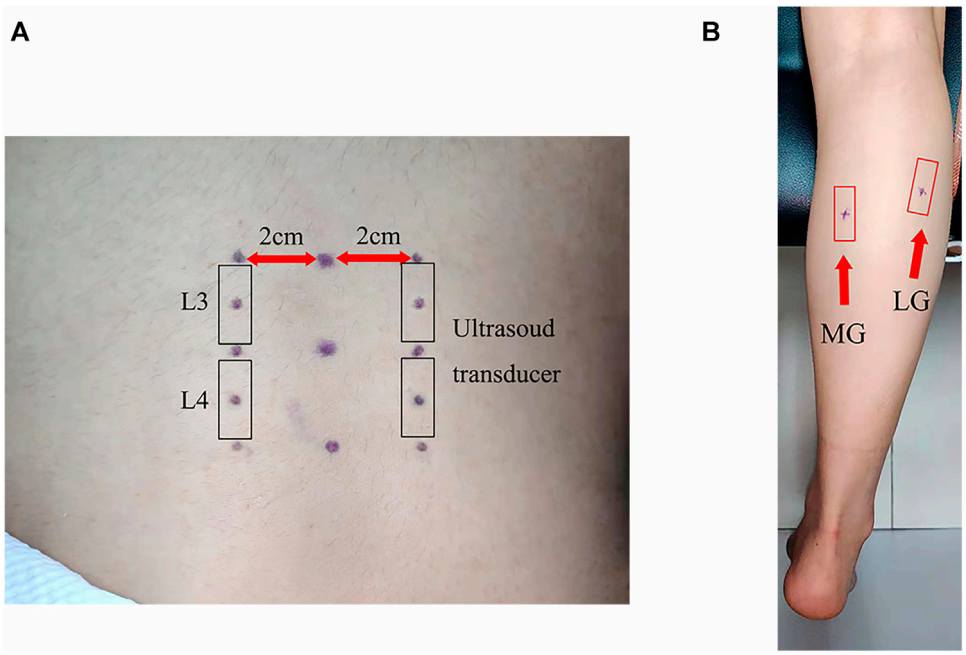

FIGURE 1 | Setting out plan of the ultrasound transducer: **(A)** thoracolumbar fascia and erector spinae and **(B)** medial gastrocnemius and lateral gastrocnemius.

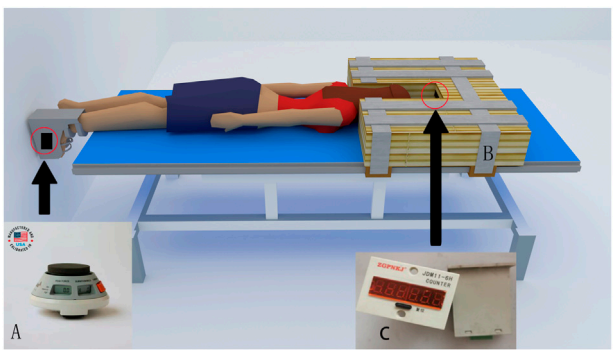

FIGURE 2 | The posture and equipment used for measurement: **(A)** ergometer, **(B)** wooden block, and **(C)** monitor.

measurement range from 0 to 300 kPa. The ergometer is HOGGAN Scientific microFET2 (wireless manual muscle tester; manufactured and calibrated in the USA), which converts the pressure signal into pounds through the pressure sensor and displays it on the screen.

Experimental Protocol

In this experiment, SWE was used to measure the stiffness of TLF, ES, MG, and LG. The lumbar tissue (TLF and ES) stiffness was measured at the third and fourth lumbar vertebra levels (L3 and L4). Firstly, the L4 spinous process was palpated according to the body surface markers, and the L3 spinous process and the L2 spinous process were palpated upward in turn. Then, B-mode ultrasound was used for confirmation and correction, and an oil pen was used to mark the measuring points 2 cm away from the midpoint of L2-3 and L3-4. The measurement site of MG was located at 30% of the length from the medial popliteal fossa to the lateral malleolus and that of LG was located at 30% of length from the lateral popliteal fossa to the medial malleolus. These measuring parts were marked with an oil pen (**Figure 1**).

During the measurement period, all participants remained in the prone position with the hands at both sides of their body, the lower limbs straight, and the ankle joint at 90° position (**Figure 2**). After the participants were enrolled in the study, we conducted isometric plantar-flexion instruction for all participants. The participants were required to contract only the plantar-flexors (MG and LG) during isometric plantar-flexion and not the auxiliary muscle (hamstrings and GMax). The participants repeatedly practiced isometric plantar-flexion until they could easily use the plantar-flexors to complete the plantar-flexion.

The experiment was carried out according to the following steps: (1) the participants walked to the ultrasound room on the 4th floor of the hospital, they were fixed on a special bed according to the test requirements, their ankles were fixed at 90° with a special ankle foot orthosis (an ergometer at the bottom), their shoulder was fixed with a wooden block, and then they rested in the prone position for 5 min; (2) the stiffness of TLF, ES, MG, and LG was measured by SWE; (3) the participants were required to perform the maximum isometric plantar-flexion, and the ergometer value was recorded, which was the MVIC. The calculation of resistance value required for each contraction was as follows: 20% MVIC = 0.2 MVIC, 40% MVIC = 0.4 MVIC, and 60% MVIC = 0.6 MVIC. At each contraction, the participants were informed of the target resistance. The participants viewed the resistance value through the screen and kept the displayed value at the target value; (4) SWE was used to monitor

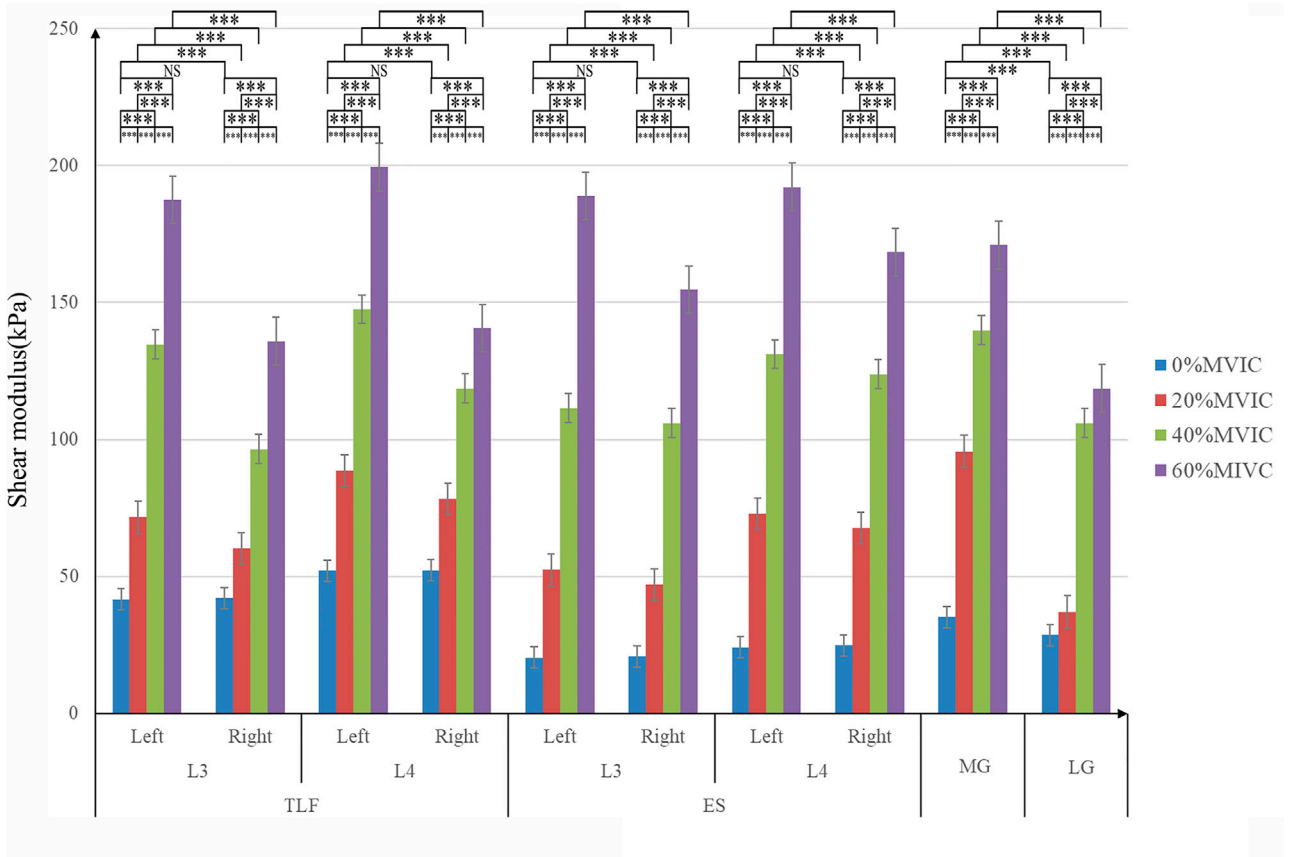

FIGURE 3 | Stiffness variation of each tissue under different resistance conditions. ***, significant intergroup difference ($p < 0.001$); NS, non-significant intergroup difference ($p > 0.05$).

the stiffness of the measured point until the stiffness value recovers to the value measured in step (2); (5) the participants were asked to perform 20% MVIC isometric plantar-flexion, and the stiffness of TLF, ES, MG, and LG were measured; (6) after repeating step (4), the participants were instructed to perform isometric plantar-flexion with 40% MVIC, and the stiffness of TLF, ES, MG, and LG was measured; and (7) after repeating step (4), the participants were ordered to perform 60% MVIC isometric plantar-flexion, and the stiffness of TLF, ES, MG, and LG was measured.

In the process of image acquisition, the B-mode was used to obtain clear images, and then the preset SWE mode was used to quantify the stiffness of each tissue. Each MVIC contraction was held for 8 s (5 s of stable image and elastic value and 3 s of intercepted image). The measurements were carried out in the order of MG, LG, TLF, and ES. One position was measured for each contraction, and between two contractions, SWE was used to monitor the stiffness of the measured point until the stiffness value recovered to the original stiffness (the value measured in step 2), then followed by the next contraction. Another researcher used the region of interest (ROI; system tool for automatically quantifying the shear modulus) of Aiexplorer software to obtain the shear modulus (kPa) from the intercepted image. The size of the ROIs of TLF was set to 1 mm, three adjacent ROIs were set for each measurement area to read data, and the size of ROI of ES, MG, and LG were set to 5 mm (**Supplementary Figures S1-S3**). Each measuring point is measured three times, and the average value was taken and used for further analyses.

Statistical Analysis

SPSS 21.0 software (version 21.0, Chicago, IL, USA) was used for statistical analysis. The statistical data was the average of the three measurements, and all statistical data were expressed as mean ± standard deviation (SD). The Shapiro–Wilk test was used for normal distribution of stiffness and stiffness percentage change data, and all data conformed to normal distribution. The one way-ANOVA with stiffness (the same measuring position) as the dependent variable and 0% MVIC, 20% MVIC, 40% MVIC, and 60%MVIC as the independent variables was used to judge whether there were differences in stiffness between different MVICs (**Figure 3**). When the one-way ANOVA was significant (**Supplementary Table S1**), *post-hoc* Tukey's test was performed (**Supplementary Table S2**). The paired *t*-test was performed to verify the difference in lumbar tissue stiffness (the same tissue and lumbar vertebra level) between the dominant and nondominant sides (**Figure 3**). The significance level of the statistical data difference was set as $p = 0.05$.

Pearson's correlation was used to calculate the correlation coefficients (*r*-values) of stiffness percentage change between

TABLE 1 | Tissue stiffness phase percentage change (mean ± SD, %).

Measurement position			0–20% MVIC	20–40% MVIC	40–60% MVIC
TLF	L3	Left	73.49 ± 21.78	88.00 ± 4.55	39.43 ± 4.98
		Right	44.03 ± 24.83	60.75 ± 15.11	41.54 ± 9.97
	L4	Left	71.41 ± 19.96	66.74 ± 5.97	35.12 ± 3.92
		Right	50.67 ± 16.06	51.31 ± 8.35	19.18 ± 6.96
ES	L3	Left	160.01 ± 55.18	114.88 ± 17.28	69.78 ± 6.01
		Right	130.71 ± 52.98	128.65 ± 26.67	45.91 ± 5.89
	L4	Left	204.58 ± 50.99	81.00 ± 10.12	46.33 ± 7.51
		Right	174.64 ± 49.36	84.97 ± 17.24	36.47 ± 16.77
	MG	—	175.83 ± 52.76	46.87 ± 9.57	22.23 ± 6.26
	LG	—	31.34 ± 18.73	188.90 ± 39.92	12.63 ± 13.14

SD, standard deviation (kPa); TLF, thoracolumbar fascia; ES, erector spinae; L3, third lumbar vertebra levels; L4, fourth lumbar vertebra levels; MG, medial gastrocnemius; LG, lateral gastrocnemius.

different tissues. The raw values of stiffness reflected the absolute change of tissue under mechanical force loaded, in which it was easy to ignore the stiffness characteristics of the tissue itself. The stiffness percentage change was calculated by the ratio of absolute change of tissue stiffness with its initial stiffness, which truly reflected the influence of the mechanical force on the tissue itself. Therefore, we chose the stiffness percentage change of different tissues to calculate the correlation coefficients as follows: *Stiffness percentage change (%) = (measured stiffness − original stiffness) ÷ original stiffness* × 100% The stiffness percentage change of each measured position was compared to the stiffness percentage change of MG for the same test conditions. The correlation strength of the *r*-value was set to $r < 0.3$ for weak correlation, $0.3 \leq r \leq 0.6$ for moderate correlation, and $r > 0.6$ for a strong correlation. The statistical significance level was set as $p = 0.05$.

RESULTS

Effect of Different Isometric Plantar-Flexion Resistance on Tissue Stiffness

The relationship between tissue stiffness and different isometric plantar-flexion resistance is shown in **Figure 3**; **Supplementary Figure S4**. The stiffness of TLF, ES, MG, and LG increased significantly with the increase of resistance ($p < 0.001$, **Figure 3**). In the condition of no resistance, there was no significant difference in the stiffness between the nondominant and dominant sides of TLF and ES ($p > 0.05$, **Figure 3**), and MG stiffness was significantly higher than LG ($p < 0.001$, **Figure 3**). With the increase of resistance, the stiffness of nondominant TLF and ES was always greater than that of the dominant side ($p < 0.001$, **Figure 3**).

Characteristics of Tissue-Stiffness-Phased Percentage Change Under Continuous Loading Resistance

The characteristics of tissue-stiffness-phased percentage change are shown in **Table 1**. The stiffness of ES and MG increased

TABLE 2 | The correlation between the stiffness percentage changes of each tissue (mean ± SD, %).

Measurement parts			0–20% MVIC			0–40% MVIC			0–60% MVIC		
			Percentage change	*r*-values	*p*-values	Percentage change	*r*-values	*p*-values	Percentage change	*r*-values	*p*-values
TLF	L3	Left	73.49 ± 21.78	0.936	0.000	226.69 ± 45.70	0.913	0.000	353.69 ± 51.29	0.847	0.000
		Right	44.03 ± 24.83	0.943	0.000	130.93 ± 40.91	0.898	0.000	225.36 ± 64.92	0.850	0.000
	L4	Left	71.41 ± 19.96	0.912	0.000	185.32 ± 30.53	0.927	0.000	285.75 ± 44.72	0.883	0.000
		Right	50.67 ± 16.06	0.839	0.000	128.31 ± 29.56	0.877	0.000	170.40 ± 23.20	0.768	0.000
ES	L3	Left	160.01 ± 55.18	0.910	0.000	450.89 ± 82.36	0.907	0.000	831.82 ± 116.02	0.858	0.000
		Right	130.71 ± 52.98	0.926	0.000	418.66 ± 94.99	0.889	0.000	656.62 ± 138.90	0.868	0.000
	L4	Left	204.58 ± 50.99	0.930	0.000	446.75 ± 65.19	0.925	0.000	702.95 ± 125.01	0.887	0.000
		Right	174.64 ± 49.36	0.884	0.000	401.15 ± 54.98	0.743	0.000	576.86 ± 44.97	0.809	0.000
	MG	—	175.83 ± 52.76	1	—	302.91 ± 66.83	1	—	392.95 ± 91.29	1	—
	LG	—	31.34 ± 18.73	0.800	0.000	276.53 ± 54.80	0.703	0.001	320.53 ± 57.57	0.588	0.006

SD, standard deviation (kPa); TLF, thoracolumbar fascia; ES, erector spinae; L3, third lumbar vertebra levels; L4, fourth lumbar vertebra levels; MG, medial gastrocnemius; LG, lateral gastrocnemius.

sharply when the resistance appears, and then the stiffness-phased percentage change decreased. The stiffness-phased percentage change of LG began to increase sharply at approximately 40% MVIC resistance. The phased percentage change of TLF stiffness increased continuously between 0 and 40% MVIC and decreased between 40 and 60% MVIC.

Correlation Between the Stiffness of Lumbar Tissue and Lower Limb Under Different Resistance

Each stiffness percentage change of every measurement position was compared with the stiffness percentage change of MG for the same test conditions (**Table 2**). The results showed that the stiffness percentage change of TLF (r = 0.768–0.936, p < 0.001) and ES (r = 0.743–0.930, p < 0.001) has a strong correlation with the stiffness percentage change of MG under different resistance. The correlation of hardness percentage change between LG and MG was moderate and strong (r = 0.588–0.800, p < 0.001).

DISCUSSION

The purpose of this study was to elucidate the stiffness changes of the lower limb muscle and lumbar tissue during isometric plantar-flexion so as to better understand the interaction between different tissues in the myofascial tensegrity network. This study found that the stiffness changes of the lower limb muscle and lumbar tissue during isometric plantar-flexion had the following characteristics: (1) the stiffness of the TLF, ES, MG, and LG increased with the increase of isometric resistance; (2) there was a strong correlation between the stiffness percentage change of the lumbar tissue and MG; and (3) the stiffness percentage change of the nondominant lumbar tissue was greater than that of the dominant lumbar tissue.

The muscle and fascia tissues do not exist in isolation in structure and function but function together in body movement through a mutual connection forming a myofascial tension network to connect all parts of the body as a whole (Stackhouse et al., 2013)—for example, Barker *et al.* dissected and analyzed the connection structure between the waist, back, and hip and found that TLF is directly connected with the gluteus maximus in the area near the posterior superior iliac spine (PSIS) and S3 spinous process. The aponeurosis of ES extends to be part of the origin of GMax, and the GMax extends downward to be part of the origin of iliotibial tract (Barker et al., 2014). Wilke *et al.* induced a significant displacement of semimembranosus and its fascia band through passive ankle back extension, suggesting that mechanical force can be transmitted from the ankle joint to the dorsal thigh and affect the parallel muscles contained in the dorsal thigh fascia band (biceps femoris and semitendinosus muscle and semimembranosus) during passively stretching the gastrocnemius (Wilke et al., 2020). The anatomical study of Tuncay *et al.* showed that the gastrocnemius and hamstring muscles communicate with each other at the popliteal fossa through the deep fascia of the popliteal fossa (Tuncay et al., 2007). Their results established a possible path for studying the long-distance interaction between the dorsal side of the lower limb muscle and lumbar tissue. The order of the model from distal to proximal is gastrocnemius, deep popliteal fascia, hamstring, dorsal thigh fascia band, GMax, TLF, and ES. In this study, the stiffness of TLF, ES, MG, and LG increased with the increase of plantar isometric bending resistance. The stiffness increase rate of MG was always closely related to the stiffness increase rate of the lumbar tissue (TLF and ES). The mechanical properties of the muscle and fascia depend on the change of their own tension. Tissue stiffness is one of the important indicators to evaluate tissue tension (Swanson, 2013). Therefore, our results preliminarily show that there is a long-distance interaction between the dorsal side of the lower limb muscle and lumbar tissue in the myofascial tensegrity network, and MG, LG, ES, and TLF play a synergistic role in plantar-flexion.

There was no significant difference in lumbar tissue stiffness between the dominant side and the non-dominant side in the resting state, but after the beginning of plantar flexion, the lumbar tissue stiffness of the nondominant side was always greater than that of the dominant side. We speculate that the reason for this difference may be that the plantar flexion movement on the dominant side changes the tension distribution of the lumbar tissues on both sides. Previous studies have shown that passive dorsiflexion of the ankle can induce joint displacement of the gastrocnemius, semimembranosus, and quadriceps femoris (Huang et al., 2018; Wilke et al., 2020). The contraction of Gmax can affect the contralateral latissimus dorsi muscle through TLF and ES (Carvalhais et al., 2013). In an anatomical study, the shallow lamina of TLF crosses the midline at the L4-S2 level and connected with the contralateral sacrum, posterior superior iliac spine, iliac bone, and GMax (Vleeming et al., 1995). Thus, our results reinforce earlier findings of the interaction between different tissues in the myofascial tension network. In addition, as Weisman *et al.* observed, the myoelectric activity of the nondominant side of the PSIS level was significantly higher than that of the dominant side during the maximum resistance plantar-flexion of the dominant foot, indicating that the impulse conduction generated by the lower extremity tissue tension may complete the cross before reaching the PSIS level (Weisman et al., 2014). The studies of Stecco *et al.* have shown that the fascia can sense the tension produced by the contraction of the proximal muscle and transmit the signal to the distance, leading to the activation of the distal muscle (Stecco et al., 2009). Because the fascia has rich proprioceptive innervation and free nerve endings, the stretching of the fascia could activate the corresponding proprioceptors and compress or stretch the free nerve endings (Mense, 2019; Garofolini and Svanera, 2019). Therefore, the interaction between the dorsal side of the lower limb muscle and lumbar tissue may be realized by tension change and nerve signal transmission in myofascial tension network. In the exercise test, the cross-activation mode for the contralateral muscles of the trunk and lower limbs has been proven to be a factor to stabilize the trunk balance (Stevens et al., 2007; García-Vaquero et al., 2012). From the perspective of the whole-body mechanics adjustment, the trunk may have a tendency of dominant flexion when the dominant isometric plantar-flexion occurs. Therefore,

the tension structure of the nondominant trunk can increase the tension to fight against the coming shortening of the dominant side and maintain the balance of the body. No matter what the movement mode is, the human trunk always ensures normal function through the overall regulation of the activation mode. This also shows the importance of studying the whole-body mechanics regulation mode, and the study of the myofascial tensegrity network is just one of these links.

Plantar-flexion is an important part of walking, running, jumping, and other activities. ln the process of the foot pushing off the ground, it is accompanied by isometric plantar-flexion and a continuous increase of plantar-flexion myodynamia (Li et al., 2018). Therefore, studying the effect of isometric plantar-flexion on tissue stiffness can clarify the adjustment strategy of different tissues in isometric plantar-flexion. After analyzing the stiffness-phased percentage change of various tissues at different resistances, we found that the stiffness-phased percentage change of ES and MG is much higher than that of TLF and LG when the resistance changed from 0 to 20%MVIC, which indicates that MG is the main generation part of plantar-flexion tension, and ES is the lumbar tissue most affected by the change of lower limb tension at the initial stage of resistance rising. When the resistance changed from 20 to 40%MVIC, the stiffness-phased percentage change of LG increased significantly and that of MG decrease significantly. We speculate that, when the resistance changes from 20 to 40%, the output strategies of MG and LG are redistributed, the force output of MG tends to be stable, and LG improves the strength of the force output. Because MG and LG are laterally adjacent and converge on the Achilles tendon, the lateral disturbance of adjacent muscles and tension transmission between tendons may be the reason for this phenomenon, which needs further research to verify (Huijing and Baan, 2001). Moreover, when the resistance reaches 60% MVIC, the stiffness-phased percentage change of TLF, ES, MG, and LG decreased significantly, indicating that the stiffness changes of each tissue tended to be stable.

LIMITATIONS

There are some limitations to this study. First, we failed to measure the thigh portion of the myofascial tensegrity network due to technical reasons. Second, the ankle 90° fixator covers the distal end of the soleus muscle and the Achilles tendon, so we could not evaluate these two areas. Third, only female participants were recruited. In our preliminary experiments, the tissue stiffness of 40 and 60% MVIC in male participants often exceeded the measuring range of the instrument. Therefore, only female individuals were recruited in this study. We need to develop instruments with a larger measuring range to meet the needs of future research. Fourth, although we fully trained the participants to not contract the auxiliary muscles, due to the lack of EMG monitoring equipment, we cannot confirm that this was the case. In the next experiment, we will introduce an EMG device to objectively monitor the muscle activity. Finally, the results of this study were only applicable to healthy young people. We will gradually carry out research on injured people in the future.

CONCLUSION

This study quantified stiffness values of the TLF, ES, MG, and LG in healthy humans during isometric plantar-flexion against different resistances using the SWE. We found a moderate to strong correlation between TLF, ES, MG, and LG during isometric plantar-flexion, which provides preliminary data for exploring the interaction between different tissues in the myofascial tensegrity network. Through the study of different resistance conditions, we know that the change of local force will have a synergistic effect on other parts of the myofascial tensegrity network, which provides a valuable reference for us to understand the overall regulation mode of the myofascial tensegrity network of injury more comprehensively.

DATA AVAILABILITY STATEMENT

The raw data supporting the conclusion of this article will be made available by the authors without undue reservation.

ETHICS STATEMENT

The studies involving human participants were reviewed and approved by the Ethics Committee of the Guangdong Provincial Hospital of Chinese Medicine. The patients/participants provided their written informed consent to participate in this study.

AUTHOR CONTRIBUTIONS

BC contributed to conceptualization, methodology, investigation, validation, visualization, data curation, writing—original draft, and formal analysis. SC and MX contributed to investigation and project administration. ZZ and CL contributed to writing—review, supervision, and resources.

ACKNOWLEDGMENTS

The SWE equipment for this article was provided by the Guangdong Provincial Hospital of Chinese Medicine. We are grateful to Ming Lin and Weixin Deng for the medical screening of participants and to the students of the Guangzhou University of Chinese Medicine for being the participants in the study. Thanks for the support of Guangdong Provincial Bureau of Traditional Chinese Medicine (no. 20201240) and Shenzhen Special Fund for Introducing High-Level Medical Team Project (SZSM201502044).

SUPPLEMENTARY MATERIAL

The supplementary material for this article can be found online at: https://www.frontiersin.org/articles/10.3389/fbioe.2021.810250/full#supplementary-material

REFERENCES

Barker, P. J., Hapuarachchi, K. S., Ross, J. A., Sambaiew, E., Ranger, T. A., and Briggs, C. A. (2014). Anatomy and Biomechanics of Gluteus Maximus and the Thoracolumbar Fascia at the Sacroiliac Joint. *Clin. Anat.* 27 (2), 234–240. doi:10.1002/ca.22233

Bordoni, B., Walkowski, S., Morabito, B., and Varacallo, M. A. (2019). Fascial Nomenclature: An Update. *Cureus* 11 (9), 5718. doi:10.7759/cureus.5718

Carvalhais, V. O. d. C., Ocarino, J. d. M., Araújo, V. L., Souza, T. R., Silva, P. L. P., and Fonseca, S. T. (2013). Myofascial Force Transmission between the Latissimus Dorsi and Gluteus Maximus Muscles: an *In Vivo* experiment. *J. Biomech.* 46 (5), 1003–1007. doi:10.1016/j.jbiomech.2012.11.044

Chen, B., Liu, C., Lin, M., Deng, W., and Zhang, Z. (2021). Effects of Body Postures on the Shear Modulus of Thoracolumbar Fascia: a Shear Wave Elastography Study. *Med. Biol. Eng. Comput.* 59 (2), 383–390. doi:10.1007/s11517-021-02320-2

Cresswell, A. G., Löscher, W. N., and Thorstensson, A. (1995). Influence of Gastrocnemius Muscle Length on Triceps Surae Torque Development and Electromyographic Activity in Man. *Exp. Brain Res.* 105 (2), 283–290. doi:10.1007/BF00240964

Creze, M., Nordez, A., Soubeyrand, M., Rocher, L., Maître, X., and Bellin, M.-F. (2018). Shear Wave Sonoelastography of Skeletal Muscle: Basic Principles, Biomechanical Concepts, Clinical Applications, and Future Perspectives. *Skeletal Radiol.* 47, 457–471. doi:10.1007/s00256-017-2843-y

Fukunaga, T., Roy, R. R., Shellock, F. G., Hodgson, J. A., Day, M. K., Lee, P. L., et al. (1992). Physiological Cross-Sectional Area of Human Leg Muscles Based on Magnetic Resonance Imaging. *J. Orthop. Resofficial Publication Orthopaedic Res. Soc.* 10 (6), 928–934. doi:10.1002/jor.1100100623

Fukunaga, T., Kubo, K., Kawakami, Y., Fukashiro, S., Kanehisa, H., and Maganaris, C. N. (2001). *In Vivo* behaviour of Human Muscle Tendon during Walking. *Proc. R. Soc. Lond. B* 268 (1464), 229–233. doi:10.1098/rspb.2000.1361

García-Vaquero, M. P., Moreside, J. M., Brontons-Gil, E., Peco-González, N., and Vera-Garcia, F. J. (2012). Trunk Muscle Activation during Stabilization Exercises with Single and Double Leg Support. *J. Electromyogr. Kinesiol. Official J. Int. Soc. Electrophysiological Kinesiol.* 22 (3), 398–406. doi:10.1016/j.jelekin.2012.02.017

Garofolini, A., and Svanera, D. (2019). Fascial Organisation of Motor Synergies: a Hypothesis. *Eur. J. Transl. Myol.* 29 (3), 8313. doi:10.4081/ejtm.2019.8313

Gennisson, J.-L., Deffieux, T., Fink, M., and Tanter, M. (2013). Ultrasound Elastography: Principles and Techniques. *Diagn. Interv. Imaging* 94, 487–495. doi:10.1016/j.diii.2013.01.022

Huang, J., Qin, K., Tang, C., Zhu, Y., Klein, C. S., Zhang, Z., et al. (2018). Assessment of Passive Stiffness of Medial and Lateral Heads of Gastrocnemius Muscle, Achilles Tendon, and Plantar Fascia at Different Ankle and Knee Positions Using the MyotonPRO. *Med. Sci. Monit.* 24, 7570–7576. doi:10.12659/msm.909550

Huijing, P. A., and Baan, G. C. (2001). Myofascial Force Transmission Causes Interaction between Adjacent Muscles and Connective Tissue: Effects of blunt Dissection and Compartmental Fasciotomy on Length Force Characteristics of Rat Extensor Digitorum Longus Muscle. *Arch. Physiol. Biochem.* 109 (2), 97–109. doi:10.1076/apab.109.2.97.4269

Huijing, P. A. (20092007). Epimuscular Myofascial Force Transmission: A Historical Review and Implications for New Research. International Society of Biomechanics Muybridge Award Lecture, Taipei, 2007. *J. Biomech.* 42 (1), 9–21. doi:10.1016/j.jbiomech.2008.09.027

Li, Y., Ko, J., Walker, M. A., Brown, C. N., Schmidt, J. D., Kim, S.-H., et al. (2018). Does Chronic Ankle Instability Influence Lower Extremity Muscle Activation of Females during landing? *J. Electromyogr. Kinesiol.* 38, 81–87. doi:10.1016/j.jelekin.2017.11.009

Liu, C.-L., Zhou, J.-P., Sun, P.-T., Chen, B.-Z., Zhang, J., Tang, C.-Z., et al. (2020). Influence of Different Knee and Ankle Ranges of Motion on the Elasticity of Triceps Surae Muscles, Achilles Tendon, and Plantar Fascia. *Sci. Rep.* 10 (1), 6643. doi:10.1038/s41598-020-63730-0

Mense, S. (2019). Innervation of the Thoracolumbar Fascia. *Eur. J. Transl Myol* 29 (3), 8297. doi:10.4081/ejtm.2019.8297

Rosager, S., Aagaard, P., Dyhre-Poulsen, P., Neergaard, K., Kjaer, M., and Magnusson, S. P. (2002). Load-displacement Properties of the Human Triceps Surae Aponeurosis and Tendon in Runners and Non-runners. *Scand. J. Med. Sci. Sports* 12, 90–98. doi:10.1034/j.1600-0838.2002.120205.x

Stackhouse, S. K., Eisennagel, A., Eisennagel, J., Lenker, H., Sweitzer, B. A., and McClure, P. W. (2013). Experimental Pain Inhibits Infraspinatus Activation during Isometric External Rotation. *J. Shoulder Elbow Surg.* 22 (4), 478–484. doi:10.1016/j.jse.2012.05.037

Stecco, A., Antonio, S., Gilliar, W., Wolfgang, G., Hill, R., Robert, H., et al. (2013). The Anatomical and Functional Relation between Gluteus Maximus and Fascia Lata. *J. Bodyw. Mov. Ther.* 17 (4), 512–517. doi:10.1016/j.jbmt.2013.04.004

Stecco, A., Macchi, V., Stecco, C., Porzionato, A., Ann Day, J., Delmas, V., et al. (2009). Anatomical Study of Myofascial Continuity in the Anterior Region of the Upper Limb. *J. Bodywork Movement Therapies* 13 (1), 53–62. doi:10.1016/j.jbmt.2007.04.009

Stecco, C., Porzionato, A., Macchi, V., Stecco, A., Vigato, E., Parenti, A., et al. (2008). The Expansions of the Pectoral Girdle Muscles onto the Brachial Fascia: Morphological Aspects and Spatial Disposition. *Cells Tissues Organs* 188 (3), 320–329. doi:10.1159/000121433

Stevens, V. K., Coorevits, P. L., Bouche, K. G., Mahieu, N. N., Vanderstraeten, G. G., and Danneels, L. A. (2007). The Influence of Specific Training on Trunk Muscle Recruitment Patterns in Healthy Subjects during Stabilization Exercises. *Man. Ther.* 12 (3), 271–279. doi:10.1016/j.math.2006.07.009

Swanson, R. L. (2013). Biotensegrity: A Unifying Theory of Biological Architecture with Applications to Osteopathic Practice, Education, and Research-A Review and Analysis. *J. Am. Osteopath. Assoc.* 113 (1), 34–52. doi:10.7556/jaoa.2013.113.1.34

Tuncay, I., Kucuker, H., Uzun, I., and Karalezli, N. (2007). The Fascial Band from Semitendinosus to Gastrocnemius: the Critical point of Hamstring Harvesting an Anatomical Study of 23 Cadavers. *Acta Orthopaedica* 78 (3), 361–363. doi:10.1080/17453670710013933

Vleeming, A., Pool-Goudzwaard, A. L., Stoeckart, R., van Wingerden, J.-P., and Snijders, C. J. (1995). The Posterior Layer of the Thoracolumbar Fascia|Its Function in Load Transfer from Spine to Legs. *Spine* 20 (7), 753–758. doi:10.1097/00007632-199504000-00001

Weinfeld, S. B. (2014). Achilles Tendon Disorders. *Med. Clin. North America* 98 (2), 331–338. doi:10.1016/j.mcna.2013.11.005

Weisman, M. H. S., Haddad, M., Lavi, N., and Vulfsons, S. (2014). Surface Electromyographic Recordings after Passive and Active Motion along the Posterior Myofascial Kinematic Chain in Healthy Male Subjects. *J. Bodywork Movement Therapies* 18 (3), 452–461. doi:10.1016/j.jbmt.2013.12.007

Wilke, J., Debelle, H., Tenberg, S., Dilley, A., and Maganaris, C. (2020). Ankle Motion Is Associated with Soft Tissue Displacement in the Dorsal Thigh: An *In Vivo* Investigation Suggesting Myofascial Force Transmission across the Knee Joint. *Front. Physiol.* 11, 180. doi:10.3389/fphys.2020.00180

Wilke, J., Krause, F., VogtBanzer, L. W., and Banzer, W. (2016). What Is Evidence-Based about Myofascial Chains: A Systematic Review. *Arch. Phys. Med. Rehabil.* 97 (3), 454–461. doi:10.1016/j.apmr.2015.07.023

Conflict of Interest: The authors declare that the research was conducted in the absence of any commercial or financial relationships that could be construed as a potential conflict of interest.

frontiers in Bioengineering and Biotechnology

ORIGINAL RESEARCH
published: 14 February 2022
doi: 10.3389/fbioe.2022.789629

Overstretching Expectations May Endanger the Success of the "Millennium Surgery"

Alwina Bender[1], *Philipp Damm*[1]*, *Hagen Hommel*[2] *and Georg N. Duda*[1]

[1]*Berlin Institute of Health at Charité-Universitätsmedizin Berlin, Julius-Wolff-Institute, Berlin, Germany,* [2]*Department of Orthopaedics, Märkisch-Oderland Hospital, Brandenburg Medical School Theodor Fontane, Wriezen, Germany*

Total hip arthroplasty (THA) is an extremely successful treatment strategy. Patient expectations, however, have increased; if not properly guided by surgeons, at present, patients expect next to pain-free restoration of the joint and a fast return to work and sports. While the revision rates after THA also increased in younger patients, knowledge on musculoskeletal loads still remains sparse, and the current recommendations on postoperative rehabilitation are based on expert opinions only. The aim of this study was to unravel biomechanical contact conditions in "working age" (<60 years, 53.5 ± 3.0 years) and "retirement age" (>60 years, 67.7 ± 8.6 years) patients during activities recommended post-THA. We hypothesized that working age patients would show substantially increased hip contact loads compared to older patients. The *in vivo* joint contact force (F_{res}) and torsion torque (M_{tors}), reflecting the main contact load situation, experienced during activities of daily living and sports activities were measured in a unique group of 16 patients with instrumented THA. We summarized patient activities and sports recommendations after THA mentioned within the literature using PubMed (without claim of completeness). The measurements showed that younger working age patients experienced significant ($p = 0.050$) increased M_{tors} (21.52 ± 9.11 Nm) than older retirement age patients (13.99 ± 7.89 Nm) by walking. Bowling, as a recommended low-impact sport, was associated with F_{res} of up to 5436 N and M_{tors} of up to 108 Nm in the working age group, which were higher than the F_{res} (5276 N) and M_{tors} (71 Nm) during high-impact soccer. Based on our results, age was proven to be a discriminator in joint loading, with working age patients presenting with increased loads compared to retirement age patients, already during daily activities. The current patient recommendations have led to further increased joint loadings. If THA cannot be delayed in a patient, we propose counselling patients on a carefully considered return to sports, focusing on low-impact activities, as indicated hereby. The findings from this work illustrate the need to provide critical feedback to patient expectations when returning to work and sports activities. Patients returning to more intensive sports activities should be carefully monitored and advised to avoid as much overloading as possible.

Keywords: total hip arthroplasty, loads, sport activities, activity of daily living, age

OPEN ACCESS

Edited by:
Rafael Reimann Baptista, Pontifical Catholic University of Rio Grande do Sul, Brazil

Reviewed by:
Denitsa Docheva, University Medical Center Regensburg, Germany
Alexandre Terrier, Swiss Federal Institute of Technology Lausanne, Switzerland

***Correspondence:**
Philipp Damm
philipp.damm@bih-charite.de

Specialty section:
This article was submitted to Biomechanics, a section of the journal Frontiers in Bioengineering and Biotechnology

Received: *05 October 2021*
Accepted: *07 January 2022*
Published: *14 February 2022*

Citation:
Bender A, Damm P, Hommel H and Duda GN (2022) Overstretching Expectations May Endanger the Success of the "Millennium Surgery". Front. Bioeng. Biotechnol. 10:789629. doi: 10.3389/fbioe.2022.789629

1 INTRODUCTION

The "operation of the century"—total hip arthroplasty (THA) (Learmonth et al., 2007)—has been demonstrated to be extremely effective for decades (Jenkins et al., 2013). THA provides a reliable solution for one of the most common disabling diseases in humans: end-stage osteoarthritis (OA) (Woolf et al., 2003; Kurtz, 2007; Pabinger and Geissler, 2014). The growing number of OA patients, their rising expectations, and an ever-growing number of younger patients seeking this surgery explain the further predicted increase in the annual number of THA surgeries (Kurtz et al., 2009; Bashinskaya et al., 2012; Nemes et al., 2014; Culliford et al., 2015; Pilz et al., 2018; Sloan et al., 2018). The incidence rate growth ranges from 25% (Pilz et al., 2018) to 132% (Sloan et al., 2018), with a 7-fold growth rate for patients <64 years (Pabinger and Geissler, 2014).

Despite the overall increase in numbers and younger patients, the lifetime of a functional hip joint arthroplasty has remained at 15–20 years over the last decades (Junnila et al., 2016; Swarup et al., 2018). Originally, THA was implemented to reduce acute pain and allow painless mobility in daily life in older patients with degenerated joints (Wright et al., 1994). For these patients, long-lasting success rates have been realized. Due to the good functional THA lifetime, new materials and design, the restriction to offer THA to older patients has been dropped and more and more younger patients now seek such end-stage therapy. At the same time, a change in work and leisure behavior took place: less physically hard work, reduction in working hours, and more attention to sports and recreational activities. In addition, patient expectations have dramatically changed over the last decades. Beyond pain reduction, the present expectations include returning not only to full functional and recreational activities (Healy et al., 2008; Mancuso et al., 2009) in daily life but also to work and sport (Hoorntje et al., 2018), or eventually to start with new activities (Schmidutz et al., 2012).

Despite all these changes, aseptic loosening remains the most common failure mode in primary THA (Ben-Shlomo et al., 2019; Burke et al., 2019; Australian Orthopaedic Association National Joint Replacement Registry (AOANJRR) 2019), especially in younger patients (Ben-Shlomo et al., 2019; Kuijpers et al., 2020). The growing number of younger compared to older patients (Australian Orthopaedic Association National Joint Replacement Registry (AOANJRR), 2019; Swedish Hip Arthroplasty Register, 2019; Norwegian National Advisory Unit Report on Arthroplasty and Hip Fractures, 2019; Danish Hip Arthroplasty Register, 2020; Canadian Institute for Health Information, 2019; Dutch Arthroplasty Register (LROI), 2019; Ben-Shlomo et al., 2019; Finnish Arthroplasty Register for National Institute of Health and Welfare, 2020) with inferior outcomes has caused an unavoidable increase in the number of THA revisions (Bayliss et al., 2017; Rajaee et al., 2018). With each additional revision surgery, the risk of implant-associated infections increases threefold (Swedish Hip Arthroplasty Register (2019); Kuijpers et al., 2020).

With the increasing number of younger patients (Pabinger and Geissler, 2014; Pilz et al., 2018; Sloan et al., 2018) seeking THA, their increased expectations for joint function and return to activity (Healy et al., 2008; Mancuso et al., 2009), their longer life expectancy (Cutler et al., 2006; Roser, 2019), and the increased economic benefit of performing such surgery, the overarching success that THA has seen in previous years may be endangered. Thus, the basic biomechanical conditions of increased joint loads in younger THA patients make serious considerations of a well-balanced recovery and expectation management essential for its long-term success.

Using a unique worldwide group of patients with telemetric THA that allows measuring *in vivo* hip contact loads (Damm et al., 2010) and comparing against recommendations on postoperative activities (Schneider et al., 2006; Bohannon, 2007; Tudor-Locke et al., 2008; Koenen et al., 2014; Bergmann et al., 2016; Oehler et al., 2016; Hoorntje et al., 2018), we hypothesized that, across a patient cohort, age is a discriminator for THA joint contact loads with younger patients showing higher loads.

2 MATERIALS AND METHODS

2.1 Patients With Telemetric Total Hip Arthroplasty

In vivo loading data for THA during activities of daily living (ADL), sports, and work are rare (Bergmann et al., 1998; Bergmann et al., 2010; Bergmann et al., 2016). To identify the *in vivo* loads in THA, we used a previously described technology (Bergmann et al., 1988; Bergmann et al., 1993; Graichen et al., 1999; Damm et al., 2010; Bergmann et al., 2016; Georg Bergmann et al., 2018b). Sixteen patients with end-stage OA received between 1988 and 2013 instrumented hip implants with three different telemetric data transmission capabilities (implant types I, II, and III; **Figure 1**). The centrum–collum–diaphyseal (CCD) angle was 135° in all patients (**Figure 1**).

We used telemetric data collected in previous studies since 1990 in our well-established internal archive of *in vivo* data without new measurements. Some of the *in vivo* data have been published earlier (Bergmann et al., 2016; Damm et al., 2017; Kutzner et al., 2017). The studies were approved by our ethics committee and registered at the German Clinical Trials Register (DRKS00000563). All patients gave written informed consent prior to participation in this study and to have their images published.

Based on a subjective assessment of activity level, all patients were considered more or less active than the average activity level of the patients in the group (**Figure 1**). There were no changes in the activity level pre- and postoperatively.

The patients were divided into "working age" (<60 years, 53.6 ± 3.0 years) and "retirement age" (>60 years, 67.7 ± 8.6 years) groups based on their age at implantation and the lowest limit of effective retirement age in OECD (Organisation for Economic Co-operation and Development) countries. According to the *t*-test, there was a significant difference in age at implantation between the two groups [$t(7.1) = 4.15$, $p = .004$, 95% CI = 6.17–22.20], with Cohen's effect size $d_s = 2.32$. The primary aim of THA in all 16 patients was pain reduction without expectation in return to sport (RTS). Two retirement age and 7 working age patients returned to work within 24 months postoperatively.

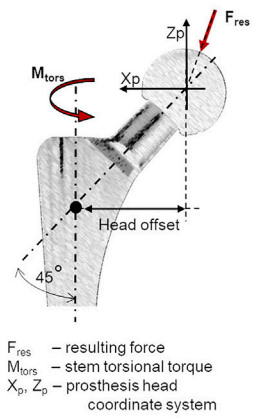

Patient	Implant type	Head offset [mm]	Age at surgery [Y]	Sex	Body weight at 12 month PO [kg]	BMI at 12 month PO [kg/m²]	THA approach	Activity level	Group
EBL	I	42.4	83	m	62	22.8	dorsal	more	'retirement age'
IBL	I	42.4	76	w	84	29.6	anterolateral	less	'retirement age'
KWR	II	43.8	61	m	72	27.0	anterolateral	more	'retirement age'
RHR	II	43.8	63	w	60	23.9	anterolateral	less	'retirement age'
H2R	III	42.0	61	m	75	26.4	transgluteal	more	'retirement age'
H5L	III	39.3	62	w	87	30.9	transgluteal	more	'retirement age'
H6R	III	39.3	68	m	84	26.8	transgluteal	more	'retirement age'
Average 'retirement age'			**67.7**		**74.9**	**26.8**			
HSR	II	43.8	55	m	82	29.0	anterolateral	more	'working age'
PFL	II	43.8	49	m	98	33.0	anterolateral	less	'working age'
H1L	III	39.3	55	m	73	24.5	transgluteal	less	'working age'
H3L	III	39.3	59	m	91	32.1	transgluteal	less	'working age'
H4L	III	44.8	50	m	85	25.6	transgluteal	more	'working age'
H7R	III	44.8	52	m	95	29.1	transgluteal	more	'working age'
H8L	III	42.0	55	m	80	27.0	transgluteal	more	'working age'
H9L	III	42.0	54	m	118	37.2	transgluteal	more	'working age'
H10R	III	42.1	53	w	98	38.6	transgluteal	more	'working age'
Average 'working age'			**53.5**		**91.1**	**30.7**			

FIGURE 1 | Coordinate system of the hip implant and the *in vivo* loading as the resultant contact force (F_{res}) and torsional torque (M_{tors}) and details of the patients wearing telemetric implants and their group distribution. Implant types: *I*—hip implant with one 4-channel transmitter technology (Bergmann et al., 1988) (since 1988); *II*—hip implant with two 8-channel transmitter technology (Graichen et al., 1999) (since 1997); and *III*—hip implant with one 9-channel transmitter technology (Graichen et al., 2007) (since April 2010).

The resultant *in vivo* joint contact force (F_{res}) acting on the implant head and the torsion torque relative to the stem (M_{tors}), reflecting the main contact load situation at the stem–bone interface, were analyzed. F_{res} represents the sum of forces crossing from the acetabulum to the proximal femur *via* the head of the implant, and M_{tors} indicates the torsion torque acting around the implant stem (**Figure 1**). Notably, M_{tors} is derived from forces measured in the prosthesis coordinate system:

$$M_{tors} = F_{ypr} * L_x + M_{zpr},$$

where F_{ypr} is the force in the anterior–posterior directions (in Newton), M_{zpr} is moment in the mediolateral direction (in Newton*meter), and L_x is the implant-specific head offset (in meters) (**Figure 1**).

Since the measured contact force and torsional torque values were compared with ISO norms to estimate whether the *in vivo* loads were of high, intermediate, or low impact, all values were considered in Newton and Newton*meter, respectively.

2.2 Registry Data, Self-Reported Return to Sport, and Return to Work

In order to analyze the changes in the activities and expectations of patients after THA, sports recommendations after THA, and the THA failure rates by age group in the last 30 years, several arthroplasty registries and studies to self-reported return to sport (RTS) and return to work (RTW) as the studies on sports recommendation after THA were analyzed. All respective studies were extracted from the PubMed and ScienceDirect databases. Despite a thorough search, we do not claim to have reviewed all of the published literature.

This overview summarized THA revision rate data from 10 registries (Ben-Shlomo et al., 2019; Australian Orthopaedic Association National Joint Replacement Registry (AOANJRR), 2019; Canadian Institute for Health Information, 2019; Dutch Arthroplasty Register (LROI), 2019; Norwegian National Advisory Unit Report on Arthoplasty and Hip Fractures, 2019; Danish Hip Arthroplasty Register, 2020; Finnish Arthroplasty Register for National Institute of Health and Welfare, 2020) (**Supplementary Material S1**), 10 studies on recommendations regarding sports after THA (McGrory et al., 1995; Healy et al., 2001; Franke et al., 2006; Klein et al., 2007; Healy et al., 2008; Swanson et al., 2009; Laursen et al., 2014; Bradley et al., 2017; Meester et al., 2018; Vu-Han et al., 2020) (**Supplementary Material S2**), 17 studies on RTS (Dubs et al., 1983; Mont et al., 1999; Hatterji et al., 2004; Huch et al., 2005; Suckel and Best, 2006; Arbuthnot et al., 2007; Schmidutz et al., 2012; Lefevre et al., 2013; Abe et al., 2014; Raguet et al., 2015; Innmann et al., 2016; Piccolo et al., 2016; Karampinas et al., 2017; Hara et al., 2018; Batailler et al., 2019; Jassim et al., 2019; Ortmaier et al., 2019), and 19 on RTW (Danielsson, 1965; Nevitt et al., 1984; Johnsson and Persson, 1986; Visuri et al., 1987; Suarez et al., 1996; Mobasheri et al., 2006; Bohm, 2010; Nunley et al., 2011; Buchau et al., 2013; Clyde et al., 2013; Sankar et al., 2013; Truszczyńska et al., 2014; Kleim et al., 2015; Leichtenberg et al., 2016; Pop et al., 2016; Tilbury et al., 2016; Drobniewski et al., 2017; Boersma et al., 2019; Laasik et al., 2019) (**Supplementary Material S3**).

2.3 Sport Recommendation Evidence

Expert sports recommendations were not uniform in the published literature. Different terms and numbers of intermediate levels between the recommended or allowed and non-recommended sports were used.

To provide an overview of experts' sports recommendations, we introduced "sport recommendation evidence" (SRE) with five levels: SRE 1 for "allow"/"allowed"/"recommended"/"unlimited"; SRE 2 for "allowed with experience"/"experience"; SRE 3 for "occasional"/"intermediate"/"depends"; SRE 4 for "no conclusion"/"undecided"/"no advice"; and SRE 5 for "not recommended"/"not allowed"/"discouraged." For known percentages of expert opinions on certain sports, we calculated the SRE as a weighted average (**Supplementary Material S2**).

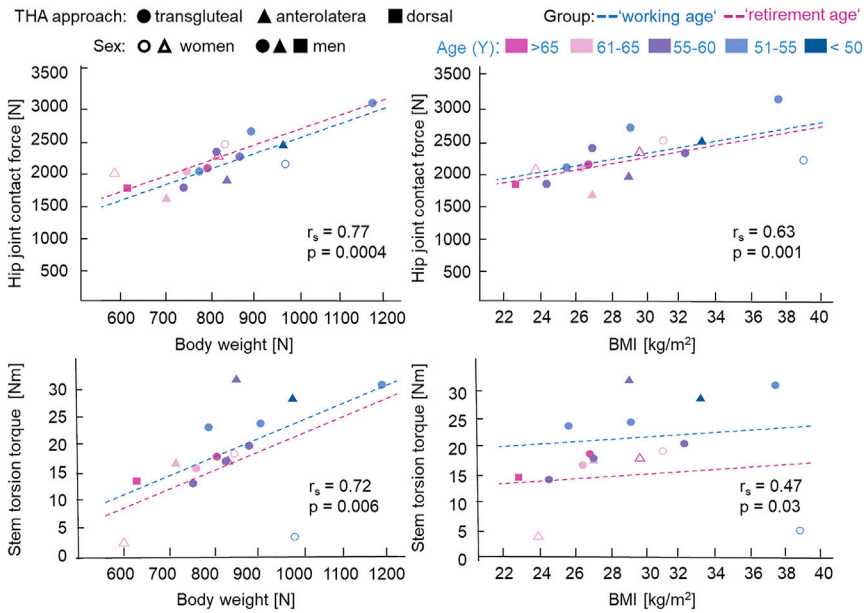

FIGURE 2 | Influence of body weight (BW), body mass index (BMI), and age on the maximal hip joint contact force and stem torsion torque during normal walking with self-selected comfortable speed. For total hip arthroplasty (THA) approach, *circle* denotes transqluteal, *triangle* denotes anterolateral, and *rectangle* denotes dorsal. *Unfilled circle* or *triangle* represents women, while *filled circle*, *triangle*, or *rectangle* represents men. Age at implantation is shown from *magenta* (>65 years) to *blue* (<50 years) in 5-year steps. r_s is the Spearman's rank correlation coefficient (one-tailed) for all patients (working age and retirement age groups) with *p*-values. Analysis of covariance (ANCOVA) with separated regression lines by groups: *dashed blue lines* for working age (<60 years) and *dashed magenta lines* for retirement age (>60 years).

2.4 Statistical Analyses of *In Vivo* Data

All evaluations were performed in R software (version 4.0.2) (R Core Team, 2021) in RStudio IDE (RStudio, Boston, MA, United States). We used *t*-tests, Spearman's rank correlation coefficient (r_s), and the Kolmogoroff–Smirnov test for group differences, which were evaluated using the stats package (R software).

For the analysis of covariance (ANCOVA), the R script as proposed in Wollschläger (2017) was applied. The 95% confidence interval (CI), *p*-value, and effect size were reported. A $p < .05$ was considered significant.

3 RESULTS

3.1 Relevance of Body Weight and Age in Maximal Total Hip Arthroplasty Contact Forces and Torsional Torques

Our data showed no relationship between the THA approach (dorsal, transgluteal, or anterolateral) or sex and implant loading (**Figures 2**, **3**).

The younger working age patient group had, on average, a higher body weight (BW)/body mass index (BMI) (91.1 ± 13.3 kg, BMI = 30.7 ± 4.9) than the older retirement age group (74.9 ± 10.9 kg, BMI = 26.8 ± 2.9). The *t*-test indicated a significant difference in BW/BMI between both groups [BW: $t(13.9) = 2.69$, $p = 0.018$, 95% CI = 3.31–29.20; BMI: $t(13.1) = 1.98$, $p = .069$, 95% CI = −.35 to 8.16)], with a strong Cohen's effect size (BW: $d_s = 1.32$; BMI: $d_s = .93$).

Spearman's rank correlation test showed a significant positive correlation between the maximal joint contact force, F_{res}, and BW/BMI (BW: $r_s = .77$, $p < .001$; BMI: $r_s = .63$, $p = .001$) and between the maximal stem torsion torque, M_{tors}, and BW/BMI (BW: $r_s = .72$, $p = .006$; BMI: $r_s = .47$, $p = .03$) during normal walking with self-selected speed for all our patients (**Figure 2**), which meant a significant strong (for $r_s = .77$, .63, or .72) to moderate (for $r_s = .47$) correlation.

Since the data points in **Figure 2** were color-coded gradually from magenta for age >65 years to blue for age <50 years, it can be observed that the working age group tended to have higher F_{res} and M_{tors}. The influence of age on F_{res} and M_{tors} was assessed using ANCOVA with BW/BMI as the confounder. ANCOVA showed a significant dependency of F_{res} [$F(1, 7, 9) = 5.07$, $p = .042$, with partial η_p^2 as effect size = .064] and a lower dependency of M_{tors} [$F(1, 7, 9) = 3.60$, $p = .080$, with effect size $\eta_p^2 = .016$] on age group at walking. The regression lines for both groups are shown in **Figure 2** and

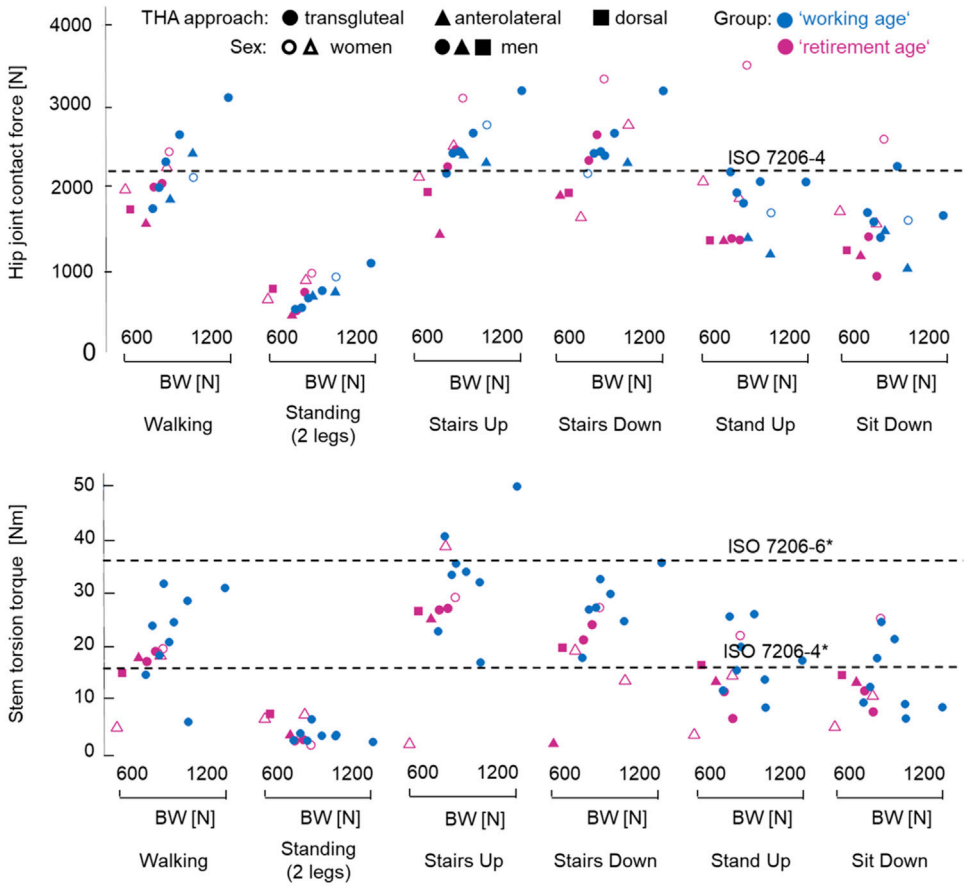

FIGURE 3 | Age-related differences in the maximal hip joint contact force, F_{res} (in newton), and maximal torsion torque, M_{tors} (in Newton*meter), during various activities of daily living (ADL). For total hip arthroplasty (THA) approach, *circle* denotes transqluteal, *triangle* denotes anterolateral, and *rectangle* denotes dorsal. *Empty circle* or *triangle* represents women, while *filled circle*, *triangle*, or *rectangle* represents men. For group by age at implantation, the retirement age group (>60 years) is shown as magenta and the working age group (<60 years) shown as blue.

demonstrated a tendency of higher contact force and torsion torque values for the working age group; only for $F_{res} = f(BW)$ did the regression line for the retirement age group lie higher than that for the working age group.

3.2 *In Vivo* Joint Loads During Activities of Daily Living

Since the revision rates in younger patients were higher and there were indications of age-related differences in the movement patterns due to changes in muscular coordination, it is necessary to consider differences between these groups. For comparison, the 12-month postoperative F_{res} and M_{tors} for each patient and ADL were used.

While the maximal F_{res} in the working age group (2,327 ± 441 N) tended to be higher, but demonstrated no significant differences compared to the retirement age group (2,057 ± 291 N) by walking at self-selected speed, comparison of the maximal M_{tors} between the groups resulted in significantly higher torsional torque values in the working age group (21.52 ± 9.11 Nm) than in the retirement age group (13.99 ± 7.89 Nm) for this activity. The Kolmogorov–Smirnov test for maximal M_{tors} revealed significant differences (D = .625, p = .050).

While there were trends toward higher maximal contact force and torsion torque values in the working age group across all activities (**Figure 3**), no significant differences were identified in all other considered ADL. However, the force values during ADL were higher than that of the test standard for the implant stem (ISO7206-4) and lower than that for the neck (ISO7206-6). According to standards ISO7206-6 and ISO7206-4, the maximal individual test M_{tors} values in our patient group were 37.4 and 16 Nm, respectively. Almost all ADL in our measurements showed values higher than 16 Nm and lower than 37.4 Nm. However, the M_{tors} values were partly higher than those of the test standards during stair climbing. Patients with lower BW/BMI showed, in some cases, higher (stairs down/stand up) or similar (stairs up) F_{res} and M_{tors} (stairs up/down).

3.3 Changes in Patient Age and Expectations

Data on the cumulative revision rates from arthroplasty registries for different age groups, for both men and women, were compared (Ben-Shlomo et al., 2019; Australian Orthopaedic Association National Joint Replacement Registry (AOANJRR), 2019; Canadian Institute for Health Information, 2019; Danish Hip Arthroplasty Register, 2020; Finnish Arthroplasty Register for National Institute of Health and Welfare, 2020; Dutch Arthroplasty Register (LROI), 2019; Norwegian National Advisory Unit Report on Arthoplasty and Hip Fractures, 2019). The revision rates at 1 year postoperative time for patients <55 years (.92%–2.1% for males and .92%–2.0% for females) were similar or slightly lower than those for patients >75 years (.98%–2.6% for males and .71%–2.03% for females). At 5 years postoperative time, the revision rates for patients <55 years (3.33%–5.5% for males and 3.11%–7.0% for females) were higher than those for patients >75 years (2.05%–4.08% for males and 1.48%–4.33% for females). At 20–25 years postoperatively, the cumulative revision rates for younger patients (<55 years) (23.7%–44.3% for males and 24.5%–51% for females) were significantly higher than those for older patients (>75 years) (13.2%–25.6% for males and 9.1%–17.5% for females) (for more details, see **Supplementary Material S1**).

The age of THA patients was analyzed in some studies (Kurtz et al., 2009; BQS—Bundesgeschäftsstelle Qualitätssicherung gGmbH, 2009; IQTIG–Institut für Qualitätssicherung und Transparenz im Gesundheitswesen, 2018). These studies revealed that every sixth to fifth THA patient is younger than 60 years. Five studies (Bashinskaya et al., 2012; Nemes et al., 2014; Culliford et al., 2015; Pilz et al., 2018; Sloan et al., 2018) have shown a tendency toward younger patients.

Several studies analyzed the expectations of patients after THA (Wright et al., 1994; Mancuso et al., 2009; Ghomrawi et al., 2011; Hepinstall et al., 2011; Judge et al., 2011; Scott and Biant, 2012; Koenen et al., 2014; Mancuso et al., 2017; Jassim et al., 2019). The studies of Koenen et al., (2014), Wright et al., (1994), and Mancuso et al., (2009) showed that higher expectations in THA were related to younger age (Gandhi et al., 2010; Scott and Biant, 2012). Two studies reported age-independent high expectations (Hepinstall et al., 2011; Koenen et al., 2014). At least six studies reported high patient expectations of full recovery in ADL and sports (Mancuso et al., 2009; Ghomrawi et al., 2011; Scott and Biant, 2012; Koenen et al., 2014; Mancuso et al., 2017; Jassim et al., 2019). Oehler et al., (2016) showed the overall increasing level of activities of the THA patients in their study.

3.4 Sports-Related Recommendations After Total Hip Arthroplasty

Sports after THA is a significant health factor for patients. Based on 10 studies published between 1995 and 2020 (McGroryet al., 1995; Healy et al., 2001; Franke et al., 2006; Klein et al., 2007; Healy et al., 2008; Swanson et al., 2009; Laursen et al., 2014; Bradley et al., 2017; Meester et al., 2018; Vu-Han et al., 2020), we compiled an overview of sports recommendations after THA over the past 20–30 years (**Supplementary Material S2**).

The sports activity recommendations in all 10 studies have been developed on the basis of expert opinions (Healy et al., 2001; Klein et al., 2007; Healy et al., 2008; Reeves et al., 2009) and divided sports into three severity levels according to the assumed load levels (Vail et al., 1996; Schmidutz et al., 2012): low, intermediate, and high impact for low, intermediate, and high expected loads, respectively. There was no uniform opinion on sports classifications (Klein et al., 2007; Schmidutz et al., 2012; Hara et al., 2018) with

- Cross-country skiing was classified as "potentially low" by Klein et al. (2007) and as "intermediate" by Schmidutz et al. (2012).
- Aerobics was classified as "intermediate" by Hara et al. (2018), while Klein et al. (2007) distinguished between low-impact aerobics, which was classified as "intermediate impact," and high-impact aerobics, which was classified as "high impact."

The number and type of sports activities considered also differed between studies. McGrory et al. (1995) considered 28 activities, Healy et al. (2008) considered 36, and the study by Meester et al. (2018) considered 41 sports activities with recommendations for patients >65 and <65 years.

Expert recommendations varied between "allow"/"allowed"/"recommended"/"unlimited"/"without limitation" and "not recommended"/"not allowed"/"discouraged" with 1–3 steps in between. To allow a comparison of expert sports recommendations, we introduced SRE with values between SRE 1 for "allow"/"allowed"/"recommended"/"unlimited"/"without limitation" and SRE 5 for "not recommended"/"not allowed"/"discouraged" (see *Materials and Methods* and **Supplementary Material S2**). A comparison between the different recommendations indicated changes in expert opinions within the last 20–30 years. A change within the SRE values can be observed in multiple cases, as in the following:

- For hiking: from SRE 2 ("allowed with experience"/"experience"/"with training") in McGrory et al. (1995) to SRE 1 ("allow"/"allowed"/"recommended"/"unlimited"/"without limitation") in Bradley et al. (2017) and Vu-Han et al. (2020)
- For tennis doubles: from SRE 3 ("occasional"/"intermediate"/"depends") (McGrory et al., 1995) to SRE 2 (Healy et al., 2008; Meester et al., 2018)
- For dancing (ballet und square/jazz): from SRE 4 ("no conclusion"/"undecided"/"no advice") (McGrory et al., 1995; Healy et al., 2001) to SRE 1(Meester et al., 2018; Vu-Han et al., 2020)
- For jogging: from SRE 5 ("not recommended"/"not allowed"/"discouraged") (Healy et al., 2001; Klein et al., 2007) to SRE 2 (Laursen et al., 2014; Vu-Han et al., 2020)

In **Supplementary Material S2**, more data collected on sports activity recommendations after THA can be found.

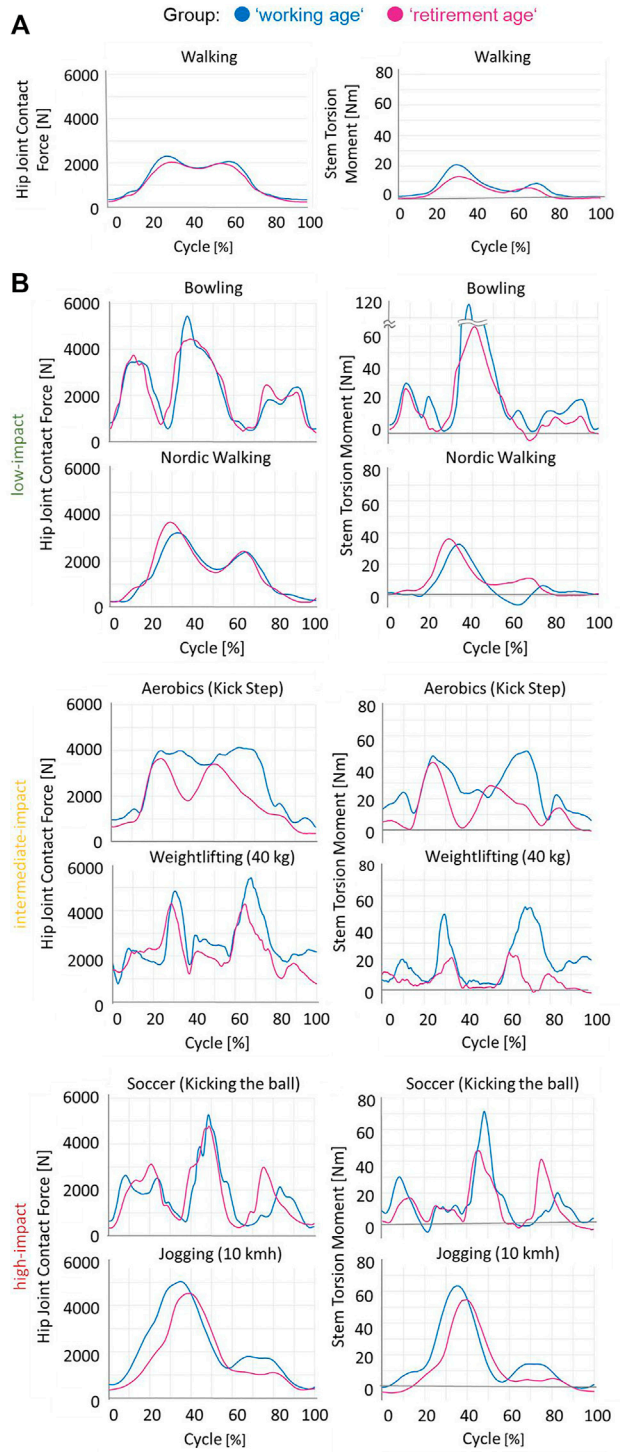

FIGURE 4 | (A) Mean *in vivo* hip joint contact force and stem torsion torque curves during walking (ADL, **Figure 3**). **(B)** Examples of the *in vivo* measured hip joint contact force and torsion torque values for some low-, intermediate-, and high-impact sporting activities, as classified in **Supplementary Material S2**, for one patient per group, working age (*blue*) and retirement age (*magenta*).

3.5 Self-Reported Return to Sports After Total Hip Arthroplasty

Data from 17 studies on RTS sorted by impact were summarized (**Supplementary Materials S2 and S3**). Two of the 17 studies reported RTS before 2000 postoperatively relative to preoperatively. In the study from 1983 (Dubs et al., 1983) with 110 THA patients, 102% of the patients returned to low-impact sports (>100% means that patients had not performed sports before THA and began sports participation after), 50% returned to intermediate-impact, and 40% to high-impact sports. The studies after 2000 with up to 420 THA patients showed an RTS of 90%–180% for low-impact, 40%–140% for intermediate-impact, and 10%–100% for high-impact sports activities.

3.6 Self-Reported Return to Work After Total Hip Arthroplasty

From the 19 studies on self-reported RTW for patients <65 years at the time of surgery, five studies were published before 2000 and reported RTW between 25% (Suarez et al., 1996) and 68% (Nevitt et al., 1984). The other 14 studies were published after 2000 and reported RTW between 59% (Truszczyńska et al., 2014) and 96%(Mobasheri et al., 2006). The summarized RTW value for five studies before 2000 was at 43% and for the 14 studies after 2000 was at 90%.

3.7 *In Vivo* Loads During Sporting Activities

To obtain an impression of the magnitude of F_{res} and M_{tors}, we present in **Figure 4** the results of our first *in vivo* data collected during activities that were ranked according to the above classifications into low-, intermediate-, and high-impact sports levels.

In the <60 years group, not only the higher maximum but also the average contact force and torsion torque values across the entire movement cycle were increased, with clear differences between age groups:

–Additional "in-betweens–low points" in F_{res} and M_{tors} in aerobic exercise and
–Significantly "flatter" curve of the M_{tors} in weightlifting in elderly patients.

There were a limited number of measurements available at present, and the maximum estimated M_{tors} and F_{res} values were determined for two subjects per group (**Figure 5**). All sports activities were performed by more active patients (**Figure 1**) who had undergone a transgluteal THA approach, except golf (anterolateral) and cross-country skiing (dorsal).

High loads (F_{res} and M_{tors}) occurred in both high-impact (F_{res} = 5276 N, M_{tors} = 71 Nm at soccer) and low-impact (F_{res} = 5436 N, M_{tors} = 108 Nm at bowling) sports. Therefore, patients in the working age group tended to have higher F_{res} and M_{tors}.

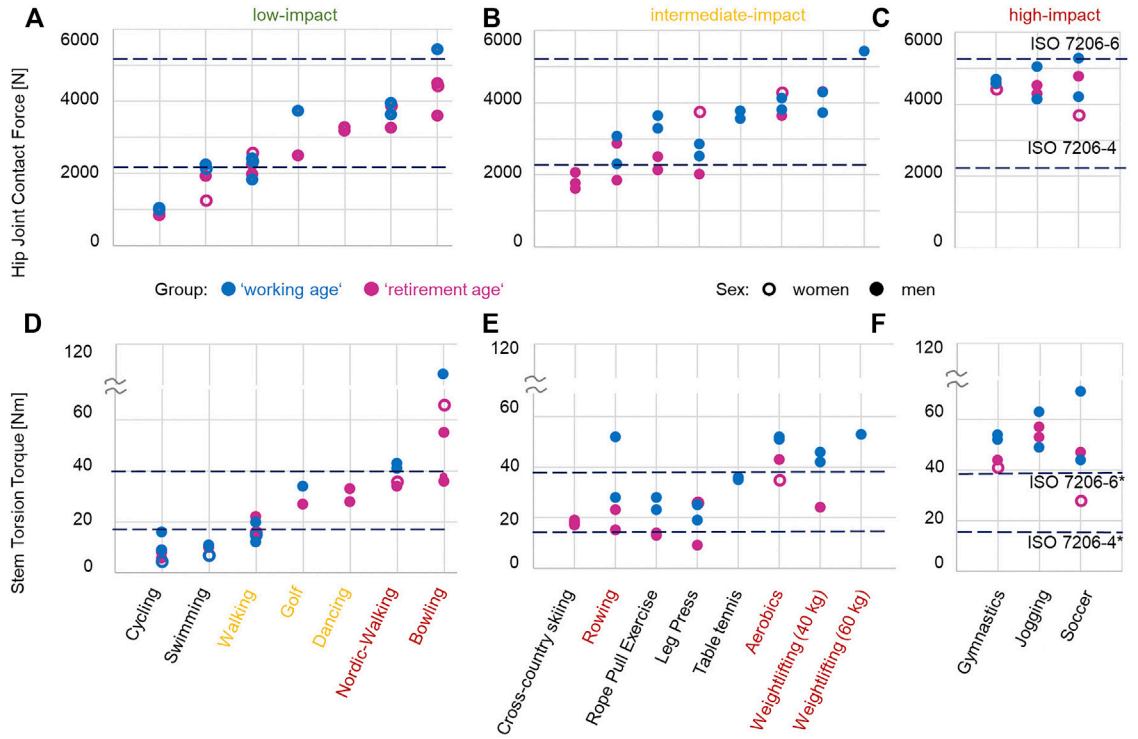

A, D – low-impact sports; **B, E** – intermediate-impact sports; **C, F** – high-impact sports as classified by figure in Supplement 2.
Dotted blue line in **A, B, C** – ISO 7206-4 and ISO 7206-6 norms for contact forces; dotted blue line in **D, E, F** - torsional torque according to ISO 7206-6 and ISO 7206-4 for maximal head offset in the group of patients with telemetric implants = 44.8mm (ISO 7206-6* and ISO 7206-4*).

FIGURE 5 | Examples of the *in vivo* measured hip joint contact force **(A–C)** and torsion torque **(D–F)** values for some sporting activities. One to three examples per group, retirement age (*magenta*) or working age (*blue*), are drawn. *Filled circle* and *empty circle* denote men and women, respectively. *Red* low- and intermediate-impact activities show high-impact contact force and torsion torque values. *Yellow* low-impact activities show intermediate-impact contact force and torsion torque values.

In bowling, rowing, and soccer, patients from the working age group with BMI of 25.6 (H4L) showed higher F_{res} and M_{tors} than patients with BMI of 26.4 (H2R), 26.5 (H6R), or 30.9 (H5L).

4 DISCUSSION

THA has shown a documented track record of being a successful therapy for late-stage OA so far and has been proven to be an instant solution for patients suffering from pain. However, various studies have confirmed that today's THA patients are more active than those who underwent THA in the 1980s–1990s (Bohannon, 2007; Naal and Impellizzeri, 2010; Hoorntje et al., 2018). They are more active in ADL and frequently return to work after surgery, but they also return to sports and have high expectations for the endurance and survival of their joint replacement.

In this study, the differences in the contact force and stem torsion torque values between working age and retirement age THA patients were explored in a small but unique group of patients with telemetric THA. The small number of patients is a limitation of this study. However, this unique worldwide group provided an insight into tendencies in THA loading conditions for younger and older THA patients.

A high BMI is a significant risk factor for several diseases (NCD Risk Factor Collaboration, 2016). The rate of obese THA patients with BMI > 30 and significantly higher complication rates (Jakubowitz et al., 2009; Zhang et al., 2012) increased (Culliford et al., 2015; Buirs et al., 2016). Several studies showed age-related changes in movement patterns and suggested that these were due to altered muscular coordination and performance (Hortobágyi et al., 2011; Novak and Brouwer, 2011; Chiu et al., 2015). It was discussed that this should ultimately also lead to altered loads in the large joints of the lower extremity (Hortobágyi et al., 2011).

Our patient groups reflected the current situation in the population (Finucane et al., 2011; Hales et al., 2017): the working age group had, on average, a higher BW/BMI (91.1 kg, BMI = 30.7) than the retirement age group (74.9 kg, BMI = 26.8). However, our measurements revealed that BW was an essential, but not the only, factor in the THA loading conditions: in bowling, rowing, and soccer, as in some ADL (stairs down/up and stand up), patients with low BMI showed the highest loading.

Our measurements confirmed the intuitive assumption that working age patients experience higher contact forces and torsion torques than do retirement age patients. This statement refers to ADL (**Figure 3**) and the aforementioned

examples of sport activities (**Figures 4**, **5**). The loads—even during ADL, such as stair climbing M_{tors}—may exceed the thresholds defined in ISO7206-6 for preclinical testing for THA in younger patients.

Other potential influencing parameters, such as a change in lean muscle volume of the gluteal muscles (Damm et al., 2018; Heller et al., 2001), could affect the contact force and torsion torque values [like a reversed effect for $F_{res} = f(BW)$] (**Figure 2**), but could not be controlled in this study and were not taken into account here.

Various registries revealed higher revision rates for younger patients than for older patients (Ben-Shlomo et al., 2019; Australian Orthopaedic Association National Joint Replacement Registry (AOANJRR) 2019; Swedish Hip Arthroplasty Register, 2019; Norwegian National Advisory Unit Report on Arthoplasty and Hip Fractures, 2019; Danish Hip Arthroplasty Register, 2020; Canadian Institute for Health Information, 2019;Dutch Arthroplasty Register (LROI) 2019; Finnish Arthroplasty Register for National Institute of Health and Welfare, 2020) (**Supplementary Material S1**) for both males and females, especially from 3 to 5 years postoperatively. Other studies have shown that the higher expectations in THA (Wright et al., 1994; Mancuso et al., 2009; Koenen et al., 2014) were related to younger age (Gandhi et al., 2010; Scott and Biant, 2012) and that every sixth to fifth patient was younger than 60 years (BQS—Bundesgeschäftsstelle Qualitätssicherung gGmbH, 2009; Kurtz et al., 2009; IQTIG—Institut für Qualitätssicherung und Transparenz im Gesundheitswesen, 2018), with a continuous trend toward younger patients (Bashinskaya et al., 2012; Nemes et al., 2014; Culliford et al., 2015; Pilz et al., 2018; Sloan et al., 2018). The reported age-independent high expectations in Hepinstall et al. (2011) and Koenen et al. (2014) may be explained by the overall increasing level of activities even in patients above 60 years of age (Oehler et al., 2016).

In general, patients today come with high expectations of full recovery of daily and sporting activities (Mancuso et al., 2009; Ghomrawi et al., 2011; Scott and Biant, 2012; Koenen et al., 2014; Mancuso et al., 2017; Jassim et al., 2019). Patient expectations were characterized by a desire to maintain relevant mobility for a long-term perspective with limited acceptance of any postoperative constraints on their preoperative activity levels (Mancuso et al., 2009; Mancuso et al., 2017). In some reports, patients even associated THA with restoration of greater athletic endurance (Judge et al., 2011; Mancuso et al., 2017; Jassim et al., 2019). Fulfilling these expectations appeared to correlate well with postoperative satisfaction with THA (Scott and Biant, 2012).

Without a doubt, engaging in sports has beneficial effects on reducing the risk of cardiovascular diseases and maintaining bone quality and neuromuscular coordination (Haskell et al., 2007; Global Recommendations on Physical Activity for Health, 2012). Contrary to the original recommendation (Charnley, 1979)—which discouraged patients from anything more strenuous than walking—the current recommendations suggest RTS activity (Swanson e al., 2009; Laursen et al., 2014; Meester et al., 2018).

Due to the lack of *in vivo* data, sports activity recommendations after THA have been widely developed on an expert opinion basis (Healy e al., 2001; Klein et al., 2007; Healy et al., 2008; Reeves et al., 2009) and divided sports into low, intermediate, and high impact (Vail et al., 1996; Schmidutz et al., 2012) for low, intermediate, and high expected loads, respectively. There is no uniform opinion on sports classifications (Klein et al., 2007; Schmidutz et al., 2012; Hara et al., 2018), nor have these classifications remained unchanged over the years (McGrory et al., 1995; Healy et al., 2001; Healy et al., 2008; Meester et al., 2018). **Supplementary Material S2** gives an overview of the recommendations (McGrory et al., 1995; Healy et al., 2001; Klein et al., 2007; Healy et al., 2008; Swanson et al., 2009; Laursen et al., 2014; Bradley et al., 2017; Meester et al., 2018; Vu-Han et al., 2020), without claiming to be a complete overview. It quickly becomes visible that the recommendations are not uniform and that they differ among authors: 20–25 years ago, only a few sporting activities were "recommended" (McGrory et al., 1995; Healy et al., 2008), while today, the number has substantially increased (Klein et al., 2007; Laursen et al., 2014; Bradley et al., 2017; Meester et al., 2018; Vu-Han et al., 2020). Expert opinion-based recommendations have changed over the years, from being rather "conservative" to now being more "risk-friendly." However, the published recommendations do not refer to *in vivo* loads or clinical registry or cohort data, and it remains unclear on what scientific basis were these recommendations formulated (Klein et al., 2007; Laursen et al., 2014; Bradley et al., 2017; Meester et al., 2018; Vu-Han et al., 2020).

Only a few studies reported RTS before 2000 (Dubs et al., 1983; Mont et al., 1999). The data after 2000 showed the same trend as 3 years before (Hoorntje et al., 2018) in terms of increased sports activities. Many patients practice increasingly high-impact sports (McGrory et al., 1995; Jassim et al., 2014; Hoorntje et al., 2018; Vu-Han et al., 2020). A study in a wider population (Bonnin et al., 2018) showed that approximately 20% of patients participated in strenuous sports and that 76% were motivated.

The summarized data from 19 studies on self-reported RTW for patients <65 years at the time of surgery (**Supplementary Material S3**) showed that significantly fewer patients returned to work until 2000. After 2000, on average, approximately 90% returned to work, which confirmed the trend identified in systematic reviews (Kuijer et al., 2009; Tilbury et al., 2014; Hoorntje et al., 2018) and can be explained at least in part by the fact that the number of younger patients of working age has increased. Many of them switched to less heavy-duty work (Hoorntje et al., 2018), although the actual loads experienced during work were generally unknown. While we do not claim to have reviewed all of the published literature, this overview provide a survey of the changes in activity and recommended activity after THA over the past two decades.

The *in vivo* loads during sporting activities were mostly unknown, except for those activities measured in our small cohort of patients (Kutzner, et al., 2017; Damm et al., 2017; Kutzner et al., 2017; Haffer et al., 2021). However, there is evidence that joint friction differed markedly between ADL and sports activities (Georg Bergmann, et al., 2018a). It can be expected that sports will also lead to higher F_{res} and M_{tors}. Therefore, it is not surprising that sport activities generally lead to experiencing higher loads. However, the levels of torsional torque were unexpected: while the maximum force levels across all activities were roughly comparable, the maximal torsional torque, M_{tors}, measured in

low-impact sports was even higher than that in some activities considered to be of high impact. Maximum M_{tors} was observed during bowling, previously classified (Ritter and Meding, 1987) as a low-impact sport (**Supplementary Material S2**).

In specific sport activities, the loads were even higher than those of the preclinical test standard loads for neck failure testing (ISO7206-6). M_{tors} exceeded the levels defined by both ISO standards in our patients. Only in swimming and cycling were the maximal F_{res} and M_{tors} within the preclinical test standards for THA. In the <60 years group, not only the high load maxima but also the load levels experienced across the entire cycles of various sport activities were increased compared to those in the retirement age group (**Figure 4**).

These measurements are only first impressions of the load patterns during sporting activities. Additional investigations of such telemetrically instrumented patients will be necessary to gain an in-depth understanding of the influence of specific sports activities on biomechanical conditions and consequences on a tissue level, such as at the implant–bone interface, in the various age groups.

Mobility and sports activity are vital for patients with THA to achieve a balanced life and to meet their expectations. Several reviews have shown a trend toward increased self-reported sport activities with increasing intensity (Schmidutz et al., 2012; Bonnin et al., 2018; Hoorntje et al., 2018). Patients performing judo (Lefevre et al., 2013) and jogging (Abe et al., 2014) and many other sports activities were not at all covered (Schmidutz et al., 2012; Bonnin et al., 2018).

With this overview, we aimed to open a debate on the current postoperative recommendations. The data on *in vivo* loads, specifically the increased torsional torque in working age patients and its further increase even in the so-called low-impact sports activities, make it necessary to revisit the current "guidelines" for RTS after THA. Our measurements suggest that only swimming and cycling are at load levels below those of ADL and can be considered "low impact" in any postoperative setting. Only such activities should be "recommended" to those patients in whom a low-impact sport appears to be necessary. In all other activities, we found load levels higher than those experienced during ADL. *In vivo* loads during work were mostly unknown, but it can be supposed that these loads may be reflected in some of the sport activities that we were able to measure, especially for the working age patients.

The calculated revision risk (Bayliss et al., 2017) for patients <60 years at primary surgery appeared to be up to 35%, resulting in younger patients also having an increased re-revision risk (Lübbeke et al., 2007; Ben-Shlomo et al., 2019), while the lifetime risk for patients >70 years was much lower (1%–6%) (Bayliss et al., 2017). With further increases in other factors, such as activity level, number of patients working after surgery, and life expectancy, it can be expected that the lifetime risk of revision for younger patients may even be higher. Consequently, the revision and re-revision numbers are expected to rise further in the next decade.

From a biomechanical perspective, THA, as the ultimate solution, should be delayed as much as possible, taking into account the consequences of OA such as pain (Vergara et al., 2011), impact on ADL (Palazzo et al., 2016; Clynes et al., 2019), mental well-being (Vina and Kwoh, 2018), and the risk of all-cause mortality (Palazzo et al., 2016; Kendzerska et al., 2018). If THA cannot be delayed in a patient, we propose reconsidering the current recommendations critically and making patients aware of the risk of potential implant loosening during full return to sports. Moreover, recommendations of sportive activities should be mainly focused on low-impact activities, as indicated here. If patients have to do heavy physical work or are nevertheless interested in intermediate-/high-impact sports, they should be aware of the implications this may have on the longevity of THA. The findings from this paper and the data from http://www.OrthoLoad.com may help guide patient expectations.

Various registries revealed higher revision rates for younger patients than for older patients. Patients today come with higher expectations, and current recommendations suggesting RTS activity showed that the contact force and torsional torque values were increased in younger (working age) compared to older (retirement age) patients for daily and sporting activities. If patients engage in intermediate- or high-impact sports despite being informed of the implications, they have to be closely monitored clinically and radiologically. Further study of the biomechanical loading in sports and work is needed.

DATA AVAILABILITY STATEMENT

The datasets presented in this study can be found in online repositories. The names of the repository/repositories and accession number(s) can be found below: https://orthoload.com/database/.

ETHICS STATEMENT

The studies involving human participants were reviewed and approved by the Etikkomission Charité—Universitätsmedizin Berlin. The patients/participants provided written informed consent to participate in this study.

AUTHOR CONTRIBUTIONS

PD and GD contributed to the conception and design of the study. AB evaluated the data, performed the statistical analysis, and wrote the first draft of the manuscript. HH contributed to clinical relevance of the manuscript. All authors contributed to manuscript revision, read, and approved the submitted version.

FUNDING

This work was supported by the German Research Society (DA 1786/5-1), the German Federal Ministry of Education and Research (BMBF 01EC1905D, BMBF—workHealth, Subproject 3), and the OrthoLoadClub.

SUPPLEMENTARY MATERIAL

The Supplementary Material for this article can be found online at: https://www.frontiersin.org/articles/10.3389/fbioe.2022.789629/full#supplementary-material

REFERENCES

Abe, H., Sakai, T., Nishii, T., Takao, M., Nakamura, N., and Sugano, N. (2014). Jogging after Total Hip Arthroplasty. *Am. J. Sports Med.* 42 (1), 131–137. doi:10.1177/0363546513506866

Arbuthnot, J. E., McNicholas, M. J., Dashti, H., and Hadden, W. A. (2007). Total Hip Arthroplasty and the Golfer. *The J. Arthroplasty* 22 (4), 549–552. doi:10.1016/j.arth.2006.05.030

Australian Orthopaedic Association National Joint Replacement Registry (AOANJRR) (2019). *Hip, Knee & Shoulder Arthroplasty-Annual Report 2019*. Adelaide: AOA. Available at: https://aoanjrr.sahmri.com/annual-reports-2019.

Bashinskaya, B., Zimmerman, R. M., Walcott, B. P., and Antoci, V. (2012). Arthroplasty Utilization in the United States Is Predicted by Age-specific Population Groups. *ISRN Orthopedics* 2012, 1–8. doi:10.5402/2012/185938

Batailler, C., Rozinthe, A., Mercier, M., Bankhead, C., Gaillard, R., and Lustig, S. (2019). Return to Sport after Bilateral Single Stage Total Hip Arthroplasty Using the Direct Anterior Approach: A Case Control Study. *J. Arthroplasty* 34 (12), 2972–2977. doi:10.1016/j.arth.2019.06.054

Bayliss, L. E., Culliford, D., Monk, A. P., Glyn-Jones, S., Prieto-Alhambra, D., Judge, A., et al. (2017). The Effect of Patient Age at Intervention on Risk of Implant Revision after Total Replacement of the Hip or Knee: A Population-Based Cohort Study. *The Lancet* 389 (10077), 1424–1430. doi:10.1016/S0140-6736(17)30059-4

Ben-Shlomo, Y., Blom, A., Boulton, C., Brittain, R., Clark, E., Craig, R., et al. (2019). National Joint Registry for England, Wales, Northern Ireland and the Isle of Man - 2019 16th Annual Report. Available at: www.njrreports.org.uk.

Bergmann, G., Bender, A., Dymke, J., Duda, G., and Damm, P. (2016). Standardized Loads Acting in Hip Implants. *PLOS ONE* 11 (5), e0155612. doi:10.1371/journal.pone.0155612

Bergmann, G., Bender, A., Dymke, J., Duda, G. N., and Damm, P. (2018a). Physical Activities that Cause High Friction Moments at the Cup in Hip Implants. *J. Bone Jt. Surg.* 100 (19), 1637–1644. doi:10.2106/JBJS.17.01298

Bergmann, G., Graichen, F., and Rohlmann, A. (1998). "Loads Acting at the Hip Joint," in *Hip Surgery. Materials and Developments*, Editor M. E. Cabanela (London, United Kingdom: Dunitz Ltd), 1–8.

Bergmann, G., Graichen, F., and Rohlmann, A. (1993). Hip Joint Loading during Walking and Running, Measured in Two Patients. *J. Biomech.* 26 (8), 969–990. doi:10.1016/0021-9290(93)90058-M

Bergmann, G., Graichen, F., Rohlmann, A., Bender, A., Heinlein, B., Duda, G. N., et al. (2010). Realistic Loads for Testing Hip Implants. *Bio-Medical Mater. Eng.* 20 (2), 65–75. doi:10.3233/BME-2010-0616

Bergmann, G., Graichen, F., Siraky, J., Jendrzynski, H., and Rohlmann, A. (1988). Multichannel Strain Gauge Telemetry for Orthopaedic Implants. *J. Biomech.* 21 (2), 169–176. doi:10.1016/0021-9290(88)90009-7

Bergmann, G., Kutzner, I., Bender, A., Dymke, J., Trepczynski, A., Duda, G. N., et al. (2018b). Loading of the Hip and Knee Joints during Whole Body Vibration Training. *PLOS ONE* 13 (12), e0207014. doi:10.1371/journal.pone.0207014

Boersma, A. R., Brouwer, S., Koolhaas, W., Brouwer, R. W., Zijlstra, W. P., Van Beveren, J., et al. (2019). No Association between Preoperative Physical Activity Level and Time to Return to Work in Patients after Total Hip or Knee Arthroplasty: A Prospective Cohort Study. *PLoS ONE* 14 (9), e0221932–13. doi:10.1371/journal.pone.0221932

Bohannon, R. W. (2007). Number of Pedometer-Assessed Steps Taken Per Day by Adults: A Descriptive Meta-Analysis. *Phys. Ther.* 87 (12), 1642–1650. doi:10.2522/ptj.20060037

Bohm, E. R. (2010). The Effect of Total Hip Arthroplasty on Employment. *J. Arthroplasty* 25 (1), 15–18. doi:10.1016/j.arth.2008.11.011

Bonnin, M. P., Rollier, J.-C., Chatelet, J.-C., Ait-Si-Selmi, T., Chouteau, J., Jacquot, L., et al. (2018). Can Patients Practice Strenuous Sports after Uncemented Ceramic-On-Ceramic Total Hip Arthroplasty? *Orthopaedic J. Sports Med.* 6 (4), 232596711876392–232596711876398. doi:10.1177/2325967118763920

BQS - Bundesgeschäftsstelle Qualitätssicherung gGmbH. (2009). *BQS-bundesauswertung 2008 Hüft-Endoprothesen-Erstimplantation Qualitätsindikatoren*. Available at: https://sqg.de/upload/CONTENT/Qualitaetsberichte/2008/.

Bradley, B. M., Moul, S. J., Doyle, F. J., and Wilson, M. J. (2017). Return to Sporting Activity after Total Hip Arthroplasty-A Survey of Members of the British Hip Society. *J. Arthroplasty* 32 (3), 898–902. doi:10.1016/j.arth.2016.09.019

Buirs, L. D., Van Beers, L. W. A. H., Scholtes, V. A. B., Pastoors, T., Sprague, S., Poolman, R. W., et al. (2016). Predictors of Physical Functioning after Total Hip Arthroplasty: A Systematic Review. *BMJ Open* 6 (9), e010725. doi:10.1136/bmjopen-2015-010725

Burke, N. G., Gibbons, J. P., Cassar-Gheiti, A. J., Walsh, F. M., and Cashman, J. P. (2019). Total Hip Replacement-The Cause of Failure in Patients under 50 Years Old? *Ir J. Med. Sci.* 188 (3), 879–883. doi:10.1007/s11845-018-01956-8

Canadian Institute for Health Information (2019). "Hip and Knee Replacements in Canada - Canadian Joint Replacement Registry (CJRR) 2017-2019 Annual Report." in *Canadian Joint Replacement Registry (CJRR)*. Available at: https://www.cihi.ca/en/canadian-joint-replacement-registry-cjrr.

Charnley, J. (1979). *Low Friction Arthroplasty of the Hip*. Berlin, Germany: Springer Berlin Heidelberg. doi:10.1007/978-3-642-67013-8

Chatterji, U., Ashworth, M. J., Lewis, P. L., Dobson, P. J., Chatterji, U., Ashworth, M. J., et al. (2004). Effect of Total Hip Arthroplasty on Recreational and Sporting Activity. *ANZ J. Surg.* 74 (6), 446–449. doi:10.1111/j.1445-1433.2004.03028.x

Chiu, S.-L., Chang, C.-C., Dennerlein, J. T., and Xu, X. (2015). Age-Related Differences in Inter-joint Coordination during Stair Walking Transitions. *Gait & Posture* 42 (2), 152–157. doi:10.1016/j.gaitpost.2015.05.003

Clyde, C. T., Goyal, N., Matar, W. Y., Witmer, D., Restrepo, C., and Hozack, W. J. (2013). Workers' Compensation Patients after Total Joint Arthroplasty. *J. Arthroplasty* 28 (6), 883–887. doi:10.1016/j.arth.2013.01.036

Clynes, M. A., Jameson, K. A., Edwards, M. H., Cooper, C., and Dennison, E. M. (2019). Impact of Osteoarthritis on Activities of Daily Living: Does Joint Site Matter? *Aging Clin. Exp. Res.* 31 (8), 1049–1056. doi:10.1007/s40520-019-01163-0

Culliford, D., Maskell, J., Judge, A., Cooper, C., Prieto-Alhambra, D., and Arden, N. K. (2015). Future Projections of Total Hip and Knee Arthroplasty in the UK: Results from the UK Clinical Practice Research Datalink. *Osteoarthritis and Cartilage* 23 (4), 594–600. doi:10.1016/j.joca.2014.12.022

Cutler, D., Deaton, A., and Lleras-Muney, A. (2006). The Determinants of Mortality. *J. Econ. Perspect.* 20 (3), 97–120. doi:10.1257/jep.20.3.97

Damm, P., Dymke, J., Bender, A., Duda, G., and Bergmann, G. (2017). *In Vivo* Hip Joint Loads and Pedal Forces during Ergometer Cycling. *J. Biomech.* 60, 197–202. doi:10.1016/j.jbiomech.2017.06.047

Damm, P., Graichen, F., Rohlmann, A., Bender, A., and Bergmann, G. (2010). Total Hip Joint Prosthesis for *In Vivo* Measurement of Forces and Moments. *Med. Eng. Phys.* 32 (1), 95–100. doi:10.1016/j.medengphy.2009.10.003

Damm, P., Zonneveld, J., Brackertz, S., Streitparth, F., and Winkler, T. (2018). Gluteal Muscle Damage Leads to Higher *In Vivo* Hip Joint Loads 3 Months after Total Hip Arthroplasty. *PLOS ONE* 13 (1), e0190626. doi:10.1371/journal.pone.0190626

Danielsson, L. (1965). Arthroplasty of the Hip According to Thompson and Moore. *Acta Orthopaedica Scand.* 35 (1–4), 348–357. doi:10.3109/17453676508989365

Danish Hip Arthroplasty Register (2020). The Danish Hip Arthroplasty Register (DHR), 2019 National Annual Report. Available at: http://www.dhr.dk.

Del Piccolo, N., Carubbi, C., Mazzotta, A., Sabbioni, G., Filanti, M., Stagni, C., et al. (2016). Return to Sports Activity with Short Stems or Standard Stems in Total Hip Arthroplasty in Patients Less Than 50 Years Old. *HIP Int.* 26 (Suppl. 1), S48–S51. doi:10.5301/hipint.5000404

Drobniewski, M., Borowski, A., Krasińska, M., Sibiński, M., and Synder, M. (2017). Return to Work after Surgical Treatment of Coxarthrosis by Total Cementless Hip Arthroplasty. *Ortop Traumatol. Rehabil.* 19 (4), 349–360. doi:10.5604/01.3001.0010.4644

Dubs, L., Gschwend, N., and Munzinger, U. (1983). Sport after Total Hip Arthroplasty. *Arch. Orth. Traum. Surg.* 101 (3), 161–169. doi:10.1007/bf00436765

Dutch Arthroplasty Register (LROI) (2019). Online LROI Annual Report 2019. Available at: www.lroi-report.

Finnish Arthroplasty Register for National Institute of Health And Welfare (2020). Finnish Arthroplasty Register - ENDOnet. Available at: https://www.thl.fi/far/#index.

Finucane, M. M., Stevens, G. A., Cowan, M. J., Danaei, G., Lin, J. K., Paciorek, C. J., et al. (2011). National, Regional, and Global Trends in Body-Mass index since 1980: Systematic Analysis of Health Examination Surveys and Epidemiological

Studies with 960 Country-Years and 9·1 Million Participants. *The Lancet* 377 (9765), 557–567. doi:10.1016/S0140-6736(10)62037-5

Franke, H., Berg, A., Halle, M., Mayer, F., Nowacki, P., Predel, G., et al. (2006). Bewegung Und Sport Mit Endoprothese. *Deutsche Z. Für Sportmedizin* 57 (7/8), VII–VIII.

Gandhi, R., Dhotar, H., Davey, J. R., and Mahomed, N. N. (2010). Predicting the Longer-Term Outcomes of Total Hip Replacement. *J. Rheumatol.* 37 (12), 2573–2577. doi:10.3899/jrheum.100149

Ghomrawi, H. M. K., Dolan, M. M., Rutledge, J., and Alexiades, M. M. (2011). Recovery Expectations of Hip Resurfacing Compared to Total Hip Arthroplasty: A Matched Pairs Study. *Arthritis Care Res.* 63 (12), 1753–1757. doi:10.1002/acr.20626

Global Recommendations on Physical Activity for Health (2012). World Health Organization. Vol. 66, Available at: http://apps.who.int//44399.

Graichen, F., Arnold, R., Rohlmann, A., and Bergmann, G. (2007). Implantable 9-Channel Telemetry System for *In Vivo* Load Measurements with Orthopedic Implants. *IEEE Trans. Biomed. Eng.* 54 (2), 253–261. doi:10.1109/TBME.2006.886857

Graichen, F., Bergmann, G., and Rohlmann, A. (1999). Hip Endoprosthesis for *In Vivo* Measurement of Joint Force and Temperature. *J. Biomech.* 32 (10), 1113–1117. doi:10.1016/S0021-9290(99)00110-4

Haffer, H., Popovic, S., Martin, F., Hardt, S., Winkler, T., and Damm, P. (2021). *In Vivo* Loading on the Hip Joint in Patients with Total Hip Replacement Performing Gymnastics and Aerobics Exercises. *Sci. Rep.* 11 (1), 13395. doi:10.1038/s41598-021-92788-7

Hales, C. M., Carroll, M. D., Fryar, C. D., and Ogden, C. L. (2017). Prevalence of Obesity Among Adults and Youth: United States, 2015-2016. *NCHS Data Brief* 288. 18, Available at: https://www.cdc.gov/nchs/products/databriefs/db288.htm.

Hara, D., Hamai, S., Komiyama, K., Motomura, G., Shiomoto, K., and Nakashima, Y. (2018). Sports Participation in Patients after Total Hip Arthroplasty vs Periacetabular Osteotomy: A Propensity Score-Matched Asian Cohort Study. *J. Arthroplasty* 33 (2), 423–430. doi:10.1016/j.arth.2017.08.035

Haskell, W. L., Lee, I.-M., Pate, R. R., Powell, K. E., Blair, S. N., Franklin, B. A., et al. (2007). Physical Activity and Public Health. *Med. Sci. Sports Exerc.* 39 (8), 1423–1434. doi:10.1249/mss.0b013e3180616b27

Healy, W. L., Iorio, R., and Lemos, M. J. (2001). Athletic Activity after Joint Replacement. *Am. J. Sports Med.* 29 (3), 377–388. doi:10.1177/03635465010290032301

Healy, W. L., Sharma, S., Schwartz, B., and Iorio, R. (2008). Athletic Activity after Total Joint Arthroplasty. *The J. Bone Jt. Surgery-American Volume* 90 (10), 2245–2252. doi:10.2106/JBJS.H.00274

Heller, M. O., Bergmann, G., Deuretzbacher, G., Claes, L., Haas, N. P., and Duda, G. N. (2001). Influence of Femoral Anteversion on Proximal Femoral Loading: Measurement and Simulation in Four Patients. *Clin. Biomech.* 16 (8), 644–649. doi:10.1016/S0268-0033(01)00053-5

Hepinstall, M. S., Rutledge, J. R., Bornstein, L. J., Mazumdar, M., and Westrich, G. H. (2011). Factors that Impact Expectations before Total Knee Arthroplasty. *J. Arthroplasty* 26 (6), 870–876. doi:10.1016/j.arth.2010.09.010

Hoorntje, A., Janssen, K. Y., Bolder, S. B. T., Koenraadt, K. L. M., Daams, J. G., Blankevoort, L., et al. (2018). The Effect of Total Hip Arthroplasty on Sports and Work Participation: A Systematic Review and Meta-Analysis. *Sports Med.* 48 (7), 1695–1726. doi:10.1007/s40279-018-0924-2

Hortobágyi, T., Finch, A., Solnik, S., Rider, P., DeVita, P., Hortobagyi, T., et al. (2011). Association between Muscle Activation and Metabolic Cost of Walking in Young and Old Adults. *Journals Gerontol. Ser. A: Biol. Sci. Med. Sci.* 66A (5), 541–547. doi:10.1093/gerona/glr008

Huch, K., Müller, K. A. C., Stürmer, T., Brenner, H., Puhl, W., Günther, K. P., et al. (2005). Sports Activities 5 Years after Total Knee or Hip Arthroplasty: The Ulm Osteoarthritis Study. *Ann. Rheum. Dis.* 64 (12), 1715–1720. doi:10.1136/ard.2004.033266

Innmann, M. M., Weiss, S., Andreas, F., Merle, C., and Streit, M. R. (2016). Sports and Physical Activity after Cementless Total Hip Arthroplasty with a Minimum Follow-Up of 10 Years. *Scand. J. Med. Sci. Sports* 26 (5), 550–556. doi:10.1111/sms.12482

IQTIG – Institut für Qualitätssicherung und Transparenz im Gesundheitswesen (2018). Bundesauswertung Zum Erfassungsjahr 2017 Hüftendoprothesenversorgung Impressum. Available at: https://www.iqtig.org.

Jakubowitz, E., Seeger, J. B., Kretzer, J. P., Heisel, C., Kleinhans, J. A., and Thomsen, M. (2009). The Influence of Age, Bone Quality and Body Mass Index on Periprosthetic Femoral Fractures: A Biomechanical Laboratory Study. *Med. Sci. Monit.* 15 (11), BR307–12. Available at: http://www.ncbi.nlm.nih.gov/pubmed/19865047.

Jassim, S. S., Douglas, S. L., and Haddad, F. S. (2014). Athletic Activity after Lower Limb Arthroplasty. *Bone Jt. J.* 96-B (7), 923–927. doi:10.1302/0301-620X.96B7.31585

Jassim, S. S., Tahmassebi, J., Haddad, F. S., and Robertson, A. (2019). Return to Sport after Lower Limb Arthroplasty - Why Not for All?. *Wjo* 10 (2), 90–100. doi:10.5312/wjo.v10.i2.90

Jenkins, P. J., Clement, N. D., Hamilton, D. F., Gaston, P., Patton, J. T., and Howie, C. R. (2013). Predicting the Cost-Effectiveness of Total Hip and Knee Replacement. *Bone Jt. J.* 95-B (1), 115–121. doi:10.1302/0301-620X.95B1.29835

Johnsson, R., and Persson, B. M. (1986). Occupation after Hip Replacement for Arthrosis. *Acta Orthopaedica Scand.* 57 (3), 197–200. doi:10.3109/17453678608994374

Judge, A., Cooper, C., Arden, N. K., Williams, S., Williams, S., Hobbs, N., et al. (2011). Pre-Operative Expectation Predicts 12-Month Post-Operative Outcome Among Patients Undergoing Primary Total Hip Replacement in European Orthopaedic Centres. *Osteoarthritis and Cartilage* 19 (6), 659–667. doi:10.1016/j.joca.2011.03.009

Junnila, M., Laaksonen, I., Eskelinen, A., Pulkkinen, P., Ivar Havelin, L., Furnes, O., et al. (2016). Implant Survival of the Most Common Cemented Total Hip Devices from the Nordic Arthroplasty Register Association Database. *Acta Orthopaedica* 87 (6), 546–553. doi:10.1080/17453674.2016.1222804

Karampinas, P. K., Papadelis, E. G., Vlamis, J. A., Basiliadis, H., and Pneumaticos, S. G. (2017). Comparing Return to Sport Activities after Short Metaphyseal Femoral Arthroplasty with Resurfacing and Big Femoral Head Arthroplasties. *Eur. J. Orthop. Surg. Traumatol.* 27 (5), 617–622. doi:10.1007/s00590-016-1897-1

Kendzerska, T., King, L. K., Lipscombe, L., Croxford, R., Stanaitis, I., and Hawker, G. A. (2018). The Impact of Hip and Knee Osteoarthritis on the Subsequent Risk of Incident Diabetes: A Population-Based Cohort Study. *Diabetologia* 61 (11), 2290–2299. doi:10.1007/s00125-018-4703-2

Kleim, B. D., Malviya, A., Rushton, S., Bardgett, M., and Deehan, D. J. (2015). Understanding the Patient-Reported Factors Determining Time Taken to Return to Work after Hip and Knee Arthroplasty. *Knee Surg. Sports Traumatol. Arthrosc.* 23 (12), 3646–3652. doi:10.1007/s00167-014-3265-1

Klein, G. R., Levine, B. R., Hozack, W. J., Strauss, E. J., Hozack, W. J., Strauss, E. J., et al. (2007). Return to Athletic Activity after Total Hip Arthroplasty. *J. Arthroplasty* 22 (2), 171–175. doi:10.1016/j.arth.2006.09.001

Koenen, P., Bäthis, H., Schneider, M. M., Fröhlich, M., Bouillon, B., and Shafizadeh, S. (2014). How Do We Face Patients' Expectations in Joint Arthroplasty?. *Arch. Orthop. Trauma Surg.* 134 (7), 925–931. doi:10.1007/s00402-014-2012-x

Krischak, G., Kaluscha, R., Kraus, M., Tepohl, L., Nusser, M., and Nusser, M. (2013). Rückkehr in das Erwerbsleben nach Hüfttotalendoprothese. *Unfallchirurg* 116 (8), 755–759. doi:10.1007/s00113-013-2424-z

Kuijer, P. P. F. M., De Beer, M. J. P. M., Houdijk, J. H. P., and Frings-Dresen, M. H. W. (2009). Beneficial and Limiting Factors Affecting Return to Work after Total Knee and Hip Arthroplasty: A Systematic Review. *J. Occup. Rehabil.* 19 (4), 375–381. doi:10.1007/s10926-009-9192-1

Kuijpers, M. F. L., Hannink, G., van Steenbergen, L. N., Schreurs, B. W., and Schreurs, B. W. (2020). Outcome of Revision Hip Arthroplasty in Patients Younger Than 55 years: An Analysis of 1,037 Revisions in the Dutch Arthroplasty Register. *Acta Orthopaedica* 91, 165–170. doi:10.1080/17453674.2019.1708655

Kurtz, S. M., Lau, E., Ong, K., Zhao, K., Kelly, M., Bozic, K. J., et al. (2009). Future Young Patient Demand for Primary and Revision Joint Replacement: National Projections from 2010 to 2030. *Clin. Orthopaedics Relat. Research®* 467 (10), 2606–2612. doi:10.1007/s11999-009-0834-6

Kurtz, S., Ong, K., Lau, E., Mowat, F., and Halpern, M. (2007). Projections of Primary and Revision Hip and Knee Arthroplasty in the United States from 2005 to 2030. *J. Bone Jt. Surg.* 89 (4), 780–785. doi:10.2106/JBJS.F.00222

Kutzner, I., Richter, A., Gordt, K., Dymke, J., Damm, P., Duda, G. N., et al. (2017). Does Aquatic Exercise Reduce Hip and Knee Joint Loading? *In Vivo* Load Measurements with Instrumented Implants. *PLoS ONE* 12 (3), e0171972–14. doi:10.1371/journal.pone.0171972

Laasik, R., Lankinen, P., Kivimäki, M., Aalto, V., Saltychev, M., Mäkelä, K., et al. (2019). Return to Work after Primary Total Hip Arthroplasty: A Nationwide Cohort Study. *Acta Orthopaedica* 90 (3), 209–213. doi:10.1080/17453674.2019.1591081

Laursen, M. K., Andersen, J. B., Andersen, M. M., Simonsen, O. H., and Laursen, M. B. (2014). Danish Surgeons Allow the Most Athletic Activities after Total Hip and Knee Replacement. *Eur. J. Orthop. Surg. Traumatol.* 24 (8), 1571–1577. doi:10.1007/s00590-014-1442-z

Learmonth, I. D., Young, C., and Rorabeck, C. (2007). The Operation of the Century: Total Hip Replacement. *The Lancet* 370 (9597), 1508–1519. doi:10.1016/S0140-6736(07)60457-7

Lefevre, N., Rousseau, D., Bohu, Y., Klouche, S., and Herman, S. (2013). Return to Judo after Joint Replacement. *Knee Surg. Sports Traumatol. Arthrosc.* 21 (12), 2889–2894. doi:10.1007/s00167-012-2064-9

Leichtenberg, C., Tilbury, C., Kuijer, P., Verdegaal, S., Wolterbeek, R., Nelissen, R., et al. (2016). Determinants of Return to Work 12 Months after Total Hip and Knee Arthroplasty. *Annals* 98 (6), 387–395. doi:10.1308/rcsann.2016.0158

Lübbeke, A., Katz, J. N., Perneger, T. V., Hoffmeyer, P., Lübbeke, A., Katz, J. N., et al. (2007). Primary and Revision Hip Arthroplasty: 5-Year Outcomes and Influence of Age and Comorbidity. *J. Rheumatol.* 34 (2), 394–400. [Epub ahead of print].

Mancuso, C. A., Jout, J., Salvati, E. A., and Sculco, T. P. (2009). Fulfillment of Patients' Expectations for Total Hip Arthroplasty. *J. Bone Jt. Surgery-American Volume* 91 (9), 2073–2078. doi:10.2106/JBJS.H.01802

Mancuso, C. A., Wentzel, C. H., Ghomrawi, H. M. K., and Kelly, B. T. (2017). Hip Preservation Surgery Expectations Survey: A New Method to Measure Patients' Preoperative Expectations. *Arthrosc. J. Arthroscopic Relat. Surg.* 33 (5), 959–968. doi:10.1016/j.arthro.2016.11.012

McGrory, B. J., Stuart, M. J., and Sim, F. H. (1995). Participation in Sports after Hip and Knee Arthroplasty: Review of Literature and Survey of Surgeon Preferences. *Mayo Clinic Proc.* 70 (4), 342–348. doi:10.4065/70.4.342

Meester, S. B., Wagenmakers, R., van den Akker-Scheek, I., and Stevens, M. (2018). Sport Advice Given by Dutch Orthopaedic Surgeons to Patients after a Total Hip Arthroplasty or Total Knee Arthroplasty. *PLoS ONE* 13 (8), e0202494–12. doi:10.1371/journal.pone.0202494

Mobasheri, R., Gidwani, S., and Rosson, J. (2006). The Effect of Total Hip Replacement on the Employment Status of Patients under the Age of 60 Years. *annals* 88 (2), 131–133. doi:10.1308/003588406X95129

Mont, M. A., Laporte, D. M., Mullick, T., Silberstein, C. E., and Hungerford, D. S. (1999). Tennis after Total Hip Arthroplasty. *Am. J. Sports Med.* 27 (1), 60–64. doi:10.1177/03635465990270011801

Naal, F. D., and Impellizzeri, F. M. (2010). A Systematic Review, Florian D Naal, and Franco M ImpellizzeriHow Active Are Patients Undergoing Total Joint Arthroplasty?: A Systematic Review. *Clin. Orthopaedics Relat. Research®* 468 (7), 1891–1904. doi:10.1007/s11999-009-1135-9

NCD Risk Factor Collaboration (2016). Trends in Adult Body-Mass Index in 200 Countries from 1975 to 2014: A Pooled Analysis of 1698 Population-Based Measurement Studies with 19·2 Million Participants. *The Lancet* 387 (10026), 1377–1396. doi:10.1016/S0140-6736(16)30054-X

Nemes, S., Gordon, M., Rogmark, C., and Rolfson, O. (2014). Projections of Total Hip Replacement in Sweden from 2013 to 2030. *Acta Orthopaedica* 85 (3), 238–243. doi:10.3109/17453674.2014.913224

Nevitt, M. C., Epstein, W. V., Masem, M., and Murray, W. R. (1984). Work Disability before and after Total Hip Arthroplasty. *Arthritis Rheum.* 27 (4), 410–421. doi:10.1002/art.1780270408

Norwegian National Advisory Unit Report on Arthoplasty and Hip Fractures (2019). *Norwegian National Advisory Unit Report on Arthoplasty and Hip Fractures 2019*.

Novak, A. C., and Brouwer, B. (2011). Sagittal and Frontal Lower Limb Joint Moments during Stair Ascent and Descent in Young and Older Adults. *Gait & Posture* 33 (1), 54–60. doi:10.1016/j.gaitpost.2010.09.024

Nunley, R. M., Ruh, E. L., Zhang, Q., Della Valle, C. J., Engh, C. A., Parvizi, J., et al. (2011). Do Patients Return to Work after Hip Arthroplasty Surgery. *J. Arthroplasty* 26 (Suppl. 6), 92–98. doi:10.1016/j.arth.2011.03.038

Oehler, N., Schmidt, T., and Niemeier, A. (2016). Endoprothetischer Gelenkersatz Und Sport. *Sportverletz Sportschaden* 30 (04), 195–203. doi:10.1055/s-0042-119109

Ortmaier, R., Pichler, H., Hitzl, W., Emmanuel, K., Mattiassich, G., Plachel, F., et al. (2017). Return to Sport after Short-Stem Total Hip Arthroplasty. *Clin. J. Sport Med.* Publish Ahead of Print (6), 451–458. doi:10.1097/JSM.0000000000000532

Pabinger, C., and Geissler, A. (2014). Utilization Rates of Hip Arthroplasty in OECD Countries. *Osteoarthritis and Cartilage* 22 (6), 734–741. doi:10.1016/j.joca.2014.04.009

Palazzo, C., Nguyen, C., Lefevre-Colau, M.-M., Rannou, F., and Poiraudeau, S. (2016). Risk Factors and Burden of Osteoarthritis. *Ann. Phys. Rehabil. Med.* 59 (3), 134–138. doi:10.1016/j.rehab.2016.01.006

Pilz, V., Hanstein, T., and Skripitz, R. (2018). Projections of Primary Hip Arthroplasty in Germany until 2040. *Acta Orthopaedica* 89 (3), 308–313. doi:10.1080/17453674.2018.1446463

Pop, T., Czenczek-Lewandowska, E., Lewandowski, B., Leszczak, J., Podgórska-Bednarz, J., and Baran, J. (2016). Occupational Activity in Patients 10 Years after Hip Replacement Surgery. *Ortop Traumatol. Rehabil.* 18 (4), 327–336. doi:10.5604/15093492.1220824

Raguet, M., Pierson, C., and Pierson, A. (2015). La course à pied " hors norme » est-elle possible avec une prothèse totale de hanche ?. *J. de Traumatologie Du Sport* 32 (1), 3–14. doi:10.1016/j.jts.2015.01.005

Rajaee, S. S., Campbell, J. C., Mirocha, J., and Paiement, G. D. (2018). Increasing Burden of Total Hip Arthroplasty Revisions in Patients between 45 and 64 Years of Age. *J. Bone Jt. Surg.* 100 (6), 449–458. doi:10.2106/JBJS.17.00470

R Core Team (2021). *R: A Language and Environment for Statistical Computing*. Vienna, Austria: R Foundation for Statistical Computing. Available at: https://www.R-project.org/.

Reeves, N. D., Spanjaard, M., Mohagheghi, A. A., Baltzopoulos, V., and Maganaris, C. N. (2009). Older Adults Employ Alternative Strategies to Operate within Their Maximum Capabilities when Ascending Stairs. *J. Electromyogr. Kinesiol.* 19 (2), e57–e68. doi:10.1016/j.jelekin.2007.09.009

Ritter, M. A., and Meding, J. B. (1987). Total Hip Arthroplasty: Can the Patient Play Sports Again?. *Orthopedics* 10 (10), 1447–1452. doi:10.3928/0147-7447-19871001-15

Roser, M. (2019). Life Expectancy." Published Online at OurWorldInData.Org. Available at: https://ourworldindata.org/life-expectancy.

Sankar, A., Davis, A. M., Palaganas, M. P., Beaton, D. E., Badley, E. M., Palaganas, M. P., et al. (2013). Return to Work and Workplace Activity Limitations Following Total Hip or Knee Replacement. *Osteoarthritis and Cartilage* 21 (10), 1485–1493. doi:10.1016/j.joca.2013.06.005

Schmidutz, F., Grote, S., Pietschmann, M., Weber, P., Mazoochian, F., Fottner, A., et al. (2012). Sports Activity after Short-Stem Hip Arthroplasty. *Am. J. Sports Med.* 40 (2), 425–432. doi:10.1177/0363546511424386

Schneider, P. L., Bassett, D. R., Thompson, D. L., Pronk, N. P., and Bielak, K. M. (2006). Effects of a 10,000 Steps Per Day Goal in Overweight Adults. *Am. J. Health Promot.* 21 (2), 85–89. doi:10.4278/0890-1171-21.2.85

Scott, C. E. H., Bugler, K. E., Clement, N. D., MacDonald, D., Howie, C. R., and Biant, L. C. (2012). Patient Expectations of Arthroplasty of the Hip and Knee. *The J. Bone Jt. Surg. Br. volume* 94-B (7), 974–981. doi:10.1302/0301-620X.94B7.28219

Sloan, M., Premkumar, A., and Sheth, N. P. (2018). Projected Volume of Primary Total Joint Arthroplasty in the u.s., 2014 to 2030. *J. Bone Jt. Surg.* 100 (17), 1455–1460. doi:10.2106/JBJS.17.01617

Suarez, J., Arguelles, J., Costales, M., Arechaga, C., Cabeza, F., and Vijande, M. (1996). Factors Influencing the Return to Work of Patients after Hip Replacement and Rehabilitation. *Arch. Phys. Med. Rehabil.* 77 (3), 269–272. doi:10.1016/S0003-9993(96)90110-0

Suckel, A., and Best, R. (2006). Der Golfsport mit Hüft- und Knietotalendoprothesen. *Sportverletz Sportschaden* 20 (3), 127–131. doi:10.1055/s-2006-926996

Swanson, E. A., Schmalzried, T. P., and Dorey, F. J. (2009). Activity Recommendations after Total Hip and Knee Arthroplasty. *J. Arthroplasty* 24 (6), 120–126. doi:10.1016/j.arth.2009.05.014

Swarup, I., Lee, Y.-y., Chiu, Y.-f., Sutherland, R., Shields, M., and Figgie, M. P. (2018). Implant Survival and Patient-Reported Outcomes after Total Hip Arthroplasty in Young Patients. *J. Arthroplasty* 33 (9), 2893–2898. doi:10.1016/j.arth.2018.04.016

Swedish Hip Arthroplasty Register (2019). *Swedish Hip Arthroplasty Register Annual Report 2018*. doi:10.18158/H1BdmrOWu

Tilbury, C., Holtslag, M. J., Tordoir, R. L., Leichtenberg, C. S., Verdegaal, S. H. M., Kroon, H. M., et al. (2016). Outcome of Total Hip Arthroplasty, but Not of Total Knee Arthroplasty, Is Related to the Preoperative Radiographic Severity of Osteoarthritis. *Acta Orthopaedica* 87 (1), 67–71. doi:10.3109/17453674.2015.1092369

Tilbury, C., Schaasberg, W., Plevier, J. W. M., Fiocco, M., Nelissen, R. G. H. H., Vliet Vlieland, T. P. M., et al. (2014). Return to Work after Total Hip and Knee Arthroplasty: A Systematic Review. *Rheumatology* 53 (3), 512–525. doi:10.1093/rheumatology/ket389

Truszczyńska, A., Rąpała, K., Tarnowski, A., and Kucharczyk, W. (2013). Analysis of Factors Influencing Return to Work after Total Hip Arthroplasty. *Ortop Traumatol. Rehabil.* 15 (5), 459–467. doi:10.5604/15093492.1084360

Tudor-Locke, C., Hatano, Y., Pangrazi, R. P., and Kang, M. (2008). Revisiting "How Many Steps Are Enough?. *Med. Sci. Sports Exerc.* 40 (Suppl. ment), S537–S543. doi:10.1249/MSS.0b013e31817c7133

United Kingdom National Joint Registry (2017). National Joint Registry for England, Wales, Northern Ireland and the Isle of Man, *National Joint Registry 14th Annual Report 2017*, Vol. 1821. Available at: http://www.njrreports.org.uk/Portals/0/PDFdownloads/NJR.

Vail, T. P., Mallon, W. J., Mallon, W. J., and Liebelt, R. A. (1996). Athletic Activities after Joint Arthroplasty. *Sports Med. Arthrosc. Rev.* 4 (3), 298. doi:10.1097/00132585-199600430-00010

Vergara, I., Bilbao, A., Gonzalez, N., Escobar, A., and Quintana, J. M. (2011). Factors and Consequences of Waiting Times for Total Hip Arthroplasty. *Clin. Orthopaedics Relat. Res.* 469 (5), 1413–1420. doi:10.1007/s11999-010-1753-2

Vina, E. R., and Kwoh, C. K. (2018). Epidemiology of Osteoarthritis: Literature Update. *Physiol. Behav.* 30 (2), 160–167. doi:10.1097/BOR.0000000000000479. Epidemiology

Visuri, T., Koskenvuo, M., and Lindholm, T. S. (1987). Return to Work and Working Capacity after Total Hip Replacement. *Int. J. Rehabil. Res.* 10 (4), 434–438. doi:10.1097/00004356-198712000-00014

Vu-Han, T., Hardt, S., Ascherl, R., Gwinner, C., Perka, C., Han, T. Vu., et al. (2020). Recommendations for Return to Sports after Total Hip Arthroplasty Are Becoming Less Restrictive as Implants Improve. *Arch. Orthop. Trauma Surg.* 141, 507–497. doi:10.1007/s00402-020-03691-1

Wollschläger, D. (2017). *Grundlagen Der Datenanalyse Mit R. Statistik*. Berlin, Heidelberg: Springer Berlin Heidelberg. doi:10.1007/978-3-662-53670-4

Woolf, A. D., Pfleger, B., and Pfleger, B. (2003). Burden of Major Musculoskeletal Conditions. *Bull. World Health Organ.* 81 (9), 646–656. doi:10.1590/S0042-96862003000900007

Wright, J., Rudicel, S., and Feinstein, A. (1994). Ask Patients what They Want. Evaluation of Individual Complaints before Total Hip Replacement. *J. Bone Jt. Surg. Br. volume* 76-B (2), 229–234. doi:10.1302/0301-620X.76B2.8113282

Zhang, Z.-j., Kang, Y., Zhang, Z.-q., Yang, Z.-b., He, A.-s., Fu, M., et al. (2012). The Influence of Body Mass Index on Life Quality and Clinical Improvement after Total Hip Arthroplasty. *J. Orthopaedic Sci.* 17 (3), 219–225. doi:10.1007/s00776-012-0197-9

Conflict of Interest: The authors declare that the research was conducted in the absence of any commercial or financial relationships that could be construed as a potential conflict of interest.

Publisher's Note: All claims expressed in this article are solely those of the authors and do not necessarily represent those of their affiliated organizations, or those of the publisher, the editors and the reviewers. Any product that may be evaluated in this article, or claim that may be made by its manufacturer, is not guaranteed or endorsed by the publisher.

frontiers in Bioengineering and Biotechnology

ORIGINAL RESEARCH
published: 18 March 2022
doi: 10.3389/fbioe.2022.799836

Predicting Sit-to-Stand Adaptations due to Muscle Strength Deficits and Assistance Trajectories to Complement Them

Vinay Kumar[1]*, *Takahide Yoshiike*[2] *and Tomohiro Shibata*[1]*

[1]Department of Human Intelligence Systems, Graduate School of Life Science and Systems Engineering, Kyushu Institute of Technology, Kitakyushu, Japan, [2]Honda R&D Co., Ltd., Saitama, Japan

Sit-to-stand (STS) transition is one of the most bio-mechanically challenging task necessary for performing activities of daily life. With muscle strength being the most dominant, many co-occurring factors influence how individuals perform STS. This study investigates the STS changes and STS failure caused by strength deficits using the trajectories generated employing an open-loop single shooting optimization framework and musculoskeletal models. The strength deficits were introduced by simultaneously scaling the maximum isometric strength of muscles in steps of 20%. The optimization framework could generate successful STS transitions for models with up to 60% strength deficits. The joint angle kinematics, muscle activation patterns, and the ground reaction forces from the 0% strength deficit model's STS transition match those observed experimentally for a healthy adult in literature. Comparison of different strength deficit STS trajectories shows that the vasti muscle saturation leads to reduced activation of the antagonistic hamstring muscle, and consequently, the gluteus maximus muscle saturation. Subsequently, the observation of reduced hamstring activation and the motion tracking results are used to suggest the vasti muscle weakness to be responsible for STS failure. Finally, the successful STS trajectory of the externally assisted 80% strength deficit model is presented to demonstrate the optimization framework's capability to synthesize assisted STS transition. The trajectory features utilization of external assistance as and when needed to complement strength deficits for successful STS transition. Our results will help plan intervention and design novel STS assistance devices.

Keywords: sit-to-stand, musculoskeletal model, strength deficit, single shooting optimization, open loop controller, assist-as-needed

OPEN ACCESS

Edited by:
Marcus Fraga Vieira,
Universidade Federal de Goiás, Brazil

Reviewed by:
Burak Ozsoy,
Stoparkinson Healthcare Systems, Turkey
Sarah Seko,
University of California, San Francisco, United States

***Correspondence:**
Vinay Kumar
vinaym815@gmail.com
Tomohiro Shibata
tom@brain.kyutech.ac.jp

Specialty section:
This article was submitted to Biomechanics, a section of the journal Frontiers in Bioengineering and Biotechnology

Received: *22 October 2021*
Accepted: *18 February 2022*
Published: *18 March 2022*

Citation:
Kumar V, Yoshiike T and Shibata T (2022) Predicting Sit-to-Stand Adaptations due to Muscle Strength Deficits and Assistance Trajectories to Complement Them. Front. Bioeng. Biotechnol. 10:799836. doi: 10.3389/fbioe.2022.799836

1 INTRODUCTION

Sit-to-stand (STS) transition is a precursor to walking, hence critical for performing daily life activities and an independent lifestyle. Lower extremity strength plays an important role in human STS, and its deficits are thought to limit the STS functionality. Studies have shown that the lower extremity strength is a strong predictor of the ability of older adults to perform STS from the lowest possible chair height (Hughes et al., 1996; Schenkman et al., 1996). This study aims to identify the STS changes and the STS failure caused by lower extremity strength deficits and the external assistance trajectories that can complement them for successful STS transition.

The decline in muscle strength often co-occurs with other physiological and psychological impediments such as reduced balance, joint pain, and depression, making it difficult to access its independent effect on STS using experiments (Lord et al., 2002). Also, besides subject-specific factors, STS is influenced by many extrinsic factors like foot placement, knee position, and chair height, making designing and conducting experiments complex. Some past studies have used STS trajectories generated using optimization and human models to avoid the complications of experiments. Pandy et al. (1995) presented a cost function that generates STS trajectories with similar muscle activations to those of experiments. Bobbert et al. (2016) and Yokota et al. (2016) searched for trajectories that reduced loads on the muscles and the knee joint. However, the studies mentioned above have made either minimal or no observations about STS changes caused by strength deficits. Further, these studies have also not investigated how strength deficits might lead to unsuccessful STS.

Many older individuals incapable of independent STS transition can perform the same when assisted externally. This external assistance can help maintain or recover lower extremity strength when provided in an assist-as-needed manner. Thus it is desirable to generate reference assistance trajectories that assist as and when needed and by the amount that is needed. Mombaur and Hoang (2017) and Geravand et al. (2017) have used optimization to discover assistance trajectories that support part of the user's weight during STS and squat-to-stand motions, respectively. However, both the studies use human models with independently torque actuated joints. The hamstrings and the rectus femoris are two biarticular muscles that play an essential role in the STS transition. Their biarticularity couples the torques produced at the hip and knee joints. This coupling should not be ignored, especially when generating reference STS assistance trajectories, as it may lead to assistance profiles that over actuates one of these muscles, leading to muscle contracture and eventually lower back issues. The coupling is also crucial for accurately investigating the STS changes and the STS failure caused by the strength deficits. Thus, musculoskeletal models with varying degrees of strength deficits are used in this study to generate assisted and unassisted STS trajectories.

In this study, the single shooting optimization framework used to generate STS trajectories is detailed first, followed by the tools used to analyze them. Subsequently, the joint angle, the muscle activation, and the ground and seat reaction force patterns from the 0% strength deficit model's STS trajectory are contrasted against those observed experimentally for a healthy adult in literature for validation. Then, the different strength deficit trajectories are compared to observe the STS changes caused by strength deficits, followed by an investigation of the STS failure using motion-tracking results. Finally, the successful STS trajectory of an externally assisted musculoskeletal model, incapable of performing unaided STS transition, is presented to demonstrate the optimization framework's ability to generate externally assisted STS trajectory. The findings of this study will help plan intervention and design novel STS assistance devices that operate in an assist-as-needed manner.

Within the single shooting optimization framework, we have parameterized the open-loop excitation trajectories of the actuators similarly to Pandy et al. (1995), and Yokota et al. (2016). The excitation trajectories are used to integrate the system's equation of motion of the equation forward in time to generate the resultant motion. The cost function evaluated on the resultant motion is then used to tune the actuator's excitation trajectories. Another possible optimization framework's structure is in whom the optimization is performed over the joint angle space. The tuning of joint angle trajectories is based on the solutions of inverse dynamics for skeletal models and the solutions of inverse dynamics and static optimization for musculoskeletal models. Such frameworks are used for STS synthesis in Sadeghi et al. (2013); Norman-Gerum and McPhee (2018); Yang and Ozsoy (2020), to discover STS trajectories with minimum actuator efforts in Yoshioka et al. (2007, 2012), and to predict the unilateral grab-rail assisted STS trajectories of a virtually unhealthy adult in Yang and Ozsoy (2021); Ozsoy and Yang (2021). Direct collocation is another potential optimization framework. This framework performs optimization over both the joint angle and the actuator excitation space (Bobbert et al., 2016). We selected open-loop single shooting trajectory optimization for its straightforward implementation and effortless extension to incorporate closed-loop controllers in future works.

It is difficult to identify and detail all of the parameters that shape the STS trajectories generated using optimization. For example, Bobbert et al. (2016), and Yokota et al. (2016) does not contain information about the initial guesses to the optimization algorithm, while Pandy et al. (1995) does not include information about the mechanical limits used to restrict the motion to the physiologically plausible range. Therefore we have made all the source code and results from this study public at https://github.com/ShibataLab/PredictiveSTS.

2 METHODS

An overview of the single shooting optimization framework used to generate STS trajectories in this study is shown in **Figure 1**. The framework tunes the values of decision variables using the aCMA-ES algorithm (Arnold and Hansen, 2010). aCMA-ES is a stochastic gradient-free optimization algorithm that adapts a Gaussian distribution towards low energy regions. It was selected for its enhanced robustness to locally optimal solutions compared to the gradient-based algorithms. At each generation, aCMA-ES samples a batch of candidate solutions from the Gaussian being adapted. Subsequently, the cost function values are evaluated for all the candidates on the respective forward simulations. aCMA-ES then adapts the Gaussian based on the cost function values and samples the next batch of candidate solutions and so on until one of the stopping criteria is met.

In **subsection 2.1**, the musculoskeletal models used with the optimization framework to generate STS trajectories are detailed. **Subsection 2.2** includes the details of the decision variables and the termination criteria used with the optimization framework,

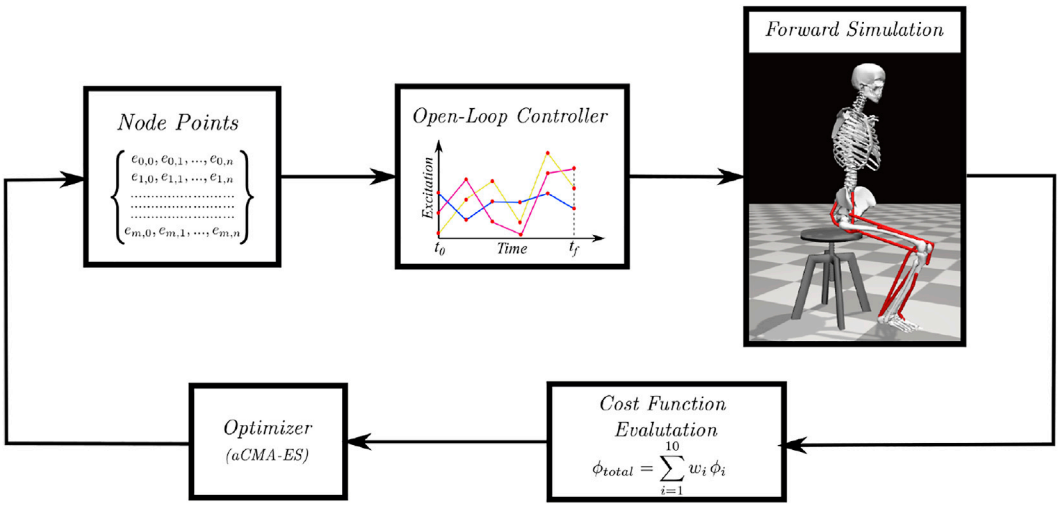

FIGURE 1 | Overview of single shooting optimization framework. The red dots in the open-loop controller represents the node points obtained from the discretization of excitation trajectories.

while **subsection 2.3** describes the cost function. **Subsection 2.4** includes a summary of the motion-tracking setup used to investigate the STS failure. The final **subsection 2.5**, details the steps used to process the experimental data against whom the 0% strength deficit model's STS trajectory is validated. We refer to the STS trajectories as the model's trajectories for conciseness, even though the models were only a single component of the optimization framework.

2.1 Musculoskeletal Model

Musculoskeletal models with different strength deficits for this study were obtained by simultaneously scaling the maximum isometric strengths of the muscles present within the base model. The base model, also shown in **Figure 2**, is a simplified version of the LaiArnold2017 model (Lai et al., 2017). The LaiArnold2017 model represents an average-sized adult male of mass 75 *Kg* and height 170 *cm*. The base model is 2D with eight hill-type muscles and three degrees of freedom, while the source model is 3D with 80 hill type muscles and 37 degrees of freedom. The simplifications were needed to make the optimization problem computationally tractable. The following paragraphs detail some of these simplifications along with other modelling details.

From the LaiArnold2017 model, the left leg and the associated muscles were removed. The masses of arms, forearms, hands and the head were lumped to the torso's center of mass (COM). The mass and inertia of the torso after lumping were halved to account for the missing left leg and the associated muscles. The right foot was fixed to the ground using a weld joint. Then the degrees of freedom corresponding to the sagittal plane motion of the ankle, knee, hip and lumbar joints were added. The 0° angle of the hip, knee, ankle and lumbar joints corresponds model standing upright. From 0°, the positive joint angles correspond to ankle dorsiflexion, knee flexion, hip flexion, and lumbar extension; and the negative joint angles correspond to the opposite. The lumbar joint was locked to −10°, for reasons explained in **subsection 2.5** and thus, the model effectively has three degrees of freedom. The lower extremity muscles with similar functions were combined to single muscle-tendon units as realized in Ong et al. (2019). **Figure 2** shows insertion points and the paths of the resultant muscles included in the model, i.e., gluteus maximus (GMAX), biarticular hamstrings (HAMS), iliopsoas (ILPSO), biarticular rectus femoris (RF), vasti (VAS), biarticular gastrocnemius (GAS), soleus (SOL), and tibialis anterior (TA). **Table 1** lists the maximum isometric strengths for the muscles included in the base model along with the acronyms. At the beginning of simulations, the muscle states were set by equilibrating the muscle-tendon units with the default activation of 0.05.

The chair-body contact interactions were modelled using a point on point kinematic constraint between the femur head and the chair. During simulation, the kinematic constraint was disabled if the vertical reaction forces required to maintain it turned non-compressive or satisfied the slipping condition. The seat kinematic constraint, once disabled, could not be re-engaged and thus prevented the optimization from getting stuck into local optima with multiple chair rises. The model had nonlinear torsional springs representing ligaments at the hip, knee, and ankle joints, limiting the motions to physiologically plausible ranges. They generated torques when the hip joint flex beyond 120°or extends below 30°, or the knee joint flex beyond 140° or extend beyond 0°, or the ankle dorsiflex beyond 30° or plantarflex beyond 40°. These ranges are from the LaiArnold2017 model. The remaining torsional spring parameters are from Ong et al. (2019).

External assistance was introduced at the torso's COM in the musculoskeletal model that failed to perform unassisted STS transition. The rationale behind introducing it at the torso is explained in **subsection 3.3**. For implementation simplicity, the external assistance was modelled using two independent point forces acting in the vertical and horizontal directions. Their respective magnitudes were limited to the 0–200 *N* range. Before computing actuation, the excitation signals to point forces were passed through first-order activation dynamics. It made the external assistance trajectories smooth and thus

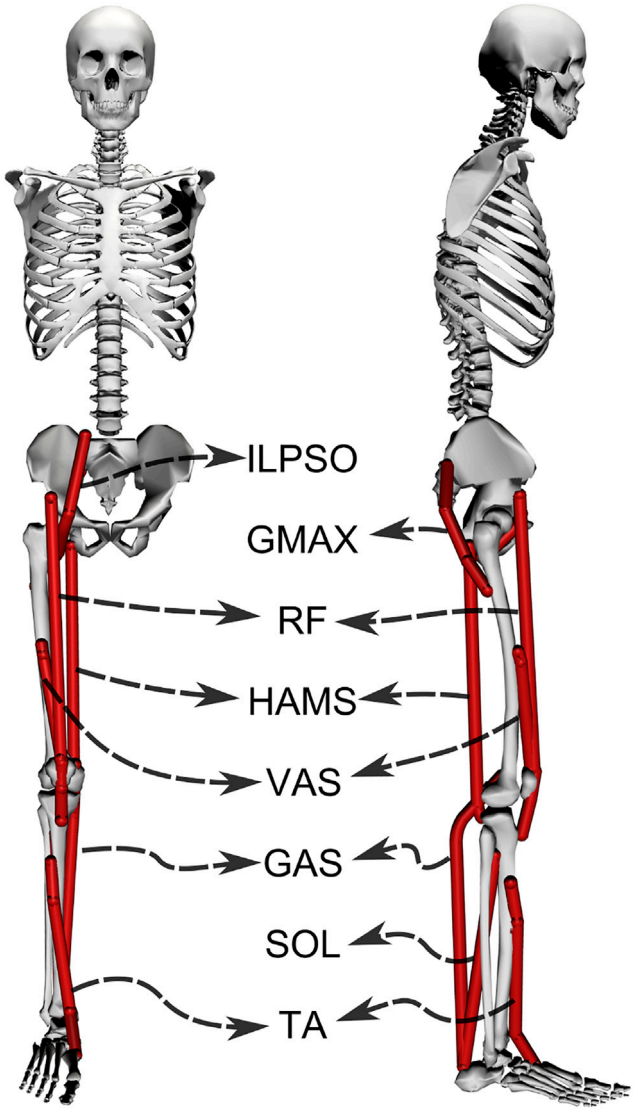

FIGURE 2 | A planar musculoskeletal model for sit-to-stand. The model's musculotendon actuators (red lines) represents the major uniarticular and biarticular muscle groups that drive the sit-to-stand motion in the sagittal plane, i.e., iliopsoas (ILPSO), gluteus maximus (GMAX), biarticular rectus femoris (RF), biarticular hamstrings (HAMS), vasti (VAS), gastrocnemius (GAS), soleus (SOL), and tibialis anterior (TA). The model has three degrees of freedom distributed at the hip, knee and ankle joints.

reduced the optimization framework's sensitivity to the values of individual assistance force decision variables. The first-order activation dynamics had a time constant of 0.1 s. The OpenSim API (Delp et al., 2007) was used to formulate the musculoskeletal model's equation of motion and their forward integration.

2.2 Optimization Setup

The optimization framework tuned the STS duration (t_f) and the node point values obtained by discretizing the excitation trajectories of the actuators present within the musculoskeletal model. The discretization was performed using piecewise linear functions with a fixed time step of 0.1 s between consecutive nodes. The upper limit for simulation duration ($t_{\max}$) was selected to be 1.6 s, similar to Yokota et al. (2016). All the musculoskeletal models had eight hill-type muscles, and the externally assisted musculoskeletal model had two additional point actuators. At t_0, the actuators had their default activation. Thus, the optimization problem had 129 decision variables when generating unassisted STS trajectories and 161 decision variables when generating assisted STS trajectories.

As mentioned before, aCMA-ES is a stochastic gradient-free optimization algorithm that adapts a Gaussian distribution towards low energy regions. The node point values corresponding to the model sitting in a chair were used as the initial guess for the mean of the Gaussian. The algorithm was restarted if the number of generations exceeded 4,000 or if the improvement in the cost values was lower than 1.0 for the best candidate solutions over the immediate 250 generations. At each restart, the generation counter and the covariance matrix were reset to default, and the mean was set to the been-seen candidate solution till then. Four restarts were performed to account for the stochasticity of the optimization algorithm and the non-linearity optimization space before selecting the optimal candidate solution. We used the *libcmaes* library (CMA-ES, 2013) for the aCMA-ES algorithm.

2.3 Cost Function

The cost function we selected to engender STS transition is a linear combination of ten different terms and can be expressed as follows:

$$\phi_{total} = \sum_{i=1}^{10} w_i \phi_i \tag{1}$$

where w_i is the relative weight of ith cost term, i.e., ϕ_i. The mathematical expressions for the ten cost terms are given in **Eqs 2–12**. Please refer to **Table 2** for the list of symbols used in these equations. All the elements associated with different costs were computed in SI units.

$$\phi_1 = \frac{d\left(C_f, C_{goal}\right)}{d\left(C_0, C_{goal}\right)} \tag{2}$$

TABLE 1 | Muscles included in the model, their acronyms and their respective maximum isometric strengths for the 0% strength deficit model.

Muscle	Acronym	Maximum isometric strength (N)
Iliopsoas	ILPSO	2697.3
Gluteus maximus	GMAX	3337.6
Biarticular rectus femoris	RF	2191.7
Biarticular hamstrings	HAMS	4105.5
Vasti	VAS	9594.0
Biarticular gastrocnemius	GAS	4690.6
Soleus	SOL	7925.0
Tibialis anterior	TA	2116.8

TABLE 2 | List of symbols.

Variable	Description
t	Time
$..(t)$	Value of a expression .. at time t
$\|..\|$	The absolute value expression ..
t_0	Simulation start time
t_f	Simulation final time
t_{max}	Upper limit of t_f
t_{SR}	Time of seat release
C_0	Center of mass position at t_0
C_f	Center of mass position at t_f
C_{goal}	Center of mass position for standing posture
$d\ (C_1, C_2)$	Euclidean distance between center of mass positions at t_1 and t_2
α	% Sit to stand completion
$F_{chair,y}$	y component of constraint force applied by the chair on the femur head
τ	Time constant
a_i	Activation of actuator i
$\|F_{Assist}\|$	Magnitude of external assistance
$T_{n,limit}$	Torque generated by the torsional limit spring at the nth joint
$F_{feet,n}$	Component of force applied along n direction by the ground on the feet
ZMP_x	x coordinate of feet force zero moment point
$\dot{\theta}_j$	Velocity of joint j
$Feet_x$	x coordinate of the mid point between heel and toes
mg	Weight of musculoskeletal model

$$\phi_2 = [1-\alpha]\int_{t_0}^{t_f} \frac{e^{t/\tau}}{\tau\left[e^{t_f/\tau}-1\right]} F_{chair,y}(t)dt \tag{3}$$

$$\phi_3 = \sqrt{\frac{\sum_i \int_{t_0}^{t_f} a_i(t)^2 dt}{\sum i}} \tag{4}$$

$$\phi_4 = \sqrt{\frac{\sum_i \int_{t_0}^{t_f} \dot{a}_i(t)^2 dt}{\sum i}} \tag{5}$$

$$\phi_5 = \int_{t_0}^{t_f} \|F_{Assist}(t)\|dt \tag{6}$$

$$\phi_6 = \sum_n \int_{t_0}^{t_f} |T_{n,limit}(t)|dt \tag{7}$$

$$\phi_7 = \alpha \max_{\{t_0,t_f\}}\left(0, |F_{feet,x}(t)| - \mu F_{feet,y}(t)\right) \tag{8}$$

$$\phi_8 = \alpha \max_{\{t_0,t_f\}} |ZMP_x(t) - Feet_x(t)|dt \tag{9}$$

$$\phi_9 = \alpha\left[|\dot{\theta}_{hip}(t_f)| + |\dot{\theta}_{knee}(t_f)| + |\dot{\theta}_{ankle}(t_f)|\right] \tag{10}$$

$$\phi_{10} = \alpha\begin{bmatrix} |\max_{\{t_{SR},t_f\}}\left(F_{feet,y}(t)\right) - mg| + \\ |\min_{\{t_{SR},t_f\}}\left(F_{feet,y}(t)\right) - mg| + \\ |F_{feet,y}(t_f) - mg| \end{bmatrix} \tag{11}$$

$$\alpha = 1 - \frac{\min\left(d(C_f, C_{goal}), d(C_0, C_{goal})\right)}{d(C_0, C_{goal})} \tag{12}$$

Cost ϕ_1 is the ratio of euclidean distances between the goal and t_f COM positions, and the goal and t_0 COM positions. The goal COM position corresponds to the model standing upright. Cost ϕ_2 penalizes the model staying in contact with the chair. Cost ϕ_2 features an increasing exponential and thus penalizes the chair contact interactions more during the later part of simulation than prior. Costs ϕ_3 and ϕ_4 penalize the control effort and its rate of change, respectively. Cost ϕ_5 demotivates excessive use of external assistance. It was set to zero for the unassisted STS trajectories. Cost ϕ_6 discourages hyper-flexion and hyper-extension of joints. Costs ϕ_7 and ϕ_8 respectively penalize the feet contact forces that would lead to slip or tipping over the heel or toes. Cost ϕ_9 penalizes the body motion at t_f while cost ϕ_{10} penalizes the excessive body accelerations.

The scalar α represents STS progress and is illustrated in **Figure 3**. While learning to perform STS, the optimization first comes across unstable trajectories. Costs ϕ_7 to ϕ_{10} are scaled by α to prevent them from hindering the exploration of unstable STS trajectories for stable ones. It can be seen in **Figure 4** that during the initial generations, the value of α is closer to zero as C_f is far away from C_{goal}. Then as the optimization progresses, cost ϕ_2 moves the model out chair and cost ϕ_1 moves it towards standing posture. This moves C_f towards C_{goal}, and the value of α and so the contribution costs ϕ_7 to ϕ_{10} increases. As the model learns to stand up, an increasing amount of control effort is required and thus, the relative contributions of costs ϕ_3 and ϕ_4 increase with optimization progress. The values of relative weights associated with different costs, i.e., w_i, were determined by trial and error and listed in **Table 3** along with other cost function related hyperparameters. **Supplementary Figure S1** of the supplementary material shows the generated STS trajectories are reasonably robust to the w_i values.

2.4 Motion Tracking Setup

The OpenSim CMC tool-based motion tracking was used to investigate the STS failure in this study. The CMC tool computes the actuator excitation levels at user-specified time intervals that will drive the generalized coordinates ($\vec{q}$) of the musculoskeletal model towards a desired kinematic trajectory ($\vec{q}_{\exp}$) in the presence of external forces. At any given time t, the CMC tool first computes the desired acceleration $\ddot{\vec{q}}^*$ using the following proportional derivative control law:

$$\ddot{\vec{q}}^*(t+T) = \ddot{\vec{q}}_{\exp}(t+T) + \vec{k}_v\left[\dot{\vec{q}}_{\exp}(t) - \dot{\vec{q}}(t)\right] + \vec{k}_p\left[\vec{q}_{\exp}(t) - \vec{q}(t)\right] \tag{13}$$

where, $\vec{k}_v$ and $\vec{k}_p$ are the feedback gains on the velocity and position errors, respectively. Since the forces that muscles apply cannot change instantaneously, the desired accelerations are computed some small-time T in the future. Then, CMC tool uses static optimization to distribute the load across synergistic actuators using static optimization. CMC tool offers two formulations for static optimization referred to as slow target and fast target. We used the fast target formulation. It minimizes the sum of squared controls augmented by a set of equality constraints which can be mathematically represented as follows:

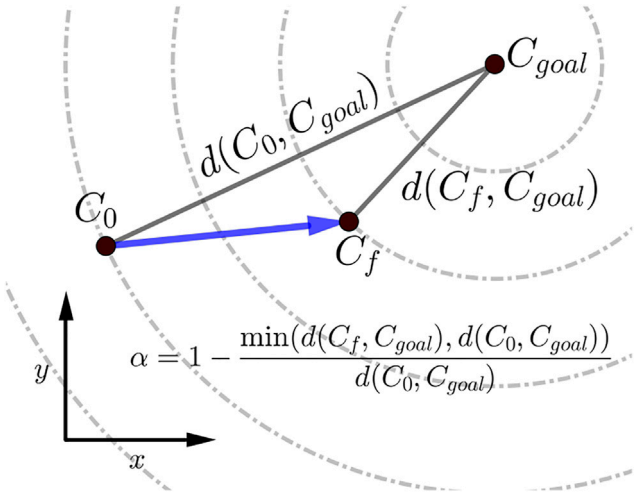

FIGURE 3 | Scalar α, used within the cost expressions, represents the percentage of STS completion and ranges between 0 and 1. The dashed circles show the states that are equidistant from the C_{goal}.

$$J = \sum_{i=1} e_i^2 \tag{14}$$

$$C_j = \ddot{q}_j^* - \ddot{q}_j \forall j \tag{15}$$

where e_i is the control input/excitation of ith actuator at time t and q_j is the jth generalized coordinate. Since for many $\ddot{q}_j^*$ the muscles might not be able to produce sufficient forces, ideal torque actuators are added to the musculoskeletal model to prevent the fast target formulation from failing. Usually, the forces/torques produced per unit control effort for the ideal actuators is much lower than muscles. In such setups, following **Eq. 14**, ideal torque actuators produce significant force/torque only when the muscles are saturated, and hence they are also referred to as reserve actuators. Since the CMC tool does not support event-based disabling of kinematic constraints, the seat forces were computed during the forward simulation and then supplied as external forces.

2.5 Experimental Data Processing

We have used the experimental data recordings of Lao et al. (2019) and Lao et al. (2020) to validate the 0% strength deficit model's STS trajectory generated. The experimental data contains optical marker trajectories, surface EMG signals and the ground and seat-pan reaction forces for 12 healthy adult subjects performing assisted and unassisted STS. Since the experimental data does not contain functional trials needed to scale musculoskeletal models, we have used the recordings of the subject with height and weight closest to our model. The selected subject weighs 71 *Kg* and is 169 *cm* tall. The source musculoskeletal model represents an adult male of mass 75 *Kg* and height 170 *cm*.

The unassisted STS recordings have six trials under each of four conditions, i.e., arms folded across chest, arms hanging freely next to the body, natural STS, and slow pace imitating assisted STS. We used the 18 trials belonging to the first three categories. The optical markers were fixed to the musculoskeletal model on the average marker positions of the T-pose trial. This musculoskeletal model with registered optical markers was used for inverse kinematics. We defined the beginning and the end of STS as the times when hip flexion and hip extensions velocities smoothed with a rolling window of 0.1 s were respectively higher or lower than 20°/*s*. The resulting joint trajectories from the 18 trials are shown in **Supplementary Figure S2**. The mean initial posture observed in experiments is compared to the initial posture used to generate STS trajectories in **Figure 5**. As can be observed, the simulation model was moved slightly forward towards the feet, and the lumbar joint was locked to −10°. The adjustments were made to compensate for the non-actuated lumbar joint. Also, the simulation's initial posture is easier to stand up from due to the torso lying closer to the feet.

The sEMG signals were processed by first passing through a fourth-order Butterworth bandpass filter with 10 and 350 Hz cutoff frequencies. Then they were rectified and subsequently passed through a fourth-order Butterworth lowpass filter of 3 Hz cutoff frequency. Finally, the signals were normalized using the peak values from the maximum voluntary control trials. The ground and seat reaction force trajectories were not processed. **Supplementary Figures S3, S4** respectively illustrate the sEMG and ground and seat reaction force trajectories from the 18 trails used in this study.

3 RESULTS

The optimization could generate successful STS trajectories for the 0, 20, 40 and 60% strength deficit models. However, for the 80% strength deficit model, the optimization could generate successful STS trajectories only when the model was assisted externally. The STS trajectories are divided into the three phases suggested in Millington et al. (1992) to facilitate discussions. Phase 1 starts with the trunk flexion and ends when the model loses contact with the chair. Phase 2 starts with the knee extension and ends when the hip joint is maximally flexed. Phase 3 begins with the reversal of trunk flexion to extension and ends with the model standing upright. The vertical black dotted lines in **Figures 6–12** marks the transition between the three phases.

The results are organized into three subsections. In **subsection 3.1** the kinematics and dynamics of the 0% strength deficit model's STS trajectory are discussed and contrasted against the experimental observations. **Subsection 3.2** details the adaptations and STS failure caused by muscle strength deficits. **Subsection 3.3** discusses the features of the externally assisted 80% strength deficit model's STS trajectory. Please refer to **Figures 6–11**; **Table 4** during the following subsections for details. The resultant joint torques, in **Figure 11**; **Table 4**, were obtained using inverse dynamical analysis of the STS trajectories. During inverse dynamical analysis, the muscles forces were excluded, while the seat constraint and assistance forces were supplied as external forces. The resultant joint torques and the contributions of different muscles to them were computed using OpenSim (Delp et al., 2007).

3.1 Unassisted STS Trajectory of 0% Strength Deficit Model

The joint angle, the muscle excitation, the COM position and velocity, the feet force zero moment point (*ZMP*), and the contact

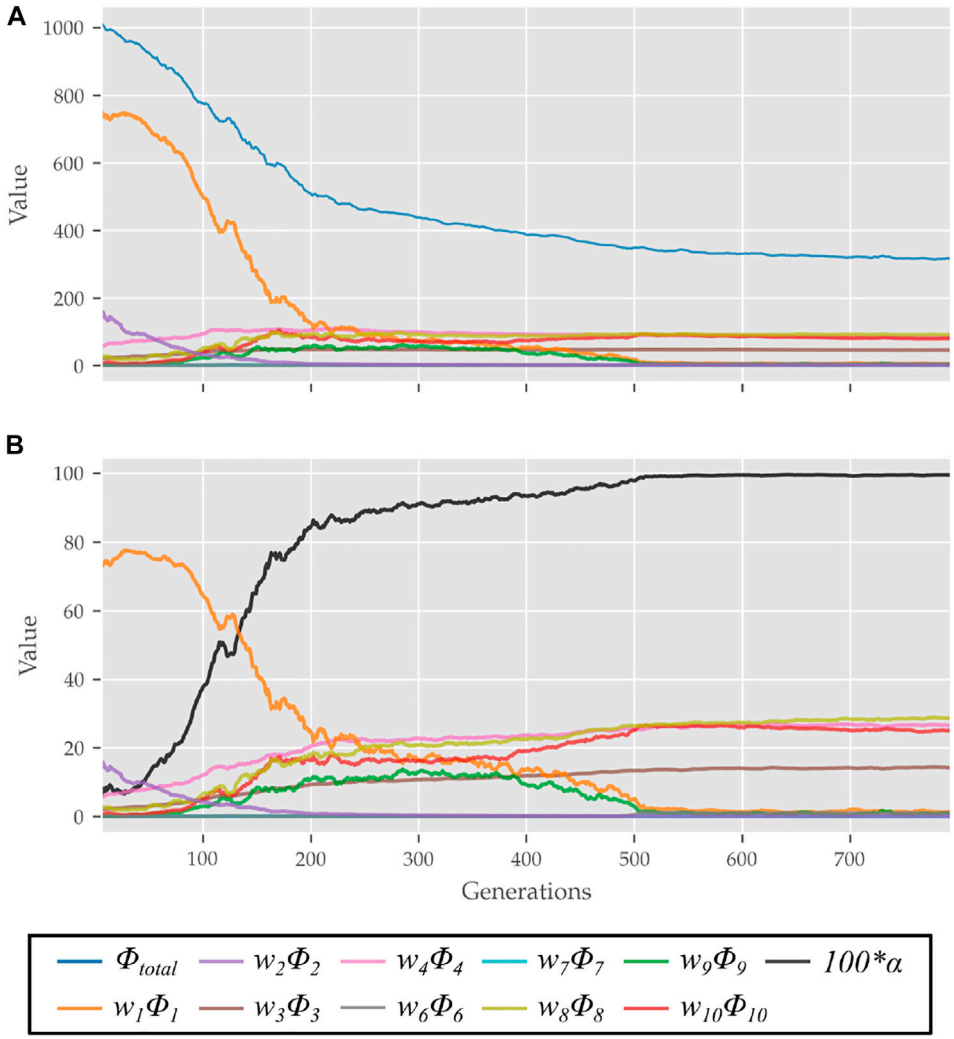

FIGURE 4 | (A) Evolution of different costs and **(B)** their relative contributions to the total cost for the best candidates observed during optimization using the 0% strength deficit model. The costs were smoothed using a rolling average of 10 generations for this plot.

TABLE 3 | Cost function hyperparameters.

Variable	Value
τ	$t_{max}/8$
w_1	800
w_2	1.2
w_3	175
w_4	70
w_5	5
w_6	10
w_7	0.1
w_8	1,000
w_9	6
w_{10}	0.3

force trajectories associated with the 0% strength deficit model's STS trajectory are respectively illustrated in **Figures 6–10**. The STS motion is initiated by activating the ILPSO and RF muscles (**Figure 7**). Their activation generates torque around the hip joint and flexes the torso forward (**Figure 11**). It is followed by the deactivation of ILPSO and RF muscles and gradually increasing activations of the GMAX and HAMS muscles. Due to the trunk's forward flexion, the COM's horizontal velocity increases and peaks (**Figure 8**) before the activations of the GMAX and HAMS muscles increase to control the torso's forward flexion. Also, the activation of VAS muscle increases to prepare for seat-off. Phase 1 ends when the VAS muscle has generated sufficient torques around the knee joint to lift the musculoskeletal model off the chair. The seat off takes place with the body's COM lying behind feet force ZMP (**Figure 9**). During phase 2, the GMAX and HAMS muscle activations increase until the hip flexion velocity reduces to zero. At this point, the trunk is maximally flexed, and phase 2 comes to an end. The knee joint extends only slightly during phase 2. The peak VAS, GMAX and HAMS muscle activations occur during phase 2. During phase 3, the activation of GMAX, HAMS, and VAS muscles slowly taper

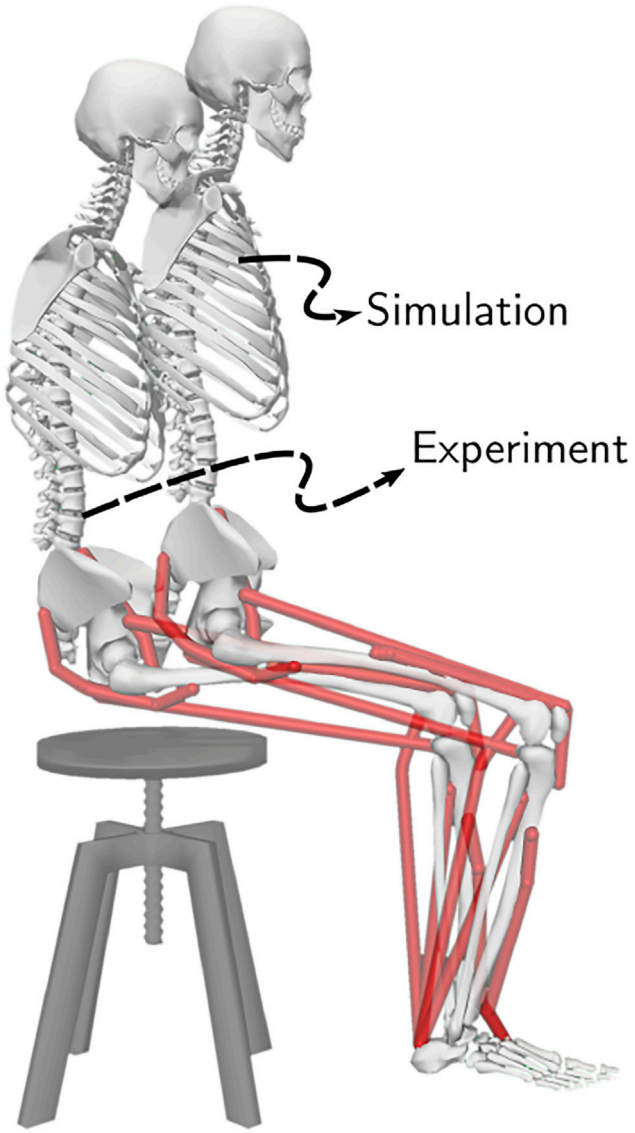

FIGURE 5 | The initial posture used to generate STS trajectories and the mean initial posture observed during experiments. The model was moved slightly forward for simulation to compensate for its non-actuated lumbar joint.

off because smaller forces are required to continue standing up due to an increasing fraction of body weight being borne by bone alignment. These patterns lead to the extension of both the hip and knee joints until the standing posture is achieved. At the end of phase 3, increased activation is observed in ILPSO, RF, and TA muscles to stop the hip, knee and ankle joints from extending past the upright posture. Also, during the latter half of phase 3, the body's COM reaches the feet support polygon. The SOL muscles see almost negligible activation; however, it produces significant passive fiber forces during the first two phases and a significant part of the third phase. Significant TA muscle activations are present during all three phases. These activations produce the force needed to balance the counteracting SOL and GAS muscle forces.

The joint angle trajectories of 0% strength deficits are contrasted against those observed experimentally for a healthy adult in **Figure 6B**. The general shape of the hip and knee joint angle trajectories matches those of experiments. The discrepancies in the joint angle trajectories primarily result from the different initial postures (**Figure 5**). The mean initial posture from experiments requires the lumbar joint extension from −30° to nearly 0°. Our model did not include lumbar joint actuation for the reasons of modelling simplification. The initial posture was modified to compensate for the non-actuated lumbar joint by moving the model slightly forward and locking the lumbar joint with 10° of flexion.

The muscle activation patterns of the 0% strength deficit model's STS trajectory are compared to those of experiments in **Figure 7**. The general shape of activation patterns for the STS critical muscles, i.e., GMAX, HAMS and VAS, matches the experiments. The higher activation of VAS muscle than experiments during the first half of phase 1 is potentially due to cost term ϕ_2. Muscle RF features higher activation during STS initiation as the model did not feature trunk muscles. The higher activation of TA muscle than experiments is potentially due to the passive fiber forces induced in the SOL muscle by the initial posture. Experimental data features a small peak in the TA, GAS and SOL muscle activations during phase 2. This peak is absent in the generated STS. The experimental data did not include EMG signal for ILPSO muscle. The peak activations of all the muscles except RF and TA are within the two standard deviations of the peaks observed experimentally.

The seat and feet contact force trajectories of the 0% strength deficit model's STS transition are compared to the experimental observations in **Figure 10**. The lower seat-pan forces than experiments are most potentially because of the point on point constraint-based formulation. The flattening in the peak feet forces for simulation is because of the cost term ϕ_{10} and the absence of control noise. Also, the seat-off in simulation occurs earlier than in the experiments because the simulation's initial posture requires less horizontal momentum to stand up, and the kinematic constraint-based seat force formulation makes its development easier.

3.2 STS Adaptations and Failure

With strength deficits, the STS duration and the peak VAS, GMAX, RF, ILPSO and TA muscle activations increase (**Table 4**; **Figure 11**). The peak HAMS muscle activation increases with muscle weakness up to 40% and then decreases for the 60%. The peak VAS muscle activation is higher than that of GMAX muscle up to 40% strength deficits and is equal for the 60% strength deficit. The decrease in the peak HAMS muscle activation from 40 to 60% strength deficit is to alleviate the saturated VAS muscle antagonistic at the knee joint. It is evident from the contribution of HAMS muscle to peak resultant knee torques dropping from −112.17% for the 40% strength deficit to −30.99% for the 60% strength deficit. The reduced HAMS muscle activation saturates the GMAX muscle as they work together to control the hip flexion. It is demonstrated by the contributions of HAMS muscle to the peak resultant hip torques dropping from

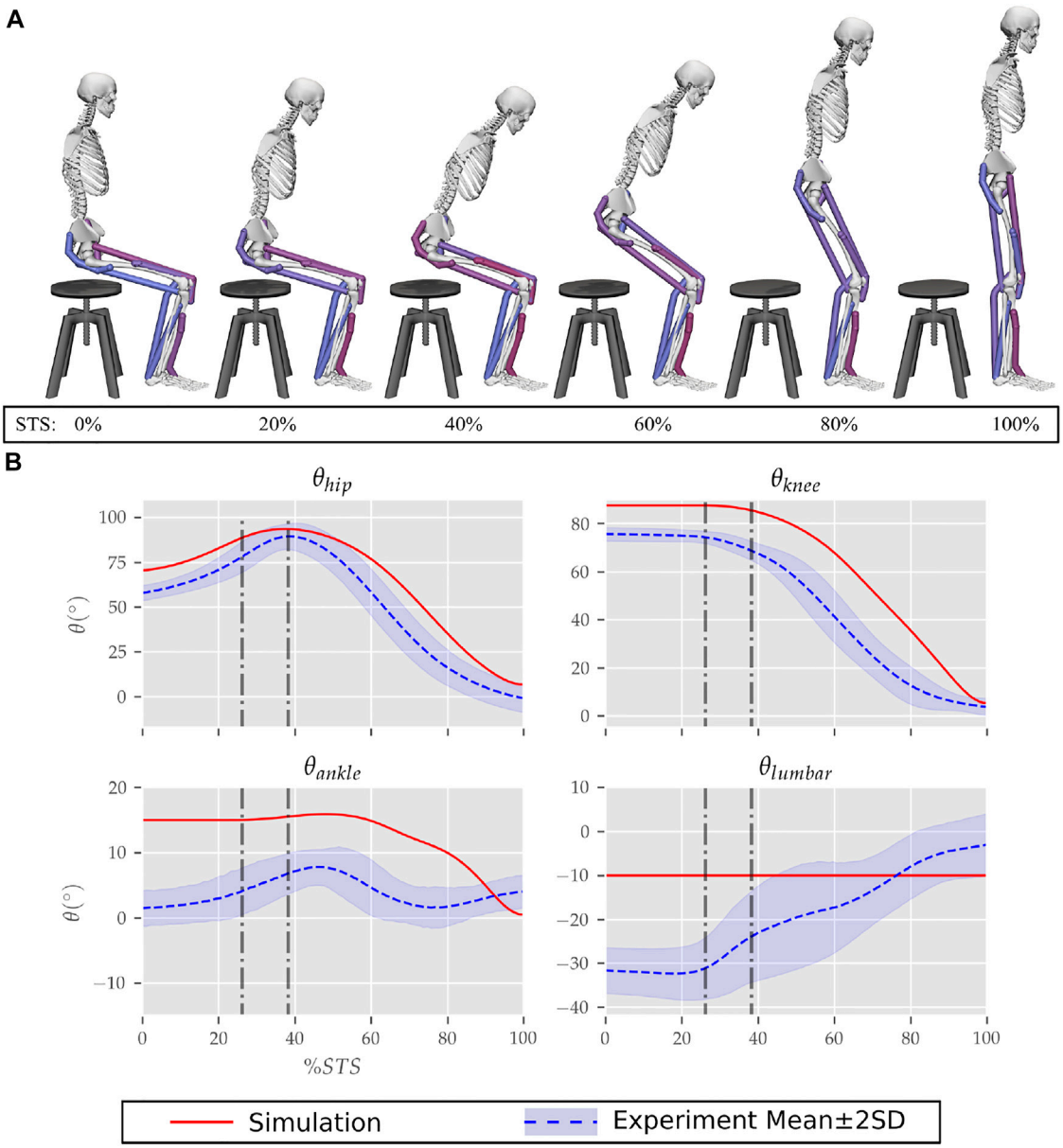

FIGURE 6 | (A) Different postures observed during the 0% strength deficit model's STS transition and **(B)** the comparison of associated joint angle trajectories against experimental observations. The first vertical dotted line marks the point when the model lost contact with the chair, and the second vertical dotted line marks the posture with maximum hip flexion.

70.26% for the 40% strength deficit to 54.7% for the 60% strength deficit. Also, a reduction in the peaks of COM velocity, ground reaction forces, and GMAX, HAMS and VAS muscle forces is observed from the 40–60% strength deficits. Bobbert et al. (2016) also observes that with strength deficits, the STS duration increases, while the peak COM vertical velocity, peak GMAX, and VAS muscle forces decrease. However, Bobbert et al. (2016) does not observe any significant reduction in HAMS muscle activation. It is potentially because Bobbert et al. (2016) used the immediately prior solutions as the initial guess for the subsequent optimization. Besides STS duration and peak muscle activation, we do not observe consistent trends from the 0–40% strength deficits. It is most potentially because the optimizations converged to different locally optimal solutions for each model.

The optimization framework failed to generate STS transitions using the 80% strength deficit model. We suspected the GMAX or the VAS muscle to be responsible for this failure as they were getting saturated for the 60% strength deficit model's STS trajectory (**Figure 11**). We tracked the 60% strength deficit model's successful STS trajectory using the 80% strength deficit and two

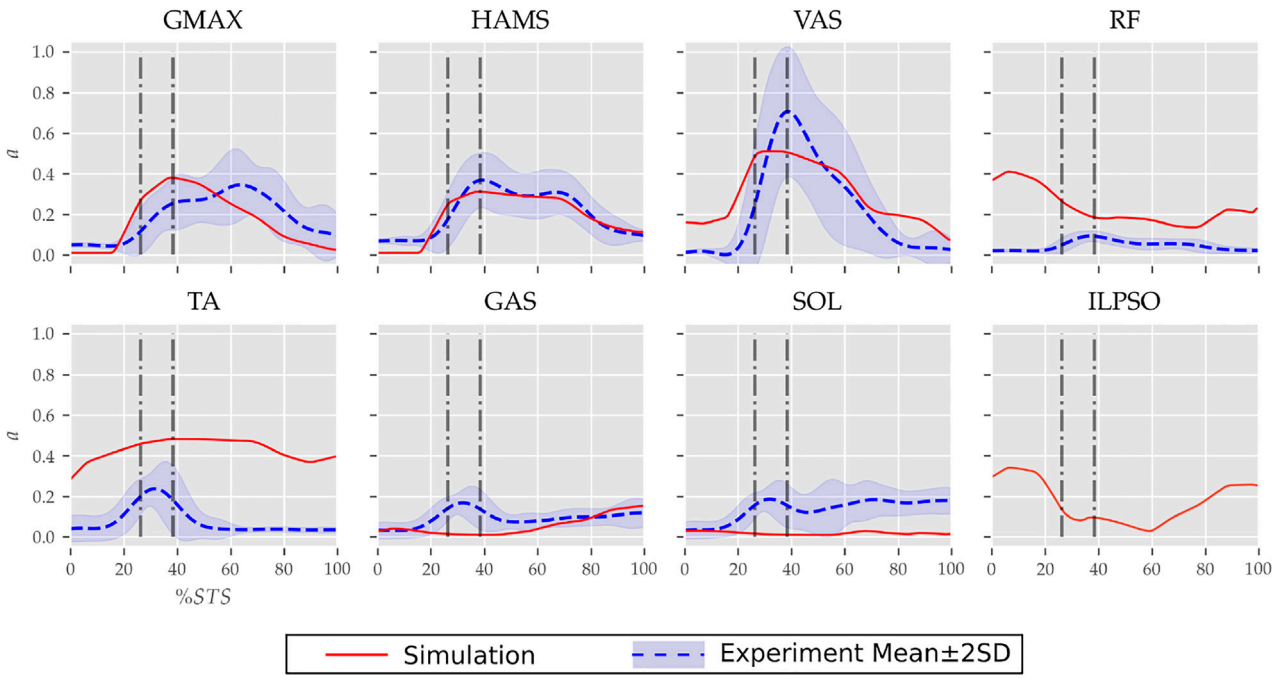

FIGURE 7 | Muscle activation trajectories associated with the 0% strength deficit model's STS transition and those recorded experimentally.

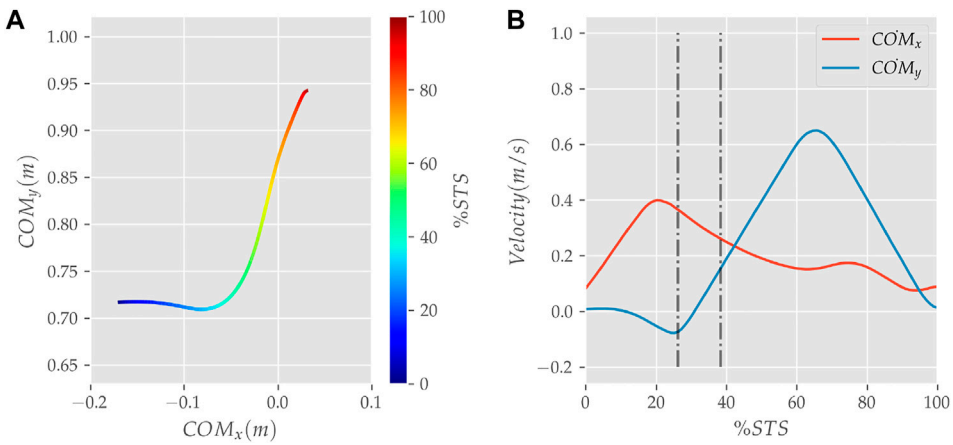

FIGURE 8 | (A) Evolution of COM position and **(B)** velocity for the 0% strength deficit model's STS transition.

different reserve actuator setups. In the first setup, the optimal torque, i.e., torques generated per unit control effort, for the hip and knee torque actuators were $100Nm$ and $1Nm$ respectively, while for the second setup, they were $1Nm$ and $100Nm$. The first setup favored the utilization of the hip reserve actuator, while the second setup favored the utilization of the knee reserve actuator. The first setup's motion-tracking features a peak torque of $-19.81Nm$ by the knee reserve actuator and increased activation of both VAS and RF muscles. The second setup-based motion-tracking features a peak torque of $-12.05Nm$ by the hip reserve actuator and increased HAMS and GMAX activations. The lower magnitude of reserve actuator in the second setup suggests that the STS failure occurred because of VAS muscle weakness. Also, the observation that peak VAS muscle activation is greater than or equal to that of GMAX muscle supports this hypothesis.

3.3 Externally Assisted STS Transition

During the motion tracking of the previous subsection, it was observed that assisting the musculoskeletal model primarily at the hip joint lead to increased RF muscle activation, while assisting it primarily at the knee joint lead to increased HAMS muscle activation. As STS transition is performed

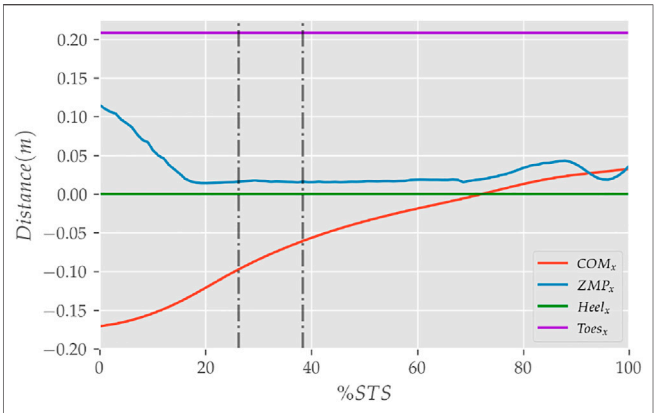

FIGURE 9 | The zero moment point (feet forces) and the body's COM trajectories from the 0% strength deficit model's STS transition.

several times a day, assisting only at the hip or the knee joint has a high potential to cause the RF or the HAMS muscle contracture. Both the muscles cross the hip joint, and their contracture can cause back pain issues if not diagnosed. Thus the external assistance was introduced at the torso COM in the 80% strength deficit model. Also, assisting the model at the torso center of mass is a good approximation for assisting a human at the underarms area. The underarms area is easily graspable, and assistance using it helps simplify the design of probable STS assistance devices.

Physical assistance can help maintain or recover lower extremity strength when provided in an assist-as-needed manner. Thus while generating the assisted STS trajectories, the over-utilization of external assistance was penalized (**Eq. 6**). **Figure 12** shows the body postures, the assistance forces, and muscle activation for the externally assisted 80% strength deficit model's STS trajectory. The trajectory features utilization of external assistance when the VAS and GMAX muscle starts getting saturated, i.e., the model uses external assistance only when needed. The peak magnitudes of external assistance's vertical and horizontal components are 36.50 and 44.51% of the body's weight. The STS trajectory features reduced peaks of COM velocities, resultant hip and knee joint torques and the VAS, GMAX, and HAMS muscle forces. The seat-off takes place with the torso more upright than unassisted models.

4 DISCUSSION

This paper presented and analyzed the sit-to-stand (STS) trajectories generated using an open-loop single shooting optimization and musculoskeletal models with different strength deficits. The strength deficits were introduced by simultaneously scaling the maximum isometric strength of all the muscles in steps of 20%. The optimization could successfully generate STS trajectories for models with up to 60%strength deficits. The muscle activation patterns for the 0% strength deficit model agree reasonably with the experimental observations for a healthy adult. A reduction in the peak HAMS muscle activation is observed when the VAS muscle, antagonistic across the knee joint, gets saturated due to the strength deficits. The reduced HAMS muscle activation saturated the GMAX muscle. After clinical validation, the reduced ratio of peak HAMS to GMAX muscle activation can be used to plan intervention. Then, the motion-tracking results were used to suggest the VAS muscle weakness to be responsible for optimization's failure to generate STS trajectories using the 80% strength deficit model. The motion tracking results were also used to motivate the introduction of external assistance at the torso's centre of mass (COM). The optimization could generate successful STS trajectories for the externally assisted 80% strength deficit model. The optimal trajectory featured the utilization of external assistance in an assist-as-needed manner. We have made the source code for optimization public to speed up the design of future assist-as-needed STS care devices. Finally, the findings of this study should be observed with caution as they have many inherent assumptions. The most significant among them are discussed in the following next paragraphs, followed by our probable future research directions.

Many experimental studies report that the elderly follow a stabilization strategy in which they move the body's COM over the feet support polygon before getting off the chair. Like the

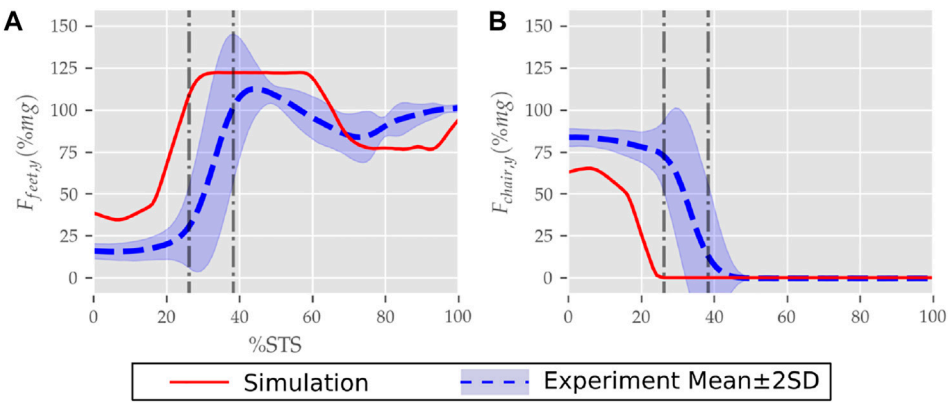

FIGURE 10 | (A) Feet and **(B)** seat contact forces observed during the STS trajectory of the 0% strength deficit model and the experiments.

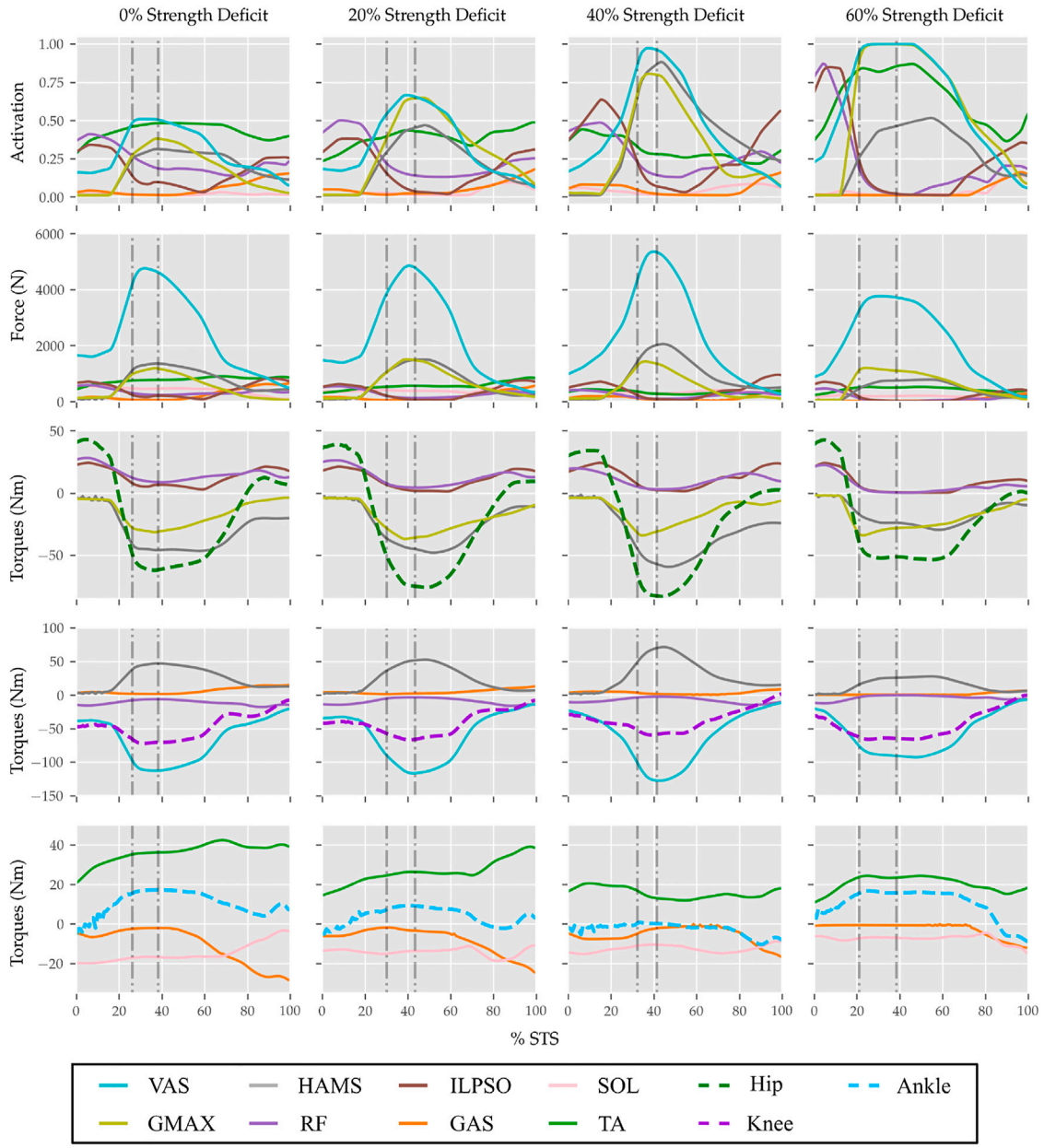

FIGURE 11 | Muscle activations, muscle forces, and their respective contributions to the resultant joint torques from the STS trajectories of 0, 20, 40 and 60% strength deficit models.

mean initial posture of our experiments, the stabilisation strategy requires significant lumbar motion. For our musculoskeletal model, the body's COM lies just 1.15 *cm* inside the feet support polygon when the trunk is maximally flexed while maintaining chair contact. Thus the elimination of the lumbar joint and the feet-ground relative degree of freedom, even though also made by Pandy et al. (1995), Bobbert et al. (2016), and Yokota et al. (2016), might have been oversimplifications for predicting STS trajectories of the elderly adults.

The strength deficits were introduced by simultaneously scaling all the muscles' maximum isometric strength. However, the strengths of all the muscles do not deteriorate by the same ratio. Also, scaling the maximum isometric forces is not the only way to introduce strength deficits. For example, the peak muscle activations could have been limited to the same effect. Thus the strength deficit modelling, even though made similarly by Bobbert et al. (2016) and Yokota et al. (2016), should be investigated for more accurate predictions.

We assumed a sagittal plane of symmetry. However, it has been shown that even for healthy adults, one leg is usually more dominant than the other. Also, significant asymmetries may arise when one of the upper extremities grabs surfaces for assistance.

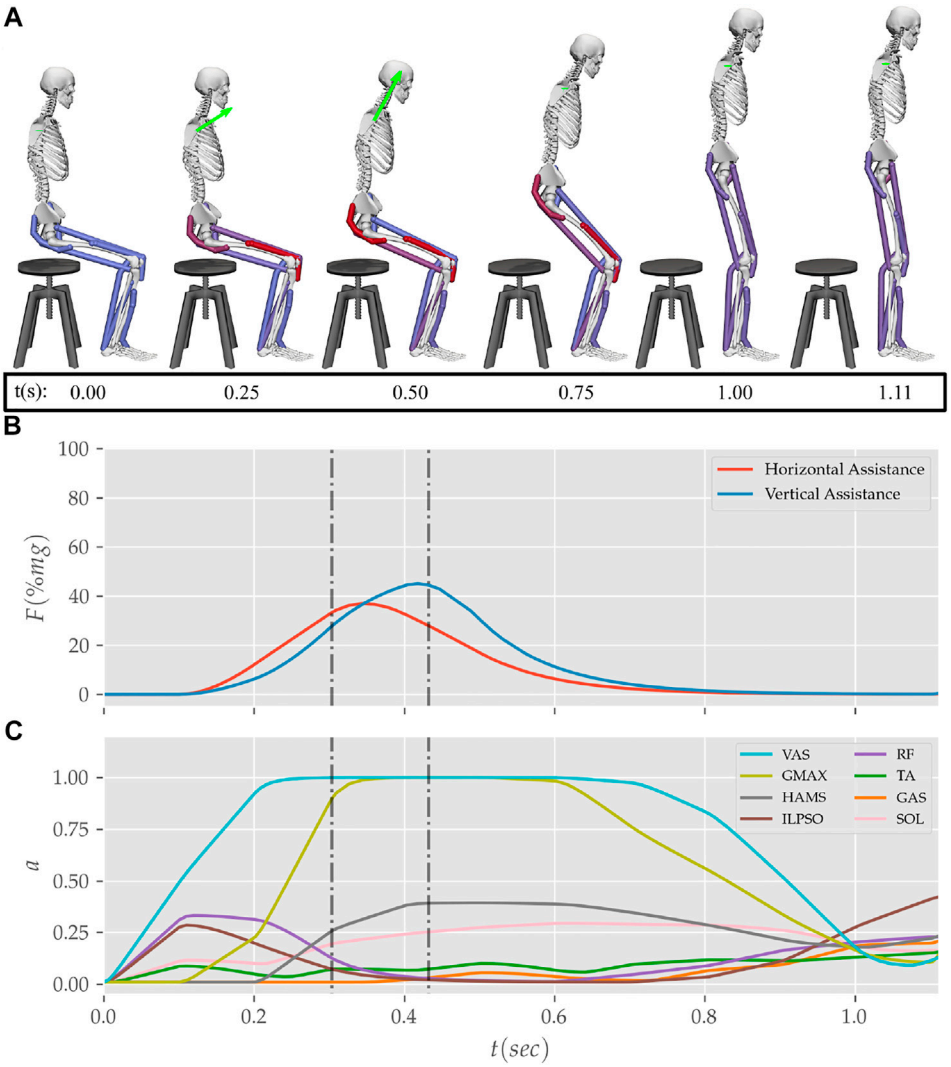

FIGURE 12 | (A) Postures, **(B)** external assistance and **(C)** muscle activation trajectories from the STS transition of the externally assisted 80% strength deficit model. The green arrow in **(A)** represents the resultant external assistance force.

TABLE 4 | Properties of the 0, 20, 40, 60% and externally assisted 80% strength deficit model's STS trajectories. Rows five, six, eight and nine show contributions of muscles to peak resultant joint torques.

# Row	Property	0% strength deficit	20% strength deficit	40% strength deficit	60% strength deficit	80% strength deficit assisted
1	STS duration (s)	1.14	1.23	1.33	1.47	1.11
2	Peak COM Horizontal Velocity (*m/s*)	0.40	0.42	0.42	0.39	0.43
3	Peak COM Vertical Velocity (*m/s*)	0.65	0.71	0.65	0.55	0.42
4	Peak Hip Torque (*Nm*)	−62.17	−76.10	−83.28	−53.58	−35.59
5	GMAX Peak Hip Torque (*Nm*)	−31.60	−35.12	−30.03	−26.17	−20.96
6	HAMS Peak Hip Torque (*Nm*)	−45.91	−47.15	−58.51	−29.31	−15.44
7	Peak Knee Torque (*Nm*)	−72.02	−66.73	−59.22	−65.86	−42.19
8	VAS Peak Knee Torque (*Nm*)	−111.26	−115.92	−125.02	−85.51	−42.36
9	HAMS Peak Knee Torque (*Nm*)	44.40	50.34	66.43	20.41	2.69
10	Peak VAS Force (*N*)	4754.10	4857.40	5355.19	3765.91	1907.14
11	Peak GMAX Force (*N*)	1194.27	1513.42	1437.11	1206.33	615.33
12	Peak HAMS Force (*N*)	1366.03	1505.99	2058.45	782.31	340.31

Thus, the optimization framework needs to be extended to use the 3D musculoskeletal model to generate more realistic assisted and unassisted STS trajectories. Other musculoskeletal model-related critical assumptions that must be validated are simplifying the muscle groups to single musculotendon units and the control level decoupling of muscles.

Perfect coordination between the musculoskeletal model and the external assistance was assumed. It led to an optimal assisted STS transition with 1.11*sec* STS duration and is unrealistic to replicate. The optimization framework should be extended to include sensory noise and delay in external assistance formulation to synthesize realistically replicable STS trajectories. The maximum simulation duration needs to be extended beyond 1.6*sec*. The chair height and the initial posture heavily influence the STS transitions, and the results of this study are a function of them.

The cost function used in this study is not unique in its capability to engender STS. Further, even for the selected cost function, the relative weights of the different cost terms should have been chosen using inverse optimal control. The relative weights were selected using trial and error because of the computationally demanding nature of the optimization. The generated STS trajectories are local optimal solutions of nonlinear non-convex optimizations. The optimization's failure to generate STS using the 80% strength deficit model might have been due to the unsuccessful search rather than muscle saturation.

We plan to design a kinematic events-based closed-loop STS controller in the future. We also plan to investigate the torque and muscle actuated lumbar joint models for STS trajectories with more accurate joint kinematics and dynamics. Finally, we intend to extend the optimization framework to include sensory noise and delay for the more realistic models of assist-as-needed STS care devices.

DATA AVAILABILITY STATEMENT

The source code and the data used in this study are available at https://github.com/ShibataLab/PredictiveSTS.

AUTHOR CONTRIBUTIONS

Conceptualization: VK, TY, and TS; Methodology: VK; Software: VK; Data Analysis: VK; Validation: TS; Writing—original draft preparation: VK; Writing—review and editing: VK, TY, and TS; Funding acquisition: TS; Resources: TY and TS; Supervision: TS.

ACKNOWLEDGMENTS

We would like to thank Tamei Tomoya (Associate Professor, Center for Mathematical and Data Sciences, Kobe University) for sharing the experimental data with us.

SUPPLEMENTARY MATERIAL

The Supplementary Material for this article can be found online at: https://www.frontiersin.org/articles/10.3389/fbioe.2022.799836/full#supplementary-material

REFERENCES

Arnold, D. V., and Hansen, N. (2010). "Active Covariance Matrix Adaptation for the (1+ 1)-Cma-Es," in *Proceedings of the 12th Annual Conference on Genetic and Evolutionary Computation* (Portland, OR: ACM Digital Library), 385–392. doi:10.1145/1830483.1830556

Bobbert, M. F., Kistemaker, D. A., Vaz, M. A., and Ackermann, M. (2016). Searching for Strategies to Reduce the Mechanical Demands of the Sit-To-Stand Task with a Muscle-Actuated Optimal Control Model. *Clin. Biomech.* 37, 83–90. doi:10.1016/j.clinbiomech.2016.06.008

CMA-ES (2013). Libcmaes. Available at: https://github.com/CMA-ES/libcmaes.

Delp, S. L., Anderson, F. C., Arnold, A. S., Loan, P., Habib, A., John, C. T., et al. (2007). Opensim: Open-Source Software to Create and Analyze Dynamic Simulations of Movement. *IEEE Trans. Biomed. Eng.* 54, 1940–1950. doi:10.1109/tbme.2007.901024

Geravand, M., Korondi, P. Z., Werner, C., Hauer, K., and Peer, A. (2017). Human Sit-To-Stand Transfer Modeling towards Intuitive and Biologically-Inspired Robot Assistance. *Auton. Robot* 41, 575–592. doi:10.1007/s10514-016-9553-5

Hughes, M. A., Myers, B. S., and Schenkman, M. L. (1996). The Role of Strength in Rising from a Chair in the Functionally Impaired Elderly. *J. Biomech.* 29, 1509–1513. doi:10.1016/s0021-9290(96)80001-7

Lai, A. K. M., Arnold, A. S., and Wakeling, J. M. (2017). Why Are Antagonist Muscles Co-activated in My Simulation? a Musculoskeletal Model for Analysing Human Locomotor Tasks. *Ann. Biomed. Eng.* 45, 2762–2774. doi:10.1007/s10439-017-1920-7

Lao, B., Tamei, T., and Ikeda, K. (2019). Characterizing Strategic Contributions of Physical Therapy to Natural Standing Motion in the Muscle Synergy Space. *Annu. Int. Conf. IEEE Eng. Med. Biol. Soc.* 2019, 2311–2315. doi:10.1109/EMBC.2019.8857541

Lao, B., Tamei, T., and Ikeda, K. (2020). Data-efficient Framework for Personalized Physiotherapy Feedback. *Front. Comput. Sci.* 2, 3. doi:10.3389/fcomp.2020.00003

Lord, S. R., Murray, S. M., Chapman, K., Munro, B., and Tiedemann, A. (2002). Sit-to-stand Performance Depends on Sensation, Speed, Balance, and Psychological Status in Addition to Strength in Older People. *Journals Gerontol. Ser. A: Biol. Sci. Med. Sci.* 57, M539–M543. doi:10.1093/gerona/57.8.m539

Millington, P. J., Myklebust, B. M., and Shambes, G. M. (1992). Biomechanical Analysis of the Sit-To-Stand Motion in Elderly Persons. *Arch. Phys. Med. Rehabil.* 73, 609–617.

Mombaur, K., and Ho Hoang, K.-L. (2017). How to Best Support Sit to Stand Transfers of Geriatric Patients: Motion Optimization under External Forces for the Design of Physical Assistive Devices. *J. Biomech.* 58, 131–138. doi:10.1016/j.jbiomech.2017.04.037

Norman-Gerum, V., and McPhee, J. (2018). Constrained Dynamic Optimization of Sit-To-Stand Motion Driven by Bézier Curves. *J. Biomech. Eng.* 140. doi:10.1115/1.4041527

Ong, C. F., Geijtenbeek, T., Hicks, J. L., and Delp, S. L. (2019). Predicting Gait Adaptations Due to Ankle Plantarflexor Muscle Weakness and Contracture Using Physics-Based Musculoskeletal Simulations. *Plos Comput. Biol.* 15, e1006993. doi:10.1371/journal.pcbi.1006993

Ozsoy, B., and Yang, J. (2021). Assisted Spatial Sit-To-Stand Prediction—Part 2: Virtual Injured Elderly Individuals. *J. Comput. Inf. Sci. Eng.* 21, 061009. doi:10.1115/1.4050473

Pandy, M. G., Garner, B. A., and Anderson, F. C. (1995). Optimal Control of Non-ballistic Muscular Movements: a Constraint-Based Performance Criterion for Rising from a Chair. *J. Biomechanical Eng.* 117, 15–26. doi:10.1115/1.2792265

Sadeghi, M., Emadi Andani, M., Bahrami, F., and Parnianpour, M. (2013). Trajectory of Human Movement during Sit to Stand: a New Modeling Approach Based on Movement Decomposition and Multi-phase Cost Function. *Exp. Brain Res.* 229, 221–234. doi:10.1007/s00221-013-3606-1

Schenkman, M., Hughes, M. A., Samsa, G., and Studenski, S. (1996). The Relative Importance of Strength and Balance in Chair Rise by Functionally Impaired Older Individuals. *J. Am. Geriatr. Soc.* 44, 1441–1446. doi:10.1111/j.1532-5415.1996.tb04068.x

Yang, J., and Ozsoy, B. (2021). Assisted Spatial Sit-To-Stand Prediction-Part 1: Virtual Healthy Elderly Individuals. *J. Comput. Inf. Sci. Eng.* 21, 041002. doi:10.1115/1.4048128

Yang, J., and Ozsoy, B. (2020). Three Dimensional Unassisted Sit-To-Stand Prediction for Virtual Healthy Young and Elderly Individuals. *Multibody Syst. Dyn.* 49, 33–52. doi:10.1007/s11044-019-09699-9

Yokota, H., Ohshima, S., and Mizuno, N. (2016). Sit-to-stand Motion Analysis Using Multiobjective Genetic Algorithm Based on Musculoskeletal Model Simulation. *IEEJ J. IA* 5, 236–244. doi:10.1541/ieejjia.5.236

Yoshioka, S., Nagano, A., Himeno, R., and Fukashiro, S. (2007). Computation of the Kinematics and the Minimum Peak Joint Moments of Sit-To-Stand Movements. *Biomed. Eng. Online* 6, 26–14. doi:10.1186/1475-925X-6-26

Yoshioka, S., Nagano, A., Hay, D. C., and Fukashiro, S. (2012). The Minimum Required Muscle Force for a Sit-To-Stand Task. *J. Biomech.* 45, 699–705. doi:10.1016/j.jbiomech.2011.11.054

Conflict of Interest: TY was employed by the company Honda R&D Co. Ltd.

The remaining authors declare that the research was conducted in the absence of any commercial or financial relationships that could be construed as a potential conflict of interest.

frontiers | Frontiers in Sports and Active Living

SYSTEMATIC REVIEW
published: 13 April 2022
doi: 10.3389/fspor.2022.873718

The Effect of Eccentric vs. Traditional Resistance Exercise on Muscle Strength, Body Composition, and Functional Performance in Older Adults: A Systematic Review With Meta-Analysis

Klemen Čretnik[1], *Jernej Pleša*[1], *Žiga Kozinc*[1,2], *Stefan Löfler*[3] *and Nejc Šarabon*[1,2,4,5]*

[1] Faculty of Health Sciences, University of Primorska, Izola, Slovenia, [2] Andrej Marušič Institute, University of Primorska, Koper, Slovenia, [3] Ludwig Boltzmann Institute for Rehabilitation Research, St. Pölten, Austria, [4] Human Health Department, InnoRenew CoE, Izola, Slovenia, [5] Laboratory for Motor Control and Motor Behavior, S2P, Science to Practice, Ltd., Ljubljana, Slovenia

OPEN ACCESS

Edited by:
Rafael Reimann Baptista,
Pontifical Catholic University of Rio Grande do Sul, Brazil

Reviewed by:
Masatoshi Nakamura,
Niigata University of Health and Welfare, Japan
Pierre Clos,
INSERM U1093 Cognition, Action et Plasticité Sensomotrice, France

***Correspondence:**
Nejc Šarabon
nejc.sarabon@fvz.upr.si

Specialty section:
This article was submitted to Exercise Physiology, a section of the journal Frontiers in Sports and Active Living

Received: 11 February 2022
Accepted: 09 March 2022
Published: 13 April 2022

Citation:
Čretnik K, Pleša J, Kozinc Ž, Löfler S and Šarabon N (2022) The Effect of Eccentric vs. Traditional Resistance Exercise on Muscle Strength, Body Composition, and Functional Performance in Older Adults: A Systematic Review With Meta-Analysis. Front. Sports Act. Living 4:873718. doi: 10.3389/fspor.2022.873718

The effects of eccentric exercise (ECC) in older adults have received limited scientific attention, considering the ample evidence for its effectiveness in general and athletic populations. The purpose of this paper is to review the effects of ECC exercise modalities vs. traditional or concentric (CON) exercise on muscle strength, body composition and functional performance in older adults. Inclusion criteria regarding the age was >55 years. Three major scientific literature databases (PubMed, Scopus and Web of Science) were screened for trials comparing the effect of ECC and CON exercise programs, and 19 papers were included in the meta-analysis. ECC and CON training programs were typically matched by the duration of each session. The difference between ECC and CON was expressed as standardized mean difference (SMD). Regarding isometric knee strength, the pooled effect favored ECC (SMD = 0.50), but was not statistically significant ($p = 0.160$). ECC exercise elicited greater improvements in timed up and go test (SMD = −0.68; $p = 0.004$), 2-min sit-stand test (SMD = 0.53; $p = 0.030$) and 30-s sit-stand test (SMD = 0.81; $p = 0.002$), but not in 6-min walking test (SMD = 0.01; $p = 0.960$). The effects on body composition and muscle architecture were unclear (SMD = −1.44 to 1.95; $p = 0.060$–0.689). In conclusion, our literature review indicates that ECC exercise is superior to, or at least as good as CON exercise for preserving health and overall function in older adults.

Keywords: elderly, sarcopenia, eccentric training, eccentric exercise, older adults

INTRODUCTION

Aging is associated with numerous physiological and morphological changes, related to declines in functional abilities and susceptibility to age-related diseases, which negatively influences the quality of life and independency (Deschenes, 2004; Capodaglio et al., 2005). Exercise interventions have been shown to improve cardiovascular health, decrease occurrence of sarcopenia and decrease

fragility and risk of falling (Macaluso and De Vito, 2004; Benichou and Lord, 2016). Structured exercise is regarded as an effective method to prevent, delay, or attenuate the effect of aging, especially in terms of functional ability and physiological changes (Viña et al., 2016).

A plethora of factors needs to be considered in exercise prescription. One of such important factors is the type of muscle contraction. Muscular actions during resistance exercise may be isometric (i.e., the muscle length is maintained during activation), concentric (i.e., the muscle shortens during activation) and eccentric (i.e., the muscle lengthens during activation), all of which present distinct physiological, neural and mechanical characteristics and responses (Peake et al., 2005; Raman et al., 2012). It has been argued that any training regime that maximizes muscle strength will ultimately improve functional abilities (Malbut-Shennan and Young, 1999). On the other hand, many studies indicate that eccentric-focused training on eccentric ergometer promotes greater gains in muscle strength and hypertrophy when compared to conventional strength training (slow concentric and eccentric actions) performed in "standard" training regime of 10 repetitions per set (LaStayo et al., 2003; Mueller et al., 2009). Furthermore, LaStayo et al. (2014) reported that low-intensity endurance-focused eccentric contractions in eccentric cycling can result in large muscle hypertrophy in older adults. On the other hand, the study by Lewis et al. (2018) showed that the strength gains may not differ between training modalities (ECC and CON cycling) when the intensities are matched in middle-aged sedentary males. Nevertheless, this information should be carefully considered, because the participants in the study are middle age males, which means that the results could be different for older adults. Moreover, Gault and Willems (2013), reported that endurance eccentric exercises (e.g., eccentric cycling, downstairs walking) are adequate for elderly adults to reduce risk of falls and to improve their quality of life. It is also important to note that many tasks that are associated with a high risk of falling, such as descending stairs, relay heavily on eccentric muscle contractions.

In addition to superior effect of eccentric over traditional resistance exercise regarding strength and hypertrophy adaptations, studies reporting lower rate of perceived effort in eccentric compared concentric exercise (Lindstedt et al., 2001; LaStayo et al., 2003). Similar results have been shown for eccentric cycling compared to concentric cycling at the same intensity at given heart rate or oxygen consumption (LaStayo et al., 1999; Peñailillo et al., 2014; Clos et al., 2019). The most important drawback of eccentric exercise is a the possibility of exercise-induced muscle damage (Hody et al., 2013; Jamurtas et al., 2013). Moreover, eccentric exercise is sometimes somewhat more difficult to implement in contrast to conventional exercise methods because a) of safety reasons (eccentric exercises are usually performed at higher intensity, thus it is recommended that exercise is performed with the help of exercise practitioner or "spotter") and b) lack of appropriate equipment. Given that both advantages and drawbacks of eccentric exercise have been identified, investigating the effect of eccentric-focused exercise in contrast to conventional resistance exercise is important to provide practitioners with optimal and comprehensive guidelines.

In contrast to general and athletic populations, older adults have received less scientific attention in relation to the effect of eccentric exercise. The effect of exercise interventions in older adults has been evaluated through different testing methods, such as functional ability tests (timed-up-and go test (TUGT), 5-repetition sit-to-stand, walking speed, etc.), body composition (muscle mass, fat mass, muscle cross-section area, etc.) and tests of motor abilities (e.g., strength, endurance, balance, etc.). Performance in functional tasks such as TUGT and 5-repetition sit-to-stand can be used to predict the risk for recurrent falls (Buatois et al., 2008). Moreover, performance of everyday functional tasks such as crossing the road or carrying bags from the store are also, to some extent, associated with isokinetic strength (Doherty, 2003). Two very recent systematic reviews focused on the effect of eccentric training in healthy older adults (Molinari et al., 2019; Kulkarni et al., 2021). Molinari et al. (2019) included 5 studies with muscle strength outcomes, and reported similar effects of eccentric exercises and traditional resistance exercises, with the data slightly favoring the former. Kulkarni et al. (2021) examined 10 studies and reported that eccentric exercises can be as effective as conventional exercises in older adults for improving functional performance. In sum, existing reviews are showing the potential of eccentric exercise to elicit similar improvement in comparison to traditional resistance exercise. In light of advantages of eccentric exercise, such as lower energy expenditure, it could be suggested that eccentric exercise should be incorporated in resistance exercise programs for older adults. However, only limited number of variables have been included in existing reviews, thus further analysis is needed to provide broader view about the effects of eccentric exercise and eccentric training modalities compared to traditional training type on basic motor capabilities, body composition and functional ability in older adults. Based on that, the objective of this paper is to review the effects of eccentric exercise modalities vs. traditional resistance exercise on muscle strength, body composition and functional performance in older adults. In accordance with the previous evidence, we hypothesized that eccentric exercise will have similar effect on functional performance, muscle strength and body composition, compared to traditional resistance exercise.

METHODS

Search Strategy

The search was performed in October 2021. Three major scientific literature databases (PubMed, Scopus and Web of Science) were screened, using the following search term: (eccentric exercise OR flywheel OR isoinertial exercise OR eccentric training) AND (older adults OR elderly OR elders OR old age OR aging). The records were imported into Mendeley (version 1.19.8) to remove the duplicates, and then exported into

Microsoft Excel software. The search strategy was carried out in three stages: (1) assessing the eligibility of the papers based on the title, (2) assessing the eligibility of the papers based on the abstract and (3) assessing the eligibility of the papers based on the full text. Both reviewers assess all papers. At all three stages, two reviewers carried out the procedures independently. In case of non-agreement in stages 1.-2., any papers that were identified by only one reviewer were carried over to the next phase. In stage 3., potential disagreements were resolved by additional discussion and consultation of the third reviewer.

Inclusion Criteria

The inclusion criteria are structured according to the PICOS tool (Methley et al., 2014), as follows:

- **P (population):** older adults, aged > 55 years. We excluded patients with neurological diseases (e.g., Parkinson's disease), but we also considered patients with metabolic and cardiovascular diseases.
- **I (Intervention):** Resistance exercise interventions focusing on (or emphasizing) eccentric contraction. This includes flywheel training and functional tasks such as loaded stair descent. Duration of the intervention > 4 weeks.
- **C (Comparison):** Resistance exercise interventions, performed in a traditional manner or emphasizing concentric contraction.
- **(Outcome):** Outcomes describing muscle performance (muscle strength or power), body composition outcomes (e.g., lean mass, muscle thickness, body fat mass) and functional performance tests (e.g., 6-min walking test, sit-stand tests, stair walking, etc.).
- **S (Study design):** Interventional clinical trials, with at least two groups (eccentric and traditional/concentric exercise groups).

Data Extraction

The data extraction was carried out independently by two reviewers and disagreements were resolved through consultation with other reviewers. The extracted data included: (a) baseline and post-intervention means and standard deviations for all eligible outcome measures for eccentric and concentric groups; percent changes were considered instead of pre-post data when available (b) baseline demographics of participants (gender, age, body height, body mass, body mass index); (c) intervention characteristics (target body area (upper, lower or whole-body), duration of the intervention, number of sessions per week, volume (number of exercises, sets, and repetitions), breaks between exercises and sets, supervision, and progression of exercise difficulty). Data were carefully entered into Microsoft Excel 2016 (Microsoft, Redmond, WA, USA). If the data were presented in a graphical rather than tabular form, we used Adobe Illustrator Software (version CS5, Adobe Inc., San Jose, CA, USA) to accurately determine the means and standard deviations. In case of missing data, the corresponding author of the respective article was contacted by e-mail. If no response was received after 7 days, the author was contacted again. If the author did not reply to the second inquiry, the data was considered irretrievable.

Assessment of the Quality of the Included Studies

Two reviewers evaluated the quality of the included studies using the PEDro scale (Maher et al., 2003), which assesses study quality based on a 0–10 scale. Potential disagreements between the reviewers were resolved by consulting the other authors. Studies scoring from 9 to 10 were considered as "excellent," 6 to 8 as "good," 4 to 5 as "fair," and <4 as "poor" quality. The PEDro scale was selected because it was developed to assess the quality of clinical trial studies evaluating physical therapy interventions.

Data Analysis

The main data analyses were carried out in Review Manager (Version 5.3, Copenhagen: The Nordic Cochrane Center, The Cochrane Collaboration, London, UK). Before the results were entered into the meta-analytical model, the pre-post differences and pooled standard deviations were calculated according to the following formula $SD = \sqrt{[(SD_{pre}^2 + SD_{post}^2) - (2 \times r \times SD_{pre} \times SD_{post})}$. The correction value (r), which represents the pre-test–post-test correlation of outcome measures, was conservatively set at 0.75. It should be noted that a change in the correction value in the range between 0.5 and 0.9 had little effect on the pooled SD and would not change the outcomes of the meta-analyses. For the meta-analysis, the inverse variance method for continuous outcomes with a random-effects model was used. The effect sizes were expressed as standardized mean difference (SMD). For SMD, the respective 95% confidence intervals were also calculated and reported.

The analysis compared the effects of the eccentric exercise and traditional resistance exercise or concentric exercise interventions. Statistical heterogeneity among studies was determined by calculating the I^2 statistics. According to Cochrane guidelines, the I^2 statistics of 0% to 40% might not be important, 30 to 60% may represent moderate heterogeneity, 50–90% may represent substantial heterogeneity, and 75–100% indicates considerable heterogeneity. The threshold for statistical significance was set at $p \leq 0.05$ for the pooled effect size. Sensitivity analysis was performed by examining the effect of exclusion of studies one-by-one from the analyses.

RESULTS

Search Summary

The initial search yielded 3,188 records (PubMed = 1,200; Scopus = 97; Web of science = 1,891). After the duplicates were removed, 2,521 records were left for examination. Based on the title, Reviewer 1 identified 264 potentially relevant papers, and Reviewer 2 identifies 242. Most of the papers were overlapping between the reviewers, thus, the sum of the identified papers was 332. In the next step, based on the abstract reading, Reviewer 1 identified 61 potentially relevant papers, and Reviewer 2 identified 57. At this stage, the reference lists of relevant reviews were also scrutinized, and 1 additional paper was included. In total, 73 papers were included for a full-text examination. Both reviewers identified 18 eligible papers with a complete agreement, thus, 19 papers were included into the meta-analysis. The search is summarized on the Flowchart in **Figure 1**.

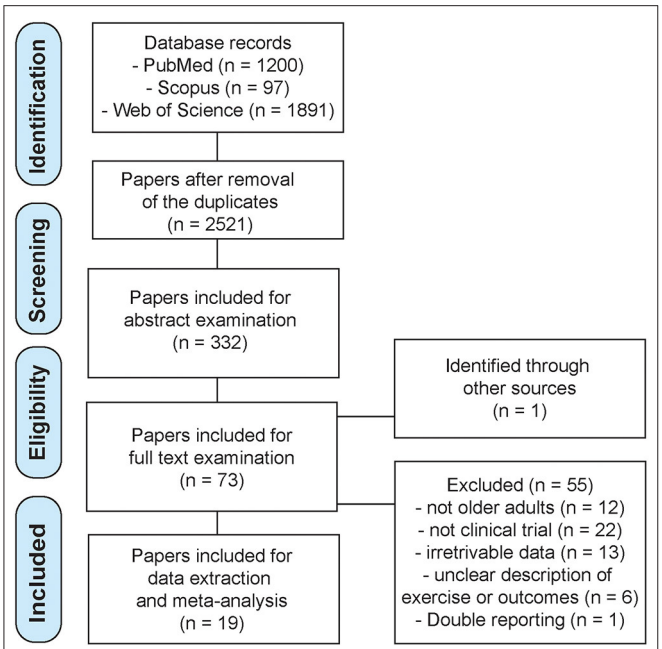

FIGURE 1 | Flowchart with search protocol summary.

Supplementary Table 1 also includes the list of papers included at each stage, as well as the extracted data. **Table 1** includes basic information regarding the included studies.

Assessment of Study Quality

All of the studies received the PEDro score in the 3–6 range. Two studies received a score of 3 points, indicating "poor" quality. One study received the score of 6, indicating "good" quality. The remaining studies were of "fair" quality (9 studies with a score of 4; 7 studies with a score of 5). The mean PEDro score was 4.4 ± 0.8. Overall, the evidence presented in this review may be considered to be of "fair" quality. The most common items that almost all studies failed to satisfy were blinding of the subjects, therapists and assessors. Exercise intensity and type of the exercise (whole body only or single-joint task) were not part of the sorting criteria.

Muscle Strength

Isometric muscle strength assessments were included in 12 studies, involving 149 participants in eccentric exercise groups and 148 participants in traditional resistance or concentric exercise groups (**Figure 2**). The overall effect, although favoring the eccentric exercise group (SMD = 0.50), was not statistically significant ($p = 0.160$). Moreover, the heterogeneity across the studies was high ($I^2 = 87$ %). Sensitivity analysis showed that the exclusion of one study that favored concentric exercise (Onambélé et al., 2008) swayed the pooled effect enough to be statistically significant ($p = 0.030$) in favor of eccentric exercise (SMD = 0.71). Isometric ankle extension strength was assessed in two studies (with 33 participants in total for each group). The results are in favor of eccentric exercise with moderate effect (SMD = 0.92), but the difference between the exercise types was not statistically significant ($p = 0{,}200$), and the two studies were very heterogeneous ($I^2 = 84$ %) (**Figure 2**).

Body Composition and Muscle Architecture

Body fat percentage and body fat mass were considered in three studies, with a total number of 47 participants in eccentric exercise groups and 48 participants in in traditional resistance or concentric exercise groups Although the overall effect was large (SMD = −1.44) and showing decreases in body fat with eccentric exercise, it was statistically not significant ($p = 0.220$). A closer inspection of the data revealed that two studies showed almost no difference between the exercise types, while one study pointed heavily toward fat-lowering effect of eccentric exercise in comparison to traditional resistance or concentric exercise. Accordingly, the heterogeneity between the studies was very high ($I^2 = 95$ %). Lean leg mass was reported in two studies (with 50 and 49 participants in total for eccentric and concentric/traditional exercise groups, respectively) (**Figure 3**). The difference between the exercise modes was negligible (SMD = 0.08; $p = 0.680$).

Four studies compared the effect of eccentric and traditional resistance or concentric exercise on quadriceps muscle thickness (28 and 25 participants in total within eccentric and concentric/traditional groups, respectively) (**Figure 3**). The overall effect tended to support the superiority of eccentric exercise (SMD = 0.63), but was not statistically significant ($p = 0.200$) and the heterogeneity among the studies was high ($I^2 = 63$ %). The results for thigh circumference and thigh mass were pooled together from four studies, involving a total of 48 and 49 participants in eccentric and traditional resistance or concentric exercise groups, respectively. Three studies indicated larger thigh circumference/mass increases in eccentric group with large effect sizes (SMD = 1.16–1.95), however, one study pointed in the opposite direction (SMD = −0.39), yielding a large pooled effect that tended toward better effects in eccentric groups (SMD = 1.07), but slightly above the threshold for statistical significance ($p = 0.060$). The heterogeneity among the studies was high ($I^2 = 63\%$) (**Figure 3**), with three studies favoring eccentric and one study favoring traditional resistance. In a sensitivity analysis, the exclusion of the latter study (Mueller et al., 2011) resulted in statistically significant effect ($p < 0.001$) favoring eccentric exercise (SMD = 1.57). One study also involved the measurement of pennation angle and fascicle length of the vastus lateralis muscle. There was a large effect in favor of traditional resistance or concentric exercise for pennation angle (SMD = 2.65), while the opposite was true for the fascicle length (SMD = 1.25) (both $p < 0.01$).

Mobility and Function

The 6-min walking test was performed in 7 studies, involving a total of 97 participants in each group. The studies indicate no difference between the intervention groups on 6-min walking test (SMD = 0.01; $p = 0.960$). The heterogeneity among the studies was moderate ($I^2 = 54$ %). On the contrary, statistically significant ($p = 0.002$) moderate effect (SMD = 0.81) in favor of

TABLE 1 | Overview of the studies included into meta-analyses.

Study	Intervention	Basic participant data	Exercise type	Outcome	Main conclusion
Casillas et al., 2016	7 weeks, 3 times/week, 32 min/session	*n* = 42 (21 ECC; 21 CON) Age = 63.7 ± 10.1 ECC; 61.83 ± 8.5 CON BMI = 25.4 ± 3.8 ECC; 25.8 ± 3.7 Height = 171.1 ± 6.7 ECC; 170.4 ± 8.2 CON Weight = 74.5 ± 13.1 ECC; 75.2 ± 13.2 CON	ECC cycling vs. CON cycling	Isometric quadriceps torque, isometric triceps surae torque, peak work rate, 6MWT	Improvement in peak work and 6MWT was the same for the both groups. Maximal strength in triceps surae was increased only in ECC group.
Katsura et al., 2019	8 weeks, 3 times/week, 90 min/session	*n* = 17 (9 ECC; 8 CON) Age = 72 ± 6.6 ECC; 71.1 ± 4.5 CON BMI = 23.5 ± 4.5 ECC, 22.9 ± 1.5 CON Height = 160.8 ± 10.9 ECC; 155.5 ± 5.5 CON Weight = 60.3 ± 9.8 ECC; 55.4 ± 5.4 CON	ECC whole body exercises vs. CON whole body exercises	Isometric quadriceps torque, 30 s chair stand test, TUG, muscle volume of quadriceps femoris, 2 min step test, sit and reach test	ECC training was more effective for improvement of lower limb strength, mobility, muscle volume and postural stability in older adults when compared with CON training.
LaStayo et al., 2009	12 weeks, 3 times/week, 30 min/session	*n* = 17 (9 ECC; 8 CON) Age = 67 ± 8.8 ECC; 68 ± 8.7 CON BMI = 32.4 ± 4.4 ECC; 33.5 ± 5.4 CON	ECC lower body exercises vs. CON lower body exercises	Isometric quadriceps torque, 6MWT, TUG, muscle volume of quadriceps femoris, stair descent, stair ascent	Increase in muscle size and strength and improvement in functional ability tasks were greater in ECC group.
Mueller et al., 2009	12 weeks, 2 times/week, 35–45 min/session	*n* = 46 (23 ECC; 23 CON) Age = 80.3 ± 0.7 ECC; 80.1 ± 0,8 CON BMI = 23.5 ± 0.6 ECC; 24.3 ± 1 CON Height = 168 ± 2 ECC; 167 ± 2 CON Weight = 66.1 ± 1.8 ECC; 67.7 ± 2.6 CON	ECC ergometer training vs. conventional resistance training	Isometric quadriceps torque, TUG, Berg balance scale, Total fat mass	Maximal isometric leg extension strength, loss of body fat and thigh fat were significantly improved only in ECC group. Authors concluded that both ECC and CON training are beneficial for the elderly with regard to muscle function and structural improvements.
Mueller et al., 2011	12 weeks, 2 times/week, 40 min/session	*n* = 27 (13 ECC; 14 CON) Age = 80.3 ±1 ECC; 79.9 ± 1 Height = 168 ± 2.4 ECC; 169.8 ± 2.4 CON Weight = 68.5 ± 2.7 ECC; 74.9 ± 3.4 CON	ECC ergometer training vs. conventional resistance training	Isometric quadriceps torque, Thigh mass, Total fat mass	Both ECC and CON training regimes showed similar functional improvements, with ECC group being at least as effective or more effective as CON group.
Quinlan et al., 2021	8 weeks, 3 times/week, 60 min/session	*n* = 17 (9 ECC; 8 CON) Age = 67.5 ± 1.5 ECC; 69.1 ± 3.0 CON BMI = 24.7 ± 2.9 ECC; 25.7 ± 2.2 CON Height = 176 ± 8.8 ECC; 175 ± 3.3 CON Weight = 76.8 ± 10.4 ECC; 79.2 ± 8.5 CON	ECC leg press vs. CON leg press	Isometric quadriceps torque	Strength increase was similar between both groups.
Reeves et al., 2009	14 weeks, 3 times/week, 10 min/session	*n* = 19 (10 ECC; 9 CON) Age = 67 ± 2 ECC; 74 ± 3 CON Height = 168 ± 12 ECC; 163 ± 10 CON Weight = 74 ± 15 ECC; 70 ± 16 CON	ECC knee extension vs. CON knee extension	Volume of quadriceps femoris, Knee extensor pennation angle, knee extensor fascial length	Increase of fascial length was greater in ECC group. conversely, pennation angle significantly increased only in CON group. In ECC group, eccentric muscle strength was increased, with no change in concentric torque, and vice versa for CON group (increased concentric torque with no change in eccentric torque). Isometric torque increased to a similar extent in both groups.
Regnersgaard et al., 2021	6 weeks, 3 times/week, 45–60 min/session	*n* = 21 (7 ECC; 7 ECC*, 7 CON) Age = 71 ± 1 ECC; 70 ± 1 ECC*; 70 ± 1 CON BMI = 27 ± 0.7 ECC; 25.4 ± 1.7 ECC*; 24.8 ± 2 CON Weight = 73.8 ± 3.1 ECC; 73.4 ± 7 ECC*; 65.1 ± 6.6 CON	Stair ascent vs. Stair descent vs. Stair descent with 15% of persons additional weight (ECC*)	6MWT, 30 s chair stand test, Thigh mass	Leg muscle mass increased more in ECC*and ECC compared to CON. 6MWT and 30 s chair stand test increased more in ECC*compared to other groups. Carrying extra weight while descending star walking do not increase RPE, but still resulted in greater responses compared with CON.

(Continued)

TABLE 1 | Continued

Study	Intervention	Basic participant data	Exercise type	Outcome	Main conclusion
Steiner et al., 2004	8 weeks, 3 times/week, 30 min/session	*n* = 12 (6 ECC; 6 CON) Age = 55 ± 2.6 ECC; 56 ± 3.5 CON BMI = 27.6 ± 1.3 ECC; 27.1 ± 1.9 CON Height = 173 ± 3.9 ECC; 169 ± 0.8 CON Weight = 83 ± 8.1 ECC; 77 ± 1.9 CON	ECC ergometer training vs. standard cycle ergometer	Isometric quadriceps torque, Quadriceps lean tissue cross section area	Muscle mass increased significantly in both groups. Strength parameters improved only in ECC group, while fiber size increased only in CON group.
Symons et al., 2005	12 weeks, 3 times/week, 30 min/session	*n* = 19 (9 ECC; 10 CON) Age = 70.5 ± 5.2 ECC; 71,8 ± 3.1 CON Height = 166.1 ± 9.1 ECC; 168.9 ± 10.3 CON Weight = 80.7 ± 11.6 ECC; 78.5 ± 11.2 CON	ECC isokinetic training vs. CON isokinetic training	Isometric quadriceps torque	Both groups were effective in increasing strength and improving stair-climbing performance. ECC training was not superior to CON training.
Theodorou et al., 2013	6 weeks, 3 times/week, 12 min/session	*n* = 12 (6 ECC; 6 CON) Age = 66.8 ± 1.7 ECC; 64.8 ± 2.3 CON Weight = 85.8 ± 3.1 ECC; 82.1 ± 2.3 CON	Stair ascent vs. Stair descent	Isometric quadriceps torque	Both groups increased muscle strength. Stair descending appears to be less demanding than stair ascending, while changes in muscle strength are similar or even greater.
Besson et al., 2013	7 weeks, 3 times/week, 32 min/session	*n* = 30 (15 ECC; 15 CON) Age = 63.3 ± 10.1 ECC; 60.7 ± 11.8 CON Height = 170.9 ± 7.8 ECC; 170 ± 7 CON Weight = 70.3 ± 15.6 ECC; 74.7 ± 14.5 CON	ECC cycling vs. CON cycling	6MWT	Distance in 6MWT improved in both groups with ECC group being slightly better. ECC training induces functional improvement similar to conventional training, with lower demand on the cardiovascular system during exercise.
Bourbeau et al., 2020	10 weeks, 3 times/week, 30 min/session	*n* = 20 (10 ECC; 10 CON) Age = 68.5 ± 5.6 ECC; 65.2 ± 5 CON BMI = 24.9 ± 5.4 ECC; 25.8 ± 5.8 CON Height = 170.9 ± 10 ECC; 170 ± 8 CON Weight = 73.2 ± 20.4 ECC; 74.6 ± 18.3 CON	ECC cycling vs. CON cycling	Isometric quadriceps torque, 6MWT, stair ascent, steps per day	Muscle strength improved only in ECC group. Training-induced improvement for the 6MWD was observed only in the ECC group. Improvement in the total number of daily step counts from baseline were observed only after ECC training.
Chen et al., 2017a,b	12 weeks, 2 times/week, 5–60 min/session	*n* = 30 (15 ECC; 15 CON) Age = 66.4 ± 6.8 ECC; 66.5 ± 6.8 CON BMI = 26.2 ± 1.1 ECC; 26.1 ± 0.8 CON Height = 155.2 ± 5.8 ECC; 155.2 ± 5.8 CON Weight = 62.7 ± 6.4 ECC; 62.8 ± 5.1 CON	Stair ascent vs. Stair descent	Isometric quadriceps torque, 6MWT, 30 s chair stand test, TUG, 2-min step test, Thigh mass, Body mass	Muscle strength increased more in ECC group. Moreover, results of many functional ability tests show significantly greater improvement for ECC group compared to CON group.
Chen et al., 2017a	12 weeks, once per week, 10–100 min/session	*n* = 26 (13 ECC; 13 CON) Age = 65.9 ± 4.7 ECC & CON BMI = 25.5 ± 2.9 ECC & CON Height = 164.7 ± 5 ECC & CON Weight = 70.5 ± 8 ECC & CON	ECC knee extension vs. CON knee extension	Isometric quadriceps torque, 6MWT, 30 s chair stand test, TUG, 2-min step test, Thigh mass, Postural balance	Muscle strength and functional ability performance (e.g., 30 s chair stand, TUGT, balance) improved greater in ECC group compared to CON group. Eccentric exercise training was more effective than concentric exercise training to improve health and functional fitness in older adults.
Gault et al., 2012	12 weeks, 3 times/week, 30 min/session	*n* = 26 (13 ECC; 11 CON) Age = 67 ± 4 ECC & CON BMI = 26.6 ± 3.9 ECC & CON Height = 170 ± 9 ECC & CON Weight = 77.2 ± 13.9 ECC & CON	Downhill treadmill walking vs. level treadmill walking	TUG	Improvements in functional ability tests were substantial and similar in both groups.

(Continued)

TABLE 1 | Continued

Study	Intervention	Basic participant data	Exercise type	Outcome	Main conclusion
Gluchowski et al., 2017	8 weeks, 2 times/week	*n* = 22 (11 ECC; 11 CON) Age = 67 ± 4.5 ECC & CON Height = 169 ± 8.6 ECC & CON Weight = 75 ± 15.3 ECC & CON	ECC leg press vs. CON leg press	Stair descent, Leg soft tissue lean mass, Total fat mass	Muscle strength and functional ability tasks equally improved in all groups. Body composition significantly improved only in ECC group, with no statistical differences between groups (ECC, CON, eccentric based group).
Onambélé et al., 2008	12 weeks, 3 times/week	*n* = 24 (12 ECC; 12 CON) Age = 69.6 ± 1.1 ECC; 70.2 ± 1.5 CON BMI = 24.3 ± 2 ECC; 24.1 ± 2.5 CON	Flywheel VS inertial load machine	Isometric quadriceps torque, triceps surae maximal isometric torque, eyes open ML sway, eyes open AP sway	ECC group significantly increased quadriceps and triceps surae strength, while CON group increased only triceps surae strength. ECC training results in greater improvements in muscular strength and balance compared to CON group.
Jacobs et al., 2014	12 weeks, 3 times/week, 60 min/session	*n* = 77 (39 ECC; 38 CON) Age = 76.2 ± 7.4 ECC; 74.6 ± 6.2 CON BMI = 27.1 ± 4.8 ECC; 29.1 ± 6.2 CON	ECC ergometer stepper vs. Leg press and straight leg exercise	Leg soft tissue lean mass	No differences in intermuscular adipose tissue (IMAT) were observed over time, and there were no differences in IMAT response between intervention groups. Moreover, participants in CON group lost a significant amount of lean tissue in the 9 months after intervention, while participants in the ECC group did not.

ECC, eccentric exercise; CON, concentric exercise; BMI, body mass index; 6MWT, six-min walking test; TUGT, timed up and go test.

eccentric exercise was shown for the 30-s sit-stand test (**Figure 4**), which was tested in four studies, involving 44 participants in eccentric exercise groups and 43 participants in traditional resistance or concentric exercise groups. The heterogeneity among the studies was low ($I^2 = 19$ %). Two studies (44 and 43 participants in eccentric and traditional resistance or concentric exercise groups) included the stair descent test and tended to support a somewhat favorable effect of eccentric compared to traditional resistance or concentric exercise (SMD = −0.46), but not reaching statistical significance ($p = 0.179$). The two studies were homogenous ($I^2 = 0$%). Moreover, two studies (involving a total number of 19 participants in each group) reported the results of stair ascent test (**Figure 4**). The difference between the exercise modes was trivial (SMD = 0.03; $p = 0.930$). Three studies reported on the 2-min stepping test results (37 participants in eccentric exercise groups, 36 in traditional resistance or concentric exercise groups) (**Figure 4**). The overall effect favored the eccentric exercise (SMD = 0.53) and was statistically significant ($p = 0.03$). The studies reported very consistent results, as shown by negligible heterogeneity ($I^2 = 0$ %). TUGT was included in six studies (82 and 78 participants in eccentric and traditional resistance or concentric exercise groups, respectively). Similar to 30-s sit-stand, the results for TUGT were also statistically significantly ($p = 0.004$) better after eccentric exercise than traditional resistance or concentric exercise interventions (SMD = −0.68), and the heterogeneity among the studies was low ($I^2 = 22$ %).

DISCUSSION

The purpose of this systematic review with meta-analysis was to examine the effects of eccentric exercise interventions in contrast to traditional resistance or concentric exercise interventions on muscle strength, body composition, muscle architecture, mobility, and function in older adults. We included 18 interventional clinical trials that had at least two intervention groups (eccentric and traditional resistance or concentric intervention group). The main findings of our systematic review are as follows: (a) for muscle strength, the pooled effect favored eccentric exercise, but the difference to traditional resistance or concentric was not statistically significant; (b) the results regarding body composition and muscle architecture were unclear and pooled from a smaller number of studies; (c) for mobility and function, the results were diverse, with the effects either in favor of eccentric exercise, or showing no difference between the intervention groups. In sum we examined a wide variety of tests and yielded different results. Because of this fact we cannot say with absolute certainty that eccentric exercises are superior to traditional resistance or concentric exercises and therefore cannot entirely reject nor accept our hypothesis. Although the results support the somewhat favorable effect of eccentric exercises, there are still a few questions that remain open.

The studies examined a wide variety of functional tests, including tests that emphasize aerobic capacity (6MWT, 2-min stepping test) and tests that assess functional performance

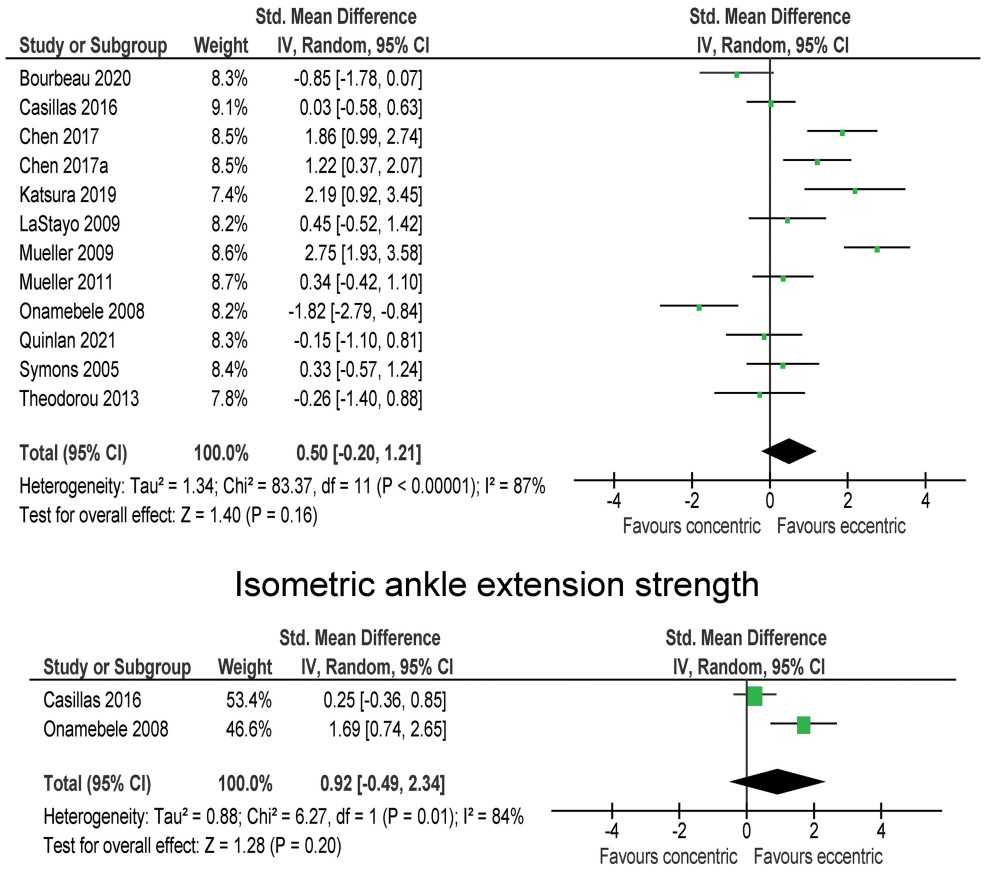

FIGURE 2 | The effect of eccentric vs. concentric exercise on muscle strength outcomes.

and mobility (TUGT, 30-s sit-stand test, stair descending and stair ascending). Seven studies examined the effect of eccentric exercise on 6MWT. All the studies were in agreement that the effect of eccentric resistance training is similar to that of traditional resistance or concentric exercise. Some studies have speculated that the improvements in eccentric training are due to an increased contribution of anaerobic metabolism during eccentric training and a consequent improvement of its capacity. Adaptation of anaerobic capacity would particularly benefit shorter functional tests, such as 30-s sit-stand test (Besson et al., 2013; Laroche et al., 2013). On the other hand, it has been proposed that involvement of elastic components in eccentric exercise could improve movement efficiency, which is associated with reduced metabolic cost (LaStayo et al., 1999; Lindstedt et al., 2001) and could contribute to improvement in all functional tests. Namely, as eccentric exercise is associated with lower metabolic costs, it presumably enables higher force and power outputs to be reached during training, which would in turn elicit higher adaptations in muscle capacity. Even within endurance tests, such as 6MWT, greater anaerobic capacity could improve the performance, as resistance exercise interventions have been shown numerous times to improve economy of endurance activities (Hartman et al., 2007; Hunter et al., 2021). The 2-min stepping test was improved for ∼10% in the eccentric exercise groups and ∼5% in traditional resistance or concentric exercise group (Chen et al., 2017a,b; Katsura et al., 2019). Thus, both interventions improved the 2-min stepping test results, but the eccentric training group was even more effective (SMD = 0.53).

The TUGT and the 30-s sit-stand test are the among the most frequently used and scientifically supported tests for assessing overall function in older adults (Beauchet et al., 2011; Bennell et al., 2011; Barry et al., 2014). We found greater improvement in TUGT with eccentric exercise ($p = 0.004$; SMD = −0.68) compared to traditional resistance or concentric exercise. That was also the case with 30-s sit to stand test ($p = 0.002$; SMD = 0.81). However, it appears that the effects on maximal strength are similar in both groups although there was some tendency for larger effects in eccentric groups. One of the most common issues in older adults is sarcopenia, which is associated with a decreased quality of life, lower exercise tolerance and decreased levels physical activity levels in general (Maltais et al., 2014). Therefore, increasing or maintaining muscle mass and muscle strength need to be considered as a priority when planning training protocols for older adults. It is well-documented that resistance exercise is a

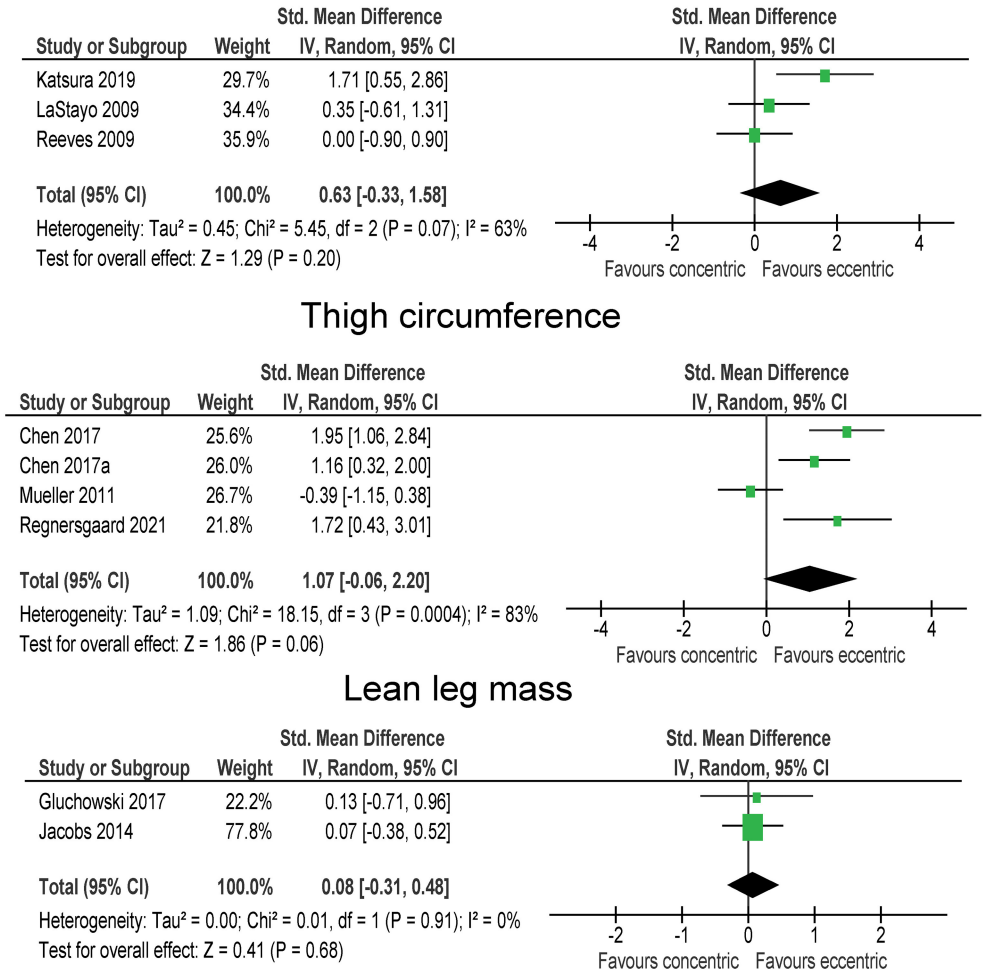

FIGURE 3 | The effect of eccentric vs. concentric exercise on outcomes related to body composition.

very effective low-cost tool for preventing and treating sarcopenia and chronic diseases (Booth et al., 2012; Pedersen and Saltin, 2015; Ciolac and Rodrigues-da-Silva, 2016). As we can see from this systematic review, eccentric exercise can be as effective or even more effective than traditional resistance or concentric exercise. Of note, care should be taken when prescribing the quantity and intensity of exercise to avoid or minimize the risk of muscle damage and associated muscle soreness. Clos et al. (2021) came to a conclusion that when exercises are performed at the same power output, eccentric cycling elicits less intense perceptions of effort and muscle pain than concentric cycling. Maximal voluntary torque on the other hand showed a similar decline. When clinicians base the eccentric exercises on the rating of perceived exertion they should be very careful, given that most participants exhibit more neuromuscular performance decline after eccentric exercises (Clos et al., 2021).

The interventions considered in this review included either high-load eccentric resistance exercises, or low-load cyclic tasks performed in eccentric conditions or with accentuated eccentric portion of the movement (downhill walking, stair descending, and eccentric cycling). Downhill or downstairs walking is emerging as an effective type of eccentric exercise for the elderly. Assuming that training protocol is carried out where an elevator or any kind of assistance that helps the trainee to ascend is available, the intervention requires little additional equipment. Chen et al. (2017a) reported that descending stair walking improved muscle function, physical fitness, balance, cardiorespiratory fitness, lipid profiles, bone mineral density, and insulin sensitivity more than ascending stair walking in elderly obese women. In addition to providing great health and fitness benefits, downhill/downstairs walking is also metabolically less demanding than uphill/upstairs walking (Theodorou et al., 2013; Chen et al., 2017b; Regnersgaard et al., 2021). There is a wide variety of other means to perform eccentric exercise, such as working on resistance-training machines, performing everyday tasks in a way to emphasize eccentric contraction

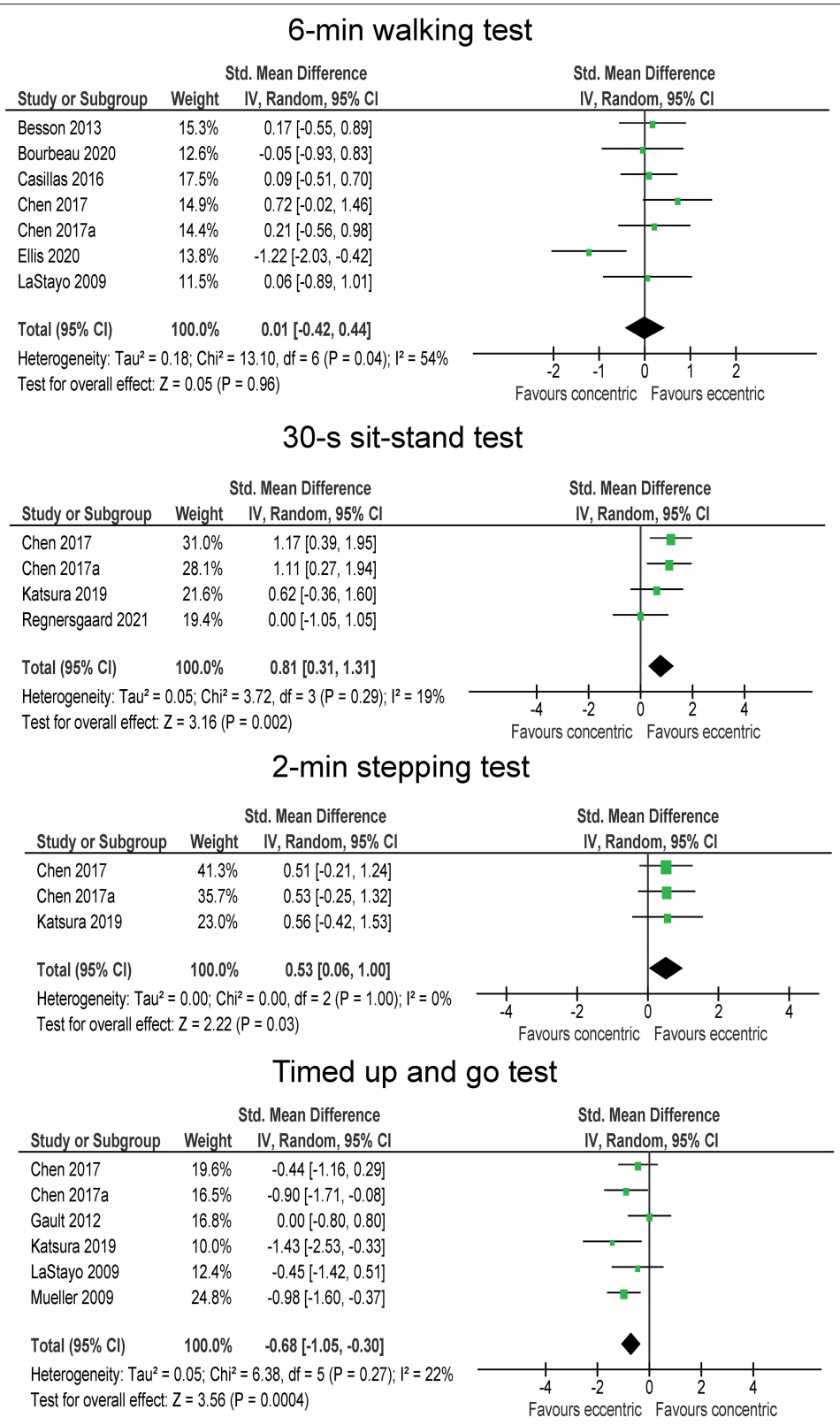

FIGURE 4 | The effect of eccentric vs. concentric exercise on outcomes related to function and mobility.

(e.g., sitting slowly down on a chair), or working on an eccentric cycle-ergometer. As said, one of the most important tasks of clinicians is that they dose the exercise correctly and that exercise is personalized by monitoring the rating of perceived exertion. Across the studies included in this review, the exercise was progressed gradually as fitness improved; either by pre-determined progression plan, or by tracking the rating of perceived exertion. Studies in this review mostly used the intensity corresponding to "somewhat hard" to "hard" exertion (between 9 and 13) on a Borg scale.

There are also a few limitations of this review to consider. The interventions were relatively short-term (6–12 weeks), which means that the differences between eccentric and traditional resistance or concentric exercise regarding long-term effects in older adults are not known. Moreover, several outcomes in the meta-analyses were pooled from a limited number of studies. In addition, subgroup analyses were not feasible due to the low number of studies. A few limitations also arise from the fact that there is sometimes hard to distinguish between ECC-only and ECC-emphasized exercise training protocols. It does raise an interesting question for further research on the topic, whether ECC-only training is more beneficial than merely emphasizing the ECC part of the exercise. Finally, the workload match between the exercise groups has to be questioned. Several studies used Borg scale, usually permitting some variation (e.g., 9–11 units). Some studies allowed participants to self-select the intensity (Gault and Willems, 2013) and very few used load prescription based on % repetition maximum (Reeves et al., 2009). It is not always clear how exercise programs should be matched to examine pure difference due to contraction type and maintain the ecological validity at the same time.

CONCLUSION

In conclusion, our literature review indicates that there are a few tests in which eccentric training is superior or at least equal to traditional resistance or concentric training in maintaining health and overall function in older adults. The tests that showed the most effects for shorter (anaerobic) tests such as 30-s sit-stand test and TUGT. On the other hand, longer (aerobic) tests showed less improvements. When examining the papers, we also came to a conclusion that eccentric exercise is safe for frail and sick individuals. This type of exercise has to be well-planned and constantly monitored by clinicians. When progressing the exercise, one of the more useful tools to use is a combination of RPE, increasing quantity and a gradual increase in amount and intensity within a training protocol.

DATA AVAILABILITY STATEMENT

The original contributions presented in the study are included in the article/**Supplementary Material**, further inquiries can be directed to the corresponding authors.

AUTHOR CONTRIBUTIONS

KČ, JP, SL, ŽK, and NŠ conceptualized the idea. KČ and JP carried out the review and wrote the manuscript. NŠ and ŽK were overviewing the review procedure. NŠ, SL, and ŽK analyzed the collected data and finalized the manuscript. All authors contributed to the article and approved the submitted version.

FUNDING

We want to acknowledge the support of the European Regional Development Fund and Physiko- and Rheumatherapie Institute through the Centre of Active Ageing project in the Interreg Slovakia–Austria cross-border cooperation program (partners: Faculty for Physical Education and Sports, Comenius University in Bratislava: Institute for Physical Medicine and Rehabilitation, Physiko- and Rheumatherapie GmbH). NŠ and ŽK acknowledge the University of Primorska's suppirt through internal research program KINSPO (2990-1-2/2021). The funders had no role in study conceptualization, data acquisition, data analysis or manuscript preparation.

SUPPLEMENTARY MATERIAL

The Supplementary Material for this article can be found online at: https://www.frontiersin.org/articles/10.3389/fspor.2022.873718/full#supplementary-material

REFERENCES

Barry, E., Galvin, R., Keogh, C., Horgan, F., and Fahey, T. (2014). Is the Timed Up and Go test a useful predictor of risk of falls in community dwelling older adults: a systematic review and meta-analysis. *BMC Geriatr.* 14:14. doi: 10.1186/1471-2318-14-14

Beauchet, O., Fantino, B., Allali, G., Muir, S. W., Montero-Odasso, M., and Annweiler, C. (2011). Timed up and go test and risk of falls in older adults: a systematic review. *J. Nutr. Heal. Aging* 15, 933–938. doi: 10.1007/s12603-011-0062-0

Benichou, O., and Lord, S. R. (2016). Rationale for strengthening muscle to prevent falls and fractures: a review of the evidence. *Calcif. Tissue Int.* 98, 531–545. doi: 10.1007/s00223-016-0107-9

Bennell, K., Dobson, F., and Hinman, R. (2011). Measures of physical performance assessments: Self-Paced Walk Test (SPWT), Stair Climb Test (SCT), Six-Minute Walk Test (6MWT), Chair Stand Test (CST), Timed Up and Go (TUG), Sock Test, Lift and Carry Test (LCT), and car task. *Arthritis Care Res.* 63, S350–S370. doi: 10.1002/acr.20538

Besson, D., Joussain, C., Gremeaux, V., Morisset, C., Laurent, Y., Casillas, J. M., et al. (2013). Eccentric training in chronic heart failure: feasibility and functional effects. Results of a comparative study. *Ann. Phys. Rehabil. Med.* 56, 30–40. doi: 10.1016/j.rehab.2013.01.003

Booth, F. W., Roberts, C. K., and Laye, M. J. (2012). Lack of exercise is a major cause of chronic diseases. *Compr. Physiol.* 2, 1143–1211. doi: 10.1002/cphy.c110025

Bourbeau, J., Sena, R. D. S., Taivassalo, T., Richard, R., Jensen, D., Baril, J., et al. (2020). Eccentric versus conventional cycle training to improve muscle strength

in advanced COPD: a randomized clinical trial. *Respir Physiol Neurobiol.* 276:103414. doi: 10.1016/j.resp.2020.103414

Buatois, S., Miljkovic, D., Manckoundia, P., Gueguen, R., Vançon, G., Perrin, P., et al. (2008). Five times sit to stand test is a predictor of recurrent falls in healthy community-living subjects aged 65 and older. *J. Am. Geriatr. Soc.* 56, 1575–1577. doi: 10.1111/j.1532-5415.2008.01777.x

Capodaglio, P., Capodaglio, E. M., Ferri, A., Scaglioni, G., Marchi, A., and Saibene, F. (2005). Muscle function and functional ability improves more in community-dwelling older women with a mixed-strength training programme. *Age Ageing* 34, 141–147. doi: 10.1093/ageing/afi050

Casillas, J. M., Besson, D., Hannequin, A., Gremeaux, V., Morisset, C., Tordi, N., et al. (2016). Effects of an eccentric training personalized by a low rate of perceived exertion on the maximal capacities in chronic heart failure: A randomized controlled trial. *Eur. J. Phys. Rehabil. Med.* 52, 159–168.

Chen, T. C., Hsieh, C. C., Tseng, K. W., Ho, C. C., and Nosaka, K. (2017b). Effects of descending stair walking on health and fitness of elderly obese women. *Med. Sci. Sports Exerc.* 49, 1614–1622. doi: 10.1249/MSS.0000000000001267

Chen, T. C. C., Tseng, W. C., Huang, G. L., Chen, H. L., Tseng, K. W., and Nosaka, K. (2017a). Superior effects of eccentric to concentric knee extensor resistance training on physical fitness, insulin sensitivity and lipid profiles of elderly men. *Front. Physiol.* 8:209. doi: 10.3389/fphys.2017.00209

Ciolac, E. G., and Rodrigues-da-Silva, J. M. (2016). Resistance training as a tool for preventing and treating musculoskeletal disorders. *Sport. Med.* 46, 1239–1248. doi: 10.1007/s40279-016-0507-z

Clos, P., Laroche, D., Stapley, P. J., and Lepers, R. (2019). Neuromuscular and perceptual responses to sub-maximal eccentric cycling. *Front. Physiol.* 10:354. doi: 10.3389/fphys.2019.00354

Clos, P., Mater, A., Laroche, D., and Lepers, R. (2021). Concentric versus eccentric cycling at equal power output or effort perception: neuromuscular alterations and muscle pain. *Scand. J. Med. Sci. Sports* 32, 45–59. doi: 10.1111/sms.14053

Deschenes, M. R. (2004). Effects of aging on muscle fibre type and size. *Sport. Med.* 34, 809–824. doi: 10.2165/00007256-200434120-00002

Doherty, T. J. (2003). Physiology of aging invited review: aging and sarcopenia. *J. Appl. Physiol.* 95, 1717–1727. doi: 10.1152/japplphysiol.00347.2003

Gault, M. L., Clements, R. E., and Willems, M. E. T. (2012). Functional mobility of older adults after concentric and eccentric endurance exercise. *Eur. J. Appl. Physiol.* 112, 3699–3707. doi: 10.1007/s00421-012-2338-4

Gault, M. L., and Willems, M. E. T. (2013). Isometric strength and steadiness adaptations of the knee extensor muscles to level and downhill treadmill walking in older adults. *Biogerontology* 14, 197–208. doi: 10.1007/s10522-013-9423-x

Gluchowski, A., Dulson, D., Merien, F., Plank, L., and Harris, N. (2017). Comparing the effects of two distinct eccentric modalities to traditional resistance training in resistance trained, higher functioning older adults. *Exp. Gerontol.* 98, 224–229. doi: 10.1016/j.exger.2017.08.034

Hartman, M. J., Fields, D. A., Byrne, N. M., and Hunter, G. R. (2007). Resistance training improves metabolic economy during functional tasks in older adults. *J. Strength Cond. Res.* 21, 91–5. doi: 10.1519/00124278-200702000-00017

Hody, S., Rogister, B., Leprince, P., Laglaine, T., and Croisier, J. L. (2013). The susceptibility of the knee extensors to eccentric exercise-induced muscle damage is not affected by leg dominance but by exercise order. *Clin. Physiol. Funct. Imaging* 33, 373–380. doi: 10.1111/cpf.12040

Hunter, G. R., Singh, H., Martins, C., Baranauskas, M. N., and Carter, S. J. (2021). Stretch-shortening cycle potentiation and resistance training-induced changes in walking economy/ease and activity-related energy expenditure in older women. *J. Strength Cond. Res.* 35, 1345–1349. doi: 10.1519/JSC.0000000000003975

Jacobs, J. L., Marcus, R. L., Morrell, G., and LaStayo, P. (2014). Resistance exercise with older fallers: Its impact on intermuscular adipose tissue. *Biomed Res. Int.* 2014:398960. doi: 10.1155/2014/398960

Jamurtas, A. Z., Garyfallopoulou, A., Theodorou, A. A., Zalavras, A., Paschalis, V., Deli, C. K., et al. (2013). A single bout of downhill running transiently increases HOMA-IR without altering adipokine response in healthy adult women. *Eur. J. Appl. Physiol.* 113, 2925–2932. doi: 10.1007/s00421-013-2717-5

Katsura, Y., Takeda, N., Hara, T., Takahashi, S., and Nosaka, K. (2019). Comparison between eccentric and concentric resistance exercise training without equipment for changes in muscle strength and functional fitness of older adults. *Eur. J. Appl. Physiol.* 119, 1581–1590. doi: 10.1007/s00421-019-04147-0

Kulkarni, D., Gregory, S., and Evans, M. (2021). Effectiveness of eccentric-biased exercise interventions in reducing the incidence of falls and improving functional performance in older adults: a systematic review. *Eur. Geriatr. Med.* doi: 10.1007/s41999-021-00571-8. [Epub ahead of print].

Laroche, D., Joussain, C., Espagnac, C., Morisset, C., Tordi, N., Gremeaux, V., et al. (2013). Is it possible to individualize intensity of eccentric cycling exercise from perceived exertion on concentric test? *Arch. Phys. Med. Rehabil.* 94, 1621–1627.e1. doi: 10.1016/j.apmr.2012.12.012

LaStayo, P., Marcus, R., Dibble, L., Frajacomo, F., and Lindstedt, S. (2014). Eccentric exercise in rehabilitation: safety, feasibility, and application. *J. Appl. Physiol.* 116, 1426–1434. doi: 10.1152/japplphysiol.00008.2013

LaStayo, P. C., Ewy, G. A., Pierotti, D. D., Johns, R. K., and Lindstedt, S. (2003). The positive effects of negative work: increased muscle strength and decreased fall risk in a frail elderly population. *J. Gerontol. Ser. A Biol. Sci. Med. Sci.* 58, M419–424. doi: 10.1093/gerona/58.5.M419

LaStayo, P. C., Meier, W., Marcus, R. L., Mizner, R., Dibble, L., and Peters, C. (2009). Reversing muscle and mobility deficits 1 to 4 years after tka: A pilot study. *Clin. Orthop. Relat. Res.* 467, 1493–1500. doi: 10.1007/s11999-009-0801-2

LaStayo, P. C., Reich, T. E., Urquhart, M., Hoppeler, H., and Lindstedt, S. L. (1999). Chronic eccentric exercise: improvements in muscle strength can occur with little demand for oxygen. *Am. J. Physiol. Regul. Integr. Comp. Physiol.* 276, R611–615. doi: 10.1152/ajpregu.1999.276.2.R611

Lewis, M. C., Peoples, G. E., Groeller, H., and Brown, M. A. (2018). Eccentric cycling emphasising a low cardiopulmonary demand increases leg strength equivalent to workload matched concentric cycling in middle age sedentary males. *J. Sci. Med. Sport* 21, 1238–1243. doi: 10.1016/j.jsams.2018.05.009

Lindstedt, S. L., LaStayo, P. C., and Reich, T. E. (2001). When active muscles lengthen: properties and consequences of eccentric contractions. *News Physiol. Sci.* 16, 256–261. doi: 10.1152/physiologyonline.2001.16.6.256

Macaluso, A., and De Vito, G. (2004). Muscle strength, power and adaptations to resistance training in older people. *Eur. J. Appl. Physiol.* 91, 450–472. doi: 10.1007/s00421-003-0991-3

Maher, C. G., Sherrington, C., Herbert, R., Moseley, A. M., and Elkins, M. (2003). Reliability of the PEDro scale for rating quality of randomized controlled trials. *Phys. Ther.* 83, 713–721. doi: 10.1093/ptj/83.8.713

Malbut-Shennan, K., and Young, A. (1999). The physiology of physical performance and training in old age. *Coron. Artery Dis.* 10, 37–42. doi: 10.1097/00019501-199901000-00007

Maltais, F., Decramer, M., Casaburi, R., Barreiro, E., Burelle, Y., Debigare, R., et al. (2014). An official American thoracic society/european respiratory society statement: update on limb muscle dysfunction in chronic obstructive pulmonary disease. *Am. J. Respir. Crit. Care Med.* 189, e15–62. doi: 10.1164/rccm.201402-0373ST

Methley, A. M., Campbell, S., Chew-Graham, C., McNally, R., and Cheraghi-Sohi, S. (2014). PICO, PICOS and SPIDER: a comparison study of specificity and sensitivity in three search tools for qualitative systematic reviews. *BMC Health Serv. Res.* 14:579. doi: 10.1186/s12913-014-0579-0

Molinari, T., Steffens, T., Roncada, C., Rodrigues, R., and Dias, C. P. (2019). Effects of eccentric-focused versus conventional training on lower limb muscular strength in older adults: a systematic review with meta-analysis. *J. Aging Phys. Act.* 27, 823–830. doi: 10.1123/japa.2018-0294

Mueller, M., Breil, F. A., Lurman, G., Klossner, S., Flück, M., Billeter, R., et al. (2011). Different molecular and structural adaptations with eccentric and conventional strength training in elderly men and women. *Gerontology* 57, 528–538. doi: 10.1159/000323267

Mueller, M., Breil, F. A., Vogt, M., Steiner, R., Klossner, S., Hoppeler, H., et al. (2009). Different response to eccentric and concentric training in older men and women. *Eur. J. Appl. Physiol.* 107, 145–153. doi: 10.1007/s00421-009-1108-4

Onambélé, G. L., Maganaris, C. N., Mian, O. S., Tam, E., Rejc, E., McEwan, I. M., et al. (2008). Neuromuscular and balance responses to flywheel inertial versus weight training in older persons. *J. Biomech.* 41, 3133–3138. doi: 10.1016/j.jbiomech.2008.09.004

Peake, J., Nosaka, K., and Suzuki, K. (2005). Characterization of inflammatory responses to eccentric exercise in humans. *Exerc. Immunol. Rev.* 11, 64–85.

Pedersen, B. K., and Saltin, B. (2015). Exercise as medicine - Evidence for prescribing exercise as therapy in 26 different chronic diseases. *Scand. J. Med. Sci. Sport.* 25, 1–72. doi: 10.1111/sms.12581

Peñailillo, L., Blazevich, A., and Nosaka, K. (2014). Energy expenditure and substrate oxidation during and after eccentric cycling. *Eur. J. Appl. Physiol.* 114, 805–814. doi: 10.1007/s00421-013-2816-3

Quinlan, J. I., Franchi, M. V., Gharahdaghi, N., Badiali, F., Francis, S., Hale, A., et al. (2021). Muscle and tendon adaptations to moderate load eccentric vs. *concentric resistance exercise in young and older males. GeroSci.* 43, 1567–1584. doi: 10.1007/s11357-021-00396-0

Raman, J., MacDermid, J. C., and Grewal, R. (2012). Effectiveness of different methods of resistance exercises in lateral epicondylosis - a systematic review. *J. Hand Ther.* 25, 5–26. doi: 10.1016/j.jht.2011.09.001

Reeves, N. D., Maganaris, C. N., Longo, S., and Narici, M. V. (2009). Differential adaptations to eccentric versus conventional resistance training in older humans. *Exp. Physiol.* 94, 825–833. doi: 10.1113/expphysiol.2009.046599

Regnersgaard, S., Knudsen, A. K., Lindskov, F. O., Mratinkovic, M., Pressel, E., Ingersen, A., et al. (2021). Down stair walking: a simple method to increase muscle mass and performance in 65+ year healthy people. *Eur. J. Sport Sci.* 22, 279–288. doi: 10.1080/17461391.2020.1856936

Steiner, R., Meyer, K., Lippuner, K., Schmid, J. P., Saner, H., and Hoppeler, H. (2004). Eccentric endurance training in subjects with coronary artery disease: A novel exercise paradigm in cardiac rehabilitation? *Eur. J. Appl. Physiol.* 91, 572–578. doi: 10.1007/s00421-003-1000-6

Symons, T. B., Vandervoort, A. A., Rice, C. L., Overend, T. J., and Marsh, G. D. (2005). Effects of maximal isometric and isokinetic resistance training on strength and functional mobility in older adults. *J. Gerontol. - Ser. A Biol. Sci. Med. Sci.* 60, 777–781. Available online at: http://www.embase.com/search/results?subaction=viewrecord&from=export&id=L40881186

Theodorou, A. A., Panayiotou, G., Paschalis, V., Nikolaidis, M. G., Kyparos, A., Mademli, L., et al. (2013). Stair descending exercise increases muscle strength in elderly males with chronic heart failure. *BMC Res. Notes* 6:87. doi: 10.1186/1756-0500-6-87

Viña, J., Rodriguez-Mañas, L., Salvador-Pascual, A., Tarazona-Santabalbina, F. J., and Gomez-Cabrera, M. C. (2016). Exercise: the lifelong supplement for healthy ageing and slowing down the onset of frailty. *J. Physiol.* 594, 1989–1999. doi: 10.1113/JP270536

Conflict of Interest: NŠ was employed by company S2P, Science to Practice, Ltd. The company hand no role in conceptualization of the study, data acquisition, article writing nor any other phase of the study.

The remaining authors declare that the research was conducted in the absence of any commercial or financial relationships that could be construed as a potential conflict of interest.

frontiers | Frontiers in Physiology

ORIGINAL RESEARCH
published: 20 April 2022
doi: 10.3389/fphys.2022.833809

Low-Intensity Resistance Exercise Combined With Blood Flow Restriction is More Conducive to Regulate Blood Pressure and Autonomic Nervous System in Hypertension Patients—Compared With High-Intensity and Low-Intensity Resistance Exercise

Yan Zhao[1], *Yuchan Zheng*[1], *Xiaohuan Ma*[1], *Lili Qiang*[2], *Aicui Lin*[3]* *and Mo Zhou*[4]*

[1]School of Sports and Health, Nanjing Sport Institute, Nanjing, China, [2]Rehabilitation Hospital of Huishan District of Wuxi, Wuxi, China, [3]Department of Science and Technology, Nanjing First Hospital, Nanjing Medical University, Nanjing, China, [4]Department of Rehabilitation, Nanjing First Hospital, Nanjing Medical University, Nanjing, China

Background: The effect of resistance exercise on the autonomic nervous system of patients with hypertension has not been identified.

Objective: To explore a suitable resistance training method for hypertension patients to regulate blood pressure (BP) and autonomic nervous system function.

Method: Forty-five hypertension patients aged between 55 and 70 years were randomly equally divided into three groups: the high-intensity resistance exercise (HE) group, the low-intensity resistance exercise combined with blood flow restriction (LE-BFR) group, and the low-intensity resistance exercise (LE) group. All patients performed quadriceps femoris resistance exercise. The exercise intensity of HE, LE-BFR and LE group was 65, 30 and 30% of one repetition maximum (1RM), respectively. The LE-BFR group used pressure cuffs to provide 130% of systolic pressure to the patient's thighs during resistance exercise. The training program was 20 times/min/set with a 1-min break after each set, and was conducted five sets/day and 3 days/week, lasting for 12 weeks. The heart rate (HR), BP, root-mean-square of difference-value of adjacent RR intervals (RMSSD), low frequency (LF) and high frequency (HF) were evaluated before and after the first training and the last training.

Result: Significant differences in HR were observed in both recovery states after the first and last training ($p < 0.01$). After 12 weeks of training, the recovery speed of HR in the LE-BFR group increased significantly ($p < 0.01$). The systolic blood pressures in the HE and LE-BFR group were significantly reduced ($p < 0.05$ and $p < 0.01$), and the differences among groups were significant ($p < 0.01$). In the last recovery state, the RMSSD of the LE group was significantly lower than that in the first recovery state ($p < 0.01$). The LF/HF ratios of the HE and LE groups in the resting and recovery states were increased significantly (all $p < 0.01$). LF/HF ratios in the LE-BFR group in the resting and recovery state were decreased significantly (both $p < 0.01$).

Edited by:
Marcus Fraga Vieira, Universidade Federal de Goiás, Brazil

Reviewed by:
Ana Cristina Silva Rebelo, Universidade Federal de Goiás, Brazil
Samuel Oxford, Coventry University, United Kingdom
In cheol Jeong, Icahn School of Medicine at Mount Sinai, United States

***Correspondence:**
Aicui Lin
linaicui@126.com
Mo Zhou
zhoumo3480@126.com

Specialty section:
This article was submitted to Exercise Physiology, a section of the journal Frontiers in Physiology

Received: *12 December 2021*
Accepted: *02 March 2022*
Published: *20 April 2022*

Citation:
Zhao Y, Zheng Y, Ma X, Qiang L, Lin A and Zhou M (2022) Low-Intensity Resistance Exercise Combined With Blood Flow Restriction is More Conducive to Regulate Blood Pressure and Autonomic Nervous System in Hypertension Patients—Compared With High-Intensity and Low-Intensity Resistance Exercise. Front. Physiol. 13:833809. doi: 10.3389/fphys.2022.833809

Conclusion: Compared to HE and LE, LE-BFR could effectively decrease systolic pressure and regulate the autonomic nervous system function in hypertension patients.

Keywords: hypertension, autonomic nervous system, resistance exercise, blood flow restriction, blood pressure

1 INTRODUCTION

Hypertension is an important public health problem worldwide and is considered the main risk factor for cardiovascular diseases (Mozaffarian et al., 2015). The autonomic nervous system (ANS) plays an important role in regulating blood pressure (BP). Studies have found that imbalance and dysregulation of the ANS, manifested as enhanced sympathetic activity (Li et al., 2020; Esler, 2011), precede the occurrence of hypertension and develop concurrently with hypertension (Hering et al., 2016; Mancia and Grassi, 2014; Zubcevic et al., 2019). Therefore, it is important to modify the imbalance and dysregulation of the ANS for hypertension patients with sympathetic predominant states.

Exercise helps to lower BP, but patients with arterial hypertension were advised to avoid high levels of acute cardiovascular stress (Vale et al., 2018) because of the sympathetic predominance. Even though aerobic exercise was demonstrated to be able to inhibit sympathetic predominance (Esler, 2011), the effect of resistance exercise on decreasing sympathetic activity has not yet been identified in previous studies (Trevizani et al., 2018).

A transient research has found high-intensity resistance exercise (HE) can lead to a significant increase in systolic blood pressure (SBP) after the exercise, while low-intensity resistance exercise (LE) cannot, but LE can lead to a significant increase in the low frequency/high frequency (LF/HF) ratio (Vale et al., 2018). Hence, it remains unclear whether high-intensity and low-intensity exercise are unfavorable to patients with hypertension, and the exploration of resistance exercise suitable for hypertensive patients is required to reduce BP and avoid cardiovascular disease risks.

Low-intensity resistance exercise combined with blood flow restriction (LE-BFR) has been widely implemented to investigate its cardiovascular effect, but most of the research explored the cardiovascular effect on healthy adults. Early et al. found LE-BFR could lower SBP in healthy young adults (Early et al., 2020). However, studies on LE-BFR in hypertension patients are rare (Cerqueira et al., 2021).

This study aimed to analyze and compare the impacts of HE, LE, and LE-BFR on BP and ANS in hypertension patients, and to provide the most efficacious resistance exercise procedure that could reduce BP and avoid cardiovascular disease risks for hypertension patients.

2 METHODS

2.1 Participants

Forty-five hypertension patients aged between 55 and 70 years, including 16 men and 29 women, were voluntarily included. Patients with the following features were excluded: 1) body mass index (BMI) > 28; 2) abnormal electrocardiogram in the resting state and after exercise; 3) with musculoskeletal disorders; 4) with physical exercises more than twice a week; 5) SBP ≥180 mmHg and/or diastolic blood pressure (DBP) ≥ 100 mmHg in resting state; 6) special diet control. Patients were included in this study only when the clinical evaluation showed that they had no restrictions on participating in physical exercise. A written informed consent was obtained from each patient after they understood the detailed description of all procedures. This study was approved by the Ethics Committee for Human Experiments of Rehabilitation hospital of Huishan in Wuxi, Jiangsu, China (ID: HK-LLWYH-202002).

2.2 Trial Design

2.2.1 Groups

Patients were randomly equally divided into three groups: HE, LE-BFR, and LE groups.

2.2.2 One Repetition Maximum

The one repetition maximum (1RM) of quadriceps femoris was evaluated by the Isokinetic Muscle Strength Evaluation Training System (SYSTEM4, BIODEX Co., Ltd., New Jersey, United States). Before the evaluation, each patient underwent a 15 minutes of lower limb muscle stretching as warm-up and then sat on the chair of the isokinetic dynamometer with one lower leg perpendicular to the ground. Before the evaluation, all patients participated in an adaptation session. When doing adaptation exercises, the patients performed ten contractions of quadriceps femoris to move the knee joint from 90° flexion to 0° extension without load. During the evaluation, the patients performed three contractions of quadriceps femoris to move the knee joint from 90° flexion to 0° extension. The instrument calculated the 1RM by the strength of contraction. The 1RM of both legs was evaluated, and the higher value was selected as the patient's evaluation result. An assessment was conducted every 4 weeks to help the subjects adjust their exercise intensity.

2.2.3 Measurement of Cardiac ANS Function

The autonomic modulation index of the cardiovascular system was obtained by FIRSTBEAT (Version 4.7.3.1, Firstbeat Technologies Ltd., Jyväskylä, Finland). Time domain variables examined included the mean heart rate (HR) and the root-mean-square of difference-value of adjacent RR intervals (RMSSD). Frequency domain indicators examined included low frequency (LF; 0.04–0.15 Hz) and high frequency (HF; 0.15–0.50 Hz) values. In addition, the LF/HF ratio was calculated to represent the sympathovagal balance (Task Force, 1996).

Participants were required to avoid drinking any liquids containing caffeine and/or alcohol within 2 h before the assessment. All evaluations were performed at least 2 h after a

meal. The index of ANS in the resting states were obtained 0–15 min before the first and the last trainings. In order to get the indicators of ANS in the recovery state on the same time period, RMSSD, LF and HF were obtained 10–20 min after the first and the last trainings. HR in the recovery state was collected 10–30 min after the training, as it turned stable 10 min after the training.

2.2.4 Blood Flow Restriction Intervention

Blood pressures were measured 0–15 min before the first and last trainings in the resting state. For patients in the LE-BFR group, inflatable pressure cuffs (KAATSUMASTER, Kaatsu Japan Co., Ltd., Tokyo, Japan) were used to wrap around the upper third of both thighs to restrict blood flow. When patients performed exercises, the pressure cuffs were inflated and the pressure was 130% of the subjects' SBP (Zhao et al., 2021). The pressure cuffs were removed after each set of exercise.

2.3 Training Program

The resistance exercises in each group were conducted by contracting quadriceps femoris, leading to the extension of knee joints on the isokinetic dynamometer. The exercise intensity of patients in the HE group was 65% of 1RM, and that in the LE group and LE-BFR group was 30% of 1RM. During exercises, patients in the LE-BFR group underwent blood occlusions by inflating the pressure cuffs. The resistance exercise program was 20 times/min/set, with a 1-min break after each set and a number of five sets/day. The exercise frequency was 3 days/week, for a total of 12 weeks. Each repetition was completed within 3 s, with the rhythm controlled by a metronome. Both legs of the patients were trained and their daily physical activities were not intervened.

2.4 Statistical Analyses

The measurement data were expressed as mean ± standard deviation (SD). Differences within each group were analyzed using the paired *t* test. Differences among three groups were analyzed by one-way ANOVA, and the LSD method was used for multiple comparisons. The *p*-value reported was two-sided, and the differences with a *p*-value <0.05 was considered statistically significant, while *p*-value <0.01 was considered highly statistically significant. All statistical analyses were performed using SPSS software (version 13.0, SPSS, Chicago, IL, United States).

3 RESULTS

3.1 Basic Characteristics

Before the training started, there were no significant differences among groups in terms of age, height, body mass, and other characteristics (**Table 1**).

3.2 Effects of Different Exercise Modes on HR

After 12 weeks of training, HR in the resting state didn't vary significantly in the three groups ($p > 0.05$) (**Figure 1A**).

After the first training, HR in the recovery state in the LE group (71.5 ± 6.2 b·min^{-1}) was significantly lower than that in the LE-BFR (90.2 ± 5.2 b·min^{-1}) and HE groups (96.3 ± 12.3 b·min^{-1}) (both $p < 0.01$). After 12 weeks of training, HR in the recovery state in the LE-BFR group decreased significantly ($p < 0.01$), and HR in the HE group (91.6 ± 11.4 b·min^{-1}) was significantly higher than that in the LE-BFR (73.9 ± 8.0 b·min^{-1}) and LE groups (75.1 ± 7.5 b·min^{-1}) (both $p < 0.01$) (**Figure 1B**).

3.3 Effects of Different Exercise Modes on BP

Before the training, there were no significant differences in BP among groups ($p > 0.05$). After 12 weeks of training, SBP in the HE (148.1 ± 11.4 vs. 142.9 ± 4.9 mmHg, $p < 0.05$) and LE-BFR groups (144.7 ± 7.9 vs. 129.7 ± 7.6 mmHg, $p < 0.01$) were significantly decreased compared to that before resistance training. SBP in the LE-BFR group was significantly lower than that in the HE (148.1 ± 11.4 mmHg) and LE groups (140.9 ± 5.2 mmHg) (both $p < 0.01$) (**Figure 2A**). There were no significant differences in DBP among groups before and after the trainings ($p > 0.05$) (**Figure 2B**).

3.4 Effects of Different Exercise Modes on RMSSD

In terms of RMSSD, there were no significant differences among groups in the resting states before the training and 12 weeks after the training or in the recovery states after the first training ($p > 0.05$) (**Figures 3A, B**). After 12 weeks of training, RMSSD in the LE group in the recovery state was decreased significantly (20.4 ± 3.2 vs. 16.7 ± 4.5 m, $p < 0.01$). Comparing the recovery state after the first and last training, there was no significant decrease of RMSSD in the HE group (17.7 ± 11.0 vs. 15.3 ± 5.3 m, $p > 0.05$), and no significant increase of RMSSD in the LE-BFR group (19.1 ± 5.9 vs. 19.9 ± 4.9 m, $p > 0.05$). However, there was significant difference in RMSSD in the recovery state between the HE and LE-BFR groups after the last training ($p < 0.05$) (**Figures 3B, D**).

3.5 Effects of Different Exercise Modes on LF/HF Ratio

Before the training, there were no significant differences in LF/HF ratio among groups ($p > 0.05$). After 12 weeks of training, in terms of LF/HF ratio in resting state, significant increases were observed in the HE (1.5 ± 0.3 vs. 2.8 ± 0.5, $p < 0.01$) and LE groups (1.5 ± 0.3 vs. 1.7 ± 0.4, $p < 0.01$), whereas significant decrease was observed in the LE-BFR group (1.5 ± 0.2 vs. 0.7 ± 0.1, $p < 0.01$). Moreover, there were significant differences in LF/HF ratio among groups ($p < 0.01$) (**Figure 4A**). In the recovery state after the first training, LF/HF ratio in the HE group was significantly higher than that in the LE-BFR and LE groups (both $p < 0.01$) (**Figure 4B**). In the recovery state after the last training, significant increases in LF/HF ratio were observed in the HE (2.5 ± 0.4 vs. 5.4 ± 1.0, $p < 0.01$) and LE groups (1.6 ± 0.3 vs. 1.8 ± 0.3, $p < 0.01$), while significantly decreased LF/HF ratio was

TABLE 1 | Characteristics of participants included in the study.

Variables	LE group	LE-BFR group	HE group
Age (years)	61.0 ± 4.3	63.0 ± 5.2	61.7 ± 3.6
Height (m)	158.7 ± 5.4	160.7 ± 3.5	158.0 ± 8.4
Body mass (kg)	65.0 ± 10.1	60.0 ± 6.2	63.9 ± 8.6
Body mass index (kg/m^2)	25.7 ± 2.9	23.2 ± 2.0	25.5 ± 2.7
1RM (kg)	38.2 ± 2.5	36.4 ± 4.7	39.8 ± 3.9
Heart rate (b/min)	72.0 ± 6.7	73.0 ± 4.8	69.9 ± 6.6
SBP (mmHg)	145.9 ± 9.3	144.7 ± 7.9	148.1 ± 11.4
DBP (mmHg)	77.2 ± 5.5	74.5 ± 5.4	75.9 ± 9.8
Fasting blood glucose (mmol/L)	6.5 ± 1.2	6.0 ± 1.1	6.0 ± 0.8
Total cholesterol (mmol/L)	4.7 ± 1.0	5.0 ± 1.3	4.9 ± 0.7
Triglyceride (mmol/L)	1.7 ± 1.0	1.6 ± 0.8	1.8 ± 0.9
Low density lipoprotein (mmol/L)	2.6 ± 1.0	3.1 ± 1.1	3.0 ± 0.7
Proportion of hypertension (%)	100.0	100.0	100.0
Proportion of hyperlipidemia (%)	40.0	60.0	46.7
Proportion of hyperglycemia (%)	60.0	40.0	26.7

Data are presented as mean ± standard deviation.
1RM, One-repetition maximum; SBP, systolic blood pressure; DBP, diastolic blood pressure.

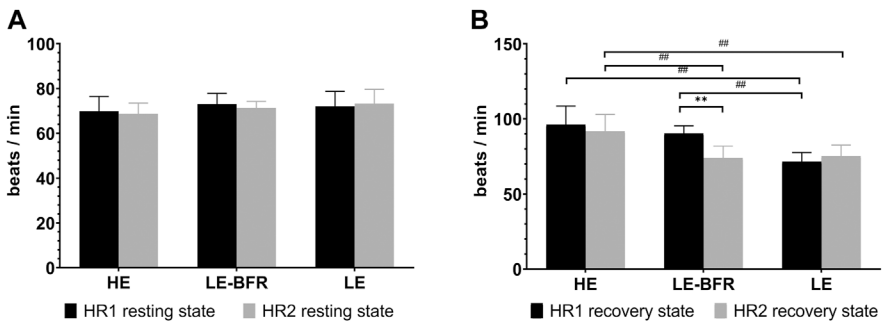

FIGURE 1 | (A) HR in the resting state before the first and last training. **(B)** HR in the recovery state after the first and last training. HR1 resting state, HR in the resting state before the first training. HR2 resting state, HR in the resting state before the last training. HR1 recovery state, HR in the recovery state after the first training. HR2 recovery state, HR in the recovery state after the last training. Data are presented as the mean ± standard deviation (SD). $^{**}p < 0.01$, significantly different from baseline. $^{\#\#}p < 0.01$, significantly different among groups.

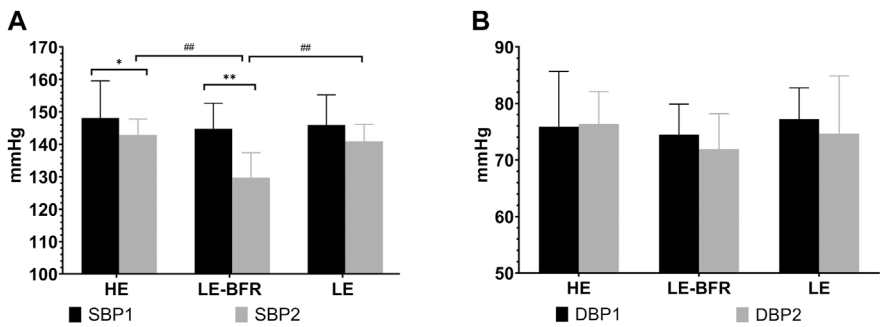

FIGURE 2 | (A) SBP in the resting state before the first and the last training. **(B)** DBP in the resting state before the first and the last training. SBP1, SBP before the first training. SBP2, SBP before the last training. DBP1, DBP before the first training. DBP2, DBP before the last training. Data are presented as the mean ± standard deviation (SD). $^{*}p < 0.05$, $^{**}p < 0.01$, significantly different from baseline. $^{\#\#}p < 0.01$, significantly different among groups.

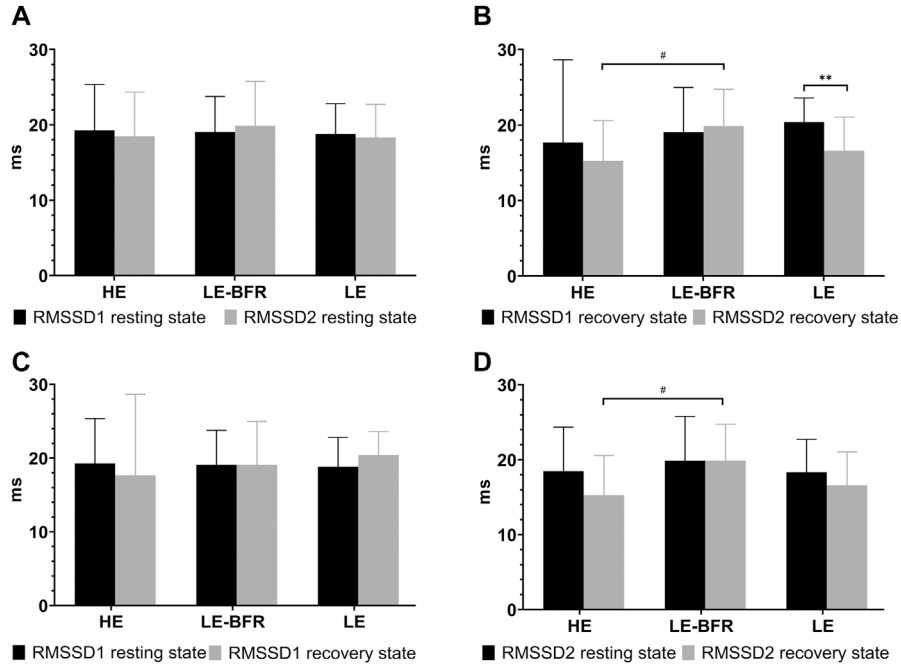

FIGURE 3 | (A) RMSSD in the resting state before the first and the last training. **(B)** RMSSD in the recovery state after the first and the last training. **(C)** RMSSD before and after the first training. **(D)** RMSSD before and after the last training. RMSSD1 resting state, RMSSD in the resting state before the first training. RMSSD2 resting state, RMSSD in the resting state before the last training. RMSSD1 recovery state, RMSSD in the recovery state after the first training. RMSSD2 recovery state, RMSSD in the recovery state after the last training. Data are presented as the mean ± standard deviation (SD). $^{**}p < 0.01$, significantly different from baseline. $\#p < 0.05$, significantly different among groups.

observed in the LE-BFR group (1.8 ± 0.3 vs. 0.7 ± 0.1, $p < 0.01$). There were significant differences in LF/HF ratio among groups ($p < 0.01$) (**Figure 4B**).

In the recovery state after the first training, compared to the resting state, LF/HF ratios in the HE and LE-BFR groups were increased significantly (both $p < 0.01$). Moreover, LF/HF ratio in the HE group was higher than that in the LE-BFR and LE groups (both $p < 0.01$) (**Figure 4C**). In the resting state before the last training, LF/HF ratio was increased in the HE group compared to the LE group ($p < 0.01$), and in the LE group compared to the LE-BFR group ($p < 0.01$). In the recovery state after the last training, compared to the resting state before the last training, LF/HF ratio in the HE group was increased significantly ($p < 0.01$), but no significant difference in LF/HF ratio between LE-BFR and LE groups were observed ($p > 0.05$). There were significant differences in LF/HF ratio among the three groups ($p < 0.01$) (**Figure 4D**). As shown in **Table 2**, HF in the HE group was decreased very significantly ($p < 0.01$) and HF in the LE-BFR group was increased very significantly ($p < 0.01$) after the training, which led to the highly significant change of LF/HF ratios among the groups.

4 DISCUSSION

This study aimed to find out the resistance exercise type that was beneficial for regulating BP and ANS, and that could avoid higher cardiovascular risk. It was suggested that compared to HE and LE, LE-BFR could more effectively regulate SBP and the imbalance and dysregulation of the ANS in hypertension patients. It was also indicated that when hypertension patients used resistant exercise to decrease SBP in the resting state, LE-BFR was the most effective exercise type compared to HE and LE, leading to less cardiovascular risk.

Both high BP and high HR are risk factors of cardiovascular, however, this research didn't find the decrease of SBP related to HR in the resting states. In this research, there was no significant difference between the resting HR before and after the training.

HR recovery rate reflects the balance of the autonomic nervous system (Silva et al., 2021). Previous studies have found slow HR recovery rate after exercise is associated with increased risk for arrhythmia and other cardiovascular morbidities and mortality, while increased HR recovery rate is associated with improved prognosis and lower mortality related to cardiovascular disease (Heffernan et al., 2007; Smith et al., 2005; Stein et al., 2005; Task Force, 1996; Tsuji et al., 1996; Zhang et al., 2016). Cardiovascular and neurovegetative adaptations to exercise training through alteration in sympathovagal balance lead to changes in HR recovery (Suzic et al., 2017). After the first training, the HR recovery rate of the HE and LE-BFR groups was slower than that of the LE group, implying that for hypertension patients without exercise habits, the cardiovascular risk caused by temporary HE and LE-BFR was higher than that by LE. After 12 weeks of training, the HR recovery rate of the LE-BFR group was

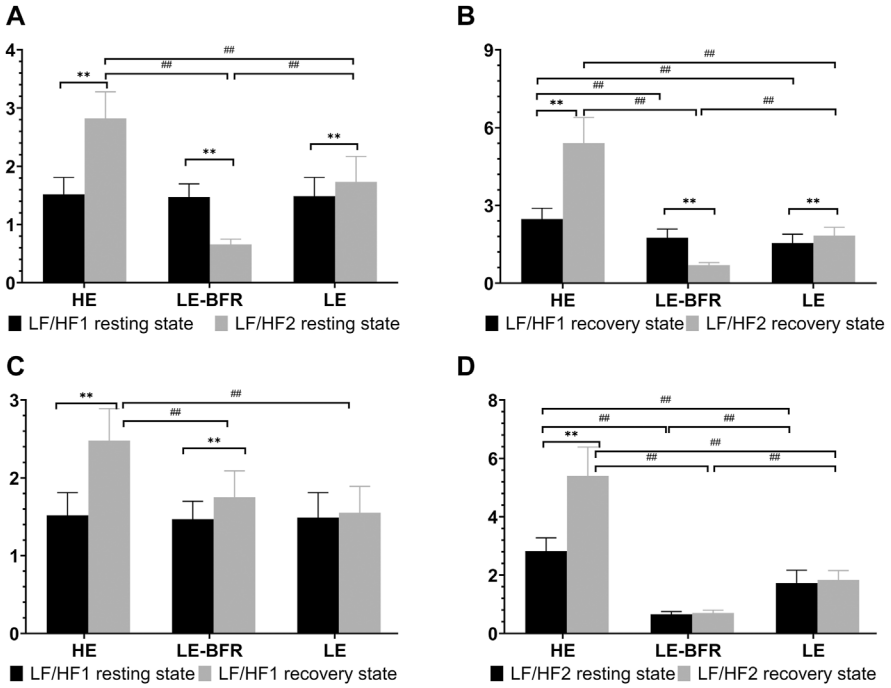

FIGURE 4 | (A) LF/HF in the resting state. **(B)** LF/HF in the recovery state. **(C)** LF/HF before and after the first training. **(D)** LF/HF before and after the last training. LF/HF1 resting state, LF/HF in the resting state before the first training. LF/HF2 resting state, LF/HF in the resting state before the last training. LF/HF1 recovery state, LF/HF in the recovery state after the first training. LF/HF2 recovery state, LF/HF in the recovery state after the last training. Data are presented as the mean ± standard deviation (SD). $^{**}p < 0.01$, significantly different from baseline. $^{\#\#}p < 0.01$, significantly different among groups.

TABLE 2 | Parameters of LF and HF in the resting and recovery states.

Variables	Groups	Resting state	Recovery state
LF1 (μn)	HE	577.21 ± 53.92$^{\#\#}$	564 ± 55.61$^{\#\#}$
	LE-BFR	510.56 ± 42.59	498.57 ± 50.82
	LE	502.36 ± 60.51	506.92 ± 47.26
LF2 (μn)	HE	555.96 ± 59.3	567.64 ± 36.08
	LE-BFR	429.29 ± 45.06$^{\#\#**}$	442.02 ± 42.51$^{\#\#,*}$
	LE	559.76 ± 41.96**	566.8 ± 36.07**
HF1 (μn)	HE	386.96 ± 44.68$^{\#\#}$	232.23 ± 36.28$^{\#\#}$
	LE-BFR	352.34 ± 45.31	294.22 ± 57.19
	LE	344.7 ± 38.83	337.85 ± 58.87$^{\#\#}$
HF2 (μn)	HE	199.97 ± 22.7$^{\#\#**}$	107.55 ± 16.18$^{\#\#**}$
	LE-BFR	653.29 ± 50.46$^{\#\#**}$	633.08 ± 57.96$^{\#\#**}$
	LE	335.15 ± 54.92	316.82 ± 49.32

LF1, LF, of the first training; LF2, LF, of the last training; HF1, HF, of the first training; HF2, HF, of the last training.

Data are presented as the mean ± standard deviation.

$^{*}p < 0.05$ *vs. baseline,* $^{**}p < 0.01$ *vs. baseline.*

$^{\#\#}p<0.01$ *among groups.*

significantly improved, and there was no difference in this value between the LE and LE-BFR group. In addition, the HR of HE group was even higher than that of the LE-BFR and LE groups. This finding indicated that LE-BFR could result in better adaptability of the cardiovascular function, thereby lowering cardiovascular risk. However, HE could cause higher cardiovascular risks compared to LE-BFR and LE.

High SBP is the leading cause of death and disability worldwide (Lim et al., 2012). The meta-analysis by Naci et al. (2019) pointed out that middle to high intensity resistance exercises could effectively reduce BP. Consistent with their research, the present study suggested that HE could effectively decrease SBP. Furthermore, our research found LE-BFR could also decrease SBP, and the effect of LE-BFR was more significant compared to the HE and LE modes. These results demonstrated that LE-BFR could exert better antihypertensive effects in subjects compared to HE. For people who are not able to perform high intensity resistant exercises, they can reduce their BP by LE-BFR training.

RMSSD is a parameter to evaluate parasympathetic activity. In the present study, RMSSD in the resting state didn't change significantly. This result was similar to the findings from several previous studies. The study by Takahashi et al. (2009) included 17 healthy old men who conducted high intensity resistant exercises for 12 weeks and showed that RMSSD in the resistant exercise group didn't change significantly. Millar et al. (2013) suggested similar results of RMSSD in the resting state with our findings when they inspected elderly hypertension patients who performed low intensity resistant exercises for 12 weeks. The findings about RMSSD by Gerage et al. (2013) also consistent with our results. The difference between us is their subjects were elderly healthy women but our subjects were elderly hypertension patients. However, the conclusions of the study by Caruso et al. (2015) on RMSSD in the resting state in elderly patients with coronary heart disease was different with our results. They

showed that RMSSD in resting state had increased after low intensity resistant exercises for 8 weeks. The cause of the difference might be the different exercise forms, exercise volume and detection time.

In the present study, the RMSSD in the recovery state after the first training was the highest in the LE group, and the lowest in the HE group. Although there were no significant differences among groups, the trend was consistent with the result of the transient study by Okuno et al. (2014), which covered about 20–29 years healthy men. In their study, there were significant differences among groups. The possible reason of significant differences in their study was that the exercise intensity of their subjects was 10% higher than ours, and the subjects must exercise to exhaustion in the last set. The article by Isidoro et al. (2017) on healthy men aged 20–35 years also showed that transient high intensity resistant exercises could reduce RMSSD significantly. The difference between their and our results might come from the fact that all limbs of subjects in their research should exercise and the total exercise volume was different. Taken together, it was suggested that RMSSD could not be used as an independent indicator to evaluate cardiovascular risk. RMSSD might indicate an increase in cardiovascular risk only when other parameters of the ANS prompted this risk with decreasing RMSSD.

LF is a parameter to express sympathetic and vagal modulations simultaneously, and this index represents sympathetic modulations best. HF is an indicator of vagal modulation. LF/HF ratio is a parameter to evaluate the sympathovagal balance (Task Force, 1996). Enhanced sympathetic and weakened parasympathetic predominance regulations are associated with increased cardiovascular risk (Mourot et al., 2004; Seiler et al., 2007; Lima et al., 2011). In the present study, after 12 weeks of training, both in the resting state and the recovery state, LF/HF ratio in the HE and LE groups increased significantly, whereas this value in the LE-BFR group decreased significantly. This indicated that patients in the LE-BFR group had significantly improved ANS, while those in the HE and LE groups didn't show this advantage. The study of Lima et al. (2011) about HE only also showed that LF/HF ratio increased after HE. However, the study by Bellavere et al. (2018) showed that after HE for 4 months, the LF/HF ratio of subjects with type II diabetes decreased. The transient high-intensity resistance training proposed by Isidoro et al. (2017) also showed a decreased LF/HF ratio. The difference might come from different modes of exercise, which was supported by the study by Morishima et al. (2018). They compared low-intensity high-repetition and high-intensity low-repetition resistance exercises, and the results verified that the intensity, number of repetition, and intermittent resting time were important factors affecting BP and endothelial function after exercise. However, their study didn't involve the indicators for ANS. Moreover, the difference in detection time might also affect the results.

Although LF/HF ratios in both HE and LE groups increased significantly, there was also difference between them. LF increased significantly in the LE group while HF decreased significantly in the HE group after 12 weeks of training. The LF/HF ratio in HE group increased greatly (1.52–2.82 in the resting state; 2.48 to 5.40 in the recovery state), but the LF/HF ratio in LE group was still in normal range (1.49–1.73 in the resting state; 1.55 to 1.83 in the recovery state). Because the long-term follow-up study about heart rate variability and mortality (Kuo et al., 2018) demonstrated high LF/HF ratio was an independent risk factor for mortality and LF/HF ratio >2.6 was associated with a higher mortality, our research indicates LE and LE-BFR was safer than HE.

This study was the first to compare BP and ANS in hypertension patients after performing three types of resistant exercises for 12 weeks. Those are different from others. We found LE-BFR had the most obvious effect on reducing SBP and adjusting sympathetic-parasympathetic balance, and was associated with lower cardiovascular risk compared to HE and LE. There are some limitations in the present study. For example, BP in the recovery state wasn't measured. Additionally, although the effects of 12 weeks of training was examined, the long-term effects of resistance exercise needed to be further observed. Furthermore, no biochemical indicators related to ANS were detected, making it difficult to identify the causes of the changes in RMSSD, LF and HF.

DATA AVAILABILITY STATEMENT

The raw data supporting the conclusions of this article will be made available by the authors, without undue reservation.

ETHICS STATEMENT

The studies involving human participants were reviewed and approved by the Ethics Committee for Human Experiments of Rehabilitation hospital of Huishan. The patients/participants provided their written informed consent to participate in this study.

AUTHOR CONTRIBUTIONS

AL and MZ designed the study; YZ wrote the manuscript; YCZ, XM, and LQ performed the experiment; AL, MZ, and YZ critically revised the manuscript; All authors read and approved the final manuscript.

FUNDING

This work was supported by the National Natural Science Foundation of China (Grant number 81101456); the Nanjing Medical Science and Technique Development Foundation (Grant number YKK19073); the Natural Science Foundation of the Jiangsu Higher Education Institutions of China (Grant number 18KJA320002) and research project of kinesiology laboratory of Nanjing Sport Institute (Grant number SYS202105).

REFERENCES

Bellavere, F., Cacciatori, V., Bacchi, E., Gemma, M. L., Raimondo, D., Negri, C., et al. (2018). Effects of Aerobic or Resistance Exercise Training on Cardiovascular Autonomic Function of Subjects with Type 2 Diabetes: A Pilot Study. *Nutr. Metab. Cardiovasc. Dis.* 28, 226–233. doi:10.1016/j.numecd.2017.12.008

Caruso, F. R., Arena, R., Phillips, S. A., Bonjorno, J. C., Jr., Mendes, R. G., Arakelian, V. M., et al. (2015). Resistance Exercise Training Improves Heart Rate Variability and Muscle Performance: a Randomized Controlled Trial in Coronary Artery Disease Patients. *Eur. J. Phys. Rehabil. Med.* 51, 281–289.

Cerqueira, M. S., Costa, E. C., Santos Oliveira, R., Pereira, R., and Brito Vieira, W. H. (2021). Blood Flow Restriction Training: To Adjust or Not Adjust the Cuff Pressure over an Intervention Period? *Front. Physiol.* 12, 678407. doi:10.3389/fphys.2021.678407

Early, K. S., Rockhill, M., Bryan, A., Tyo, B., Buuck, D., and McGinty, J. (2020). Effect of Blood Flow Restriction Training on Muscular Performance, Pain and Vascular Function. *Intl J. Sports Phys. Ther.* 15, 892–900. doi:10.26603/ijspt20200892

Esler, M. (2011). The Sympathetic Nervous System through the Ages: from Thomas Willis to Resistant Hypertension. *Exp. Physiol.* 96, 611–622. doi:10.1113/expphysiol.2011.052332

Gerage, A., Forjaz, C. L., Nascimento, M., Januário, R. S., Polito, M., and Cyrino, E. (2013). Cardiovascular Adaptations to Resistance Training in Elderly Postmenopausal Women. *Int. J. Sports Med.* 34, 806–813. doi:10.1055/s-0032-1331185

Heffernan, K. S., Fahs, C. A., Shinsako, K. K., Jae, S. Y., and Fernhall, B. (2007). Heart Rate Recovery and Heart Rate Complexity Following Resistance Exercise Training and Detraining in Young Men. *Am. J. Physiology-Heart Circulatory Physiol.* 293, H3180–H3186. doi:10.1152/ajpheart.00648.2007

Hering, D., Kara, T., Kucharska, W., Somers, V. K., and Narkiewicz, K. (2016). Longitudinal Tracking of Muscle Sympathetic Nerve Activity and its Relationship with Blood Pressure in Subjects with Prehypertension. *Blood Press.* 25, 184–192. doi:10.3109/08037051.2015.1121708

Isidoro, N. J., Santana, M. D. R., Valenti, V. E., Garner, D. M., and de Abreu, L. C. (2017). Cardiac Autonomic Recovery after Strength Exercise in Lower and Upper Limbs. *Acta Cardiologica* 72, 467–473. doi:10.1080/00015385.2017.1335454

Kuo, G., Chen, S.-W., Huang, J.-Y., Wu, C.-Y., Fu, C.-M., Chang, C.-H., et al. (2018). Short-term Heart Rate Variability as a Predictor of Long-Term Survival in Patients with Chronic Hemodialysis: A Prospective Cohort Study. *J. Formos. Med. Assoc.* 117, 1058–1064. doi:10.1016/j.jfma.2018.09.006

Li, Y., Wei, B., Liu, X., Shen, X. Z., and Shi, P. (2020). Microglia, Autonomic Nervous System, Immunity and Hypertension: Is There a Link? *Pharmacol. Res.* 155, 104451. doi:10.1016/j.phrs.2019.104451

Lim, S. S., Vos, T., Flaxman, A. D., Danaei, G., Shibuya, K., Adair-Rohani, H., et al. (2012). A Comparative Risk Assessment of burden of Disease and Injury Attributable to 67 Risk Factors and Risk Factor Clusters in 21 Regions, 1990-2010: a Systematic Analysis for the Global Burden of Disease Study 2010. *Lancet* 380, 2224–2260. doi:10.1016/S0140-6736(12)61766-8

Lima, A. H. R. d. A., Forjaz, C. L. d. M., Silva, G. Q. d. M., Menêses, A. L., Silva, A. J. M. R., and Ritti-Dias, R. M. (2011). Efeito agudo da intensidade Do exercício de força na modulação autonômica cardíaca pós-exercício. *Arq. Bras. Cardiol.* 96, 498–503. doi:10.1590/s0066-782x2011005000043

Mancia, G., and Grassi, G. (2014). The Autonomic Nervous System and Hypertension. *Circ. Res.* 114, 1804–1814. doi:10.1161/circresaha.114.302524

Millar, P. J., Levy, A. S., McGowan, C. L., McCartney, N., and MacDonald, M. J. (2013). Isometric Handgrip Training Lowers Blood Pressure and Increases Heart Rate Complexity in Medicated Hypertensive Patients. *Scand. J. Med. Sci. Sports* 23, 620–626. doi:10.1111/j.1600-0838.2011.01435.x

Morishima, T., Tsuchiya, Y., Iemitsu, M., and Ochi, E. (2018). High-intensity Resistance Exercise with Low Repetitions Maintains Endothelial Function. *Am. J. Physiology-Heart Circulatory Physiol.* 315, H681–H686. doi:10.1152/ajpheart.00281.2018

Mourot, L., Bouhaddi, M., Tordi, N., Rouillon, J. D., and Regnard, J. (2004). Short- and Long-Term Effects of a Single Bout of Exercise on Heart Rate Variability: Comparison between Constant and Interval Training Exercises. *Eur. J. Appl. Physiol.* 92, 508–517. doi:10.1007/s00421-004-1119-0

Mozaffarian, D., Benjamin, E. J., Go, A. S., Arnett, D. K., Blaha, M. J., Cushman, M., et al. (2015). American Heart Association Statistics & S. Stroke StatisticsHeart Disease and Stroke Statistics--2015 Update: a Report from the American Heart Association. *Circulation* 131, e29–322. doi:10.1161/cir.0000000000000152

Naci, H., Salcher-Konrad, M., Dias, S., Blum, M. R., Sahoo, S. A., Nunan, D., et al. (2019). How Does Exercise Treatment Compare with Antihypertensive Medications? A Network Meta-Analysis of 391 Randomised Controlled Trials Assessing Exercise and Medication Effects on Systolic Blood Pressure. *Br. J. Sports Med.* 53, 859–869. doi:10.1136/bjsports-2018-099921

Okuno, N. M., Pedro, R. E., Leicht, A. S., de Paula Ramos, S., and Nakamura, F. Y. (2014). Cardiac Autonomic Recovery after a Single Session of Resistance Exercise with and without Vascular Occlusion. *J. Strength Cond Res.* 28, 1143–1150. doi:10.1519/jsc.0000000000000245

Seiler, S., Haugen, O., and Kuffel, E. (2007). Autonomic Recovery after Exercise in Trained Athletes. *Med. Sci. Sports Exerc.* 39, 1366–1373. doi:10.1249/mss.0b013e318060f17d

Silva, É. P., Soares, B. A., Reimberg, M. M., Ritti-Dias, R., Nascimento, K. S., Anjos, F. S., et al. (2021). Heart Rate Recovery in Asthmatic Children and Adolescents after Clinical Field Test. *BMC Pulm. Med.* 21, 61. doi:10.1186/s12890-020-01355-9

Smith, L. L., Kukielka, M., and Billman, G. E. (2005). Heart Rate Recovery after Exercise: a Predictor of Ventricular Fibrillation Susceptibility after Myocardial Infarction. *Am. J. Physiology-Heart Circulatory Physiol.* 288, H1763–H1769. doi:10.1152/ajpheart.00785.2004

Stein, P. K., Domitrovich, P. P., Huikuri, H. V., Kleiger, R. E., and Cast, I. (2005). Traditional and Nonlinear Heart Rate Variability Are Each Independently Associated with Mortality after Myocardial Infarction. *J. Cardiovasc. Electrophysiol.* 16, 13–20. doi:10.1046/j.1540-8167.2005.04358.x

Suzic Lazic, J., Dekleva, M., Soldatovic, I., Leischik, R., Suzic, S., Radovanovic, D., et al. (2017). Heart Rate Recovery in Elite Athletes: the Impact of Age and Exercise Capacity. *Clin. Physiol. Funct. Imaging* 37, 117–123. doi:10.1111/cpf.12271

Takahashi, A. C. M., Melo, R. C., Quitério, R. J., Silva, E., and Catai, A. M. (2009). The Effect of Eccentric Strength Training on Heart Rate and on its Variability during Isometric Exercise in Healthy Older Men. *Eur. J. Appl. Physiol.* 105, 315–323. doi:10.1007/s00421-008-0905-5

Task Force (1996). Heart Rate Variability. Standards of Measurement, Physiological Interpretation, and Clinical Use. Task Force of the European Society of Cardiology and the North American Society of Pacing and Electrophysiology. *Eur. Heart J.* 17, 354–381.

Trevizani, G. A., Seixas, M. B., Benchimol-Barbosa, P. R., Vianna, J. M., da Silva, L. P., and Nadal, J. (2018). Effect of Resistance Training on Blood Pressure and Autonomic Responses in Treated Hypertensives. *J. Strength Cond Res.* 32, 1462–1470. doi:10.1519/jsc.0000000000001995

Tsuji, H., Larson, M. G., Venditti, F. J., Manders, E. S., Evans, J. C., Feldman, C. L., et al. (1996). Impact of Reduced Heart Rate Variability on Risk for Cardiac Events. *Circulation* 94, 2850–2855. doi:10.1161/01.cir.94.11.2850

Vale, A. F., Carneiro, J. A., Jardim, P. C. V., Jardim, T. V., Steele, J., Fisher, J. P., et al. (2018). Acute Effects of Different Resistance Training Loads on Cardiac Autonomic Modulation in Hypertensive Postmenopausal Women. *J. Transl Med.* 16, 240. doi:10.1186/s12967-018-1615-3

Zhang, D., Shen, X., and Qi, X. (2016). Resting Heart Rate and All-Cause and Cardiovascular Mortality in the General Population: a Meta-Analysis. *Can. Med. Assoc. J.* 188, E53–E63. doi:10.1503/cmaj.150535

Zhao, Y., Lin, A., and Jiao, L. (2021). Eight Weeks of Resistance Training with Blood Flow Restriction Improve Cardiac Function and Vascular Endothelial Function in Healthy Young Asian Males. *Int. Health* 13, 471–479. doi:10.1093/inthealth/ihaa089

Zubcevic, J., Richards, E. M., Yang, T., Kim, S., Sumners, C., Pepine, C. J., et al. (2019). Impaired Autonomic Nervous System-Microbiome Circuit in Hypertension. *Circ. Res.* 125, 104–116. doi:10.1161/circresaha.119.313965

Conflict of Interest: The authors declare that the research was conducted in the absence of any commercial or financial relationships that could be construed as a potential conflict of interest.

Publisher's Note: All claims expressed in this article are solely those of the authors and do not necessarily represent those of their affiliated organizations, or those of the publisher, the editors and the reviewers. Any product that may be evaluated in this article, or claim that may be made by its manufacturer, is not guaranteed or endorsed by the publisher.

frontiers | Frontiers in Bioengineering and Biotechnology

ORIGINAL RESEARCH
published: 04 May 2022
doi: 10.3389/fbioe.2022.872258

Characterization of Changes in Subchondral Bone Tissue Density of the Ankle Joint in Taekwondo Players

Guanghua Xu, Hongyu Liu and Lifu Zhang*

Institute of Sport and Exercise Medicine, North University of China, Taiyuan, China

Background: It has been found that ankle joint impingement can cause articular cartilage injury, and the change of subchondral bone density and distribution under long-term stress loading can reflect the stress interaction of the articular surface and the difference in bone remodeling degree and predict the location of cartilage injury.

Objective: To investigate the bone density distribution pattern of ankle joint subchondral bone under mechanical stress loading of Taekwondo, the volume proportion of bone tissue with different bone densities, and the distribution characteristics of bone remodeling position.

Study design: A controlled laboratory study.

Methods: Computed tomography data were collected from the feet of 10 normal subjects (control group) and 10 high-level Taekwondo athletes. First, the distribution pattern of the high-density area of the articular surface was determined by computed tomography osteoabsorptiometry and the nine-grid anatomical region localization method. Second, the percentage of bone volume (%BTV) and the distribution trend of bone tissue were measured.

Result: In the present study, it was found that there were high-density areas in the 1st, 2nd, 3rd, 4th, 6th, 7th, and 9th regions of the distal tibia of Taekwondo athletes, and the distribution track was consistent with the high-density areas of the talar dome surface (1st, 2nd, 3rd, 4th, 6th, 7th, and 9th regions). In Taekwondo athletes, the percentage of bone tissue volume in the distal tibia and talus with high and moderate bone density was significantly higher than that in the control group ($p < 0.05$).

Conclusion: The impact stress, ground reaction force, intra-articular stress, lower limb movement technology, lower limb muscle, and tendon stress caused by Taekwondo lead to special pressure distribution patterns and bone tissue remodeling in the ankle.

Keywords: Taekwondo, distal tibial, talus dome, bone density distribution, bone remodeling, computed tomography osteoabsorptiometry

OPEN ACCESS

Edited by:
Chiarella Sforza,
University of Milan, Italy

Reviewed by:
Giovanni Corsetti,
University of Brescia, Italy
Abdelwahed Barkaoui,
International University of Rabat, Morocco

****Correspondence:***
Hongyu Liu
lhyxianjd@163.com

Specialty section:
This article was submitted to Biomechanics, a section of the journal Frontiers in Bioengineering and Biotechnology

Received: *09 February 2022*
Accepted: *07 April 2022*
Published: *04 May 2022*

Citation:
Xu G, Liu H and Zhang L (2022) Characterization of Changes in Subchondral Bone Tissue Density of the Ankle Joint in Taekwondo Players. Front. Bioeng. Biotechnol. 10:872258. doi: 10.3389/fbioe.2022.872258

INTRODUCTION

Taekwondo sports technology is complex and diverse. In particular, Taekwondo athletes need to use their bodies to obtain effective hitting scores by rotating their trunks and hitting their opponent's head and chest (Watta, 2021) with their feet. This means that the lower limbs of Taekwondo athletes may be affected by mechanical factors: impact stress and ground reaction force after jumping and landing. In addition, the technical characteristics of Taekwondo lower limbs are strong leg strength, fast-hitting speed, flexible footwork, and hitting opponents in movement. The technical movements of Taekwondo include lower limb hitting techniques such as roundabout kick, side kick, back kick, down split kick, and push kick. According to the statistics of researchers, 98% of the scores of competitive Taekwondo athletes in Taekwondo competitions come from leg blows (Jakubiak and Saunders, 2008). This shows that the score of Taekwondo depends on the hitting of lower limbs; the more difficult the hitting action is, the more concentrated it is on the head, and the higher the hitting score will be obtained.

Early studies conducted kinematic analysis on the lower limb kicking of Taekwondo athletes and found that the impact force of Taekwondo athletes' roundhouse kick is about 1,000 N–3,000 N. The impact force of contestants is higher than that of noncontestants, and the leg impact stress of nonmedal contestants is far lower than that of medal winners (Falco et al., 2009; Estevan et al., 2011; Thibordee and Prasartwuth, 2014). However, there were also studies that Taekwondo athletes need a certain vertical take-off height before hitting (Pieter et al., 2012), but Taekwondo athletes must accept the ground reaction force of 6 times their body weight after taking off and hitting the target and landing. If one leg lands barefoot, it may further increase the risk of lower limb injury, and the reaction force changes with the increase of body weight (Ryu and Lee, 2021). Therefore, the strong ground reaction after jumping and landing may act not only on the lower limb arch but also on the ankle. The lower limbs of amateur Taekwondo players are the most common injury parts, while the head of professional players is the most common injury part. Epidemiological investigations have found that Taekwondo athletes will have sports injuries such as laceration, contusion, hematoma, cartilage injury, or fracture during the Olympic Games. This is not surprising because Taekwondo athletes usually lack protection for their lower limbs, and the landing after kicking and jumping may transmit large impact and reaction forces (Gartland et al., 2001; Jeong et al., 2019).

Previous studies have found that the distribution pattern of subchondral bone mineral density is considered to reflect stress distribution on the joint surface and subchondral bone under long-term stress loading. Computed tomography osteoabsorptiometry (CTOAM) technology can not only obtain the distribution form of intra-articular mechanical stress but also evaluate the changes of joint mechanical stress after surgery or injury. As a basic clinical research method, this technology is not invasive and has the characteristics of high efficiency and safety for subjects (Müller-Gerbl et al., 1989). At present, there is a lack of image anatomical research on the changes in bone morphology and bone tissue of athletes' lower limbs under Taekwondo stress loading. Therefore, the purpose of this study is to analyze the distribution pattern of the high-density area of subchondral bone, the volume percentage of bone tissue, and bone remodeling characteristics of the subchondral bone of the ankle in the two groups by using CTOAM. Let us assume that the impact stress, ground reaction force, intra-articular stress, lower limb movement technology, and lower limb muscle and tendon stress caused by Taekwondo lead to special pressure distribution patterns and bone tissue remodeling in the ankle.

TABLE 1 | Basic characteristics of subjects.

	Control	Taekwondo	*p* value
Number	10	10	
Dominant foot	Right	Right	
Age (yrs)	20.80 ± 0.92	21.10 ± 0.88	0.406
Height (cm)	178.90 ± 2.63	179.00 ± 2.63	0.933
Weight (kg)	67.30 ± 2.21	67.40 ± 2.27	0.922
Training age (yrs)	0	≥8	

Data are expressed as mean ± SD.

METHODS

Data Collection

The study has been approved by the institutional ethics review committee of the North University of China. Informed consent to participate in the study was obtained from each participant. The height, weight, age, and training history of 10 male Taekwondo athletes (Taekwondo group; Taekwondo National Championship) and 10 male non-Taekwondo athletes (control group) were investigated (**Table 1**). All Taekwondo athletes have more than 8 years of training history. All subjects volunteered to participate in the experiment and underwent lower extremity CT image scanning (LightSpeed VCT, GE Healthcare, Waukesha, WI, United States; tube voltage: 120 KV, tube current: 250 mA; slice thickness: 0.625 mm). This study has excluded any foot and ankle diseases, discomfort symptoms, and trauma history.

Computed Tomography Osteoabsorptionmetry

The obtained CT image data were exported in DICOM format and transmitted to Material Mimics 21.0 (Materialise, Leuven, Belgium) for postprocessing. Then, we took the high-density area on the articular surface of the distal tibia and the high-density area on the surface of the talar dome as the region of interest (ROI), and each density area was defined as Hounsfield Unit (HU, which defined as X-ray attenuation;

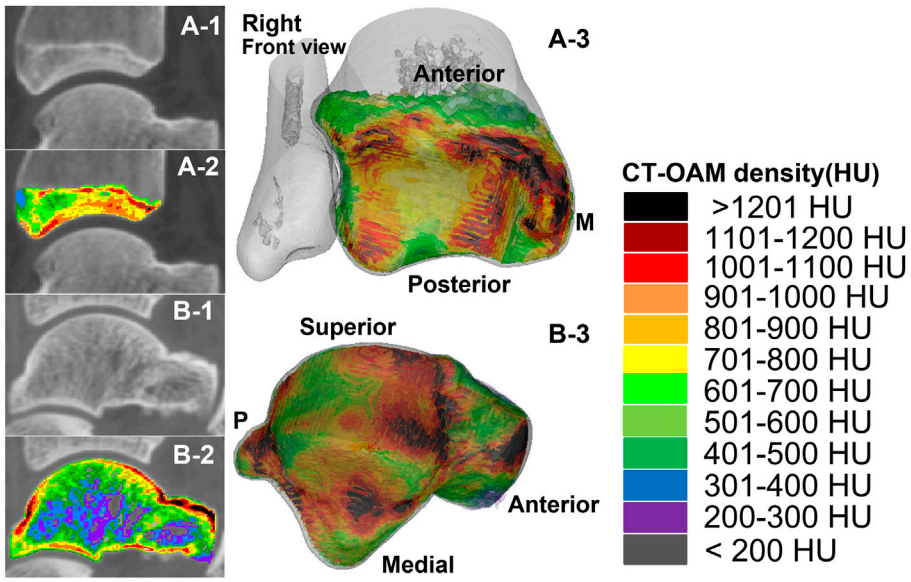

FIGURE 1 | The measurement range and reconstruction model of the subchondral bone of the distal tibia and the talus in the two groups of subjects. A-1 and A-2 were computed tomography (CT) images and CTOAM images of the distal tibia; A-3 is the reconstructed image of each bone density tissue of the distal tibia. B-1 and B-2 were computed tomography (CT) images and CTOAM images of the talus; B-3 is the image of bone density tissue of the talus after reconstruction.

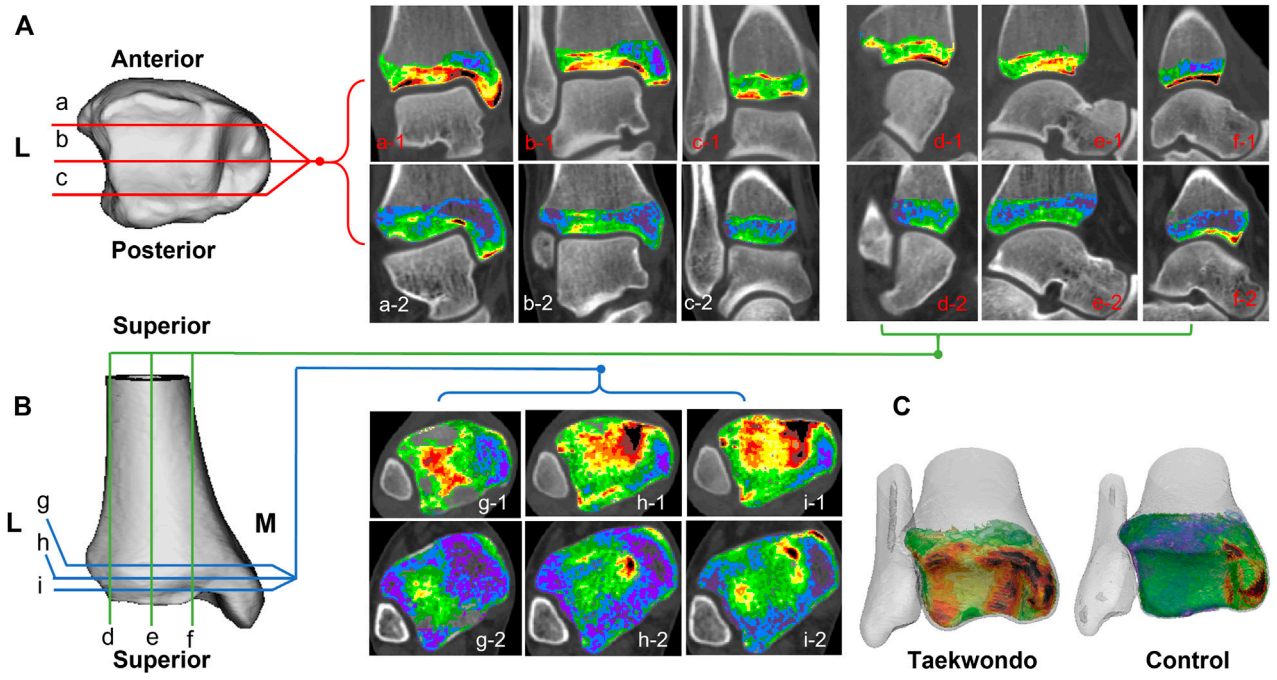

FIGURE 2 | Computed tomographic images of the distribution of different bone density bone tissues in the distal tibia in two groups. **(A)** is a schematic diagram of the coronal tomographic images of the tibia; **(B)** is a schematic diagram of the sagittal and axial tomographic images of the talus; **(C)** is a schematic diagram of the superimposed bone tissue of each bone density within the distal tibia. a1–c1 are the coronal images of the Taekwondo; d1–f1 are the sagittal images of the Taekwondo; g1–i1 are the axial images of the Taekwondo; a2–c2 control coronal images; d2–f2 control sagittal images; g2–i2 control axial images.

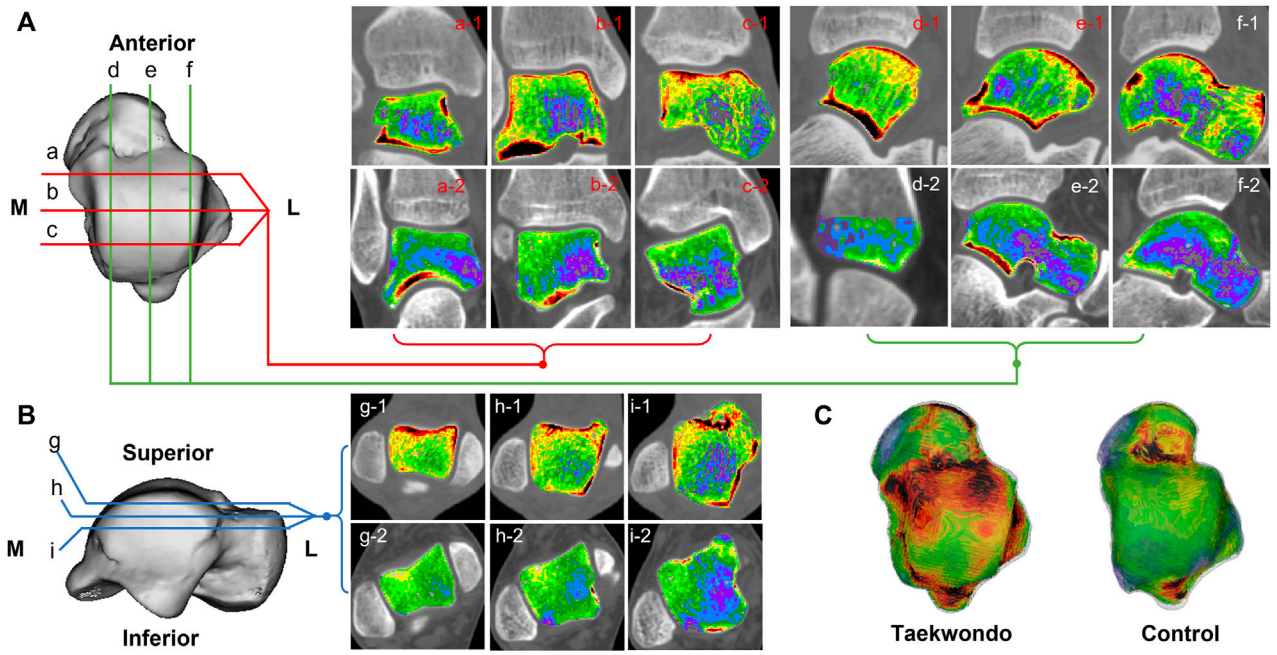

FIGURE 3 | Computed tomographic images of the distribution of bone tissue of different bone densities in the talus of two groups. **(A)** is a schematic diagram of the coronal and sagittal tomographic images of the talus; **(B)** is a schematic diagram of the axial tomographic images of the talus; **(C)** is a schematic diagram of the superimposed bone tissue of each bone density in the talus. a1–c1 are the coronal images of Taekwondo; d1–f1 are the sagittal images of Taekwondo; g1–i1 are the axial images of Taekwondo; a2–c2 control group coronal images; d2–f2 control group sagittal images; g2–i2 control group axial images.

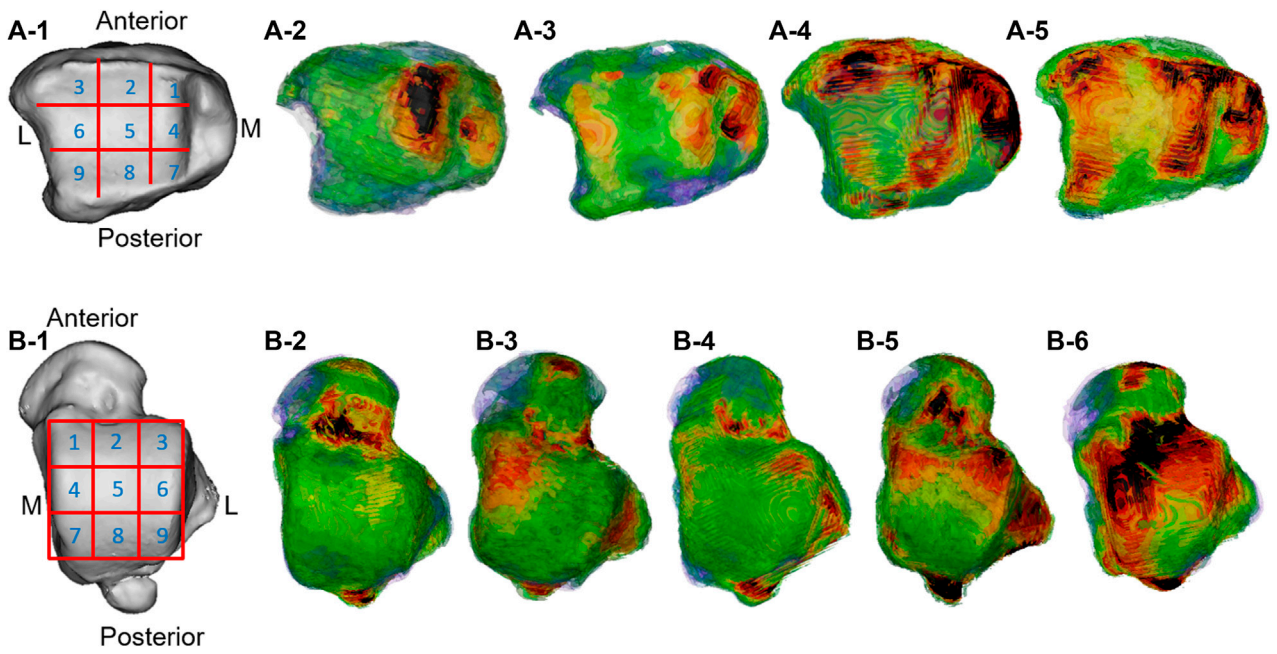

FIGURE 4 | Distribution pattern of the high-density zone of the distal tibial articular surface and talar talus. A-1 and B-1 are the division pattern of the high-density zone of the distal tibial articular surface and talar talus; A-2 was the medial center; A-3 was the medial–lateral center; A-4 was the ring; A-5 was comprehensive; B-2 was blank; B-3 was the medial center; B-4 was lateral center; B-5 was medial–lateral center; B-6 was ring type.

TABLE 2 | Distal tibial articular surface and talus dome high-density area classification data.

Position	Distal tibia				Talar dome			
Groups	Control group		Taekwondo		Control group		Taekwondo	
High-density area	Number (20)	Frequency (%)	Number (20)	Frequency (%)	Number (20)	Frequency (%)	Number (20)	Frequency (%)
1	17	85%	20	100%	15	75%	18	90%
2	2	10%	15	75%	11	55%	14	70%
3	4	20%	20	100%	12	60%	18	90%
4	12	60%	19	95%	7	35%	16	80%
5	3	15%	6	30%	2	10%	6	30%
6	5	25%	13	65%	7	35%	18	90%
7	13	65%	20	100%	5	25%	14	70%
8	5	25%	17	85%	1	5%	4	20%
9	4	20%	14	70%	7	45%	15	75%
Blank	0	0	0	0	4	20%	0	0
Medial center	12	60%	0	0	4	20%	0	0
Lateral center	0	0	0	0	2	10%	0	0
Medial–lateral center	7	35%	0	0	10	50%	8	40%
Ring	1	5%	14	70%	0	0	12	60%
Comprehensive	0	0	6	30%	0	0	0	0

TABLE 3 | Comparison of the bone volume of each bone density zone in the distal tibia subchondral bone between the groups (%).

Density classifications	Unit:HU	Right		*p* value	Left		*p* value
		Control	Taekwondo		Control	Taekwondo	
Low bone density	200–300	16.90 ± 11.63	4.99 ± 2.17	**0.001**	13.01 ± 7.83	4.66 ± 2.10	**0.008**
	301–400	25.79 ± 9.75	14.33 ± 3.04	**0.005**	20.38 ± 5.89	13.06 ± 2.08	**0.003**
	401–500	24.13 ± 4.93	18.47 ± 3.55	**0.011**	21.87 ± 3.44	19.81 ± 3.07	0.174
	501–600	18.39 ± 2.36	18.36 ± 1.96	0.974	15.37 ± 2.32	17.48 ± 1.87	0.105
Medium bone density	601–700	12.79 ± 3.35	15.39 ± 2.53$^{\#\#}$	0.066	10.89 ± 3.28	13.70 ± 2.04	**0.033**
	701–800	7.96 ± 3.06	11.10 ± 1.59$^{\#}$	**0.012**	7.53 ± 2.87	10.19 ± 1.19	**0.019**
	801–900	4.67 ± 2.08	8.12 ± 1.66$^{\#\#}$	**0.001**	4.69 ± 2.22	7.14 ± 1.24	**0.009**
High bone density	901–1000	2.62 ± 1.28	5.45 ± 1.32	**0.001**	2.66 ± 1.50	4.99 ± 1.46	**0.002**
	1,001–1,100	1.55 ± 0.92	3.68 ± 0.99	**0.001**	1.41 ± 0.85	3.63 ± 1.47	**0.001**
	1,101–1,200	0.97 ± 0.68	2.59 ± 0.75	**0.001**	0.95 ± 0.73	2.60 ± 1.28	**0.002**
	1,201–maximum	1.16 ± 0.95	2.50 ± 0.66	**0.004**	1.24 ± 1.13	2.74 ± 1.03	**0.006**

The statistical results are expressed as mean ± SD. $^{\#\#}$ and $^{\#}$ indicate statistically significant p *values of <0.01 and <0.05 in Taekwondo vivo, respectively. %BTV: percentage change in bone tissue volume for each bone density within the distal tibial subchondral bone.*

To indicate that the data comparisons are different, we put boldface on the P values that are significantly different.

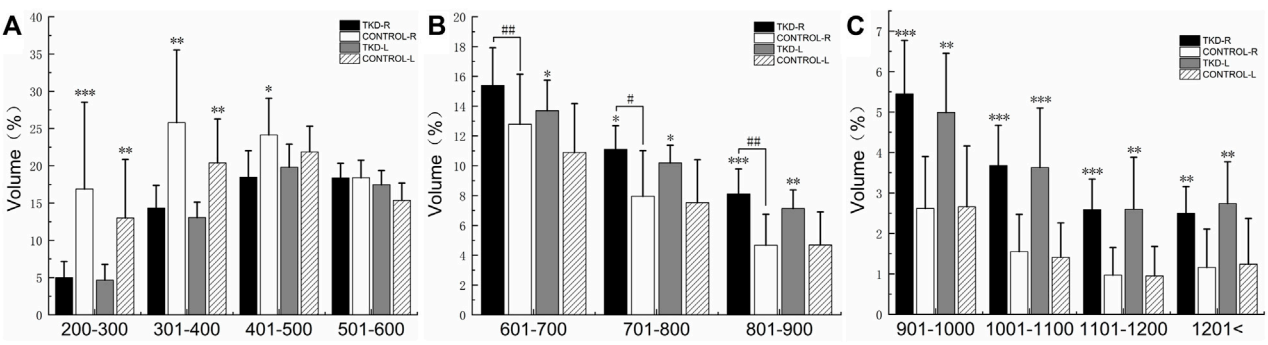

FIGURE 5 | Comparison of the bone volume of each bone density zone in the distal tibia subchondral bone between the groups (%). **(A)** is the bone volume of low bone density; **(B)** is the bone volume of medium bone density; **(C)** is the bone volume of high bone density (***, **, and * indicate statistically significant *p* values of <0.001, <0.01, and <0.05 vs. control group; $^{\#\#}$ and $^{\#}$ indicate statistically significant *p* values of <0.01 and <0.05 in Taekwondo in vivo, respectively).

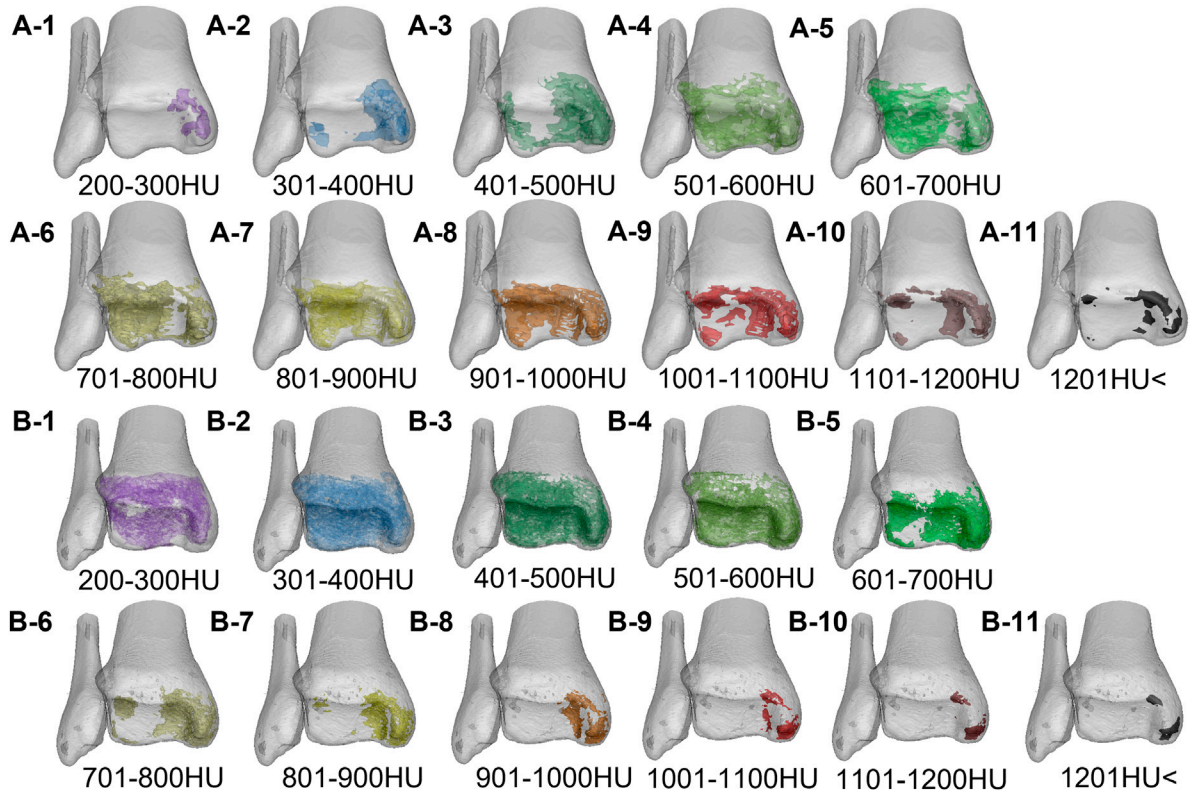

FIGURE 6 | The volume distribution of bone tissue with different bone densities in the distal tibia of the two groups. A1–A11 is the Taekwondo group; B1–B11 is the control group.

water is 0, and dense bone is 1000). The range of bone mineral density in the articular surface of the distal tibia and that in the subchondral bone of the talus was divided into 11 equal intervals, and each interval was given different colors: black indicated high density and purple indicated low density (Müller-Gerbl et al., 1989; Onodera et al., 2012). Finally, we stacked the bone mask data of each interval to obtain the mapping image of each bone density interval of the whole subchondral bone of the ankle.

Distribution Patterns of Bone Tissue With Different Densities Within the Subchondral Bone of the Ankle Joint

First, by the regional growth function in Mimics software, the bone masks of each density interval of the distal tibia and subchondral bone of the talus were extracted, and then the extracted bone masks of each density interval were successively reconstructed into the corresponding bone tissue model. Second, the bone tissue models of the distal tibia and subchondral talus were applied with visible function and transparency function (low and medium bone density bone tissue has high transparency; high bone density has medium transparency). Finally, in order to determine the distribution pattern of different bone density bone tissue within the subchondral bone of the ankle joint in the two subjects, we took three tomographic image sections, sagittal, coronal, and axial (medial, middle, and lateral; anterior, middle, and posterior; superior, middle, and inferior), on the articular surface of the distal tibia and the articular surface of the talus in each of the two subjects and observed the distribution of bone tissue of different bone densities within the distal tibia and talar articular surfaces in the computed tomography images.

Evaluation of the Distribution Pattern of High Bone Density Areas on the Ankle Joint Surface

In order to divide the distribution pattern of subchondral bone high bone density areas on the articular surface of the distal tibia, we divided the reconstructed bone tissue model of the articular surface of the distal tibia and talar dome into nine anatomical regions (Raikin et al., 2007; Elias et al., 2009) to determine the frequency, distribution pattern, and quantity percentage of high bone density areas on the articular surface of the distal tibia and talar dome.

Quantitative Analysis of the Volume Percentage of the Ankle Subchondral Bone

In the images, we took the volume of bone tissue of distal tibia (growth plate to the articular surface) and subchondral bone tissue of talus as the volume of bone tissue of interest and

TABLE 4 | Comparison of the bone volume of each bone density zone in the talus subchondral bone between the groups (%).

Density classifications	Unit: HU	Right		*p* value	Left		*p* value
		Control	Taekwondo		Control	Taekwondo	
Low bone density	200–300	12.67 ± 5.59	6.28 ± 2.12	**0.006**	12.37 ± 5.92	5.73 ± 1.81	**0.006**
	301–400	19.18 ± 3.69	13.19 ± 2.09	**0.001**	18.70 ± 3.23	12.14 ± 3.38	**0.001**
	401–500	20.03 ± 2.48	17.18 ± 1.89	**0.010**	21.21 ± 4.96	16.95 ± 2.06	**0.022**
	501–600	16.84 ± 2.01	16.37 ± 1.78	0.584	16.08 ± 1.20	16.61 ± 1.76	0.448
Medium bone density	601–700	12.13 ± 2.00	14.51 ± 1.08	**0.005**	11.79 ± 1.85	14.53 ± 0.99	**0.001**
	701–800	8.04 ± 2.70	11.98 ± 1.87	**0.001**	7.97 ± 2.57	11.86 ± 1.65	**0.001**
	801–900	5.03 ± 2.35	8.36 ± 1.41	**0.001**	4.94 ± 2.36	9.04 ± 1.76	**0.001**
High bone density	901–1000	2.79 ± 1.49	5.09 ± 0.88	**0.001**	2.95 ± 1.69	5.68 ± 1.35	**0.001**
	1,001–1,100	1.51 ± 1.03	2.97 ± 1.66	**0.001**	1.80 ± 1.33	3.37 ± 0.96	**0.007**
	1,101–1,200	0.87 ± 0.74	1.89 ± 0.62	**0.003**	1.04 ± 0.83	2.03 ± 0.62	**0.008**
	1,201–maximum	0.90 ± 0.98	2.16 ± 0.93	**0.019**	1.16 ± 1.24	2.06 ± 0.97	0.052

The statistical results are expressed as mean ± SD. %BTV: percentage change in bone tissue volume for each bone density within the talus subchondral bone. To indicate that the data comparisons are different, we put boldface on the P values that are significantly different.

compared and analyzed the volume percentage difference of bone tissue of distal tibia and subchondral bone tissue of the talus between the two groups (bone tissue volume percentage, % BTV). First, we reconstructed the bone mask between the distal tibial growth plate and the articular surface and the bone mask between the subchondral bone of the talus into a three-dimensional model (**Figure 1**) and derived the bone tissue volume data of each density interval. Second, sum the volume of the distal tibia and subchondral bone tissue of the talus in each bone density interval to obtain the total volume of the distal tibia and subchondral bone tissue of the talus. Finally, the %BTV in the ankle joint surface is obtained through calculation. The formula is as follows:

$$\%BTV = \frac{volume\ of\ bone\ tissue\ with\ a\ certain\ density\ in\ distal\ tibia\ or\ talus}{total\ volume\ of\ subchondral\ bone\ tissue\ of\ distal\ tibia\ or\ talus}.$$

Statistical Analysis

The measurement results were first tested by Kolmogorov–Smirnov to see whether the data of the two groups conformed to normal distribution. If the data conformed to normal distribution, Student's *t*-test was used to compare the experimental and control groups. If the distribution did not conform to normal distribution, then the Mann–Whitney *U*-test was used for comparison between groups, the Wilcoxon signed rank test was used for comparison within the experimental group, and statistical results were expressed as mean ± SD, with $p < 0.05$ as statistically significant. IBM SPSS Statistics 25.0 software was used.

RESULTS

Comparison of Basic Characteristics Between Groups

The characteristics of the subjects are shown in **Table 1**. There was no significant difference in age, height, and weight between the two groups of subjects.

Assessment of the Distribution Pattern of Bone Tissue With Different Densities Under the Cartilage of the Ankle Joint

In the sagittal, coronal, and axial images, the bone tissue of each bone density in the distal tibia and talus showed a mixed lamellar–concentric distribution in both groups of subjects, and the bone tissue density was higher on the side close to the articular surface in **Figures 2** and **3**.

Comparison of Frequency and Distribution Patterns of the High-Density Zone of the Distal Tibia and Talus Dome Articular Surface in the Three-Dimensional Mode

The high-density measurement patterns of the two groups of subjects are shown in **Figure 4**, and the location and distribution patterns of the high-density areas of the distal tibia and the talar dome surface of the two groups are further analyzed in **Table 2**.

In the present study, it was found that there were high-density areas in the 1st, 2nd, 3rd, 4th, 6th, 7th, and 9th regions of the distal tibia of Taekwondo athletes, and the distribution track was consistent with the high-density areas of the talar dome surface (1st, 2nd, 3rd, 4th, 6th, 7th, and 9th regions).

Comparison of the Volume Percentage of the Bone Density of the Distal Tibia Epiphysis and Talus Subchondral Bone Between the Two Groups

%BTV of the moderate and high bone mineral density of subchondral bone of distal tibia in the Taekwondo group was higher than that in the control group ($p > 0.05$). The right distal tibia of the Taekwondo group had a higher %BTV of moderate bone mineral density in the subchondral bone than the left distal tibia of the Taekwondo group ($p > 0.05$). %BTV of low bone density bone tissue of distal tibial subchondral bone in the control group was higher than that in the Taekwondo group ($p > 0.05$) in **Table 3** and **Figures 5** and **6**.

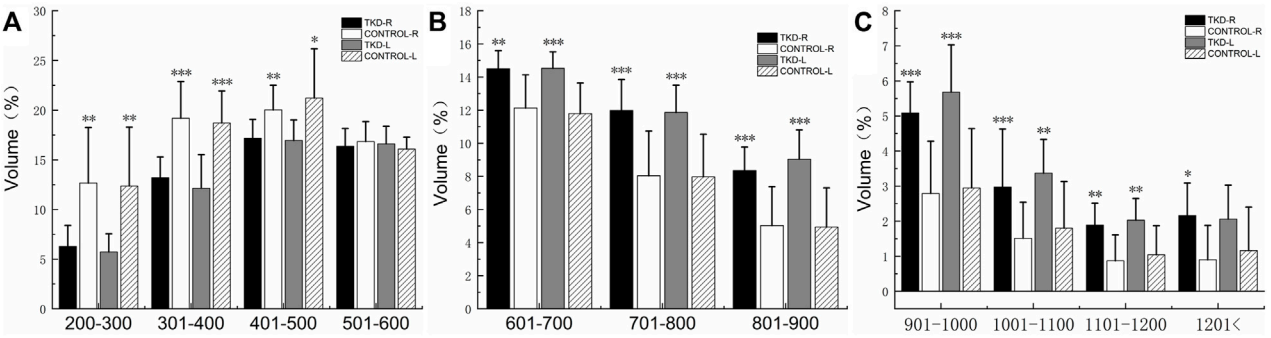

FIGURE 7 | Comparison of the bone volume of each bone density zone in the talus subchondral bone between the groups (%). **(A)** is the bone volume of low bone density; **(B)** is the bone volume of medium bone density; **(C)** is the bone volume of high bone density (***, **, and * indicate statistically significant p values of <0.001, <0.01, and <0.05 in the control group).

%BTV with the moderate and high bone density of subchondral bone of talus in the Taekwondo group was higher than that in the control group ($p > 0.05$). %BTV with the low bone density of subchondral bone of talus in the control group was higher than that in the Taekwondo group ($p > 0.05$) in **Table 4** and **Figures 7** and **8**.

DISCUSSION

The Stress Distribution of Ankle Joint Surface Between Taekwondo and Control Subjects Was Different

In the plantar flexion–internal rotation of the ankle, the posteromedial region of the talus contacts the distal tibia. When the ankle is dorsiflexion, the talus slides posteriorly toward the tibia. In ankle plantar flexion, the talus slides forward to the tibia (Stormont et al., 1985; Hayes et al., 2006; Kobayashi et al., 2015). Therefore, as the ankle moves from dorsiflexion to plantar flexion, the contact trajectory between the talus and the tibia is posteriorly anterior to the tibia (Driscoll et al., 1994; Omori et al., 2004). In the aforementioned experiments, cadaver specimens were used to measure the difference in stress distribution and joint motion pattern of the distal tibia. *In vivo*, bone joints are also filled with bone joint fluid to lubricate them, helping them to complete rolling, friction, impact, sliding, and other single and composite actions. In the present study, it was found that there were high-density areas in the 1st, 2nd, 3rd, 4th, 6th, 7th, and 9th regions of the distal tibia of Taekwondo athletes, and the distribution track was consistent with the high-density areas of the talar dome surface (1st, 2nd, 3rd, 4th, 6th, 7th, and 9th regions). In addition, we also noticed that some Taekwondo athletes had higher bone density distribution in the second region of the talus and talus articular surface. Therefore, we believe that Taekwondo athletes' take off movement in a short period of time, and gravity reaction force after landing, lower limb mobility technology, and long-term impact stress loading lead to the high-density distribution of the distal tibial articular surface and talar dome area. Finally, we also observed several unreported distribution types of high-density areas (Leumann et al., 2015; Deml et al., 2017; Shiota et al., 2020), such as blank area and annular high-density area on the talar dome of subjects in the control group and Taekwondo group, and annular and comprehensive high-density area on the distal tibia. We suggested that the control subjects may not have a long-term or high-intensity exercise habit and therefore do not develop a large area of high density in the medial to lateral area of the talar dome surface. Differences in the distribution of medial–lateral high-density in the distal tibia and talus cartilage may also be related to the subjects' gait cycle, skeletal morphology, joint stress pattern, genetics, and shoe type. In addition, according to the frequency of high-density areas on the articular surface of the distal tibia and talar dome surface, the 1st, 4th, and 7th regions of the normal stress part of the distal tibia and the 1st, 4th, and 9th regions of the talar dome surface were selected as the reference sites in the control group. The stress position of the distal tibial articular surface and talar dome surface of Taekwondo athletes is based on the normal stress area. After long-term stress loading of the joint, part of the middle region and part of the lateral region (low-stress area) high-density area increases, that is, the ankle joint surface of Taekwondo athletes shows a whole stress state.

Generally speaking, from the perspective of functional anatomy, the joint surfaces of the ankle move with each other in the form of extrusion, collision, and friction, which can lead to obvious contact stress distribution on the joint surfaces of the two. This change is very consistent with the report that the contact pressure distribution of the ankle joint moves from the middle to the anterior region of the talar dome surface from the first peak to the second peak of the standing stage. During the standing period of ankle gait, the contact stress on the talar dome surface mainly concentrates on the middle region of the talar dome surface. The maximum load was detected in the anterolateral region of the talar dome during the thrust phase of the ankle gait. During the transition from plantar flexion to dorsiflexion, the lateral load of the talus increases and the medial load decreases (Michelson et al., 2001; Suckel et al., 2010; Park et al., 2019). In addition, the range of plantar flexion of the ankle joint is 40–50°, while the range of dorsiflexion is about 20°. The 20° dorsiflexion range left by Taekwondo athletes after jumping

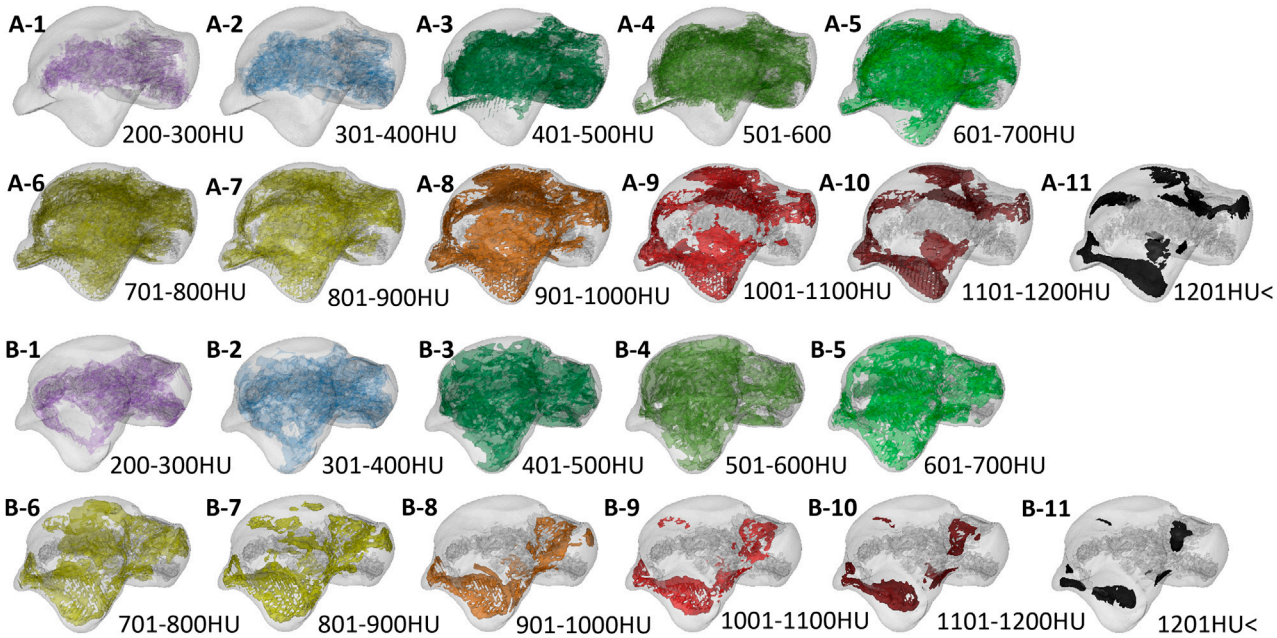

FIGURE 8 | The volume distribution of bone tissue with different bone densities in the talus subchondral bone of the two groups. A1–A11 is the Taekwondo group; B1–B11 is the control group.

and landing may lead to the high-density regional distribution phenomenon in the 1st, 2nd, 3rd, 4th, 6th, 7th, and 9th regions of the talus. In the field of sports medicine research, some scholars think that there was a higher risk of cartilage damage lesions in the medial region 4th and lateral region 6th of the talar dome surface and region 4th on the medial distal side of the tibia, and main factors of cartilage damage may be due to form a violent collision between two bone, articular cartilage, as a result of increased ankle internal stress loading damage (Raikin et al., 2007; Elias et al., 2009). Generally speaking, the ankle can cushion the impact of landing. However, some studies have found that depending on the height of the jumping landing, the ankles of subjects need to bear 6–10 times the weight of ground reaction force when their legs land, resulting in high-intensity vibration of the joints (Zhang et al., 2000; Ryu and Lee, 2021). The number of ground reaction forces varies with the type of ballet technique (McPherson et al., 2019). And, the ground reaction force explains the force exerted by the ankle joint on the ground and the feedback of that force. Most lower limb injuries in athletes occur after landing on one leg, and the ankle joint is unable to withstand the impact stress of landing (Olsen et al., 2004; Ryu and Lee, 2021). This suggests that Taekwondo athletes may be potential patients with an ankle cartilage injury. Therefore, it is recommended that Taekwondo athletes receive regular medical imaging during training to reduce the potential risk of cartilage damage.

Compared with the experimental results of Shiota et al. (2020), the distribution pattern of the high-density area of the tibial ankle joint of Taekwondo athletes is similar to that of soccer players. Although soccer and Taekwondo belong to lower limb sports, soccer players have a shorter time dribbling the ball and running distance, while running without the ball more time. Soccer players, however, wear professional sneakers to play on grass, which makes it possible to cushion the ankle to some extent. In addition, when Taekwondo athletes wear electronic protective gear on their lower limbs, they only get the score of hitting, but it does not provide much protection to the feet of Taekwondo athletes. As a result, large areas of high bone density are distributed in the ankle joint of Taekwondo athletes.

The Mechanical Stress of Taekwondo Promotes the Difference in Ankle Bone Remodeling Distribution

In the sagittal, coronal, and axial images, the bone tissue of each bone density in the distal tibia and talus showed a mixed lamellar–concentric distribution in both groups of subjects, and the bone tissue density was higher on the side close to the articular surface. Compared with the control group, the moderate and high bone volume of ankle joint subchondral bone in the Taekwondo group was significantly increased. It indicates that long-term stress loading results in a high degree of remodeling of the subchondral bone of the ankle joint of athletes, and the remodeling position of the bone is located in the stress position of the joint. According to the age and training history of the subjects, the participants of the high-level Taekwondo athletes have more than 8 years of training history on average. Moving the training history forward to the beginning of the training period, the mechanical stress stimulation resulting from Taekwondo

training or competition at the same age may accelerate the pubertal bone development and remodeling process in athletes. After Taekwondo athletes take off and hit the target, their bodies must receive 6 times of their own ground reaction force after landing. If they land on one foot and gain weight, the risk of lower limb injury will be further increased (Ryu and Lee, 2021). The athlete keeps the jump-landing posture during training and competition, which causes the ankle, knee, and hip joints to continuously suffer from the body and ground gravity and ground reaction force, resulting in the collision between the talus and the distal tibia, resulting in the ankle surface bone remodeling phenomenon. According to Wolfe's law (Wolff, 2010) and research findings, long-term high-intensity exercise stress may lead to adaptive changes in bone (Lara et al., 2016). Impact exercise intervention in adult women found ossification in the distal tibia, while resistance training had a greater impact on the strength of the femoral shaft and proximal femur (Lambert et al., 2020).

Early studies have found that subchondral ossification of the distal end of long bones over time may indicate a functional adaptation of the distal tibial articular surface to joint load, but may also lead to articular cartilage damage and osteoarthritis (Muir et al., 2006). However, recent studies have found that the bone mineral density of the spine and lower limb (vertebral body, femoral neck, and femoral trochanter) of retired soccer players is significantly higher than that of the control group, and the prevalence of knee osteoarthritis is lower than that of nonathletes, suggesting that low bone mineral density and advanced age are the main influencing factors of knee osteoarthritis (Lv et al., 2018). In Taekwondo athletes after early training, the volume remodeling level of the distal tibia and subtalus bone tissue is constantly improved to resist stress stimulation. Some studies have found that, with the change in biomechanical environment, the modeling and remodeling of subchondral bone is faster, while the conversion rate of articular cartilage is relatively low (Intema et al., 2010; Goldring, 2012; Zhen and Cao, 2014). In general, subchondral bone has greater stiffness and strength than articular cartilage and can absorb much of the stress transferred from the articular surface and provide biomechanical support to cartilage (Zhen and Cao, 2014). Therefore, we can know that reducing the stress carrying capacity of subchondral bone (bone density) can lead to changes in the stress distribution of articular cartilage, thus increasing the probability of articular cartilage injury. Studies have found that patients with osteoporosis and osteoarthritis of subchondral bone remodeling can lead to serious abnormal cartilage damage, and abnormal subchondral bone remodeling damaged the normal biomechanical environment, exacerbating the cartilage injury risk; this shows that the stress load transfer mechanism in the subchondral bone and articular cartilage plays a key role in the functional unit (Chu et al., 2019). Subchondral bone remodeling with a good stress transfer effect may reduce the high-intensity stress carried by articular cartilage. However, it is puzzling that Taekwondo athletes did not show any ankle injury or ankle pain symptoms before the CT scan. This may be related to the arch of the foot and the muscles and ligaments around the ankle joint of Taekwondo athletes, which buffer the stress and provide support and nutrition for the ankle joint (Guimarães et al., 2018; Rice et al., 2019; Sutter et al., 2019), thus reducing the probability of joint injury to a certain extent.

Mechanical Stress in Taekwondo Promotes the Distribution of High-Density Bone in Other Parts of Ankle Joint

The current study demonstrates that, outside the zone of interest at the distal tibia and talar dome, we noted areas of high density at the tibial medial malleolus tip and the head of the talus, the lateral tuberosity, and the outer ankle surface. We thought the Taekwondo athletes after landing, ankle joint instability there may be a moment in (including ankle inversion and eversion action in the coronal plane), ankle plantar flexion and backstretch displacement, landing back within the asymmetric stress and arch deformation after extrusion (e.g., from the boat joints), the surrounding ligament pull on the ankle, and leading to the aforementioned areas appear large bone remodeling phenomenon. Compressive strain, tensile strain, hydrostatic pressure, shear strain, and hydrodynamics are considered to be important mechanical loading cues that regulate bone regeneration and remodeling (Goodship and Kenwright, 1985; Carter et al., 1988; Leucht et al., 2007; Hara et al., 2018). Earlier studies found that when subjects landed on one side, they increased the range of motion of the ankle joint, the impact absorption of the surrounding muscle tissue, the risk of injury, and the total energy absorption after landing by 11%, suggesting that there was a significant amount of passive energy transferred from both sides during a one-sided landing (Weinhandl et al., 2010). Athletes with chronic ankle instability had a significant ankle valgus angle at initial landing, suggesting a preference for additional ankle valgus angles during landing to avoid ankle sprain due to ankle rollover (Lin et al., 2019). After Taekwondo athletes take off and land, the instantaneous instability of the ankle joint in the coronal plane (including ankle varus and valgus) may cause the tension of ligaments attached to the inside and outside of the ankle joint to be pulled alternately. Bone remodeling was caused by the impact of the fibula lateral malleolus tip and talar dome, as well as the medial malleolus tip and talus lateral malleolus surface of the distal tibia. The high-density area and bone remodeling of the talus and lateral tuberosity may be caused by the intercompression of the talus navicular bone joints in the arch of the foot, the mutual pulling of the talus and navicular bone by the talus dorsal ligament, the intercompression of the calcaneal posterior articular surface and the posterior talus joint, and the tension of the talus, and the calcaneus posterior ligament. Early studies using MRI resonance found that during the training period of military recruits, a large number of bone stress injuries occurred in the talus of the foot of lower limbs, and all of them were concentrated in the upper region of the talus (Sormaala et al., 2006). However, it has been found that an increase in hindfoot valgus and a decrease in forefoot valgus may exacerbate the shear stress in the middle third of the navicular bone. If the forefoot valgus angle is reduced, the pressure on the talus increases. The medial rotation of the talus causes the talus to exert force on the

lateral side of the navicular bone. However, it has been found that an increase in hindfoot valgus and a decrease in forefoot valgus may exacerbate the shear stress in the middle third of the navicular bone as posterior valgus is increased (Arndt et al., 2007; Becker et al., 2018). The findings of the present study are consistent with those reported by Mueller et al. (2014). In the three-dimensional model of the talus and the two-dimensional images of the coronal surface of the navicular bone, high-density zones were observed in the posterior articular surface of the talus and in the talonavicular surface. Based on our current results, we conclude that the interaction between the talus and navicular bone can be used to transfer and release the intra-articular stress generated by the human arch of the talus. However, it has been found that an increase in hindfoot valgus and a decrease in forefoot valgus may exacerbate the shear stress in the middle third of the navicular bone. The talus–navicular joint pulls the talonavicular ligament during movement, resulting in a high-density distribution of the head of the talus. The high-density distribution of the external ankle surface of the talus is mainly caused by the interaction between the internal fibula surface and the external talus ankle surface, the friction of the calcaneal ligament, and the traction of the talocalcaneal lateral ligament. In addition, the posterior articular surface of the calcaneus and the talus forms the subtalar joint, and the plantar-flexion motion of the calcaneus pulled by the Achilles tendon results in the interaction between the posterior articular surface of the calcaneus and the talus, resulting in a high-density distribution of the posterior articular surface of the talus. The mechanical relationship between the talar head and the navicular bone remains unclear and needs to be further investigated by bone and joint biomechanics and finite element analysis of cadaveric specimens.

LIMITATION

For the current studies, this study has several limitations. 1) The corresponding biomechanical experiment was not carried out in this test, and the stress parameters generated by Taekwondo athletes' striking and footwork movement were not obtained. 2) As far as the present study is concerned, the experiment fails to determine which direct or indirect factors will lead to the high-density stress distribution of the distal tibial bone of the ankle joint of Taekwondo athletes.

CONCLUSION

The impact stress, ground reaction force, intra-articular stress, lower limb movement technology, lower limb muscle, and tendon stress caused by Taekwondo lead to special pressure distribution patterns and bone tissue remodeling in the ankle. The distal tibia and talus bone transformation rule for low density in bone tissue to medium density bone tissue to high-density and medium-density bone tissue. The stress points on the articular surface of the ankle joint are the 1st, 4th, and 7th regions of the distal tibia, and the 1st, 3rd, 4th, and 7th regions of the talar dome surface. The ankle joint of Taekwondo athletes is comprehensively stressed based on the normal stress point, to improve the area of high density near the area of low stress. Because Taekwondo athletes have a large area of high-density distribution and high bone remodeling on the distal tibia and talus joint surface, we suggest that coaches and athletes should receive CT images and MRI examinations regularly to observe the wear of athletes' articular cartilage.

DATA AVAILABILITY STATEMENT

The raw data supporting the conclusions of this article will be made available by the authors, without undue reservation.

ETHICS STATEMENT

The studies involving human participants were reviewed and approved by the ethics committee certificate from the North University of China. The patients/participants provided their written informed consent to participate in this study. Written informed consent was obtained from the individual(s) for the publication of any potentially identifiable images or data included in this article.

AUTHOR CONTRIBUTIONS

GX completed the experiment and wrote the manuscript. GX and HL directed the design test and repaired the manuscript. HL provided research information. The rest of the authors put forward valuable opinions on the whole subject design. All authors contributed to the article and approved the submitted version.

ACKNOWLEDGMENTS

We would like to express our sincere thanks to engineer Zhao Xi of Siemens Healthineers China, Wang Haohao of the Department of Orthopedics at Shanxi Medical University, Wang Qiuyuan of China-Japan Friendship Hospital, and Lin Dongxin of the National Key Discipline of Human Anatomy at Southern Medical University for their comments and suggestions.

REFERENCES

Arndt, A., Wolf, P., Liu, A., Nester, C., Stacoff, A., Jones, R., et al. (2007). Intrinsic Foot Kinematics Measured *In Vivo* during the Stance Phase of Slow Running. *J. Biomech.* 40 (12), 2672–2678. doi:10.1016/j.jbiomech.2006.12.009

Becker, J., James, S., Osternig, L., and Chou, L.-S. (2018). Foot Kinematics Differ between Runners with and without a History of Navicular Stress Fractures. *Orthopaedic J. Sports Med.* 6 (4), 232596711876736. doi:10.1177/2325967118767363

Carter, D. R., Blenman, P. R., and Beaupré, G. S. (1988). Correlations between Mechanical Stress History and Tissue Differentiation in Initial Fracture Healing. *J. Orthop. Res.* 6 (5), 736–748. doi:10.1002/jor.1100060517

Chu, L., Liu, X., He, Z., Han, X., Yan, M., Qu, X., et al. (2019). Articular Cartilage Degradation and Aberrant Subchondral Bone Remodeling in Patients with Osteoarthritis and Osteoporosis. *J. Bone Miner Res.* 35 (3), 505–515. doi:10.1002/jbmr.3909

Deml, C., Eichinger, M., van Leeuwen, W. F., Erhart, S., Euler, S. A., and Brunner, A. (2017). Does Intra-articular Load Distribution Change after Lateral Malleolar Fractures? an *In Vivo* Study Comparing Operative and Non-operative Treatment. *Injury* 48 (4), 854–860. doi:10.1016/j.injury.2017.02.035

Driscoll, H. L., Christensen, J. C., and Tencer, A. F. (1994). Contact Characteristics of the Ankle Joint. Part 1. The normal Joint. *J. Am. Podiatr Med. Assoc.* 84 (10), 491–498. doi:10.7547/87507315-84-10-491

Elias, I., Raikin, S. M., Schweitzer, M. E., Besser, M. P., Morrison, W. B., and Zoga, A. C. (2009). Osteochondral Lesions of the Distal Tibial Plafond: Localization and Morphologic Characteristics with an Anatomical Grid. *Foot Ankle Int.* 30 (6), 524–529. doi:10.3113/fai.2009.0524

Estevan, I., Álvarez, O., Falco, C., Molina-García, J., and Castillo, I. (2011). Impact Force and Time Analysis Influenced by Execution Distance in a Roundhouse Kick to the Head in Taekwondo. *J. Strength Cond Res.* 25 (10), 2851–2856. doi:10.1519/jsc.0b013e318207ef72

Falco, C., Alvarez, O., Castillo, I., Estevan, I., Martos, J., Mugarra, F., et al. (2009). Influence of the Distance in a Roundhouse Kick's Execution Time and Impact Force in Taekwondo. *J. Biomech.* 42 (3), 242–248. doi:10.1016/j.jbiomech.2008.10.041

Gartland, S., Malik, M. H. A., and Lovell, M. E. (2001). Injury and Injury Rates in Muay Thai Kick Boxing. *Br. J Sport Med* 35 (5), 308–313. doi:10.1136/bjsm.35.5.308

Goldring, S. R. (2012). Alterations in Periarticular Bone and Cross Talk between Subchondral Bone and Articular Cartilage in Osteoarthritis. *Ther. Adv. Musculoskelet.* 4 (4), 249–258. doi:10.1177/1759720x12437353

Goodship, A., and Kenwright, J. (1985). The Influence of Induced Micromovement upon the Healing of Experimental Tibial Fractures. *The J. Bone Jt. Surg. Br. volume* 67-B (4), 650–655. doi:10.1302/0301-620x.67b4.4030869

Guimarães, B. R., Pimenta, L. D., Massini, D. A., Dos Santos, D., Siqueira, L. O. D. C., Simionato, A. R., et al. (2018). Muscle Strength and Regional Lean Body Mass Influence on mineral Bone Health in Young Male Adults. *Plos One* 13 (1), e0191769. doi:10.1371/journal.pone.0191769

Hara, E. S., Okada, M., Nagaoka, N., Hattori, T., Iida, L. M., Kuboki, T., et al. (2018). Chondrocyte Burst Promotes Space for mineral Expansion. *Integr. Biol.* 10 (1), 57–66. doi:10.1039/c7ib00130d

Hayes, A., Tochigi, Y., and Saltzman, C. L. (2006). Ankle Morphometry on 3D-CT Images. *Iowa Orthop. J.* 26, 1–4.

Intema, F., Hazewinkel, H. A. W., Gouwens, D., Bijlsma, J. W. J., Weinans, H., Lafeber, F. P. J. G., et al. (2010). In Early OA, Thinning of the Subchondral Plate Is Directly Related to Cartilage Damage: Results from a Canine ACLT-Meniscectomy Model. *Osteoarthritis and Cartilage* 18 (5), 691–698. doi:10.1016/j.joca.2010.01.004

Jakubiak, N., and Saunders, D. H. (2008). The Feasibility and Efficacy of Elastic Resistance Training for Improving the Velocity of the Olympic Taekwondo Turning Kick. *J. Strength Cond Res.* 22 (4), 1194–1197. doi:10.1519/jsc.0b013e31816d4f66

Jeong, H. S., O'Sullivan, D. M., Lee, S. C., and Lee, S. Y. (2019). Safety Evaluation of Protective Equipment for the Forearm, Shin, Hand and Foot in Taekwondo. *J. Sports Sci. Med.* 18 (2), 376–383.

Kobayashi, T., Suzuki, E., Yamazaki, N., Suzukawa, M., Akaike, A., Shimizu, K., et al. (2015). *In Vivo* Talocrural Joint Contact Mechanics with Functional Ankle Instability. *Foot & Ankle Specialist* 8 (6), 445–453. doi:10.1177/1938640015585967

Lambert, C., Beck, B. R., Harding, A. T., Watson, S. L., and Weeks, B. K. (2020). Regional Changes in Indices of Bone Strength of Upper and Lower Limbs in Response to High-Intensity Impact Loading or High-Intensity Resistance Training. *Bone* 132, 115192. doi:10.1016/j.bone.2019.115192

Lara, B., Salinero, J. J., Gutiérrez, J., Areces, F., Abián-Vicén, J., Ruiz-Vicente, D., et al. (2016). Influence of Endurance Running on Calcaneal Bone Stiffness in Male and Female Runners. *Eur. J. Appl. Physiol.* 116 (2), 327–333. doi:10.1007/s00421-015-3285-7

Leucht, P., Kim, J.-B., Wazen, R., Currey, J. A., Nanci, A., Brunski, J. B., et al. (2007). Effect of Mechanical Stimuli on Skeletal Regeneration Around Implants. *Bone* 40 (4), 919–930. doi:10.1016/j.bone.2006.10.027

Leumann, A., Valderrabano, V., Hoechel, S., Göpfert, B., and Müller-Gerbl, M. (2015). Mineral Density and Penetration Strength of the Subchondral Bone Plate of the Talar Dome: High Correlation and Specific Distribution Patterns. *J. Foot Ankle Surg.* 54 (1), 17–22. doi:10.1053/j.jfas.2014.09.035

Lin, J. Z., Lin, Y. A., and Lee, H. J. (2019). Are Landing Biomechanics Altered in Elite Athletes with Chronic Ankle Instability. *J. Sports Sci. Med.* 18 (4), 653–662.

Lv, H., Chen, W., Yuwen, P., Yang, N., Yan, X., and Zhang, Y. (2018). Multivariate Analysis of Factors Related to Radiographic Knee Osteoarthritis Based on the Comparison between Football Players and Matched Nonsportsmen. *Int. Orthopaedics (Sicot)* 42 (3), 519–527. doi:10.1007/s00264-018-3797-y

McPherson, A. M., Schrader, J. W., and Docherty, C. L. (2019). Ground Reaction Forces in Ballet Differences Resulting from Footwear and Jump Conditions. *J Dance Med. Sci.* 23 (1), 34–39. doi:10.12678/1089-313x.23.1.34

Michelson, J. D., Checcone, M., Kuhn, T., and Varner, K. (2001). Intra-articular Load Distribution in the Human Ankle Joint during Motion. *Foot Ankle Int.* 22 (3), 226–233. doi:10.1177/107110070102200310

Mueller, F., Hoechel, S., Klaws, J., Wirz, D., and Müller-Gerbl, M. (2014). The Subtalar and Talonavicular Joints: a Way to Access the Long-Term Load Intake Using Conventional CT-data. *Surg. Radiol. Anat.* 36 (5), 463–472. doi:10.1007/s00276-013-1205-2

Muir, P., McCarthy, J., Radtke, C. L., Markel, M. D., Santschi, E. M., Scollay, M. C., et al. (2006). Role of Endochondral Ossification of Articular Cartilage and Functional Adaptation of the Subchondral Plate in the Development of Fatigue Microcracking of Joints. *Bone* 38 (3), 342–349. doi:10.1016/j.bone.2005.08.020

Müller-Gerbl, M., Putz, R., Hodapp, N., Schulte, E., and Wimmer, B. (1989). Computed Tomography-Osteoabsorptiometry for Assessing the Density Distribution of Subchondral Bone as a Measure of Long-Term Mechanical Adaptation in Individual Joints. *Skeletal Radiol.* 18 (7), 507–512. doi:10.1007/BF00351749

Olsen, O.-E., Myklebust, G., Engebretsen, L., and Bahr, R. (2004). Injury Mechanisms for Anterior Cruciate Ligament Injuries in Team Handball. *Am. J. Sports Med.* 32 (4), 1002–1012. doi:10.1177/0363546503261724

Omori, G., Kawakami, K., Sakamoto, M., Hara, T., and Koga, Y. (2004). The Effect of an Ankle Brace on the 3-dimensional Kinematics and Tibio-Talar Contact Condition for Lateral Ankle Sprains. *Knee Surg. Sports Traumatol. Arthrosc.* 12 (5), 457–462. doi:10.1007/s00167-004-0493-9

Onodera, T., Majima, T., Iwasaki, N., Kamishima, T., Kasahara, Y., and Minami, A. (2012). Long-term Stress Distribution Patterns of the Ankle Joint in Varus Knee Alignment Assessed by Computed Tomography Osteoabsorptiometry. *Int. Orthopaedics (Sicot)* 36 (9), 1871–1876. doi:10.1007/s00264-012-1607-5

Park, S., Lee, S., Yoon, J., and Chae, S.-W. (2019). Finite Element Analysis of Knee and Ankle Joint during Gait Based on Motion Analysis. *Med. Eng. Phys.* 63, 33–41. doi:10.1016/j.medengphy.2018.11.003

Pieter, W., Fife, G. P., and O'Sullivan, D. M. (2012). Competition Injuries in Taekwondo: a Literature Review and Suggestions for Prevention and Surveillance. *Br. J. Sports Med.* 46 (7), 485–491. doi:10.1136/bjsports-2012-091011

Raikin, S. M., Elias, I., Zoga, A. C., Morrison, W. B., Besser, M. P., and Schweitzer, M. E. (2007). Osteochondral Lesions of the Talus: Localization and Morphologic Data from 424 Patients Using a Novel Anatomical Grid Scheme. *Foot Ankle Int.* 28 (2), 154–161. doi:10.3113/fai.2007.0154

Rice, P. E., Needle, A. R., Leicht, Z. S., Zwetsloot, K. A., and McBride, J. M. (2019). Bone Health, Muscle Properties and Stretch-Shortening Cycle

Function of Young and Elderly Males. *J. Musculoskelet. Neuronal Interact* 19 (4), 389–395.

Ryu, S., and Lee, T.-k. (2021). Biomechanical Parameters that May Influence Lower Limb Injury during Landing in Taekwondo. *Medicina* 57 (4), 373. doi:10.3390/medicina57040373

Shiota, J., Momma, D., Yamaguchi, T., and Iwasaki, N. (2020). Long-term Stress Distribution Patterns across the Ankle Joint in Soccer Players: A Computed Tomography Osteoabsorptiometry Study. *Orthopaedic J. Sports Med.* 8 (11), 232596712096308. doi:10.1177/2325967120963085

Sormaala, M. J., Niva, M. H., Kiuru, M. J., Mattila, V. M., and Pihlajamäki, H. K. (2006). Bone Stress Injuries of the Talus in Military Recruits. *Bone* 39 (1), 199–204. doi:10.1016/j.bone.2005.12.001

Stormont, D. M., Morrey, B. F., An, K.-N., and Cass, J. R. (1985). Stability of the Loaded Ankle. *Am. J. Sports Med.* 13 (5), 295–300. doi:10.1177/036354658501300502

Suckel, A., Muller, O., Wachter, N., and Kluba, T. (2010). *In Vitro* measurement of Intraarticular Pressure in the Ankle Joint. *Knee Surg. Sports Traumatol. Arthrosc.* 18 (5), 664–668. doi:10.1007/s00167-009-1040-5

Sutter, T., Toumi, H., Valery, A., El Hage, R., Pinti, A., and Lespessailles, E. (2019). Relationships between Muscle Mass, Strength and Regional Bone mineral Density in Young Men. *Plos One* 14 (3), e0213681. doi:10.1371/journal.pone.0213681

Thibordee, S., and Prasartwuth, O. (2014). Effectiveness of Roundhouse Kick in Elite Taekwondo Athletes. *J. Electromyogr. Kinesiol.* 24 (3), 353–358. doi:10.1016/j.jelekin.2014.02.002

Watta, E. (2021). *Know Your Sport: Olympic Taekwondo Rules, Scoring and Equipment A Rundown of Olympic Taekwondo Rules, Equipment, Scoring and the Different Belts*. Nairobi, Madrid: The International Olympic Committee (IOC).

Weinhandl, J. T., Joshi, M., and O'Connor, K. M. (2010). Gender Comparisons between Unilateral and Bilateral Landings. *J. Appl. Biomech.* 26 (4), 444–453. doi:10.1123/jab.26.4.444

Wolff, J. (2010). The Classic: On the Inner Architecture of Bones and its Importance for Bone Growth: (Ueber die innere Architectur der Knochen und ihre Bedeutung für die Frage vom Knochenwachsthum). *Clin. Orthopaedics Relat. Res.* 468 (4), 1056–1065. doi:10.1007/s11999-010-1239-2

Zhang, S.-N., Bates, B. T., and Dufek, J. S. (2000). Contributions of Lower Extremity Joints to Energy Dissipation during Landings. *Med. Sci. Sports Exerc.* 32 (4), 812–819. doi:10.1097/00005768-200004000-00014

Zhen, G., and Cao, X. (2014). Targeting TGFβ Signaling in Subchondral Bone and Articular Cartilage Homeostasis. *Trends Pharmacol. Sci.* 35 (5), 227–236. doi:10.1016/j.tips.2014.03.005

Conflict of Interest: The authors declare that the research was conducted in the absence of any commercial or financial relationships that could be construed as a potential conflict of interest.

Publisher's Note: All claims expressed in this article are solely those of the authors and do not necessarily represent those of their affiliated organizations or those of the publisher, the editors, and the reviewers. Any product that may be evaluated in this article, or claim that may be made by its manufacturer, is not guaranteed or endorsed by the publisher.

frontiers | Frontiers in Bioengineering and Biotechnology

ORIGINAL RESEARCH
published: 12 May 2022
doi: 10.3389/fbioe.2022.877347

Predicting the Internal Knee Abduction Impulse During Walking Using Deep Learning

*Issam Boukhennoufa[1], Zainab Altai[2], Xiaojun Zhai[1], Victor Utti[2], Klaus D McDonald-Maier[1] and Bernard X. W. Liew[2]**

[1]School of Computer Science and Electrical Engineering, University of Essex, Colchester, United Kingdom, [2]School of Sport, Rehabilitation and Exercise Sciences, University of Essex, Colchester, United Kingdom

Knee joint moments are commonly calculated to provide an indirect measure of knee joint loads. A shortcoming of inverse dynamics approaches is that the process of collecting and processing human motion data can be time-consuming. This study aimed to benchmark five different deep learning methods in using walking segment kinematics for predicting internal knee abduction impulse during walking. Three-dimensional kinematic and kinetic data used for the present analyses came from a publicly available dataset on walking (participants n = 33). The outcome for prediction was the internal knee abduction impulse over the stance phase. Three-dimensional (3D) angular and linear displacement, velocity, and acceleration of the seven lower body segment's center of mass (COM), relative to a fixed global coordinate system were derived and formed the predictor space (126 time-series predictors). The total number of observations in the dataset was 6,737. The datasets were split into training (75%, n = 5,052) and testing (25%, n = 1685) datasets. Five deep learning models were benchmarked against inverse dynamics in quantifying knee abduction impulse. A baseline 2D convolutional network model achieved a mean absolute percentage error (MAPE) of 10.80%. Transfer learning with InceptionTime was the best performing model, achieving the best MAPE of 8.28%. Encoding the time-series as images then using a 2D convolutional model performed worse than the baseline model with a MAPE of 16.17%. Time-series based deep learning models were superior to an image-based method when predicting knee abduction moment impulse during walking. Future studies looking to develop wearable technologies will benefit from knowing the optimal network architecture, and the benefit of transfer learning for predicting joint moments.

Keywords: gait biomechanics, knee joint moments, machine learning, neural network, time-series

OPEN ACCESS

Edited by:
Rezaul Begg,
Victoria University, Australia

Reviewed by:
Yaodong Gu,
Ningbo University, China
Chi-Wen Lung,
Asia University, Taiwan
Abdelrahman Zaroug,
Western Health, Australia

****Correspondence:***
Bernard X. W. Liew
bl19622@essex.ac.uk
liew_xwb@hotmail.com

Specialty section:
This article was submitted to Biomechanics, a section of the journal Frontiers in Bioengineering and Biotechnology

Received: *16 February 2022*
Accepted: *19 April 2022*
Published: *12 May 2022*

Citation:
Boukhennoufa I, Altai Z, Zhai X, Utti V, McDonald-Maier KD and Liew BXW (2022) Predicting the Internal Knee Abduction Impulse During Walking Using Deep Learning. Front. Bioeng. Biotechnol. 10:877347. doi: 10.3389/fbioe.2022.877347

1 INTRODUCTION

Knee joint moments are commonly calculated to provide an indirect measure of knee joint loads (Webster et al., 2012; Richards et al., 2018a; Robinson et al., 2021), with the frontal plane moment being the most implicated as a risk factor for the onset, exacerbation, and relapse of knee pathologies. For example, in knee osteoarthritis (OA), a greater external knee adduction moment (KAM) has been linked with accelerated disease progression (Henriksen et al., 2014). In contrast, a greater external knee abduction moment has been linked with a greater risk of developing patellofemoral pain and anterior cruciate ligament (ACL) injuries (Myer et al., 2015). Researchers have begun

TABLE 1 | Non-exhaustive list of studies using macine learning to predicting knee moments.

Study	Predictors	Outcome	Machine-learning algorithm	Performance error	Performance error—scaled*
Boswell et al. (2021)	3D positions of 13 anatomical landmarks	Peak external knee adduction moment	Fully connected neural network (10 hidden layers)	MAE: 0.53% (BW.Ht)	0.15 Nm/kg
Favre et al. (2012)	12 kinematic and kinetic variables	External knee adduction moment waveform	Multi-layer perceptron neural network (1 hidden layer)	MAD: 0.36% (Bw.Ht)	0.06 Nm/kg
Wang et al. (2020)	4 demographic, 24 kinematic variables	External knee adduction moment waveform	Fully connected neural network (10 hidden layers)	MAE: 0.002 Nm/(BW.Ht)	0.03 Nm/kg
He et al. (2019b)	24 plantar pressure variables	External knee adduction moment waveform	Multi-layer perceptron neural network (1 hidden layer)	RMSE: 0.36% (BW.Ht)	0.06 Nm/kg
Stetter et al. (2020)	16 kinematic variables	Peak external knee adduction moment	Fully connected neural network (2 hidden layer)	Difference: 0.11 Nm/kg	0.11 Nm/kg

**Scaled based on 1.70 m tall participant.*

Abbreviations: MAE, mean absolute error; MAD, mean absolute deviation; RMSE, root mean squared error

coupling real-time biofeedback of the KAM, together with provision of specific gait modification strategies in people with knee OA during walking, and this resulted in up to 14% reduction in peak KAM (Richards et al., 2018b).

Inverse dynamics represent the "Gold Standard" to calculate knee joint moments (Ren et al., 2008; Holder et al., 2020; Baltzopoulos, 2021). A shortcoming of inverse dynamics approaches is that the process of collecting and processing human motion data can be time-consuming (Ren et al., 2008; Holder et al., 2020; Baltzopoulos, 2021). The traditional methods to calculate knee joint moments makes it clinically impractical for large scale implementation. To circumvent the need to use inverse dynamics, researchers have turned to machine learning to predict knee joint moments (Favre et al., 2012; Aljaaf et al., 2016; He Z. et al., 2019; Mundt et al., 2020a; Mundt et al., 2020b; Stetter et al., 2020; Wang et al., 2020; Boswell et al., 2021)—which we term, the ML approach.

The most common ML method used to predict joint moments is neural networks (He Z. et al., 2019; Stetter et al., 2020; Wang et al., 2020; Boswell et al., 2021). Some studies adopt a shallow network architecture with one/two "hidden" layers (Favre et al., 2012; He Z. et al., 2019; Stetter et al., 2020), whilst others used deeper layers (Wang et al., 2020; Boswell et al., 2021). Studies have used kinematics captured using markerless motion capture (Boswell et al., 2021), a combination of inertial measurement units (IMUs) and plantar pressure insoles (He Z. et al., 2019), and IMUs alone (Stetter et al., 2020; Wang et al., 2020) as predictors. Currently, body kinematics obtained *via* IMUs represent the best variables used for predicting joint moments, compared to variables like plantar pressure from insoles and ground reaction forces from force plates. This is because IMUs, in contrast to pressure insoles, are commercially ubiquitous and cost-effective, and are the most accurate commercial devices to capture kinematics when compared to three-dimensional motion capture (Slade et al., 2022). Also, IMUs in contrast with force plates can be used in free-living environments. Outcomes that have been predicted include the peak value (He Z. et al., 2019; Boswell et al., 2021), the waveform (Stetter et al., 2020; Wang et al., 2020), and the moment integral (Stetter et al., 2020) of KAM. Reported prediction accuracies for KAM during walking range 0.03 Nm/kg to 0.15 Nm/kg (**Table 1**).

Most studies that used neural networks contain fully connected layers as their model architecture (Favre et al., 2012; He Z. et al., 2019; Stetter et al., 2020; Wang et al., 2020; Boswell et al., 2021). A limitation of fully connected layered neural networks is that more parameters have to be learned, thereby increasing computation time, compared to convolutional networks. Another limitation of fully connected layered neural networks in biomechanics is that they cannot accommodate temporal variables. To circumvent this limitation, researchers have opted to treat each value of a time-series as independent observations (Stetter et al., 2020), which ignores the inherent correlation in temporal biomechanics data.

Boswell et al. (2021) trialed different time-series neural network architectures (e.g., long short-term memory [LSTM]) but reported these to be inferior to a fully connected network. The findings of Boswell et al. (2021) was surprising given that LTSM are examples of time-series models that takes into account the information (e.g., correlation) from adjacent time-points to model the relationship between the predictors and outcome. The lack of benefit of using a LTSM model over a fully connected network could be explained by the relatively shallow number of layers (2 LTSM layers) (Boswell et al., 2021), which may have precluded learning an adequate representation of the prediction problem. However, a well-known problem of having deep layers in a neural network is the "vanishing gradient" issue (Veit et al., 2016), which states at deeper layers, there is incrementally lesser amount of information available for learning new relationships.

In this work, we employed more sophisticated time-series models consisting of the InceptionTime (Ismail Fawaz et al., 2020) and TS-ResNet (Wang et al., 2017), which till this current work to the authors knowledge, have not been used in biomechanics. These network architectures have been inspired by the popular Inception-v4 and the Resnet architecture that performed outstandingly in the computer vision domain. InceptionTime combines five deep learning models, each consisting of multiple Inception blocks (Ismail Fawaz et al., 2020). The inceptionTime outperformed other neural network architectures (convolutional neural networks [CNN], LSTM, bidirectional [BiLSTM], CNN-LSTM, and Gated Recurrent Units [GRU]) in human activity recognition (Pantawong et al., 2021). TS-ResNet enables very deep layers by adding connections that skip over some layers, to slow the rate of learning reaching saturation, and thus avoid the degradation problem. TS-ResNet outperformed eight

neural network architectures on 97 time-series datasets (Ismail Fawaz et al., 2019). Both these networks have not been used in joint moment estimation which is therefore a contribution of this work. In addition, time-series data can also first be encoded into images using Gramian Angular Field (GMF) and then fed into neural network architectures typically used for image-based datasets—a technique that significantly improved human activity recognition compared to traditional CNN models (Boukhennoufa et al., 2021a).

A challenge when using ML in biomechanics is the sample size. When the sample size is small, the ML model may generalize poorly for new observations. Current studies have used data from a very small cohort of 10 (Liu et al., 2009) to a larger cohort of 106 participants (Wang et al., 2020). However, even though a sample size of 100 participants is considered large clinically, it pales in comparison to non-clinical ML research [e.g., millions of samples (Simonyan and Zisserman, 2014)]. A novel ML method to manage the issue of small sample sizes is transfer learning (Weiss et al., 2016). Transfer learning takes advantage of "knowledge" from existing large pre-trained ML models, with the collected biomechanical data used for fine-tuning (Johnson et al., 2019). Pre-trained models such as the VGG network, have been trained on 1.3 million ImageNet images and 1000 object classes (Simonyan and Zisserman, 2014).

Transfer learning achieved a Pearson correlation of 0.94–0.97 (Johnson et al., 2019), which was similar to the correlation of 0.96 when using a custom CNN model (Wang et al., 2020) for predicting knee abduction/adduction moments during walking. Interestingly, a direct benchmark study in running reported that transfer learning resulted in poorer correlation compared to a custom CNN model (Liew et al., 2021). However, the previous study converted the time-series to images for modelling which could have introduced "noise" to the original data (Liew et al., 2021). To our knowledge, no studies have benchmarked the performance of different state-of-art time-series and image-based network architectures, and transfer learning for predicting knee joint moments in walking.

The potential clinical benefit of being able to quantify knee joint moments in the field warrants a systematic investigation of the optimal network architectures that maximizes prediction performance. Given that a previous study has reported that moment integrals (i.e., impulse) provide a better indication of joint load than peak moment values (Kean et al., 2012), this study aimed to benchmark different neural network architectures in using walking segment kinematics in predicting internal knee abduction impulse during walking. The decision to report internal and not external moments will be explained in the Methods section. We hypothesized that transfer learning will perform better than a simple custom CNN model in predicting internal knee abduction impulse.

2 MATERIALS AND METHODS

2.1 Design

This was a secondary analysis of a publicly available dataset, using a single session, cross-sectional laboratory study design (Fukuchi et al., 2018). Hence, no ethical approval was required for the conductance of this secondary analysis.

2.2 Dataset

The data came from a public dataset of 42 healthy adults walking on a treadmill, the details of which can be found in the original open-source publication (Fukuchi et al., 2018). Nine out of the 42 participants from the walking dataset were excluded from the present study. These participants had simultaneous bilateral foot contacts on the same force plate, resulting in an absence of consecutive good foot contact strides which lasted >50% of the walking duration. The 50% threshold was determined by the authors to minimize manual identification of foot contact events, to increase processing replicability (Liew et al., 2019).

Participants performed unshod walking on a dual-belt, force-instrumented treadmill (300 Hz, FIT; Bertec, Columbus, OH, United States), and motion was captured with 12 opto-electronic cameras (150 Hz, Raptor-4; Motion Analysis Corporation, Santa Rosa, CA, United States) (Fukuchi et al., 2018). This dataset was deemed feasible for this study given that the primary aim is to determine the optimal network architecture for using time-series kinematic measures to predict knee joint moment impulse. Walking occurred over eight controlled speeds: 40%, 55%, 70%, 85%, 100%, 115%, 130%, and 145% of each participant's self-determined dimensionless speed (Froude number). The associated absolute walking speeds for all eight conditions for each participant were reported by the authors (Fukuchi et al., 2018). Marker trajectories and ground reaction force (GRF) were low passed filtered at a matched frequency of 6 Hz (4th Order, zero-lag, Butterworth) (Liew et al., 2019). A seven-segment lower limb, 6DOF joint model was developed in Visual 3D software (C-motion Inc., Germantown, MD, United States) (Liew et al., 2019). A force plate threshold of 50N was used to determine gait events of initial contact and toe-off.

Three-dimensional (3D) angular and linear displacement, velocity, and acceleration of the seven segment's center of mass (COM), relative to a fixed global coordinate system were derived and formed the predictor space (126 time-series predictors).These kinematic predictors were used as it represented predictors can potentially be measured using IMUs. Internal moments are automatically calculated in Visual 3D. Hence, the internal knee abduction moment (inverse of the external KAM) was calculated using inverse-dynamics and expressed in the proximal segment's reference frame (Schache and Baker, 2007) (negative values indicated internal knee abduction moment).

2.3 Machine Learning Modeling

All analyses were done using Python (version 3.7.0), with packages (Numpy v1.19.5, Pandas v1.1.5, Scipy v1.4.1). All ML models were trained using either Keras (version 2.4.0) or Tsai (version 0.2.2) from fastai with Google Collab's Tesla V100 GPU, 25 GB RAM.

2.4 Generic Pre-processing

All time-series (predictors and outcome) were segmented between initial contact and toe-off (Liew et al., 2019). For the outcome, the area under the (negative) internal knee abduction moment curve for each time-series segment was calculated to provide a measure of knee abduction impulse. The knee abduction impulse was normalized to each participant's body mass (Nm.s/kg). Given that the stance duration between each

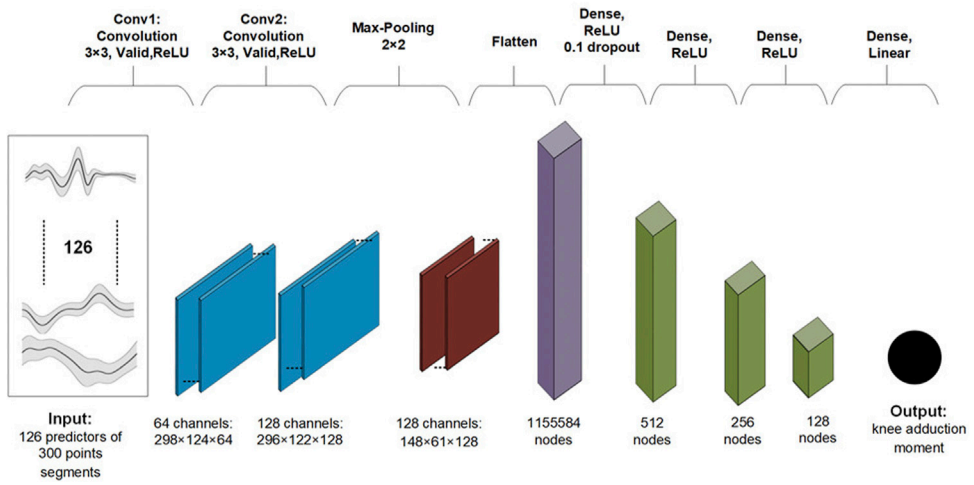

FIGURE 1 | Baseline two dimensional convolutional neural network architecture.

step, each speed condition, and participants were different, each time-series segment had a different number of data points. We zero-padded the time-series segments to have an equal number of data points as that of the longest time-series segment (Dwarampudi and Reddy, 2019; Pogson et al., 2020).

We explored three different pre-processing methods and their influence on prediction performance: 1) using raw time-series data as predictors, 2) normalizing the time-series predictors to a range from 0 to 1, and 3) standardizing the time-series predictors to a mean of 0 and standard deviation of 1. Although scaling of predictors (e.g., to a mean of 0 and standard deviation 1) is commonly advocated in ML (Burdack et al., 2020), our exploratory analysis revealed that using raw time-series as predictors provided the best prediction performance, and this was subsequently used in formal ML modelling.

The total number of observations in the dataset was 6,737 corresponding to 6,737 participant-steps. The predictor dataset was organised into a 3D array of shape 6737 × 126 × 300, where the second dimension was the number of predictors, and the third dimension was the number of time points. The outcome dataset was organised into a 1D vector of length 6737. Both the predictor and outcome datasets were split into training (75%, n = 5,052) and testing (25%, n = 1685) datasets (Wouda et al., 2018). The training dataset contains 75% of all the participants' data with all the controlled speeds while the test dataset contains the rest of the dataset over the controlled speeds. This allows the model to learn from all the different cases to permit a more robust generalisation for each distinct instance. Our method of ML model development relies on a scenario that a participant comes for a baseline biomechanics assessment to develop a personalised model for the prediction of future instances of knee joint loads.

2.5 Algorithms

The following architectures were evaluated: 1) A 2D CNN-based model used as a baseline model, 2) InceptionTime model, 3) transfer learning, 4) the TS-Resnet model, and 5) the combination GADF-xResnet18. We have specifically selected the TS-Resnet, the InceptionTime and the combination GADF-xResnet18 as they have been very successful in dealing with other TS domains such as in activity recognition (Boukhennoufa et al., 2021a; Boukhennoufa et al., 2021b) and we wanted to investigate the performance in predicting the knee abduction moment impulse.

2.5.1 2D CNN Model

The baseline 2D CNN model architecture can be found in **Figure 1**. Convolutional layers in a neural network are designed to learn a hierarchical representation of local features (e.g., peaks) of the predictors (Indolia et al., 2018). Advantages of convolutional layers over fully connected layers include having to learn much fewer parameters, better generalizability, and better scalability to big datasets. The model hyperparameters were selected based on initial exploratory analysis. Neural network (NN) weights were initialized with Xavier initialization (Glorot and Bengio, 2010). The Xavier initialization method is calculated as a random number with a uniform probability distribution (U) between the range $-\frac{1}{\sqrt{n}}$ and $\frac{1}{\sqrt{n}}$, where n is the number of inputs to the node.

$$weight = U\left[-\frac{1}{\sqrt{n}}, \frac{1}{\sqrt{n}}\right]$$

A batch size of 64, 100 epochs of training repetitions, a learning rate of $3e^{-3}$, and an Adam optimiser were used. We used the mean squared error as the loss criteria.

For the other neural network models, a different method to find the appropriate learning rate, which has been termed cyclical learning rates, was used (Smith, 2017). The loss was plotted with respect to an increasing value of the learning rate. The learning rate was chosen to be in the interval that resulted in the lowest loss, which was found to be between $8e^{-3}$ and $1e^{-1}$. The learning rate took the value of $8e^{-3}$ at the first epoch and then gradually increased to reach a final value of $1e^{-1}$ at the last epoch. In conjunction with the cyclical method, it was found that after only ten epochs the loss stabilises and therefore 10 epochs were chosen, and a batch size of 128. weights were initialized with Xavier initialisation. The three models used are described below:

2.5.2 InceptionTime

InceptionTime consists of an ensemble of deep CNN models, inspired by the Inception-v4 architecture for computer vision (Ismail Fawaz et al., 2020). The composition of an Inception network contains two different residual blocks. For the Inception network, each block is comprised of three Inception modules rather than traditional fully convolutional layers. Each residual block's input is transferred *via* a shortcut linear connection to be added to the next block's input. Following these residual blocks, we employed a Global Average Pooling layer that averages the output multivariate time-series over the whole time dimension. Each inception module contains a bottleneck 1D CNN layer with 32 output channels, a stride of 1 and a kernel size of 1 to reduce parameter dimensionality. The bottleneck layer is followed by three 1D CNN layers with an output channel of 32, a kernel size of 39, 19, 9 consecutively, a padding of 19, 9 and 4, with a stride of 1 in all the cases. The final layer of the InceptionTime network consists of a linear layer to output the internal knee abduction moment impulse.

2.5.3 Transfer Learning InceptionTime

The InceptionTime model previously defined that was pre-trained on datasets from the UCR archive (Dau et al., 2019). Only two layers were tuned from the InceptionTime model - the first input layer to ensure that the required dimensions of the data conformed to our dataset; and the last layer in which the activation function was changed to linear to predict the continuous outcome of knee abduction moment impulse.

2.5.4 TS-Resnet

ResNet allows using very deep structures which minimises the problems of vanishing gradients and accuracy saturation, by adding shortcut connections in each residual block to enable the gradient flow directly through the bottom layers (He et al., 2016). A residual block is a stack of layers set in such a way that the output of a layer is taken and added to another layer deeper in the block. The non-linearity is then applied after adding it together with the output of the corresponding layers in the main path. A time-series residual block is comprised of stacking three 1D CNN layers followed by a batch normalization layer and a ReLU activation layer. The number of filters for the CNN layers in each residual block are 64 then 128 then 256. The final ResNet stacks three residual blocks followed by a global average pooling layer and finally a linear activation layer to predict the knee abduction moment impulse.

2.5.5 GADF-xResnet18

This model required the 1D time-series predictors to be converted into 2D images. To do so, we used the Gramian Angular Difference Fields (GADF) algorithm (Wang and Oates, 2015), which takes as an input the $6737 \times 126 \times 300$ time-series sequences and outputs 6737×126 images of sizes 300×300 i.e: 6,737 images for each of the 126 predictors. GADF is a time-series encoding method that represents each time-series into 2D polar coordinates presented in a matrix-form called the Gramian matrix. Each element of this matrix is the difference (GADF) of their sine values. This mapping maintains the temporal dependency of the time-series. This was undertaken for both the training and testing predictor datasets.

The images encoded using GADF was than fed into the xResNet18 model (He T. et al., 2019) which is an improvement of the conventional ResNet18 that consists of 1) moving the stride 2 from the first convolutional layer to the second convolutional layer in the residual block, 2) removing the 7×7 convolution in the input layer of the network and replacing it with three consecutive 3×3 convolutions, and finally 3) adding a 1×1 convolution of stride 2 at the end of the residual block to reduce the number of parameters.

2.5.6 Predictive Performance

Prediction performance of the knee abduction impulse was calculated on our test dataset using the metrics of the root mean squared error (RMSE, Nm.s/kg), the mean average error (MAE, Nm.s/kg), and the mean absolute percentage error (MAPE, %), and the normalized root mean squared Error (NRMSE, %) (Gholami et al., 2020). The RMSE was computed using

$$RMSE = \sqrt{\frac{\sum_{i=1}^{N} \| y(i) - \hat{y}(i) \|^2}{N}}$$

where y is the observed knee abduction moment, $\hat{y}$ is the predicted moment and N is the number of observations in the test dataset.

The MAE was computed using:

$$MAE = \frac{\sum_{i=1}^{N} y \| (i) - \hat{y}(i) \|}{N}$$

The MAPE was computed using:

$$MAPE = \frac{1}{N} \sum_{i=1}^{N} \left\| \frac{y(i) - \hat{y}(i)}{y(i)} \right\|$$

And finally, the NRMSE which is the RMSE divided by a measure spread. In this work we divide the RMSE by the difference between min and the max of the knee abduction.

$$NRMSE\ (\%) = \frac{RMSE}{MAX - MIN} \times 100$$

The maximum and minimum values are reported below in the result section.

3 RESULTS

For the 33 included participants (female = 15, male = 18), the mean (standard deviation [SD]) age was 39.42 (17.87) years, height was 1.67 m (0.12 m), and body mass was 67.66 kg (12.44 kg). The mean knee abduction moment was −28.06 Nm.s/kg, standard deviation was 11.55 Nm.s/kg, the interquartile range was 15.17 Nm.s/kg, with a variation range (max -min) of 86.94 Nm.s/kg (maximum −88.14 Nm.s/kg, minimum −1.20 Nm.s/kg). The mean (SD) waveforms of our

TABLE 2 | Regression models performance.

	Training set loss (Nm.s/kg)	Validation set loss (Nm.s/kg)	Test set MAE (Nm.s/kg)	Test set RMSE (Nm.s/kg)	Test set MAPE (%)	Test set NRMSE (%)
Baseline model	8.91	16.97	2.78	3.46	10.80	3.98
InceptionTime	6.70	6.05	1.76	2.46	8.61	2.83
Transfer learning	6.54	5.59	1.70	2.36	8.28	2.71
TS-ResNet	5.28	6.10	1.77	2.47	8.65	3.15
GADF-xResnet	19.89	21.33	3.45	4.62	16.17	5.31

126 predictors normalized 100% timepoints of the stance phase, on our dataset can be found in the **Supplementary Material S1**.

Table 2 shows the performance of the five ML models. MAPE and MAE are measures of how far the model's predictions are off from observed values on average. The baseline model achieved 10.80% with the predicted value spreading on average 2.78 Nm.s/kg from the observed values. Transfer learning with inceptionTime was the best performing model, achieving the best MAPE of 8.28%, which translates to the predicted value spreading on average 1.70 Nm.s/kg from the observed values. In contrast, training the inceptionTime model from scratch resulted in a slightly lower performance compared to transfer learning, with a MAPE of 8.61%. The GADF-xResnet 18 model performed worse than the baseline model with a MAPE of 16.17%. This means that converting a time-series to images did not improve ML prediction performances.

4 DISCUSSION

The ability to quantify joint moments in the field may revolutionize the clinical management of musculoskeletal disorders where tissue loading has been implicated as a risk factor for the onset, exacerbation, and symptomatic relapse. In partial support of our hypothesis, transfer learning resulted in the best prediction performance of the outcome of knee abduction impulse during walking. However, in contrast to our hypothesis, the GADF-xResnet model was the worst-performing algorithm.

The only other study to our knowledge that investigated the accuracy of ML in predicting KAM impulse was Stetter et al. (2020), which reported an average observed value of 69.16 Nm.s/kg, and a predicted value of 64.23 Nm.s/kg—a difference of 4.93 Nm.s/kg. Given that performance metrics (RMSE, MAE) were not reported for KAM impulse (Stetter et al., 2020), we used the difference in average values as the performance metric for comparison. The performance in predicting KAM impulse in the previous study (Stetter et al., 2020) was worse than all our models tested in the present study. The worse performance by Stetter et al. (2020) could be due to two reasons. First, the previous study used IMU time-series predictors (Stetter et al., 2020) which may be noisier than our kinematic predictors. Second, Stetter et al. (2020) performed validation whereby the training and testing data independent (i.e., subject data in training set not in testing set). However, our training and testing data were dependent, the reason for which was explained in the methods section. Third, they used a fully connected layered neural network model which may not adequately harness the temporal information within the variables (Stetter et al., 2020). As previously mentioned, Boswell et al. (2021) reported that a fully connected network was superior to LTSM network, but the poorer performance of the latter could be an insufficient number of layers. Future investigations are needed to benchmark different types of network architectures on different biomechanical datasets to determine when different modeling approaches would be superior.

Converting the time-series kinematic predictors to images *via* the GADF resulted in the worst prediction performance. This contrasted with another study that reported an improvement in activity classification accuracy from 94% using time-series predictors, to 97% when converting time-series into images as predictors (Boukhennoufa et al., 2021a). The GADF transformed the time-series predictor (300 time points) into 2D images of dimensions 300 × 300 pixels. It is likely that the greater input dimension of the transformed images would require a model with more layers to learn an increased number of parameters, compared to using the original time-series. Another possible reason is that transforming the time series data into images is more fructuous in classification models as opposed to regression models. The ResNet model used in the present study had 18 layers, whilst a previous study used the VGG16 model which had 16 layers (Boukhennoufa et al., 2021a). However, Boukhennoufa et al. (2021a), had only 6 time-series predictors, compared to 126 time-series predictors in the present study. This means that the combination of a high number of predictors coupled with a greater input dimension size means that the number of layers used in our ResNet model was potentially insufficient to learn the parameters.

Another finding of the present study was that our baseline CNN model performed worse than InceptionTime and TS-ResNet, using the same time-series predictors. Both InceptionTime and TS-ResNet contain shortcut residual connections between convolutional layers, whilst our baseline CNN model does not. The benefit of having residual connections within the network is that makes training a deep neural network much easier by reducing the vanishing gradient effect (He et al., 2016). In addition, the high performance of InceptionTime may be attributed to having multiple parallel convolutional layers, each with different filter lengths, learning different latent hierarchical features of the time-series. The benefit of having multiple parallel layers may be analogous to the benefit of ensemble machine learning techniques like

boosting—combining the results of multiple weak learners. InceptionTime, when compared to the baseline model, combines multiple extracting structures with different window sizes, which allows the former to extract a more diverse set of features from the predictors than the latter, thereby improving the prediction performance using InceptionTime. In a consistent manner, TS-ResNet's deep architecture also allows to learn a plethora of features that are associated with this dataset. In contrast, the baseline model likely did not allow to learn the features as well as with InceptionTime and TS-ResNet due to its shallower architecture.

Interestingly, our finding that transfer learning resulted in the best prediction performance was not supported by another study, albeit conducted in running (Liew et al., 2021). In a previous study, the multivariate time-series kinematic predictors were transformed into static images using cubic spline interpolation (Liew et al., 2021). The purpose of the interpolation was so that the predictor dimension fitted the input dimensions of the VGG16 image model used for transfer learning (Liew et al., 2021). For example, from an original array of 490 [observations] × 101 [gait cycle] × 9 [variables] × 3 [axes], the data was transformed into a 490 × 150 × 150 × 3 shape (Liew et al., 2021). This pre-processing step could have introduced excessive noise into the predictors, thereby affecting the prediction performance of transfer learning.

This study has the following limitations. First, we did not perform hyperparameter tuning, and the selected hyperparameters were selected based on the experience of the authors. Hence, our findings can be said to provide a more conservative estimate of the predictive performance of deep and transfer learning models. Second, we used predictors derived from optoelectronic systems, which can still be time-consuming to use in the clinics. Wearable sensors or markerless motion capture represent the most clinically feasible methods of measuring body motions. Whether the performance of the ML approach using these newer technologies would match that of traditional optoelectronic systems needs to be investigated. Third, our model was developed using data collected from treadmill walking, and the performance may be different in overground walking. Lastly, our models were trained to predict a specific load metric, the internal knee abduction impulse. Whether the present study's findings would similarly translate to other knee load metrics (e.g., peaks), or indeed the entire time-series curve, will need to be investigated.

5 CONCLUSION

We used different state-of-the-art deep learning algorithms to predict knee abduction moment impulse in healthy individuals walking. We found that time-series based deep learning models were superior to an image-based method when predicting knee abduction moment impulse during walking. Also, transfer learning improved the predictive model performance even though the two models are derived from different domain disciplines. Our results support the viability of combining ML with kinematic inputs to quantify biomechanical kinetic measures outside the laboratory. Future studies looking to develop wearable technologies will benefit from knowing the optimal network architecture, and the benefit of transfer learning for predicting joint moments.

DATA AVAILABILITY STATEMENT

The data and code for this study can be found on the lead author's GitHub page (https://github.com/el3oss19/dataset).

ETHICS STATEMENT

Ethical review and approval was not required for the study on human participants in accordance with the local legislation and institutional requirements. Written informed consent for participation was not required for this study in accordance with the national legislation and the institutional requirements.

AUTHOR CONTRIBUTIONS

Conceptualization—IB, BL; Data Curation-IB, Formal Analysis—IB, BL, Funding Acquisition-BL, KM, Methodology-IB, BL, XZ, Project Administration—BL, XZ, Software-IB, Supervision- KM, VU, BL, XZ, Validation-IB, XJ, BL, ZA Visualization-IB, BL, Writing—Original Draft Preparation—All authors, Writing—Review and Editing-All authors

FUNDING

This work is partially supported by the UK Engineering and Physical Sciences Research Council through grants EP/R02572X/1, EP/P017487/1, EP/P015956/1 and EP/V034111/1. ZA is supported by The Academy of Medical Sciences, UK, Springboard Award (SBF006\1019).

SUPPLEMENTARY MATERIAL

The Supplementary Material for this article can be found online at: https://www.frontiersin.org/articles/10.3389/fbioe.2022.877347/full#supplementary-material

Supplementary Figure S1 | Time-normalized stance-phased plots of the kinematic predictors used for deep learning. Abbreviations: PL—pelvis; TH—thigh; SK—shank; FT—foot; R—right limb; L—left limb; Lin—linear; Ang—angular; displ—displacement; vel—velocity; accl—acceleration; x—anterior-posterior axis; y—vertical axis; z—medial-lateral axis. Units: angular displacement (°), angular velocity (°/s), angular acceleration (°/s^2), linear displacement (m), linear velocity (m/s), linear acceleration (m/s^2).

REFERENCES

Aljaaf, A. J., Hussain, A. J., Fergus, P., Przybyla, A., and Barton, G. J. (2016). "Evaluation of Machine Learning Methods to Predict Knee Loading from the Movement of Body Segments," in *International Joint Conference on Neural Networks* (Vancouver, BC, Canada : IJCNN), 5168–5173. doi:10.1109/ijcnn.2016.7727882

Baltzopoulos, V. (2021). Inverse Dynamics, Joint Reaction Forces and Loading in the Musculoskeletal System: Guidelines for Correct Mechanical Terms and Recommendations for Accurate Reporting of Results. *Sports Biomech.* 20, 1–14. doi:10.1080/14763141.2020.1841826

Boswell, M. A., Uhlrich, S. D., Kidziński, Ł., Thomas, K., Kolesar, J. A., Gold, G. E., et al. (2021). A Neural Network to Predict the Knee Adduction Moment in Patients with Osteoarthritis Using Anatomical Landmarks Obtainable from 2D Video Analysis. *Osteoarthr. Cartil.* 29, 346–356. doi:10.1016/j.joca.2020.12.017

Boukhennoufa, I., Zhai, X., Mcdonald-Maier, K., Utti, V., and Jackson, J. (2021a). "Improving the Activity Recognition Using GMAF and Transfer Learning in Post-stroke Rehabilitation Assessment," in *IEEE 19th World Symposium on Applied Machine Intelligence and Informatics* (Herl'any, Slovakia: SAMI), 391–398. doi:10.1109/sami50585.2021.9378670

Boukhennoufa, I., Zhai, X., Utti, V., Mcdonald-Maier, K., and Jackson, J. (2021b). "A Comprehensive Evaluation of State-Of-The-Art Time-Series Deep Learning Models for Activity-Recognition in Post-stroke Rehabilitation Assessment," in Proceeding of the 43rd Annual International Conference of the IEEE Engineering in Medicine and Biology Society, Mexico, 1-5 Nov. 2021 (IEEE). doi:10.1109/embc46164.2021.9630462

Burdack, J., Horst, F., Giesselbach, S., Hassan, I., Daffner, S., and Schöllhorn, W. I. (2020). Systematic Comparison of the Influence of Different Data Preprocessing Methods on the Performance of Gait Classifications Using Machine Learning. *Front. Bioeng. Biotechnol.* 8, 260. doi:10.3389/fbioe.2020.00260

Dau, H. A., Bagnall, A., Kamgar, K., Yeh, C.-C. M., Zhu, Y., Gharghabi, S., et al. (2019). The UCR Time Series Archive. *IEEE/CAA J. Autom. Sin.* 6, 1293–1305. doi:10.1109/jas.2019.1911747

Dwarampudi, M., and Reddy, N. (2019). Effects of Padding on LSTMs and CNNs. *arXiv*.

Favre, J., Hayoz, M., Erhart-Hledik, J. C., and Andriacchi, T. P. (2012). A Neural Network Model to Predict Knee Adduction Moment during Walking Based on Ground Reaction Force and Anthropometric Measurements. *J. Biomechanics* 45, 692–698. doi:10.1016/j.jbiomech.2011.11.057

Fukuchi, C. A., Fukuchi, R. K., and Duarte, M. (2018). A Public Dataset of Overground and Treadmill Walking Kinematics and Kinetics in Healthy Individuals. *PeerJ* 6, e4640. doi:10.7717/peerj.4640

Gholami, M., Napier, C., and Menon, C. (2020). Estimating Lower Extremity Running Gait Kinematics with a Single Accelerometer: A Deep Learning Approach. *Sensors* 20, 2939. doi:10.3390/s20102939

Glorot, X., and Bengio, Y. (2010). "Understanding the Difficulty of Training Deep Feedforward Neural Networks," in *Proceedings of the Thirteenth International Conference on Artificial Intelligence and Statistics*. Editors T. Yee Whye and T. Mike (Chia Laguna Resort, Sardinia, Italy: Proceedings of Machine Learning Research: PMLR).

He, K., Zhang, X., Ren, S., and Sun, J. (2016). "Deep Residual Learning for Image Recognition," in Proceedings Of the IEEE Conference on Computer Vision and Pattern Recognition*)*, 770–778. doi:10.1109/cvpr.2016.90

He, T., Zhang, Z., Zhang, H., Zhang, Z., Xie, J., and Li, M. (2019a). "Bag of Tricks for Image Classification with Convolutional Neural Networks," in Proceedings Of the IEEE/CVF Conference On Computer Vision And Pattern Recognition, Long Beach, CA*)*, 558–567. doi:10.1109/cvpr.2019.00065

He, Z., Liu, T., and Yi, J. (2019b). A Wearable Sensing and Training System: Towards Gait Rehabilitation for Elderly Patients with Knee Osteoarthritis. *IEEE Sensors J.* 19, 5936–5945. doi:10.1109/jsen.2019.2908417

Henriksen, M., Creaby, M. W., Lund, H., Juhl, C., and Christensen, R. (2014). Is There a Causal Link between Knee Loading and Knee Osteoarthritis Progression? A Systematic Review and Meta-Analysis of Cohort Studies and Randomised Trials. *BMJ Open* 4, e005368. doi:10.1136/bmjopen-2014-005368

Holder, J., Trinler, U., Meurer, A., and Stief, F. (2020). A Systematic Review of the Associations between Inverse Dynamics and Musculoskeletal Modeling to Investigate Joint Loading in a Clinical Environment. *Front. Bioeng. Biotechnol.* 8, 603907. doi:10.3389/fbioe.2020.603907

Indolia, S., Goswami, A. K., Mishra, S. P., and Asopa, P. (2018). Conceptual Understanding of Convolutional Neural Network- A Deep Learning Approach. *Procedia Comput. Sci.* 132, 679–688. doi:10.1016/j.procs.2018.05.069

Ismail Fawaz, H., Forestier, G., Weber, J., Idoumghar, L., and Muller, P.-A. (2019). Deep Learning for Time Series Classification: a Review. *Data Min. Knowl. Disc* 33, 917–963. doi:10.1007/s10618-019-00619-1

Ismail Fawaz, H., Lucas, B., Forestier, G., Pelletier, C., Schmidt, D. F., Weber, J., et al. (2020). InceptionTime: Finding AlexNet for Time Series Classification. *Data Min. Knowl. Disc* 34, 1936–1962. doi:10.1007/s10618-020-00710-y

Johnson, W. R., Mian, A., Lloyd, D. G., and Alderson, J. A. (2019). On-field Player Workload Exposure and Knee Injury Risk Monitoring via Deep Learning. *J. Biomechanics* 93, 185–193. doi:10.1016/j.jbiomech.2019.07.002

Kean, C. O., Hinman, R. S., Bowles, K. A., Cicuttini, F., Davies-Tuck, M., and Bennell, K. L. (2012). Comparison of Peak Knee Adduction Moment and Knee Adduction Moment Impulse in Distinguishing between Severities of Knee Osteoarthritis. *Clin. Biomech.* 27, 520–523. doi:10.1016/j.clinbiomech.2011.12.007

Liew, B. X. W., Morris, S., and Netto, K. (2019). Defining Gait Patterns Using Parallel Factor 2 (PARAFAC2): A New Analysis of Previously Published Data. *J. Biomechanics* 90, 133–137. doi:10.1016/j.jbiomech.2019.04.035

Liew, B. X. W., Rügamer, D., Zhai, X., Wang, Y., Morris, S., and Netto, K. (2021). Comparing Shallow, Deep, and Transfer Learning in Predicting Joint Moments in Running. *J. Biomechanics* 129, 110820. doi:10.1016/j.jbiomech.2021.110820

Liu, Y., Shih, S.-M., Tian, S.-L., Zhong, Y.-J., and Li, L. (2009). Lower Extremity Joint Torque Predicted by Using Artificial Neural Network during Vertical Jump. *J. Biomechanics* 42, 906–911. doi:10.1016/j.jbiomech.2009.01.033

Mundt, M., Koeppe, A., David, S., Witter, T., Bamer, F., Potthast, W., et al. (2020a). Estimation of Gait Mechanics Based on Simulated and Measured IMU Data Using an Artificial Neural Network. *Front. Bioeng. Biotechnol.* 8, 41. doi:10.3389/fbioe.2020.00041

Mundt, M., Thomsen, W., Witter, T., Koeppe, A., David, S., Bamer, F., et al. (2020b). Prediction of Lower Limb Joint Angles and Moments during Gait Using Artificial Neural Networks. *Med. Biol. Eng. Comput.* 58, 211–225. doi:10.1007/s11517-019-02061-3

Myer, G. D., Ford, K. R., Di Stasi, S. L., Foss, K. D. B., Micheli, L. J., and Hewett, T. E. (2015). High Knee Abduction Moments Are Common Risk Factors for Patellofemoral Pain (PFP) and Anterior Cruciate Ligament (ACL) Injury in Girls: Is PFP Itself a Predictor for Subsequent ACL Injury? *Br. J. Sports Med.* 49, 118–122. doi:10.1136/bjsports-2013-092536

Pantawong, J., Jitpattanakul, A., and Mekruksavanich, S. (2021). "Enhancement of Human Complex Activity Recognition Using Wearable Sensors Data with InceptionTime Network," in Proceeding of the2nd International Conference on Big Data Analytics and Practices (IBDAP)), Bangkok, Thailand, 26-27 Aug. 2021 (IEEE), 12–16. doi:10.1109/IBDAP52511.2021.9552133

Pogson, M., Verheul, J., Robinson, M. A., Vanrenterghem, J., and Lisboa, P. (2020). A Neural Network Method to Predict Task- and Step-specific Ground Reaction Force Magnitudes from Trunk Accelerations during Running Activities. *Med. Eng. Phys.* 78, 82–89. doi:10.1016/j.medengphy.2020.02.002

Ren, L., Jones, R. K., and Howard, D. (2008). Whole Body Inverse Dynamics over a Complete Gait Cycle Based Only on Measured Kinematics. *J. BIomechanics* 41, 2750–2759. doi:10.1016/j.jbiomech.2008.06.001

Richards, R. E., Andersen, M. S., Harlaar, J., and Van Den Noort, J. C. (2018a). Relationship between Knee Joint Contact Forces and External Knee Joint Moments in Patients with Medial Knee Osteoarthritis: Effects of Gait Modifications. *Osteoarthr. Cartil.* 26, 1203–1214. doi:10.1016/j.joca.2018.04.011

Richards, R. E., Van Den Noort, J. C., Van Der Esch, M., Booij, M. J., and Harlaar, J. (2018b). Effect of Real-Time Biofeedback on Peak Knee Adduction Moment in Patients with Medial Knee Osteoarthritis: Is Direct Feedback Effective? *Clin. Biomech.* 57, 150–158. doi:10.1016/j.clinbiomech.2017.07.004

Robinson, M. A., Sharir, R., Rafeeuddin, R., Vanrenterghem, J., and Donnelly, C. J. (2021). The Non-sagittal Knee Moment Vector Identifies 'at Risk' Individuals that the Knee Abduction Moment Alone Does Not. *Sports Biomech.* 20, 1–11. doi:10.1080/14763141.2021.1903981

Schache, A. G., and Baker, R. (2007). On the Expression of Joint Moments during Gait. *Gait Posture* 25, 440–452. doi:10.1016/j.gaitpost.2006.05.018

Simonyan, K., and Zisserman, A. (2014). Very Deep Convolutional Networks for Large-Scale Image Recognition. *arXiv*.

Slade, P., Habib, A., Hicks, J. L., and Delp, S. L. (2022). An Open-Source and Wearable System for Measuring 3D Human Motion in Real-Time. *IEEE Trans. Biomed. Eng.* 69, 678–688. doi:10.1109/tbme.2021.3103201

Smith, L. N. (2017). Cyclical Learning Rates for Training Neural Networks in IEEE winter conference on applications of computer vision (WACV) (IEEE).

Stetter, B. J., Krafft, F. C., Ringhof, S., Stein, T., and Sell, S. (2020). A Machine Learning and Wearable Sensor Based Approach to Estimate External Knee Flexion and Adduction Moments during Various Locomotion Tasks. *Front. Bioeng. Biotechnol.* 8, 9. doi:10.3389/fbioe.2020.00009

Veit, A., Wilber, M. J., and Belongie, S. (2016). Residual Networks Behave like Ensembles of Relatively Shallow Networks. *Adv. neural Inf. Process. Syst.* 29. doi:10.48550/arXiv.1605.06431

Wang, C., Chan, P. P. K., Lam, B. M. F., Wang, S., Zhang, J. H., Chan, Z. Y. S., et al. (2020). Real-Time Estimation of Knee Adduction Moment for Gait Retraining in Patients with Knee Osteoarthritis. *IEEE Trans. Neural Syst. Rehabil. Eng.* 28, 888–894. doi:10.1109/tnsre.2020.2978537

Wang, Z., and Oates, T. (2015). "Imaging Time-Series to Improve Classification and Imputation," in *Proceedings of the 24th International Conference on Artificial Intelligence* (Buenos Aires, Argentina: AAAI Press).

Wang, Z., Yan, W., and Oates, T. (2017). "Time Series Classification from Scratch with Deep Neural Networks: A Strong Baseline," in *International Joint Conference on Neural Networks (IJCNN),* Anchorage, AK. doi:10.1109/ijcnn.2017.7966039

Webster, K. E., Mcclelland, J. A., Palazzolo, S. E., Santamaria, L. J., and Feller, J. A. (2012). Gender Differences in the Knee Adduction Moment after Anterior Cruciate Ligament Reconstruction Surgery. *Br. J. Sports Med.* 46, 355–359. doi:10.1136/bjsm.2010.080770

Weiss, K., Khoshgoftaar, T. M., and Wang, D. (2016). A Survey of Transfer Learning. *J. Big Data* 3, 9. doi:10.1186/s40537-016-0043-6

Wouda, F. J., Giuberti, M., Bellusci, G., Maartens, E., Reenalda, J., Van Beijnum, B. F., et al. (2018). Estimation of Vertical Ground Reaction Forces and Sagittal Knee Kinematics during Running Using Three Inertial Sensors. *Front. Physiol.* 9, 218. doi:10.3389/fphys.2018.00218

Conflict of Interest: The authors declare that the research was conducted in the absence of any commercial or financial relationships that could be construed as a potential conflict of interest.

Publisher's Note: All claims expressed in this article are solely those of the authors and do not necessarily represent those of their affiliated organizations, or those of the publisher, the editors and the reviewers. Any product that may be evaluated in this article, or claim that may be made by its manufacturer, is not guaranteed or endorsed by the publisher.

frontiers | Frontiers in Bioengineering and Biotechnology

BRIEF RESEARCH REPORT
published: 25 May 2022
doi: 10.3389/fbioe.2022.890004

Effects of Elbow Crutch Locomotion on Gluteus Medius Activation During Stair Ascending

*Carlos De la Fuente[1,2,3], Alejandro Neira[4], Gustavo Torres[1], Rony Silvestre[3], Matias Roby[3,5], Roberto Yañez[3,5], Sofia Herrera[1], Virgina Martabit[1], Isabel McKay[1] and Felipe P. Carpes[2]**

[1]Departamento de Cs. de la Salud, Facultad de Medicina, Pontificia Universidad Católica de Chile, Santiago, Chile, [2]Laboratory of Neuromechanics, Universidade Federal do Pampa, Uruguaiana, Brazil, [3]Servicio de Biomecánica, Centro de Innovación, Clínica MEDS, Santiago, Chile, [4]Escuela Kinesiología, Facultad de Ciencias, Universidad Mayor, Santiago, Chile, [5]Traumatología, Clínica MEDS, Santiago, Chile

Crutches can help with the locomotion of people with walking disorders or functional limitations. However, little is known about hip muscle activation during stair ascending using different crutch locomotion patterns in people without disorders and limitations. Thus, we determined the acute effects of elbow crutch locomotion on gluteus medius (GM) activity during stair ascending. This comparative analytic cross-sectional study enrolled ten healthy men (22.0 ± 0.47 years). Participants climbed up the stairs with elbow crutches using one or two crutches, with ipsilateral or contralateral use, and after loading or unloading a limb. EMG signals were recorded from anterior, middle, and posterior portions of the GM and compared between the crutch conditions. The Kruskal–Wallis test and Dunn's multiple comparison test were performed (α = 5%). The activation of the GM increased with the ipsilateral use of crutches, with two crutches and three points, and when all the load depended only on one limb. GM activation decreased with contralateral use and in the unload limb. In conclusion, ascending stairs with elbow crutches alters the GM activation. The more critical factors were choosing the crutches' lateral use, the number of crutches, and if the limb is loaded or unloaded while ascending the stairs. Our findings can be helpful to increase or decrease the GM activation for those who use or will use crutches.

Keywords: Gluteus Medius, EMG, assistive device, stairs, locomotion

OPEN ACCESS

Edited by:
Rafael Reimann Baptista, Pontifical Catholic University of Rio Grande do Sul, Brazil

Reviewed by:
Leonardo Alexandre Peyré-Tartaruga, Federal University of Rio Grande do Sul, Brazil
Eduardo Mendonca Scheeren, Pontifícia Universidade Católica do Paraná, Brazil

***Correspondence:**
Felipe P. Carpes
carpes@unipampa.edu.br

Specialty section:
This article was submitted to Biomechanics, a section of the journal Frontiers in Bioengineering and Biotechnology

Received: *04 March 2022*
Accepted: *21 April 2022*
Published: *25 May 2022*

Citation:
De la Fuente C, Neira A, Torres G, Silvestre R, Roby M, Yañez R, Herrera S, Martabit V, McKay I and Carpes FP (2022) Effects of Elbow Crutch Locomotion on Gluteus Medius Activation During Stair Ascending. Front. Bioeng. Biotechnol. 10:890004. doi: 10.3389/fbioe.2022.890004

INTRODUCTION

The elbow or Canadian crutch is a nonaxillary assisted device often used in rehabilitation (Rasouli and Reed, 2020). Its design combines forearm and axillary support, providing stability through the upper extremity with the elbow flexed (Rasouli and Reed, 2020). Locomotion with crutches tries to assist users with daily life tasks and movement of patients during rehabilitation, disability, aging, and recovery from acute injuries (Sanders et al., 2018). For instance, the use of crutches by the elderly can help with their locomotion and increase their independence (Harper et al., 2018). Nevertheless, there are substantial effects on energy expenditure and mechanical work assumptions when elbow crutches are used during locomotion (Thys et al., 1996; Halsey et al., 2012).

Although crutches can assist with the locomotion of people with walking disorders or limitations, the use of crutches may affect activation muscle patterns, i.e., muscles acting for frontal plane stabilization. In this regard, a recent study found a negative relation between gluteus medius (GM)

activation and dynamical stability (margins-of-stability) using poles during walking (Peyré-Tartaruga et al., 2022). The change in the activation of muscles acting in the frontal plane has critical functional implications for the hip and pelvis stability (Semciw et al., 2016; Buckthorpe et al., 2019). The GM stabilizes the pelvis and controls the hip adduction and internal rotation (Ebert et al., 2017). Unfortunately, crutch locomotion may alter the GM activity during weight-bearing and unipedal postures (Jebsen, 1967; Hsue and Su, 2010; Ebert et al., 2017), leading to altered lower limb joint control. The most used locomotion pattern is one crutch on the contralateral side to increase the support base, providing better balance and reducing mediolateral displacement of the center of mass (Jebsen, 1967; Hsue and Su, 2010). However, there are many locomotion patterns with crutches combining the delay between the crutches and foot placement (when the foot lands after the crutch), the number of concurrent points of contact (total number of points in contact with the ground), laterality (one crutch moving at a time), or the load/unload of the limb (Rasouli and Reed, 2020).

For example, walking stairs requires additional strength, a range of motion, balance, and coordination compared with gait at the ground level (Hsue and Su, 2010). However, little is known about how the neuromuscular system responds to the increased demand. Stair ascent involves a hip extension combined with adduction followed by abduction and forward contralateral rotation of the pelvis while the center of mass ascents against gravity (Hsue and Su, 2010; Hall et al., 2017). Elbow crutches increase the mediolateral displacement of the center of mass when walking up the stairs (Hsue and Su, 2010) since it might influence GM activity. Previous studies have addressed the effects of crutch use on energy expenditure, ground reaction forces during locomotion at the ground level, and the activity of ankle and knee muscles (Carpentier et al., 2001; Halsey et al., 2012; Moran et al., 2015; Watanabe et al., 2018; Rasouli and Reed, 2020). However, little is known about the GM activity during stair ascent. When not using crutches, the GM is activated later at the instant of the foot landing on the stairs (Brindle et al., 2003). Its function is pelvis and hip stabilization to reduce the center of mass oscillation (Hsue and Su, 2010; Benedetti et al., 2012).

The knowledge about GM activation while walking up the stairs using different crutch locomotion patterns is important to help manage activation exercises and acquire occupational skills for those experiencing long- and short-term use of crutches (Ebert et al., 2017) since understanding how GM can acutely adapt its neuromuscular activity is a fundamental first step. Therefore, here, we aimed to determine the effect of elbow crutch locomotion on GM muscle activity during stair ascending. We hypothesized that GM activation depends on choosing the crutches' lateral use, the number of crutches, and if the limb is loaded or unloaded while ascending the stairs.

MATERIALS AND METHODS

Study Design

To study the effects of elbow crutch locomotion on GM muscle activity during stair ascending, we have focused our study on nonimpaired people who can provide us with typical neuromuscular adaptations of the nervous and the motor system. Participants were recruited from the local community. Each participant provided written consent to be included in this study, which was approved by ethics committee no. 200721006 from the Pontificia Universidad Católica de Chile and conducted following the Declaration of Helsinki.

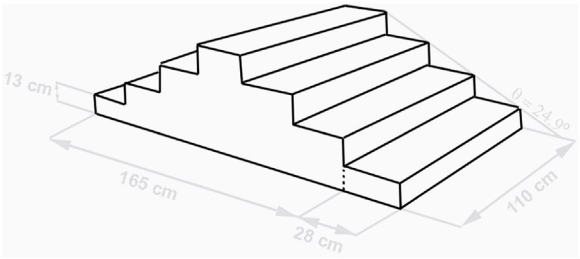

FIGURE 1 | Staircase dimensions. The experimental environment conditions of the study.

Participants

The volunteers should be men aged between 18 and 25 years old, achieving at least 72 points in the lower extremity functional scale (Repo et al., 2017) and having a fully functional joint range of motion in the sagittal plane. Data were collected from 10 healthy men with an age of 22.0 ± 0.47 years, body mass of 68.8 ± 10.9 kg, height of 1.70 ± 0.06 m, BMI of 23.8 ± 3.3 kg/m^2, and lower extremity functional scale score of 79.0 ± 1.5 points, and participants without any orthopedic commitment or postural alteration including cavus and flat foot and without experience with the use of elbow crutches in the past participated in this cross-sectional study. As a similar experimental setup and population were not found in the literature, we measured the post hoc power. We measured the post hoc power in multiples of 5, and we stopped the recruitment when the post hoc power was equal to or more than 0.80.

Participants were oriented to come to the laboratory using comfortable clothes (to avoid limitation in the range of motion), to avoid wearing shoes with a height higher than 4 cm (Hapsari and Xiong, 2016), to not fast for more than 4 h, to refrain from vigorous physical exercise, to not take alcohol in the 72 h preceding the tests, and to sleep for at least 6 h in the night before the tests. Participants were excluded if they reported pain or discomfort of any type during the trials. For data collection, they performed different patterns of elbow crutch locomotion while ascending stairs at a self-selected speed. The neuromuscular activation from the GM was recorded while performing stair ascent with different patterns of locomotion with crutches.

Staircase Design and Crutch

The motor task consisted of ascending a wood custom-made staircase with four symmetrical steps built according to the standards described in National Law of Housing and Urbanism no. 1305 (Chilean Mistry, 1992), imitating the local conditions of the stairs. The step had a rise of 13 cm, run of 28 cm,

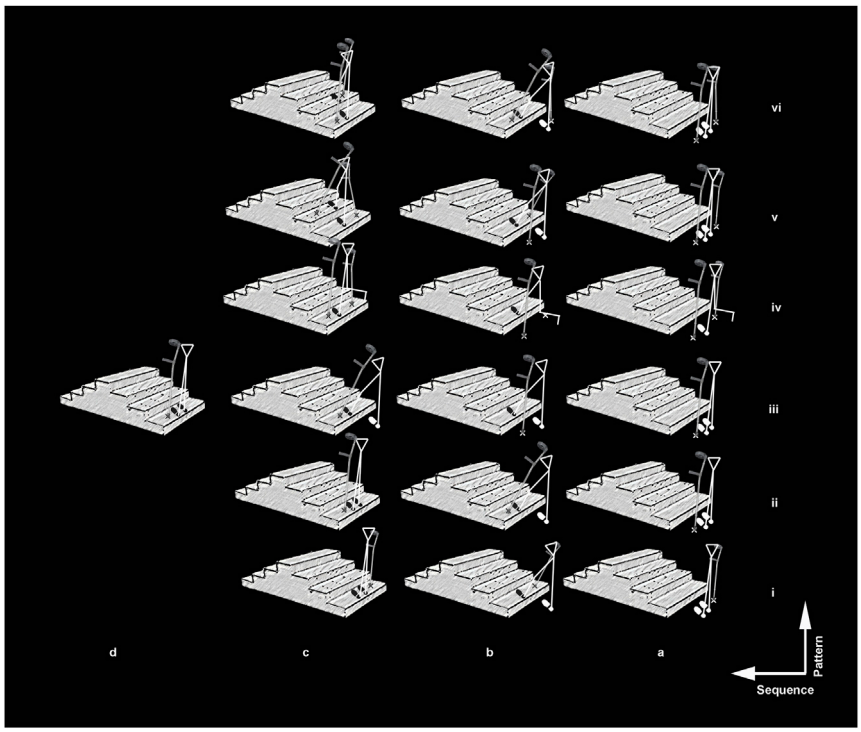

FIGURE 2 | Crutch locomotion patterns. The image shows a half of the kinematic patterns using crutches in the study (n = 6) from i to vi. The total number of crutch locomotion patterns was 12, which resulted from changing the limb side to start the movement. In addition, the figure shows the movement sequence from letter a to d. Finally, the weight-bearing of the limb and crutch over the ground is indicated with a print stick figure and Canadian crutches. The stair ascending control (without crutches, n = 2) were omitted.

and a width of 110 cm, resulting in a stair angle (slope) of 24.9° (**Figure 1**). The participants used an aluminum elbow crutch with a rubber tip and a plastic forearm cuff and handle (**Figure 1**). The height was defined as the vertical distance from the ground to the greater trochanter anatomical reference, with 20° of elbow flexion (Hsue and Su, 2010).

Crutch Locomotion

Two weeks before data collection, all participants were familiarized with the measurements and the locomotion using crutches as well as control conditions. The familiarization sessions were performed three times a week, lasted 1 h, and were always conducted by the same researcher. The familiarization was performed to ensure correct learning of the locomotion pattern of stair ascent with and without (control condition) the elbow crutches. During each familiarization session, locomotion was videotaped to show the patterns used and to reinforce the learning. Before data collection, all participants achieved the criteria of fluid locomotion, no falls, and complete foot contact on the steps (Inoue et al., 2012).

For data collection, the participant was bipedally positioned, standing in the front and 28 cm away from the first step of the stairs. Following a verbal "go" command, the participant ascended the stairs at a self-selected speed (Hsue and Su, 2010). In this study, twelve experimental conditions and two control conditions that resulted in fourteen conditions in total were studied (see **Figure 2** and **Table 1**), with 10 min of rest in between. The ascending was performed in a random order to reduce fatigue effects (Hsue and Su, 2010). All conditions were tested on the same day to avoid the effects of EMG sensor shift. Three valid trials, which mean no loss of control and balance during ascending, were considered for data analysis. In addition, a control ascending was added, obtaining two control conditions, one for each limb.

Measurements

Data with respect to age, height, BMI, and lower extremity functional scale (Repo et al., 2017) were collected during the familiarization sessions. The neuromuscular activity was recorded by surface electromyography (EMG) from the anterior, middle, and posterior portions of the GM. With the participant standing, the surface electrodes for the anterior region were placed at 50% of the distance between the anterosuperior iliac spine and the greater trochanter for the anterior fiber of the GM, the electrodes for the middle fibers were placed at 50% of the distance between the greater trochanter and the iliac crest, and the electrodes for the posterior fibers were placed at 33% of the distance between the posterior ilium and the greater trochanter (Otten et al., 2015). Electrodes were placed after the skin was

TABLE 1 | Details of the different conditions for crutch locomotion during stair ascending.

Crutch condition	Support Base	Crutch side	Movement and conditions
One-crutch	Three-points	Right	Left foot stepped up first with a contralateral crutch (condition 1) followed by the right foot (condition 8)
One-crutch	Three-points	Left	Left foot stepped up first with an ipsilateral crutch (condition 9) followed by the right foot (condition 2)
One-crutch	Three-points	Left	Left foot stepped up first without a crutch followed by a delayed ipsilateral crutch (condition 3), after which the right foot is stepped up (condition 10)
Two-crutches	Three-points	Both sides	Left foot stepped up first without crutches followed by two-crutches (condition 4), while the right leg is unloaded (condition 11)
Two-crutches	Four-points	Both sides	Left foot stepped up first with a contralateral crutch (condition 5) followed by the right foot with a contralateral crutch (condition 12)
Two-crutches	Four-points	Both sides	Left foot stepped up first with an ipsilateral crutch (condition 6) followed by the right foot with a contralateral crutch (condition 13)
Control	Two-points	Without	The locomotion control strategy was added, establishing two conditions for limbs and normal stair walking: left foot stepped up first (condition 7) followed by the right foot (condition 14)

shaved and cleaned according to the "Surface Electromyography for the Non-Invasive Assessment of Muscles" guidelines (Hermens et al., 2000). After the placement of each electrode, the participant was requested to perform a maximal isometric test to check the selective action of the GM according to the sensor placement (Semciw et al., 2014; Otten et al., 2015). The quality of the signal was checked visually before any recording.

EMG Acquisition and Treatment

The raw EMG signals were collected using a Trigno Wireless 16-Channel EMG system (Delsys Inc., Boston, United States) and with CMRR >80 dB, a gain of 1,000, an interelectrode distance of 10 mm, and a sampling rate of 2000 Hz through the software Nexus 1.8.5 (Vicon Motion Systems Ltd., United Kingdom). For offline processing, the EMG signals were mean-centered and filtered with a band-pass of 20–450 Hz with a second-order Butterworth filter (Semciw et al., 2014). The magnitude of muscle activation was estimated by applying a root mean square envelope with a window length of 250 ms and sliding 1 sample using a custom-made script written in Matlab 2016a software (Mathwork Inc., United States). The ICA algorithm was used to separate the independent basal noise of the whole EMG signals (Zheng and Hu, 2019). The EMG signals were normalized to each lower limb to the respective peak root mean square (rms) value obtained during the control condition for stair ascent (Dwyer et al., 2013).

Statistical Analysis

Data normality was checked using the Shapiro–Wilk test. EMG data showed a nonparametric distribution. Therefore, these are reported as median ± interquartile range. The muscle activation between the different gluteus medius regions was compared using the one-way Kruskal–Wallis test and Dunn's multiple comparison test with an alpha of 5% after Bonferroni's correction due to normality assumptions. The *p*-values were summarized using a connection graph to better understand the multiple statistical differences between conditions (Bastian et al., 2009). All statistical analyses were performed using the Matlab software 2016a (Mathworks, Inc., United States). The posteriori statistical power was estimated using G*Power software version 3.1.9.2 (Universitat Dusseldorf, Dusseldorf, Germany).

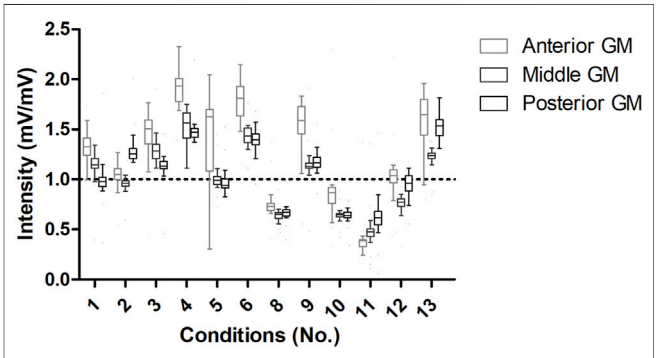

FIGURE 3 | EMG intensity of crutch patterns locomotion. The horizontal line indicates the median reference of the control condition. When EMG intensities are above and below the horizontal line, there was more and less activation for the portions of the GM than under the control condition, respectively. GM, gluteus medius.

RESULTS

EMG data were normalized to the control condition from each limb. The anterior GM activation was higher under conditions 1, 2, 3, 4, 5, 6, 9, and 13 than under control conditions. The middle portion of the GM showed higher activation under conditions 1, 3, 4, 6, 9, and 13 than under control conditions. The posterior portion of the GM showed higher activation under conditions 2, 3, 4, 6, 9, and 13 than under control conditions. In contrast, the other conditions for all regions showed lower median values than the control conditions.

Activation of anterior ($p < 0.001$), middle ($p < 0.001$), and posterior ($p < 0.001$) portions of the GM increased with the ipsilateral use of crutches and in the loaded extremity using two crutches with three support points (see **Figures 3**, **4**). In contrast, activation of anterior ($p < 0.001$), middle ($p < 0.001$), and posterior ($p < 0.001$) portions of the GM decreased in the unloaded extremity and also when one-contralateral crutch supports the ascent of the stairs or provides support in a contralateral manner while the other limb ascends (see **Figures 3**, **4**). The posteriori statistical power was 0.99.

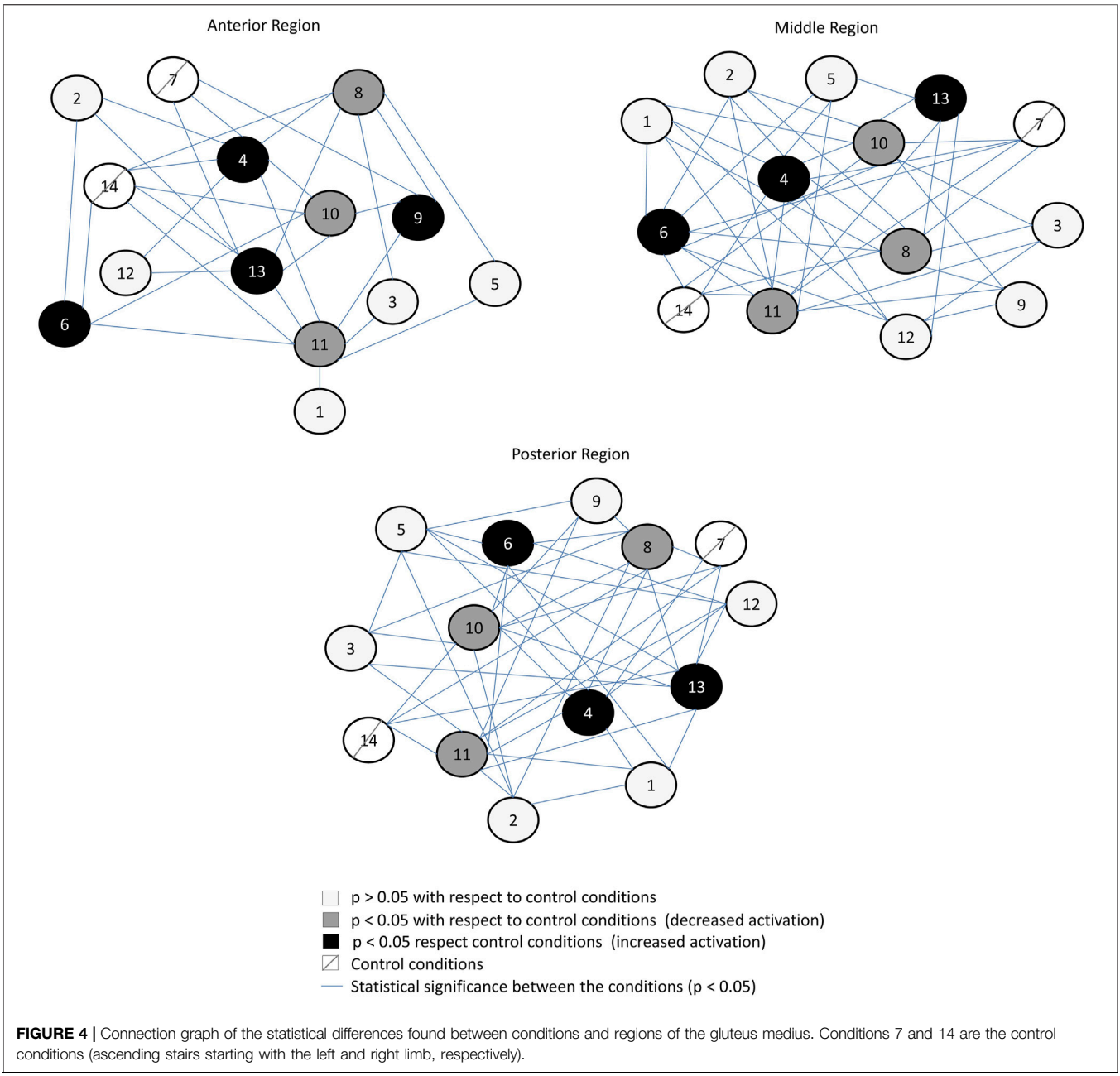

FIGURE 4 | Connection graph of the statistical differences found between conditions and regions of the gluteus medius. Conditions 7 and 14 are the control conditions (ascending stairs starting with the left and right limb, respectively).

DISCUSSION

In this study, we demonstrate that different locomotion crutch patterns affect the GM muscle activity during stair ascending because changes in rms with respect to the control conditions were observed. The rms of the EMG signal is a measure of muscle excitation caused by the sarcolemma depolarization of activated motor units, which is the main component of the EMG signal and the result of the sum of different muscle fiber excitations (Vigotsky et al., 2017). Thus, our findings can be grouped by the lateral use of crutches (higher activation for ipsilateral use), the number of crutches (higher activation with two crutches and three points), and the load/unload of the extremity (higher activation in the loaded limb). The contralateral use and unloaded limb reduced GM activation. As far as we know, this is the first study to determine the effects of the different patterns of locomotion using elbow crutches during stair ascent on GM activation. Our findings have important implications for guiding the management of the crutch locomotion for the community.

Higher GM activation was found for stair ascent using two crutches with three points in the loaded limb (**Figure 2**, see 4th condition). This pattern is frequently recommended in clinics for "going up with the uninvolved limb first" (Jebsen, 1967). The increase in GM activation is in coherence with the increase in mechanical work required for body displacement with a unilateral stance when the center of mass is located further

back, such as that observed for squat exercises that also increase GM activity (Bolgla et al., 2016; Ebert et al., 2017).

The stair ascent using two ipsilateral crutches with four points also increased GM activity. This pattern implies two symmetrical conditions (6th and 13th conditions) where the ipsilateral crutch acts as a pivot, is closer to the center of mass, and permits the contralateral limb to oscillate while it ascents to the next step (Jebsen, 1967; Hsue and Su, 2010). Studies simulating gait found that hip abductor weakness results in compensatory movements of the pelvis (Borrelli and Haslach, 2014). We hypothesize that higher GM activation likely occurred to provide pelvis stability in the frontal plane while rotating forward during the ascent movement (Jebsen, 1967; Heim et al., 2000; Lee et al., 2014) and more significant mediolateral displacement of the center of mass (Hsue and Su, 2010), similar to the strategies used during unilateral stance tasks (Bolgla et al., 2016; Ebert et al., 2017; Moore et al., 2019).

Mechanical constraints due to the use of crutches also account for higher GM activation. Under the ipsilateral crutch condition, the perpendicular distance between the crutches and the GM is lower since it requires a larger hip abductor movement to ascent the stairs (Borrelli and Haslach, 2014). Pelvis hiking has been associated with larger mediolateral displacement of the center of mass and indicates abductor weakness (Svehlík et al., 2012). We consider that identifying the crutch locomotion patterns leading to increased GM activity can help manage muscle activation, for example, in geriatric populations or patients with neuromuscular impairment (Hsue and Su, 2010).

Stair ascent using two crutches with three points resulted in lower GM activity in the unloaded limb. We hypothesize that the GM stabilizing role is combined with the activation of abductors' muscles to generate the coactivation necessary to avoid excessive movement of the contralateral pelvis associated with larger displacement of the center of mass and instability (Lewis et al., 2017). The other two patterns eliciting lower GM activation occurred in the delayed limb (**Figure 2**, see 8th and 10th conditions). Both patterns created a triangular base of support using three points with one crutch. The first condition had a higher angle located in the upper step, and the second condition had a higher angle located in the back step during the ascent. Both strategies suggest that the passive moment produced by the crutch reduces GM activity in the delayed limb. Lower muscle activity under this condition agrees with decreased active mechanical work during gait with assistive devices (Ajemian et al., 2004; Borrelli and Haslach, 2014) and the increased base of support provided by the crutch aids (van der Veen et al., 2020). These strategies are taught mainly in physiotherapy schools as options to manage acute lower limb injuries and avoid overload in tissues with low resistance in healing processes resulting from fractures (Sanders et al., 2018).

The higher activity of the anterior region of the GM in most patterns suggests that its recruitment helps control the contralateral forward pelvis rotation during stair ascending (Semciw et al., 2014). The higher activation of this region may result in the challenge to control the forward contralateral pelvis movement during the ascent, whereas the activation of the medial fibers is more related to frontal stabilization (Semciw et al., 2013; Semciw et al., 2014), and posterior fibers stabilize the head of the femur especially because its fiber orientation permits active control of anterior instabilities (Semciw et al., 2013; Safran, 2019). In general, the crutch locomotion patterns elicit more instability, increasing the GM activity, which we interpret as a highlight of the role of this muscle in helping to achieve a more stable movement pattern. Therefore, appropriate conduct would be needed when impaired activation and instability behaviors exist, for example, in patients operated with hip arthroscopies (Safran, 2019) or acute muscle inhibitions due to joint edema (Rice et al., 2014).

Currently, there is a lack of scientific knowledge for the prescription of assistive devices. Our results may help better manage early muscle deficits due to rest under acute injuries (Maguire et al., 2016) or long-time adaptation in the elderly population using assistive devices (Allen, 2001; Allen et al., 2001; Hamel and Cavanagh, 2004). We acknowledge that EMG crosstalk can limit our experiment (Semciw et al., 2014). Another limitation is the movement of the fibers under the skin during hip movements. We used interelectrode distances and the location of sensors standardized according to the literature to minimize these effects. We also conducted a normalization and low level of step rise to control the excessive displacement of the fiber under the skin.

CONCLUSION

The more important factors affecting the activation of the motor unit pool of the GM during elbow crutch locomotion for ascending stairs were the lateral use of crutches, the number of crutches, and the load/unload of extremity. Ascending stairs using two crutches with three points in the unloaded limb elicited lower activation than that observed for the loaded extremity. This novel knowledge may have utility in increasing the activity of frontal pelvis–hip stabilizers when crutches are used.

DATA AVAILABILITY STATEMENT

The datasets presented in this study can be found in online repositories. The names of the repository/repositories and accession number(s) can be found below: https://www.researchgate.net/publication/357092654_Effects_of_different_elbow_crutches_locomotion_patterns_on_anterior_middle_and_posterior_Gluteus_Medius_activation_during_stair_ascending_data.

ETHICS STATEMENT

The studies involving human participants were reviewed and approved by the Pontificia Universidad Catolica de Chile

committee. The patients/participants provided their written informed consent to participate in this study.

AUTHOR CONTRIBUTIONS

CF, AN, and FC contributed toward conceptualization, methodology, software, validation, formal analysis, investigation, resources, data curation, writing the original draft, review and editing, visualization, supervision, and project administration. SH, VM, GT, RS, MR, RY, and IM contributed toward methodology, software, investigation, writing the original draft, and visualization.

FUNDING

The "I Concurso Investigación Interdisciplina de Ciencias de la Salud de la Pontificia Univerisidad Catolica de Chile" partially funded the development of this study.

ACKNOWLEDGMENTS

CF acknowledges the support of the Pontificia Universidad Catolica de Chile.

REFERENCES

Ajemian, S., Thon, D., Clare, P., Kaul, L., Zernicke, R. F., and Loitz-Ramage, B. (2004). Cane-assisted Gait Biomechanics and Electromyography after Total Hip Arthroplasty. *Archives Phys. Med. Rehabilitation* 85 (12), 1966–1971. doi:10.1016/j.apmr.2004.04.037

Allen, S. M. (2001). Canes, Crutches and Home Care Services: the Interplay of Human and Technological Assistance. *Policy Brief. Cent. Home Care Policy Res.* (4), 1–6.

Allen, S. M., Foster, A., and Berg, K. (2001). Receiving Help at Home: the Interplay of Human and Technological Assistance. *Journals Gerontology Ser. B Psychol. Sci. Soc. Sci.* 56 (6), S374–S382. doi:10.1093/geronb/56.6.s374

Bastian, M., Heymann, S., and Jacomy, M. (2009). "Gephi : An Open Source Software for Exploring and Manipulating Networks," in International AAAI Conference on Weblogs and Social Media.2

Benedetti, M. G., Agostini, V., Knaflitz, M., and Bonato, P. (2012). "Muscle Activation Patterns during Level Walking and Stair Ambulation," in *Applications of EMG in Clinical and Sports Medicine*. [Internet]. 2012 Jan 11 [cited 2020 Aug 2]; Available at: https://www.intechopen.com/books/applications-of-emg-in-clinical-and-sports-medicine/muscle-activation-patterns-during-level-walking-and-stair-ambulation.

Bolgla, L. A., Cruz, M. F., Roberts, L. H., Buice, A. M., and Pou, T. S. (2016). Relative Electromyographic Activity in Trunk, Hip, and Knee Muscles during Unilateral Weight Bearing Exercises: Implications for Rehabilitation. *Physiother. Theory Pract.* 32 (2), 130–138. doi:10.3109/09593985.2015.1092059

Borrelli, J., and Haslach, H. W. (2014). "Rationale for a Modified Crutch Use Methodology for Individuals with Weak or Paralyzed Hip Abductor Muscles," in *American Society of Mechanical Engineers Digital Collection*. [cited 2020 Aug 2]. Available at: https://fluidsengineering.asmedigitalcollection.asme.org/IDETC-CIE/proceedings/IDETC-CIE2013/55966/V07AT10A003/253302.

Brindle, T. J., Mattacola, C., and McCrory, J. (2003). Electromyographic Changes in the Gluteus Medius during Stair Ascent and Descent in Subjects with Anterior Knee Pain. *Knee Surg. Sports Traumatol. Arthrosc.* 11 (4), 244–251. doi:10.1007/s00167-003-0353-z

Buckthorpe, M., Stride, M., and Villa, F. D. (2019). Assessing and Treating Gluteus Maximus Weakness - A Clinical Commentary. *Intl J. Sports Phys. Ther.* 14 (4), 655–669. doi:10.26603/ijspt20190655

Carpentier, A., Duchateau, J., and Hainaut, K. (2001). Motor Unit Behaviour and Contractile Changes during Fatigue in the Human First Dorsal Interosseus. *J. Physiol.* 534 (Pt 3), 903–912. doi:10.1111/j.1469-7793.2001.00903.x

Chilean Mistry (1992). "Chilean Mistry of Housing and Urbanism," in *Housing and Urbanism Law*. [Internet]. Chilean Mistry of housing and urbanism. 1992 [cited 2020 Aug 2]. Available at: https://www.leychile.cl/Navegar?idNorma=8201.

Dwyer, M. K., Stafford, K., Mattacola, C. G., Uhl, T. L., and Giordani, M. (2013). Comparison of Gluteus Medius Muscle Activity during Functional Tasks in Individuals with and without Osteoarthritis of the Hip Joint. *Clin. Biomech.* 28 (7), 757–761. doi:10.1016/j.clinbiomech.2013.07.007

Ebert, J. R., Edwards, P. K., Fick, D. P., and Janes, G. C. (2017). A Systematic Review of Rehabilitation Exercises to Progressively Load the Gluteus Medius. *J. Sport Rehabil.* 26 (5), 418–436. doi:10.1123/jsr.2016-0088

Hall, M., Wrigley, T. V., Kean, C. O., Metcalf, B. R., and Bennell, K. L. (2017). Hip Biomechanics during Stair Ascent and Descent in People with and without Hip Osteoarthritis. *J. Orthop. Res.* 35 (7), 1505–1514. doi:10.1002/jor.23407

Halsey, L. G., Watkins, D. A. R., and Duggan, B. M. (2012). The Energy Expenditure of Stair Climbing One Step and Two Steps at a Time: Estimations from Measures of Heart Rate. *PLoS ONE* 7 (12), e51213. doi:10.1371/journal.pone.0051213

Hamel, K. A., and Cavanagh, P. R. (2004). Stair Performance in People Aged 75 and Older. *J. Am. Geriatr. Soc.* 52 (4), 563–567. doi:10.1111/j.1532-5415.2004.52162.x

Hapsari, V. D., and Xiong, S. (2016). Effects of High Heeled Shoes Wearing Experience and Heel Height on Human Standing Balance and Functional Mobility. *Ergonomics* 59 (2), 249–264. doi:10.1080/00140139.2015.1068956

Harper, N. G., Wilken, J. M., and Neptune, R. R. (2018). Muscle Function and Coordination of Amputee Stair Ascent. *J. Biomech. Eng.* 140 (1). doi:10.1115/1.4037791

Heim, M., Wershavski, M., Martinowitz, U., Chechick, A., and Azaria, M. (2000). Elbow Joint, Crutches and Locomotion: Special Reference to Persons with Haemophilia. *Haemophilia* 6 (5), 556–561. doi:10.1046/j.1365-2516.2000.00387.x

Hermens, H. J., Freriks, B., Disselhorst-Klug, C., and Rau, G. (2000). Development of Recommendations for SEMG Sensors and Sensor Placement Procedures. *J. Electromyogr. Kinesiol.* 10 (5), 361–374. doi:10.1016/s1050-6411(00)00027-4

Hsue, B.-J., and Su, F.-C. (2010). The Effect of Cane Use Method on Center of Mass Displacement during Stair Ascent. *Gait Posture* 32 (4), 530–535. doi:10.1016/j.gaitpost.2010.07.015

Inoue, K., Hobara, H., and Wada, T. (2012). "Effects of Foot Placement on the Lower Extremity in the Swing Phase during Stair Ascending: Implications for Transfemoral Prostheses," in Proceeding of the 2012 ICME International Conference on Complex Medical Engineering (Kobe, Japan: CME), 32–37. doi:10.1109/iccme.2012.6275644

Jebsen, R. H. (1967). Use and Abuse of Ambulation Aids. *JAMA* 199 (1), 5–10. doi:10.1001/jama.1967.03120010049008

Lee, S.-K., Lee, S.-Y., and Jung, J.-M. (2014). Muscle Activity of the Gluteus Medius at Different Gait Speeds. *J. Phys. Ther. Sci.* 26 (12), 1915–1917. doi:10.1589/jpts.26.1915

Lewis, C. L., Laudicina, N. M., Khuu, A., and Loverro, K. L. (2017). The Human Pelvis: Variation in Structure and Function during Gait. *Anat. Rec.* 300 (4), 633–642. doi:10.1002/ar.23552

Maguire, C., Sieben, J. M., Scheidhauer, H., Romkes, J., Suica, Z., and de Bie, R. A. (2016). The Effect of Crutches, an Orthosis TheraTogs, and No Walking Aids on the Recovery of Gait in a Patient with Delayed Healing Post Hip Fracture: A Case Report. *Physiother. Theory Pract.* 32 (1), 69–81. doi:10.3109/09593985.2015.1075640

Moore, D., Pizzari, T., McClelland, J., and Semciw, A. I. (2019). Rehabilitation Exercises for the Gluteus Medius Muscle Segments: An Electromyography Study. *J. Sport Rehabil.* 28, 1–4. doi:10.1123/jsr.2018-0340

Moran, J., Murphy, A., Murphy, D., Austin, A., Moran, D., Cronin, C., et al. (2015). The Energy Expenditure of Non-weight Bearing Crutch Walking on the Level and Ascending Stairs. *Gait Posture* 42 (1), 23–26. doi:10.1016/j.gaitpost.2014.10.024

Otten, R., Tol, J. L., Holmich, P., and Whiteley, R. (2015). Electromyography Activation Levels of the 3 Gluteus Medius Subdivisions during Manual Strength Testing. *J. Sport Rehabil.* 24 (3), 244–251. doi:10.1123/jsr.2013-0149

Peyré-Tartaruga, L. A., Boccia, G., Feijó Martins, V., Zoppirolli, C., Bortolan, L., and Pellegrini, B. (2022). Margins of Stability and Trunk Coordination during Nordic Walking. *J. Biomech.* 134, 111001. doi:10.1016/j.jbiomech.2022.111001

Rasouli, F., and Reed, K. B. (2020). Walking Assistance Using Crutches: A State of the Art Review. *J. Biomechanics* 98, 109489. doi:10.1016/j.jbiomech.2019.109489

Repo, J. P., Tukiainen, E. J., Roine, R. P., Ilves, O., Järvenpää, S., and Häkkinen, A. (2017). Reliability and Validity of the Finnish Version of the Lower Extremity Functional Scale (LEFS). *Disabil. Rehabilitation* 39 (12), 1228–1234. doi:10.1080/09638288.2016.1193230

Rice, D. A., McNair, P. J., Lewis, G. N., and Dalbeth, N. (2014). Quadriceps Arthrogenic Muscle Inhibition: the Effects of Experimental Knee Joint Effusion on Motor Cortex Excitability. *Arthritis Res. Ther.* 16 (6), 502. doi:10.1186/s13075-014-0502-4

Safran, M. R. (2019). Microinstability of the Hip-Gaining Acceptance. *J. Am. Acad. Orthop. Surg.* 27 (1), 12–22. doi:10.5435/jaaos-d-17-00664

Sanders, M., Bowden, A. E., Baker, S., Jensen, R., Nichols, M., and Seeley, M. K. (2018). The Influence of Ambulatory Aid on Lower-Extremity Muscle Activation during Gait. *J. Sport Rehabil.* 27 (3), 230–236. doi:10.1123/jsr.2016-0148

Semciw, A. I., Neate, R., and Pizzari, T. (2014). A Comparison of Surface and Fine Wire EMG Recordings of Gluteus Medius during Selected Maximum Isometric Voluntary Contractions of the Hip. *J. Electromyogr. Kinesiol.* 24 (6), 835–840. doi:10.1016/j.jelekin.2014.08.015

Semciw, A. I., Pizzari, T., Murley, G. S., and Green, R. A. (2013). Gluteus Medius: an Intramuscular EMG Investigation of Anterior, Middle and Posterior Segments during Gait. *J. Electromyogr. Kinesiol.* 23 (4), 858–864. doi:10.1016/j.jelekin.2013.03.007

Semciw, A., Neate, R., and Pizzari, T. (2016). Running Related Gluteus Medius Function in Health and Injury: A Systematic Review with Meta-Analysis. *J. Electromyogr. Kinesiol.* 30, 98–110. doi:10.1016/j.jelekin.2016.06.005

Svehlík, M., Kraus, T., Steinwender, G., Zwick, E. B., and Linhart, W. E. (2012). Pathological Gait in Children with Legg-Calvé-Perthes Disease and Proposal for Gait Modification to Decrease the Hip Joint Loading. *Int. Orthop.* 36 (6), 1235–1241. doi:10.1007/s00264-011-1416-2

Thys, H., Willems, P. A., and Saels, P. (1996). Energy Cost, Mechanical Work and Muscular Efficiency in Swing-Through Gait with Elbow Crutches. *J. Biomechanics* 29 (11), 1473–1482. doi:10.1016/0021-9290(96)84543-x

van der Veen, S. M., Hammerbeck, U., and Hollands, K. L. (2020). How Accuracy of Foot-Placement Is Affected by the Size of the Base of Support and Crutch Support in Stroke Survivors and Healthy Adults. *Gait Posture* 76, 224–230. doi:10.1016/j.gaitpost.2019.12.007

Vigotsky, A. D., Halperin, I., Lehman, G. J., Trajano, G. S., and Vieira, T. M. (2017). Interpreting Signal Amplitudes in Surface Electromyography Studies in Sport and Rehabilitation Sciences. *Front. Physiol.* 8, 985. doi:10.3389/fphys.2017.00985

Watanabe, K., Kouzaki, M., Ogawa, M., Akima, H., and Moritani, T. (2018). Relationships between Muscle Strength and Multi-Channel Surface EMG Parameters in Eighty-Eight Elderly. *Eur. Rev. Aging Phys. Act.* 15, 3. doi:10.1186/s11556-018-0192-z

Zheng, Y., and Hu, X. (2019). Interference Removal from Electromyography Based on Independent Component Analysis. *IEEE Trans. Neural Syst. Rehabil. Eng.* 27 (5), 887–894. doi:10.1109/tnsre.2019.2910387

Conflict of Interest: The authors declare that the research was conducted in the absence of any commercial or financial relationships that could be construed as a potential conflict of interest.

Publisher's Note: All claims expressed in this article are solely those of the authors and do not necessarily represent those of their affiliated organizations, or those of the publisher, the editors, and the reviewers. Any product that may be evaluated in this article, or claim that may be made by its manufacturer, is not guaranteed or endorsed by the publisher.

frontiers | Frontiers in Bioengineering and Biotechnology

ORIGINAL RESEARCH
published: 09 June 2022
doi: 10.3389/fbioe.2022.858610

Patellar Tendon Shear Wave Velocity Is Higher and has Different Regional Patterns in Elite Competitive Alpine Skiers than in Healthy Controls

Tobias Götschi[1,2*†], *Jonas Hanimann*[3,4†], *Nicole Schulz*[1,2], *Simon Huser*[3,4], *Victoria Held*[3,4], *Walter O. Frey*[3,4], *Jess G. Snedeker*[1,2] *and Jörg Spörri*[3,4]

[1]Department of Orthopedics, Balgrist University Hospital, University of Zurich, Zurich, Switzerland, [2]Institute for Biomechanics, ETH Zurich, Zurich, Switzerland, [3]Sports Medical Research Group, Department of Orthopedics, Balgrist University Hospital, University of Zurich, Zurich, Switzerland, [4]University Centre for Prevention and Sports Medicine, Balgrist University Hospital, University of Zurich, Zurich, Switzerland

OPEN ACCESS

Edited by:
Chiarella Sforza,
University of Milan, Italy

Reviewed by:
Cheng-Feng Lin,
National Cheng Kung University, Taiwan
Gianluca Vernillo,
University of Milan, Italy

***Correspondence:**
Tobias Götschi
tobias.goetschi@balgrist.ch

[†]These authors have contributed equally to this work and share first authorship

Specialty section:
This article was submitted to Biomechanics, a section of the journal Frontiers in Bioengineering and Biotechnology

Received: 20 January 2022
Accepted: 18 May 2022
Published: 09 June 2022

Citation:
Götschi T, Hanimann J, Schulz N, Huser S, Held V, Frey WO, Snedeker JG and Spörri J (2022) Patellar Tendon Shear Wave Velocity Is Higher and has Different Regional Patterns in Elite Competitive Alpine Skiers than in Healthy Controls. Front. Bioeng. Biotechnol. 10:858610. doi: 10.3389/fbioe.2022.858610

Competitive alpine skiers are exposed to enormous forces acting on their bodies–particularly on the knee joint and hence the patellar tendon - during both the off-season preparation and in-season competition phases. However, factors influencing patellar tendon adaptation and regional pattern differences between alpine skiers and healthy controls are not yet fully understood, but are essential for deriving effective screening approaches and preventative countermeasures. Thirty elite competitive alpine skiers, all members of the Swiss Alpine Ski Team, and 38 healthy age-matched controls were recruited. A set of two-dimensional shear wave elastography measurements of the PT was acquired and projected into three-dimensional space yielding a volumetric representation of the shear wave velocity profile of the patellar tendon. Multivariate linear models served to quantify differences between the two cohorts and effects of other confounding variables with respect to regional shear wave velocity. A significant ($p < 0.001$) intergroup difference was found between skiers (mean ± SD = 10.4 ± 1.32 m/s) and controls (mean ± SD = 8.9 ± 1.59 m/s). A significant sex difference was found within skiers ($p = 0.024$), but no such difference was found in the control group ($p = 0.842$). Regional SWV pattern alterations between skiers and controls were found for the distal region when compared to the mid-portion ($p = 0.023$). Competitive alpine skiers exhibit higher SWV in all PT regions than healthy controls, potentially caused by long-term adaptations to heavy tendon loading. The presence of sex-specific differences in PT SWV in skiers but not in controls indicates that sex effects have load-dependent dimensions. Alterations in regional SWV patterns between skiers and controls suggest that patellar tendon adaptation is region specific. In addition to the implementation of 3D SWE, deeper insights into long-term tendon adaptation and normative values for the purpose of preventative screening are provided.

Keywords: knee, tendinopathy, shear wave elastography, injury prevention, athletes, alpine ski racing

1 INTRODUCTION

Tendons transmit the forces from muscles to the skeleton and are thus crucial for human locomotion. Similar to other connective tissues, tendons are able to respond to various intrinsic and extrinsic stimuli through morphological and material property adaptations. Among others, tendon loading, age (Carroll et al., 2008; Hsiao et al., 2015), sex (Magnusson et al., 2007), body mass index (BMI) (Gumina et al., 2014) and nutritional habits (Scott et al., 2015; Korntner et al., 2017) are factors influencing tendon properties.

Repetitive exertion of tensile stress on tendons can promote tendon remodeling and thickening (Bohm et al., 2015), involving both collagen synthesis and degradation (Magnusson et al., 2010). Additionally, upregulated enzymatic cross-linking increases the structural integrity of the tissue (Svensson et al., 2016; Passini et al., 2021). Repetitive excessive overloading and inadequate repair mechanisms can, however, induce cumulated tendon damage and trigger degenerative pathological processes (Cook and Purdam, 2009), including an increase in collagen type III fibers, fibrocartilaginous changes through the decomposition of glycosaminoglycans (GAGs), neovascularization and tenocyte rounding and proliferation (Maffulli et al., 2000; Fredberg and Stengaard-Pedersen, 2008; Attia et al., 2014; Snedeker and Foolen, 2017). Compared to collagen type I fibers, collagen type III fibers exhibit a reduced ability to form cross-links, thus decreasing fiber orientation and mechanical strength within the tendon (Maffulli et al., 2000). GAGs contain highly hydrophilic side chains and therefore increase the water content within the tendon. These degenerative adaptations deteriorate the mechanical properties of the pathologic tendons (Seo et al., 2015; Ooi et al., 2016; Finnamore et al., 2019) and favor traumatic tendon injuries (Cook and Purdam, 2009; Yasui et al., 2017). From a screening and injury prevention perspective, however, both physiological and pathological processes are crucial since tendon pathologies move along a partially reversible continuum (Cook and Purdam, 2009).

Physiological adaptations contribute to athletic performance (energy storage-releasing capacity of tendon) (Mcguigan et al., 2006; Van Hooren and Zolotarjova, 2017; Groeber et al., 2021), whereas pathological developments can jeopardize an athletic career (Kettunen et al., 2002; Lian et al., 2005; Zwerver et al., 2011). Transferring the forces exerted by M. quadriceps femoris from the lateral apex of the patella to the tibial tuberosity and, hence, being involved in many daily and sports-related activities, the patellar tendon (PT) bears high volumes of heavy loads. Substantial differences in morphological and mechanical PT properties between team sports athletes (i.e., Volleyball and basketball players) and the general population were reported (Zhang et al., 2015; Bayliss et al., 2016). In particular, high magnitude loading, such as exercising close to the maximal strength capacities, induced significant tendon adaptation (Malliaras et al., 2013; Bohm et al., 2015).

One cohort exposed to high PT loads during both the off-season preparation and in-season competition phases are competitive alpine skiers. During the preparation phase, plyometric and heavy weight exercises are frequently performed, both exerting large loads on the PT (Hydren et al., 2013). On-snow training and competition can require skiers to perform 33,000 turns per season, whereby the ground reaction force peaks at up to 4 times body weight (Supej and Holmberg, 2010; Gilgien et al., 2018). These forces act–due to the constantly flexed knee position–strongly on the knee extensor muscle-tendon unit and, thus, the PT (Alhammoud et al., 2020). Therefore, healthy competitive alpine skiers are considered a suitable cohort for the detection of physiological PT adaptations. However, it is not yet clear whether differences in tendon adaptation can be observed between competitive alpine skiers and healthy controls and to what extent other factors act on tendon properties within the two groups.

Ultrasound (US) shear wave elastography allows on-site assessment of tissue mechanical properties. A focused acoustic radiation impulse induces tissue displacement that propagates perpendicularly to the direction of the impulse and can be observed with high frame rate (3–18 kHz) brightness mode (B-mode) US and appropriate tracking algorithms (Hein and O'brien, 1993). The instantaneous group shear wave velocity (SWV) can be mapped on a regular grid superimposed onto the B-mode US image and is related to the tissues' elastic properties (Nightingale, 2011). In detecting pathological and traumatic conditions of musculoskeletal structures, the quantitative assessment of elastic properties has proven valuable (Taljanovic et al., 2017). Particularly in depicting tendon damage and degeneration as well as predicting impeding structural failure, shear wave elastography (SWE) shows great potential (Aubry et al., 2015).

Tissue property assessments using US SWE are commonly performed in a two-dimensional (2D) manner. In particular, the investigation of larger structures is impeded by the limited field of view (FOV); therefore, the results are highly position dependent. In particular, tendon imaging requires accurate spatial referencing, as pathological characteristics in structural composition and architecture are typically spatially confined (Johnson et al., 1996; Khan et al., 1996; Pearson and Hussain, 2014). To overcome these limitations, we have previously implemented and validated an approach for three-dimensional US shear wave velocity mapping (Götschi et al., 2021). The technique allows sampling of larger structures primarily limited by the maximum measurement depth of the system and enables off-line analysis of distinct subregions (Götschi et al., 2021).

Based on this background, the current study was undertaken to 1) investigate differences in PT SWV in competitive alpine skiers compared to age-matched healthy control subjects, to 2) evaluate sex-specific differences in PT SWV, and to 3) describe potential differences in regional SWV patterns in both cohorts. Considering the literature and the high training volumes and loads in competitive alpine skiers, an increased SWV in the skier cohort compared to the control group was hypothesized. For the reasons stated above, it was also expected that the PT of male subjects would have a higher SWV than that of female subjects.

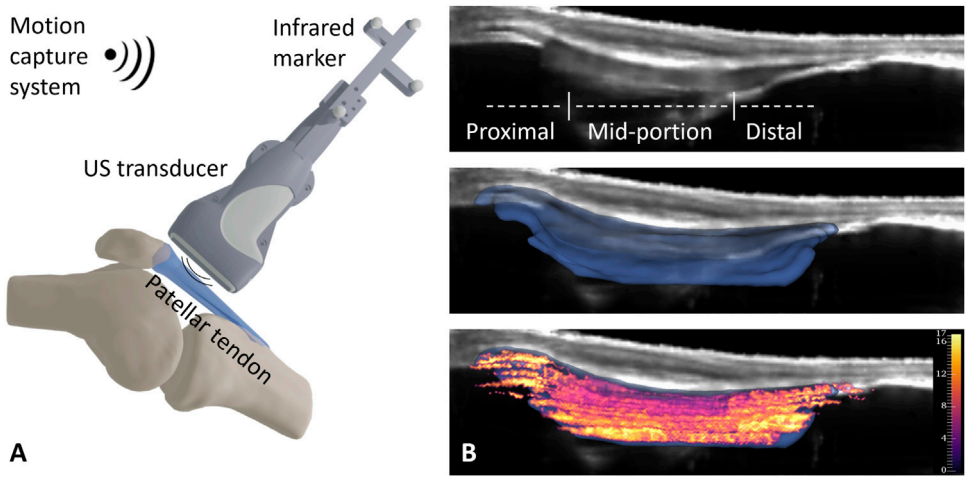

FIGURE 1 | Schematic depiction of the ultrasound shear wave elastography analysis. **(A)** Ultrasound B-mode and shear wave elastography measurements were acquired with a linear ultrasound probe equipped with optical markers. **(B)** Two-dimensional measurements were projected into three-dimensional space to yield volumetric B-mode and shear wave elastography representations (top image). The patellar tendon was segmented (middle image), and the segmentation was applied to the shear wave elastography volume (bottom image).

TABLE 1 | Baseline characteristics.

Parameter	*Control Group (n = 38, female: 20)*	*Skier Group (n = 30, female: 14)*	*Overall (n = 68, female: 34)*	*p value*	
Age [years]	24.9 ± 2.50	23.6 ± 2.50	24.4 ± 2.57	0.982	ns
Weight [kg]	65.9 ± 10.3	73.7 ± 10.7	69.3 ± 11.1	0.002	**
Height [cm]	172 ± 8.71	173 ± 9.37	172 ± 8.95	0.324	ns
BMI [kg/m^2]	22.2 ± 2.18	24.5 ± 1.81	23.2 ± 2.32	<0.001	**

Data are expressed as the mean ± SD (**): $p < 0.01$ *(ns):* $p > 0.05$.

TABLE 2 | Inference models identified group membership as the only significant predictor for shear wave velocity of the entire study population in all assessed tendon regions.

Tendon region	*Predictor*	*Estimate [ms^{-1}]*	*Std-Error [ms^{-1}]*	*p value*	
Overall	Skier group	1.495	0.328	< 0.001	**
	Sex	0.263	0.325	0.422	ns
Proximal	Skier group	1.184	0.357	0.002	**
	Sex	0.116	0.366	0.753	ns
	Tendon length	0.054	0.028	0.061	ns
Mid-portion	Skier group	1.401	0.359	< 0.001	**
	Sex	0.256	0.365	0.486	ns
	Tendon length	0.045	0.028	0.117	ns
Distal	Skier group	2.202	0.447	< 0.001	**
	Sex	0.023	0.443	0.959	ns

(**): $p < 0.01$, *(ns):* $p > 0.05$.

MATERIALS AND METHODS

Participants and Study Design

Thirty-nine elite competitive alpine skiers (skier group), all members of the Swiss Alpine Ski Team, and 38 age-matched healthy controls were recruited for the conduction of this case–control study. In winter, i.e., during the competition period, the training of elite competitive alpine skiers typically includes 1 to 3 on-snow competitions and/or on-snow training sessions, as well as 7 to 14 off-snow training sessions per week (Gilgien et al., 2018). In summer, i.e., during the off-season training period, they train an average of 5–9 sessions on-snow and 6 to 18 sessions off-snow per week, resulting in a total of 14–21 h of training per week (Gilgien et al., 2018). During the first

TABLE 3 | Predictive factors of shear wave velocity in the skier group. In the control group, no predictive factors were identified.

Target	Predictor	Estimate	Std- error	*p* value	
Skier Group					
Proximal	Male sex	0.927 ms-1	0.524 ms-1	0.088	ns
	Tendon length	0.058	0.034	0.102	ns
	BMI	–0.212	0.141	0.144	ns
Mid-portion	Age	–0.172 ms-1year-1	0.087 ms-1year-1	0.057	ns
	Male sex	1.080 ms-1	0.428 ms-1	0.018	*
Distal	Male sex	0.035 ms-1	0.678 ms-1	0.960	ns

(*): p < *0.05, (ns):* p > *0.05.*

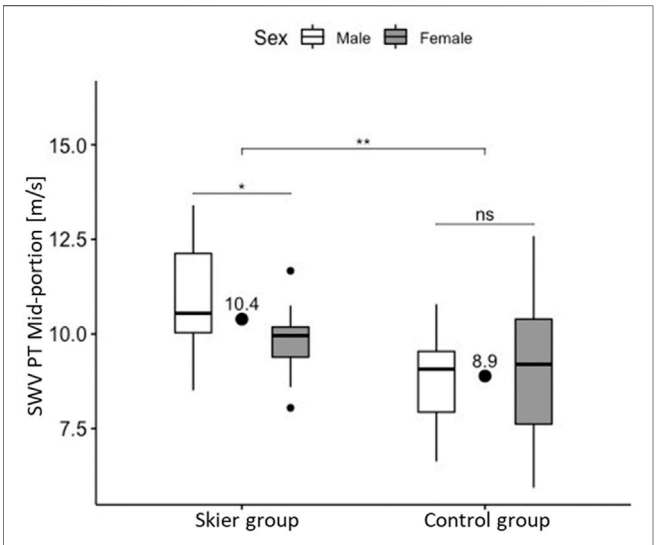

FIGURE 2 | Shear wave velocity of the midportion of the patellar tendon as a function of group membership and sex. (●): Group averages. Box: Median, interquartile range, range and outliers (*): $p < 0.05$ (**): $p < 0.01$ (ns): $p > 0.05$.

part of the off-season training period, in which also the present study was conducted, there is a particular focus on physical conditioning with 2–4 sessions of endurance training, 2–4 sessions of strength training, 1,2 sessions of explosive strength training and plyometrics, 2,3 sessions of agility and motor training, 3–5 sessions of stability and mobility training, and 1,2 sessions of cross training in other sports (Gilgien et al., 2018). The following inclusion criterion was applied: Physically active defined as more than one session of intense physical activity or more than 30 min of moderate physical activity per week. The number of participants recruited was limited by the number of active national competitive alpine skiers as part of the Swiss Alpine Ski Team. All skiers were monitored for health problems in a two-weekly interval with the Oslo Trauma Research Center (OSTRC) questionnaire for a minimum of 9 months prior to and up to the day of testing. Exclusion criteria were: 1) manifested signs of tendon disease or systemic pathology relevant to the purpose of the study; 2) acute PT tendon complaints; or 3) "severe" traumatic knee injuries leading to long-term training absences of more than 28 days (Fuller et al., 2006) within the 9 months preceding the US assessments. The medical records were verified and updated during an additional check-up by a medical doctor prior to SWV assessments. Nine subjects from the skier group were excluded, as they met exclusion criteria; 4 were excluded due to exclusion criteria 2, and 5 were excluded due to exclusion criteria 3. SWE assessments in the skier group were performed at the start of the off-season training period in May. Controls were particularly recruited to be healthy and not having experienced patellar tendon-related knee pain within the last 12 months. All subjects were informed of the aim of the study and provided written consent. The study was approved by the local ethics committee (KEK-ZH-NR: 2017-01395).

Ultrasound Assessment

US assessments and data processing were performed exactly as described in our validation study, which revealed *good* interoperator reliability (ICC of 0.736) and *very good* interday reliability (ICC of 0.904) (Götschi et al., 2021). One assessment was performed for each tendon by an experienced examiner; in total, 4 examiners were involved. The participant was in the supine position with adjustable support underneath the knee and a knee flexion angle of approximately 20°, and the right patellar tendon was examined (Martinoli, 2010). A US device (Aixplorer® Ultimate, Supersonic Imagine, Aix-en-Provence, France) capable of high frame-rate US acquisition equipped with a linear transducer (SL18-5) was used. The US transducer was held perpendicular to the skin, and parallel alignment with the fiber axis was ensured by observing and maximizing the fibrillar appearance of the intratendinous structure. Position and orientation of the US transducer was tracked throughout the scanning procedure with optical markers attached to it and an optical tracking system (FusionTrack 500, Atracsys LLC) (**Figure 1A**). 2D SWE and US brightness-mode (B-mode) data were projected into 3D space and aggregated using a weighted averaging scheme to yield a 3D voxel representation of the measurement (MATLAB 2020a; The MathWorks, Inc., Natick, MA, United States). The tendon was then segmented in the US B-mode volume, and the SWE volume was masked accordingly (3D slicer, version 4.10.2, (Kikinis et al., 2014). To allow analysis of distinct PT regions, the masked SWE reconstruction was divided into three regions with two cuts positioned at a distance of 10 mm from the proximal and distal insertion (**Figure 1B**), analogous to the approach described in our validation study (Götschi et al., 2021). Briefly, the area of

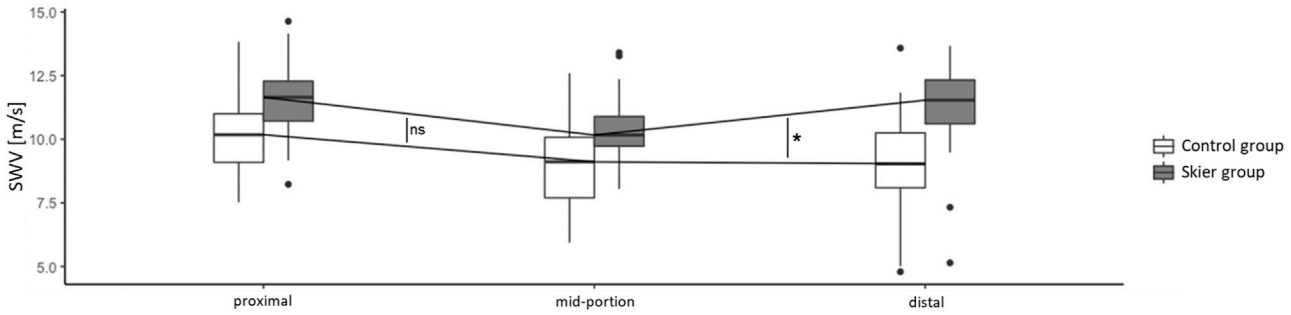

FIGURE 3 | Regional shear wave velocity in both study groups. Box: Median, interquartile range, range and outliers.

interest was identified using landmarks placed during manual segmentation of the volume. Accordingly, the most distal point of attachment of the patella to the patellar tendon and the most proximal point of attachment of the tibia were marked for the proximal and distal sections of the PT. Further analysis was performed based on mean values for the respective regions.

Statistical Analysis

To estimate the association of group membership while correcting for other potentially confounding variables with regional SWV, a multivariate approach is needed. Given the sample size available, including all factors of interest (including interaction effects) in one linear model may yield erroneous estimates due to overfitting. Hence, we opted for an alternative approach where we determined the linear model for inference by selecting the set of predictors with the best predictive performance in a leave-one-out validation scheme (maximum adjusted R^2). Consequently, for factors not included in the final models, no effect estimates are available. Univariate comparisons between groups were conducted with independent samples t tests. Statistical analysis was performed with R (Team, 2021), and statistical significance was set at $\alpha = 0.05$.

RESULTS

Baseline Characteristics

The baseline characteristics of both study groups are summarized in **Table 1**.

Overall Study Population

Linear regression modeling revealed group membership to be the only determining factor of SWV over the entire study population for all assessed tendon regions (overall, proximal, mid-portion, and distal), with skiers displaying higher SWV (**Table 2**).

Predictive Factors of Shear Wave Velocity in Each Study Group

When assessing each study group separately, in the skier group, both subject age and sex were retained in the final regression model for the midportion region of the PT (**Table 3**). In the control group, no predictors for mid-portion SWV were identified.

Figure 2 visualizes shear wave velocity differences between groups as well as the significant sex effect in the skier group and the absence thereof in the control group.

Regional Shear Wave Velocity Patterns in Patellar Tendons

We found that the regional difference in SWV between the distal and mid-portion PTs differed between the skier and control groups ($p = 0.023$). The two groups, however, did not differ with regard to the regional delta between the proximal and PT mid-portions ($p = 0.599$, **Figure 3**).

DISCUSSION

This study found higher PT SWV in competitive alpine skiers than in healthy controls. No demographic factors were predictive of SWV in the entire study cohort. Male skiers had a higher SWV than female skiers, whereas no such difference was found in the control group. Furthermore, skiers displayed a larger SWV decrease from the distal tendon to its mid-portion.

Higher Shear Wave Velocity in Competitive Alpine Skiers Than Healthy Controls

Physiological tendon hypertrophy and remodeling in response to altered loading regimes allows the tendon to cope with increased training volume and intensity. Moreover, optimization of muscle tendon unit performance requires both muscle and tendon to adapt, whereas the tendon is responsible for effective force transmission. In this context, lower tendon hysteresis has been reported in ski jumpers and runners compared to control subjects (Wiesinger et al., 2017). Pathological adaptations, on the other hand, lead to deterioration of the tendon structure, limiting the capacity for physical performance and increasing the risk of tendon rupture (Cook and Purdam, 2009; Ooi et al., 2016; Yasui et al., 2017). Competitive alpine skiers are exposed to tremendous loads both during off-season training and in the competition season (Supej and Holmberg, 2010; Hydren et al.,

2013; Gilgien et al., 2018). High accelerations combined with forward pushed, highly flexed knees induce large forces acting on the knee joint and, in particular, the PT (Alhammoud et al., 2020). Moreover, compared to other sports, particularly in competition situations the demands on the PT in alpine skiers are relatively high (90–120 s of high-intensity loading of the quadriceps muscles with peak ground reaction forces of up to four times body weight) (Supej and Holmberg, 2010). Therefore, off-snow training modalities are also designed to meet these unique demands, making extensive adaptations of the PT in skiers theoretically sound. Finally, such extraordinary demands can overwhelm the system's capacity for adaptation, which may manifest in a high prevalence of overuse complaints in this cohort (Fröhlich et al., 2020; Fröhlich et al., 2021). A closer understanding of the adaptive processes in response to long-term repetitive loading with regard to PT material properties is crucial in prevention and early detection strategies.

Influence of Demographic Factors

When assessing intercohort differences, adjustment of cofounding variables such as demographic factors is necessary. To do so, the selection of linear models with the best predictive performance is a suitable method (Stone, 1974). In our dataset, the effect of the tendon loading regime (i.e., group membership) outweighed biological factors such as weight, height, sex, age, tendon CSA, and tendon length. Zhang et al. reported lower stiffness in the PT of athletes; however, the inclusion criteria for the athletic cohort was a minimum of 4 h of exercise per week; hence, the inclusion criteria for the control and athlete groups are not comparable with our study (Zhang et al., 2015). Other studies agree with our finding: Increased PT SWV in athletes has been reported when compared to nonathletic cohorts (Zhang et al., 2015; Bayliss et al., 2016; Mersmann et al., 2017; Cristi-Sanchez et al., 2019; Dirrichs et al., 2019; Selcuk Can et al., 2021). A quantitative comparison of relative magnitude from our study shows a 1.17 times higher SWV in PT in skiers compared to the control group, whereas it is 1.47 when calculated with the results from Selcuk Can et al. (Selcuk Can et al., 2021). The difference may be explained by the different activity levels of the control and athlete groups in the two studies, but nevertheless, the two factors are in a similar range.

Potential Influence of Different Loading Regimes

Furthermore, increased tendon SWV values have been reported to result from altered loading regimes (Malliaras et al., 2013; Bohm et al., 2015), confirming the tendon's ability to adapt to load and supporting our finding that the loading regime is the main factor inducing physiological tendon adaptation. Interestingly, a sex-specific difference in SWV was only found in the skier group, which may indicate that high loads must be present to elicit sex-specific adaptation mechanisms. Some studies suggest that there is a sex-specific difference in mechanical tendon properties (Kubo et al., 2003; Onambele et al., 2007; Tas et al., 2017), while others do not (Burgess et al., 2009; O'brien et al., 2010; Morrison et al., 2015); hence, in the literature, there is no consensus in this regard. On the one hand, hormone-based effects on tendon adaptation have been described: Acute exercise-induced increase of tendon collagen synthesis is inhibited by estrogen (Magnusson et al., 2007) and is therefore diminished in magnitude and time, compared with men (Miller et al., 2007). On the other hand, male subjects are both heavier and suspected to be able to generate higher knee extension moments than female subjects, leading to increased PT forces and subsequently inducing PT adaptation. In agreement with this hypothesis, Arampatzis et al. found a positive correlation between maximal knee extension moment and PT stiffness (Arampatzis et al., 2007). Another study found increased PT stiffness in heavy loaded legs, whereas no effect was found in light loaded legs (Kongsgaard et al., 2007). Furthermore, no significant correlation between knee extension torque and PT stiffness has been found in subjects with no specific training engagement (Mannarino et al., 2018), thus supporting our hypothesis. The literature states that female sex is a protective factor regarding patellar tendinopathies, referring to team sport athletes (Morton et al., 2017). Since the difference in PT SWV was observed in competitive alpine skiers but not in the control group, it may be assumed that lower forces applied in female recreational athletes and, therefore, overuse complaints at the PT occur less frequently.

Differences in Regional Patellar Tendon Shear Wave Velocity

In the current study, different regional patterns in the PT SWV were found between skiers and controls, with significant differences between the delta from the mid-portion to the distal region. Functionally and clinically, proximal regions, mid-portions, and distal regions differ, and thus, it is expected that SWV as a quantification for tendon adaptation (i.e., collagen cross-linking) reflects the heterogeneous regional characteristics. Interestingly, Kongsgaard and others found an increase in proximal PT CSA after light and heavy training in healthy untrained men but a distal increase in CSA only after heavy training, with the training consisting of knee extension exercise (Kongsgaard et al., 2007). Since our study included only physically active subjects and yet the athletic cohort performs heavier physical activity, our finding is reflected by the results from Kongsgaard et al. (Kongsgaard et al., 2007). The precise structural adaptations that underlie elevated tendon SWV are currently unclear; nevertheless, the nonuniform adaptation behavior along the PT in response to the loading regime cannot be neglected. Thus, further research should implement a more sophisticated view regarding loading magnitude with regard to regional adaptations.

Study Limitations

This study has limitations to be considered. Physical activity levels of control subjects were not quantified on a continuous scale, and thus, there are potentially highly active subjects included in the control group. Since high-level athletes usually have more muscle mass than recreational athletes, BMI between these groups significantly differs, hence representing a cofounding factor. Furthermore, a challenge in assessing tendon SWV is the alignment between the transducer and tendon fiber orientation. Despite greatest caution in aligning

the transducer to the fiber orientation, situations where the fibers are not colinear over the entire measurement frame cannot be compensated for. Finally, tendon loading in the hours prior to or during the measurement was not controlled for; therefore, we asked the subjects to remain relaxed in the measurement position for 5 minutes and refrain from strenuous physical activity 24 h prior to the assessment. An interesting aspect that cannot be concluded from the present study and requires further investigation is whether there are differences in the SWV profiles of skiers in the different periods of a season.

CONCLUSION

Competitive alpine skiers showed higher SWV values in PT than physically active control subjects. The tendon loading regime is likely a main cause for the observed adaptations. Within skiers, males showed higher SWV values than females in the control group; however, no sex-specific difference was found. Hence, the intracohort analysis indicates that vast loading magnitudes and volumes are required to elicit such effects. Differences in the regional SWV pattern in the two cohorts indicate PT tissue adaptations to be dependent on the anatomical location. Translating our findings toward clinical applications and prevention strategies, screening and appropriate strength exercise might represent a fundamental component; however, normative data for different cohorts are fundamental in turns of a meaningful screening program.

DATA AVAILABILITY STATEMENT

The datasets presented in this article are not readily available because their access is restricted to protect the interests of the project partner Swiss-Ski and their athletes. Requests to access the datasets should be directed to joerg.spoerri@balgrist.ch.

ETHICS STATEMENT

The study was reviewed and approved by the local ethics committee (KEK-ZH-NR: 2017-01395). The patients/participants provided their written informed consent to participate in this study.

AUTHOR CONTRIBUTIONS

JSp and TG conceptualized and designed the study. JSp, NS, and SH recruited the participants and organized the data collection. TG, NS, SH, VH and JSp collected the data. TG, JH, NS, SH, and VH processed the data, and JH and TG performed the statistical analysis. All authors substantially contributed to the interpretation of the data. TG and JH drafted the current manuscript; all authors revised it critically, approved the final version of the manuscript, and agreed to be accountable for all aspects of the work.

FUNDING

This study was generously supported by the Balgrist Foundation, Swiss-Ski, the "Stiftung Passion Schneesport", and the "Stiftung zur Förderung des alpinen Skisportes in der Schweiz".

ACKNOWLEDGMENTS

We would also like to thank all participants, parents, and coaches involved. Imaging was performed with equipment maintained by the Swiss Centre for Musculoskeletal Imaging, SCMI, Balgrist Campus AG, Zürich.

REFERENCES

Alhammoud, M., Hansen, C., Meyer, F., Hautier, C., and Morel, B. (2020). On-Field Ski Kinematic According to Leg and Discipline in Elite Alpine Skiers. *Front. Sports Act. Living* 2, 56. doi:10.3389/fspor.2020.00056

Arampatzis, A., Karamanidis, K., Morey-Klapsing, G., De Monte, G., and Stafilidis, S. (2007). Mechanical Properties of the Triceps Surae Tendon and Aponeurosis in Relation to Intensity of Sport Activity. *J. Biomechanics* 40, 1946–1952. doi:10.1016/j.jbiomech.2006.09.005

Attia, M., Scott, A., Carpentier, G., Lian, Ø., Van Kuppevelt, T., Gossard, C., et al. (2014). Greater Glycosaminoglycan Content in Human Patellar Tendon Biopsies Is Associated with More Pain and a Lower VISA Score. *Br. J. Sports Med.* 48, 469–475. doi:10.1136/bjsports-2013-092633

Aubry, S., Nueffer, J.-P., Tanter, M., Becce, F., Vidal, C., and Michel, F. (2015). Viscoelasticity in Achilles Tendonopathy: Quantitative Assessment by Using Real-Time Shear-Wave Elastography. *Radiology* 274, 821–829. doi:10.1148/radiol.14140434

Bayliss, A. J., Weatherholt, A. M., Crandall, T. T., Farmer, D. L., Mcconnell, J. C., Crossley, K. M., et al. (2016). Achilles Tendon Material Properties Are Greater in the Jump Leg of Jumping Athletes. *J. Musculoskelet. Neuronal Interact.* 16, 105–112.

Bohm, S., Mersmann, F., and Arampatzis, A. (2015). Human Tendon Adaptation in Response to Mechanical Loading: a Systematic Review and Meta-Analysis of Exercise Intervention Studies on Healthy Adults. *Sports Med. - Open* 1, 7. doi:10.1186/s40798-015-0009-9

Burgess, K. E., Pearson, S. J., Breen, L., and Onambélé, G. N. L. (2009). Tendon Structural and Mechanical Properties Do Not Differ between Genders in a Healthy Community-Dwelling Elderly Population. *J. Orthop. Res.* 27, 820–825. doi:10.1002/jor.20811

Carroll, C. C., Dickinson, J. M., Haus, J. M., Lee, G. A., Hollon, C. J., Aagaard, P., et al. (20081985). Influence of Aging on the *In Vivo* Properties of Human Patellar Tendon. *J. Appl. Physiology* 105, 1907–1915. doi:10.1152/japplphysiol.00059.2008

Cook, J. L., and Purdam, C. R. (2009). Is Tendon Pathology a Continuum? A Pathology Model to Explain the Clinical Presentation of Load-Induced Tendinopathy. *Br. J. Sports Med.* 43, 409–416. doi:10.1136/bjsm.2008.051193

Cristi-Sánchez, I., Danes-Daetz, C., Neira, A., Ferrada, W., Yáñez Díaz, R., and Silvestre Aguirre, R. (2019). Patellar and Achilles Tendon Stiffness in Elite Soccer Players Assessed Using Myotonometric Measurements. *Sports Health* 11, 157–162. doi:10.1177/1941738118820517

Dirrichs, T., Schrading, S., Gatz, M., Tingart, M., Kuhl, C. K., and Quack, V. (2019). Shear Wave Elastography (SWE) of Asymptomatic Achilles Tendons: A Comparison between Semiprofessional Athletes and the Nonathletic General Population. *Acad. Radiol.* 26, 1345–1351. doi:10.1016/j.acra.2018.12.014

Finnamore, E., Waugh, C., Solomons, L., Ryan, M., West, C., and Scott, A. (2019). Transverse Tendon Stiffness Is Reduced in People with Achilles Tendinopathy: A Cross-Sectional Study. *PLoS One* 14, e0211863. doi:10.1371/journal.pone.0211863

Fredberg, U., and Stengaard-Pedersen, K. (2008). Chronic Tendinopathy Tissue Pathology, Pain Mechanisms, and Etiology with a Special Focus on Inflammation. *Scand. J. Med. Sci. Sports* 18, 3–15. doi:10.1111/j.1600-0838.2007.00746.x

Fröhlich, S., Helbling, M., Fucentese, S. F., Karlen, W., Frey, W. O., and Spörri, J. (2021). Injury Risks Among Elite Competitive Alpine Skiers Are Underestimated if Not Registered Prospectively, over the Entire Season and Regardless of whether Requiring Medical Attention. *Knee Surg. Sports Traumatol. Arthrosc.* 29, 1635–1643. doi:10.1007/s00167-020-06110-5

Fröhlich, S., Peterhans, L., Stern, C., Frey, W. O., Sutter, R., and Spörri, J. (2020). Remarkably High Prevalence of Overuse-Related Knee Complaints and MRI Abnormalities in Youth Competitive Alpine Skiers: a Descriptive Investigation in 108 Athletes Aged 13-15 Years. *BMJ Open Sport Exerc Med.* 6, e000738. doi:10.1136/bmjsem-2020-000738

Fuller, C. W., Ekstrand, J., Junge, A., Andersen, T. E., Bahr, R., Dvorak, J., et al. (2006). Consensus Statement on Injury Definitions and Data Collection Procedures in Studies of Football (Soccer) Injuries. *Br. J. Sports Med.* 40, 193–201. doi:10.1136/bjsm.2005.025270

Gilgien, M., Reid, R., Raschner, C., Supej, M., and Holmberg, H.-C. (2018). The Training of Olympic Alpine Ski Racers. *Front. Physiol.* 9, 1772. doi:10.3389/fphys.2018.01772

Götschi, T., Schulz, N., Snedeker, J. G., Hanimann, J., Franchi, M. V., and Spörri, J. (2021). Three-Dimensional Mapping of Shear Wave Velocity in Human Tendon: A Proof of Concept Study. *Sensors (Basel)* 21, 1655. doi:10.3390/s21051655

Groeber, M., Stafilidis, S., and Baca, A. (2021). The Effect of Stretch-Shortening Magnitude and Muscle-Tendon Unit Length on Performance Enhancement in a Stretch-Shortening Cycle. *Sci. Rep.* 11, 14605. doi:10.1038/s41598-021-94046-2

Gumina, S., Candela, V., Passaretti, D., Latino, G., Venditto, T., Mariani, L., et al. (2014). The Association between Body Fat and Rotator Cuff Tear: the Influence on Rotator Cuff Tear Sizes. *J. Shoulder Elb. Surg.* 23, 1669–1674. doi:10.1016/j.jse.2014.03.016

Hein, I. A., and O'brien, W. D. (1993). Current Time-Domain Methods for Assessing Tissue Motion by Analysis from Reflected Ultrasound Echoes-A Review. *IEEE Trans. Ultrason. Ferroelect., Freq. Contr.* 40, 84–102. doi:10.1109/58.212556

Hsiao, M.-Y., Chen, Y.-C., Lin, C.-Y., Chen, W.-S., and Wang, T.-G. (2015). Reduced Patellar Tendon Elasticity with Aging: *In Vivo* Assessment by Shear Wave Elastography. *Ultrasound Med. Biol.* 41, 2899–2905. doi:10.1016/j.ultrasmedbio.2015.07.008

Hydren, J. R., Volek, J. S., Maresh, C. M., Comstock, B. A., and Kraemer, W. J. (2013). Review of Strength and Conditioning for Alpine Ski Racing. *Strength & Cond. J.* 35, 10–28. doi:10.1519/ssc.0b013e31828238be

Johnson, D. P., Wakeley, C. J., and Watt, I. (1996). Magnetic Resonance Imaging of Patellar Tendonitis. *J. Bone Jt. Surg. Br.* 78-B, 452–457. doi:10.1302/0301-620x.78b3.0780452

Kettunen, J. A., Kvist, M., Alanen, E., and Kujala, U. M. (2002). Long-Term Prognosis for Jumper's Knee in Male Athletes: Prospective Follow-Up Study. *Am. J. Sports Med.* 30, 689–692. doi:10.1177/03635465020300051001

Khan, K. M., Bonar, F., Desmond, P. M., Cook, J. L., Young, D. A., Visentini, P. J., et al. (1996). Patellar Tendinosis (Jumper's Knee): Findings at Histopathologic Examination, US, and MR Imaging. Victorian Institute of Sport Tendon Study Group. *Radiology* 200, 821–827. doi:10.1148/radiology.200.3.8756939

Kikinis, R., Pieper, S. D., and Vosburgh, K. G. (2014). "3D Slicer: A Platform for Subject-specific Image Analysis, Visualization, and Clinical Support," in *Intraoperative Imaging and Image-Guided Therapy*. Editor F. A. Jolesz (New York, NY: Springer New York), 277–289. doi:10.1007/978-1-4614-7657-3_19

Kongsgaard, M., Reitelseder, S., Pedersen, T. G., Holm, L., Aagaard, P., Kjaer, M., et al. (2007). Region Specific Patellar Tendon Hypertrophy in Humans Following Resistance Training. *Acta Physiol.* 191, 111–121. doi:10.1111/j.1748-1716.2007.01714.x

Korntner, S., Kunkel, N., Lehner, C., Gehwolf, R., Wagner, A., Augat, P., et al. (2017). A High-Glucose Diet Affects Achilles Tendon Healing in Rats. *Sci. Rep.* 7, 780. doi:10.1038/s41598-017-00700-z

Kubo, K., Kanehisa, H., and Fukunaga, T. (2003). Gender Differences in the Viscoelastic Properties of Tendon Structures. *Eur. J. Appl. Physiol.* 88, 520–526. doi:10.1007/s00421-002-0744-8

Lian, Ø. B., Engebretsen, L., and Bahr, R. (2005). Prevalence of Jumper's Knee Among Elite Athletes from Different Sports: a Cross-Sectional Study. *Am. J. Sports Med.* 33, 561–567. doi:10.1177/0363546504270454

Maffulli, N., Ewen, S. W. B., Waterston, S. W., Reaper, J., and Barrass, V. (2000). Tenocytes from Ruptured and Tendinopathic Achilles Tendons Produce Greater Quantities of Type III Collagen Than Tenocytes from Normal Achilles Tendons: An *In Vitro* Model of Human Tendon Healing. *Am. J. Sports Med.* 28, 499–505. doi:10.1177/03635465000280040901

Magnusson, S. P., Hansen, M., Langberg, H., Miller, B., Haraldsson, B., Kjoeller Westh, E., et al. (2007). The Adaptability of Tendon to Loading Differs in Men and Women. *Int. J. Exp. Pathol.* 88, 237–240. doi:10.1111/j.1365-2613.2007.00551.x

Magnusson, S. P., Langberg, H., and Kjaer, M. (2010). The Pathogenesis of Tendinopathy: Balancing the Response to Loading. *Nat. Rev. Rheumatol.* 6, 262–268. doi:10.1038/nrrheum.2010.43

Malliaras, P., Kamal, B., Nowell, A., Farley, T., Dhamu, H., Simpson, V., et al. (2013). Patellar Tendon Adaptation in Relation to Load-Intensity and Contraction Type. *J. Biomechanics* 46, 1893–1899. doi:10.1016/j.jbiomech.2013.04.022

Mannarino, P., Lima, K. M. M., Fontenelle, C. R. C., Matta, T. T., De Salles, B. F., Simão, R., et al. (2018). Analysis of the Correlation between Knee Extension Torque and Patellar Tendon Elastic Property. *Clin. Physiol. Funct. Imaging* 38, 378–383. doi:10.1111/cpf.12424

Martinoli, C. (2010). Musculoskeletal Ultrasound: Technical Guidelines. *Insights Imaging* 1, 99–141. doi:10.1007/s13244-010-0032-9

Mcguigan, M. R., Doyle, T. L. A., Newton, M., Edwards, D. J., Nimphius, S., and Newton, R. U. (2006). Eccentric Utilization Ratio: Effect of Sport and Phase of Training. *J. Strength Cond. Res.* 20, 992–995. doi:10.1519/r-19165.1

Mersmann, F., Charcharis, G., Bohm, S., and Arampatzis, A. (2017). Muscle and Tendon Adaptation in Adolescence: Elite Volleyball Athletes Compared to Untrained Boys and Girls. *Front. Physiol.* 8, 417. doi:10.3389/fphys.2017.00417

Miller, B. F., Hansen, M., Olesen, J. L., Schwarz, P., Babraj, J. A., Smith, K., et al. (2007). Tendon Collagen Synthesis at Rest and after Exercise in Women. *J. Appl. Physiology* 102, 541–546. doi:10.1152/japplphysiol.00797.2006

Morrison, S. M., Dick, T. J. M., and Wakeling, J. M. (2015). Structural and Mechanical Properties of the Human Achilles Tendon: Sex and Strength Effects. *J. Biomechanics* 48, 3530–3533. doi:10.1016/j.jbiomech.2015.06.009

Morton, S., Williams, S., Valle, X., Diaz-Cueli, D., Malliaras, P., and Morrissey, D. (2017). Patellar Tendinopathy and Potential Risk Factors. *Clin. J. Sport Med.* 27, 468–474. doi:10.1097/jsm.0000000000000397

Nightingale, K. (2011). Acoustic Radiation Force Impulse (ARFI) Imaging: a Review. *Cmir* 7, 328–339. doi:10.2174/157340511798038657

O'brien, T. D., Reeves, N. D., Baltzopoulos, V., Jones, D. A., and Maganaris, C. N. (2010). Mechanical Properties of the Patellar Tendon in Adults and Children. *J. Biomech.* 43, 1190–1195. doi:10.1016/j.jbiomech.2009.11.028

Onambélé, G. N. L., Burgess, K., and Pearson, S. J. (2007). Gender-specific *In Vivo* Measurement of the Structural and Mechanical Properties of the Human Patellar Tendon. *J. Orthop. Res.* 25, 1635–1642. doi:10.1002/jor.20404

Ooi, C. C., Richards, P. J., Maffulli, N., Ede, D., Schneider, M. E., Connell, D., et al. (2016). A Soft Patellar Tendon on Ultrasound Elastography Is Associated with Pain and Functional Deficit in Volleyball Players. *J. Sci. Med. Sport* 19, 373–378. doi:10.1016/j.jsams.2015.06.003

Passini, F. S., Jaeger, P. K., Saab, A. S., Hanlon, S., Chittim, N. A., Arlt, M. J., et al. (2021). Shear-stress Sensing by PIEZO1 Regulates Tendon Stiffness in Rodents and Influences Jumping Performance in Humans. *Nat. Biomed. Eng.* 5, 1457–1471. doi:10.1038/s41551-021-00716-x

Pearson, S. J., and Hussain, S. R. (2014). Region-specific Tendon Properties and Patellar Tendinopathy: a Wider Understanding. *Sports Med.* 44, 1101–1112. doi:10.1007/s40279-014-0201-y

Scott, A., Zwerver, J., Grewal, N., De Sa, A., Alktebi, T., Granville, D. J., et al. (2015). Lipids, Adiposity and Tendinopathy: Is There a Mechanistic Link? Critical Review. *Br. J. Sports Med.* 49, 984–988. doi:10.1136/bjsports-2014-093989

Selcuk Can, T., Ozdemir, S., and Yilmaz, B. K. (2021). Shear-Wave Elastography of Patellar Ligament and Achilles Tendon in Semiprofessional Athletes: Comparing with the Nonexercising Individuals. *J. Ultrasound Med.* (Online ahead of print). doi:10.1002/jum.15908

Seo, J.-B., Yoo, J.-S., and Ryu, J.-W. (2015). Sonoelastography Findings of Supraspinatus Tendon in Rotator Cuff Tendinopathy without Tear:

Comparison with Magnetic Resonance Images and Conventional Ultrasonography. *J. Ultrasound* 18, 143–149. doi:10.1007/s40477-014-0148-8

Snedeker, J. G., and Foolen, J. (2017). Tendon Injury and Repair - A Perspective on the Basic Mechanisms of Tendon Disease and Future Clinical Therapy. *Acta Biomater.* 63, 18–36. doi:10.1016/j.actbio.2017.08.032

Stone, M. (1974). Cross-Validatory Choice and Assessment of Statistical Predictions. *J. R. Stat. Soc. Ser. B Methodol.* 36, 111–133. doi:10.1111/j.2517-6161.1974.tb00994.x

Supej, M., and Holmberg, H.-C. (2010). How Gate Setup and Turn Radii Influence Energy Dissipation in Slalom Ski Racing. *J. Appl. Biomech.* 26, 454–464. doi:10.1123/jab.26.4.454

Svensson, R. B., Heinemeier, K. M., Couppé, C., Kjaer, M., and Magnusson, S. P. (2016). Effect of Aging and Exercise on the Tendon. *J. Appl. Physiol. (1985)* 121, 1237–1246. doi:10.1152/japplphysiol.00328.2016

Taljanovic, M. S., Gimber, L. H., Becker, G. W., Latt, L. D., Klauser, A. S., Melville, D. M., et al. (2017). Shear-Wave Elastography: Basic Physics and Musculoskeletal Applications. *Radiographics* 37, 855–870. doi:10.1148/rg.2017160116

Tas, S., Yilmaz, S., Onur, M. R., Soylu, A. R., Altuntas, O., and Korkusuz, F. (2017). Patellar Tendon Mechanical Properties Change with Gender, Body Mass Index and Quadriceps Femoris Muscle Strength. *Acta Orthop. Traumatol. Turc* 51, 54–59.

Team, R. C. (2021). *R: A Language and Environment for Statistical Computing*. Vienna, Austria: R Foundation for Statistical Computing. Available at: https://www.R-project.org/.

Van Hooren, B., and Zolotarjova, J. (2017). The Difference between Countermovement and Squat Jump Performances: A Review of Underlying Mechanisms with Practical Applications. *J. Strength & Cond. Res.* 31, 2011–2020. doi:10.1519/jsc.0000000000001913

Wiesinger, H.-P., Rieder, F., Kösters, A., Müller, E., and Seynnes, O. R. (2017). Sport-Specific Capacity to Use Elastic Energy in the Patellar and Achilles Tendons of Elite Athletes. *Front. Physiol.* 8, 132. doi:10.3389/fphys.2017.00132

Yasui, Y., Tonogai, I., Rosenbaum, A. J., Shimozono, Y., Kawano, H., and Kennedy, J. G. (2017). The Risk of Achilles Tendon Rupture in the Patients with Achilles Tendinopathy: Healthcare Database Analysis in the United States. *Biomed. Res. Int.* 2017, 7021862. doi:10.1155/2017/7021862

Zhang, Z. J., Ng, G. Y. F., and Fu, S. N. (2015). Effects of Habitual Loading on Patellar Tendon Mechanical and Morphological Properties in Basketball and Volleyball Players. *Eur. J. Appl. Physiol.* 115, 2263–2269. doi:10.1007/s00421-015-3209-6

Zwerver, J., Bredeweg, S. W., and Van Den Akker-Scheek, I. (2011). Prevalence of Jumper's Knee Among Nonelite Athletes from Different Sports. *Am. J. Sports Med.* 39, 1984–1988. doi:10.1177/0363546511413370

Conflict of Interest: The authors declare that the research was conducted in the absence of any commercial or financial relationships that could be construed as a potential conflict of interest.

Publisher's Note: All claims expressed in this article are solely those of the authors and do not necessarily represent those of their affiliated organizations, or those of the publisher, the editors and the reviewers. Any product that may be evaluated in this article, or claim that may be made by its manufacturer, is not guaranteed or endorsed by the publisher.

frontiers | Frontiers in Physiology

ORIGINAL RESEARCH
published: 13 June 2022
doi: 10.3389/fphys.2022.916924

Age Differences in Recovery Rate Following an Aerobic-Based Exercise Protocol Inducing Muscle Damage Among Amateur, Male Athletes

*Irit Markus[1], Keren Constantini[1], Nir Goldstein[1], Roee Amedi[1], Yael Bornstein[1], Yael Stolkovsky[2], Merav Vidal[2], Shahar Lev-Ari[2], Roy Balaban[3], Stav Leibou[4], Tamar Blumenfeld-Katzir[5], Noam Ben-Eliezer[5,6,7], David Peled[6], Yaniv Assaf[6,8,9], Dennis Jensen[10], Naama Constantini[11], Gal Dubnov-Raz[12], Israel Halperin[1] and Yftach Gepner[1]**

[1]Department of Epidemiology and Preventive Medicine, School of Public Health, Sackler Faculty of Medicine, and Sylvan Adams Sports Institute, Tel-Aviv University, Tel-Aviv, Israel, [2]Department of Health Promotion, School of Public Health, Sackler Faculty of Medicine, Tel-Aviv University, Tel-Aviv, Israel, [3]Department of Clinical Microbiology and Immunology, Sackler School of Medicine, Tel Aviv University, Tel-Aviv, Israel, [4]Sackler School of Medicine, Tel Aviv University, Tel-Aviv, Israel, [5]Department of Biomedical Engineering, Tel Aviv University, Tel Aviv, Israel, [6]Sagol School of Neuroscience, Tel Aviv University, Tel-Aviv, Israel, [7]Center for Advanced Imaging Innovation and Research (CAI2R), New-York University Langone Medical Center, New York, NY, United States, [8]Department of Neurobiology, Faculty of Life Sciences, Tel-Aviv, Israel, [9]The Strauss Center for Neuroimaging, Tel Aviv University, Tel Aviv, Israel, [10]Clinical Exercise & Respiratory Physiology Laboratory, Department of Kinesiology and Physical Education, Faculty of Education, McGill University, Montreal, QC, Canada, [11]Shaare Zedek Medical center affiliated to the Hebrew University, Jerusalem, Israel, [12]Sports and Exercise Medicine Clinic, Sheba Medical Center, Sackler Faculty of Medicine, Tel Aviv, Israel

OPEN ACCESS

Edited by:
Rafael Reimann Baptista,
Pontifical Catholic University of Rio Grande do Sul, Brazil

Reviewed by:
Datao Xu,
Ningbo University, China
Brittany Counts,
Indiana University Bloomington School of Medicine, United States

***Correspondence:**
Yftach Gepner
gepner@tauex.tau.ac.il

Specialty section:
This article was submitted to Exercise Physiology, a section of the journal Frontiers in Physiology

Received: 10 April 2022
Accepted: 30 May 2022
Published: 13 June 2022

Citation:
Markus I, Constantini K, Goldstein N, Amedi R, Bornstein Y, Stolkovsky Y, Vidal M, Lev-Ari S, Balaban R, Leibou S, Blumenfeld-Katzir T, Ben-Eliezer N, Peled D, Assaf Y, Jensen D, Constantini N, Dubnov-Raz G, Halperin I and Gepner Y (2022) Age Differences in Recovery Rate Following an Aerobic-Based Exercise Protocol Inducing Muscle Damage Among Amateur, Male Athletes. Front. Physiol. 13:916924. doi: 10.3389/fphys.2022.916924

Purpose: Compare recovery rates between active young (Y) and middle-aged (MA) males up to 48H post aerobically based, exercise-induced muscle damage (EIMD) protocol. A secondary aim was to explore the relationships between changes in indices associated with EIMD and recovery throughout this timeframe.

Methods: Twenty-eight Y (n = 14, 26.1 ± 2.9y, 74.5 ± 9.3 kg) and MA (n = 14, 43.6 ± 4.1y, 77.3 ± 12.9 kg) physically active males, completed a 60-min downhill running (DHR) on a treadmill at −10% incline and at 65% of maximal heart rate (HR). Biochemical, biomechanical, psychological, force production and muscle integrity (using MRI diffusion tensor imaging) markers were measured at baseline, immediately-post, and up to 48H post DHR.

Results: During the DHR, HR was lower ($p < 0.05$) in MA compared to Y, but running pace and distance covered were comparable between groups. No statistical or meaningful differences were observed between groups for any of the outcomes. Yet, Significant ($p <$ 0.05) time-effects within each group were observed: markers of muscle damage, cadence and perception of pain increased, while TNF-a, isometric and dynamic force production

Abbreviations: CK, creatine kinase; CRP, c-reactive protein; EIMD, exercise induced muscle damage; IL1-RA, interleukin receptor antagonist 1; IL-6, interleukin 6; DHR, downhill running; DTI, diffusion tensor imaging; LDH, lactate dehydrogenase; TNF—α, tumor necrosis factor α; VAS, visual analog scale; CMJ, countermovement jump; VO2max, maximal oxygen uptake; MA, middle age; MVC, maximal voluntary contraction; MRI, magnetic resonance imaging; ROF, rate of fatigue; RPE, rated perceived exertion; Y, young.

and stride-length decreased. Creatine-kinase at 24H-post and 48H-post were correlated ($p < 0.05$, r range = –0.57 to 0.55) with pain perception, stride-length, and cadence at 24H-post and 48H-post. Significant ($p < 0.05$) correlations were observed between isometric force production at all time-points and IL-6 at 48H-post DHR (r range = –0.62 to (–0.74).

Conclusion: Y and MA active male amateur athletes recover in a comparable manner following an EIMD downhill protocol. These results indicate that similar recovery strategies can be used by trainees from both age groups following an aerobic-based EIMD protocol.

Keywords: aging, downhill running, muscle damage, inflammation, pain perception, recovery

1 INTRODUCTION

It is well established that aging has deleterious effects on recovery rate following various exercise protocols (Dedrick and Clarkson, 1990; Ploutz-Snyder et al., 2001). This is mainly because aging is associated with decreased muscle mass and function, increased low-grade chronic inflammation, and weakened immune function (Chung et al., 2009; Woods et al., 2012; Lavin et al., 2020). Moreover, some research suggests that middle-aged individuals are less likely to engage in physical activity compared to younger individuals (Shin et al., 2018). In addition, previous studies showed that lifelong chronic physical activity can reduce chronic inflammation and improve immune and muscle functions (Minuzzi et al., 2019; Lavin et al., 2020). Studies that have compared the recovery rates between younger and middle-aged or older (>50y) trained individuals following resistance exercise protocols, found that the decline in recovery rates begin at ~40 years of age (Korhonen et al., 2006; Fell and Williams, 2008; Gordon et al., 2017). For example, a comparison in recovery rates between younger and older sedentary adults following an eccentric resistance exercise protocol, found that the older adults suffer from higher rates of eccentric-induced muscle dysfunction (Ploutz-Snyder et al., 2001). To date, however, most such research has focused on resistance exercise. It remains to be determined whether endurance modes of exercise have similar age-related effects on recovery rate as resistance exercise among young and middle-aged individuals.

The mean age of recreational athletes participating in endurance sports increased over the last few decades, emphasizing the importance of developing a deeper understanding of the recovery rates in middle-aged and older individuals (Lehto, 2016). This is, in part, because insufficient recovery following exercise may result in impaired immune function (Peake et al., 2017) and cardiovascular instability (Romero et al., 2017). Subjective measures such as perception of pain and rate of fatigue were reported to be significantly higher in older (45 ± 6y) compared to younger (24 ± 5y) group of well-trained athletes following three consecutive days of 30-min cycling time trials (Fell et al., 2008). However, changes in objective outcomes, including range of motion, markers of muscle damage such as levels of circulating muscle proteins, and performance tests did not differ between younger (27 ± 2) and older (58 ± 2) trained adults following a 45-min downhill run. That study (Hayashi et al., 2019), however, did not assess inflammatory markers or examine changes in muscle integrity (for example via magnetic resonance imaging; MRI) in order to evaluate differences in the effect of exercise-induced muscle damage (EIMD) between age groups at the muscle fibers level.

Unaccustomed, aerobic-based exercise that predominantly includes eccentric contractions can cause structural muscle damage within the activated muscle fibers (Clarkson and Hubal, 2002; Tee et al., 2007). At the cellular level, the consequences of EIMD may include damage to structural proteins, myofibrils and muscle cell membranes, and thus impair excitation-contraction coupling (Fernandes et al., 2019; Markus et al., 2021). Subsequently, muscle strength and function are likely to be impaired (Dedrick and Clarkson, 1990; Lavin et al., 2020). This implication can also affect kinematics indices, as previous studies showed cadence and stride length are considerably altered following EIMD protocols (Kyrolainen et al., 2000; Vernillo et al., 2015). These kinematics changes could therefore shed light on the recovery processes following EIMD induced by running protocols. Taken together, quantifying the aforementioned damaging effects on muscle strength and kinematic indices can provide an effective means to identify age-related differences in recovery rates following muscle-damaging exercise (Pokora et al., 2014; Hayashi et al., 2019). Specifically, the recovery rate following EIMD can be assessed by objective evaluation of muscle proteins and inflammatory markers in the circulation, reduction in muscle strength, biomechanical measures, and performance tests, and by subjective measures such as perception of pain and rating of fatigue. Another objective method to directly assess muscle damage is by diffusion tensor imaging (DTI), which is a highly sensitive and non-invasive MRI technique that can detect exercise-induced changes in muscle structure by quantifying the magnitude and direction of water diffusion and its direction within the muscle fiber (Froeling et al., 2015; Gepner et al., 2017). To date, no studies used DTI to evaluate the effects of age on the rate of recovery following EIMD. Furthermore, to the best of our knowledge, the relationship between changes in the various biochemical, performance, biomechanical, and perceptual markers

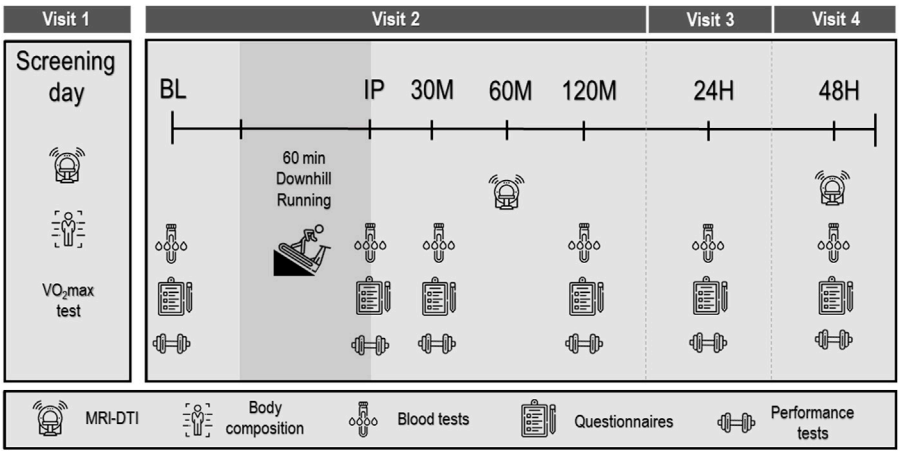

FIGURE 1 | Experimental protocol. Baseline (BL), immediately post (IP), 30 min (30 M), 120 min (120 M), 24 h (24H) and 48 h (48H) post downhill running protocol. VO2max: maximal O2 consumption; MRI-DTI: magnetic resonance imaging diffusion tensor imaging.

throughout the recovery period from an aerobic-based protocol causing EIMD remains unclear.

Thus, the primary aim of this study was to compare biochemical, performance, biomechanical and perceptual markers as well as muscle integrity following EIMD between young (Y) and middle-aged (MA) amateur male athletes. We chose these families of variables as they are strongly linked to recovery rates following EIMD protocols (Kyrolainen et al., 2000; Froeling et al., 2015; Gordon et al., 2017; Hayashi et al., 2019; Markus et al., 2021). We hypothesized that the degree of EIMD—as measured by biochemical, biomechanical, perceptual and muscle integrity markers—would be greater in MA amateur athletes compared to their Y counterpart, and that the abovementioned parameters will return to baseline levels earlier in the latter group compared to the former. A secondary aim was to explore the relationships between changes in these indices immediately post and up to 48H following a downhill running protocol designed to induce muscle damage.

2 METHODS

2.1 Study Population

Twenty-eight apparently healthy, recreationally competitive male runners and triathletes were recruited to participate in this study and were divided into two age-based groups: a young group (Y, $n = 14$; age range 18–30 years old), and a middle-aged group (MA, $n = 14$; age range 35–50 years old). All participants performed endurance exercise training at least four times per week and regularly competed in long distance running and/or triathlon events. Exclusion criteria included smoking, prescribed medications, or a self-reported history of chronic pulmonary, cardiac, metabolic, or orthopedic conditions.

2.2 Ethical Approval

The nature of the experiments was explained to all participants who provided written informed consent prior to study initiation. The study was approved by Shaare Zedek Medical Center (IRB#0345–19) and Tel Aviv University Ethical committee (#0000400–4), and is registered in www.ClinicalTrial.gov (NCT04025723).

2.3 Experimental Design

Participants visited the laboratory on four separate occasions (**Figure 1**). Visit 1, which served to screen participants, included filling an inform consent, health and physical activity level questionnaires, baseline MRI scan of the thigh muscles, anthropometric measurement, and a graded running exercise test to volitional exhaustion (i.e., maximal O_2 consumption [VO_2max] test). Visits 2–4 were performed on three consecutive days, while Visits 1 and 2 were separated by at least 48 h and all visits were completed within 14 days. During Visit 2 participants initially underwent a series of baseline (BL) measurements that included—in the following order—blood tests, questionnaires (visual analog scale of muscle soreness and rate of fatigue), force production/performance tests (counter movement jump, maximal isometric voluntary contraction), and a biomechanical assessment). Next, participants completed a 60-min downhill running (DHR) protocol, as detailed below. To assess recovery rate, the same series of measurements performed prior to the DGR protocol was conducted immediately (IP), 30 min (30 M-post), 120 min (120 M-post), 24 h (24H-post), and 48 h (48H-post) post the DHR protocol (i.e., a blood draw, assessment of running biomechanics and perceptual questionnaires, force production/performance tests). To assess muscle fiber integrity, MRI-DTI scans were performed on the screening day (prior to the DHR protocol), 60 M-post and 48H-post the DHR protocol (Visits 1, 2 and 4, respectively). Participants were instructed to refrain from consuming alcohol and caffeine, and avoid exercising for 24 h before lab visits 1 and 2 and between visits 2–4. Participants were also asked to fast for two hours prior to each lab visit.

2.4 Graded Exercise Test

On visit 1, participants performed a graded exercise test to exhaustion on a motorized treadmill (Saturn 100/300, h/p/

cosmos, Nussdorf-Traunstein, Germany) using an individualized protocol. For the first 5–6 min of the test, speed was increased every 1 min until reaching a comfortable speed (i.e., a speed at which each participant could easily run for 1 h). Then, the grade of the treadmill was increased 2% every 1 min until participants reached volitional exhaustion, defined as the point during exercise at which the participant (voluntarily) expressed inability to continue exercising despite strong verbal encouragement. Ventilatory and metabolic measurements were collected during the graded protocol using breath-by-breath analysis (Quark Cardiopulmonary Exercise Testing, Cosmed, Rome, Italy) while subjects breathed through an oro-nasal facemask (7450 Series, Hans Rudolph, Kansas City, MO, United States). Heart rate (HR) was continuously monitored using a chest strap (Garmin®, model Acc, HRM-Dual, Kansas City, MO, United States). VO_2max was determined as the highest 30-s average O_2 uptake (VO_2) achieved during exercise (as previously done by other, such as Bailey et al. (2009)), while meeting two of the following three criteria: 1) an HR ≥ 90% age-predicted maximum, 2) an RER ≥1.10, and 3) a plateau in VO_2 ≤ 150 ml with increased workload (Howley et al., 1995). Maximal HR (HRmax) was determined as the highest HR recorded during the test.

2.5 Downhill Running Protocol

Participants performed a 5-min warm-up at 0% grade while speed was increased every 30 s until the target HR of 65% of HRmax was reached. Following the warm-up, the slope of the treadmill was reduced to −10% (Byrnes et al., 1985; Peake et al., 2005; Hayashi et al., 2019) for 55 min with the running speed adjusted throughout the test so that each participant's HR remained at 65% HRmax (±5 beats/min). Every 10 min, participants were asked to rate their perceived exertion (RPE) on the Borg 6–20 scale (Borg, 1982). HR, speed (km/h), and distance (km) were recorded every 10 min.

2.6 Anthropometric Assessment

Body mass, waist circumference, fat mass and lean body mass were measured using bioelectrical impendence analysis (BIA; SECA© Medical Body Composition Analyzer, mBCA 515, Hamburg, Germany). Height was measured using a stadiometer (SECA 274).

2.7 Force Production/Performance Tests

The participants were familiarized with the performance tests on Visit 1 and, following a standardized warm-up (50% effort for two times), were asked to complete these tests at all six time points.

2.7.1 Maximal Voluntary Isometric Contraction (MVC)

Participants performed three knee extensions MVCs with one minute rest between each of the three trials. Lying on a treatment bed in the supine position, a padded strap was secured around their right ankle with the other side of the strap secured to a metal rod in the bed with the knee fixed at a 90° angle. Participants were instructed to extend their knee as forcefully as possible for 5 s. Force data were collected by the strain gauge (Chronojump®, Barcelona, Spain) and recorded by Chronojump® software at a sampling frequency of 80 Hz. The highest value obtained during the three trials was used. If the two best measurements differed by more than 10%, participants were asked to perform a fourth trial.

2.7.2 Countermovement Jump (CJM)

Participants were instructed to put their hands on their waist and jump as high as possible, while maintaining their legs shoulder-width apart, with no restrictions on how low they needed to squat prior to jumping. This test was repeated three times with one minute of rest between jumps. Jump height was calculated by flight time, using a jumping gate (Optogait, Microgate, Bolzano, Italy). The highest value obtained during the three trials was used. If the two best measurements differed by more than 10%, participants were asked to perform a fourth trial.

2.8 Biomechanics Assessment

At all six time points (BL, IP, 30 M-post, 120 M-post, 24H-post and 48H-post) participants from both age groups were asked to walk for 1 min at a fixed speed of 6 km/h and run for 2 min at 9 km/h at grade of 0% on a treadmill (Gaitway© mad, h/p/cosmos, Nussdorf-Traunstein, Germany). Stride length and cadence were measured using built-in pressure sensors within the treadmill (Zebris©, Munich, Germany). Data were recorded during the last 30 s of the running phase using Noraxon software (Noraxon Inc., Scottsdale, AZ, United States) at a frequency of 100 Hz and analyzed using Myoforce (Noraxon Inc., Scottsdale, AZ, United States).

2.9 Perceptual Questionnaires

2.9.1 Perception of Pain in the Quadriceps Muscle

Prior to all performance and biomechanics tests, participants were asked to quantify their degree of pain in the quadriceps muscle of the right thigh on a 15 cm v*isual analog scale* (VAS). Participants provided their levels of pain by making a mark on a horizontal line that ranged from "no pain at all" to "maximal pain" anchored at each end of the VAS.

2.9.2 Rate of Fatigue (ROF) Scale

Prior to all performance and biomechanics tests and following the VAS questionnaire, participants were asked to rate their level of fatigue, which was measured on an 11-point numerical scale with empirically derived accompanying descriptor and diagrammatic components of ROF (Micklewright et al., 2017).

2.9.3 Rating of Perceived Exertion (RPE)

Every 10 min during the DHR protocol, participants were asked to rate their perceived exertion on a numerical scale from 6–20 by the question "*Rate the level of effort you are currently feeling*", where 6 represents "no exertion at all" and 20 is "maximal exertion" (Borg, 1982).

2.10 Blood Collection and Biochemical Analysis

A total of 20 ml of blood was obtained at each of the six time points in two, 10 ml Vacutainer® tubes: one containing ethylenediamine tetraacetic acid (EDTA) and the other a

serum tube, for plasma and serum samples, respectively. Plasma samples were subsequently centrifuged twice at 1,500 g for 10 min at 4°C, while serum was kept at room temperature for 1 h then centrifuged at 1,300 g for 10 min. Samples were aliquoted into 1.8-ml microcentrifuge tubes and frozen at −80°C until analyzed. Interleukin (IL) 6, IL-10, tumor necrosis factor (TNF-α), and IL-1 receptor antagonist (RA) were analyzed by a high-sensitivity cytokine multiplex assay (Luminex, Cat no. FCSTM09-02; R & D Systems, Inc., Minneapolis, MN, United States) on a MAGPIX instrument (Luminex, Austin, TX, United States) according to the manufacturer's instructions. Extrapolation analysis for missing data was performed by a linear model in Analyst v5.1 Flex software (MILLIPLEX™, Carlisle, MA). Creatine kinase (CK), lactic dehydrogenase (LDH), and C-reactive protein (CRP) were analyzed by a Roche clinical chemistry and immunochemistry analyzer (Roche Diagnostics, Cobas® c111, Indianapolis, IN, United States).

2.11 MRI-Scans

DTI scans were performed on Magnetom Prisma 3T Siemens scanner at the Alfredo Federico Strauss Center located at Tel Aviv University. MRI data were obtained at BL, 60 M-post and 48H-post the DHR protocol. The distal quarter of the right thigh was positioned at the center of the coil and was scanned for 45 min. Four muscles were chosen to evaluate the anterior (rectus femoris and vastus lateralis) and posterior (biceps femoris and semitendinosus) compartments of the thigh muscles. Muscle integrity was assessed using DTI, a protocol that is sensitive to subclinical signs of muscle injury and changes in the tissue, as we and other have previously shown (Froeling et al., 2015; Oudeman et al., 2016; Biglands et al., 2020). Data obtained from MRI DTI scans can be used to calculate parameters that are sensitive to tissue changes following EIMD (Froeling et al., 2015), such as fractional anisotropy and mean diffusivity by evaluating the quality and direction of water diffusion in a given voxel, thus providing information about the integrity of the area of skeletal muscle scanned (Keller et al., 2020).

2.12 Statistical Analysis

Differences in baseline characteristics between study groups were compared using *t*-test for continuous variables, or chi-square tests for categorical variables. For each marker of muscle damage (e.g., biochemical, force production/performance, rating of fatigue and perception of pain, biomechanical, and MRI-DTI parameters), changes at each time point following the DHR protocol relative to baseline (Δ%) were analyzed using a two factor (time x group) repeated measures analysis of variance (ANOVA). In the event of a significant F-ratio, least significant difference (LSD) *post-hoc* analyses were used for pairwise comparisons. Correlations between selected muscle damage and inflammatory biomarkers (e.g., CK, CRP, IL-6, TNF-a), performance (CMJ, MVC) and subjective (VAS) measures were evaluated using Pearson *r* correlations. These correlations were performed on data from the entire cohort combined and, except for VAS, assessed as percentage change relative to baseline (Δ%). Sample size calculation was based on changes in muscle strength as a result of EIMD between young and middle-aged males (Gordon et al., 2017) using a Winpepi software. On the basis of $\alpha = 0.05$ and $\beta = 0.2$ with 80% power, the minimum number of subjects that were needed was 14 in each age group, with a total of 28 participants. Significance required an alpha level of $p \leq 0.05$. All data were analyzed by using IBM SPSS Statistics v25 software (SPSS, Inc., Chicago, IL, United States). Data are reported as mean ± SD, unless otherwise specified.

3 RESULTS

Study population characteristics, including training experience, weekly training volume are presented in **Table 1**. As expected, HRmax was significantly ($p < 0.001$) higher in the Y group compared to the MA group. Accordingly, during the DHR protocol HR was consistently higher in the Y group vs. MA ($p < 0.001$; **Figure 2**). RPE was only significantly ($p < 0.05$) higher in the MA group compared to Y at the 10 and 40 min marks (**Figure 2**) while distance and pace were not different between age groups.

3.1 Performance Tests: MVC and CMJ

No group effect was found for either MVC or CMJ. A significant time effect ($p < 0.001$) was observed for peak torque during MVC in both the MA and Y groups (F = 6.274 and F = 12.356, respectively; **Figure 3**). A significant ($p < 0.05$) time effect was also observed in CMJ for both the MA and Y groups (F = 3.961 and F = 4.125, respectively). The Y group showed a significant ($p < 0.05$) reduction in peak power of ~10% at all time points post, while MA showed a moderate yet significant ($p < 0.05$) decrease of ~5% only at 30 M-post, 24H-post and 48H-post.

3.2 Biomechanics Assessment: Cadence and Step Length

No group effect was found for either step length or cadence. Significant ($p < 0.05$) time effects were detected in both MA and Y groups for step length (F = 6.419 and F = 2.932, respectively; **Figure 3**). A significant ($p < 0.05$) time effect for cadence was observed only in the MA group (F = 7.393).

3.3 Perceptual Questionnaires: Rating of Fatigue and Soreness

No group effect was found for either step length or cadence. A significant ($p < 0.05$) time effect (F = 2.752) was observed for the ROF questioner in the Y group and was significantly higher, at 30 M-post and 120 M-post compere to baseline. A significant ($p < 0.05$) time effect for the VAS questioner, was observed in both groups (MA: F = 11.236; Y: F = 18.466) and was significantly higher at IP, 30M, 120M, 24H and 48H-post protocol in both groups.

3.4 Biochemical Analysis: Blood Markers of EIMD

No group effect was found for blood markers of EIMD. There was a significant ($p < 0.05$) time effect for CK (MA: F = 16.017; Y: F = 16.233) and LDH (MA: F = 4.505; Y: F = 3.813) (**Figure 4**). CK reached a peak 24H-post DHR protocol, with a more pronounced elevation in the Y group. CRP reached a peak 24H-post DHR

TABLE 1 | Baseline characteristics of the study population across age groups

	Young (18–30y)	Middle age (35–50y)	*p* value
	n = 14	*n* = 14	
Age (y)	26.1 ± 2.9	43.6 ± 4.1	< 0.001
Height (cm)	174.5 ± 0.1	175.5 ± 0.1	0.632
Weight (kg)	74.5 ± 9.3	77.3 ± 12.9	0.520
BMI (kg/m^2)	24.1 ± 2.5	25.3 ± 3.7	0.311
Waist circumference (cm)	82.8 ± 6.2	91.4 ± 10.4	0.014
Fat mass (%)	14.1 ± 4.3	19.2 ± 9.0	0.083
Lean body mass (kg)	60.4 ± 7.1	58.8 ± 7.1	0.552
Resting heart rate (bpm)	56 ± 9	52 ± 10	0.337
Maximal heart rate (bpm)	189 ± 7	174 ± 9	<0.001
VO_2max (ml/kg/min)	50.4 ± 6.1	46.5 ± 6.4	0.111
Systolic blood pressure (mmHg)	117 ± 11	122 ± 8	0.159
Diastolic blood pressure (mmHg)	69 ± 6	75 ± 8	0.053
Night time sleep (h)	6.8 ± 0.9	6.1 ± 1.2	0.087
Training years (y)	4.6 ± 4.3	10.2 ± 8.5	0.039
Weekly exercise (min)	558 ± 268	442 ± 183	0.206
Reported weekly running (km)	40 ± 27	54 ± 27	0.215
Resistance training (Yes)	9 (60.0%)	6 (40.0%)	0.363
Downhill experience (Yes)	0 (0.0%)	11 (71.4%)	<0.001

All data are reported as mean ± SD. Night time sleep—average of three nights.

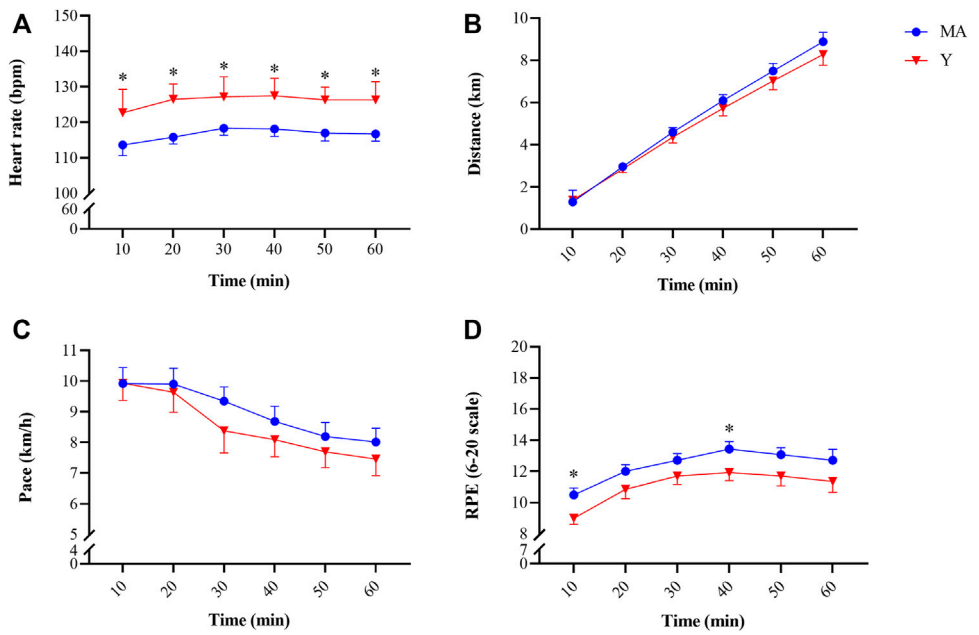

FIGURE 2 | Changes in heart rate [panel **(A)**], distance covered [panel **(B)**], pace [panel **(C)**] and rating of perceived exertion [panel **(D)**] recoded every 10 min during the 60-min downhill running protocol. * Significant ($p < 0.05$) difference between young (Y; red triangle) and middle-age (MA; blue circles) groups. All data are reported as mean ± SEM.

protocol, with a more significant elevation only occurring in the MA group.

3.5 Inflammatory Markers

There were no differences between age groups in any blood markers at baseline and no group effect was found for inflammatory markers, except for IL-6 at a single time point (see below). A significant ($p < 0.05$) time effect for CRP was observed within MA group (F = 4.067; **Figure 4**). In both groups, CRP peaked at 24H-post DHR, but the elevation was significant ($p < 0.05$) only for the MA group. In the MA group there was a significant ($p < 0.05$) time effect (F = 4.004) for IL-6. There was a significant ($p < 0.05$) difference in IL-6 between groups at 30 M-post. No time effect was observed for TNF-α and IL-1RA.

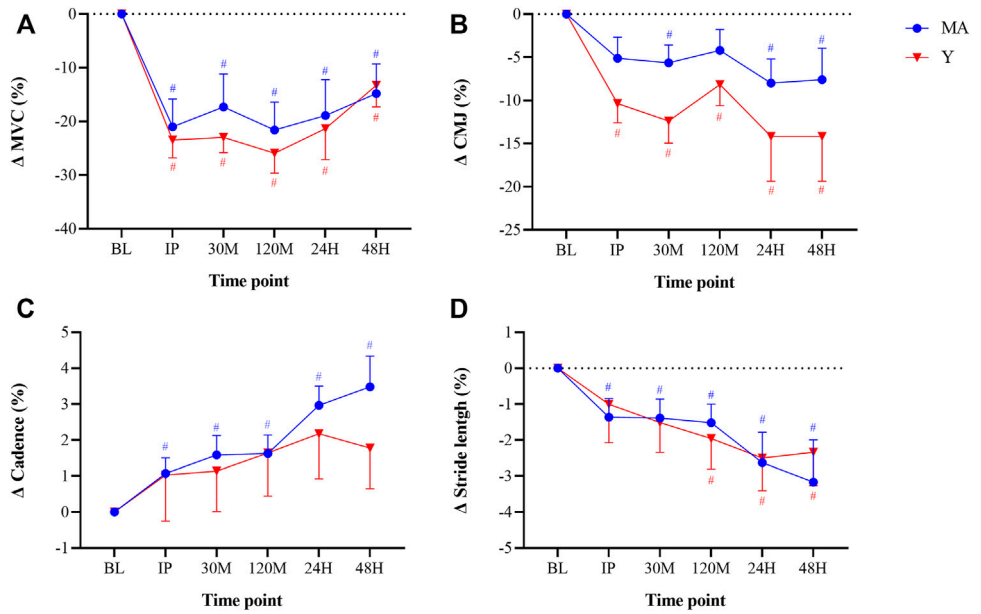

FIGURE 3 | Changes in maximal voluntary contraction [MVC; panel **(A)**], counter movement jump [CMJ; panel **(B)**], cadence [panel **(C)**], and stride length [panel **(D)**] relative to baseline (BL). Cadence and stride length were recorded while running at a constant pace of 9 km/h. Measurements were taken as BL, immediately post (IP), 30min (30 M), 120 min (120 M), 24 h (24H) and 48 h (48H) following a 60 min downhill running protocol. Young (Y; red triangle) and middle-age (MA; blue circles) groups. Dotted horizontal line represents no change compared to BL. # Significant ($p < 0.05$) difference compared with BL within each group. All data are reported as mean ± SEM.

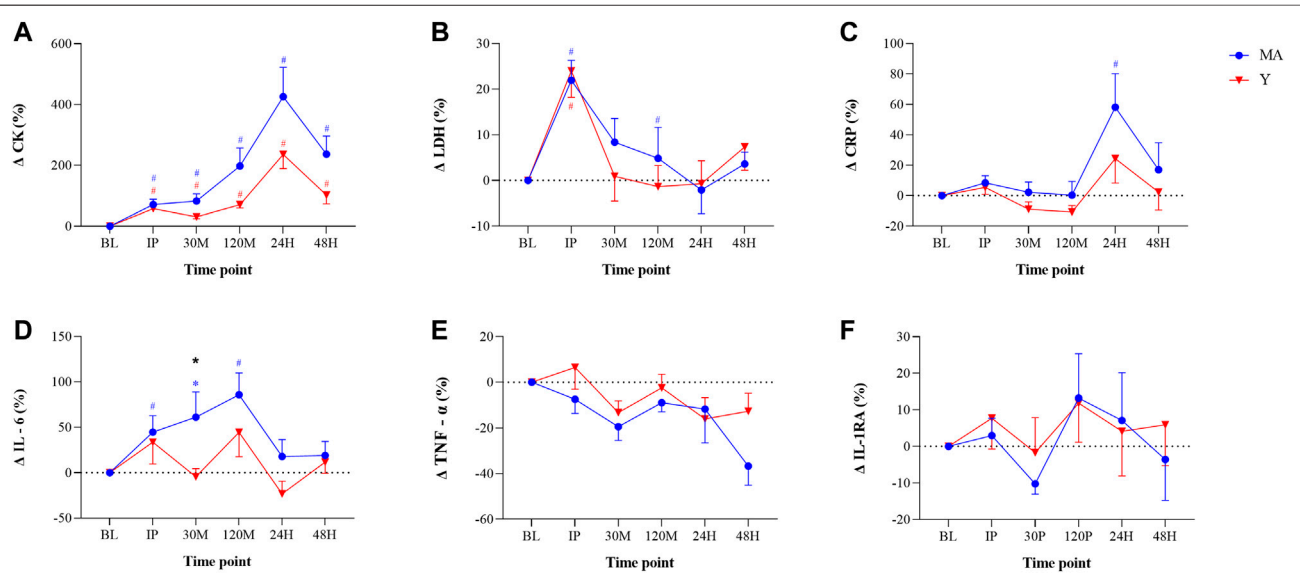

FIGURE 4 | Changes in blood markers of muscle damage and inflammation: Creatine kinase [CK; panel **(A)**], Lactate dehydrogenase [LDH; panel **(B)**], C-reactive protein [CRP; panel **(C)**] Interleukin-6 [IL-6; panel **(D)**], Tumor necrosis factor-α [TNF-α; panel **(E)**], and IL-1 receptor antagonist [IL-1RA; panel **(F)**] relative to baseline (BL). Measurements were taken as BL, immediately post (IP), 30 min (30 M), 120 min (120 M), 24 h (24H) and 48 h (48H) following a 60 min downhill running protocol. Young (Y; red triangle) and middle-age (MA; blue circles) groups. Dotted horizontal line represents no change compared to BL. # Significant ($p < 0.05$) difference compared with BL within each group. * Significant ($p < 0.05$) difference between groups at given time point. All data are reported as mean ± SEM.

3.6 MRI-DTI Scans

There was no time or group effect for any of the other MRI analyses ($p > 0.05$). There was a significant ($p < 0.05$) time effect for mean diffusivity in the rectus femoris (F = 7.025) and vastus lateralis (F = 4.515) muscles of the Y group. Changes in the parameters obtained from MRI-DTI analyses are shown in (**Figure 5**).

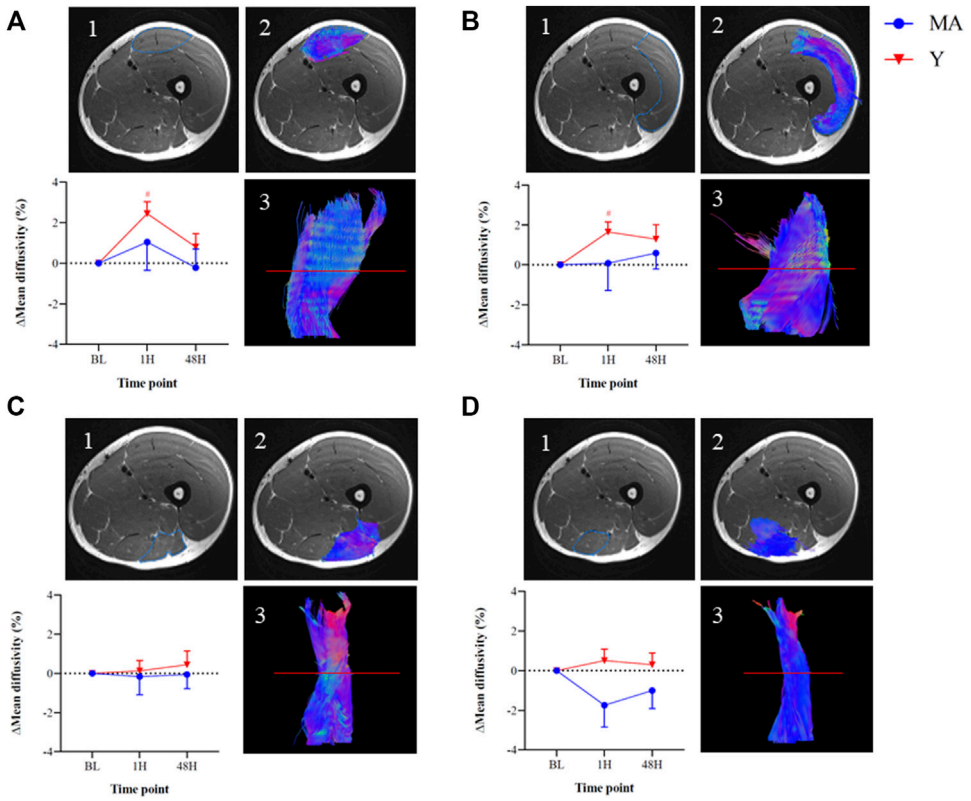

FIGURE 5 | Changes in mean diffusivity within the thigh muscles of the right leg relative to baseline (BL) measured using magnetic resonance imaging diffusion tensor imaging (MRI DTI) imaging: Rectus femoris [panel **(A)**], Vastus lateralis [panel **(B)**], Biceps femoris [panel **(C)**], and Semitendinosus [panel **(D)**]. The images represent an MRI-DTI analysis of the thigh muscles of one representative young participant at BL. 1. Region-of-interest on an axial slice 2. Colored region-of-interest on an axial slice 3. Tractography of individual muscle using DTI analysis on sagittal slice, based on the axial slice (red line). The colors within the images represent; Blue—Superior/cranial or Inferior/caudal, Green—Anterior or Posterior, Red—Distal or Proximal. Measurements were taken as BL, 1 h (1H) and 48 h (48H) following a 60 min downhill running protocol. Young (Y; red triangle) and middle-age (MA; blue circles) groups. Dotted horizontal line represents no change compared to BL. # Significant ($p < 0.05$) difference compared with BL within each group. All data are reported as mean ± SEM.

3.7 Correlations

Elevated CK concentrations at 24H-post (Δ335%) and 48H-post (Δ175%) were statistically correlated ($p < 0.05$) with the following measures at 24H-post and 48H-post (**Figure 6**): increases in VAS ($r = 0.44$ and 0.45, respectively), decreases in stride-length ($r = -0.57$ and -0.42, respectively), and increases in cadence ($r = 0.55$ and 0.45, respectively).

Ratings of perception of pain (assessed via a VAS), were statistically correlated with cadence at 120M, 24H and 48H-post ($r = 0.45$, $r = 0.43$ and $r = 0.40$, respectively; $p < 0.05$ for all). Stride length was negatively correlated with VAS at 120M and 24H-post ($p < 0.05$; $r = -0.44$, $r = -0.47$, respectively).

Significant correlations were also observed between performance measures and inflammatory cytokines: first, elevated levels (Δ16%) of IL-6 at 48H-post DHR protocol were statistically ($p < 0.05$) correlated with greater reductions (Δ -14 to -24%) in isometric force production (i.e., MVC) at all time points ($r = -0.62$ to -0.74; **Figure 7**). Second, changes in the pro-inflammatory cytokine TNF-a at 48H-post were statistically ($p < 0.05$) correlated with changes in dynamic force production (i.e., CMJ) at 30M to 48H-post ($r = -0.45$ to −0.57), where those whose TNF-a levels were reduced to a greater extent were able to better maintain peak CMJ force (**Figure 7**). No significant correlations were found between MRI-DTI to blood markers, subjective perception or performance.

4 DISCUSSION

This study was designed to comprehensively evaluate the differences in recovery rates between Y and MA amateur, male athletes, following an endurance-based protocol intended to induce muscle damage. While all participants demonstrated signs of considerable muscle damage as a result of the DHR protocol, surprisingly, and as opposed to our hypothesis, no differences in any of the outcomes were observed between the Y and MA groups at any given time point following DHR. These similarities in recovery patterns could suggested that an active lifestyle and consistent training throughout many years - as practiced by the MA group in this study - can negate some of the age-related effects associated with slower recovery rates with

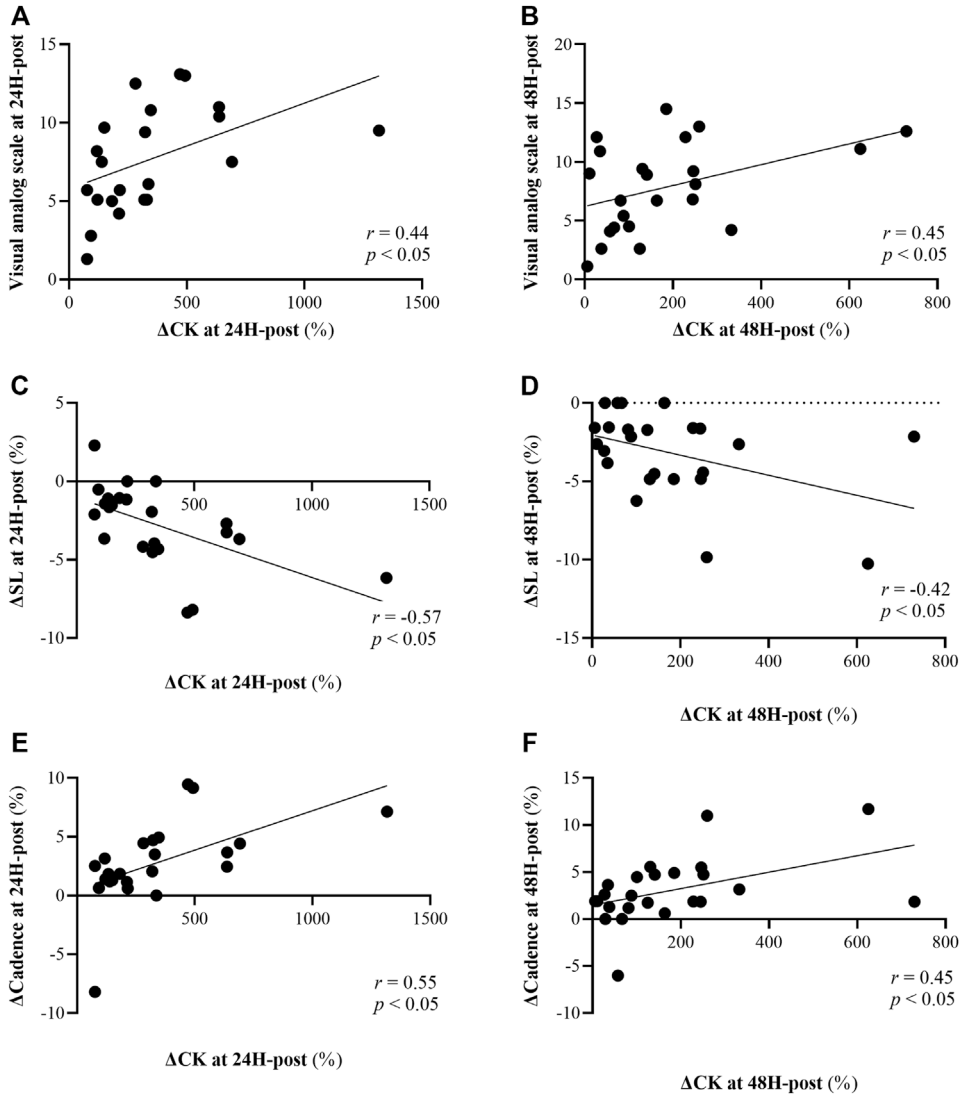

FIGURE 6 | Correlations between changes in creatine kinase (CK) at 24H-post (left panels) and 48H-post (right panels) 60 min downhill running (DHR) protocol relative to baseline and: Visual analog scale (15 point scale) at 24H-post [panel **(A)**] and 48H-post [panel **(B)**] DHR, changes in stride length (SL) at 24H-post [panel **(C)**] and 48H-post [panel **(D)**] DHR compared to baseline, and changes cadence at 24H-post [panel **(E)**] and 48H-post [panel **(F)**] DHR compared to baseline.

aging. Additionally, our findings that biomarkers of muscle damage and inflammation were strongly correlated with heightened perception of pain, alterations in running biomechanics and impairments in force production abilities, have important practical implications. Specifically, it can be suggested that subjective scales and performance tests may be carefully used to assess the severity of muscle damage and/or predisposition to altered biomechanical patterns when invasive or advanced measures are unavailable.

Aging is associated with a state of low-grade chronic inflammation and weakened immune function (Chung et al., 2009; Woods et al., 2012; Lavin et al., 2020); thus, the ability to cope with the "physiological load" after EIMD is likely to decline with age. Yet, in our study, no significant differences between the groups were found either at baseline or following the DHR protocol in inflammatory cytokines (e.g., IL-6, IL1-RA, CRP, TNF-a) or markers that are indicative of structural damage (CK and LDH) (Markus et al., 2021) (**Figure 4**). This finding is consistent with Hayashi et al. (2019), who also reported no differences in CK between young and older trained individuals, despite a peak 24H-post DHR protocol. Additionally, although acute alterations in performance (measured by MVC and CMJ) and running biomechanics (stride length and cadence) were observed following the DHR protocol, values were not different between the groups and followed similar patterns (**Figure 3**). These findings could suggest that consistent, long-term training, as experienced by the MA group, may potentially blunt age-related effects associated with the severity of and recovery from muscle damage following aerobic-based exercise.

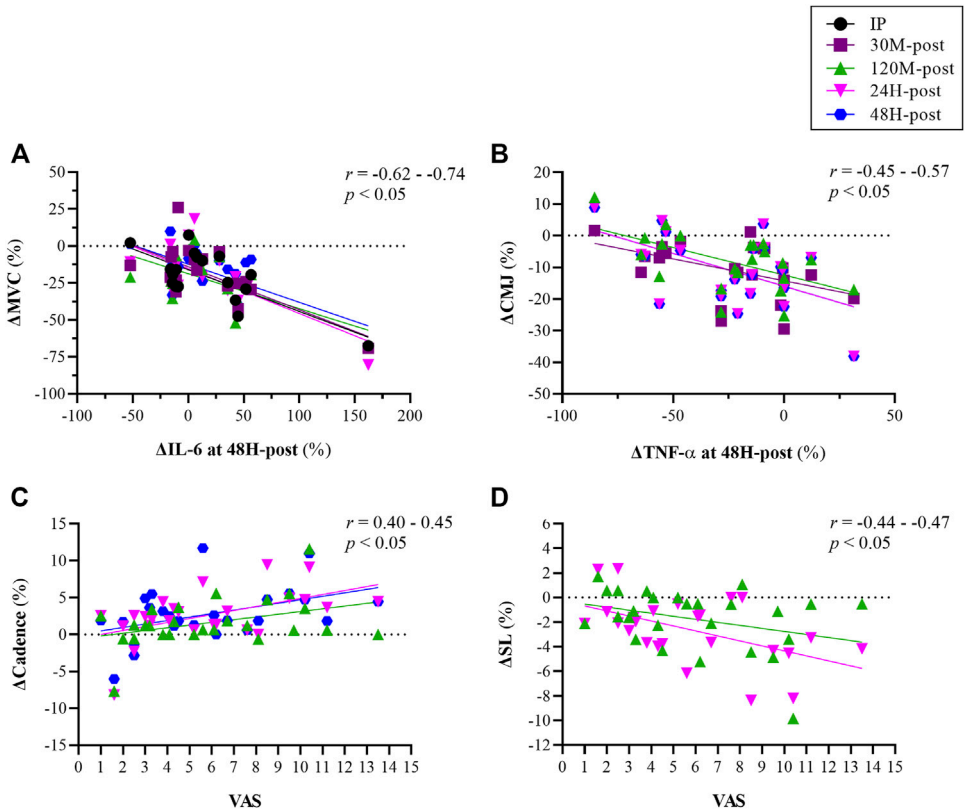

FIGURE 7 | Correlations between changes in inflammatory/biochemical markers [interleukin (IL)-6, Tumor necrosis factor-α (TNF-α)] and changes force production at various time points relative to baseline [panels **(A,B)**], and between subjective perception of pain measured assessed using a visual analog scale (VAS; 15-point scale) and changes in biomechanical indices [cadence panel **(C)**; stride length (SL) panel **(D)**] at various time points relative to baseline. Measurements were taken as baseline, immediately post (IP), 30 min (30 M), 120 min (120 M), 24 h (24H) and 48 h (48H) following a 60 min downhill running protocol. Each color represents corrolation between two variables at given time point (see legend for details).

To the best of our knowledge, this is the first study to assess differences in muscle damage between age groups following an endurance protocol via MRI-DTI technique. A scant number of studies have previously used this technique, which serves as a direct assessment of muscle integrity (as opposed, for example, to blood markers and pain scales), to evaluate muscle damage (Cermak et al., 2012; Froeling et al., 2015; Maeo et al., 2017). However, none of these studies compared age-related differences in EIMD or recovery rate. Our results showed a significant increase in mean diffusivity - a marker of microstructure changes - of the anterior department of the thigh muscles (rectus femoris and vastus lateralis) in the Y group following the DHR protocol (**Figure 5**). These results are similar to previous studies that used MRI to evaluate muscle damage (Froeling et al., 2015; Keller et al., 2020). For instance, Maeo et al. (2017) showed that 45 min of downhill running caused significant muscle damage to the knee extensors and Froeling et al. (2015) demonstrated similar changes in mean diffusivity after a marathon (42.2 km) run. Despite significant alterations in blood markers of muscle damage, muscles of the posterior department of the thigh (biceps femoris and semitendinosus) did not show any changes following the DHR protocol implemented in this study, which contrasts a previous study that examined EIMD following marathon running (Froeling et al., 2015). Future studies should implement the MRI-DTI technique as it is a powerful tool that can give deep insight into the muscle status at the fiber level.

We found a significant correlation between ΔCK and VAS at 24H and 48H-post DHR protocol (**Figure 6**). Greater ratings of subjective soreness 24–48H post EIMD has been previously shown (Gordon et al., 2017; Hayashi et al., 2019), and are likely related to severe muscle damage and associated elevated levels of CK in the bloodstream. At 24H-post DHR protocol, VAS and ΔCK were each also correlated with biomechanical measurements (**Figures 6**,**7**). The observed relationship between CK, a marker of muscle damage, and alterations in running biomechanics is physiologically sound: the micro-tears cause by EIMD, which also result in elevated CK, lead to impairments in muscle function and thus stepping patterns such as stride length and cadence. These findings have important practical implications: as measuring blood markers or gait patterns often may not be a feasible approach, coaches and athletes could instead utilize VAS to assess the severity of muscle damage and/or predisposition to altered biomechanical patterns. Thus, more informed decisions as to whether the athlete is ready to perform another high-intensity workout can be made. It is

important to consider the repeated bout effect which is known to attenuate muscle damage markers such as CK (Doma et al., 2017) due to the skeletal, neural and structural protective adaptation (Hyldahl et al., 2017), and therefore this approach should be used with caution.

Higher levels of IL-6 were found to correlate with poorer isometric force production measured via MVC, and depressed TNF-α levels were correlated with better (i.e., less reductions) in dynamic force production measured via CMJ (**Figure 7**). It could be assumed that since IL-6 is an anti-inflammatory agent, elevated levels of this cytokine could lead to greater reduction in isometric force production. On the other hand, greater reduction in the pro-inflammatory cytokine TNF-α may have resulted in better ability to maintain force during a dynamic, explosive movement such as CMJ. These results emphasize the importance of evaluating recovery following EIMD by investigating the relationships between diverse methods as suggested in previous studies (Bartolomei et al., 2017; Hayashi et al., 2019; Markus et al., 2021).

Our study is unique in its comprehensive and sensitive approach for evaluating the rate of recovery following aerobic-based protocol to induce muscle damage. We trust that the chosen protocol did indeed lead to EIMD due to the significant changes from baseline within each group in nearly all of the markers that have been assessed. While several other studies implemented a DHR protocol as well (Pokora et al., 2014; Hayashi et al., 2019), existing literature mostly consists of resistance-based training protocols (Arroyo et al., 2017; Gordon et al., 2017; Fernandes et al., 2019). This difference in study design could possibly explain the discrepancies between our study and others (Clarkson and Dedrick, 1988; Ploutz-Snyder et al., 2001), as resistance training is expected to load the neuromuscular system such that greater muscular damage occurs compared to aerobic exercise (Markus et al., 2021). Here, we specifically chose an exercise protocol that has been shown to lead to EIMD (Hamada et al., 2005; Peake et al., 2005; Pokora et al., 2014) and is aerobic in nature, as this type of training (i.e., aerobic/endurance) is commonly practiced by recreational and amateur athletes.

A limitation of our study is that we did not include a group of untrained, middle-aged participants, which may have deepened our understanding of the effects of previous training experience on recovery rate between Y and MA individuals. To the best of our knowledge, there are a limited number of studies that examined the effects of and recovery from aerobic-based EIMD between trained to untrained populations. One study Smith et al. (2007) that examined the effects of a 60 min downhill running protocol among untrained young individuals (18–30 y) showed CK values at 24H-post protocol that were nearly double those that we observed at the same time point in the young, trained group (897 ± 97 vs. 476 ± 200 IU/L, respectively). Another comparison between our study to (Smith et al., 2007) showed a threefold increase in IL-6 among the untrained group, IL-6 increased 6 h post protocol to ~29 pg/ml while in our study, we observed at 120 M-post absolute values of ~9 pg/ml. While Hayashi et al. (2019) did not report values for blood markers in the young, untrained group included in their study, the reductions in isometric strength following a downhill running protocol experienced by that group are of a smaller magnitude than those observed in our study for trained amateur athletes (10–15% vs. 20–30%, respectively). These results emphasize the attenuated response among trained populations following aerobic-based EIMD. Additionally, we followed the recovery phase only up to 48H post DHR. This decision was partly based on our understanding that participants in our study represent a population that does not usually rest for more than 48H between training sessions. Lastly, since we did not include females in this study, our findings can only be applied to males. Future studies should investigate the age-dependent differences in the extent of muscle damage and recovery rate following an aerobic/endurance-based exercise protocol among females as well.

5 CONCLUSION

Our findings demonstrate that the extent of recovery rate following EIMD, as measured using wide range of parameters, was similar between MA and Y amateur male athletes. While these results do not match our hypothesis, they could indicate that a highly active lifestyle for many years, as practiced by the MA group on this study, might preserve the capacity to recover in a similar manner to younger individuals following muscle damage induced by aerobic exercise. From a practical standpoint, similar approaches may be implemented in reference to recovery from EIMD for both middle-aged and young active males. Our results also indicated strong correlations between biochemical perturbations, heightened perception of muscle pain, and alternation in running biomechanics, and reductions in force production in the 48H following an aerobic-based muscle damaging protocol. Since invasive biochemical and inflammatory/muscle damage blood measures are often unavailable, subjective pain perception scales and force-production tests which can be performed in field settings can be carefully used to assess the severity of muscle damage.

DATA AVAILABILITY STATEMENT

The original contributions presented in the study are included in the article/Supplementary Materials, further inquiries can be directed to the corresponding author.

ETHICS STATEMENT

The studies involving human participants was reviewed and approved by the study was approved by Shaare Zedek Medical Center (IRB#0345–19) and Tel Aviv University Ethical committee (#0000400–4), and is registered in www.ClinicalTrial.gov(NCT04025723). The patients/participants provided their written informed consent to participate in this study.

AUTHOR CONTRIBUTIONS

YG, IM, NG, IH, and KC conceived the project. YG, IM, NG, IH, GD-R, NC, SL-A, NB-E, and KC designed the trial. IM, RA, YA, TB-K, and NB-E, analyzed the magnetic resonance

imaging scans. YG, IM, and NG analyzed the data. YG, IM, KC, DP, DJ, NC, and GD-R supervised the experiments. YG, IM, KC, and IH wrote the manuscript. All authors discussed the results and reviewed the manuscript and commented on the article.

FUNDING

This work was supported by a grant from the Tel Aviv University Center for AI and Data Science (TAD, 590957), and by the Tel Aviv University - McGill University Research Collaboration Fund (0601443901).

ACKNOWLEDGMENTS

The authors thank all the associates for their assistance and contribution to the development and achievement of this research. The authors thank the participants for their significant contribution.

REFERENCES

Arroyo, E., Wells, A. J., Gordon, J. A., Varanoske, A. N., Gepner, Y., Coker, N. A., et al. (2017). Tumor Necrosis Factor-Alpha and Soluble TNF-Alpha Receptor Responses in Young vs. Middle-Aged Males Following Eccentric Exercise. *Exp. Gerontol.* 100, 28–35. doi:10.1016/j.exger.2017.10.012

Bailey, S. J., Winyard, P., Vanhatalo, A., Blackwell, J. R., Dimenna, F. J., Wilkerson, D. P., et al. (2009). Dietary Nitrate Supplementation Reduces the O2cost of Low-Intensity Exercise and Enhances Tolerance to High-Intensity Exercise in Humans. *J. Appl. Physiology* 107, 1144–1155. doi:10.1152/japplphysiol.00722.2009

Bartolomei, S., Sadres, E., Church, D. D., Arroyo, E., Varanoske, A. N., Wang, R., et al. (2017). Comparison of the Recovery Response from High-Intensity and High-Volume Resistance Exercise in Trained Men. *Eur. J. Appl. Physiol.* 117, 1287–1298. doi:10.1007/s00421-017-3598-9

Biglands, J. D., Grainger, A. J., Robinson, P., Tanner, S. F., Tan, A. L., Feiweier, T., et al. (2020). MRI in Acute Muscle Tears in Athletes: Can Quantitative T2 and DTI Predict Return to Play Better Than Visual Assessment? *Eur. Radiol.* 30, 6603–6613. –11. doi:10.1007/s00330-020-06999-z

Borg, G. A. V. (1982). Psychophysical Bases of Perceived Exertion. *Med. Sci. Sports Exerc.* 14, 377–381. doi:10.1249/00005768-198205000-00012

Byrnes, W. C., Clarkson, P. M., White, J. S., Hsieh, S. S., Frykman, P. N., and Maughan, R. J. (1985). Delayed Onset Muscle Soreness Following Repeated Bouts of Downhill Running. *J. Appl. Physiology* 59, 710–715. doi:10.1152/jappl.1985.59.3.710

Cermak, N. M., Noseworthy, M. D., Bourgeois, J. M., Tarnopolsky, M. A., and Gibala, M. J. (2012). Diffusion Tensor MRI to Assess Skeletal Muscle Disruption Following Eccentric Exercise. *Muscle Nerve* 46, 42–50. doi:10.1002/mus.23276

Chung, H. Y., Cesari, M., Anton, S., Marzetti, E., Giovannini, S., Seo, A. Y., et al. (2009). Molecular Inflammation: Underpinnings of Aging and Age-Related Diseases. *Ageing Res. Rev.* 8, 18–30. doi:10.1016/j.arr.2008.07.002

Clarkson, P. M., and Dedrick, M. E. (1988). Exercise-induced Muscle Damage, Repair, and Adaptation in Old and Young Subjects. *J. Gerontology* 43, M91–M96. doi:10.1093/GERONJ/43.4.M91

Clarkson, P. M., and Hubal, M. J. (2002). Exercise-induced Muscle Damage in Humans. *Am. J. Phys. Med. Rehabilitation* 81, S52–S69. S52–S69. doi:10.1097/00002060-200211001-00007

Dedrick, M. E., and Clarkson, P. M. (1990). The Effects of Eccentric Exercise on Motor Performance in Young and Older Women. *Eur. J. Appl. Physiol.* 60, 183–186. doi:10.1007/BF00839156

Doma, K., Schumann, M., Leicht, A. S., Heilbronn, B. E., Damas, F., and Burt, D. (2017). The Repeated Bout Effect of Traditional Resistance Exercises on Running Performance across 3 Bouts. *Appl. Physiol. Nutr. Metab.* 42, 978–985. doi:10.1139/apnm-2017-0214

Fell, J., Reaburn, P., and Harrison, G. J. (2008). Altered Perception and Report of Fatigue and Recovery in Veteran Athletes. *J. Sports Med. Phys. Fit.* 48, 272–277.

Fell, J., and Williams, A. D. (2008). The Effect of Aging on Skeletal-Muscle Recovery from Exercise: Possible Implications for Aging Athletes. *J. Aging Phys. Act.* 16, 97–115. doi:10.1123/japa.16.1.97

Fernandes, J., Lamb, K., and Twist, C. (2019). Exercise-Induced Muscle Damage and Recovery in Young and Middle-Aged Males with Different Resistance Training Experience. *Sports* 7, 132. doi:10.3390/sports7060132

Froeling, M., Oudeman, J., Strijkers, G. J., Maas, M., Drost, M. R., Nicolay, K., et al. (2015). Muscle Changes Detected with Diffusion-Tensor Imaging after Long-Distance Running. *Radiology* 274, 548–562. doi:10.1148/radiol.14140702

Gepner, Y., Hoffman, J. R., Shemesh, E., Stout, J. R., Church, D. D., Varanoske, A. N., et al. (2017). Combined Effect of Bacillus Coagulans GBI-30, 6086 and HMB Supplementation on Muscle Integrity and Cytokine Response during Intense Military Training. *J. Appl. Physiology* 123, 11–18. doi:10.1152/japplphysiol.01116.2016

Gordon, J. A., Hoffman, J. R., Arroyo, E., Varanoske, A. N., Coker, N. A., Gepner, Y., et al. (2017). Comparisons in the Recovery Response from Resistance Exercise between Young and Middle-Aged Men. *J. Strength Cond. Res.* 31, 3454–3462. doi:10.1519/JSC.0000000000002219

Hamada, K., Vannier, E., Sacheck, J. M., Witsell, A. L., and Roubenoff, R. (2005). Senescence of Human Skeletal Muscle Impairs the Local Inflammatory Cytokine Response to Acute Eccentric Exercise. *FASEB J.* 19, 1–19. doi:10.1096/fj.03-1286fje

Hayashi, K., Leary, M. E., Roy, S. J., Laosiripisan, J., Pasha, E. P., and Tanaka, H. (2019). Recovery from Strenuous Downhill Running in Young and Older Physically Active Adults. *Int. J. Sports Med.* 40, 696–703. doi:10.1055/a-0951-0017

Howley, E. T., Bassett, D. R., and Welch, H. G. (1995). Criteria for Maximal Oxygen Uptake. *Med. Sci. Sports Exerc.* 27, 1292–1301. doi:10.1249/00005768-199509000-00009

Hyldahl, R. D., Chen, T. C., and Nosaka, K. (2017). Mechanisms and Mediators of the Skeletal Muscle Repeated Bout Effect. *Exerc. Sport Sci. Rev.* 45, 24–33. doi:10.1249/JES.0000000000000095

Keller, S., Yamamura, J., Sedlacik, J., Wang, Z. J., Gebert, P., Starekova, J., et al. (2020). Diffusion Tensor Imaging Combined with T2 Mapping to Quantify Changes in the Skeletal Muscle Associated with Training and Endurance Exercise in Competitive Triathletes. *Eur. Radiol.* 30, 2830–2842. doi:10.1007/s00330-019-06576-z

Korhonen, M. T., Cristea, A., Alén, M., Häkkinen, K., Sipilä, S., Mero, A., et al. (2006). Aging, Muscle Fiber Type, and Contractile Function in Sprint-Trained Athletes. *J. Appl. Physiology* 101, 906–917. doi:10.1152/japplphysiol.00299.2006

Kyröläinen, H., Pullinen, T., Candau, R., Avela, J., Huttunen, P., and Komi, P. V. (2000). Effects of Marathon Running on Running Economy and Kinematics. *Eur. J. Appl. Physiology* 82, 297–304. doi:10.1007/s004210000219

Lavin, K. M., Perkins, R. K., Jemiolo, B., Raue, U., Trappe, S. W., and Trappe, T. A. (2020). Effects of Aging and Lifelong Aerobic Exercise on Basal and Exercise-Induced Inflammation. *J. Appl. Physiology* 128, 87–99. doi:10.1152/japplphysiol.00495.2019

Lehto, N. (2016). Effects of Age on Marathon Finishing Time Among Male Amateur Runners in Stockholm Marathon 1979-2014. *J. Sport Health Sci.* 5, 349–354. doi:10.1016/j.jshs.2015.01.008

Maeo, S., Ando, Y., Kanehisa, H., and Kawakami, Y. (2017). Localization of Damage in the Human Leg Muscles Induced by Downhill Running. *Sci. Rep.* 7, 5769. doi:10.1038/s41598-017-06129-8

Markus, I., Constantini, K., Hoffman, J. R., Bartolomei, S., and Gepner, Y. (2021). Exercise-induced Muscle Damage: Mechanism, Assessment and Nutritional Factors to Accelerate Recovery. *Eur. J. Appl. Physiol.* 121, 969–992. doi:10.1007/s00421-020-04566-4

Micklewright, D., St Clair Gibson, A., Gladwell, V., and Al Salman, A. (2017). Development and Validity of the Rating-Of-Fatigue Scale. *Sports Med.* 47, 2375–2393. doi:10.1007/s40279-017-0711-5

Minuzzi, L. G., Chupel, M. U., Rama, L., Rosado, F., Muñoz, V. R., Gaspar, R. C., et al. (2019). Lifelong Exercise Practice and Immunosenescence: Master Athletes Cytokine Response to Acute Exercise. *Cytokine* 115, 1–7. doi:10.1016/j.cyto.2018.12.006

Oudeman, J., Nederveen, A. J., Strijkers, G. J., Maas, M., Luijten, P. R., and Froeling, M. (2016). Techniques and Applications of Skeletal Muscle Diffusion Tensor Imaging: A Review. *J. Magn. Reson. Imaging* 43, 773–788. doi:10.1002/jmri.25016

Peake, J. M., Neubauer, O., Walsh, N. P., and Simpson, R. J. (2017). Recovery of the Immune System after Exercise. *J. Appl. Physiology* 122, 1077–1087. doi:10.1152/japplphysiol.00622.2016

Peake, J. M., Suzuki, K., Hordern, M., Wilson, G., Nosaka, K., and Coombes, J. S. (2005). Plasma Cytokine Changes in Relation to Exercise Intensity and Muscle Damage. *Eur. J. Appl. Physiol.* 95, 514–521. doi:10.1007/s00421-005-0035-2

Ploutz-Snyder, L. L., Giamis, E. L., Formikell, M., and Rosenbaum, A. E. (2001). Resistance Training Reduces Susceptibility to Eccentric Exercise-Induced Muscle Dysfunction in Older Women. *Journals Gerontology Ser. A Biol. Sci. Med. Sci.* 56, B384–B390. doi:10.1093/gerona/56.9.b384

Pokora, I., Kempa, K., Chrapusta, S., and Langfort, J. (2014). Effects of Downhill and Uphill Exercises of Equivalent Submaximal Intensities on Selected Blood Cytokine Levels and Blood Creatine Kinase Activity. *Biol. Sport* 31, 173–178. doi:10.5604/20831862.1111434

Romero, S. A., Minson, C. T., and Halliwill, J. R. (2017). The Cardiovascular System after Exercise. *J. Appl. Physiology* 122, 925–932. doi:10.1152/japplphysiol.00802.2016

Shin, C.-N., Lee, Y.-S., and Belyea, M. (2018). Physical Activity, Benefits, and Barriers across the Aging Continuum. *Appl. Nurs. Res.* 44, 107–112. doi:10.1016/j.apnr.2018.10.003

Smith, L. L., McKune, A. J., Semple, S. J., Sibanda, E., Steel, H., and Anderson, R. (2007). Changes in Serum Cytokines after Repeated Bouts of Downhill Running. *Appl. Physiol. Nutr. Metab.* 32, 233–240. doi:10.1139/H06-106

Tee, J. C., Bosch, A. N., and Lambert, M. I. (2007). Metabolic Consequences of Exercise-Induced Muscle Damage. *Sports Med.* 37, 827–836. doi:10.2165/00007256-200737100-00001

Vernillo, G., Savoldelli, A., Zignoli, A., Skafidas, S., Fornasiero, A., La Torre, A., et al. (2015). Energy Cost and Kinematics of Level, Uphill and Downhill Running: Fatigue-Induced Changes after a Mountain Ultramarathon. *J. Sports Sci.* 33, 1998–2005. doi:10.1080/02640414.2015.1022870

Woods, J. A., Wilund, K. R., Martin, S. A., and Kistler, B. M. (2012). Exercise, Inflammation and Aging. *Aging Dis.* 3, 130–140.

Conflict of Interest: The authors declare that the research was conducted in the absence of any commercial or financial relationships that could be construed as a potential conflict of interest.

Publisher's Note: All claims expressed in this article are solely those of the authors and do not necessarily represent those of their affiliated organizations, or those of the publisher, the editors and the reviewers. Any product that may be evaluated in this article, or claim that may be made by its manufacturer, is not guaranteed or endorsed by the publisher.

frontiers | Frontiers in Physiology

TYPE Original Research
PUBLISHED 29 August 2022
DOI 10.3389/fphys.2022.919184

OPEN ACCESS

EDITED BY
Marcus Fraga Vieira,
Universidade Federal de Goiás, Brazil

REVIEWED BY
Yun-Ju Lee,
National Tsing Hua University, Taiwan
Orlando De Fernandes,
University of Evora, Portugal
Kohei Kaminishi,
The University of Tokyo, Japan

*CORRESPONDENCE
Ing-Shiou Hwang,
ensureh@gmail.com

SPECIALTY SECTION
This article was submitted to Exercise Physiology,
a section of the journal
Frontiers in Physiology

RECEIVED 15 April 2022
ACCEPTED 22 July 2022
PUBLISHED 29 August 2022

CITATION
Tsai Y-Y, Chen Y-C, Zhao C-G and Hwang I-S (2022), Adaptations of postural sway dynamics and cortical response to unstable stance with stroboscopic vision in older adults. *Front. Physiol.* 13:919184. doi: 10.3389/fphys.2022.919184

Adaptations of postural sway dynamics and cortical response to unstable stance with stroboscopic vision in older adults

Yi-Ying Tsai[1], Yi-Ching Chen[2,3], Chen-Guang Zhao[1] and Ing-Shiou Hwang[1,4]*

[1]Department of Physical Therapy, College of Medicine, National Cheng Kung University, Tainan City, Taiwan, [2]Department of Physical Therapy, College of Medical Science and Technology, Chung Shan Medical University, Taichung City, Taiwan, [3]Physical Therapy Room, Chung Shan Medical University Hospital, Taichung City, Taiwan, [4]Institute of Allied Health Sciences, College of Medicine, National Cheng Kung University, Tainan City, Taiwan

Background: Stroboscopic vision (SV), intermittent visual blocking, has recently been incorporated into postural training in rehabilitation. This study investigated interactions of postural fluctuation dynamics and cortical processing for the elderly during stabilometer stance with SV.

Methods: Thirty-five healthy elderly maintained an upright stance on a stabilometer. Along with postural fluctuation dynamics, EEG relative power and EEG-EEG connectivity were used to contrast neuromechanical controls of stabilometer stance with SV and full-vision.

Results: Compared with the full-vision, SV led to greater postural fluctuations with lower sample entropy and mean frequency (MF). SV also reduced regional power in the mid-frontal theta cluster, which was correlated to SV-dependent changes in the size of postural fluctuations. SV also enhanced the alpha band supra-threshold connectivity in the visual dorsal and frontal–occipital loops of the right hemisphere, and the supra-threshold connectivity from Fp2 positively related to variations in the MF of postural fluctuations.

Conclusion: SV adds challenge to postural regulation on the stabilometer, with the increasing regularity of postural movements and fewer corrective attempts to achieve the postural goal. The elderly shift over-reliance on visual inputs for posture control with more non-visual awareness, considering deactivation of the dorsal visual stream and visual error processing.

KEYWORDS

stroboscopic vision, EEG, functional connectivity, posture, visual feedback

Introduction

Degenerative changes in the vestibular, visual, and somatosensory systems challenge postural controls of the elderly who are prone to fall risk. The age-related sensory ambiguity impacts body-sway characteristics of older adults during upright stance, resulting in a greater sway area (or energy) of the center of pressure (COP) than that of young adults (Quijoux et al., 2021). In the presence of sensory conflicts, the mean frequency (MF) change of COP in older adults is especially evident in the anteroposterior (AP) direction, corresponding to the uncertainty of balance control (Moon et al., 2021). A relatively low level of COP entropy measures is noted in older adults, which indicates functional consequences of age-related complexity loss and inferior adaptive capacity to environmental constraints (Manor et al., 2010; Walsh, 2021). An increase in COP regularity also reflects greater attentional investment in postural control for the elderly (Donker et al., 2007). The changes in COP dynamics of older adults underlie the reorganization of cortical activities to solve balance constraints due to sensory ambiguity. The elderly exhibit more widespread oscillatory activities in the alpha, beta, and gamma bands than do young adults during static balance tests (Rubega et al., 2021). Compared to young adults, the elderly show lower increases in alpha activity without significant potentiation of the high-frequency beta wave when standing with their eyes closed (Lin et al., 2021). Also, eye closure leads to stronger frontoparietal-occipital connectivity but weaker fronto-tempo-motor connectivity of the theta, alpha, and beta bands in older adults (Chen et al., 2021b). These findings highlight the fact that brain activation in older adults during bipedal stance is reorganized in response to complete visual occlusion (Chen et al., 2021b; Lin et al., 2021). In fact, older adults are less capable of redistributing the relative sensory weighting to non-visual channels for postural control, as those non-visual sensory systems are more susceptible to degenerative changes (Bugnariu and Fung, 2007; Franz et al., 2015).

Flickering between clear and opaque frames can partially occlude visual information, resulting in an intermittent vision status known as stroboscopic vision (SV). With SV, people are forced to utilize incomplete visual information during sports activities (Bennett et al., 2018). Anecdotal behavioral studies suggest that short-term adaptation effects from practicing with stroboscopic vision may help improve skilled or semi-skilled visuomotor activities such as badminton (Hulsdunker et al., 2021) or volleyball (Kroll et al., 2020). SV is claimed to foster visual memory (Appelbaum et al., 2012) and central vision attention (Appelbaum et al., 2011) along with increasing motion extrapolation, in contrast to monotony and attentional underload in the full-vision condition (Ballester et al., 2017). However, when subjects are not well-adapted, SV can undermine visuomotor performance due to the limited visual information available. With this negative impact, SV can be integrated into postural training for patients with anterior cruciate ligament (ACL) injury (Grooms et al., 2018) and chronic ankle instability (Kim et al., 2021; Lee et al., 2021; VanDeMark et al., 2021; Han et al., 2022). SV is advocated to expedite sensory reweighting for reducing visual reliance, especially for the patients with ACL and ankle instability who may excessively weigh the visual channel to maintain an upright stance in cases of impairment of the proprioceptive or somatosensory systems (Song et al., 2016; Grooms et al., 2018). Hence, SV can be analogized to improve balance control in older people; however, little attention has been paid to the extension of SV applications (Chen et al., 2021a). There are two major debates on the functional benefits of SV-based postural training. Conforming to the analogy of sensory reweighting (Isableu et al., 2003; Kim et al., 2020), visual information block adjusts sensory contributions to postural control. Within this context, visual attention is unloaded with SV. Alternatively, SV increases visual attention (Appelbaum et al., 2011; Appelbaum et al., 2012; Grooms et al., 2015), which reinforces timing anticipation and motion coherence with vision (Hulsdunker et al., 2021). It will be of value in resolving the theoretical debate with direct neural evidence of the effects of stroboscopic vision on attentional resource allocation during postural training in older adults.

In addition to regional activities in the sensorimotor and visual cortex, posture control involves in coordinated processing of cortical activities within these spatially distinct areas, especially when the effect of visual cues is manipulated (Chen et al., 2021a; 2021b, 2022). By examining COP dynamics, regional/inter-regional EEG features, and COP-EEG interaction, this study investigated neuromechanical control of upright balance with stroboscopic vision for older people, while they were standing on a stabilometer surface with visual feedback. For intermittent visual blocking, SV was hypothesized to alter postural mechanics and impair the monitoring and correction of postural errors through variation of the mid-frontal and reverent error-related network in the theta (4–7 Hz) band (Cavanagh et al., 2012; Ozdemir et al., 2016; Pezzetta et al., 2018) during stabilometer stance. Next, if the hypothesis of sensory reweighting is supported, SV may unload visual attention and reduce motion explorations due to enhanced synchronization of the visuomotor network in the alpha (8–12 Hz) and beta (13–35 Hz) bands due to an inhibition process (Pfurtscheller et al., 1996) and a sustained active state of the sensorimotor cortex with non-visual inputs (Lin et al., 2021), respectively.

Methods

Participants

Thirty-six older adults over 60 years old (20 females and 16 males; age: 65.8 ± 2.8 years) from a university campus

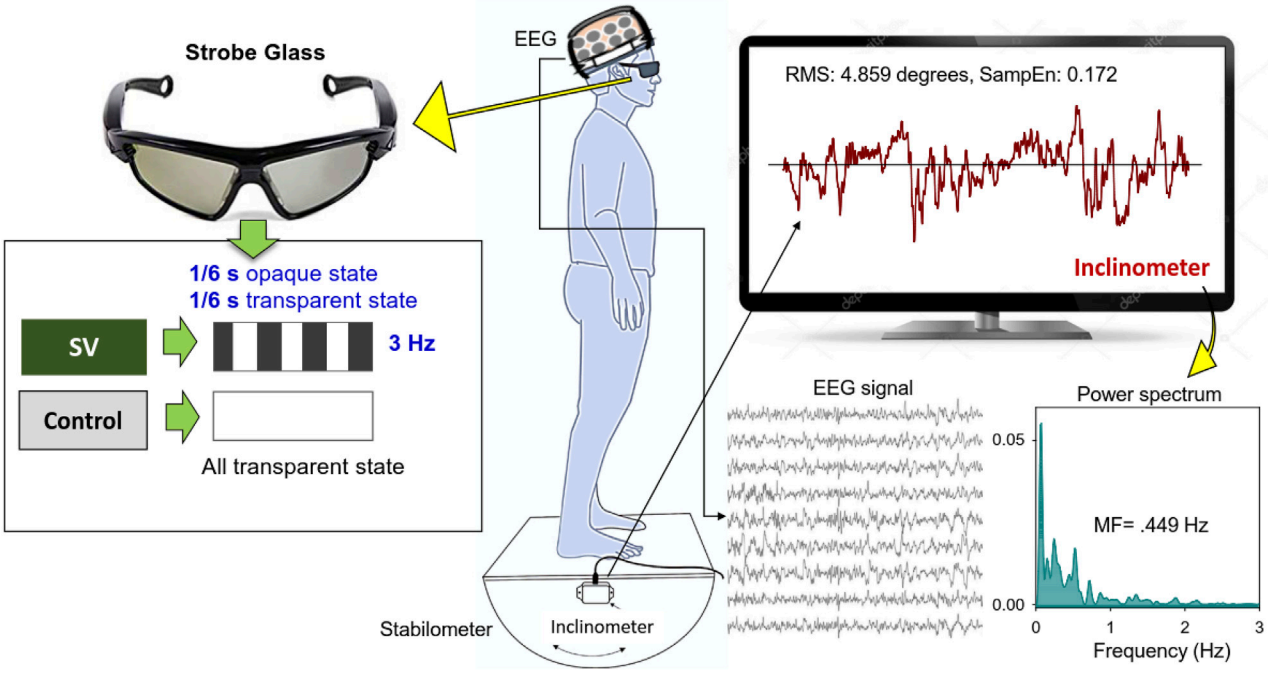

FIGURE 1
System setup and stabilometer stance with and without stroboscopic vision (SV). Under SV, the subjects regulated upright stance on the stabilometer with intermittent visual feedback of stabilometer movements at 3 Hz. In the control condition, the subjects wore stroboscopic glasses and visually tracked the stabilemeter movement trajectory with full vision.

participated in this study. One female participant failed to complete the experiment due to temporary dizziness during the experimental proceedings. Most participants were recreationally active with regular exercise habits. They had a corrected-to-normal vision (7 subjects: cataract surgery, 1 subject: glaucoma under control) and no known cognitive problems, history of falls, or diagnoses of neurological and musculoskeletal disorders requiring medication. Eleven subjects had known mild hypertension under regular medication. This study was approved by an authorized institutional human research review board at the University Hospital (A-ER-107-099-T). All subjects signed the consent form before the experiment, in accordance with the Declaration of Helsinki.

Experimental procedures

This study used a randomized, repeated measures design. Stabilometer stance, which is commonly used to train stance stability in elderly and neurological patients with balance dysfunction, served as the postural task in this study. Protected by a custom-made wooden fence, the subjects were asked to stand barefoot on a 50 cm × 58 cm wooden stabilometer (radius: 25 cm; height: 18.5 cm) (Figure 1). The stabilometer could rotate along its sagittal axis (roll maximum excursion: 20°). Subjects needed to keep the stabilometer in a horizontal position with a real-time stabilometer trajectory and a horizontal target visual feedback on the computer monitor. The subjects wore a pair of stroboscopic glasses (Visionup Athlete VA11-AF, Japan) and attempted to couple the stabilometer movement trajectory with the horizontal target line during the stabilometer stance. In the full vision condition, the stroboscopic glasses provided no opaque state, so no visual information was occluded. In the SV condition, the stroboscopic glasses provided a 1/6-s opaque state and a 1/6-s transparent state at a rate of 3 Hz to reduce half amount of visual feedback (Figure 1). The opaque/transparent ratio was 1:1. Each trial lasted 45 s. All participants completed three experimental trials for both the SV and full vision conditions in alternating order with rest periods of 3 min between trials to prevent fatigue. Half of the participants began with an SV trial and the other half began with a full vision trial.

Instrumentation setting

According to the 10-20 system of electrode placement, scalp EEG during stabilometer stance was recorded with Ag-AgCl electrodes and a 40-channel NuAmps amplifier (NeuroScan

TABLE 1 The contrast angular fluctuation of stabilometer movement dynamics between the stroboscopic vision and control conditions.

Stabilometer movement dynamics	SV	Control	*Hotelling's Statistics*	*Post-hoc test*
RMS (degree)	4.848 ± 2.013†††	2.487 ± 0.969	Wilks' $\Lambda = 0.287$, $p < 0.001$	$t_{34} = 9.036$, $p < 0.001$
SampEn	0.186 ± 0.074***	0.225 ± 0.083		$t_{34} = -3.942$, $p < 0.001$
MF (Hz)	0.308 ± 0.089***	0.398 ± 0.139		$t_{34} = -4.329$, $p < 0.001$

†††SV > Control, $p < 0.001$.
***SV < Control, $p < 0.001$.
RMS, root mean square of angular fluctuations; SampEn, sample entropy of angular fluctuations; MF, mean frequency of angular fluctuations.

Inc., EI Paso, United States) with the ground electrode located along the midline ahead of F_z. For off-line electrooculography (EOG) assessment, two electrodes were placed at the outer canthus of the left and right eyes, and two electrodes were placed infra- and supra-orbitally at the right eye. The impedances of all the electrodes were below 5 kΩ. The EEG data were recorded with a band-pass filter set at 0.1–100 Hz and a sampling rate of 1 kHz. At the same time, angular movements of the stabilometer were registered with an inclinometer (Model FAS-A, LORD MicroStrain, United States), which was fixed on the rational axis of the stabilometer. Synchronized with the scalp EEG system, the angular movements were digitized to 1 kHz with an analog-to-digital converter (Model 6341, National Instruments, United States) controlled by a Labview program (Labview v8.5, National Instruments, United States).

Data analysis

The angular stabilometer movements were first conditioned with a 4th-order low-pass Butterworth filter (cutoff frequency: 6 Hz) and down-sampled to 100 Hz (Michalak et al., 2014). At the behavior level, a set of postural fluctuation sway metrics was derived from the stabilometer movements, including root mean squared (RMS) (degree), mean frequency (MF) (Hz), and sample entropy (SampEn). MF of postural fluctuations was derived from the power spectra of the stabilometer movement, estimated with a fast Fourier transform and the Welch method with a spectral resolution of 0.02 Hz (Figure 1). The MF reflected a spectral shift in postural sway, with higher MF indicating greater stance uncertainty. Postural sway regularity was indexed with SampEn, which is an effective biomarker to index attentional investment in postural control (Donker et al., 2007; Roerdink et al., 2011). The mathematical formula of sample entropy was $SampEn(m, r, N) = -\log(\frac{\sum_{i=1}^{N-m} A_i}{\sum_{i=1}^{N-m} B_i})$, where r = 15% of the standard deviation of the force channel, m is the length of the template ($m = 2$), and N is the number of data points in the time series. A_i is the number of matches of the ith template of length $m + 1$ data points, and B_i is the number of matches of the ith template of length m data points. The values of m and r to calculate COP complexity were identical to the settings of the previous study (Ramdani et al., 2009). Attentional involvement in postural control increases the regularity (or smaller SampEn) of stabilometer movements. The postural variables were analyzed in MATLAB R2019a software (Mathworks, United States). All of the postural variables of the three trials in the SV and control conditions were averaged for each participant.

The EEG data were first filtered between 4 and 35 Hz using a zero-phase finite impulse response (FIR) filter (60 dB/octave) to remove the DC shift and potential contaminations of low-frequency postural sway under 4 Hz. EEG data in the gamma band were not analyzed, as it was susceptible to contamination by neighboring muscle activities (van Lutterveld et al., 2017). Eye blinks in the EEG were corrected with the NeuroScan 4.3 software program (NeuroScan Inc., EI Paso, TX, United States), based on a bipolar vertical EOG channel. The EEG data were segmented into 2-s epochs after the removal of ocular artifacts. Epochs surviving automated artifact rejection were visually inspected by researchers for rejection of undetected artifacts. After that, for the regional activity of the EEG, the spectral power in each epoch was calculated using Fast Fourier Transformation (FFT) with a frequency resolution of 0.2 Hz. Relative power was computed as the ratio of the power of each spectral value to the total power. The power spectra were averaged across epochs for each channel. Based on the pooled relative power, the mean peak amplitude in each sub-band (theta (4–7 Hz), alpha (8–12 Hz), and beta (13–30 Hz)) was obtained across the EEG channels. The regions of interest for various sub-bands (theta (4–7 Hz), alpha (8–12 Hz), and beta (13–30 Hz)) were denoted on the EEG channels, where the sub-band peak amplitudes were significantly different between the SV and control conditions. Three trials of the relative powers of the electrodes in the regions of interest were averaged for the SV and control conditions for all participants. The EEG power spectrum were analyzed in MATLAB R2019a software (Mathworks, United States). In addition to regional activity, we estimated the inter-regional connectivity of the EEG of the 30 electrode pairs from all sub-bands in terms of the phase-lag index (PLI). The PLI quantifies the distribution asymmetry of phase differences in the instantaneous phases of two time-series based on the Hilbert transformation. The PLI is defined thus:

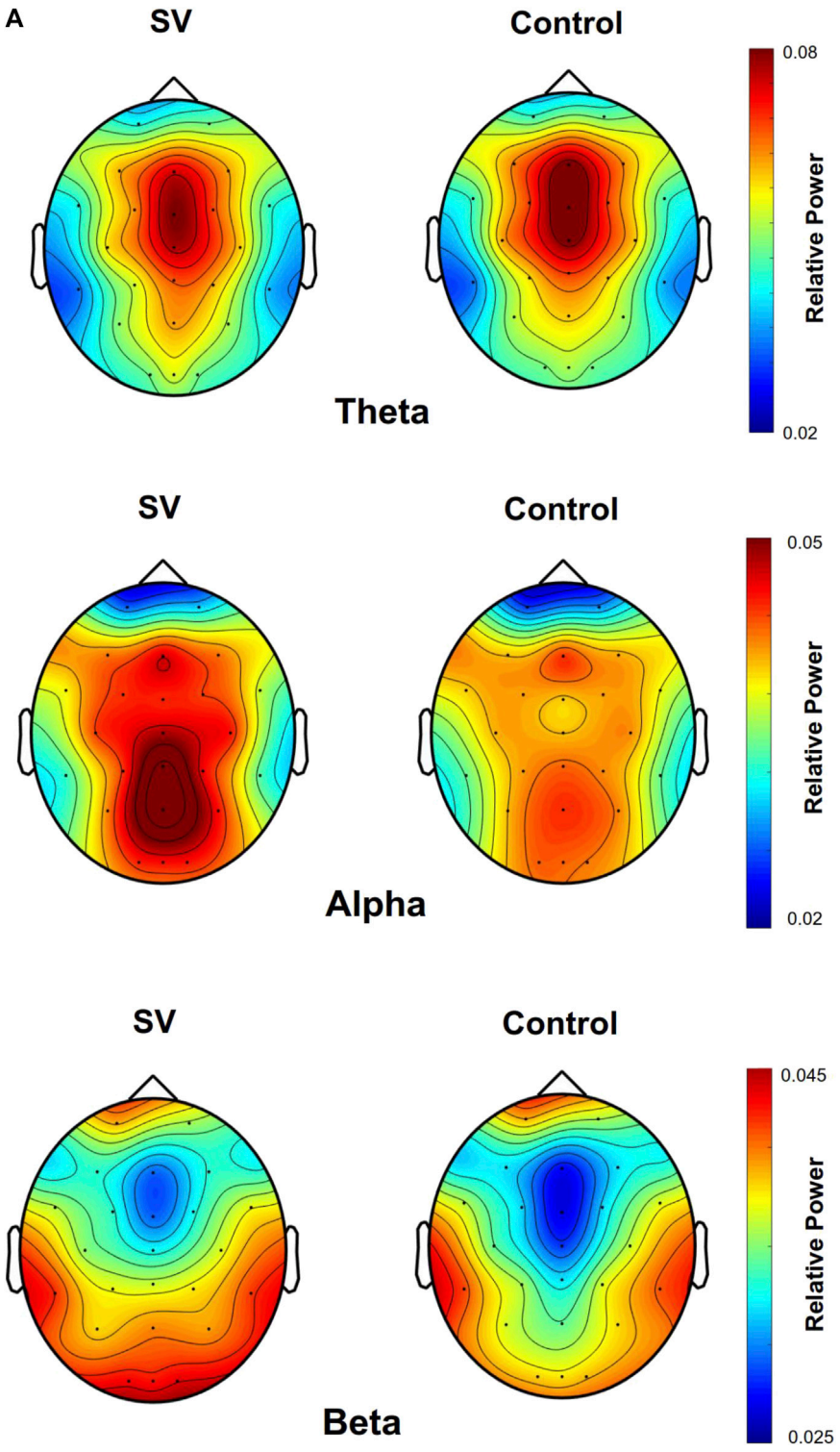

FIGURE 2A
The pooled topological spectral mapping of scalp EEG at the theta (4–7 Hz), alpha (8–12 Hz), and beta bands (13–35 Hz) in the stroboscopic vision (SV) and control conditions. Oscillatory waves in the theta and alpha bands are most evident in the mid-frontal and parietal-occipital areas, respectively. Beta oscillation is most evident in the mid-frontal and bilateral temporal areas in the control condition. Relative powers of theta, alpha, and beta bands are selectively tuned to stroboscopic vision.

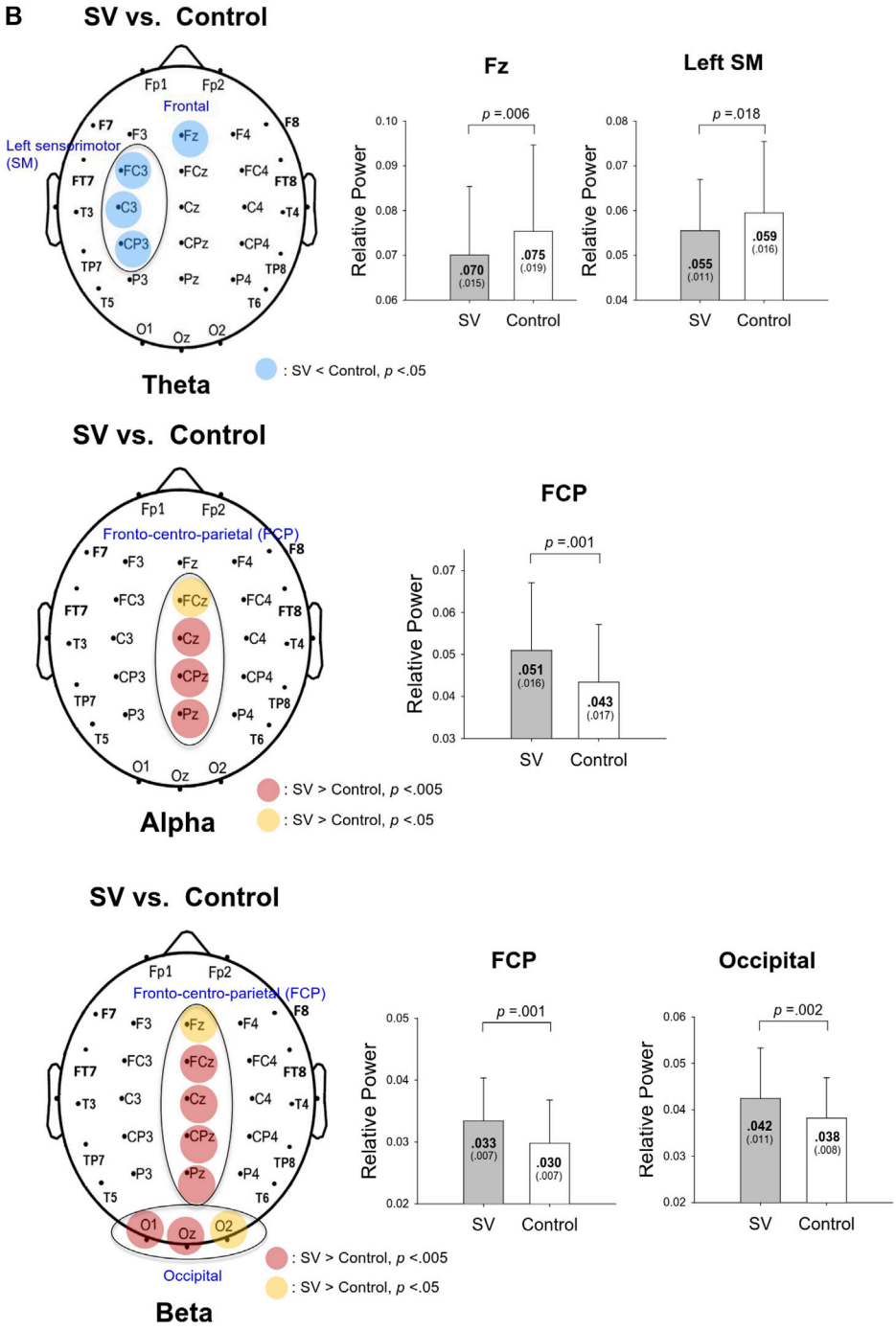

FIGURE 2B
Schematic illustration of the SV-induced changes in the relative power of scalp electrodes for the theta (top), alpha (middle), and beta (bottom) bands. The right subplots of **(B)** contrast the mean relative powers at various spectral bands in the regions of interest between the SV and control conditions. A warm color indicates greater regional activity in the SV condition than in the control condition. A cold color indicates smaller regional activity in the SV condition than in the control condition.

$PLI = |E\{sgn(\Delta\varphi(t))\}|$, where $\varphi(t)$ is the phase difference and *sgn* is a function that extracts the sign of a real number. PLI was used because it is relatively immune to volume conduction and common source noises (Stam et al., 2007). A square 30 × 30 PLI adjacent matrix for the SV and control conditions was obtained after the computation of the PLI across all electrode pairs. The

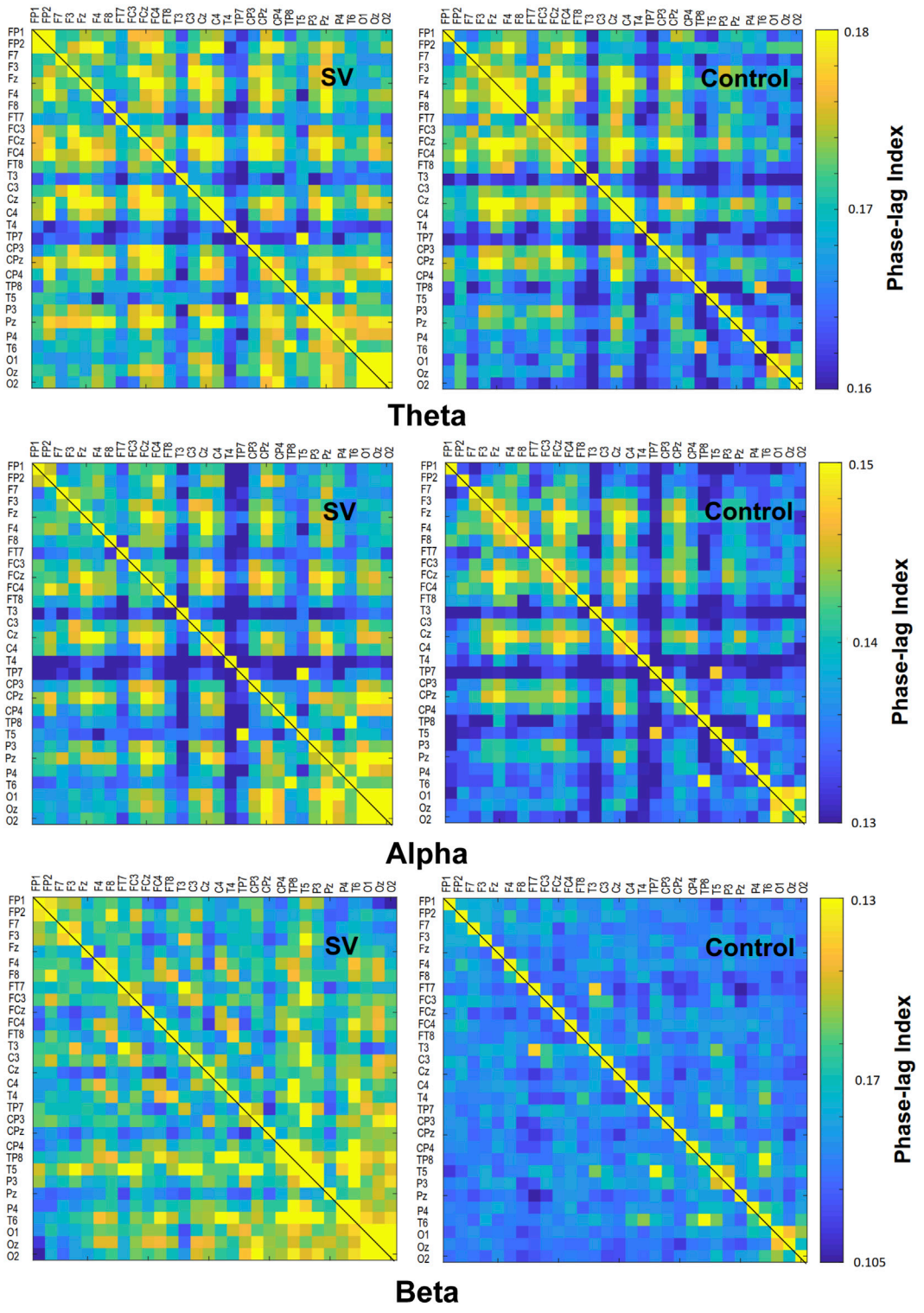

FIGURE 3
The adjacent matrices of t values contrasting the phase-lag index (PLI) values of all electrode pairs in the theta (4–7 Hz), alpha (8–12 Hz), and beta (13–35 Hz) bands between the SV and control conditions. A contrasting wiring diagram on the scalp shows the topological distributions of the supra-threshold connectivity tuned to stroboscopic vision (SV vs. Control) ($|t| > 2.898$, $p < 0.005$). (Red line: SV > Control, $p < 0.005$; Blue line: SV < Control, $p < 0.005$)

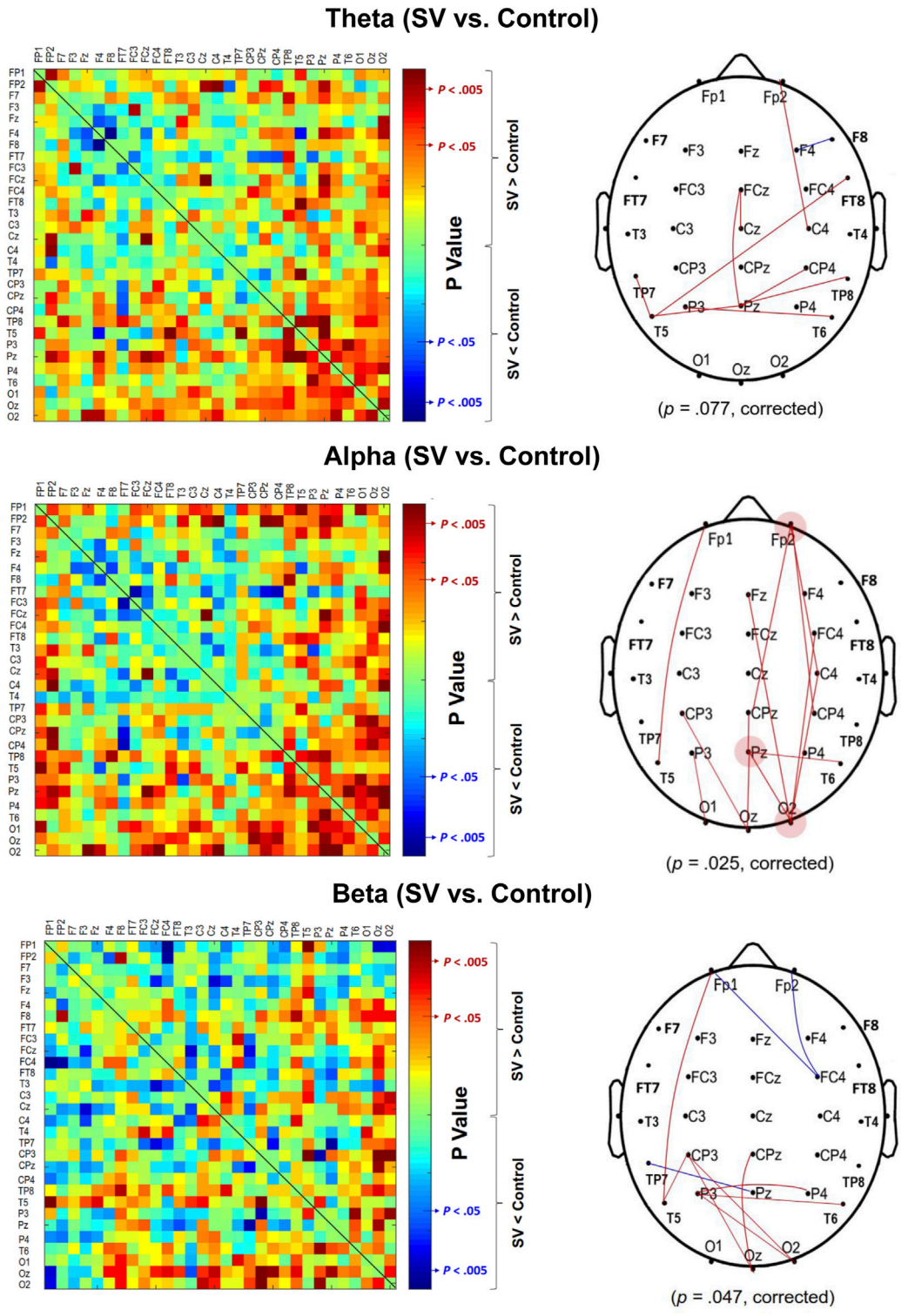

FIGURE 4
The phase-lag index (PLI) adjacent matrices represent the averaged strengths of inter-regional connectivity of the theta (4–7 Hz), alpha (8–12 Hz), and beta (13–35 Hz) bands between the SV and control conditions.

TABLE 2 Pearson's correlation between changes in regional spectral activity and stabilometer dynamics due to stroboscopic vision. The black-bolded fonts in the shaded areas indicate significant correlations of regional activity and postural sway dynamics.

Pearson's	ND-theta		ND-alpha	ND-beta	
Correlation (n = 35)	Mid-frontal	Left sensorimotor	Fronto-centro-parietal	Fronto-centro-parietal	Occipital
ND-RMS	**r = 0.355, p =0.035**	r = 0.171, p =0.326	r = −0.147, p =0.398	r = −0.263, p =0.126	r = 0.065, p =0.711
ND-SampEn	r = −0.135, p =0.349	r = −0.050, p =0.744	r = 0.025, p =0.885	r = −0.018, p = 0.918	r = 0.105, p =0.548
ND-MF	r = −0.194, p =0.265	r = −0.096, p =0.583	r = −0.096, p =0.596	r = 0.033, p =0.583	r = 0.006, p =0.972

ND, normalized differences; RMS, root mean square of angular fluctuations; MF, mean frequency of angular fluctuations; SampEn, sample entropy of angular fluctuations.

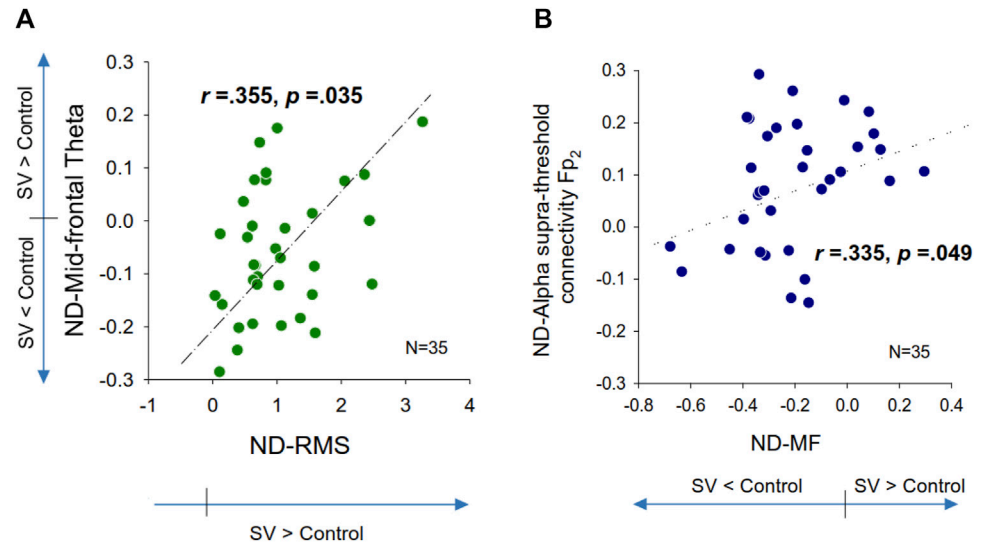

FIGURE 5
Scatter plots of normalized differences (ND) in EEG variables and normalized differences in postural fluctuation variables that are significantly correlated. **(A)** ND in mid-frontal theta vs. ND in root mean square of postural fluctuations, **(B)** ND in supra-threshold connectivity of Fp_2 in the alpha band vs. ND in mean frequency (MF) of postural fluctuations.

PLI-based functional connectivity was calculated with the HERMES function in Matlab (Niso et al., 2013).

Statistical analysis

EEG variables and the postural variables in the three experimental trials in the SV and control conditions were averaged for each subject. Hotelling's T-squared statistics were used to examine the intermittent visual effect (SV vs. control) on the postural fluctuation characteristics (RMS, MF, and SampEn). The post-hoc test for the postural variables was a paired t-test using Bonferroni correction. For EEG variables of regional activity, paired t-test was used to contrast differences in the pooled relative powers of each sub-band for the EEG channels in the regions of interest between the SV and control conditions. The strength of each connection within the PLI adjacent matrix in the SV and control conditions was first examined with a two-sample t-test. A set of supra-threshold edges ($|t_{34}| > 2.728$, $p <$ 0.005) was extracted to highlight the differences in topological distributions between the SV and control conditions. This identified all possible connected components, or subnetworks, in the matrix at this uncorrected level. In the framework of network statistics, a permutation test was performed 5,000 times to examine variations in the null distribution of the supra-threshold connectivity between the SV and control conditions. Methodological details of corrected network-based statistics were documented in the work of Zalesky et al. (2010). In fact, SV enhanced or suppressed the supra-threshold connectivity. For various EEG sub-bands [theta (4–7 Hz), alpha (8–12 Hz), and beta (13–30 Hz)], we further

TABLE 3 Pearson's correlation between changes in supra-threshold inter-regional coupling of spectral bands/key-nodes and stabilometer dynamics. Pearson's correlation between changes in supra-threshold inter-regional functional coupling ($p < 0.005$) of various spectral bands and postural sway dynamics due to stroboscopic vision. The numbers within parentheses are the edge number of each key node. The black-bolded and grey-bolded fonts in the shaded areas indicate significant and marginally-significant correlations of regional activity and postural sway dynamics, respectively.

Pearson's	ND-supra-threshold edge (theta)		ND-supra-threshold edge (alpha)	ND- ND-supra-threshold edge (beta)	
Correlation (n = 35)	Enhancement	Suppression	Enhancement	Enhancement	Suppression
ND-RMS	r = −0.041, p = 0.813	r = 0.276, p = 0.109	r = −0.220, p = 0.203	r = −0.089, p = 0.610	r = 0.234, p =0.177
ND-SampEn	r = 0.069, p = 0.693	r = −0.180, p = 0.299	r = 0.207, p = 0.232	r = 0.054, p = 0.756	r = 0.053, p =0.763
ND-MF	r = −0.059, p = 0.737	r = −0.216, p = 0.213	**r = 0.307, p = 0.073**	r = 0.236, p = 0.172	r = −0.072, p =0.680

ND, normalized differences.

TABLE 4 Pearson's correlation between changes in supra-threshold inter-regional coupling of spectral bands/key-nodes and stabilometer dynamics. Pearson's correlation between increases in supra-threshold inter-regional functional coupling of key nodes (O2, Pz, and Fp2) of alpha-band and postural sway dynamics due to stroboscopic vision. The numbers within parentheses are the edge number of each key node. The black-bolded and grey-bolded fonts in the shaded areas indicate significant and marginally-significant correlations of regional activity and postural sway dynamics, respectively.

Pearson's	ND-supra-threshold edge (alpha)		
Correlation (n = 35)	O2 (5)	Pz (4)	Fp2 (3)
ND-MF	r = 0.154, p = 0.378	r = 0.173, p = 0.320	**r = 0.335, p = 0.049**

ND, normalized differences.

calculated the mean PLI for the supra-threshold connectivity of the electrode pairs that exhibited greater connectivity strengths (SV > control) and smaller connectivity strengths (SV < control). Pearson's correlation was performed to examine the significance of correlations between the normalized differences (ND) in postural sway metrics between the SV and control conditions [(SV-control)/control)] and the ND in variations in sub-band regional activities/inter-regional connectivity. The level of significance was 0.05. Data are presented as group means ± standard deviation. All statistical analyses were performed in IBM SPSS Statistics (v.19).

Results

Table 1 shows the results of Hotelling's T-squared statistics comparing the postural fluctuation variables between the SV and control conditions during stabilometer stance. The postural fluctuation variables differed significantly with and without intermittent vision (Wilks' Λ = 0.287, $p < 0.001$). Post-hoc analysis revealed that intermittent vision led to greater RMS ($p < 0.001$), smaller SampEn ($p < 0.001$), and MF ($p < 0.001$) of postural fluctuations than full vision did.

The contrast of pooled topological distributions of the relative powers of the theta (4–7 Hz), alpha (8–12 Hz), and beta (13–35 Hz) waves between the SV and control conditions during stabilometer stance is shown in Figure 2A. The theta power was the most evident in the mid-frontal areas. A pronounced alpha wave was noted in the posterior part of the cortex (especially the parietal–occipital area). Stronger beta power was noted in the prefrontal and bilateral temporal areas. There was visible modulation of the spatial distribution of the EEG relative power with intermittent vision. Figure 2B summarizes the results of paired t tests to contrast the relative EEG powers of the theta, alpha, and beta bands at each electrode between the SV and control conditions. The theta power was smaller in the F_z (t_{34} = 2.938, p =0.006) and left sensorimotor areas (FC_3, C_3, and CP_3) ($p < 0.05$) for the SV condition (Figure 2B, top). The average relative power of three electrodes in the left sensorimotor area in the SV condition was smaller than that in the control condition (t_{34} = 2.494, p =0.018). The relative alpha power in the fronto-centro-parietal (FCP) area (FC_z, C_z, CP_z, and P_z) was enhanced with intermittent vision (Figure 2B middle). The mean relative alpha power of the electrodes in the regions of interest for the SV condition was greater than that for the control condition (t_{34} = -3.781,

p =0.001). The relative beta power in the fronto-centro-parietal (FCP) area (F_z, FC_z, C_z, CP_z, and P_z) and occipital area (O_1, O_2, and O_z) was also mediated by intermittent vision (Figure 2B, bottom). The mean relative powers of the electrodes of the FCP area (t_{34} = −3.559, p =0.001) and occipital area in the SV condition (t_{34} = −3.347, p =0.002) were greater than those in the control condition.

The contrast of the pooled PLI of EEG–EEG electrode pairs of the theta (4–7 Hz), alpha (8–12 Hz), and beta (13–35 Hz) waves between the SV and control conditions during stabilometer stance is shown in Figure 3. The inter-regional functional connectivity during stabilometer stance is represented with PLI values. The adjacent matrix of t-values in the left plots of Figure 4 describes the differences in PLI for all electrode pairs between the SV and control conditions at various sub-bands. According to the significance of the t-values, the supra-threshold connectivity ($|t_{34}| > 2.728$, $p < 0.005$) of the theta, alpha, and beta bands was labeled on the scalp map (Figure 4, right plots). The supra-threshold connectivity highlighted the most evident changes in connectivity strength due to intermittent vision in older adults. For the theta band, SV mainly potentiated a few connections in the centro-parietal-temporal area and suppressed functional connectivity between F_4 and F_8 (Figure 4, upper right). For the alpha band, all supra-threshold connectivity was enhanced with SV (Figure 4, middle right). The results of corrected network-based statistics indicated that SV could significantly affect the EEG–EEG network of the alpha (p = 0.025, corrected) and beta (p = 0.047, corrected) bands during stabilometer stance. The EEG–EEG network in the theta band was marginally tuned to SV (p = 0.077, corrected). SV potentiated supra-threshold connectivity of the theta band, except for that of the F_4–F_8 pair, which was suppressed with SV.

Table 2 summarizes the Pearson's correlations between normalized changes in regional activity and postural sway dynamics due to SV. Notably, there was a significant correlation between SV-dependent differences in the mid-frontal theta rhythm (ND-Theta, Frontal) and ND-RMS of postural fluctuations (r = 0.355, p = 0.035) (Figure 5A). Besides that, changes in EEG regional activity were not significantly correlated to other postural sway dynamics ($p > 0.05$). Table 3 summarizes the Pearson's correlations between normalized increases/decreases in supra-threshold EEG–EEG connectivity of various bands and postural sway dynamics due to SV. On account of a marginally significant correlation between ND enhancement of supra-threshold connectivity of the alpha band and the ND-MF of postural fluctuations (r = 0.307, p = 0.073), a further detailed correlation analysis was performed with consideration of the ND enhancement of the supra-threshold connectivity of the alpha band from the three key nodes (O_2, P_z, and Fp_2) (Table 4; Figure 5B). In addition, ND-MF of postural fluctuations was positively correlated with supra-threshold connectivity from Fp_2 in the alpha band (r = 0.335, p = 0.049) (Table 4; Figure 5B).

Discussion

Stroboscopic visual disruption led to changes in neuromechanical control of the elderly on the stabilometer stance, in light of variations in postural fluctuation dynamics, EEG regional activity, and EEG–EEG connectivity. Relative to full-vision, SV impaired postural stability, with smaller MF and SampEn of postural fluctuations in stabilometer stance. Notably, a decline in the mid-frontal (F_z) theta oscillation and enhancement of the supra-threshold connectivity of Fp_2 in the alpha band were correlated to SV-related changes in postural fluctuation dynamics. This study is the first to demonstrate evidence of potential postural training to reweigh sensory channels with stroboscopic vision for older adults on an uneven surface.

Stroboscopic vision-dependent variations in postural strategy

Compared to quiet stance, stabilometer stance with additional mechanical constraints varies the available sensory information and amplifies the motor command to master balance skills (Rougier et al., 2012). Stabilometer stance is commonly used to train posture control in rehabilitation clinics. Stroboscopic vision is hypothesized to be a sensory reweighting approach by reducing visual feedback (Isableu et al., 2003; Kim et al., 2020). In agreement with previous studies (Kim et al., 2020; Wohl et al., 2021; Han et al., 2022), the increment of postural fluctuation size (Table 1) suggested that the intermittent vision feedback added to balance difficulty, because of the reduction in the availability of visual input for the older adults who favor the utilization of visual information to ensure the visuospatial demands of a posture task (Woollacott et al., 1986; McChesney and Woollacott, 2000). In addition, the SV varied postural strategy, in support of declines in mean frequency and sample entropy of postural fluctuations (Table 1). The hypothesis of intermittent motor control (Miall et al., 1993) posited that postural fluctuations stem from superimposition of centrally-scaled pulse elements to tune postural responses that deviate

from the target goal. Central to this interpretation is that the older adults with SV reduced the number of corrective attempts (or reduced the frequency of motor explorations) for postural corrections (Paillard and Noe, 2015; Tsai et al., 2018; Chen et al., 2021b). According to the minimum entropy principle (Hur et al., 2019), postural fluctuations of lower entropy are less automatic due to more volitional efforts being invested in postural control (Borg and Laxaback, 2010; Roerdink et al., 2011). A low-entropy postural response is commonly seen in subjects with balance dysfunction (e.g., aged people and patients with neurological disorders) (Morrison and Newell, 2015). Hence, SV appeared to increase attentive control over the stabilometer stance in older adults. Collectively, the characteristic changes in postural fluctuations with SV were not fully compatible with the argument that greater demand is placed on visual–spatial attention with increasing motion explorations, as predicted by Hülsdünker et al. (2021). However, the behavioral observations are also not adequate to support the hypothesis of sensory reweighting for postural regulation with SV (Kim et al., 2017; Kim et al., 2020). The debates regarding SV impacts cannot be well-reconciled with the present behavioral findings.

Stroboscopic vision-dependent modulation of EEG regional activity

In line with the postural fluctuations, SV led to wide-range alterations in local EEG in the theta, alpha, and beta bands (Figure 2A). First, SV suppressed the theta power in the mid-frontal (F_z) and left sensorimotor areas (FC_3, C_3, and CP_3) (Figure 2B, top). The mid-frontal theta oscillation, which originated from the anterior cingulate cortex, plays an important role in error elaboration and task optimization (Cavanagh et al., 2012; Pezzetta et al., 2018). When visual errors are large, mid-frontal theta power is potentiated due to unintended consequences on performance (Cavanagh et al., 2012). Previous researches showed that mid-frontal theta power is involved with the organization of goal-directed movements and postural balance maintenance (Hulsdunker et al., 2015; Malcolm et al., 2021). When a subject was guided by visual feedback during stabilometer stance, the mid-frontal theta power was enhanced to elaborate worse outcomes even though the visualized errors were faked (Chen et al., 2022). In this study, the smaller mid-frontal theta oscillation in the SV condition (Figure 2B, top) implied that fewer error contexts were perceived by the older adults with intermittent blocking of visual feedback. Correlation analysis further suggested a positive correlation between the normalized difference in theta power and the normalized difference in the RMS of the postural fluctuations (Table 2; Figure 5A). For older adults with SV, those who demonstrated greater negative ND-theta (or smaller mid-frontal theta power in the SV condition) tended to have smaller SV-induced increases in postural fluctuations (smaller postural fluctuations in the SV condition) during stabilometer stance (Figure 5A). Hence, under the condition of SV, better prediction of postural errors (or fewer unexpected visual consequences of postural performance) is a prerequisite to gaining superior stance stability, which should be achieved by compensatory upregulation of proprioceptive/vestibular inputs and a reduction of the reliance on intermittent visual feedback (Wilkins and Appelbaum, 2020; Wohl et al., 2021). Balance-related increases in theta activity could also extend to the centro-parietal regions, which are involved in sensorimotor coordination for multi-segment movements (Sipp et al., 2013). In fact, we also noted a global decrease in theta power in the left sensorimotor area with SV during stabilometer stance (Figure 2B, top), although modulation of the theta power was not significantly related to changes in postural strategy (Table 2). The decrease in the theta power of the sensorimotor area likely resulted from SV-related interference in updating of motor plans with incoming visual information, as the theta power of the area emerges during active goal-seeking behaviors (Landfield et al., 1972; Caplan et al., 2003).

Tuned to visual availability, alpha power (8–12 Hz) activity is the most prominent feature in the posterior brain (Mierau et al., 2017; Chen et al., 2021b). According to the cortical idling hypothesis, increases in alpha activity over the sensorimotor area are related to sluggish execution of movements (Pfurtscheller et al., 1996). Analogous to visual occlusion in upright stance (Goh et al., 2016), the intermittent visual feedback also brought about marked augmentation of the alpha power in the sensorimotor regions during stabilometer stance (Figure 2B, middle), in relation to less visuospatial attention for postural tracking (Chen et al., 2022). The EEG observation supported that visual reliance during stabilometer stance was downregulated by SV.

For older adults, the beta power in the fronto-centro-parietal and occipital areas was also potentiated with SV (Figure 2B, bottom). The increase in beta power with SV resembles that in the work of Peterson and Ferris (2018), who reported an increase in the occipito-parietal activity of beta power due to visual rotation during standing (Peterson and Ferris, 2018). As posterior beta oscillations were enhanced with eye closure (Tse et al., 2013), the beta potentiation with SV was likely due to the fact that the older adults sustained efforts to reweight non-visual information for stance stabilization in a situation of perceptual conflict (Lin et al., 2021). However, variations in the regional activity of the alpha and beta bands were not directly causal to the modulation of postural strategies with SV (Table 2).

Stroboscopic vision-dependent modulation of EEG inter-regional activity

The modulation of postural strategies with SV tends to link with the enhancement of the suprathreshold connectivity in the alpha band (Tables 3, 4), which largely overlapped with the visual dorsal and frontal–occipital loops in the right hemisphere (Figure 4, middle right). For visual search (Pantazatos et al., 2012) and the perception of complex movements (Hipp et al., 2011), the large-scale fronto-parieto-occipital connectivity is responsible for multi-sensorimotor integration of body part location and decision making (Grol et al., 2007). Especially for older adults, visual inputs are keyed to cue usage during an unstable human stance (Mierau et al., 2017; Chen et al., 2021b). There are preliminary indications that the dorsal stream is involved with the cognitive aspect of posture control under visual guidance (Takakusaki, 2017), such as analyzing movements in space and updating the motor cortex about the extra-personal space and the internal state (Raffi and Piras, 2019). Our results can be interpreted within this context. The higher alpha supra-threshold connectivity with SV could indicate stronger inhibition of the dorsal visual stream, because intermittent visual feedback was expected to interfere with the sustenance of visuospatial attention and error perception from online visual feedback. In particular, SV significantly added to stronger alpha connectivity of C_4–Fp_2, CP_z–Fp_2, and CP_4–Fp_2, positively linked to MF of postural fluctuations (Table 4; Figure 5B). It is known that the prefrontal cortex receives reciprocal projections from various regions, such as the premotor cortex, basal ganglia, cerebellum, and thalamus (Leh et al., 2007). Associated with enhanced activation in the supplementary motor area (SMA) and the right posterior parietal cortex, right prefrontal involvement is relevant to gaze adjustments, dynamic representation of the body schema (Pellijeff et al., 2006), and adequate allocation of visuospatial attention (Mihara et al., 2008), in preparation for a forthcoming postural perturbation. This context speaks for a positive association between SV-induced enhancement of the supra-threshold connectivity of Fp_2 in the alpha band and increases in ND-MF (Figure 5B). The older adults with SV might down-weighed the visual channel and exhibited a high level of postural uncertainty, in that non-visual channels [such as the proprioceptive system (Lord et al., 1994)] more affected by aging could not fully compensate for the fractional impairment of the partially-blocked visual system.

One methodological concern of this study is to interpret the present data with joint effects of physical SV and SV-induced eye blinks. The number of eye blink in an experimental trial could increase in the SV condition. However, it is hard to distinguish those eye blinks exactly causal to the wearing of the stroboscopic glasses and natural eye blinks occurring roughly at a rate of 12 blinks/min (Bentivoglio et al., 1997). Despite the methodological concern, the wearing of the stroboscopic glasses substantially mediated posture sway dynamics and cortical responses during unstable stance for the elderly.

Conclusion

Within the context of neuromechanics, the present study suggests a role for sensory reweighting with the use of stroboscopic vision for older adults during unstable stance. The changes in postural fluctuation dynamics reveals that stroboscopic vision leads to greater stance difficulty for older adults with less complex postural responses. Mid-frontal theta oscillation declines indicate fewer error contexts are perceived and corrected by the older adults due to intermittent blocking of the visual information. The selective increases in the EEG–EEG connectivity of Fp_2 in the alpha band reflect inhibitions of visuospatial attention and functioning of the dorsal visual stream during an uneven stance. These EEG signatures explain the experimentally observed stance destabilization and postural strategy changes with greater regularity in older adults with stroboscopic vision. The corresponding cortical reorganization supports stroboscopic vision as a therapeutic approach in favor of non-visual channels for postural control of the elderly.

Data availability statement

The datasets presented in this article are not readily available because Data cannot be shared as participants were informed that their data would be stored confidentially, in accordance with the rules of the local ethics committee. Code to generate the EEG metrics is available under reasonable request. Requests to access the datasets should be directed to I-SH, ensureh@gmail.com.

Ethics statement

The studies involving human participants were reviewed and approved by the National Cheng Kung University Hospital (A-ER-107-099-T). The patients/participants provided their written informed consent to participate in this study.

Author contributions

I-SH was responsible for the study design, data analysis, and overall supervision. Y-YT participated in the study design and interpretation of the results and took the lead in writing the manuscript. Y-CC participated in the study design, statistical

analysis, and the interpretation of the results. C-GZ collected data.

Funding

This research was supported by grants from the Ministry of Science and Technology, Taiwan, R.O.C. (MOST 108-2314-B-006-071) and (109-2314-B-006 -029-MY2).

Acknowledgments

We thank all participants that took part in this study for their time.

Conflict of interest

The authors declare that the research was conducted in the absence of any commercial or financial relationships that could be construed as a potential conflict of interest.

Publisher's note

All claims expressed in this article are solely those of the authors and do not necessarily represent those of their affiliated organizations, or those of the publisher, the editors and the reviewers. Any product that may be evaluated in this article, or claim that may be made by its manufacturer, is not guaranteed or endorsed by the publisher.

References

Appelbaum, L. G., Schroeder, J. E., Cain, M. S., and Mitroff, S. R. (2011). Improved visual cognition through stroboscopic training. *Front. Psychol.* 2, 276. doi:10.3389/fpsyg.2011.00276

Appelbaum, L. G., Cain, M. S., Schroeder, J. E., Darling, E. F., and Mitroff, S. R. (2012). Stroboscopic visual training improves information encoding in short-term memory. *Atten. Percept. Psychophys.* 74 (8), 1681–1691. doi:10.3758/s13414-012-0344-6

Ballester, R., Huertas, F., Uji, M., and Bennett, S. J. (2017). Stroboscopic vision and sustained attention during coincidence-anticipation. *Sci. Rep.* 7 (1), 17898. doi:10.1038/s41598-017-18092-5

Bennett, S. J., Hayes, S. J., and Uji, M. (2018). Stroboscopic vision when interacting with multiple moving objects: Perturbation is not the same as elimination. *Front. Psychol.* 9, 1290. doi:10.3389/fpsyg.2018.01290

Bentivoglio, A. R., Bressman, S. B., Cassetta, E., Carretta, D., Tonali, P., and Albanese, A. (1997). Analysis of blink rate patterns in normal subjects. *Mov. Disord.* 12 (6), 1028–1034. doi:10.1002/mds.870120629

Borg, F. G., and Laxåback, G. (2010). Entropy of balance - some recent results. *J. NeuroEngineering Rehabil.* 7, 38. doi:10.1186/1743-0003-7-38

Bugnariu, N., and Fung, J. (2007). Aging and selective sensorimotor strategies in the regulation of upright balance. *J. NeuroEngineering Rehabil.* 4 (1), 19. doi:10.1186/1743-0003-4-19

Caplan, J. B., Madsen, J. R., Schulze-Bonhage, A., Aschenbrenner-Scheibe, R., Newman, E. L., and Kahana, M. J. (2003). Human θ oscillations related to sensorimotor integration and spatial learning. *J. Neurosci.* 23 (11), 4726–4736. doi:10.1523/jneurosci.23-11-04726.2003

Cavanagh, J. F., Figueroa, C. M., Cohen, M. X., and Frank, M. J. (2012). Frontal theta reflects uncertainty and unexpectedness during exploration and exploitation. *Cereb. Cortex* 22 (11), 2575–2586. doi:10.1093/cercor/bhr332

Chen, Y. C., Chou, Y. C., and Hwang, I. S. (2021a). Reliance on visual input for balance skill transfer in older adults: EEG connectome analysis using minimal spanning tree. *Front. Aging Neurosci.* 13, 632553. doi:10.3389/fnagi.2021.632553

Chen, Y. C., Huang, C. C., Zhao, C. C., and Hwang, I. S. (2021b). Visual effect on brain connectome that scales feedforward and feedback processes of aged postural system during unstable stance. *Front. Aging Neurosci.* 13, 679412. doi:10.3389/fnagi.2021.679412

Chen, Y. C., Tsai, Y. Y., Chang, G. C., and Hwang, I. S. (2022). Cortical reorganization to improve dynamic balance control with error amplification feedback. *J. NeuroEngineering Rehabil.* 19 (1), 3. doi:10.1186/s12984-022-00980-1

Donker, S. F., Roerdink, M., Greven, A. J., and Beek, P. J. (2007). Regularity of center-of-pressure trajectories depends on the amount of attention invested in postural control. *Exp. Brain Res.* 181 (1), 1–11. doi:10.1007/s00221-007-0905-4

Franz, J. R., Francis, C. A., Allen, M. S., O'Connor, S. M., and Thelen, D. G. (2015). Advanced age brings a greater reliance on visual feedback to maintain balance during walking. *Hum. Mov. Sci.* 40, 381–392. doi:10.1016/j.humov.2015.01.012

Goh, K. L., Morris, S., Lee, W. L., Ring, A., and Tan, T. (2016). Visual transparent & visual occlusion: An EEG and COP study. *Annu. Int. Conf. IEEE Eng. Med. Biol. Soc.* 2016, 829–832. doi:10.1109/EMBC.2016.7590829

Grol, M. J., Majdandzic, J., Stephan, K. E., Verhagen, L., Dijkerman, H. C., Bekkering, H., et al. (2007). Parieto-frontal connectivity during visually guided grasping. *J. Neurosci.* 27 (44), 11877–11887. doi:10.1523/JNEUROSCI.3923-07.2007

Grooms, D. R., Appelbaum, G., and Onate, J. (2015). Neuroplasticity following anterior cruciate ligament injury: A framework for visual-motor training approaches in rehabilitation. *J. Orthop. Sports Phys. Ther.* 45 (5), 381–393. doi:10.2519/jospt.2015.5549

Grooms, D. R., Chaudhari, A., Page, S. J., Nichols-Larsen, D. S., and Onate, J. A. (2018). Visual-motor control of drop landing after anterior cruciate ligament reconstruction. *J. Athl. Train.* 53 (5), 486–496. doi:10.4085/1062-6050-178-16

Han, S., Lee, H., Son, S. J., and Hopkins, J. T. (2022). The effects of visual feedback disruption on postural control with chronic ankle instability. *J. Sci. Med. Sport* 25 (1), 53–57. doi:10.1016/j.jsams.2021.07.014

Hipp, J. F., Engel, A. K., and Siegel, M. (2011). Oscillatory synchronization in large-scale cortical networks predicts perception. *Neuron* 69 (2), 387–396. doi:10.1016/j.neuron.2010.12.027

Hülsdünker, T., Mierau, A., Neeb, C., Kleinöder, H., and Strüder, H. K. (2015). Cortical processes associated with continuous balance control as revealed by EEG spectral power. *Neurosci. Lett.* 592, 1–5. doi:10.1016/j.neulet.2015.02.049

Hülsdünker, T., Gunasekara, N., and Mierau, A. (2021). Short- and long-term stroboscopic training effects on visuomotor performance in elite youth sports. Part 2: Brain-behavior mechanisms. *Med. Sci. Sports Exerc* 53 (5), 973–985. doi:10.1249/MSS.0000000000002543

Hur, P., Pan, Y. T., and DeBuys, C. (2019). Free energy principle in human postural control system: Skin stretch feedback reduces the entropy. *Sci. Rep.* 9 (1), 16870. doi:10.1038/s41598-019-53028-1

Isableu, B., Ohlmann, T., Crémieux, J., and Amblard, B. (2003). Differential approach to strategies of segmental stabilisation in postural control. *Exp. Brain Res.* 150 (2), 208–221. doi:10.1007/s00221-003-1446-0

Kim, K. M., Kim, J. S., and Grooms, D. R. (2017). Stroboscopic vision to induce sensory reweighting during postural control. *J. Sport Rehabil.* 26 (5). doi:10.1123/jsr.2017-0035

Kim, K. M., Kim, J. S., Oh, J., and Grooms, D. R. (2021). Stroboscopic vision as a dynamic sensory reweighting alternative to the sensory organization test. *J. Sport Rehabil.* 30 (1), 166–172. doi:10.1123/jsr.2019-0466

Kim, K. M., Estudillo-Martínez, M. D., Castellote-Caballero, Y., Estepa-Gallego, A., and Cruz-Díaz, D. (2021). Short-term effects of balance training with stroboscopic vision for patients with chronic ankle instability: A single-blinded randomized controlled trial. *Int. J. Environ. Res. Public Health* 18 (10), 5364. doi:10.3390/ijerph18105364

Kroll, M., Preuss, J., Ness, B. M., Dolny, M., and Louder, T. (2020). Effect of stroboscopic vision on depth jump performance in female NCAA Division I volleyball athletes. *Sports Biomech.*, 1–11. doi:10.1080/14763141.2020.1773917

Landfield, P. W., McGaugh, J. L., and Tusa, R. J. (1972). Theta rhythm: A temporal correlate of memory storage processes in the rat. *Science* 175 (4017), 87–89. doi:10.1126/science.175.4017.87

Lee, H., Han, S., Page, G., Bruening, D. A., Seeley, M. K., and Hopkins, J. T. (2021). Effects of balance training with stroboscopic glasses on postural control in chronic ankle instability patients. *Scand. Med. Sci. Sports* 32, 576–587. doi:10.1111/sms.14098

Leh, S. E., Ptito, A., Chakravarty, M. M., and Strafella, A. P. (2007). Fronto-striatal connections in the human brain: A probabilistic diffusion tractography study. *Neurosci. Lett.* 419 (2), 113–118. doi:10.1016/j.neulet.2007.04.049

Lin, C. L., Hsieh, Y. W., and Chen, H. Y. (2021). Age-related differences in alpha and beta band activity in sensory association brain areas during challenging sensory tasks. *Behav. Brain Res.* 408, 113279. doi:10.1016/j.bbr.2021.113279

Lord, S. R., Ward, J. A., Williams, P., and Anstey, K. J. (1994). Physiological factors associated with falls in older community-dwelling women. *J. Am. Geriatr. Soc.* 42 (10), 1110–1117. doi:10.1111/j.1532-5415.1994.tb06218.x

Malcolm, B. R., Foxe, J. J., Joshi, S., Verghese, J., Mahoney, J. R., Molholm, S., et al. (2021). Aging-related changes in cortical mechanisms supporting postural control during base of support and optic flow manipulations. *Eur J Neurosci.* 54 (12), 8139–8157. doi:10.1111/ejn.15004

Manor, B., Costa, M. D., Hu, K., Newton, E., Starobinets, O., Kang, H. G., et al. (2010). Physiological complexity and system adaptability: Evidence from postural control dynamics of older adults. *J. Appl. Physiology (1985)* 109 (6), 1786–1791. doi:10.1152/japplphysiol.00390.2010

McChesney, J. W., and Woollacott, M. H. (2000). The effect of age-related declines in proprioception and total knee replacement on postural control. *Journals Gerontology Ser. A Biol. Sci. Med. Sci.* 55 (11), M658–M666. doi:10.1093/gerona/55.11.m658

Miall, R. C., Weir, D. J., and Stein, J. F. (1993). Intermittency in human manual tracking tasks. *J. Mot. Behav.* 25 (1), 53–63. doi:10.1080/00222895.1993.9941639

Michalak, K. P., Przekoracka-Krawczyk, A., Nawrot, P., Woźniak, P., and Vieregge, P. (2014). The filtering of the posturographic signals shows the age related features. *Sci. World J.* 2014, 1–9. doi:10.1155/2014/403893

Mierau, A., Pester, B., Hülsdünker, T., Schiecke, K., Strüder, H. K., and Witte, H. (2017). Cortical correlates of human balance control. *Brain Topogr.* 30 (4), 434–446. doi:10.1007/s10548-017-0567-x

Mihara, M., Miyai, I., Hatakenaka, M., Kubota, K., and Sakoda, S. (2008). Role of the prefrontal cortex in human balance control. *Neuroimage* 43 (2), 329–336. doi:10.1016/j.neuroimage.2008.07.029

Moon, S., Huang, C. K., Sadeghi, M., Akinwuntan, A. E., and Devos, H. (2021). Proof-of-Concept of the virtual reality comprehensive balance assessment and training for sensory organization of dynamic postural control. *Front. Bioeng. Biotechnol.* 9, 678006. doi:10.3389/fbioe.2021.678006

Morrison, S., and Newell, K. M. (2015). Dimension and complexity in human movement and posture. *Nonlinear Dyn. Psychol. Life Sci.* 19 (4), 395–418.

Niso, G., Bruña, R., Pereda, E., Gutiérrez, R., Bajo, R., Maestú, F., et al. (2013). Hermes: Towards an integrated toolbox to characterize functional and effective brain connectivity. *Neuroinform* 11 (4), 405–434. doi:10.1007/s12021-013-9186-1

Ozdemir, R. A., Contreras-Vidal, J. L., Lee, B. C., and Paloski, W. H. (2016). Cortical activity modulations underlying age-related performance differences during posture-cognition dual tasking. *Exp. Brain Res.* 234 (11), 3321–3334. doi:10.1007/s00221-016-4730-5

Paillard, T., and Noé, F. (2015). Techniques and methods for testing the postural function in healthy and pathological subjects. *BioMed Res. Int.* 2015, 1–15. doi:10.1155/2015/891390

Pantazatos, S. P., Yanagihara, T. K., Zhang, X., Meitzler, T., and Hirsch, J. (2012). Frontal-occipital connectivity during visual search. *Brain Connect.* 2 (3), 164–175. doi:10.1089/brain.2012.0072

Pellijeff, A., Bonilha, L., Morgan, P. S., McKenzie, K., and Jackson, S. R. (2006). Parietal updating of limb posture: An event-related fMRI study. *Neuropsychologia* 44 (13), 2685–2690. doi:10.1016/j.neuropsychologia.2006.01.009

Peterson, S. M., and Ferris, D. P. (2018). Differentiation in theta and beta electrocortical activity between visual and physical perturbations to walking and standing balance. *eNeuro* 5 (4), 0207–0218. doi:10.1523/ENEURO.0207-18.2018

Pezzetta, R., Nicolardi, V., Tidoni, E., and Aglioti, S. M. (2018). Error, rather than its probability, elicits specific electrocortical signatures: A combined EEG-immersive virtual reality study of action observation. *J. Neurophysiology* 120 (3), 1107–1118. doi:10.1152/jn.00130.2018

Pfurtscheller, G., Stancák, A., Jr., and Neuper, C. (1996). Event-related synchronization (ERS) in the alpha band--an electrophysiological correlate of cortical idling: A review. *Int. J. Psychophysiol.* 24 (1-2), 39–46. doi:10.1016/s0167-8760(96)00066-9

Quijoux, F., Nicolaï, A., Chairi, I., Bargiotas, I., Ricard, D., Yelnik, A., et al. (2021). A review of center of pressure (COP) variables to quantify standing balance in elderly people: Algorithms and open-access code*. *Physiol. Rep.* 9 (22), e15067. doi:10.14814/phy2.15067

Raffi, M., and Piras, A. (2019). Investigating the crucial role of optic flow in postural control: Central vs. Peripheral visual field. *Appl. Sci.* 9 (5), 934–944. doi:10.3390/app9050934

Ramdani, S., Seigle, B., Lagarde, J., Bouchara, F., and Bernard, P. L. (2009). On the use of sample entropy to analyze human postural sway data. *Med. Eng. Phys.* 31 (8), 1023–1031. doi:10.1016/j.medengphy.2009.06.004

Roerdink, M., Hlavackova, P., and Vuillerme, N. (2011). Center-of-pressure regularity as a marker for attentional investment in postural control: A comparison between sitting and standing postures. *Hum. Mov. Sci.* 30 (2), 203–212. doi:10.1016/j.humov.2010.04.005

Rougier, P. R., Berger, S., Barral, S., and Rachet, O. (2012). Biomechanical analysis of postural strategies over the first two months following anterior cruciate ligament reconstruction. *Mot. Control* 16 (1), 94–105. doi:10.1123/mcj.16.1.94

Rubega, M., Formaggio, E., Di Marco, R., Bertuccelli, M., Tortora, S., Menegatti, E., et al. (2021). Cortical correlates in upright dynamic and static balance in the elderly. *Sci. Rep.* 11 (1), 14132. doi:10.1038/s41598-021-93556-3

Sipp, A. R., Gwin, J. T., Makeig, S., and Ferris, D. P. (2013). Loss of balance during balance beam walking elicits a multifocal theta band electrocortical response. *J. Neurophysiology* 110 (9), 2050–2060. doi:10.1152/jn.00744.2012

Song, K., Burcal, C. J., Hertel, J., and Wikstrom, E. A. (2016). Increased visual use in chronic ankle instability. *Med. Sci. Sports Exerc.* 48 (10), 2046–2056. doi:10.1249/mss.0000000000000992

Stam, C. J., Nolte, G., and Daffertshofer, A. (2007). Phase lag index: Assessment of functional connectivity from multi channel EEG and MEG with diminished bias from common sources. *Hum. Brain Mapp.* 28 (11), 1178–1193. doi:10.1002/hbm.20346

Takakusaki, K. (2017). Functional neuroanatomy for posture and gait control. *Jmd* 10 (1), 1–17. doi:10.14802/jmd.16062

Tsai, Y. Y., Chang, G. C., and Hwang, I. S. (2018). Adaptation of kinematic synergy and postural control to mechanical ankle constraint on an unsteady stance surface. *Hum. Mov. Sci.* 60, 10–17. doi:10.1016/j.humov.2018.04.010

Tse, Y. Y., Petrofsky, J. S., Berk, L., Daher, N., Lohman, E., Laymon, M. S., et al. (2013). Postural sway and rhythmic electroencephalography analysis of cortical activation during eight balance training tasks. *Med. Sci. Monit.* 19, 175–186. doi:10.12659/MSM.883824

van Lutterveld, R., van Dellen, E., Pal, P., Yang, H., Stam, C., and Brewer, J. (2017). Meditation is associated with increased brain network integration. *NeuroImage* 158, 18–25. doi:10.1016/j.neuroimage.2017.06.071

VanDeMark, L. H., Vander Vegt, C. B., Ford, C. B., Mihalik, J. P., and Wikstrom, E. A. (2021). Progressive visual occlusion and postural control responses in individuals with and without chronic ankle instability. *J. Sport Rehabil.* 30 (8), 1115–1120. doi:10.1123/jsr.2020-0466

Walsh, G. S. (2021). Visuomotor control dynamics of quiet standing under single and dual task conditions in younger and older adults. *Neurosci. Lett.* 761, 136122. doi:10.1016/j.neulet.2021.136122

Wilkins, L., and Appelbaum, L. G. (2020). An early review of stroboscopic visual training: Insights, challenges and accomplishments to guide future studies. *Int. Rev. Sport Exerc. Psychol.* 13 (1), 65–80. doi:10.1080/1750984X.2019.1582081

Wohl, T. R., Criss, C. R., and Grooms, D. R. (2021). Visual perturbation to enhance return to sport rehabilitation after anterior cruciate ligament injury: A clinical commentary. *Int. J. Sports Phys. Ther.* 16 (2), 552–564. doi:10.26603/001c.21251

Woollacott, M. H., Shumway-Cook, A., and Nashner, L. M. (1986). Aging and posture control: Changes in sensory organization and muscular coordination. *Int. J. Aging Hum. Dev.* 23 (2), 97–114. doi:10.2190/VXN3-N3RT-54JB-X16X

Zalesky, A., Fornito, A., and Bullmore, E. T. (2010). Network-based statistic: Identifying differences in brain networks. *Neuroimage* 53 (4), 1197–1207. doi:10.1016/j.neuroimage.2010.06.041

frontiers | Frontiers in Bioengineering and Biotechnology

TYPE Original Research
PUBLISHED 02 September 2022
DOI 10.3389/fbioe.2022.917486

OPEN ACCESS

EDITED BY
Marcus Fraga Vieira,
Universidade Federal de Goiás, Brazil

REVIEWED BY
Yann Morere,
Université de Lorraine, France
Sai Anirudh Karre,
International Institute of Information Technology, India

*CORRESPONDENCE
Lisa Delbes,
lisa.delbes@univ-amu.fr

SPECIALTY SECTION
This article was submitted to Biomechanics, a section of the journal Frontiers in Bioengineering and Biotechnology

RECEIVED 11 April 2022
ACCEPTED 11 July 2022
PUBLISHED 02 September 2022

CITATION
Delbes L, Mascret N, Goulon C and Montagne G (2022), Validation of an immersive virtual reality device accepted by seniors that preserves the adaptive behavior produced in the real world.
Front. Bioeng. Biotechnol. 10:917486.
doi: 10.3389/fbioe.2022.917486

Validation of an immersive virtual reality device accepted by seniors that preserves the adaptive behavior produced in the real world

Lisa Delbes*, Nicolas Mascret, Cédric Goulon and Gilles Montagne

Aix Marseille Univ, CNRS, ISM, Marseille, France

Falls in the elderly are a major societal issue. Virtual reality appears as a relevant tool to propose gait training programs to prevent the occurrence of falls. The use of a head-mounted display allows overground walking during fully immersive virtual training sessions. Our long-term ambition is to develop gait training programs with a head-mounted display to propose enjoyable and personalized training content for the elderly. Before proposing these programs, several methodological precautions must be taken. The first concerns the supposed similarity of the adaptive behavior produced in the real world and in virtual reality. The second concerns the acceptance of the virtual reality device before and after use. Twenty older adults performed a locomotor pointing task in three conditions including a real-world condition, a virtual-world condition consisting in a replica of the real-world condition, and a virtual condition in which the locomotor pointing task was performed in a different context. From feet positions in relation to the position of a target, gait adaptability behavior was investigated. In line with previous studies, step adjustments (needed and produced) were investigated through a combination of inter-trial and trial-by-trial analyses. The results highlighted that participants adopted the same gait adaptability behavior whatever the type of environment (real vs. virtual). Gait analyses suggested the use of a generic control mechanism based on information-movement coupling. We also demonstrated that older adults accepted the virtual reality device before and after use. With these methodological locks removed, it is now possible to design training programs in virtual reality to prevent falls in the elderly.

KEYWORDS

fall prevention, elderly, acceptance, immersive virtual reality, head-mounted display, information-movement coupling, real-world vs. virtual reality, adaptive behavior

1 Introduction

In the last decades, Virtual Reality (VR) technologies have been used in fall prevention in the elderly (Plante et al., 2003; Cano Porras et al., 2018; Sakhare et al., 2019), which is a major societal issue. One third of adults over the age of 65 fall at least once each year and half of these have repeated falls (Tinetti et al., 1988; Nevitt, 1989). When a fall occurs, the quality of life for most elderly fallers is lowered because of fear of falling, loss of mobility and independence, social isolation, and institutionalization. Because falls lead to severe injuries, hospitalization, or death among older adults, they are a significant public health issue responsible for a large proportion of health care costs (Ambrose et al., 2013; Burns et al., 2016). Most falls occur during tasks requiring a locomotor displacement in cluttered environments and thus in situations that require the production of adaptive gait (Berg et al., 1997; Robinovitch et al., 2013) and when the displacement adjustments required to deal with environmental constraints are imperfectly performed (Overstall et al., 1977; Nevitt et al., 1991; Ashburn et al., 2008).

Impaired gait adaptability (i.e., the ability to adapt gait in response to obstacles and stepping targets) is associated with a high risk of falls in older adults. Yamada et al. (2011) showed that stepping failures during a multi-target stepping task were associated with an increased risk of falling. Older people at increased risk of falling have reduced gait adaptability (i.e., poor stepping accuracy and more stepping errors) when negotiating unexpected obstacles and stepping targets (Caetano et al., 2016). Moreover, Caetano et al. (2018) compared high- and low-risk groups in a gait adaptability test in which they assessed their ability to adapt gait in response to obstacles and stepping targets under single- and dual-task conditions. They found that impaired gait adaptability is associated with a high risk of falls. All the previous studies suggest that training programs designed to improve gait adaptability are particularly relevant to prevent falls in the elderly (Nørgaard et al., 2021).

During the last decade VR technologies have been shown to be a relevant tool to prevent falls in the elderly (Cano Porras et al., 2018; Khanuja et al., 2018; Keshner et al., 2019). VR technology, defined as a numerical immersive and interactive environment provided by an interface (Burdea, 2003), has been used exponentially in gait training and motor learning in the elderly (Schultheis & Rizzo, 2001; Levin et al., 2015; Howard, 2017; Cano Porras et al., 2018). VR technology qualifies many devices characterized by different levels of immersion. Immersion was defined by Witmer & Singer (1998, *p.* 227) as "a psychological state characterized by perceiving oneself to be enveloped by, included in, and interacting with an environment that provides a continuous stream of stimuli and experiences". VR technology ranges from low-immersive devices (e.g., standard television monitors and large screens) to high-immersive devices (e.g., head-mounted display (HMD) and Computer-Assisted Virtual Environment (CAVE) systems).

In the field of fall prevention in the elderly, several low-immersive VR devices have been used to propose gait training programs. Low-immersive VR devices that couple a treadmill to a screen displaying specific virtual environments have been widely used to train gait adaptability in the elderly (Mirelman et al., 2020). Improvements in mobility were demonstrated after treadmill training in different realistic virtual environments with this kind of VR device (Shema et al., 2014; Mirelman et al., 2016). More recently, the instrumented treadmill C-mill (Forcelink BV, Culemborg, Netherlands), a treadmill on which virtual 2D targets were projected on the belt, has been used to offer the elderly a wide range of gait adaptability tasks. Van Ooijen et al. (2016) demonstrated that training with the treadmill C-mill led to large improvements in obstacle negotiation performance. Although all these low-immersive VR devices reviewed have so far led to improvements in motor and psychological components (Kamińska et al., 2018; Corregidor-Sánchez et al., 2019; Mirelman et al., 2020) by proposing interactive and personalized exercises increasing the engagement and enjoyment of older adults (Neri et al., 2017; Corregidor-Sánchez et al., 2019; Sakhare et al., 2019), they have several limitations in the field of gait adaptability training. First, the use of a treadmill imposes specific biomechanical constraints on locomotion (e.g., differences in sagittal plane kinematics and other biomechanical outcomes compared with overground locomotion—Van Hooren et al., 2020). In addition, the use of small screens induces lower engagement and enjoyment in training programs in comparison with high-immersive VR devices (Cikajlo and Peterlin Potisk, 2019).

Nowadays, high-immersive VR devices are the most recent VR devices used in gait training. High-immersive VR devices are defined as fully computer-generated environments providing a full field of view using HMD or projection-based systems such as CAVE (Huygelier et al., 2019). These fully immersive VR devices differ from other VR devices by their "high level of ecological validity resulting from the naturalistic sensory-motor interaction between the user and virtual environment" (Tieri et al., 2018, *p.* 9) and "natural interaction with the surrounding environment by using the entire body of the user that becomes, in this way, an active part of the 3D environment" (Tieri et al., 2018, *p.* 2). Delgado and Der Ananian, (2021) recently concluded that it is feasible to use a fully immersive VR device to improve gait and balance among older adults. Weber et al. (2021) also demonstrated that obstacle avoidance training in fully immersive VR could lead to gait adaptability improvements in the elderly. These high-immersive VR devices allow participants to experience virtual environments where they can freely move and walk and perform overground walking. In fall prevention in the elderly, gait adaptability training in fully immersive VR can propose scenarios that mimic real-life tasks (e.g., avoiding an obstacle, stepping over a curb or climbing stairs) with unconstrained locomotion with an enjoyable and personalized training content (Tieri et al., 2018; Sakhare et al., 2019) by

adjusting the difficulty level to individual requirements and progression.

To date, no gait training program designed to improve gait adaptability in the elderly (using fully immersive VR without the use of a treadmill) has been conducted despite the many potential advantages of this kind of training program both from a practical and a theoretical point of view. The long-term ambition of our project is precisely to test the effectiveness of this type of program. Now, several methodological precautions must be taken before developing an innovative gait training program. The first concerns the analysis of the supposed similarity of gait adaptability behavior, for a given task, in the real world and in the virtual environment. The second concerns the analysis of the acceptance of the HMD, with which older adults are not familiar. We also analyzed to what extent the context in which a task is performed in VR can have an impact on both gait adaptability behavior and the acceptance of the HMD.

1.1 Research questions

First, the overriding concern in relation to our future gait training program is the supposed similarity of gait adaptability behavior between real world and virtual world. In other words, could VR affect the gait adaptive behavior of older adults? This issue is of importance as the beneficial effects of our training program (i.e., good transfer from VR to real life) will be all the more important because the underlying perceptual-motor mechanisms when performing goal-directed locomotion tasks are very similar in the real world and in VR.

Secondly, we must ensure that the participants accept the fully immersive VR technology we plan to use in our future gait training program for the elderly. If the HMD is not accepted by older adults, it is very likely that they will not use it in the end, even if its effectiveness has been validated. That is why our second major challenge concerns the acceptance of technology before use (i.e., *a priori* perception—Hayotte et al., 2020) and its acceptance after use (Alexandre et al., 2018).

1.1.1 Similarity of gait adaptability behavior between real world and virtual world

We must ensure that the gait adaptability behavior of the elderly is the same between the real world and the fully immersive VR environment. Several studies conducted with older adults have shown contradictory results when comparing gait parameters during overground walking in real-world and in virtual environments. Muhla et al. (2020) showed that participants increased their total completion time and their total step number when they performed a Timed Up and Go task, a gold standard in fall risk assessment, in VR. Osoba et al. (2020) found that older adults decreased step length and gait speed and increased step width in VR compared with real-world, while Janeh et al. (2018) found no differences on these two gait parameters. Nevertheless, these two last studies found similar results concerning step width, with an increased width in VR compared with the real world.

It is worth noting that most of the studies which compare gait behavior produced in real-world and virtual environment have focused on very simple locomotion tasks in which participants are not asked to interact with their environment. This makes the study of adaptive behavior difficult, if not impossible. Even if gait parameters (e.g., step length and gait speed) are different between real world and fully immersive VR, gait adaptability behavior (i.e., the capacity to modulate gait parameters to deal with environmental constraints) is not necessarily affected. In our future gait training program in VR, older adults will perform several goal-directed locomotion tasks (e.g., obstacle interception or avoidance, stepping targets) previously used to study gait adaptability behavior in the elderly (Weerdesteyn et al., 2008; Caetano et al., 2016; Van Ooijen et al., 2016). In response to environmental challenges, appropriate gait adjustments are required. Regarding comparison of gait adaptability behavior between real and fully immersive virtual environments, several studies have been conducted with young adults during gait-specific tasks (Fink et al., 2007; Agethen et al., 2018; Buhler and Lamontagne, 2018). In these studies, young adults performed obstacle avoidance during overground walking in real world and VR, where the virtual environment was a replica of the real one. Young adults adopted a more conservative strategy in virtual environment (VE) (i.e., slower gait speed and larger clearance).

However, the study of gait adaptability behavior has often been limited to the analysis of gait parameters reflecting only the participant behavior (i.e., without indicators of gait adjustments related to the environment). In studies showing how gait adaptability training improves obstacle avoidance skills and prevents falls, the study of gait adaptability behavior was reduced once again to these same gait parameters. Mirelman et al. (2016) based their gait adaptability behavior analyses on gait speed and variabilities, and foot clearance during obstacle negotiation training. During obstacle avoidance training, Van Ooijen et al. (2016) investigated gait adaptability through the assessment of gait speed and avoidance performance (i.e., success rate), while Weerdesteyn et al. (2008) studied the avoidance reaction time, the distribution of avoidance, and spatial avoidance parameters such as distance and foot clearance. Moreover, Timmermans et al. (2019) conducted gait adaptability behavior analysis only on task performance during their seven walking-adaptability tasks. Additional levels of analysis are required to study gait adaptability behavior. In the studies reviewed in the previous section, the study of gait adaptability behavior was based on gait parameters (e.g., gait speed or clearance performance) but gait adjustments allowing participants to deal with environmental challenges were imperfectly investigated. A precise characterization of the evolution of the state of the agent-environment system when performing goal-directed locomotion tasks would lead to a better investigation of underlying mechanisms. According to the postulates of ecological psychology (Gibson, 1979; Warren, 1998) gait adjustments are based on a continuous coupling between information and movement. This

tight coupling between information and movement has been very well described in tasks in which the positions of the feet and/or the body must be controlled in relation to either stationary or moving objects in the surroundings (e.g., Lee et al., 1982; De Rugy et al., 2000; Montagne et al., 2000; Van Andel et al., 2018a). In an everyday-life context, the mechanisms underlying gait adjustments have been analyzed in two studies in which subjects had to step onto a curb (Van Andel et al., 2018a) and step over an obstacle (Cornus et al., 2009). In these two studies, participants' gait adjustments were analyzed by a method proposed by Montagne et al. (2000) based on the recording of successive feet positions in relation to the target to be pointed at. Based on the combination of inter-trial and trial-by-trial analyses, this method makes it possible to determine step adjustments (needed and produced). Taken together, the results obtained in these studies (e.g., Montagne et al., 2000; De Rugy et al., 2001, 2002; Cornus et al., 2009; Van Andel et al., 2018a) suggest the use of a control mechanism 1) based on a tight coupling between information and movement and 2) leading to successive adjustments depending on the state of the agent-environment system.

To sum up, the first issue addressed in this study concerns the similarity of gait adaptability behavior between real-world and virtual environments. We had to ensure that gait adaptability behavior in these two types of environments is similar before proposing our training program to elderly people. The gait adaptability behavior of older adults was investigated by a method allowing precise analysis of the successive step adjustments made to deal with task constraints in a locomotor pointing task.

1.1.2 Acceptance before and after use of the VR technology

The Technology Acceptance Model (TAM) (Davis, 1989; Venkatesh & Davis, 2000; Venkatesh & Bala, 2008) is the most widely used model to study acceptance of a technology. The TAM postulates that intention to use a technology is positively predicted by its perceived usefulness and its perceived ease of use. In the field of VR, perceived enjoyment (i.e., the perceived degree of enjoyability when using the technology) was also integrated into the TAM as a factor predicting the intention to use VR technology (Manis & Choi, 2019).

In the field of fall prevention in the elderly, the TAM has been recently used to study acceptance before use of an HMD device intended to prevent falls among the elderly (Mascret et al., 2020). The study highlighted that the intention to use an HMD was positively predicted by perceived usefulness, perceived enjoyment, and perceived ease of use and that perceived usefulness of this HMD was negatively predicted by fall-related self-efficacy (i.e., the perceived level of confidence of an individual when performing daily activities without falling) and positively predicted by self-avoidance goals (i.e., having a physical activity to avoid physical regression). However, this study was conducted using self-reported questionnaires following a presentation of the device based on a written text and several pictures. Consequently, the dynamic of its acceptance (after use) throughout gait training programs has not yet been studied. That is why the present study investigated acceptance of the VR-HMD before using it and the dynamic of its acceptance after using it during a specific gait-specific task in fully immersive VR. Among older adults, Huygelier et al. (2019) demonstrated that the participants' acceptance of an HMD increased after a first use of a few minutes, but it was not studied in the context of fall prevention with a gait adaptability task. In the present study, the aim is twofold concerning acceptance: to investigate its first level before use and whether its level changes after use.

Moreover, in older adults, some extended TAMs have been used to investigate the acceptance of VR devices including user experience (Syed-Abdul et al., 2019) which is associated with the quality of the immersive user experience in VR (Mütterlein & Hess, 2017). User experience may be influenced by cybersickness and sense of presence. Cybersickness quantifies motion sickness induced by discrepancies between visual, vestibular, and proprioceptive information (Robillard et al., 2003). Sense of presence quantifies subjective experience of being in a virtual environment (Witmer & Singer, 1998). Sagnier et al. (2020) demonstrated that cybersickness negatively predicts intention to use an HMD, while presence is not a significant predictor. But their study was conducted with young adults during an aeronautical assembly task and did not concern the field of gait training among the elderly. Given that these two feelings can affect the user experience (Tieri et al., 2018; Weech et al., 2019), we must investigate cybersickness and sense of presence in fully immersive VR in this present study.

To sum up, the second issue addressed in this study was to ensure that the participants accept the VR-HMD before use and to know whether the acceptance changes after use. We also investigated their subjective experience through the study of cybersickness and sense of presence.

1.1.3 Sub-challenge

In this study, we also wanted to investigate the influence of the virtual context on gait behavior. VR offers the possibility of developing a wide range of virtual environments. Diversified virtual environments can offer more enjoyable and engaging exercises in our future gait training program in fully immersive VR. The visual context in VR should be considered. Contextual realism can modify the ecological validity of a simulated environment (Kuliga et al., 2015; Joseph et al., 2020). Birenboim et al. (2021) recommended pretesting VE design to ensure high ecological validity in terms of behavior and wellbeing in fully immersive VR. Moreover, highly realistic VR environments led to greater positive affective and serenity responses compared with low-realism environments (Newman et al., 2022).

It is known that the visual context can affect human behavior. Studies have shown that an outdoor environment leads to greater relaxation (Anderson et al., 2017), restoration (Rogerson et al., 2016) and level of vigor (Yu et al., 2018) and to a faster and more complete recovery from stress (Yin et al.,

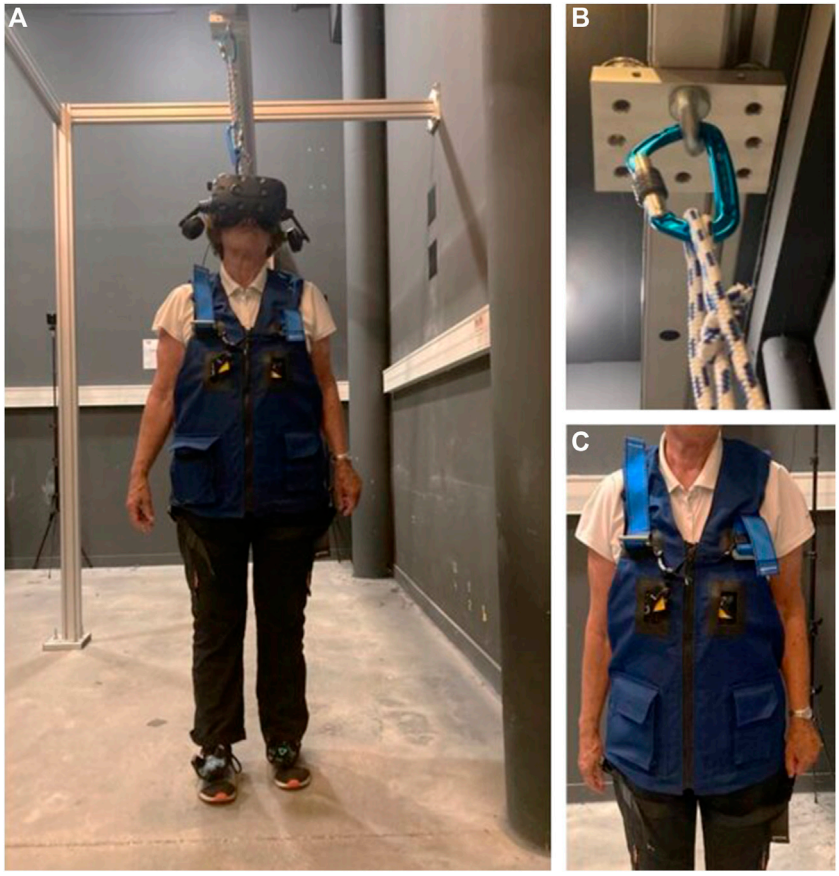

FIGURE 1
Illustrations of the test equipment. **(A)** Older adult performing the task. A wireless HTC Vive Pro® was used to display the VR environment. Two HTC Vive Pro® 2.0 trackers (placed on the feet) were used to record the positions of the feet and display virtual 3D shoes in the VR. The security system is composed of **(C)** a safety harness connected to **(B)** an in-ceiling rail by a lanyard.

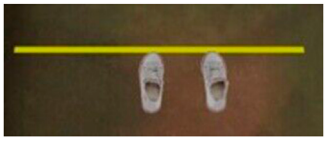

FIGURE 2
Virtual 3D shoes representing participants' feet in the virtual environment. The size of the virtual 3D shoes was adjusted to the size of the participant's feet.

2020) than an indoor environment. Moreover, Lourenço et al. (2008) showed that motivation was greater in the more enjoyable VR environment (i.e., more interesting visual and auditory interface) during a reaching task. The manipulation of the visual context may also impact gait behavior in the elderly. That is why, before proposing our gait training in different virtual environments, we must ensure that diversified virtual environments preserve gait adaptability behavior. In this present study, two different virtual environments were computed: a corresponding one (i.e., a replica of the real-world set-up) and a non-corresponding one (i.e., outdoor environment). Our non-corresponding virtual environment had the same dimensions and the same informational content as our corresponding virtual environment. In our gait-specific tasks, the available information in the visual field should be the same so as to strictly compare gait adaptability behavior in the two conditions.

1.2 Hypotheses

In summary, before developing our fully immersive VR training program to prevent falls in the elderly, several methodological precautions must be taken. First, we must ensure that gait adaptability behavior in the elderly is the same

whatever the environment (real world vs. fully immersive VR) during a locomotor pointing task. The use of an immersive VR device that preserves natural gait leads us to hypothesize that gait adaptability behavior of older adults should not be affected by the type of environment (H1). We also need to check the acceptance of the HMD (before and after its use) in the elderly during a locomotor pointing task in a fully immersive VR environment. We hypothesize that the HMD should be accepted by older adults before its use (H2) and even more after its use (H3). We also hypothesize a low level of cybersickness (H4) and a high level of sense of presence (H5) in both virtual conditions. Finally, we hypothesize that manipulating the context in which the task is performed while leaving the informational content of the environment unchanged should not affect behavior when comparing gait adaptability behavior produced in the two virtual conditions (H6).

2 Methods & materials

2.1 Experiment

2.1.1 Participants

Twenty older adults (mean age = 68.6 years, SD = 3.4 years) volunteered to take part in the experiment. Participants had normal or corrected-to-normal vision and were included in the study if they were able to walk independently, without a cane, crutch, or walker, and without help from another person. These participants had no neurological, vestibular, cardiac, pulmonary, or orthopedic disorders. These potential disorders were self-reported by the participants before the beginning of the experiment. Participants had a Montreal Cognitive Assessment (MoCA) score between 26 and 30. The MoCA cut-off score was selected based on selective criteria for intact cognition (Nasreddine et al., 2005). Participants should have never used an HMD before. Participants were not informed about the precise purpose of the study. All participants gave informed consent. The study was conducted in line with the ethical guidelines of the national ethics committee (Ethical Committee for Research no. IRB00012476-2020-25-03-51), as well as in compliance with the Declaration of Helsinki for human research and the international principles governing research on humans.

2.1.2 Instruments and material

In each condition, the participant was equipped with a security system consisting of a safety harness connected to an in-ceiling rail by a lanyard (Figures 1B,C). The in-ceiling rail only allowed rectilinear movements within a steel structure. In all the conditions, participant's feet positions were recorded by two HTC Vive Pro® foot trackers during each locomotor pointing task (Figure 1A).

2.1.2.1 VR system: HTC vive pro®

For the virtual conditions, the VR system consists of a wireless VR-HMD which displayed a VE, four trackers, and four lighthouse lasers. A computer with 2.8 GHz Intel® Core i7 processor, 8 GB of main memory, and NVIDIA® GeForce GTX 1070 graphics card was used to run the software ICE®. ICE® (Imagine, Create and Experiment) is a free 3D software developed in C++ and OpenGL for researchers who are not familiar with programming (trello link about ICE: https://trello.com/b/EtNCNrZH/ice). It is composed of "ICE_Designer" tool used to build 3D scenes with the implementation of tracking systems and of "ICE_Protocol" tool used to display the scene with the experimental settings (which scenes, in what order, participants' settings, initial conditions . . .) and to save experimental data. A wireless HTC Vive Pro® HMD was used to display a VE for the participant. This headset has a resolution of 1440 × 1600 pixels per eye (refresh rate of 90 Hz) and a diagonal field of view of 110°.

Participants' feet were presented in the VE by two virtual 3D shoes (Figure 2) with the two HTC Vive Pro® trackers placed on the feet (the same ones which recorded feet positions). For each participant, the size of the virtual 3D shoes was adjusted to the size of the participant's his/her feet in the settings of "ICE_Protocol". A supplementary tracker, placed on the floor, was used to display a blue target (120 cm wide and 2.5 cm long) and a yellow line (120 cm wide and 2.5 cm long), which marked the start area.

Four lighthouse lasers, with a span of 120° in each direction, were used to detect the position and orientation of the HMD and of the four trackers at an update rate of 120 Hz with sub-millimeter precision and accuracy for position data[1].

1 A pilot study was conducted to ensure the validity of the VR recording system by a simultaneous recording of the footfalls of 18 young participants engaged in a locomotor pointing task. The validity of the HTC Vive Pro® VR system for gait parameters was tested with the GaitRite® walkway system as a golden standard. The GaitRite® walkway system is a validated gait analysis system (Webster et al., 2005) and has excellent reliability for the quantification of gait parameters of young and older people (Menz et al., 2004). The validity was be assessed by comparing feet position data obtained by the walkway system and the VR system. Two thousand, six hundred and forty position values were recorded simultaneously by the two systems (i.e., 528 pointings x 5 steps). A linear regression analysis with position data collected by both measurement systems was computed to investigate the relationship. Two parameters are crucial to assess the validity of VR recording system: the slope of the line and the coefficient of determination (r^2). The slope of the line indicates the steepness of a line and represents the rate of change in y as x changes. In our case, a slope very close to 1 would indicate that position data recorded by the two systems are of the same magnitude. R^2 is a measure of goodness of fit and it is interpreted as the proportion of the variance in the y that is predictable from x. In our case, r2 should be very close to 1 to ensure a strong relationship between the two position data. In our study, the linear regression analysis showed a significant relationship between the position data ($p < 0.05$) recorded by the two systems with a slope of the line of 0.99 and an r^2 of 1.

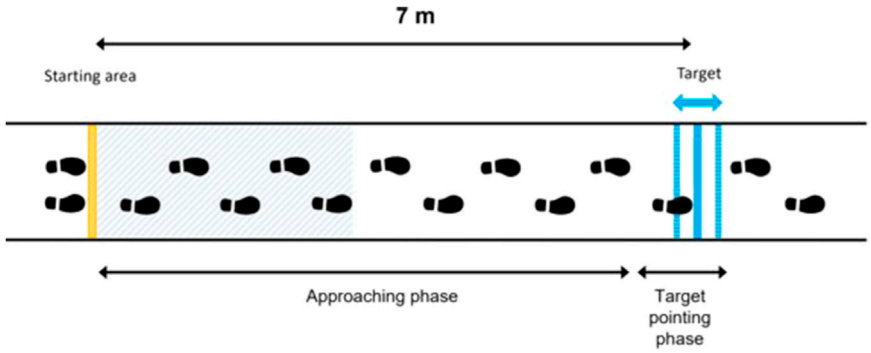

FIGURE 3
Diagram of the locomotor pointing task consisting of an approaching phase and a target-pointing phase. Participants were instructed to place themselves in the starting area and to start walking with the right leg. For each trial, participants were asked to place their right foot tip as close as possible to the lower extremity of the target while walking at a normal pace and continuing to walk subsequently. The position of the target was manipulated unbeknownst to the participants (3 different target positions: 0 ± 20 cm). The blue hatched area represents the area for calculating the average gait speed (i.e., the first five steps).

2.1.3 Protocol

The first purpose of this study was to record participants' gait parameters (by measuring feet positions) while performing a locomotor pointing task in three experimental conditions: one real-world condition (RWC) and two virtual reality conditions (VRC).

2.1.3.1 Task

The task performed in this study was a locomotor pointing task (Figure 3) which is paradigmatic when studying the mechanisms underlying goal-directed locomotion (Lee et al., 1982). The locomotor pointing task consists of two phases: an approaching phase and a target-pointing phase as in the studies of Montagne et al. (2000), De Rugy et al. (2000), Cornus et al. (2009), and Van Andel et al. (2018a). Participants were instructed to place themselves in the starting area and to start walking with the right leg. For each trial, participants were asked to place their right foot tip as close as possible to the lower extremity of the target while walking at a normal pace and continuing to walk subsequently. After each trial, participants had to return to the starting position walking at a normal pace. To avoid locomotor regularities and prevent any calibration of the distance being covered, the position of the target location was manipulated unbeknownst to the participants (3 different target positions: 0 ± 20 cm) and presented in a randomized order (6 or 7 trials for each target position condition). Instructions concerning the experimental task were given in a short explanatory video. Afterwards, participants could ask the experimenter questions and instructions could be reformulated if necessary.

2.1.3.2 Experimental conditions

For the RWC, participants had to walk in the experimental room (Figure 4A). For the VRC, two VEs were created. For the "corresponding VR" condition, the VE consisted of a reconstitution of the experimental room (Figure 4B). For the "outdoor VR" condition, the VE consisted of an outdoor environment (Figure 4C) giving rise, for a given displacement, to an identical optical flow to the other two conditions. In the VRC, participants walked in the VE wearing the VR-HMD HTC Vive Pro®.

2.1.3.3 Procedure

At the beginning of the experiment, the participants watched a short video with pictures of the VR device used (HMD), to present the VR set-up and its scientific applications. Afterward, they were equipped with the security system and HTC Vive Pro® trackers.

The experimental conditions were presented in a randomized order. Between each experimental condition, participants had a forced rest period of 10 minutes to minimize fatigue accumulation in experimental conditions.

For the three experimental conditions, the experiment was composed of a familiarization period followed by an experimental phase (Figure 5). The familiarization period was split into a calibration phase and a familiarization with the task. The calibration phase consisted of 2 minutes of free walking in the environment (without performing the pointing task). It was designed to allow participants to become familiar with their displacement in the environment. More precisely, the calibration phase was designed to allow each participant to get used to the VR interface and to ensure that participants become familiar with virtual 3D shoes representing their feet during the locomotion in VR. Afterward, the familiarization with the task consisted of successive locomotor pointing trials (minimum five). A success rate was calculated from the ratio of pointing accuracy lower than 10 cm over the last five trials. The familiarization with the task stopped when the success rate of the participants was greater than 80%. It was designed to make sure that each participant was familiar with the

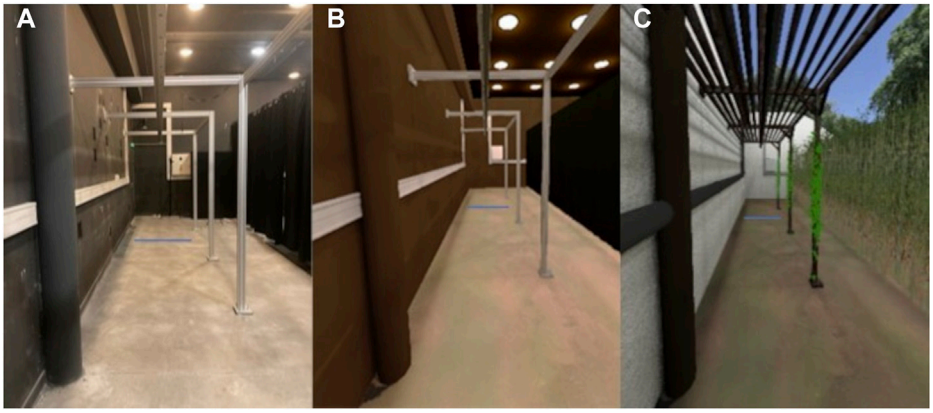

FIGURE 4
Experimental conditions. **(A)** Picture of the "real-world condition". **(B)** Screen shot of the "corresponding virtual reality condition". **(C)** Screen shot of the "outdoor virtual reality condition".

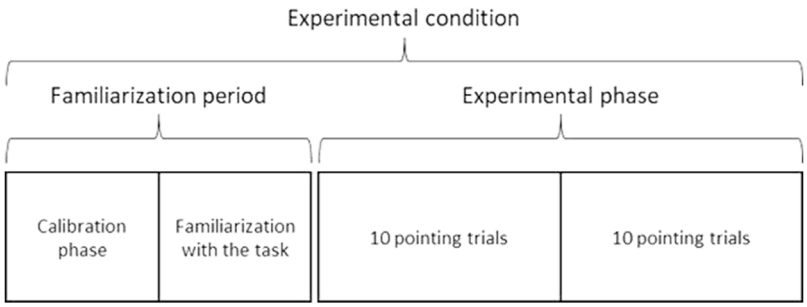

FIGURE 5
For the three experimental conditions, the experiment was composed of a familiarization period followed by an experimental phase. The familiarization period was split into a calibration phase and a familiarization with the task. The calibration phase consisted of 2 minutes of free walking in the environment. It was designed to allow participants to become familiar with their displacement in the VR environment. The familiarization with the task consisted of successive pointing trials. It was designed to make sure that each participant was familiar with the pointing locomotion task requirements and that they understood the task instructions. After the familiarization period, the experimental phase consisted of two blocks of 10 pointing trials per condition.

pointing locomotion task requirements and that they understood the task instructions. After the familiarization period, the experimental phase consisted of two blocks of 10 pointing trials per condition. Twenty trials by condition allow a substantial repetition of the task to have a good representation of the gait adaptability behavior, but it should not be large in order to avoid fatigue over the different conditions.

2.2 Outcome variables

2.2.1 Gait parameters

Gait speed, step lengths, and toe-obstacle distances were computed from the feet positions recorded by the feet trackers (Figure 6).

From these computations, several gait parameters were computed following the methodology used in previous studies (De Rugy et al., 2000; Montagne et al., 2000; Cornus et al., 2009; Van Andel et al., 2018a). Gait parameters were computed using MATLAB® (version R2017b, The MathWorks, Inc., USA). A step corresponded to two consecutive foot contacts (i.e., footfalls) of two different legs.

Several types of gait analysis were performed. A pointing accuracy analysis and a gait speed analysis were first performed. Following the procedure used by Montagne et al. (2000), Cornus et al. (2009), and Van Andel et al. (2018a), inter-trial and trial-by-trial analyses were also performed. In the inter-trial analysis, the inter-trial standard deviations of both the toe-obstacle distances and the step lengths over the target approach were computed. Two types of analysis were performed in the trial-by-trial

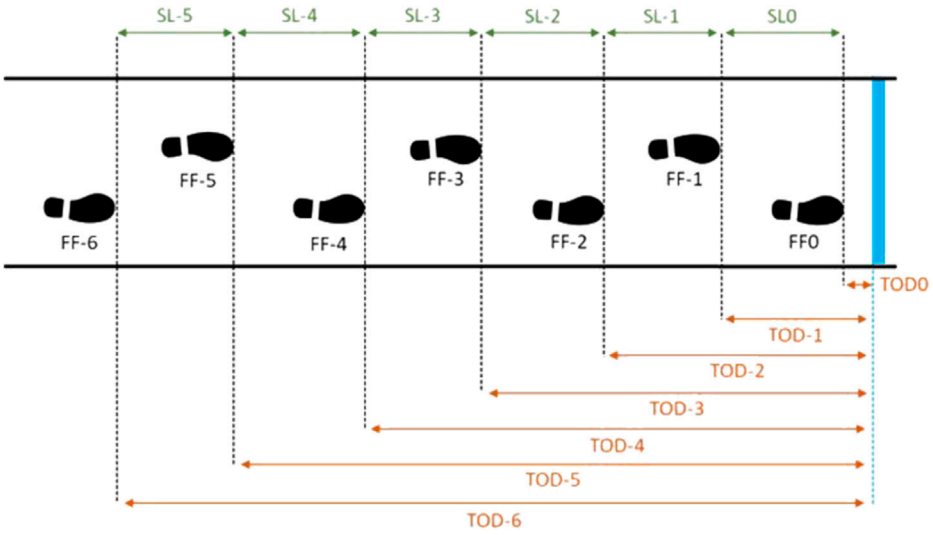

FIGURE 6
Schema of gait parameters calculation during the locomotor pointing task. The blue line represents the target. Footfall i (FFi) coding: the footfall of pointing is coded FF0. Step length (SLi) coding for each footfall i. Toe-obstacle distance (TODi) coding for each footfall i.

analysis: an inter-step number analysis and an intra-step number analysis.

2.2.1.1 Gait speed analysis

Separately for each participant, the average gait speed for the first five steps of each trial was computed. The standard deviation (within-subject inter-trial) of the gait speed was also calculated.

2.2.1.2 Pointing accuracy analysis

The pointing footfall was defined as footfall 0 (FF0). The toe-obstacle distance of FF0 represented the pointing accuracy, that is the distance between the toe and the target at last footfall. Negative values were related to pointing performances before the target (i.e., undershoot) and positive values were related to pointing performances after the target (i.e., overshoot).

The absolute and constant pointing errors were computed to measure the pointing performance (Schmidt and Lee, 1982). The following formulae explain how they are computed, with n the number of participants, xi the position of pointing i and T the position of the target.

The absolute pointing error (APE) reflects the overall accuracy without considering the direction of the error (see Eq. 1). The APE is the mean absolute value of the difference between the toe of the foot and the target at the last footfall.

$$APE = \frac{(\sum |xi - T|)}{n} \quad (1)$$

The constant pointing error (CPE) reflects the direction of the pointing errors (see Eq. 2). The CPE is the signed mean difference between the toe of the foot and the target at the last footfall (negative when the toe was before the target and positive when the toe was after the target).

$$CPE = \frac{(\sum xi - T)}{n} \quad (2)$$

2.2.1.3 Inter-trial analyses

In the inter-trial analyses, the standard deviation of the toe-obstacle distances and the standard deviation of the step lengths were measured. Separately for each participant, the toe-obstacle distance and the step length were computed for each footfall. For each footfall, the standard deviation (within-subject inter-trial) of the toe-obstacle distance and of the step length were calculated across all trials. Following previous studies in locomotor pointing, we can anticipate that during the approach to the target the step length variability increases while the toe-obstacle distance variability decreases (e.g., Lee et al., 1982; Montagne et al., 2000). The modulation of step lengths in the final steps (i.e., increase in the standard deviation of step lengths) to perform an optimal foot positioning tends to be increasingly accurate when approaching the target (i.e., decrease in the standard deviation of toe-obstacle distances). This pattern of compensatory variability underlines the need to correct the current foot position by changes in step length to perform an accurate pointing (Cornus et al., 2009; Van Andel et al., 2018a).

2.2.1.4 Trial-by-trial analyses

In the trial-by-trial analyses, each trial was analyzed separately. An inter-step number analysis and an intra-step number analysis were performed.

For the inter-step number analysis, an average pattern of step length was calculated from the mean step lengths of all 30 trials for each participant. Following Montagne et al. (2000), a threshold of 4% is established on both sides of the average pattern of step length. For each participant and each trial, adjustments were identified by comparing each step length with the average pattern of step length. Thereby, a step was characterized as a lengthening step if its length was greater than the average pattern of step length and if the difference exceeded the threshold. A step was characterized as a shortening step if its length was smaller than the average pattern of step length and if the difference exceeded the threshold.

A trial was described as regulated if at least one of its steps was characterized as a lengthening or shortening step. Three categories of regulated trials were defined: 1) lengthening trials where only lengthening steps were performed, 2) shortening trials where only shortening steps were performed, and 3) mixed trials with a combination of lengthening and shortening steps.

The intra-step number analysis was conducted to compute the amount of adjustments needed (in relation to toe-obstacle distances) and the amount of adjustments produced (in relation to step lengths) for each footfall. This analysis allowed us to determine the relationship between these two parameters and thereby to assess the strength of information-movement coupling.

The amount of adjustments needed (AN) represents the difference between the current toe-obstacle distance and the average toe-obstacle distance for that footfall. The amount of adjustments needed for footfall i (AN*i*) was the difference between the toe-obstacle distance for footfall i (TTD*i*) and the average of the toe-obstacle distance of footfall i (ATTD*i*) (Eq. 3).

$$ANi = TTDi - ATTDi \quad (3)$$

The amount of adjustments produced (AP) represents the difference between the current step length and the average of the step length for that footfall. The amount of adjustments produced at footfall i (AP*i*) was the difference between the step length of footfall i (SL*i*) and the average step length for footfall i (ASL*i*) (Eq. 4).

$$APi = SLi - ASLi \quad (4)$$

The amount of adjustments needed for the current footfall is assumed to be related to the amount of adjustments produced at the next footfall. The current difference of toe-obstacle distance (compared with the average of the toe-obstacle distance) at the current footfall should be corrected by modulation of step length at the following footfall. This relationship is used to assess the strength of information-movement coupling (De Rugy et al., 2000; Montagne et al., 2000; Cornus et al., 2009).

2.2.2 Psychological variables

2.2.2.1 Acceptance of the VR-HMD

Acceptance was measured at the beginning of the experiment (after the short video with pictures of the HMD) using self-reported questionnaires to quantify participants' acceptance of the VR-HMD before use (Appendix A), in line with the procedure of Huygelier et al. (2019). After the second VRC, they once again completed the acceptance questionnaire to quantify their acceptance of the VR-HMD after use (Appendix B). Acceptance of the VR-HMD HTC Vive Pro® before and after use was assessed through four variables: perceived usefulness, perceived ease of use, perceived enjoyment, and behavioral intention to use (Davis, 1989; Davis & Venkatesh, 1996; Manis & Choi, 2019). Participants answered the three items per variable on a Likert scale from 1 (*strongly disagree*) to 10 (*strongly agree*): perceived usefulness (e.g., "*I believe using VR hardware would help me be more effective in my locomotion*"), perceived ease of use (e.g., "*I believe using VR hardware would be easy for me*"), perceived enjoyment (e.g., "*I believe I would find using VR hardware enjoyable*"), and behavioral intention to use (e.g., "*I intend to use VR hardware within the foreseeable future*").

Internal consistency was good for each variable, with McDonald's omegas ranging from 0.82 to 0.99. McDonald's omegas were used because Cronbach's alphas have a tendency to over-estimate or under-estimate reliability (Dunn et al., 2014). McDonald's omegas for each variable, groups, and measurement times are provided in Table 1.

2.2.2.2 Cybersickness and sense of presence

Cybersickness and sense of presence were measured after the familiarization period of each virtual condition and at the end of the two pointing blocks of each virtual condition by oral questionnaires (Robillard et al., 2003). To quantify cybersickness, the experimenter asked the participants to rate verbally on a 10-point Likert scale ("*How unwell is the virtual reality making you feel?*") from 1 ("*do not feel unwell at all*") to 10 ("*feel very unwell*"). To quantify the sense of presence, the experimenter asked the participants to rate verbally on a 10-point Likert scale ("*How much do you feel that you really are present in the virtual environment you see?*") from 1 ("*not at all present*") to 10 ("*completely present*"). In this study, a short verbal 10-point Likert scale was used for repeated measurements of cybersickness and sense of presence because it is an optimal scale of response with older adults, and it has higher reliability, validity, and discrimination (Wee et al., 2008). A short scale is indeed relevant for repeated measurements as in our study.

The experimental procedure with the outcome psychological variables is summarized in Figure 7.

TABLE 1 McDonalds's omega, mean and standard deviation (SD) of the four variables of acceptance at the beginning of the experiment (T1) and after the second virtual reality condition (T2): perceived usefulness (PU), perceived ease of use (PEOU), perceived enjoyment (PE), and behavioral intention to use (BIU).

	T1		T2	
	McDonald's omega	Mean (SD)	McDonald's omega	Mean (SD)
PU	0.97	7.42 (2.53)	0.97	6.37 (2.97)
PEOU	0.95	8.02 (2.12)	0.94	9.12 (1.00)
PE	0.99	8.22 (2.55)	0.82	8.97 (1.61)
BIU	0.98	6.52 (3.01)	0.99	7.05 (3.30)

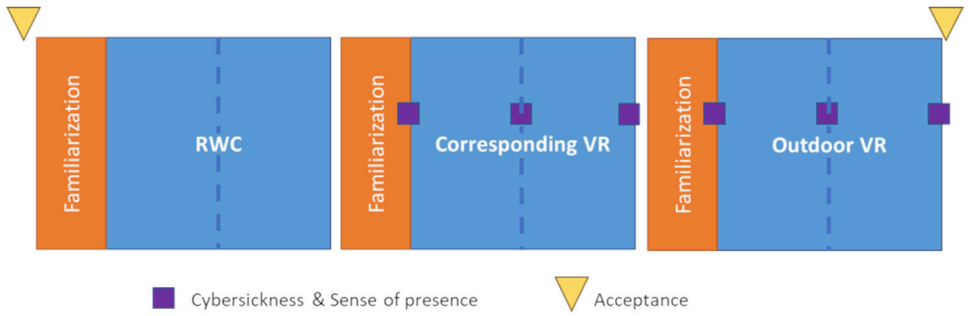

FIGURE 7
Experimental procedure in a specific order: real-world condition (RWC), corresponding virtual reality (VR) and outdoor virtual reality (VR). The experimental conditions were presented in a randomized order. The three conditions consisted of a familiarization period (in orange) and an experimental phase (in blue). The dotted blue line represents the two blocks of 10 pointing trials per condition. During the experimental phase of each condition, feet positions were recorded for each trial to compute gait parameters. Cybersickness and sense of presence were measured at the end of the familiarization period and at the end of the two pointing blocks of each virtual condition. Acceptance was measured at the beginning of the experiment to quantify acceptance before use, and once again, after the second RVC, to quantify their acceptance after use.

2.3 Statistical analyses

The statistical software JASP (Version 0.14.1, 2021) was used to run statistical analyses. The statistical level of significance was set at $\alpha = 0.05$. Non-parametric tests were used when the distribution of the data was non-normal.

For gait parameters, between conditions, differences in strategy for the participants were evaluated using non-parametric Friedman tests for gait speed, pointing accuracy, patterns of standard deviation of toe-obstacle distances and of step lengths, proportion of regulated trials, and adjustment strategies. A linear regression was calculated to assess the relationship between the amount of adjustments needed at a certain footfall and the amount of adjustments produced at the following footfall. Friedman tests were used for footfalls two by two for each condition to assess the onset of step adjustments (based on standard deviations).

For psychological variables, one-sample t tests were conducted on each variable to see if they differed significantly from the mean of the scale (i.e., 5.5). Then, for acceptance, between-times differences were evaluated using non-parametric Wilcoxon signed-rank tests.

3 Results

3.1 Gait parameters

Several analyses were conducted to study between-conditions differences in the participants' gait adaptability behavior.

3.1.1 Gait speed analysis

For the gait speed, the Friedman test revealed no significant differences between conditions ($\chi 2$ (6) > 20.569, $p = 0.153$). The participants walked at 1.07 m/s (SD = 0.02 m/s) in RWC, at 0.96 m/s (SD = 0.02 m/s) in corresponding VR, and at 0.98 m/s (SD = 0.02 m/s) in outdoor VR. They thus walked almost at the same speed whatever the condition.

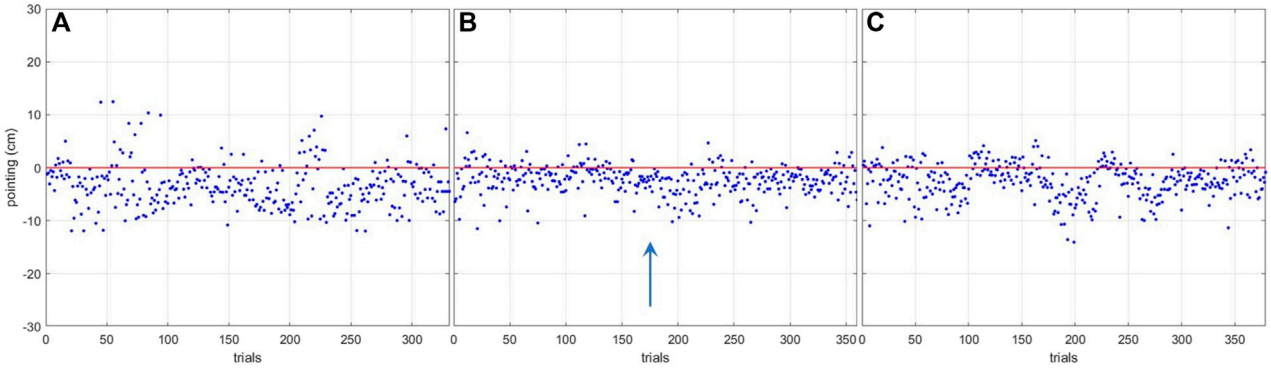

FIGURE 8
Global pointing performances in the three conditions. **(A)** real-world condition. **(B)** corresponding virtual reality condition. **(C)** outdoor virtual reality condition. The red line marks the lower extremity of the target. The blue arrow indicates the direction of the locomotor displacement.

3.1.2 Pointing accuracy analysis

Pointing accuracy analysis was based on global pointing performance across all the trials (Figure 8).

To quantify the accuracy, the APE and the CPE of the participants were computed across the different conditions.

For the APE, the Friedman test revealed a significant difference between conditions ($\chi 2$ (2) > 20.632, p <0 .001). Conover's Post Hoc test revealed a difference between the RWC condition and the VRC (p <0 .001 and p = 0.001 for corresponding VR and outdoor VR, respectively) but no difference between the VRC (p = 0.521). The participants' APEs were 4.53 cm (SD = 1.43 cm) in RW, 2.78 cm (SD = 0.86 cm) in corresponding VR, and 3.20 cm (SD = 1.66 cm) in outdoor VR. The participants had a lower absolute pointing error in VRC than in RWC.

For the CPE, the Friedman test revealed a significant difference between conditions ($\chi 2$ (2) > 8.316, p <0 .016). Conover's Post Hoc revealed a difference between the RWC condition and the VRC (p = 0.009 and p = 0.042 for corresponding VR and outdoor VR, respectively) but no difference between the VRC (p = 0.521). Participants' CPEs were −3.52 cm (SD = 1.84 cm) in RWC, −2.47 cm (SD = 0.98 cm) in corresponding VR, and -2.51 cm (SD = 2.11 cm) in outdoor VR. The results showed that participants tend to place their feet before the target in the three conditions but that the performance was better in VRC than in RWC.

3.1.3 Inter-trial analyses

Standard deviation of toe-obstacle distances (SD_{tod}) and the standard deviation of step lengths (SD_{sl}) were computed as a function of footfall number in the three experimental conditions (Figure 9). No difference was found between the patterns of the SD_{tod} and the SD_{sl} in the three conditions (all ps > 0.05). In the three conditions, at the beginning of the target approach, the SD_{tod} was high (26.11 cm on average) and decreased through the approaches with an average value of 3.64 cm at the last footfall (i.e., pointing footfall). Conversely, in the three conditions, the SD_{sl} was low (4.12 cm on average) at the beginning of the target approach and increased through the approaches with an average value of 11.51 cm at the last footfall (i.e., the pointing footfall).

Following previous studies (Berg et al., 1994; Montagne et al., 2000; Cornus et al., 2009) the onset of step adjustments (i.e., the footfall number at which gait regulation was initiated) was established as the footfall at which the SD_{tod} started to decrease and the SD_{sl} started to increase. The results showed that the onset of step adjustments was at footfall −2 on average whatever the condition. The pattern of the SD_{tod} decreased significantly at footfall −2 compared with footfall −3 (all ps <0.05) and SD_{sl} increased significantly at footfall −2 compared with footfall −3 (all ps <0 .05). The results showed that the participants initiated their step adjustments two steps before the target on the three conditions to perform an optimal foot positioning.

3.1.4 Trial-by-trial analyses

3.1.4.1 Inter-step number analysis

For the proportion of regulated trials, the Friedman test revealed no significant differences between conditions ($\chi 2$ (2) >0.758, p = 0.685). The proportion of regulated trials was 88.31% (SD = 7.45%) in RWC, 87.89% (SD = 7.87%) in corresponding VR and 88.93% (SD = 6.98%) in outdoor VR. Among regulated trials, the distribution of adjustment strategies of step length (mixed, lengthening, and shortening) was computed across the three conditions (Table 2). The Friedman test revealed no significant differences between conditions ($\chi 2$ (2) > 0.111, p = 0.946; $\chi 2$ (2) > 4.388, p = 0.111; $\chi 2$ (2) > 4.388, p = 0.111; for mixed, lengthening, and shortening trials respectively). In the three conditions, the participants adopted mostly mixed trials (almost half of trials).

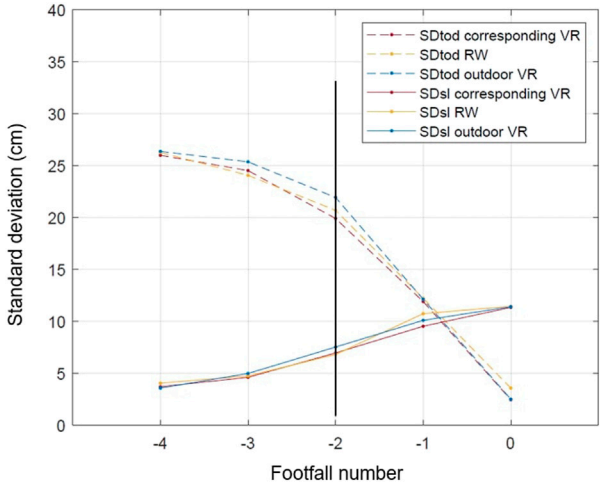

FIGURE 9
Patterns of the standard deviation of toe-obstacle distances and of step lengths as functions of footfall number. The black vertical line marks the onset of step adjustments at footfall −2. Footfall 0 is the pointing footfall. SDtod: standard deviation of toe-obstacle distances; SDsl: standard deviation of step lengths; VR: virtual reality; RW: real world.

3.1.4.2 Intra-step number analysis

Linear regression analyses showed a significant linear relationship between the amount of adjustment needed at a certain footfall and the amount of adjustment produced in the following footfall in the three conditions (Figure 10).

Relationships were significant for all footfalls in the three conditions with increasing slopes (β) and r^2 values. Slopes increase from 0.03 at footfall −4 to 0.91 at footfall 0 in RWC, from 0.08 at footfall −4 to 0.92 at footfall 0 in corresponding VR and from 0.06 at footfall −4 to 0.93 at footfall 0 in outdoor VR. At footfall 0, r^2 is close to 1 in the three conditions (0.90 in RWC, 0.96 in corresponding VR, and 0.97 in outdoor VR).

In terms of gait parameters, our first hypothesis (H1) was confirmed. We hypothesized that the participants' gait adaptability behavior is not affected by the type of environment (real-world vs. virtual). Although analyses revealed differences of absolute and constant pointing errors between RWC and VRC, these errors reflect a high level of accuracy whatever the type of environment. Analyses showed that the participants adopted the same gait adaptability behavior reflecting the use of a generic control mechanism (based on information-movement coupling) whatever the type of environment.

For the sub-challenge, (H6) was confirmed. We hypothesized that the virtual visual context does not affect gait adaptability behavior. All outcomes were similar between the two VRC.

TABLE 2 Distribution of adjustment strategies of step length (mixed (MT), lengthening (LT), and shortening (ST) trials) in the three experimental conditions (RWC: real-world condition; VR: virtual reality).

	RWC	Corresponding VR	Outdoor VR
MT (%)	45.47	49.10	47.02
LT (%)	24.39	25.93	29.30
ST (%)	30.14	24.99	23.68

3.2 Psychological variables

3.2.1 Acceptance of the VR-HMD

The results of the different variables used to examine acceptance of the VR-HMD showed that the participants accepted the device before and after use (Figure 11).

Perceived usefulness (PU) was different from the mean of the scale (i.e., 5.5) before use (p = 0.006). After use, PU was not different from the mean of the scale (p = 0.217). The VR device was considered useful before use but neither useful nor useless after use. Behavioral intention to use (BIU) was not different from the mean of the scale before use (p = 0.184). After use, BIU was different from the mean of the scale (p = 0.048). The participants did not intend to use this VR device before use but after use they intended to use it. Perceived ease of use (PEU) was different from the mean of the scale before (p < 0.001) and after (p <0 .001) use. The VR device was considered easy to use before and after use. Perceived enjoyment (PE) was different from the mean of the scale before (p <0 .001) and after (p = 0.006) use. The VR device was considered enjoyable before and after use.

Perceived usefulness (PU) was high before use (PU_{before} = 7.42) and decreased after use (PU_{after} = 6.37). A Wilcoxon test showed a significant difference (p = 0.007). Behavioral intention to use (BIU) was medium before use (BIU_{before} = 6.52) and after use (BIU_{after} = 7.05). A Wilcoxon test showed no difference (p = 0.292). Perceived ease of use (PEU) was high before use (PEU_{before} = 8.02) and increased after use (PEU_{after} = 9.12). A Wilcoxon test showed a significant difference (p = 0.033). Perceived enjoyment (PE) was high before use (PE_{before} = 8.22) and after use (PE_{after} = 8.97). A Wilcoxon test showed no difference (p = 0.183).

3.2.2 Cybersickness and sense of presence

Cybersickness was low in corresponding VR (mean = 2.40, SD = 1.69) and outdoor VR (mean = 2.23, SD = 1.36). Cybersickness was different from the mean of the scale (i.e., 5.5) in corresponding VR (p <0 .001) and in outdoor VR (p <0 .001). Participants did not experience cybersickness in the two VRC.

Sense of presence was high in corresponding VR (mean = 8.33, SD = 1.97) and outdoor VR (mean = 8.35, SD = 2.24). Sense of presence was different from the mean of the scale (i.e., 5.5) in

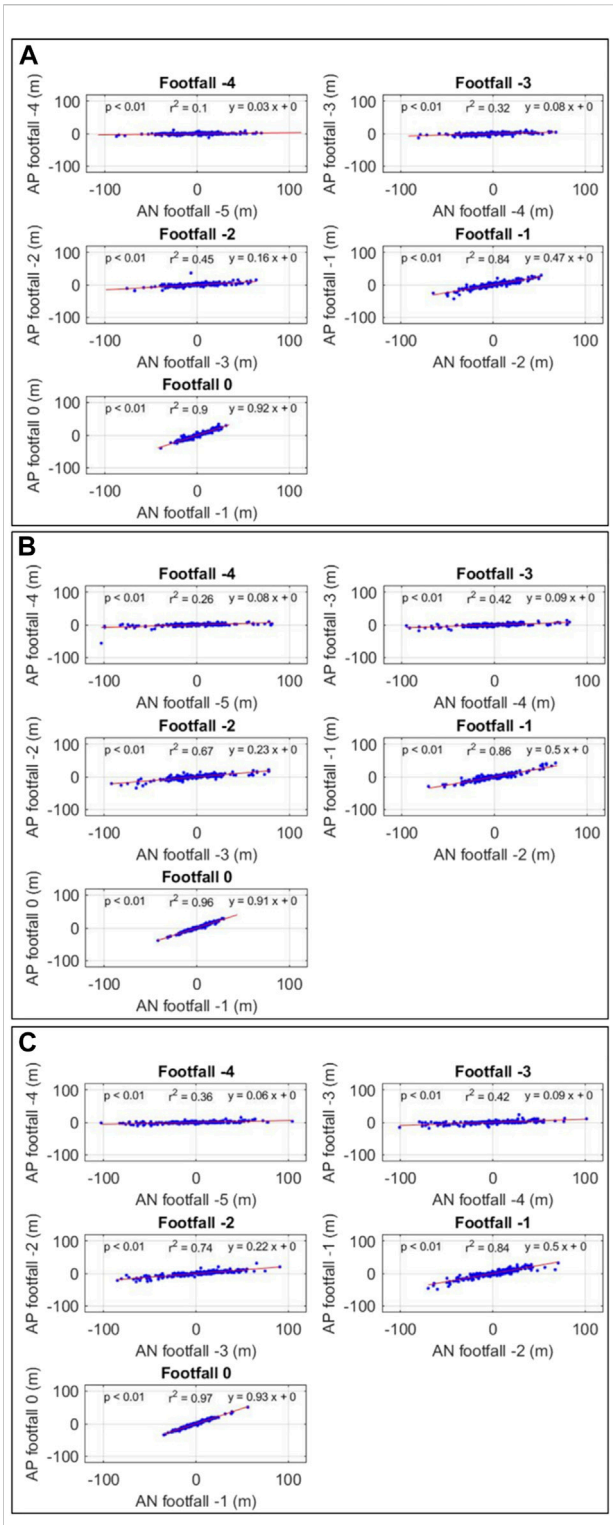

FIGURE 10
Relationship between the amount of adjustment needed (AN) at a certain footfall and the amount of adjustment produced (AP) in the following footfall. **(A)** real-world condition **(B)** corresponding virtual reality condition **(C)** outdoor virtual reality condition.

corresponding VR ($p < 0.001$) and in outdoor VR ($p < 0.001$). Participants felt present in the two VRC.

In terms of psychological variables, our hypothesis (H2) was partially confirmed. We hypothesized that the HMD would be accepted by the participants before its use. For the four different variables used to examine acceptance of the VR device, only BIU was not different from the mean of the scale before use. Our hypothesis (H3) was partially confirmed. We hypothesized an increase in HMD acceptance after use compared with its level before use) but only the PEU increased. Our hypotheses (H4) and (H5) were confirmed. We hypothesized a low level of cybersickness and a high level of sense of presence in both VRC.

4 Discussion

In the present study, we sought to ensure that gait adaptability behavior in the elderly was comparable when performing a goal-directed displacement in the real-world and in fully immersive VR. We also ensured that the participants accepted the HMD before and after use. Moreover, we investigated the influence of the visual context on gait adaptability behavior and on acceptance of this VR-HMD. Finally, we studied cybersickness and sense of presence in the two virtual environments.

4.1 Gait parameters

4.1.1 Gait speed analysis

In our study, the participants walked on average at 1.07 m/s, 0.96 m/s, and 0.98 m/s (SD = 0.02 m/s) in RWC, corresponding VR and outdoor VR, respectively. They demonstrated a similar gait speed compared with previous studies. Mirelman et al. (2016) found that their participants walked on average at 0.99 m/s during a real-world gait training on treadmill and at 1.00 m/s in low-immersive VR gait training on treadmill. Caetano et al. (2018) found that, during a gait adaptability test in the real world, the participants walked on average at 1.10 m/s (SD = 0.1 m/s) and 0.92 m/s (SD = 0.2 m/s) for low risk and high risk of falling groups, respectively. A low gait speed is a strong predictor for adverse health outcomes such as falls, functional decline, and mortality in older people (Abellan Van Kan et al., 2009) and it is adopted by high-risk older adults to approach the obstacle/target due to cognitive and motor deficits (Caetano et al., 2018). A gait speed below 1.0 m/s indicates an increased fall risk (Kyrdalen et al., 2019). In our study, gait speeds were close to 1.0 m/s in the three experimental conditions. This result can be explained by the experimental set-up. The participants walked with a safety

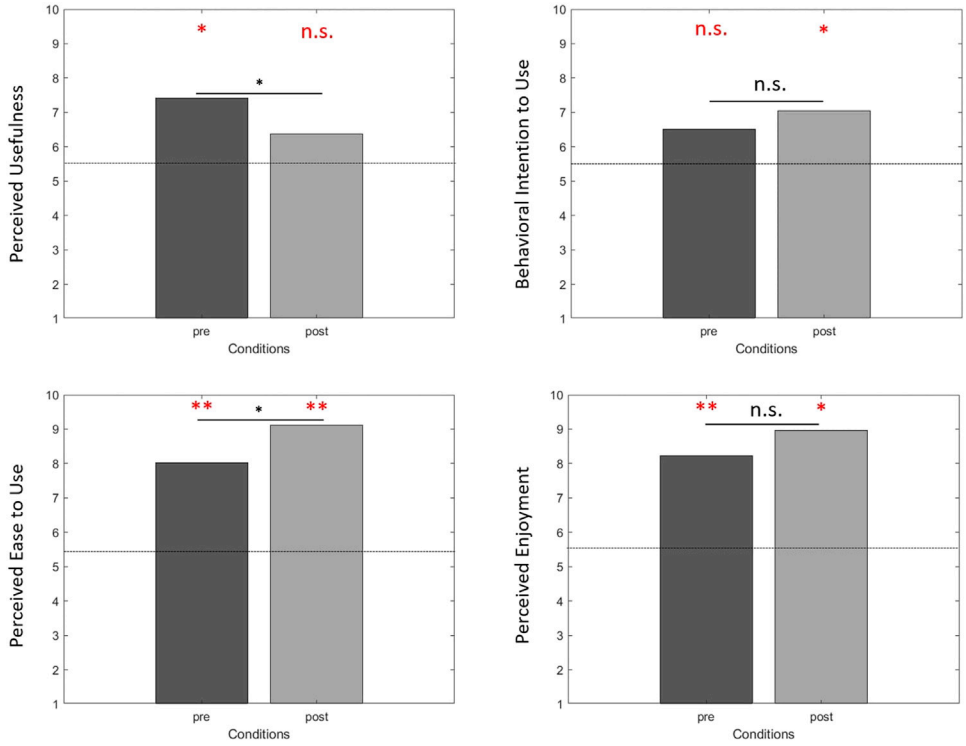

FIGURE 11
Acceptance of the virtual reality device before (pre) and after use (post). Analyses revealed that only PU after use (p = 0.217) and BIU before use (p = 0.184) were not different from the mean of the scale (i.e., dotted lines). Analyses showed differences between before and after use for PU (p = 0.007) and PEU (p = 0.033). n. s. no difference; *p < 0.05; **p < 0.001. In red, compared with the mean of the scale. In black, between conditions analyses.

harness connected to an in-ceiling rail by a lanyard and had to overcome inertia during the first steps.

In terms of gait speed comparison between real and virtual environments, we demonstrated no difference between the two types of environments, in line with Janeh et al.'s (2018) study conducted with older adults. Moreover, we found no difference between the two different virtual environments. In summary, in our study, the participants adopted the same gait speed whatever the type of environment and visual context.

4.1.2 Pointing accuracy analysis

We found that the participants had a lower APE in VRC (2.78 cm ± 0.86 cm and 3.20 cm ± 1.66 cm in corresponding VR and outdoor VR, respectively) compared with RWC (4.53 cm ± 1.43 cm). In our study, the participants were very accurate and even more so in VRC. In the three conditions, APEs were smaller than those recorded in the studies in young adults by De Rugy et al. (2000), Montagne et al. (2000), and Cornus et al. (2009) which were 15 cm, 12 cm, and 9 cm respectively. These differences could have also arisen from differences in both task and methodological constraints. In the study by De Rugy et al. (2000), participants walked on a treadmill while the virtual environment was depicted on a screen in front of them, and the target disappeared just before locomotor pointing. The disappearance of the target could have led to performance deterioration. In their long-jumping study, Montagne et al. (2000) asked their participants to jump as far as possible. It is worth mentioning that although good pointing accuracy is a necessary condition for a good jump, the very high running velocity makes accurate pointing difficult (speed-accuracy trade-off). In the study by Cornus et al. (2009), participants had to step over an obstacle, so very precise pointing was not crucial.

Furthermore, we found that the participants had a lower CPE in VRC (−2.47 cm ± 0.98 cm and −2.51 cm ± 2.11 cm in corresponding VR and outdoor VR, respectively) compared with RWC (−3.52 cm ± 1.84). The results showed that the participants tended to place their feet before the target in the three conditions. This result must be explained by the instructions given (i.e., place the right foot tip as close as possible to the lower extremity of the target).

In addition, there was no difference in the APE and the CPE between the VRC. The virtual visual context does not modify the pointing accuracy.

In summary, in our study, the participants had a high level of pointing accuracy in both real and virtual environments.

4.1.3 Inter-trial analyses

The standard deviations of both the step lengths and the toe-obstacle distances during the target approach phase were computed.

First, high values of standard deviations of toe-obstacle distances at the beginning of the target approach phase (i.e., footfall −4 and −3) reflect the fact that the target position was manipulated across trials. Moreover, our results revealed an increase in the mean standard deviation of step lengths at footfall −2 (i.e., three steps before pointing) combined with a decrease in the mean standard deviation of toe-obstacle distances, in the three experimental conditions. These inverted patterns of variability are in agreement with the results obtained in other studies based on different kinds of goal-directed locomotion tasks (Montagne et al., 2000; Cornus et al., 2009; Van Andel et al., 2018a). A precise comparison of our results with the results obtained in these studies revealed that both Van Andel et al. (2018a) and Montagne et al. (2002) also reported an increase in step length variability three steps before pointing, while the increase in variability occurred one step sooner in the study by Cornus et al. (2009). Furthermore, Montagne et al. (2000) and Cornus et al. (2009) reported a decrease in the mean standard deviation of toe-obstacle distances one step sooner than in our study. Rather than emphasizing these slight differences, which probably came from specific task constraints and differences in the methods used, we prefer to focus on the strong similarities in the patterns of variability among the different studies.

These concomitant and inverted patterns of variability could mirror some kinds of functional locomotion adaptations which have been labeled "compensatory variability" by Bootsma & van Wieringen (1990). The increase in step length variability is due to step length adjustments produced to perform an optimal foot positioning (i.e., minimize toe-obstacle distance at the last footfall). Importantly, this "compensatory variability" was not affected by the type of environment nor by the visual context. We found similar patterns of variability whatever the experimental conditions.

4.1.4 Trial-by-trial analyses

4.1.4.1 Inter-step number analysis

In our study, 88.3%, 87.9%, and 88.9% of trials were regulated in RWC, corresponding VR, and outdoor VR, respectively. The percentage of regulated trials (88.6%) was very close to the results of Van Andel et al. (2018a) (87%), but slightly greater than those obtained by Montagne et al. (2000) and Cornus et al. (2009) (77.7 and 65.9% respectively). This result demonstrates that the manipulation of the target position between trials almost always compelled the participants to regulate their displacement.

The participants adopted three different step adjustment strategies, either lengthening or shortening or mixed strategies, similar to those observed by Cornus et al. (2009) and Van Andel et al. (2018a) in pointing tasks and those observed by Montagne et al. (2000) in a long-jumping task. The percentage of mixed trials in our study (47.2% on average) was greater than those reported by Montagne et al. (2000), Cornus et al. (2009), and Van Andel et al. (2018a) (20%, 7.5 and 22% respectively). Among the non-mixed trials, in our study, the participants adopted in the same proportion lengthening trials (50.3% on average) and shortening trials (49.7% on average). However, in Cornus et al. (2009) participants adopted a higher percentage of lengthening strategy than of shortening strategy (61,1 and 38.9% respectively), whereas in Van Andel et al. (2018a) the opposite was shown (37.7% of lengthening strategy and 62.3% of shortening strategy). In our study, the participants did not adopt a specific strategy (either lengthening or shortening) to regulate their displacement, which suggested a trade-off between cautious walks with shortened steps and efficient walks with lengthening steps (Huang et al., 2010). These results indicated that the strategies adopted depend on the characteristics of the investigated population, as shown in the study by Van Andel et al. (2018b).

In summary, the participants adopted similar step adjustment strategies whatever the experimental condition. Strategies of adjustments of step lengths were not affected by the type of environment nor by the visual context.

4.1.4.2 Intra-step number analysis

The intra-step number analysis was conducted to determine the amount of adjustments needed at a given footfall (in relation to toe-obstacle distances) and the amount of adjustments produced during the next footfall (in relation to step lengths) for each footfall.

In our study, the relationship between these two variables was statistically significant from footfall −4 in the three experimental conditions. The slope of the regression lines (β) increased over the target approach from 0.06, on average, at footfall −4, to 0.95, on average, at footfall 0. Moreover, the value of R^2 increased slightly over the target approach in the three experimental conditions from 0.24, on average, at footfall −4, to 0.94, on average, at footfall 0. As in previous studies, the linearity of the relationship increased progressively from footfall −4 to footfall 0. This increasing inclination of the regression lines (i.e., increasing slopes) suggests that during the approach the amount of adjustments produced at a given footfall moves closer and closer to the amount needed (i.e., the amount to be adjusted) to succeed in the task. The current difference of toe-obstacle distance (i.e., the amount of adjustments needed) at a given footfall was rectified by a step length modulation (i.e., the amount of adjustments produced) at the following footfall. Moreover, at the last footfall (i.e., the pointing one), the inclination of the

regression line in our study was almost equal to 1 (β = 0.94), slightly above that in Cornus et al. (2009) (β = 0.84). This result underlines a strong relationship between the two variables, particularly during the last footfall. During this last footfall, the difference of toe-obstacle distance at footfall -1 was almost totally rectified by the step length modulation at the last footfall (i.e., footfall 0). These results demonstrated that the underlying control mechanism is based on a close information-movement coupling. Step length adjustments were produced gradually when needed. Adjustments produced by the participant, within a trial, depend on the current state of the agent-environment system.

In addition, our results revealed that the participants adopted this same gait adjustment behavior whatever the experimental condition. This type of analysis demonstrates the use of a generic control mechanism based on a tight coupling between information and movement and leading to successive adjustments depending on the state of the agent-environment system, in both real and virtual environments. Moreover, we found no differences in control mechanism between the two different virtual environments.

In summary, in our study, we found the control mechanism was not affected by the type of environment nor by the visual context.

4.2 Psychological variables

4.2.1 Acceptance of the VR HMD

We aimed to ensure that the participants accepted the VR device before and after its use. First of all, we found that the participants had a high perceived usefulness, perceived ease of use, and perceived enjoyment before use. The participants considered the HMD useful, easy to use, and enjoyable before use, in line with the results of Mascret et al.'s (2020) study. However, the participants did not intend to use the HMD before a first use, but they did not refuse it either. This was not so surprising because neutral attitudes toward HMD prior to a first exposure have already been found in older adults (Huygelier et al., 2019). We also showed that acceptance of the HMD was modulated after use. The participants considered the HMD easier to use and as enjoyable as before use, and they intended to use it after a first use. However, they considered the HMD neither useful nor useless after use. The decrease in perceived usefulness after use may be due to the purpose and the protocol of the present study. At the beginning of the experiment, the presentation of the VR set-up to participants with the short video focused on the role of the HMD in fall prevention, which may explain why perceived usefulness scores were high before a first use of the HMD. But after use, the participants may have considered that the pointing task performed in the study was not effectively useful for preventing fall occurrence, which was not in fact its objective. Nevertheless, perceived usefulness was not low after use; it remained around the mean of the scale. Conversely, after its first use, the participants intended to use the HMD, in line with Huygelier et al.'s (2019) study conducted with older adults. After use, increase in perceived ease of use reflects the fact that older adults feel more able to use this VR device, which is often found in the TAM literature when the technological device has a functioning adapted to the target population. Finally, high levels of perceived enjoyment before and after use highlighted the hedonic perception of the participants during VR exposition, which reinforces the numerous results identified in the literature highlighting that VR is mostly considered a hedonic technology before and after use (e.g., Manis & Choi, 2019).

4.2.2 Cybersickness and sense of presence

We found low levels of cybersickness and, conversely, high levels of sense of presence. Participants did not experience cybersickness and felt present in the two VRC. Participants did not experience potential adverse effects of virtual exposition. This result is very important in the development of our training program when we know that cybersickness negatively predicts intention to use an HMD (Sagnier et al., 2020). Moreover, the notion of the subjective experience of being in a virtual environment (by the study of sense of presence) is essential to ensure ecological validity in virtual environments (Slater, 2009; Birenboim et al., 2021). In terms of user experience, these results confirm the possibility of developing virtual gait training programs in various visual contexts for the elderly.

4.3 Limitations and directions for future studies

The present study had some limitations that might be addressed in future research.

First, although the representation only of virtual 3D shoes (representing the feet during the locomotion in VR) leads to similar gait adaptability behavior between real and virtual environments, the inclusion of an embodying avatar in our future gait training in fully immersive VR would be necessary. The representation of the user's body via an avatar in VR will enhance subjective experience of being in a virtual environment and the ecological validity of our VR environments (Slater, 2009; Grabarczyk & Pokropski, 2016).

Secondly, the healthy older adults involved in our study were relatively young, with a mean age of 68.6 years, and had never fallen. In this present study, we had to take methodological precautions on this specific population because our future training programs will concern only pre-fall participants (healthy older adults with no fall history). However, it would be interesting to extend this study to older adults with high risk of falling. Older adults who have experienced a fall are likely not to have the same gait behavior nor the same subjective experience in VR. Fall history (i.e., any fall event experienced by older adults during a specified period of time) influences older adults' behavior in VR training (Dermody et al., 2020).

Moreover, these methodological precautions should be taken with each kind of technology used, which is rarely the case in the literature. We ensured that gait adaptability behavior was not affected by the use of the VR technology which we will use in our future training programs. We also ensured that older adults accept the VR technology which we will use in our future training programs. Each VR technology (custom or high-performance devices) can have adverse effects on psychological and/or behavioral parameters. We advise those likely to deploy VR training protocols to do the same in the future.

Finally, concerning the study of psychological variables, although the completion of the questionnaires was anonymous, older adults may be subject to social desirability during self-reported questionnaires (Phillips & Clancy, 1972).

5 Conclusion

This study should allow us to take methodological precautions before developing our fully immersive VR training program intended to prevent falls in the elderly. This long-term ambition led us to carry out a multidisciplinary study with our target population. We showed that the gait adaptability behavior of older adults was the same whatever the environment (real vs. virtual) during a goal-directed locomotion task. We also demonstrated that older adults accepted the HMD before and after use, with a low level of cybersickness and a high level of sense of presence. We can now conduct our ambitious interventional study intended to propose the more relevant VR training method to develop gait adaptability in older adults.

Data availability statement

The raw data supporting the conclusions of this article will be made available by the authors, without undue reservation.

Ethics statement

The studies involving human participants were reviewed and approved by IRB00012476-2020-25-03-51. The patients/participants provided their written informed consent to participate in this study.

Author contributions

Study conception and design: LD, NM, CG, GM. Data collection: LD. Analysis and interpretation of results: LD, NM, GM. Draft manuscript preparation: LD, NM, GM. All authors reviewed the results and approved the final version of the manuscript.

Funding

This research was funded by a doctoral fellowship obtained by LD from the regional council ('Région Sud') and Prolexia company.

Acknowledgments

The authors would like to acknowledge Amélie Voron for working with our research team.

Conflict of interest

The authors declare that the research was conducted in the absence of any commercial or financial relationships that could be construed as a potential conflict of interest.

Publisher's note

All claims expressed in this article are solely those of the authors and do not necessarily represent those of their affiliated organizations, or those of the publisher, the editors and the reviewers. Any product that may be evaluated in this article, or claim that may be made by its manufacturer, is not guaranteed or endorsed by the publisher.

Supplementary material

The Supplementary Material for this article can be found online at: https://www.frontiersin.org/articles/10.3389/fbioe.2022.917486/full#supplementary-material

References

Abellan Van Kan, G., Rolland, Y., Andrieu, S., Bauer, J., Beauchet, O., Bonnefoy, M., et al. (2009). Gait speed at usual pace as a predictor of adverse outcomes in community-dwelling older people an International Academy on Nutrition and Aging (IANA) Task Force. *J. Nutr. Health Aging* 13, 881–889. doi:10.1007/s12603-009-0246-z

Agethen, P., Sekar, V. S., Gaisbauer, F., Pfeiffer, T., Otto, M., and Rukzio, E. (2018). Behavior analysis of human locomotion in the real world and virtual reality for the manufacturing industry. *ACM Trans. Appl. Percept.* 15, 1–19. doi:10.1145/3230648

Alexandre, B., Reynaud, E., Osiurak, F., and Navarro, J. (2018). Acceptance and acceptability criteria: A literature review. *Cogn. Tech. Work* 20, 165–177. doi:10.1007/s10111-018-0459-1

Ambrose, A. F., Paul, G., and Hausdorff, J. M. (2013). Risk factors for falls among older adults: A review of the literature. *Maturitas* 75, 51–61. doi:10.1016/j.maturitas.2013.02.009

Anderson, A. P., Mayer, M. D., Fellows, A. M., Cowan, D. R., Hegel, M. T., and Buckey, J. C. (2017). Relaxation with immersive natural scenes presented

using virtual reality. *Aerosp. Med. Hum. Perform.* 88, 520–526. doi:10.3357/AMHP.4747.2017

Ashburn, A., Stack, E., Ballinger, C., Fazakarley, L., and Fitton, C. (2008). The circumstances of falls among people with Parkinson's disease and the use of Falls Diaries to facilitate reporting. *Disabil. Rehabilitation* 30, 1205–1212. doi:10.1080/09638280701828930

Berg, W. P., Wade, M. G., and Greer, N. L. (1994). Visual regulation of gait in bipedal locomotion: Revisiting lee, lishman, and thomson (1982). *J. Exp. Psychol. Hum. Percept. Perform.* 20 (4), 854–863. doi:10.1037/0096-1523.20.4.854

Berg, W. P., Alessio, H. M., Mills, E. M., and Tong, C. (1997). Circumstances and consequences of falls in independent community-dwelling older adults. *Age Ageing* 26, 261–268. doi:10.1093/ageing/26.4.261

Birenboim, A., Ben-Nun Bloom, P., Levit, H., and Omer, I. (2021). The study of walking, walkability and wellbeing in immersive virtual environments. *IJERPH* 18, 364. doi:10.3390/ijerph18020364

Bootsma, J., and van Wieringen, P. C. W. (1990). Timing an attacking forehand drive in table tennis. *J. Exp. Psychol. Copyrightthe Am. Psychol. Assoc. lnc, Hum. Percept. Perform.* 16, 21–29.

Buhler, M. A., and Lamontagne, A. (2018). Circumvention of pedestrians while walking in virtual and physical environments. *IEEE Trans. Neural Syst. Rehabil. Eng.* 26, 1813–1822. doi:10.1109/TNSRE.2018.2865907

Burdea, G. (2003). Virtual rehabilitation – benefits and challenges. *Methods Inf. Med.* 42, 519–523. doi:10.1267/METH03050519

Burns, E. R., Stevens, J. A., and Lee, R. (2016). The direct costs of fatal and non-fatal falls among older adults — United States. *J. Saf. Res.* 58, 99–103. doi:10.1016/j.jsr.2016.05.001

Cano Porras, D., Siemonsma, P., Inzelberg, R., Zeilig, G., and Plotnik, M. (2018). Advantages of virtual reality in the rehabilitation of balance and gait: Systematic review. *Neurology* 90, 1017–1025. doi:10.1212/WNL.0000000000005603

Caetano, M. J. D., Lord, S. R., Brodie, M. A., Schoene, D., Pelicioni, P. H. S., Sturnieks, D. L., et al. (2018). Executive functioning, concern about falling and quadriceps strength mediate the relationship between impaired gait adaptability and fall risk in older people. *Gait Posture* 59, 188–192. doi:10.1016/j.gaitpost.2017.10.017

Caetano, M. J. D., Lord, S. R., Schoene, D., Pelicioni, P. H. S., Sturnieks, D. L., and Menant, J. C. (2016). Age-related changes in gait adaptability in response to unpredictable obstacles and stepping targets. *Gait Posture* 46, 35–41. doi:10.1016/j.gaitpost.2016.02.003

Cikajlo, I., and Peterlin Potisk, K. (2019). Advantages of using 3D virtual reality based training in persons with Parkinson's disease: A parallel study. *J. NeuroEngineering Rehabil.* 16, 119. doi:10.1186/s12984-019-0601-1

Cornus, S., Laurent, M., and Laborie, S. (2009). Perception-movement coupling in the regulation of step lengths when approaching an obstacle. *Ecol. Psychol.* 21, 334–367. doi:10.1080/10407410903320991

Corregidor-Sánchez, A. I., Segura-Fragoso, A., Rodríguez-Hernández, M., Criado-Alvarez, J. J., González-Gonzalez, J., and Polonio-López, B. (2019). Can exergames contribute to improving walking capacity in older adults? A systematic review and meta-analysis. *Maturitas* 132, 40–48. doi:10.1016/j.maturitas.2019.12.006

Davis, F. D. (1989). Perceived usefulness, perceived ease of use, and user acceptance of information technology. *MIS Q.* 13, 319. doi:10.2307/249008

Davis, F. D., and Venkatesh, V. (1996). A critical assessment of potential measurement biases in the technology acceptance model: Three experiments. *Int. J. Human-Computer Stud.* 45, 19–45. doi:10.1006/ijhc.1996.0040

De Rugy, A., Montagne, G., Buekers, M. J., and Laurent, M. (2001). Spatially constrained locomotion under informational conflict. *Behav. Brain Res.* 123, 11–15. doi:10.1016/S0166-4328(01)00185-1

De Rugy, A., Montagne, G., Buekers, M. J., and Laurent, M. (2002). Temporal information for spatially constrained locomotion. *Exp. Brain Res.* 146, 129–141. doi:10.1007/s00221-002-1155-0

De Rugy, A., Montagne, G., Buekers, M. J., and Laurent, M. (2000). The study of locomotor pointing in virtual reality: The validation of a test set-up. *Behav. Res. Methods, Instrum. Comput.* 32, 515–520. doi:10.3758/BF03200823

Delgado, F., and Der Ananian, C. (2021). The use of virtual reality through head-mounted display on balance and gait in older adults: A scoping review. *Games Health J.* 10, 2–12. doi:10.1089/g4h.2019.0159

Dermody, G., Whitehead, L., Wilson, G., and Glass, C. (2020). The role of virtual reality in improving health outcomes for community-dwelling older adults: Systematic review. *J. Med. Internet Res.* 22, e17331. doi:10.2196/17331

Dunn, T. J., Baguley, T., and Brunsden, V. (2014). From alpha to omega: A practical solution to the pervasive problem of internal consistency estimation. *Br. J. Psychol.* 105, 399–412. doi:10.1111/bjop.12046

Fink, P. W., Foo, P. S., and Warren, W. H. (2007). Obstacle avoidance during walking in real and virtual environments. *ACM Trans. Appl. Percept.* 4, 2. doi:10.1145/1227134.1227136

Gibson, J., J. (1979). *The ecological approach to visual perception*. Boston: Houghton Mifflin.

Grabarczyk, P., and Pokropski, M. (2016). Perception of affordances and experience of presence in virtual reality. *AVANT VII* 1, 25–44. doi:10.26913/70202016.0112.0002

Hayotte, M., Thérouanne, P., Gray, L., Corrion, K., and d'Arripe-Longueville, F. (2020). The French eHealth acceptability scale using the unified theory of acceptance and use of technology 2 model: Instrument validation study. *J. Med. Internet Res.* 22, e16520. doi:10.2196/16520

Howard, M. C. (2017). A meta-analysis and systematic literature review of virtual reality rehabilitation programs. *Comput. Hum. Behav.* 70, 317–327. doi:10.1016/j.chb.2017.01.013

Huang, Y., Chen, B., Wang, Q., Wei, K., and Wang, L. (2010). "Energetic efficiency and stability of dynamic bipedal walking gaits with different step lengths" in IEEE/RSJ 2010 International Conference on Intelligent Robots and Systems, IROS 2010 - Conference Proceedings, 40877–4082. doi:10.1109/IROS.2010.5650421

Huygelier, H., Schraepen, B., van Ee, R., Vanden Abeele, V., and Gillebert, C. R. (2019). Acceptance of immersive head-mounted virtual reality in older adults. *Sci. Rep.* 9, 4519. doi:10.1038/s41598-019-41200-6

Janeh, O., Bruder, G., Steinicke, F., Gulberti, A., and Poetter-Nerger, M. (2018). Analyses of gait parameters of younger and older adults during (Non-)Isometric virtual walking. *IEEE Trans. Vis. Comput. Graph.* 24, 2663–2674. doi:10.1109/TVCG.2017.2771520

Joseph, A., Browning, M. H. E. M., and Jiang, S. (2020). Using immersive virtual environments (IVEs) to conduct environmental design research: A primer and decision framework. *HERD* 13, 11–25. doi:10.1177/1937586720924787

Kamińska, M. S., Miller, A., Rotter, I., Szylińska, A., and Grochans, E. (2018). The effectiveness of virtual reality training in reducing the risk of falls among elderly people. *CIA* 13, 2329–2338. doi:10.2147/CIA.S183502

Keshner, E. A., Weiss, P. T., Geifman, D., and Raban, D. (2019). Tracking the evolution of virtual reality applications to rehabilitation as a field of study. *J. NeuroEngineering Rehabil.* 16, 76. doi:10.1186/s12984-019-0552-6

Khanuja, K., Joki, J., Bachmann, G., and Cuccurullo, S. (2018). Gait and balance in the aging population: Fall prevention using innovation and technology. *Maturitas* 110, 51–56. doi:10.1016/j.maturitas.2018.01.021

Kuliga, S. F., Thrash, T., Dalton, R. C., and Hölscher, C. (2015). Virtual reality as an empirical research tool — exploring user experience in a real building and a corresponding virtual model. *Comput. Environ. Urban Syst.* 54, 363–375. doi:10.1016/j.compenvurbsys.2015.09.006

Kyrdalen, I. L., Thingstad, P., Sandvik, L., and Ormstad, H. (2019). Associations between gait speed and well-known fall risk factors among community-dwelling older adults. *Physiother. Res. Int.* 24, e1743. doi:10.1002/pri.1743

Lee, D. N., Lishman, J. R., and Thomson, J. A. (1982). Regulation of gait in long jumping. *J. Exp. Psychol. Copyrightthe Am. Psychol. Assoc. lnc, Hum. Percept. Perform.* 8, 448–459.

Levin, M. F., Weiss, P. L., and Keshner, E. A. (2015). Emergence of virtual reality as a tool for upper limb rehabilitation: Incorporation of motor control and motor learning principles. *Phys. Ther.* 95, 415–425. doi:10.2522/ptj.20130579

Lourenço, C. B., Azeff, L., Sveistrup, H., and Levin, M. F. (2008). "Effect of environment on motivation and sense of presence in healthy subjects performing reaching tasks," in *2008 virtual rehabilitation* (Vancouver, BC: IEEE), 93–98. doi:10.1109/ICVR.2008.4625143

Manis, K. T., and Choi, D. (2019). The virtual reality hardware acceptance model (VR-HAM): Extending and individuating the technology acceptance model (TAM) for virtual reality hardware. *J. Bus. Res.* 100, 503–513. doi:10.1016/j.jbusres.2018.10.021

Mascret, N., Delbes, L., Voron, A., Temprado, J.-J., and Montagne, G. (2020). Acceptance of a virtual reality headset designed for fall prevention in older adults: Questionnaire study. *J. Med. Internet Res.* 22, e20691. doi:10.2196/20691

Mirelman, A., Maidan, I., Shiratzky, S. S., and Hausdorff, J. M. (2020). "Virtual reality training as an intervention to reduce falls," in *Falls and cognition in older persons*. Editors M. Montero-Odasso and R. Camicioli (Cham: Springer), 309–321. doi:10.1007/978-3-030-24233-6_18

Mirelman, A., Rochester, L., Maidan, I., Del Din, S., Alcock, L., Nieuwhof, F., et al. (2016). Addition of a non-immersive virtual reality component to treadmill training to reduce fall risk in older adults (V-time): A randomised controlled trial. *Lancet* 388, 1170–1182. doi:10.1016/S0140-6736(16)31325-3

Montagne, G., Buekers, M. J., De Rugy, A., Camachon, C., and Laurent, M. (2002). Control of human locomotion under various task constraints. *Exp. Brain Res.* 143 (1), 133–136. doi:10.1007/s00221-001-0990-8

Montagne, G., Cornus, S., Glize, D., Quaine, F., and Laurent, M. (2000). A perception-action coupling type of control in long jumping. *J. Mot. Behav.* 32, 37–43. doi:10.1080/00222890009601358

Menz, H. B., Latt, M. D., Tiedemann, A., Mun San Kwan, M., and Lord, S. R. (2004). Reliability of the GAITRite® walkway system for the quantication of temporo-spatial parameters of gait in young and older people. *Gait Posture* 20 (1), 20–25. doi:10.1016/S0966-6362(03)00068-7

Muhla, F., Clanché, F., Duclos, K., Meyer, P., Maïaux, S., Colnat-Coulbois, S., et al. (2020). Impact of using immersive virtual reality over time and steps in the Timed up and Go test in elderly people. *PLoS ONE* 15, e0229594. doi:10.1371/journal.pone.0229594

Mütterlein, J., and Hess, T. (2017). "Immersion, presence, interactivity: Towards a joint understanding of factors influencing virtual reality acceptance and use," in *Proceedings of the 23rd americas conference on information systems* 1. (Boston, USA: AMCIS).

Nasreddine, Z. S., Phillips, N. A., Bédirian, V., Charbonneau, S., Whitehead, V., Collin, I., et al. (2005). The montreal cognitive assessment, MoCA: A brief screening tool for mild cognitive impairment. *J. Am. Geriatrics Soc.* 53, 695–699. doi:10.1111/j.1532-5415.2005.53221.x

Neri, S. G., Cardoso, J. R., Cruz, L., Lima, R. M., de Oliveira, R. J., Iversen, M. D., et al. (2017). Do virtual reality games improve mobility skills and balance measurements in community-dwelling older adults? Systematic review and meta-analysis. *Clin. Rehabil.* 31, 1292–1304. doi:10.1177/0269215517694677

Nevitt, M. C., Cummings, S. R., and Hudes, E. S. (1991). Risk factors for injurious falls: A prospective study. *J. Gerontology* 46, 64–170. doi:10.1093/geronj/46.5.M164

Nevitt, M. C. (1989). Risk factors for recurrent nonsyncopal falls. A prospective study. *JAMA J. Am. Med. Assoc.* 261, 2663–2668. doi:10.1001/jama.261.18.2663

Newman, M., Gatersleben, B., Wyles, K. J., and Ratcliffe, E. (2022). The use of virtual reality in environment experiences and the importance of realism. *J. Environ. Psychol.* 79, 101733. doi:10.1016/j.jenvp.2021.101733

Nørgaard, J. E., Jorgensen, M. G., Ryg, J., Andreasen, J., Danielsen, M. B., Steiner, D. K., et al. (2021). Effects of gait adaptability training on falls and fall-related fractures in older adults: A systematic review and meta-analysis. *Age Ageing* 50, 1914–1924. doi:10.1093/ageing/afab105

Osoba, M. Y., Martelli, D., Prado, A., Agrawal, S. K., and Lalwani, A. K. (2020). Age-related differences in gait adaptations during overground walking with and without visual perturbations using a virtual reality headset. *Sci. Rep.* 10, 15376. doi:10.1038/s41598-020-72408-6

Overstall, P. W., Exton-Smith, A. N., Imms, F. J., and Johnson, A. L. (1977). Falls in the elderly related to postural imbalance. *BMJ* 1, 261–264. doi:10.1136/bmj.1.6056.261

Phillips, D. L., and Clancy, K. J. (1972). Some effects of "social desirability" in survey studies. *Am. J. Sociol.* 77, 921–940. doi:10.1086/225231

Plante, T. G., Aldridge, A., Bogden, R., and Hanelin, C. (2003). Might virtual reality promote the mood benefits of exercise? *Comput. Hum. Behav.* 19, 495–509. doi:10.1016/S0747-5632(02)00074-2

Robillard, G., Bouchard, S., Fournier, T., and Renaud, P. (2003). Anxiety and presence during VR immersion: A comparative study of the reactions of phobic and non-phobic participants in therapeutic virtual environments derived from computer games. *CyberPsychology Behav.* 6, 467–476. doi:10.1089/109493103769710497

Robinovitch, S. N., Feldman, F., Yang, Y., Schonnop, R., Leung, P. M., Sarraf, T., et al. (2013). Video capture of the circumstances of falls in elderly people residing in long-term care: An observational study. *Lancet* 381, 47–54. doi:10.1016/S0140-6736(12)61263-X

Rogerson, M., Gladwell, V., Gallagher, D., and Barton, J. (2016). Influences of green outdoors versus indoors environmental settings on psychological and social outcomes of controlled exercise. *IJERPH* 13, 363. doi:10.3390/ijerph13040363

Sagnier, C., Loup-Escande, E., Lourdeaux, D., Thouvenin, I., and Valléry, G. (2020). User acceptance of virtual reality: An extended technology acceptance model. *Int. J. Human–Computer Interact.* 36, 993–1007. doi:10.1080/10447318.2019.1708612

Sakhare, A. R., Yang, V., Stradford, J., Tsang, I., Ravichandran, R., and Pa, J. (2019). Cycling and spatial navigation in an enriched, immersive 3D virtual park environment: A feasibility study in younger and older adults. *Front. Aging Neurosci.* 11, 218. doi:10.3389/fnagi.2019.00218

Schmidt, R. A., and Lee, T. D. (1982). *Motor control and learning: A behavioral emphasis*. 4th ed. Champaign, IL, US: Human Kinetics.

Schultheis, M. T., and Rizzo, A. A. (2001). The application of virtual reality technology in rehabilitation. *Rehabil. Psychol.* 46, 296–311. doi:10.1037/0090-5550.46.3.296

Shema, S. R., Brozgol, M., Dorfman, M., Maidan, I., Sharaby-Yeshayahu, L., Malik-Kozuch, H., et al. (2014). Clinical experience using a 5-week treadmill training program with virtual reality to enhance gait in an ambulatory physical therapy service. *Phys. Ther.* 94, 1319–1326. doi:10.2522/ptj.20130305

Slater, M. (2009). Place illusion and plausibility can lead to realistic behaviour in immersive virtual environments. *Phil. Trans. R. Soc. B* 364, 3549–3557. doi:10.1098/rstb.2009.0138

Syed-Abdul, S., Malwade, S., Nursetyo, A. A., Sood, M., Bhatia, M., Barsasella, D., et al. (2019). Virtual reality among the elderly: A usefulness and acceptance study from taiwan. *BMC Geriatr.* 19, 223. doi:10.1186/s12877-019-1218-8

Tieri, G., Morone, G., Paolucci, S., and Iosa, M. (2018). Virtual reality in cognitive and motor rehabilitation: Facts, fiction and fallacies. *Expert Rev. Med. Devices* 15, 107–117. doi:10.1080/17434440.2018.1425613

Timmermans, C., Roerdink, M., Janssen, T. W. J., Beek, P. J., and Meskers, C. G. M. (2019). Automatized, standardized, and patient-tailored progressive walking-adaptability training: A proof-of-concept study. *Phys. Ther.* 99, 882–892. doi:10.1093/ptj/pzz013

Tinetti, M. E., Speechley, M., and Ginter, S. F. (1988). Risk factors for falls among elderly persons living in the community. *N. Engl. J. Med.* 319, 1701–1707.

Van Andel, S., Cole, M. H., and Pepping, G.-J. (2018a). Perceptual-motor regulation in locomotor pointing while approaching a curb. *Gait Posture* 60, 164–170. doi:10.1016/j.gaitpost.2017.12.006

Van Andel, S., Cole, M. H., and Pepping, G.-J. (2018b). Regulation of locomotor pointing across the lifespan: Investigating age-related influences on perceptual-motor coupling. *PLoS ONE* 13, e0200244. doi:10.1371/journal.pone.0200244

Van Hooren, B., Fuller, J. T., Buckley, J. D., Miller, J. R., Sewell, K., Rao, G., et al. (2020). Is motorized treadmill running biomechanically comparable to overground running? A systematic review and meta-analysis of cross-over studies. *Sports Med.* 50, 785–813. doi:10.1007/s40279-019-01237-z

Van Ooijen, M. W., Roerdink, M., Trekop, M., Janssen, T. W. J., and Beek, P. J. (2016). The efficacy of treadmill training with and without projected visual context for improving walking ability and reducing fall incidence and fear of falling in older adults with fall-related hip fracture: A randomized controlled trial. *BMC Geriatr.* 16, 215. doi:10.1186/s12877-016-0388-x

Venkatesh, V., and Bala, H. (2008). Technology acceptance model 3 and a research agenda on interventions. *Decis. Sci.* 39, 273–315. doi:10.1111/j.1540-5915.2008.00192.x

Venkatesh, V., and Davis, F. D. (2000). A theoretical extension of the technology acceptance model: Four longitudinal field studies. *Manag. Sci.* 46, 186–204. doi:10.1287/mnsc.46.2.186.11926

Warren, W. H. (1998). Visually controlled locomotion: 40 years later. *Ecol. Psychol.* 10, 177–219.

Weber, A., Friemert, D., Hartmann, U., Epro, G., Seeley, J., Werth, J., et al. (2021). Obstacle avoidance training in virtual environments leads to limb-specific locomotor adaptations but not to interlimb transfer in healthy young adults. *J. Biomechanics* 120, 110357. doi:10.1016/j.jbiomech.2021.110357

Webster, K. E., Wittwer, J. E., and Feller, J. A. (2005). Validity of the GAITRite® walkway system for the measurement of averaged and individual step parameters of gait. *Gait Posture* 22 (4), 317–321. doi:10.1016/j.gaitpost.2004.10.005

Wee, H.-L., Fong, K.-Y., Tse, C., Machin, D., Cheung, Y.-B., Luo, N., et al. (2008). Optimizing the design of visual analogue scales for assessing quality of life: A semi-qualitative study among Chinese-speaking Singaporeans: Optimizing the design of

visual analogue scales. *J. Eval. Clin. Pract.* 14, 121–125. doi:10.1111/j.1365-2753.2007.00814.x

Weech, S., Kenny, S., and Barnett-Cowan, M. (2019). Presence and cybersickness in virtual reality are negatively related: A review. *Front. Psychol.* 10, 158. doi:10.3389/fpsyg.2019.00158

Weerdesteyn, V., Nienhuis, B., and Duysens, J. (2008). Exercise training can improve spatial characteristics of time-critical obstacle avoidance in elderly people. *Hum. Mov. Sci.* 27, 738–748. doi:10.1016/j.humov.2008.03.003

Witmer, B. G., and Singer, M. J. (1998). Measuring presence in virtual environments: A presence questionnaire. *Presence* 7, 225–240. doi:10.1162/105474698565686

Yamada, M., Higuchi, T., Tanaka, B., Nagai, K., Uemura, K., Aoyama, T., et al. (2011). Measurements of stepping accuracy in a multitarget stepping task as a potential indicator of fall risk in elderly individuals. *Journals Gerontology Ser. A Biol. Sci. Med. Sci.* 66A, 994–1000. doi:10.1093/gerona/glr073

Yin, J., Yuan, J., Arfaei, N., Catalano, P. J., Allen, J. G., and Spengler, J. D. (2020). Effects of biophilic indoor environment on stress and anxiety recovery: A between-subjects experiment in virtual reality. *Environ. Int.* 136, 105427. doi:10.1016/j.envint.2019.105427

Yu, C.-P., Lee, H.-Y., and Luo, X.-Y. (2018). The effect of virtual reality forest and urban environments on physiological and psychological responses. *Urban For. Urban Green.* 35, 106–114. doi:10.1016/j.ufug.2018.08.013

10.3389/fbioe.2022.917486

Appendix A

QUESTIONNAIRE n°1

Comme cela a été indiqué dans la vidéo, l'objectif associé à ce casque de réalité virtuelle est d'améliorer votre déplacement et votre équilibre. Pour chaque affirmation, cochez **LA CASE** qui indique votre avis, entre « Pas du tout d'accord » et « Tout à fait d'accord » (les cases intermédiaires servent à nuancer votre réponse). Sachez qu'aucune réponse n'est juste ou fausse, **c'est votre avis qui compte**. Il est tout à fait normal que vous ayez parfois l'impression de répondre plusieurs fois à la même question.

1	**Je pense que ce casque de réalité virtuelle pourrait être utile pour améliorer mon déplacement et mon équilibre**
	Pas du tout d'accord ☐ ☐ ☐ ☐ ☐ ☐ ☐ ☐ ☐ ☐ Tout à fait d'accord
2	**Je pense que le fonctionnement de ce casque de réalité virtuelle serait pour moi facilement compréhensible**
	Pas du tout d'accord ☐ ☐ ☐ ☐ ☐ ☐ ☐ ☐ ☐ ☐ Tout à fait d'accord
3	**Je pense que l'utilisation de ce casque de réalité virtuelle serait amusante**
	Pas du tout d'accord ☐ ☐ ☐ ☐ ☐ ☐ ☐ ☐ ☐ ☐ Tout à fait d'accord
4	**Si j'avais la possibilité d'avoir facilement accès à ce casque de réalité virtuelle, je souhaiterais l'utiliser**
	Pas du tout d'accord ☐ ☐ ☐ ☐ ☐ ☐ ☐ ☐ ☐ ☐ Tout à fait d'accord
5	**Je pense qu'utiliser ce casque de réalité virtuelle pourrait faciliter l'amélioration de mon déplacement et mon équilibre**
	Pas du tout d'accord ☐ ☐ ☐ ☐ ☐ ☐ ☐ ☐ ☐ ☐ Tout à fait d'accord
6	**Je pense que ce casque de réalité virtuelle serait simple d'utilisation**
	Pas du tout d'accord ☐ ☐ ☐ ☐ ☐ ☐ ☐ ☐ ☐ ☐ Tout à fait d'accord
7	**Je pense qu'utiliser ce casque de réalité virtuelle pourrait être divertissant**
	Pas du tout d'accord ☐ ☐ ☐ ☐ ☐ ☐ ☐ ☐ ☐ ☐ Tout à fait d'accord
8	**Si j'avais la possibilité d'avoir facilement accès à ce casque de réalité virtuelle, j'aurais l'intention de l'utiliser**
	Pas du tout d'accord ☐ ☐ ☐ ☐ ☐ ☐ ☐ ☐ ☐ ☐ Tout à fait d'accord
9	**Je pense qu'utiliser ce casque de réalité virtuelle me permettrait d'améliorer mon déplacement et mon équilibre**
	Pas du tout d'accord ☐ ☐ ☐ ☐ ☐ ☐ ☐ ☐ ☐ ☐ Tout à fait d'accord
10	**Je pense que ce casque de réalité virtuelle serait facile à utiliser**
	Pas du tout d'accord ☐ ☐ ☐ ☐ ☐ ☐ ☐ ☐ ☐ ☐ Tout à fait d'accord
11	**Je pense qu'utiliser ce casque de réalité virtuelle pourrait être ludique**
	Pas du tout d'accord ☐ ☐ ☐ ☐ ☐ ☐ ☐ ☐ ☐ ☐ Tout à fait d'accord
12	**Si j'avais la possibilité d'avoir facilement accès à ce casque de réalité virtuelle, je pense que je l'utiliserais**
	Pas du tout d'accord ☐ ☐ ☐ ☐ ☐ ☐ ☐ ☐ ☐ ☐ Tout à fait d'accord

Appendix B

QUESTIONNAIRE n°2

Nous vous rappelons que l'objectif associé à ce casque de réalité virtuelle est d'améliorer votre déplacement et votre équilibre. Pour chaque affirmation, cochez **LA CASE** qui indique votre avis, entre « Pas du tout d'accord » et « Tout à fait d'accord » (les cases intermédiaires servent à nuancer votre réponse). Sachez qu'aucune réponse n'est juste ou fausse, **c'est votre avis qui compte**. Il est tout à fait normal que vous ayez parfois l'impression de répondre plusieurs fois à la même question.

1	**Je pense que ce casque de réalité virtuelle est utile pour améliorer mon déplacement et mon équilibre**
	Pas du tout d'accord ☐ ☐ ☐ ☐ ☐ ☐ ☐ ☐ ☐ ☐ Tout à fait d'accord
2	**Je pense que le fonctionnement de ce casque de réalité virtuelle est pour moi facilement compréhensible**
	Pas du tout d'accord ☐ ☐ ☐ ☐ ☐ ☐ ☐ ☐ ☐ ☐ Tout à fait d'accord
3	**Je pense que l'utilisation de ce casque de réalité virtuelle est amusante**
	Pas du tout d'accord ☐ ☐ ☐ ☐ ☐ ☐ ☐ ☐ ☐ ☐ Tout à fait d'accord
4	**Si j'avais la possibilité d'avoir facilement accès à ce casque de réalité virtuelle, je souhaiterais l'utiliser**
	Pas du tout d'accord ☐ ☐ ☐ ☐ ☐ ☐ ☐ ☐ ☐ ☐ Tout à fait d'accord
5	**Je pense qu'utiliser ce casque de réalité virtuelle peut faciliter l'amélioration de mon déplacement et mon équilibre**
	Pas du tout d'accord ☐ ☐ ☐ ☐ ☐ ☐ ☐ ☐ ☐ ☐ Tout à fait d'accord
6	**Je pense que ce casque de réalité virtuelle est simple d'utilisation**
	Pas du tout d'accord ☐ ☐ ☐ ☐ ☐ ☐ ☐ ☐ ☐ ☐ Tout à fait d'accord
7	**Je pense qu'utiliser ce casque de réalité virtuelle est divertissant**
	Pas du tout d'accord ☐ ☐ ☐ ☐ ☐ ☐ ☐ ☐ ☐ ☐ Tout à fait d'accord
8	**Si j'avais la possibilité d'avoir facilement accès à ce casque de réalité virtuelle, j'aurais l'intention de l'utiliser**
	Pas du tout d'accord ☐ ☐ ☐ ☐ ☐ ☐ ☐ ☐ ☐ ☐ Tout à fait d'accord
9	**Je pense qu'utiliser ce casque de réalité virtuelle me permet d'améliorer mon déplacement et mon équilibre**
	Pas du tout d'accord ☐ ☐ ☐ ☐ ☐ ☐ ☐ ☐ ☐ ☐ Tout à fait d'accord
10	**Je trouve que ce casque de réalité virtuelle est facile à utiliser**
	Pas du tout d'accord ☐ ☐ ☐ ☐ ☐ ☐ ☐ ☐ ☐ ☐ Tout à fait d'accord
11	**Je pense qu'utiliser ce casque de réalité virtuelle est ludique**
	Pas du tout d'accord ☐ ☐ ☐ ☐ ☐ ☐ ☐ ☐ ☐ ☐ Tout à fait d'accord
12	**Si j'avais la possibilité d'avoir facilement accès à ce casque de réalité virtuelle, je pense que je l'utiliserais**
	Pas du tout d'accord ☐ ☐ ☐ ☐ ☐ ☐ ☐ ☐ ☐ ☐ Tout à fait d'accord

Advantages of publishing in Frontiers

OPEN ACCESS
Articles are free to read for greatest visibility and readership

FAST PUBLICATION
Around 90 days from submission to decision

HIGH QUALITY PEER-REVIEW
Rigorous, collaborative, and constructive peer-review

TRANSPARENT PEER-REVIEW
Editors and reviewers acknowledged by name on published articles

Frontiers
Avenue du Tribunal-Fédéral 34
1005 Lausanne | Switzerland

Visit us: www.frontiersin.org
Contact us: frontiersin.org/about/contact

REPRODUCIBILITY OF RESEARCH
Support open data and methods to enhance research reproducibility

DIGITAL PUBLISHING
Articles designed for optimal readership across devices

FOLLOW US
@frontiersin

IMPACT METRICS
Advanced article metrics track visibility across digital media

EXTENSIVE PROMOTION
Marketing and promotion of impactful research

LOOP RESEARCH NETWORK
Our network increases your article's readership